

THE ROLE OF THE GUT-BRAIN AXIS IN AT-GENETIC-RISK AND CLINICAL ALZHEIMER'S DISEASE

By Celina Mercedes Dietrich

A Thesis submitted in Fulfilment of the Requirements for the
Degree of **Doctor of Philosophy (PhD)**



Submitted to

Norwich Medical School, University of East Anglia

Date: 27th June 2021

Abstract word count: 300

Thesis word count: 65,257

"This copy of the thesis has been supplied on condition that anyone who consults it is understood to recognise that its copyright rests with the author and that use of any information derived there from must be in accordance with current UK Copyright Law. In addition, any quotation or extract must include full attribution."

ABSTRACT

Introduction: The intestinal microbiome is emerging as an important modulator of health and disease. The Gut-Brain axis has been implicated in Alzheimer's disease (AD) and is associated with intestinal dysbiosis. It is unknown if the Gut-Brain axis is involved in the preclinical course of AD. Understanding the role of the Gut-Brain axis in an at-genetic risk AD (APO ϵ 4 carriers) may provide a microbial signature that can aid diagnosis and intervention strategies.

Aims: To examine the role of the intestinal microbiome in AD development, I assessed APO ϵ 4 carriers and non-carriers neuropsychological, cardiovascular and brain integrity at baseline and longitudinally studied their intestinal microbiome at baseline, 6- and 12-months. Finally, the APOE findings were contrasted against a cohort of clinical AD patients.

Methods and Results: Baseline results showed that APOE groups did not differ on neuropsychological, cardiovascular and brain integrity measures, with the exception of LDL being elevated in the APO ϵ 4 carriers. The baseline measurements of the microbiome via whole-genome shotgun metagenomics highlighted ten differentially abundant taxa by genotype. Longitudinally, there was increased abundance of *Prevotellaceae*, *Prevotella* and *Ruminococcus obeum* in APO ϵ 4 carriers. Functionally, differences in 20 KEGG pathways existed, including changes in energy and nitrogen metabolism. Finally, shotgun metagenomics sequencing data, indicated that the intestinal microbiota of AD patients is characterized by large-scale and taxa-specific differences versus APOE groups, including reduced α -diversity, altered taxa abundances and changes in 63 metabolic pathways.

Conclusion: Despite APOE groups being well-matched for neuropsychological, cardiovascular and brain integrity measures, except LDL, numerous taxa and functional pathways differed between the APOE cohorts on a cross-sectional and longitudinal level. Although diversity and global compositional measures were not consistently different, this indicates that microbiota changes are already present in at-genetic-risk of AD people. In the AD patient group, there was reduced diversity, distinct compositional profiles and altered taxonomy and function indicating increased intestinal microbial dysbiosis.

Access Condition and Agreement

Each deposit in UEA Digital Repository is protected by copyright and other intellectual property rights, and duplication or sale of all or part of any of the Data Collections is not permitted, except that material may be duplicated by you for your research use or for educational purposes in electronic or print form. You must obtain permission from the copyright holder, usually the author, for any other use. Exceptions only apply where a deposit may be explicitly provided under a stated licence, such as a Creative Commons licence or Open Government licence.

Electronic or print copies may not be offered, whether for sale or otherwise to anyone, unless explicitly stated under a Creative Commons or Open Government license. Unauthorised reproduction, editing or reformatting for resale purposes is explicitly prohibited (except where approved by the copyright holder themselves) and UEA reserves the right to take immediate 'take down' action on behalf of the copyright and/or rights holder if this Access condition of the UEA Digital Repository is breached. Any material in this database has been supplied on the understanding that it is copyright material and that no quotation from the material may be published without proper acknowledgement.

TABLE OF CONTENTS

LIST OF TABLES.....	9
LIST OF FIGURES.....	11
SUPPLEMENTARY LIST OF TABLES	16
SUPPLEMENTARY LIST OF FIGURES	20
ACKNOWLEDGEMENTS.....	21
LIST OF ABBREVIATIONS.....	23
CHAPTER 1: INTRODUCTION	29
Dementia: the biggest health challenge of the 21st century	29
Dementia prevalence, social and economic considerations.....	29
Dementia types.....	34
Alzheimer’s Disease pathophysiology	35
Pharmacological management of Alzheimer’s Disease	39
Approved drugs	39
Drug development	40
Unmodifiable risk factors for developing Alzheimer’s Disease	41
Ageing.....	41
Genetic risk	43
Apolipoprotein E genotype.....	43
Overview of the Apolipoprotein E gene	43
Apolipoprotein ε4 genotype increases risk for Alzheimer’s Disease	44
Apolipoprotein E allelic distribution	45
Apolipoprotein E disease mechanisms	45
Modifiable risk factors for developing Alzheimer’s Disease.....	47
The Gut-Brain axis - an emerging key player in health and disease	50
Overview	50
Microbial diversity	50
Host-microbiota functions.....	51
Gut-Brain axis interaction pathways	52
Mechanisms in Alzheimer’s Disease pathophysiology and the role of the intestinal microbiota	57
The intestinal microbiota modulates cognitive function.....	57
The intestinal microbiota may promote aggregation of Amyloid beta in the brain ...	59
Intestinal metabolites: neuroprotective and disease-promoting mechanisms	60
Reduced protective barrier function	63
Intestinal microbiota and the inflammation hypothesis	68
Existing microbiota-targeted treatment for AD	72
Observational studies in Alzheimer’s Disease mice models	73

Human studies	75
Intestinal microbiota and Apolipoprotein E genotype in Alzheimer’s Disease	86
Summary.....	88
Aims	90
Hypotheses	90
CHAPTER 2: METHODS.....	91
Ethical processes and funding.....	91
Study design.....	92
Recruitment	93
Power calculation	93
Subject identification and consent.....	93
Apolipoprotein E genotyping	95
Home visit 1	96
Home visit 2	96
Follow-up samples at 6 months (T2) and 12 months (T3).....	97
Cardiovascular risk assessment	97
Brain magnetic resonance imaging (MRI).....	97
Cognitive, behavioural, lifestyle and clinical measures.....	98
Addenbrooke’s Cognitive Examination-III.....	98
Rey–Osterrieth Complex Figure test	99
Trail Making Test	100
Spatial navigation measures	101
Cognitive Change Index	105
Cambridge Behavioural Inventory-Revised.....	106
Generalized Anxiety Disorder-7.....	107
Patient Health Questionnaire-9	108
Microbiome Questionnaire.....	108
Health questionnaire	109
Cardiovascular risk assessment – QRISK®3.....	109
Dietary assessment – Food Frequency Questionnaire.....	111
Statistical analysis of test results - generalized linear model (GLM).....	112
Magnetic Resonance Imaging analysis.....	113
Experimental design of microbiome study aspects.....	114
Sample collection, transfer and storage	114
DNA extraction	115
DNA quality control	116
Library preparation.....	116
DNA sequencing – whole metagenomic shotgun sequencing	116
Processing of sequenced data.....	117
Taxonomic and functional analysis of metagenomic sequencing data.....	120
Diversity analysis	121
Univariate differential abundance analysis	124
Multivariate differential abundance analysis	124

Functional analysis	125
CHAPTER 3: COGNITIVE, DIETARY AND HEALTH PROFILES	129
Participant recruitment, enrolment and study completion.....	129
Demographic characteristics of Apolipoprotein E groups.....	131
Cognitive and behavioural results from administered tests.....	133
Addenbrooke’s Cognitive Examination-III.....	134
Rey-Osterrich-Complex-Figure test	134
Trail Making Task	135
Supermarket Task	136
Sea Hero Quest.....	137
Cognitive and behavioural results from questionnaires.....	143
Cognitive Change Index	144
Generalized Anxiety Disorder-7.....	144
Patient Health Questionnaire-9	144
Cambridge Behavioural Inventory-Revised.....	145
Dietary, cardiovascular and general health data.....	146
Food Frequency Questionnaire	146
Microbiome Health Questionnaire	149
Cardiovascular Risk.....	149
Neuroimaging	154
Voxel based morphometry	154
Chapter Discussion.....	155
Relationship between Apolipoprotein ϵ 4 and cognition/behaviour	155
CHAPTER 4: CROSS-SECTIONAL AND LONGITUDINAL ASSESSMENT OF THE INTESTINAL MICROBIOTA PROFILES IN APOE4 CARRIERS AND NON- CARRIERS.....	162
Faecal sample collection	162
Taxonomic analysis.....	165
Descriptive summary of taxonomic profiles	165
Alpha diversity: Between-group and intra-subject variability	180
Between-group variability.....	180
Intra-subject variability	182
Beta diversity: Between-group diversity comparison.....	184
Beta diversity – Baseline (T1).....	184
Beta diversity – 6-months follow-up (T2)	186
Beta diversity – 12-months follow-up (T3)	187
Differential abundance analysis.....	189
Univariate differential abundance analysis (LEfSe).....	189
Multivariate differential abundance analysis (MaAsLin2).....	199
MaAsLin2 – Baseline (T1).....	199
MaAsLin2 – 6-months follow-up (T2)	200

MaAsLin2 – 12-months follow-up (T3)	201
MaAsLin2 – Longitudinal mixed effect model analysis of T1-T3.....	202
Predictive Functional Profiling	204
KEGG gene abundance data	204
Beta diversity of KEGG data	204
Multivariate analysis of normalized KEGG data	205
HUMAN3 functional profiles	206
Chapter discussion.....	208
Key findings	208
Detailed discussion	208
CHAPTER 5: AD PATIENT GROUP COMPARISON	219
Demographic profile of Alzheimer’s Disease patient cohort.....	219
Cognitive test performance of Alzheimer’s Disease patient cohort	220
Addenbrooke’s Cognitive Examination-III.....	221
Rey-Osterrich-Complex-Figure test	221
Trail Making Test.....	223
Cognitive and behavioural results of Alzheimer’s Disease patients from questionnaires	224
Generalized Anxiety Disorder-7.....	225
Patient Health Questionnaire-9	225
Cambridge Behaviour Inventory-Revised	225
Taxonomic profile.....	227
Descriptive summary	227
Alpha diversity	239
Beta diversity.....	240
Differential abundance analysis	244
Predictive Functional profiling	253
Beta diversity.....	253
Multivariate analysis of normalized Kyoto Encyclopedia of Genes and Genomes count data	254
HUMAN3 functional profiles	258
Chapter Discussion	260
Key findings	260
Neuropsychological and behavioural analysis	260
Diversity analysis	261
Descriptive community analysis.....	263
Differential abundance analysis	264
Microbiota functional potential.....	276
CHAPTER 6: GENERAL DISCUSSION, LIMITATIONS AND FUTURE DIRECTIONS	285
General discussion	285
Conclusion.....	290

Limitations.....	291
Study-specific limitations	291
Future directions	301
<i>BIBLIOGRAPHY</i>.....	303
<i>SUPPLEMENTARY INFORMATION</i>.....	342
Genomic DNA extraction from saliva samples.....	347
DNA quality control	347
DNA amplification	348
Brain Protocol Magnetic Resonance Imaging Sequence.....	352
Details on neuropsychological testing battery	352
Addenbrooke’s Cognitive Examination-III – detailed test description	352
Rey-Osterrich-Complex Figure test - scoring of the task	353
Sea Hero Quest – two types of level to assess spatial navigation	353
Sea Hero Quest - Statistical analysis method.....	355
Supermarket Task – detailed test description.....	356
Cognitive Change Index – detailed information on the questionnaire	358
QRISK [®] 3 – lipid measurements.....	359
Food Frequency Questionnaire – detailed description	359
Shotgun metagenomic sequencing and analysis	361
Genomic DNA extraction from faecal matter	361
Quality control of DNA from faecal matter.....	362
Library preparation.....	363
Library quality control by NOVOGENE.....	364
Data quality control by NOVOGENE	366
Processing of sequenced metagenomics data.....	367
Microbiome Analyst workflow – detailed description	367
Results neuropsychological assessment of Apolipoprotein E groups.....	368
Addenbrooke’s Cognitive Examination-III.....	368
Rey-Osterrich-Complex Figure test.....	368
Trail Making Test.....	370
Supermarket task	371
Sea Hero Quest.....	372
Cognitive Change Index	374
Generalized Anxiety Disorder-7.....	374
Patient Health Questionnaire-9	374
Cambridge Behavioural Inventory-Revised.....	375
Microbiome health questionnaire.....	375
Microbiome results of Apolipoprotein E cohorts	380
Neuropsychological results of the Alzheimer’s Disease patient group	393
Addenbrooke’s Cognitive Examination-III.....	393
Rey-Osterrich-Complex Figure.....	393
Trail Making Test.....	394
Generalized Anxiety Disorder-7.....	395

Patient Health Questionnaire-9	395
Cambridge Behavioural Inventory-Revised.....	396
Alpha diversity	396
Beta diversity.....	397

LIST OF TABLES

Table 1.1 Human studies exploring the Gut-Brain axis in Alzheimer's Disease

Table 2.1 Study inclusion and exclusion criteria

Table 2.2 Apolipoprotein E genotype frequencies in the population of the United Kingdom and study group assignment.

Table 3.1 Apolipoprotein genotype frequency in participant cohort, genetic risk for developing Alzheimer's Disease and assigned study group

Table 3.2 Primary characteristics of the Apolipoprotein E groups

Table 3.3 Neuropsychological profile of the Apolipoprotein $\epsilon 4$ carriers and non-carriers

Table 3.4 Effect of Apolipoprotein $\epsilon 4$ status on Supermarket Task performance

Table 3.5 Wayfinding performance by Apolipoprotein $\epsilon 4$ status and task level

Table 3.6 Response frequencies of flare accuracy rates by Apolipoprotein $\epsilon 4$ status, frequency distribution Pearson-chi-squared test (χ^2)

Table 3.7 Secondary neuropsychological profile of the Apolipoprotein E groups

Table 3.8 Average daily intake and standard deviation of nutrients

Table 3.9 Average daily intake and standard deviation of food groups

Table 3.10 Demographic information and clinical variables of the QRISK®3 risk prediction model by Apolipoprotein $\epsilon 4$ status

Table 3.11 QRISK®3 risk scores by Apolipoprotein $\epsilon 4$ status

Table 4.1 Relative abundances (%) of most abundant phyla across all timepoints

Table 4.2 Relative abundances (%) of most abundant families across all timepoints

Table 4.3 Relative abundances (%) of most abundant genera across all timepoints

Table 4.4 Relative abundances (%) of most abundant species across all timepoints

Table 5.1 Primary characteristics of the Alzheimer's Disease patient group compared against the two Apolipoprotein E cohorts

Table 5.2 Neuropsychological profile of the Alzheimer's Disease patient group compared against the two Apolipoprotein E cohorts

Table 5.3 Secondary neuropsychological profile of the Alzheimer's Disease patient group compared against the two Apolipoprotein E cohorts

Table 5.4 Relative abundances (%) of most abundant phyla by group

Table 5.5 Relative abundances (%) of most abundant families by group

Table 5.6 Relative abundances (%) of most abundant species by group

LIST OF FIGURES

Figure 1.1 Top 10 leading causes of death globally in 2019, figure taken from World Health Organisation Global Health Estimates (World Health Organization, 2019b)

Figure 1.2 The main leading causes of deaths in England and Wales, from 2005 to 2017, shown in percentages of total deaths. Adapted from (*England and Wales: Mortality Statistics*, 2019)

Figure 1.3 Top 10 causes of death in the United Kingdom for 2019 for both sexes and all ages from (World Health Organization, 2019a)

Figure 1.4 Processing of amyloid precursor protein (APP) by the (1) non-amyloidogenic pathway and the (2) amyloidogenic pathway which results in the generation of amyloid beta ($A\beta$). AICD: amyloid intracellular domain, α -secretase: alpha-secretase, β -secretase: beta-secretase, BACE1: beta-site APP cleaving enzyme 1, CTF: carboxy-terminal fragment, C83: 83-residue C-terminal fragment, C99: 99-residue C-terminal fragment, sAPP: soluble APP, p3: peptide 3, γ -secretase: gamma-secretase.

Figure 1.5 Schematic representation of cognitive decline as a function over increasing age as observed in healthy ageing (grey solid line) and Alzheimer's Disease (black solid line). Figure created by author, adapted from Sperling *et al.* (2011)

Figure 1.6 Schematic representation of the Apolipoprotein E gene on chromosome 19 and single nucleotide changes leading to the three isoforms $\epsilon 2$, $\epsilon 3$ and $\epsilon 4$, SNP: single nucleotide polymorphism. Figure created by author

Figure 1.7 Schematic representation of suggested modifiable (circles) and non-modifiable (squares) risk factors of AD. Microbiota modulation indicated by arrows. List not exhaustive. Figure created by author

Figure 1.8 Schematic presentation of suggested Gut-Brain interaction pathways. Figure created by author

Figure 1.9 Schematic summarizing blood-brain barrier changes in disease states, neurotoxic and neuroprotective factors modulating blood-brain barrier integrity with respect to Alzheimer's Disease pathophysiology. Figure created by author

Figure 1.10 Schematic, simplified overview of suggested mechanisms underlying lipopolysaccharide-induced inflammation. LPS: lipopolysaccharide; TLR4: Toll-like receptor 4. Figure created by author

Figure 1.11 Schematic presentation of the main microbial-driven pathways suggested to be involved in Alzheimer's Disease. Figure created by author

Figure 2.1 Study design flow chart

Figure 2.2 ROCF figure with 18 global and local elements

Figure 2.3 Egocentric (left) and allocentric (right) coding. Figure from Coughlan *et al.* (2018)

Figure 2.4 Flowchart of microbiome experimental design

Figure 2.5 MicrobiomeAnalyst workflow of KEGG gene abundance data. Figure created by author

Figure 2.6 Overall workstream of predictive functional profiling and analysis of gene abundance data. Blue: KEGG-based analysis carried out using MicrobiomeAnalyst tool and R. Green: Analysis based on HUMAnN3 relative abundance pathways, implemented in R. Figure created by author

Figure 3.1 Flowchart of study recruitment process

Figure 3.2 Consolidated Standards of Reporting Trials diagram showing the flow of participants through the study

Figure 3.3 Boxplot of “Central vs boundary navigation preference” ratio by Apolipoprotein $\epsilon 4$ status

Figure 3.4 Scatterplot with line of best fit showing age*motivation subdomain score interaction

Figure 3.5 Boxplot of (A) low-density lipoprotein levels and (B) total cholesterol levels by Apolipoprotein $\epsilon 4$ status

Figure 3.6 Example of image-processing: (A) removal of neck voxels and (B) brain mask

Figure 4.1 Scatterplot showing faecal sample collection throughout the study. Coloured dots denote sampling timepoints - red: T1, green: T2, blue: T3. Shapes denote events impacting sample collection – circle: none, triangle: sample collection affected by COVID-19, cross: antibiotics. Shaded areas denote the seasons; green = spring, yellow = summer, orange = autumn, blue = winter. Every subject keeps the same position along the y-axis

Figure 4.2 Faecal samples analyzed at T1, T2, and T3

Figure 4.3 Relative abundances of phyla at baseline, Apolipoprotein $\epsilon 4$ non-carriers (left panel), Apolipoprotein $\epsilon 4$ -carriers (right panel), shape showing kingdom affiliation, size represents relative abundances

Figure 4.4 Relative abundances (%) of phyla between Apolipoprotein E groups over time

Figure 4.5 Relative abundance of top 10 taxa at family-level at baseline, Apolipoprotein $\epsilon 4$ non-carriers (left panel), Apolipoprotein $\epsilon 4$ -carriers (right panel), shape showing kingdom affiliation, size represents relative abundances

Figure 4.6: Relative abundances (%) of families between Apolipoprotein E groups over time

Figure 4.7 Relative abundances (%) of genera between Apolipoprotein E groups over time

Figure 4.8 Top 25 most abundant species at baseline, Apolipoprotein ε4 non-carriers (left panel), Apolipoprotein ε4-carriers (right panel), shape showing kingdom affiliation, size represents relative abundance

Figure 4.9 Relative abundances (%) of families between Apolipoprotein E groups over time

Figure 4.10 Alpha diversity (measured as Shannon diversity at species-level) between the groups at T1, T2 and T3. Blue: Apolipoprotein ε4 non-carriers, red: Apolipoprotein ε4 carriers. Statistical significance $* < 0.05$

Figure 4.11 Scatterplot of Shannon diversity index, labelling of the most and least diverse samples of individual subjects at T1 (A), T2 (B), and T3 (C) by Apolipoprotein ε4 status

Figure 4.12 Non-metric multidimensional scaling on Bray-Curtis dissimilarity between the species relative-abundance intestinal microbiota profiles at baseline by (a) Apolipoprotein ε4 status, (b) sex, (c) age group. With labels denoting the centroid of points

Figure 4.13 Principal component analysis on Bray-Curtis dissimilarity between the species relative-abundance intestinal microbiota profiles at baseline by Apolipoprotein ε4 status. Ellipse showing 95% confidence interval

Figure 4.14 NMDS on Bray-Curtis dissimilarity on intestinal microbiota profiles at order-level by Apolipoprotein ε4 status (light blue = Apolipoprotein ε4 non-carriers, red = Apolipoprotein ε4 carriers) at T2. Each point denotes a sample in a reduced dimensional space and is connected with a line to the group centroid

Figure 4.15 Non-metric multidimensional scaling on Bray-Curtis dissimilarity on intestinal microbiota profiles at order-level by Apolipoprotein ε4 status (light blue = Apolipoprotein ε4 non-carriers, red = Apolipoprotein ε4 carriers) at T3. Each point denotes a sample in a reduced dimensional space and is connected with a line to the group centroid

Figure 4.16 (A) Linear Discriminant Analysis effect size of discriminative taxa between Apolipoprotein ε4 non-carriers (green) and carriers (red) at baseline. Length of bar chart represents increasing abundance and associated Linear Discriminant Analysis scores are on a log₁₀ scale. (B) Cladogram showing results using saliency and phylogenetic relatedness for a clearer visualisation. Figures generated by LEfSe

Figure 4.17 Phylogenetic overview of univariate analysis findings. (A) – (E) distinct clades. Green = significant enrichment of taxa in Apolipoprotein ε4 non-carriers, red = significant enrichment of taxa in Apolipoprotein ε4 carriers, grey = no significant association for taxa with Apolipoprotein ε4 status

Figure 4.18 Linear Discriminant Analysis effect size of discriminative taxa Apolipoprotein ε4 non-carriers (green) and carriers (red) at the 6-months follow-up. Length of bar chart represent increasing abundance and associated Linear Discriminant Analysis scores are on a log₁₀ scale

Figure 4.19: Linear Discriminant Analysis effect size of discriminative taxa between Apolipoprotein ε4 non-carriers (green) and carriers (red) at T3. Length of bar chart represent

increasing abundance and associated Linear Discriminant Analysis scores are on a log₁₀ scale

Figure 4.20 Boxplot of *Verrucomicrobia* between the Apolipoprotein E cohorts

Figure 4.21 Boxplot of (A) *Bacteroidetes* and (B) *Actinobacteria* between Apolipoprotein E cohorts

Figure 4.22 Boxplot of *Methanobacteriaceae* between Apolipoprotein E cohorts

Figure 4.23 Boxplot of (A) *Prevotellaceae*, (B) *Prevotella*, and (C) *R. obeum* between the Apolipoprotein E groups across T1-T3

Figure 4.24 Non-metric multidimensional scaling of beta diversity (Jaccard index) between the predicted KEGG metabolism by group (light blue = Apolipoprotein ε4 non-carriers, red = Apolipoprotein ε4 carriers). Each point denotes a sample in a reduced dimensional space and is connected with a line to the group centroid

Figure 5.1 Boxplot of summary Addenbrooke's Cognitive Examination-III score between the three groups, ** p<0.001

Figure 5.2 Boxplot of Rey-Osterrich-Complex-Figure recall score by participant group, ** p<0.001

Figure 5.3 Boxplot of Trail Making Test-B performance by participant group, ** p<0.001

Figure 5.4 Boxplot of Cambridge Behaviour Inventory-Revised summary frequency mean by group, ** p<0.001

Figure 5.5 Relative abundances of phyla by group: Apolipoprotein ε4 non-carriers (left panel), Apolipoprotein ε4 carriers (middle panel), Alzheimer's Disease patient group (right panel), shape showing kingdom affiliation, size represents relative abundances

Figure 5.6 Relative abundance of phyla by group (2): Apolipoprotein ε4 non-carriers (left), Apolipoprotein ε4 carriers (middle), Alzheimer's Disease patient group (right)

Figure 5.7 Relative abundances of top ten families within Alzheimer's Disease patient group. Apolipoprotein ε4 non-carriers (left panel), Apolipoprotein ε4 carriers (middle panel), Alzheimer's Disease patient group (right panel), shape showing kingdom affiliation, size represents relative abundances

Figure 5.8 Relative abundance of families by group (2), Apolipoprotein ε4 non-carriers (left), Apolipoprotein ε4 carriers (middle), Alzheimer's Disease patient group (right)

Figure 5.9 Relative abundance of species by group (2), Apolipoprotein ε4 non-carriers (left), Apolipoprotein ε4 carriers (middle), Alzheimer's Disease patient group (right)

Figure 5.10 Relative abundances of top 20 species. Apolipoprotein ε4 non-carriers (left panel), Apolipoprotein ε4 carriers (middle panel), Alzheimer's Disease patient group (right panel), shape showing kingdom affiliation, size represents relative abundances

Figure 5.11 Alpha diversity (measured as Shannon diversity index) at (A) genus-level and (B) species-level between the groups; * $p < 0.05$. Blue: Apolipoprotein $\epsilon 4$ non-carriers, red: Apolipoprotein $\epsilon 4$ carriers, yellow: Alzheimer's Disease patient group

Figure 5.12 Non-metric Multidimensional Scaling on Bray-Curtis dissimilarity between the species relative-abundance intestinal microbiota profiles by (A) group (light blue = Apolipoprotein $\epsilon 4$ non-carriers, red = Apolipoprotein $\epsilon 4$ carriers, yellow = Alzheimer's Disease patients), (B) sex (orange = female, blue = male), (C) age group (light blue = 52-60 years old, middle blue = 61-69 years old, dark blue = 75+ years old). Each point denotes a sample in a reduced dimensional space and is connected with a line to the group centroid

Figure 5.13 Linear Discriminant Analysis effect size of discriminative taxa between Apolipoprotein $\epsilon 4$ non-carriers (green), Apolipoprotein $\epsilon 4$ carriers (red) and the Alzheimer's Disease patient group (yellow). The length of bar charts represents increasing abundance. Associated Linear Discriminant Analysis scores are on a \log_{10} scale

Figure 5.14 Significant associations identified by MaAsLin2 analysis grouped by phylogeny, Clades: (A) *Actinobacteria*, (B) *Bacteroidetes*, (C) *Firmicutes*, (D) *Proteobacteria*, (E) *Viruses*. Black: associations with Alzheimer's Disease group and both Apolipoprotein E cohorts, blue: Alzheimer's Disease only with Apolipoprotein $\epsilon 4$ non-carriers, red: AD only with Apolipoprotein $\epsilon 4$ carriers, grey: no associations. Upward (increased) and downward arrow (decreased) indicate relative abundance in Alzheimer's Disease patient group compared to the APOE groups.

Figure 5.15 Non-metric Multidimensional Scaling on Jaccard index between the predicted KEGG metabolism by participant group (light blue = Apolipoprotein $\epsilon 4$ non-carriers, red = Apolipoprotein $\epsilon 4$ carriers, yellow = Alzheimer's Disease patients). Each point denotes a sample in a reduced dimensional space and is connected with a line to the group centroid

Figure 6.1 Graphical summary of the evidence for a microbial component in Alzheimer's Disease based on the current literature, findings for taxonomy and function only shown if replicated by at least one other study, \uparrow = increase, \downarrow = decrease, X = no association, \checkmark = differences exist

SUPPLEMENTARY LIST OF TABLES

- Table 7.1 Observational mice studies investigating the relationship of Alzheimer's Disease on the intestinal microbiota
- Table 7.2 Human and animal studies investigating the role of Apolipoprotein E genotype and the intestinal microbiota
- Table 7.3 External controls to determine Apolipoprotein E allelic discrimination
- Table 7.4 Reference table to determine Apolipoprotein E genotype
- Table 7.5 Excerpt of Summary of Sequencing Data information provided by NOVOGENE for three T2 samples
- Table 7.6 Multivariate regression analysis results, Addenbrooke's Cognitive Examination-III summary score
- Table 7.7 Multivariate regression analysis results, Rey-Osterrich-Complex Figure: Copy score
- Table 7.8 Multivariate regression analysis results, Rey-Osterrich-Complex Figure: Recall score
- Table 7.9 Multivariate regression analysis results, Rey-Osterrich-Complex Figure: Copy time
- Table 7.10 Person Product-moment correlation coefficient (r) between Rey-Osterrich-Complex Figure variables by group
- Table 7.11 Multivariate regression analysis results, Trail Making Test-A
- Table 7.12 Multivariate regression analysis results, Trail Making Test-B
- Table 7.13 Multivariate regression analysis results, Supermarket test
- Table 7.14 Multilevel mixed model results, Sea Hero Quest: wayfinding distance
- Table 7.15 Multilevel mixed model results, Sea Hero Quest: wayfinding duration
- Table 7.16 Multilevel mixed model results, Sea Hero Quest: wayfinding distance to border
- Table 7.17 Mixed effects ordinal logistic regression results, Sea Hero Quest: flare accuracy
- Table 7.18 Multiple regression analysis results, Cognitive Change Index: summary score
- Table 7.19 Percentage of participants experiencing anxiety by severity categories and by Apolipoprotein $\epsilon 4$ status
- Table 7.20 Multivariate regression results, Generalized Anxiety Disorder-7
- Table 7.21 Frequency distribution of depression severity by Apolipoprotein E genotype
- Table 7.22 Multivariate regression results, Patient Health Questionnaire-9
- Table 7.23 Multivariate regression results, Cambridge Behavioural Inventory-Revised: summary score

Table 7.24 Response frequencies of microbiome questionnaire by Apolipoprotein ϵ 4 status, Pearson Chi-squared (χ^2) and p-value

Table 7.25 Multivariate regression results, Low-density lipoprotein and total cholesterol

Table 7.26 Multivariate regression results, Triglycerides and High-density lipoprotein

Table 7.27 Alpha diversity by taxonomic level between the Apolipoprotein E groups at baseline (T1), 6-months follow-up (T2), 12-months follow-up (T3)

Table 7.28 Post-hoc analysis. Variance of between-sample diversity (Bray-Curtis dissimilarity distances, 999 permutations) explained by each variable assessed with cross-sectional PERMANOVA for T1 samples

Table 7.29 Variance of between-sample diversity (Bray-Curtis dissimilarity distances, 999 permutations) explained by each variable assessed with cross-sectional PERMANOVA for T2 samples

Table 7.30 Variance of between-sample diversity (Bray-Curtis dissimilarity distances, 999 permutations) explained by each variable assessed with cross-sectional PERMANOVA of T3 samples

Table 7.31 Univariate differential abundance results of Apolipoprotein ϵ 4 non-carriers for T1-T3. Significant associations in green

Table 7.32 Univariate differential abundance results of Apolipoprotein ϵ 4 carriers for T1-T3. Significant associations in red

Table 7.33 Multivariate linear regression results showing features significantly associated with Apolipoprotein ϵ 4 status, after accounting for the effect of gender and age at baseline

Table 7.34 Multivariate linear regression results showing features significantly associated with Apolipoprotein ϵ 4 status, after accounting for the effect of gender and age at T2

Table 7.35 Multivariate linear regression results showing features significantly associated with Apolipoprotein ϵ 4 status, after accounting for the effect of gender and age at T3

Table 7.36 Multivariate linear regression results showing features significantly associated with Apolipoprotein ϵ 4 status, after accounting for the effect of gender and age across all three timepoints, subject ID as random effect

Table 7.37 Kyoto Encyclopedia of Genes and Genomes modules associated with Apolipoprotein ϵ 4 status

Table 7.38 Kyoto Encyclopedia of Genes and Genomes pathways associated with Apolipoprotein ϵ 4 status

Table 7.39 HUMAnN3 Stratified pathways in Apolipoprotein E cohorts

Table 7.40 HUMAnN3 Unstratified pathways in Apolipoprotein E cohorts

Table 7.41 Variance of between-sample functional diversity (Jaccard dissimilarity distances, 999 permutations) explained by each variable assessed with cross-sectional PERMANOVA

Table 7.42 Multivariate regression results, Addenbrooke's Cognitive Examination-III

Table 7.43 Boxplot of Rey-Osterrich Complex Figure copy score by group

Table 7.44 Multivariate regression results, Rey-Osterrich Complex Figure: Copy score

Table 7.45 Multivariate regression results, Rey-Osterrich Complex Figure: Recall score

Table 7.46 Multivariate regression results, Rey-Osterrich Complex Figure: Copy time

Table 7.47 Multivariate regression results, Trail Making Test-A

Table 7.48 Multivariate regression results, Trail Making Test-B

Table 7.49 Multivariate regression results, Generalized Anxiety Disorder-7

Table 7.50 Multivariate regression results, Patient Health Questionnaire-9

Table 7.51 Multivariate regression results, Cambridge Behavioural Inventory-Revised: Domain Frequency Score

Table 7.52 Alpha diversity by taxonomic level between the two Apolipoprotein E cohorts and the Alzheimer's Disease patient group

Table 7.53 Variance of between-sample diversity (Bray-Curtis dissimilarity distances, 999 permutations) explained by each variable assessed with cross-sectional PERMANOVA

Table 7.54 Post-hoc analysis, pairwise comparisons for all pairs of level for 'group' using PERMANOVA

Table 7.55 Significant associations from univariate differential abundance analysis per group

Table 7.56 (Part 1) Multivariate analysis with significant associations for 'group', model accounts for the effect of 'age' and 'sex'. Alzheimer's Disease patient group as baseline contrast compared against Apolipoprotein $\epsilon 4$ carriers (contrast: carriers) and compared against the Apolipoprotein $\epsilon 4$ non-carriers (contrast: non-carriers)

Table 7.57 KEGG metabolisms in Alzheimer's Disease vs Apolipoprotein E cohorts

Table 7.58 KEGG modules that are enriched (\uparrow) in Alzheimer's Disease vs Apolipoprotein E cohorts

Table 7.59 KEGG modules that are decreased (\downarrow) in Alzheimer's Disease vs Apolipoprotein E cohorts

Table 7.60 KEGG pathways that are enriched (\uparrow) in Alzheimer's Disease vs Apolipoprotein E cohorts

Table 7.61 KEGG pathways that are decreased (\downarrow) in Alzheimer's Disease vs Apolipoprotein E cohorts

Table 7.62 HUMAnN3 Stratified pathways enriched in Alzheimer's Disease vs Apolipoprotein E cohorts

Table 7.63 HUMAnN3 Stratified pathways decreased in Alzheimer's Disease vs Apolipoprotein E cohorts

Table 7.64 HUMAnN3 Unstratified pathways enriched Alzheimer's Disease vs Apolipoprotein E cohorts

Table 7.65 HUMAnN3 Unstratified pathways decreased in Alzheimer's Disease vs Apolipoprotein E cohorts

Table 7.66 Post-hoc analysis. Variance of between-sample functional diversity (Jaccard dissimilarity distances, 999 permutations) explained by each variable assessed with cross-sectional PERMANOVA for T2 and Alzheimer's Disease patient samples

Table 7.67 Post-hoc analysis, pairwise comparisons for all pairs of level for "group" using PERMANOVA

SUPPLEMENTARY LIST OF FIGURES

Figure 7.1 Representative printout of allelic discrimination plot

Figure 7.2 Safety Checklist for Magnetic Resonance Imaging scanning

Figure 7.3 Maps presented in wayfinding levels 6 (A), 8 (B), 11 (C) adapted from Coughlan (2019)

Figure 7.4 Flare accuracy level modified from Coughlan (2019)

Figure 7.5 Example screenshots from the Supermarket Task

Figure 7.6 Spatial layout of supermarket response sheet modified from (Tu *et al.*, 2015)

Figure 7.7 Example page from the Food Frequency Questionnaire

Figure 7.8 Example distribution of Sequencing Quality for submitted sample H09

Figure 7.9 Example error rate distribution along reads for submitted sample H09

Figure 7.10 Example distribution of A/T/G/C content for submitted sample H09

Figure 7.11 Example composition of Raw Reads for submitted sample H09

Figure 7.12 Non-metric Multidimensional Scaling on beta diversity (Jaccard index) between the predicted (A) KEGG module and (B) KEGG pathways by group (light blue = Apolipoprotein ϵ 4 non-carriers, red = Apolipoprotein ϵ 4 carriers). Each point denotes a sample in a reduced dimensional space and is connected with a line to the group centroid

Figure 7.13 Patient Health Questionnaire-9 score by group, depression severity= none (<4), mild (5-9), moderate (10-14), moderately severe (15-19), severe (20-27)

Figure 7.14 Non-metric Multidimensional Scaling (Jaccard diversity index) between the predicted (A) KEGG module and (B) KEGG pathways by group (light blue = Apolipoprotein ϵ 4 non-carriers, red = Apolipoprotein ϵ 4 carriers, yellow = Alzheimer's Disease patients). Each point denotes a sample in a reduced dimensional space and is connected with a line to the group centroid

ACKNOWLEDGEMENTS

This work would not have been possible without the guidance and support of my primary supervisor, Professor Michael Hornberger, and my secondary supervisor, Professor Simon Carding. Thank you both very much for the opportunities that you have given me, particularly to help me push scientific boundaries and give me the confidence and courage to forge my own path.

I would also like to thank all members of Prof Hornberger's and Prof Carding's research groups with a special mention for Dr Gillian Coughlan, Dr Stephen Jeffs, Fiona Newberry, and Dr Aimee Parker.

A special thank you to my parents, without whose understanding, support and love, I would have not found the courage or determination to move to the UK to chase this dream, go through with it, and find that I can feel at home independent of geography. Thank you for everything, most importantly thank you for always believing in me.

I would also like to thank my grandmother, who has always supported me and passed on her beliefs that becoming a strong, independent woman is a foundation for a happy life. To quote one of her many proverbs – "Hol' dir die Taube auf dem Dach, was willst du denn mit dem Spatzen in deiner Hand".

A thank you cannot express my gratefulness for the unwavering support of my fiancé, Dr Nicholas Gollop, who has accompanied me from the beginning of this journey and has been there every single step of the way, whilst also doing his PhD. We have climbed mountains together, both in reality and metaphorically speaking, and I know that together nothing is insurmountable. I am excited for all that is to come.

I would like to professionally acknowledge the following groups of people for their contribution to this work: Dr Donnie Cameron, Dr David Willis, Dr Richard Green and the rest of the MRI research team, Dr Andrea Telatin, Dr Rebecca Ansorge, Dr George Savva, Mr James Goillau and Miss Catherine Essex. All of those listed were critical to this project in one way or another.

Lastly, I would also like to thank all participants of this study, who have welcomed me with kindness and have given up considerable amounts of time to participate in this research. None of this would have been possible without their commitment and I am incredibly grateful.

Supervisor Signature

I, Michael Hornberger (primary supervisor), confirm that any required taught courses have been satisfactorily completed.

Signature:

A handwritten signature in black ink, appearing to read 'M. Hornberger', written in a cursive style.

Author's Declaration

I, Celina M Dietrich, declare that the work in this thesis has not been submitted for any other award and that it is all my own work (unless otherwise stated). I also confirm that this work fully acknowledges the opinions, ideas and contributions from the work of others.

Signature:

A handwritten signature in blue ink, reading 'Celina Dietrich', written in a cursive style.

LIST OF ABBREVIATIONS

- AA – Amyloid A
- AAA – Aminoadipic acid
- ACE-III – Addenbrooke’s Cognitive Examination
- AChE – Acetylcholinesterase
- AD – Alzheimer’s Disease
- AICD – Amyloid intracellular domain
- AL – Amyloid light-chain
- ALS – Amyotrophic Lateral Sclerosis
- aMCI – Amnesic MCI
- APO ϵ – Apolipoprotein ϵ
- APP – Amyloid precursor protein
- APrP – Prion protein amyloidosis
- AST – Arcsine square root transformation
- AUC – Area Under the Curve
- A β – Amyloid beta
- α -secretase – alpha-secretase
- BACE1 – beta-site APP cleaving enzyme
- BBB – Blood-brain barrier
- BBSRC – Biotechnology and Biological Sciences Research Council
- BCRE – Bob Champion Research and Education Building
- BDNF – Brain-derived neurotrophic factor
- BET – Brain Extraction Tool
- BMI – Body Mass Index
- BMQ – Bowel Movement Quality
- BSS – Bristol Stool Scale
- bvFTD – Behavioral variant FTD

β -secretase – beta-secretase

CAA – Cerebral amyloid angiopathy

CBI-R – Cambridge-Behavioural-Inventory-Revised

CCI – Cognitive Change Index

Cdk5 – Cyclin-dependent kinase 5

CDR – Clinical dementia rating

cGMP – Cyclic guanosine monophosphate

CLR – Centred log ratio

CNS – Central nervous system

CoA – Coenzyme A

COVID-19 – Coronavirus disease of 2019

CSF – Cerebrospinal fluid

CTF – C-Terminal Fragment

CVD – Cardiovascular disease

Cypa – Cyclophilin A

D₁ – Simpson diversity index

D₂ – Inverse Simpson index

DAP – Diaminopimelic acid

DCE-MRI – Dynamic contrast-enhanced magnetic resonance imaging

Df – Degrees of freedom

DHA – Docosahexaenoic acid

DLB – Dementia with Lewy bodies

DNA – Deoxyribonucleic Acid

EA – Ethanolamine

ENS – Enteric nervous system

EPA – Eicosapentaenoic acid

EPIC – European Prospective Investigation into Cancer and Nutrition

FDR – False discovery rate

FETA – Food Frequency Questionnaire European Prospective Investigation into Cancer and Nutrition Tool for Analysis

FFQ – Food Frequency Questionnaire

FMT – Faecal matter transplant

FSL – FMRIB Software Library

FTD – Frontotemporal dementia

GABA – Gamma-Aminobutyric acid

GAD-7 – Generalized Anxiety Disorder-7

GF – Germ-Free

GI – Gastrointestinal

GLM – Generalized linear model

GM – Grey matter

GV-971 – Sodium oligomannate

H' – Shannon diversity index

H₂ – Dihydrogen

H₂S – hydrogen sulphide

HDL – High-density lipoprotein

HPA – Hypothalamic–pituitary–adrenal

HRA – Health Research Authority

HSV-1 – Herpes simplex type 1 virus

HUMAN3 – HMP Unified Metabolic Analysis Network

HXA3 – Hepoxilin A3

IATA – International Air Transport Association

IBS – Inflammatory bowel disease

Ig – Immunoglobulin

IL – Interleukin

IMP – Inosine monophosphate

IMP – Inosine-5'-phosphate

IRAS – Integrated Research Application System

JDR – Join Dementia Research

kcal – kilocalories

KEGG – Kyoto Encyclopedia of Genes and Genomes

kJ – Kilojoule

KO – KEGG orthology

LA – Linoleic acid

LDA – Linear Discriminant Analysis

LDL – Low-density lipoproteins

LPS – Lipopolysaccharides

MAMPs – Microbe-associated molecular patterns

MCI – Mild cognitive impairment

MMSE – Mini-Mental State Examination

MNI – Montreal Neurological Institute

MOTION – Microbiome of the ageing gut and its effect on human gut health and cognition

MRI – Magnetic Resonance Imaging

MRP2 – Multidrug resistance-associated protein-2

NELLC – Norfolk Elderly and Later Life Cohort

NFAT – Nuclear factor of activated T cells

NFT – Neurofibrillary tangles

NICE – National Institute for Health and Clinical Excellence

NLRP3 – NLR family pyrin domain containing 3

NMDA – N-Methyl-D-aspartate

nMDS – Non-metric multidimensional scaling

NNUH – Norfolk and Norwich University Hospital

NO – Nitric oxide

NRP – Norwich Research Park

NSAIDs – Non-steroidal anti-inflammatory drugs

OTU – Operational taxonomic unit

PAF – Weighted population attributable fraction

PCoA – Principal coordinates analysis

PD – Parkinson’s disease

PE – Phosphatidylethanolamine

PERMANOVA – Permutational multivariate analysis of variance

PET – Positron emission tomography

PG – Phosphatidylglycerol

PHQ-9 – Patient Health Questionnaire-9

PPP – Pentose phosphate pathway

PS1 – Presenilin-1

QI – Quadram Institute

R² – Squared multiple correlation

REC – Research Ethics Committee

ROCF – Rey–Osterrieth complex figure

ROS – Reactive Oxygen Species

RuMP – Ribulose monophosphate

SAMP8 – Senescence-accelerated mouse-prone 8

SAA – serum amyloid A

sAPP – soluble AA

SCD – Subjective cognitive decline

SCFAs – Short-chain fatty acids

SDP – Shotgun Data Profiling

SHQ – Sea Hero Quest

SMI – Subjective Memory Impairment

SS – Sum of squares

T2D – Type 2 Diabetes

Th1 – T helper cell type 1

TLRs – Toll-like receptors

TMA – Trimethylamine

TMAO – Trimethylamine N-oxide

TMT – Trail Making Test

TNF- α – Tumour Necrosis Factor alpha

TR – Targeted-replacement

TRACC – The demenTia Research And Care Clinic

Treg – Regulatory T cells

TUDCA – Tauroursodeoxycholic acid

UEA – University of East Anglia

UK – United Kingdom

UMP – Uridine monophosphate

p3 – peptide 3

VaD – Vascular dementia

VBM – Voxel-based morphometry

VN – Vagal nerve

γ -secretase – gamma-secretase

$\sqrt{R^2}$ – Pearson correlation

16S rRNA gene sequencing – 16S ribosomal RNA gene sequencing

5xFAD – Five familial AD mutations

6-PG/PK pathway – 6-phosphogluconate/phosphoketolase pathway

CHAPTER 1: INTRODUCTION

Dementia: the biggest health challenge of the 21st century

Today's life expectancy is without a doubt a major achievement for humankind and a reflection of the progress made in medical and other sciences (Scholey, 2017). Whilst a girl born in 1901 in the United Kingdom (UK) was expected to live to age 52.4 years, born in 2018, her life-expectancy would have climbed to 83.2 years – an increase of almost 31 years (Office for National Statistics, 2015; Public Health England, 2017). In the 21st century, the conditions and illnesses which dramatically reduced survival in early life stages, have been ameliorated and as a result, the numbers of child deaths in industrial nations are at their lowest point. It is particularly the later life stages that now confront society with new challenges in the form of age-related diseases (Scholey, 2017).

The maintenance of health and well-being in our ageing population is a critical aspect, as people continue to live longer but often with poorer health. The percentage of people aged 65 years or older in the UK was in 2000 was 15.9%, compared to 18.6% in 2019 and is predicted to reach 24% by 2040 (Office for National Statistics, 2019). Advanced age is a major risk factor for a range of neurodegenerative diseases, including dementia (Carone, Asgharian and Jewell, 2014).

Dementia prevalence, social and economic considerations

Dementia has become a global health challenge. In 2019, the worldwide prevalence of dementia was 50 million, with a current annual increase of 10 million cases per year. In the UK, more than 885,000 people were living with dementia in 2019 (Wittenberg *et al.*, 2019; Lynch, 2020). Projections estimate that by 2050 the global prevalence for dementia will be 152 million people (Lynch, 2020). In the UK is predicted to reach a prevalence of 1.6 million by 2040, which is a 8.8% of prevalence rate of the total UK population (Wittenberg *et al.*, 2019).

The driving force behind this rise is increase in life expectancy. Age is a major factor for developing dementia. Between 65 to 90 years of age dementia prevalence doubles with every five-year age increment (Corrada *et al.*, 2010). Dementia awareness is also rising, leading to higher rates of diagnosis.

In 2019, there were 55.4 million death globally. From a global perspective, seven of the ten leading causes of death are noncommunicable disease (Figure 1.1). The top leading cause of death worldwide in 2019 was ischaemic heart disease (16% of all deaths, 8.9 million deaths), followed by stroke (11% of all deaths) and chronic obstructive pulmonary disease (6% of all deaths). In 2019, Alzheimer's Disease (AD) and other dementias ranked 7th, compared to 14th in 2000 (World Health Organization, 2019b). The most common form of dementia is AD accounting for 60 to 70 percent of the cases (Boutajangout and Wisniewski, 2013; WHO, 2017).

Leading causes of death globally

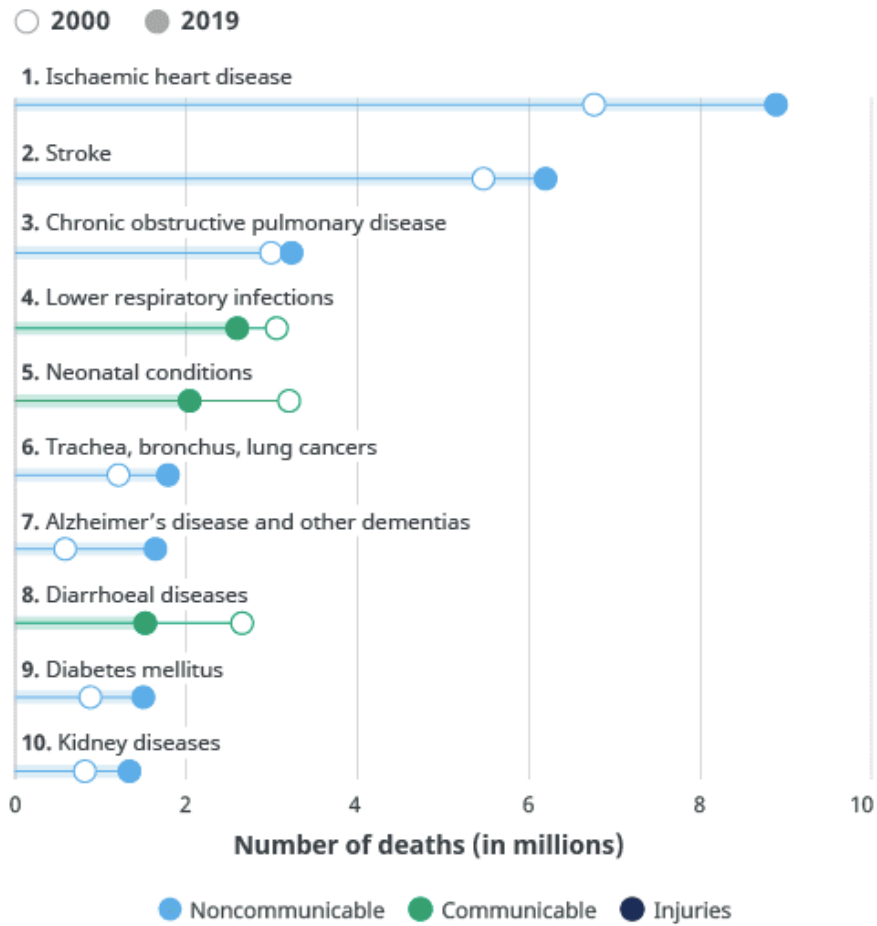


Figure 1.1 Top 10 leading causes of death globally in 2019, figure taken from World Health Organisation Global Health Estimates (World Health Organization, 2019b)

In high-income countries, all but two (ischaemic heart disease and stroke) of the top ten leading causes of death increased between 2000 and 2019. The rate of increase is by far the fastest for AD and other dementias, which ranked second in high-income countries in 2019 and accounted for 814,000 deaths (World Health Organization, 2019b).

Compared to other high-income countries, the picture of the top ten leading causes of death emerging in the UK is similar. Ischaemic heart disease and cerebrovascular disease (e.g. stroke) are following an overall downward trend as medical advances lead to considerable improvements in prevention and treatment of major diseases (Figure 1.2). This is reflected by a relative percentage decrease of 13.45% and 13.54% for ischaemic heart disease and

cerebrovascular disease, respectively, for both sexes between 2011 and 2018 (Office for National Statistics, 2020). Whereas AD and other dementias showed a relative percentage increase of 71.3% within the same timeframe in the UK.

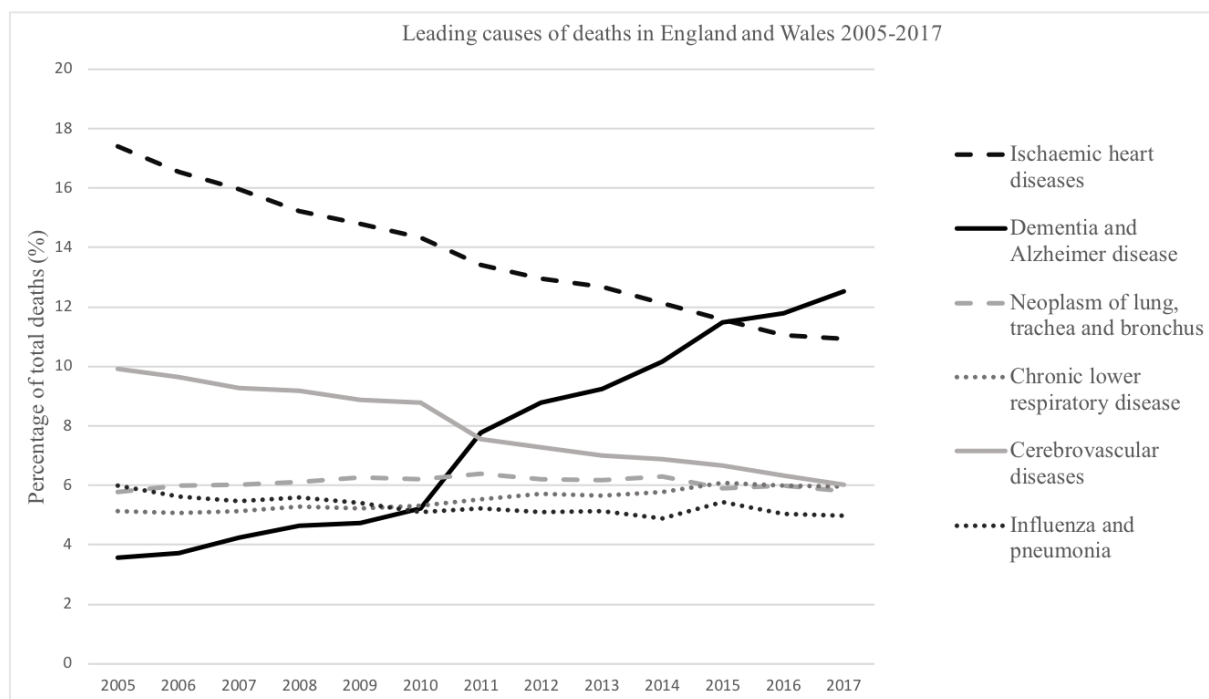


Figure 1.2 The main leading causes of deaths in England and Wales, from 2005 to 2017, shown in percentages of total deaths. Adapted from (*England and Wales: Mortality Statistics, 2019*)

In the UK, the top ten causes of death in 2019 across females and males are led by AD and other dementias with 145.3 death per 100.000 (Figure 1.3). This is followed by ischaemic heart disease (106.2 death per 100.000) and lower respiratory infection (60 per 100.000). Stroke only ranks 4th with 55.7 death per 100.000 (World Health Organization, 2019a).

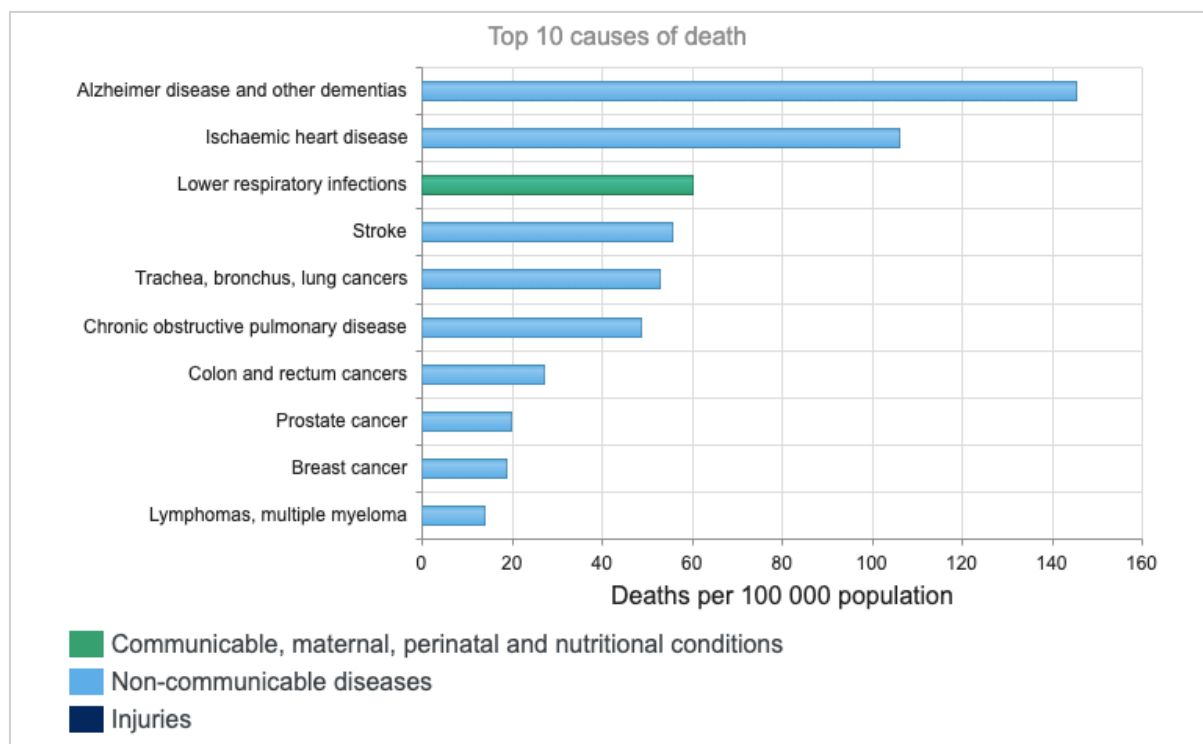


Figure 1.3 Top 10 causes of death in the United Kingdom for 2019 for both sexes and all ages from (World Health Organization, 2019a)

Although disease progression varies, dementia is ultimately fatal as it commonly leads to circulatory and respiratory system diseases (Brunnström and Englund, 2009; Boutajangout and Wisniewski, 2013; McLaren, 2015). At present, dementia is incurable with pharmacologic treatments providing modest and transient symptomatic benefit but failing to cure or stop the progressive course of dementia. From a medical perspective, all currently licensed pharmacological drugs act to provide symptomatic alleviation for some period of time but ultimately do not improve the underlying pathophysiology. The management of dementia – “dementia care” is mostly restricted to improving the individuals’ and family’s ability to cope with symptoms, provide knowledge, and alleviate stress and depression.

Dementia poses a huge challenge for the health care system, which is ill-equipped to adequately care for the amount of people with dementia. In 2009, 1 in 4 hospital beds were occupied by dementia patients in the UK (Alzheimer’s Society, 2009). Dementia care amounts to a total of £34.7 billion in 2015, of which 40% is privately funded. The cost of

social care for dementia in the UK is estimated to triple by 2040 (Wittenberg *et al.*, 2019). With increasing prevalence, both the social and economic burden of dementia will continue to grow. Not surprisingly and in view of the limited treatment options available, there has been a renewed impetus for preventative approaches towards dementia.

Dementia types

‘Dementia’ is an umbrella term used to describe several diseases which all involve progressive cognitive impairment that may include symptoms of memory loss, difficulties in planning and problem-solving, language and communication problems, as well as changes in personality, behaviour, and mood (e.g. apathy, agitation, stereotypical behaviour, depression) (Takeda, Sato and Morishita, 2014; Alzheimer Association, 2016). Cognitive symptoms are commonly categorised into five main domains: memory, executive function, language, visuospatial abilities, personality and behaviour (Cunningham *et al.*, 2015). During disease progression, symptoms (regardless of dementia subtype) broaden to affect multiple cognitive domains and intensify in later stages of the disease which consequently results in worsened functional impairment. Symptoms negatively affect daily activities and social functioning as well as the overall quality of life (Opara, 2012). The most common four subtypes of dementia are Alzheimer’s disease (~50-75%), vascular dementia (VaD, ~20%), dementia with Lewy bodies (DLB, ~5%) and frontotemporal dementia (FTD, ~5%) (Cunningham *et al.*, 2015). In addition, the pathophysiology of dementia types can overlap, termed mixed dementia. Because of the heterogeneity of symptoms and underlying pathological changes, it can prove difficult to establish a clinical diagnosis. Hence all estimates for subtypes frequencies need to be interpreted with caution (WHO, 2012).

AD is typically divided into three stages. In the early preclinical stage clinical symptoms are not apparent but underlying brain changes (increase of amyloid load, neuronal injury, oxidative stress, etc.) are ongoing. In the middle stage, people present with concerns about

their cognition (most commonly memory problems) and this is substantiated with objective evidence of mild cognitive impairment (MCI) which does not affect people's ability to go about their everyday activities (Albert *et al.*, 2011). Symptoms worsen progressively for many years and have an increasingly negative affect on daily living, until in the final stage, symptoms are so severe that the person requires full-time care.

Diagnostic criteria for AD are complex. For a diagnosis of AD, a patient needs to present with insidious onset of cognitive deficits that are supported by report or observation. Cognitive deficits need to be clearly noticeable using objective test measures and the cognitive deficit needs to affect memory and at least one other cognitive domain for amnesic AD. For non-amnesic (memory intact) presentations, the main cognitive deficit affects language or visuospatial abilities or executive functioning and one other cognitive domain (McKhann *et al.*, 2011). The most common supportive features include measurements of A β deposition (cerebrospinal fluid [CSF] levels of A β 42, or positron emission tomography [PET] imaging) or neuronal injury (CSF tau, rate of brain atrophy [hippocampal/ medial temporal areas], PET imaging) (Jack *et al.*, 2010; Albert *et al.*, 2011). These features are not only suggested to precede clinical symptoms but might also be predictive for future cognitive decline (Sperling *et al.*, 2011).

Alzheimer's Disease pathophysiology

For the past quarter of a century, the amyloid (cascade) hypothesis, first proposed by Hardy and Higgins in 1992, has been the dominant theory to explain the major pathological events that take place in AD. According to this model, the accumulation and deposition of amyloid beta (A β) peptides, which are derived from amyloid precursor protein (APP), mark the initial event and are causal for AD neuropathology (Hardy and Higgins, 1992; Kametani and Hasegawa, 2018).

There are over 25 different proteins that can form so called “amyloids” by forming insoluble, unbranched fibres consisting of β -pleated sheets which exhibit similar molecular properties such as green birefringence (following binding of the dye Congo Red) and a characteristic cross- β fibre diffraction pattern (when subjected to X-rays) (Xing and Higuchi, 2002; Eisenberg and Jucker, 2012). Some of these amyloid-forming proteins are associated with pathology that spans a range of diseases, including AD (amyloid fibril protein: $A\beta$), spongiform encephalopathies (amyloid fibril protein: prion protein amyloid [APrP]), systemic amyloid light-chain (AL) amyloidosis (amyloid fibril protein: immunoglobulin light chain protein), systemic amyloid A (AA) amyloidosis (amyloid fibril protein: serum amyloid A [SAA]) and many other types of amyloidosis (Xing and Higuchi, 2002).

The amyloid fibril involved in the pathogenesis of AD is $A\beta$. Its precursor is APP, a type-1 membrane glycoprotein, which is expressed in many tissues. Whilst it is best known for its role in AD, APP is suggested to have several important biological functions (Chen *et al.*, 2017). There are two main proteolytic processing pathways of APP: the non-amyloidogenic canonical pathway and the amyloidogenic pathway (Figure 1.4) which can be differentiated by the sequence and nature of different protease action on APP (Bergström *et al.*, 2016).

- (1) In the non-amyloidogenic pathway, APP is cleaved by α -secretase within the $A\beta$ domain and generates a membrane-bound 83-residue-long α -C-terminal fragment, α CTF (or C83), and soluble APP (sAPP) α . In fact, α CTF can subsequently be cleaved by γ -secretase, thereby generating the extracellular peptide p3 and the APP intracellular domain (AICD). Processing by α -secretase is thought to inhibit $A\beta$ formation (Zhang and Song, 2013; Bergström *et al.*, 2016; Chen *et al.*, 2017).
- (2) In the amyloidogenic pathway, the β -secretase ‘beta-site APP cleaving enzyme 1’ (BACE1) cleaves APP which produces soluble APP beta and the membrane-tethered 99-residue β -C-terminal fragment, β CTF (or C99). Further cleavage of β CTF by γ -secretase

generates an amyloid intracellular domain and a 38-42 amino acid long, soluble A β peptide (Zhang and Song, 2013; Bergström *et al.*, 2016; Chen *et al.*, 2017).

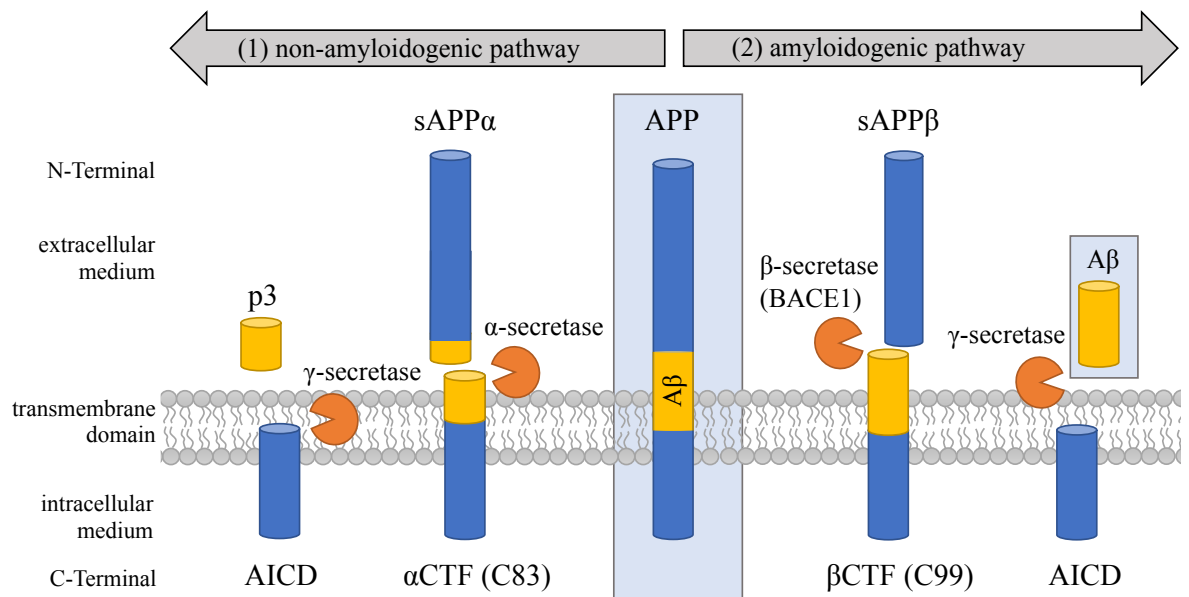


Figure 1.4 Processing of amyloid precursor protein (APP) by the (1) non-amyloidogenic pathway and the (2) amyloidogenic pathway which results in the generation of amyloid beta (A β). AICD: amyloid intracellular domain, α -secretase: alpha-secretase, β -secretase: beta-secretase, BACE1: beta-site APP cleaving enzyme 1, CTF: carboxy-terminal fragment, C83: 83-residue C-terminal fragment, C99: 99-residue C-terminal fragment, sAPP: soluble APP, p3: peptide 3, γ -secretase: gamma-secretase.

The sequence of events leading to AD begin with a decreased removal or degradation of A β from the brain (failure of clearance mechanisms). As a result, levels of A β (in particular A β 42) gradually rise and amyloid fibrils begin to form and eventually develop into senile plaques; a process termed A β amyloidosis.

These abnormal fibrous depositions initiate inflammatory responses through activated microglia and astrocytes, oxidative injury, and formation of neurofibrillary tangles (NFT) (tau pathology) resulting in widespread vascular damage and neuronal dysfunction and

neuronal cell loss (Selkoe and Hardy, 2016). NFTs, consisting mainly of hyperphosphorylated tau, has since become established as another fundamental neuropathological hallmark feature of AD, that leads to the progressive retrograde degeneration of affected neurons (Iqbal *et al.*, 2005). A spatiotemporal pattern of affected brain regions emerges during disease progression showing an early involvement of entorhinal/perirhinal cortex, that extends to sub regions (C1,CA2-3) of the hippocampus, then spreads to subiculum amygdala, thalamus, and in later stages also extends to parts of the neocortex (Braak *et al.*, 2006; Serrano-Pozo *et al.*, 2011).

Inflammation is critical in AD pathogenesis. Glial activation leads to a neuroinflammatory response in AD which may play an important role in the induction of oxidative stress (Folch *et al.*, 2018). Whilst microglia are usually suggested to have a protective role in the brain by degrading A β peptides through phagocytosis in early disease stages and thus help amyloid clearance, they may also add to the inflammatory response in later stages of the disease through release of cytokines, chemokines and free radicals which exacerbate AD disease pathology. A β in turn activates microglia activity. As a result, a positive feedback loop is created which drives inflammation in the brain (Cai, Hussain and Yan, 2014). The key role of neuroinflammation as a driving force in AD development has also emerged from epidemiological studies that show a sparing effect of non-steroidal anti-inflammatory drugs (NSAIDs), commonly used in arthritis patients, resulting in lowered AD prevalence in these patient cohorts (McGeer, Schulzer and McGeer, 1996; McGeer, Rogers and McGeer, 2016). Some evidence suggests that a main factor triggering AD is impairment of APP metabolism and that development and progression of AD are mainly attributed to tau and not A β pathophysiology (Takashima *et al.*, 1993; Roberson *et al.*, 2007; Miao *et al.*, 2009; Kametani and Hasegawa, 2018).

On a diagnostic level, one of the earliest and most typical symptoms in AD pathology is memory dysfunction, in particular impaired episodic memory. Neural correlates of episodic memory include the hippocampus, anterior thalamic nucleus, prefrontal cortex, and other regions of the medial temporal lobes. Thus, performance on neuropsychological tests may reflect the level of neurodegeneration in the central nervous system (CNS). However, recent evidence in patients suggest that brain changes might appear up to 10 years before the onset of memory deficits (Weston et al. 2016), which suggests that current cognitive factors are potentially not sensitive enough to detect earliest changes. A new approach has been to focus on spatial navigation deficits as an early diagnostic marker and to shift efforts towards pre-memory diagnostics.

Pharmacological management of Alzheimer's Disease

Approved drugs

The number of licensed drugs for AD is limited to symptomatic treatment including three acetylcholinesterase (AChE) inhibitors (donepezil hydrochloride, galantamine hydrobromide, rivastigmine tartrate) and N-Methyl-D-aspartate (NMDA) receptor antagonist (memantine) that are recommended by the National Institute for Health and Clinical Excellence (NICE) guidelines for symptomatic treatment of AD (NICE, 2018). A monotherapy using an AChE inhibitor to address the cholinergic deficit that results from the progressive loss of cholinergic neurons is usually chosen for mild to moderate cases of AD (Mesulam and Geula, 1994; Tohgi *et al.*, 1996; Ellis, 2005). Whereas memantine, which targets glutamatergic dysfunction by acting against NMDA receptor-induced toxicity that is involved in neuronal loss in AD, is prescribed for severe AD (Olin and Schneider, 2001; Areosa, Sherriff and McShane, 2005; Birks, 2006; Cunningham *et al.*, 2015; Folch *et al.*, 2018). These drugs can have a beneficial effect on cognitive functioning, aberrant behavior (if present) and improve activities of daily living. Ultimately, they do not reverse or stop the progression of the disease.

Drug development

In the 25 years since the amyloid hypothesis was postulated, over 200 clinical trials that mainly targeting different aspects of the A β cascade have failed. With a failure rate of 99.6%, AD drug development is far below the probability of success rate for clinical drug development for diseases of the CNS, which was on average 15% between 2000-2015 (Wong, Siah and Lo, 2019; Janak and Jenner, 2020). In 2020, there were a total of 33 compounds in Phase III, 78 Phase II and 32 Phase I clinical trials in the pipeline for AD (Janak and Jenner, 2020). This includes 21 anti-A β compounds (six in Phase I, eight in Phase II and seven in Phase III), next to several anti-tau immunotherapies, $\alpha/\beta/\gamma$ -Secretases and compounds targeting neurotransmission, inflammation and energy metabolism-based interventions (Janak and Jenner, 2020).

Notably, there is also several compounds emerging that are considered antimicrobials. *COR388* (Phase II/III) is an anti-microbial molecule that targets *Porphyromonas gingivalis* bacteria (known to cause periodontitis) (Dominy *et al.*, 2019). The antibiotic *Rifaxamin* (Phase II) is suggested to counter-act inflammation. Its mechanistic action is suggested to occur via lowering ammonia levels and changing the intestinal microbiota (Kowalski and Mulak, 2019). The antiviral therapy *Valaclovir* (Phase II), which is already approved for the treatment of human herpes virus 6A and 7 (Readhead *et al.*, 2018). As well as *Elavirenz* (Phase I), which is suggested to change cholesterol levels, which are a risk factor for AD and linked to Apolipoprotein E (APOE) variants (Janak and Jenner, 2020).

Reviewing the current status of drug development for AD highlights that despite a great need and huge research effort, finding a clinically effective, disease-modifying treatment for AD is extremely difficult. We also observe a shift, away from traditional anti-amyloid treatments, to interventions which target a wide scope and have novel mechanisms of action.

This is reflected by an increasing number of compounds which are classed as ‘neuroprotective/metabolic’ and newly emerging antimicrobial therapies. In China, sodium oligomannate (GV-971), which is suggested to act via altering the intestinal microbiota, was recently approved for the treatment of mild to moderate AD. The concept that AD is a disorder only of the CNS is outdated, and research and drug development are adopting a more holistic approach and are exploring many new avenues.

Unmodifiable risk factors for developing Alzheimer’s Disease

Ageing

The prevalence and probability of onset for neurodegenerative diseases including AD, Parkinson’s disease (PD), or Amyotrophic Lateral Sclerosis (ALS), rises sharply at certain age-thresholds. No other factor in the general population has such a major impact on disease incidence. Consequently, age is considered the main risk factor for AD (Mattson and Magnus, 2006; Saxena and Caroni, 2011).

The trajectories of healthy ageing and accumulation of health deficits vary between individuals and are determined by a multitude of factors of both genetic and environmental origin. Many domains of cognitive functioning decline as a function of increasing age, which can make it challenging to distinguish pathological from non-pathological cognitive ageing (see Figure 1.5).

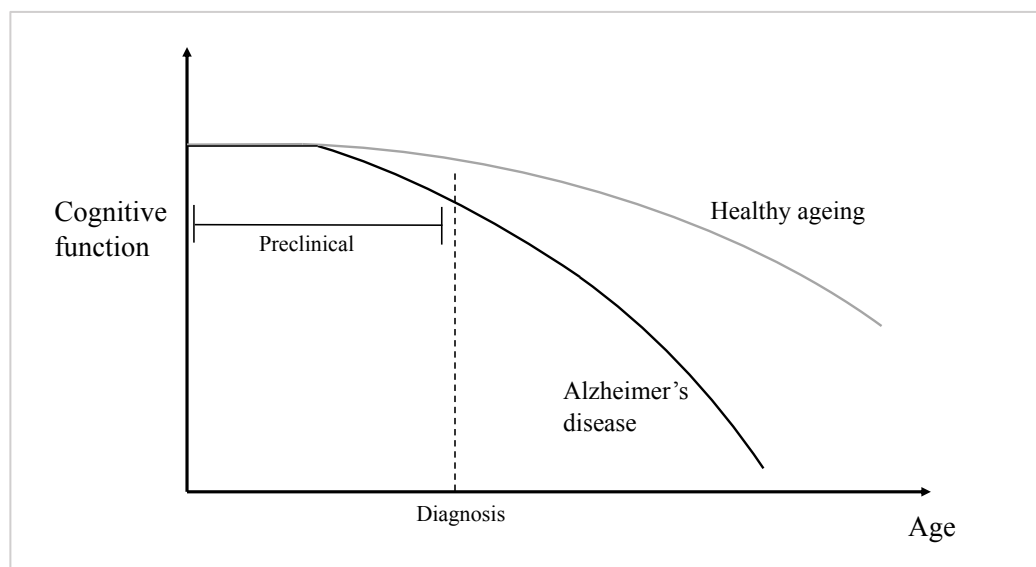


Figure 1.5 Schematic representation of cognitive decline as a function over increasing age as observed in healthy ageing (grey solid line) and Alzheimer's Disease (black solid line). Figure created by author, adapted from Sperling *et al.* (2011)

Many aspects of cognition, which are affected in AD, decline during healthy ageing and to complicate matters further, there is an overlap with the symptomatic presentation of other cognitive phenotypes such as Subjective Memory Impairment (SMI) and MCI (Scholey, 2017). Whilst SMI and MCI are not necessarily prodromal stages on the AD disease continuum, both cognitive phenotypes put people at considerably higher risk for developing AD in the future (Ward *et al.*, 2013; Jessen *et al.*, 2014).

Age-related changes of the brain lead to a gradual decline of neuropsychiatric function. This is particularly true for cognitive domains of fluid intelligence – marked by reduced information processing speed, problem solving, reasoning, and memory function – and executive function. Other cognitive domains, such as semantic memory or emotional regulation, are age-invariant and remain stable over the lifespan (Grady 2012). Natural age-related deterioration also leads to reduced cognitive reserve, diminished neuroplasticity, and moderate decline of grey matter volumes in several brain regions (Reuben *et al.* 2011). The co-occurrence of several interacting mechanisms is decisive in AD, including the emergence

of a population of neurons highly sensitive to stress and a disturbance of cellular homeostasis due to an overload of calcium which prompts a state of hyperexcitability in the glutamatergic neuronal system. The formation of neurofibrillary protein aggregates, enhanced levels of neuronal stress, calcium overload, and oxidative stress, negatively reinforce and interact with one another in a feed-forward cascade (Demuro, Parker and Stutzmann, 2010; Ghosh, Agarwal and Haggerty, 2011; Saxena and Caroni, 2011). Both genetic predisposition and advanced age are non-modifiable factors that put people at higher risk for developing dementia.

Genetic risk

There are also several genetic risk factors, which are non-modifiable and confer an increased risk for developing AD to its carrier. In the following, I am going to focus on the APOE gene and its role in AD.

Apolipoprotein E genotype

Overview of the Apolipoprotein E gene

Allelic variants of the APOE gene are the most common susceptibility genes to confer differential genetic risk for AD (Reiman *et al.*, 2020). APOE is a major glycoprotein responsible for the transport and delivery of lipids, particularly cholesterol, thereby playing a major role in lipid homeostasis and cholesterol metabolism. In the brain, APOE transports lipids from astrocytes to neurons (Liu *et al.*, 2013). The vast majority of APOE is produced in the liver, with smaller amounts produced by astrocytes, microglia, and vascular smooth muscle cells within the brain (Kanekiyo, Xu and Bu, 2014). APOE is a multifunctional protein with a central role not only in lipid handling, but also in neuronal homeostasis, which includes dendritic morphology and functioning of mitochondria (Huang and Mahley, 2014)

The APOE gene, located on chromosome 19, is polymorphic at two single nucleotides resulting in three structurally distinct isoforms – $\epsilon 2$, $\epsilon 3$, and $\epsilon 4$ (Figure 1.6) that allow for six phenotypes. A single amino acid substitution in two locations (residues 112 and 158) leads to different biological function of the isoforms. APO $\epsilon 2$ has been ascribed neuroprotective function whereas the $\epsilon 4$ allele is considered a susceptibility gene for late-onset dementia (Reiman *et al.*, 2020).

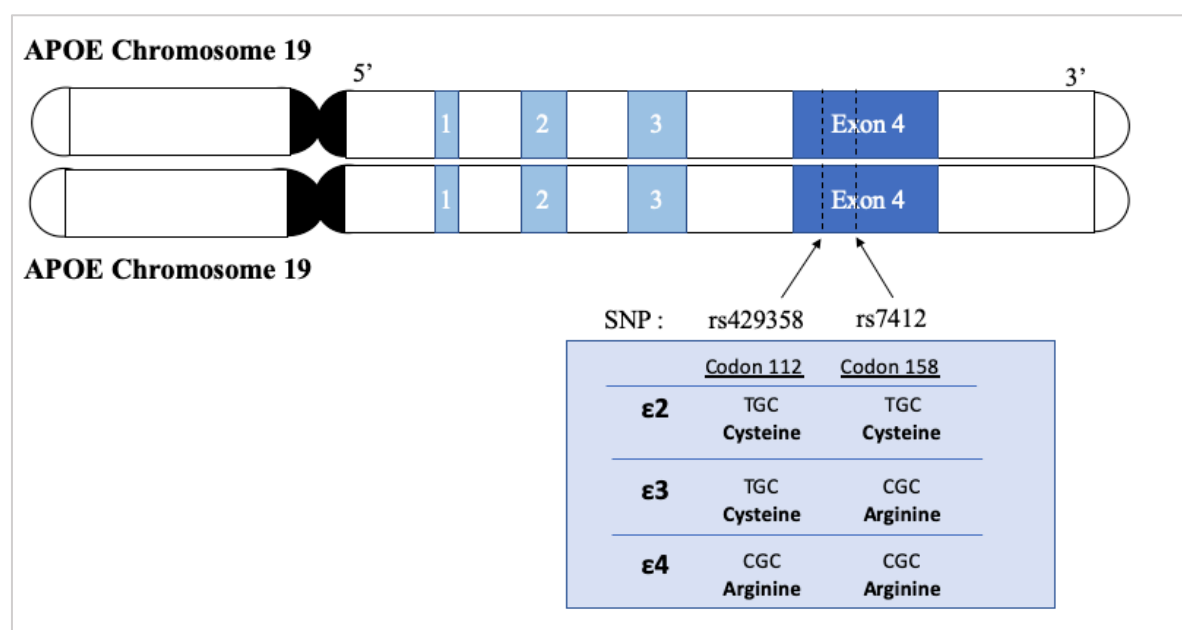


Figure 1.6 Schematic representation of the Apolipoprotein E gene on chromosome 19 and single nucleotide changes leading to the three isoforms $\epsilon 2$, $\epsilon 3$ and $\epsilon 4$, SNP: single nucleotide polymorphism. Figure created by author

Apolipoprotein $\epsilon 4$ genotype increases risk for Alzheimer's Disease

The risk for late-onset AD in individuals with APO $\epsilon 3/\epsilon 4$ and APO $\epsilon 4/\epsilon 4$ is increased three-fold and 12-fold respectively. The APO $\epsilon 4$ genotypes are also associated with lower age of disease onset (Verghese *et al.* 2011). Onset of AD is classified as either early (30-60 years old, often accounted for by an inherited single gene mutation of APP, Presenilin-1 (PS1) or PS-2 [familial AD]) or late-onset (>60 years old) (Bekris *et al.*, 2010). With a frequency of less than one in 20 patients showing clinical symptoms before the age of 60, AD is dominantly late-onset (Verghese, Castellano and Holtzman, 2011).

Apolipoprotein E allelic distribution

The APO ϵ 3 allele is the most prevalent isoform in the population, with Caucasians showing a 68-86% prevalence for this genotype (O'Donoghue *et al.*, 2018). Allelic variation worldwide for ϵ 2 and ϵ 4 is 10-23% and 4-14%, respectively (Liu *et al.*, 2013; O'Donoghue *et al.*, 2018). Estimates for the frequency distribution of the six genotypes in the UK population extrapolated from findings of 621 individuals are as follows. 52% of the population are estimated to have the APO ϵ 3/ ϵ 3 genotype, 20% have APO ϵ 2/ ϵ 3 and another 20% have APO ϵ 3/ ϵ 4, whereas only 4% have APO ϵ 2/ ϵ 4, 2% have APO ϵ 2/ ϵ 2 genotype and another 2% are homozygous for the APO ϵ 4/ ϵ 4 genotype (Singh, Singh and Mastana, 2006).

Based on these numbers approximately 22% of the general population carry at least one APO ϵ 4 allele, compared to an estimated frequency of 40-60% of AD patients (Farrer *et al.*, 1997; Wisdom, Callahan and Hawkins, 2011; Liu *et al.*, 2013), further highlighting that APO ϵ 4 confers a considerably higher risk for developing late-onset AD.

Apolipoprotein E disease mechanisms

Our understanding of the exact mechanisms underlying the association between APO ϵ 4 and AD is incomplete. APOE plays an important role in A β metabolism and may contribute to cerebral deposition of amyloid plaques. APOE is important in proteolytic clearance of soluble A β from the brain. In carriers of the APO ϵ 4 gene, this clearance mechanisms of A β is altered, possibly due to APO ϵ 4's lower binding affinity for amyloid (LaDu *et al.*, 1994; Reiman *et al.*, 2009; Castellano *et al.*, 2011), and might thereby promote A β fibril formation (Wisniewski *et al.*, 1994). This is further strengthened by the fact that A β depositions in the brain are significantly more abundant in APO ϵ 4 carriers (55-59 years old: 40.7%) compared to non-carriers (same age group: 8.2%) (Schmechel *et al.*, 1993; Polvikoski *et al.*, 1995; Kok *et al.*, 2009).

The literature suggests that APOE synthesis in the brain can be induced in response to neuronal stress or injury in order to redistribute cholesterol in the brain for neuronal repair (Gregg *et al.*, 1986). Due to its specific domain structure, APO ϵ 4 may be recognized as abnormal and may undergo proteolytic cleavage, resulting in small neurotoxic APO ϵ 4 fragments which can in turn contribute to mitochondrial dysfunction and cytoskeletal disruptions such as tau phosphorylation (Mahley, 2012). This is supported by evidence of increased APOE N-terminal fragments in the brain of AD patients (Jones *et al.*, 2011). The documented detrimental effects of APO ϵ 4 on neuronal cells are reported to include mitochondrial dysfunction, increased tau phosphorylation, intracellular trafficking of APOE, decreased dendritic spine density (Brodbeck *et al.*, 2008), and impairment of gamma-Aminobutyric acid (GABA)ergic interneurons in the hippocampus (Andrews-Zwilling *et al.*, 2010). APO ϵ 4 impacts on neuronal plasticity via the above outlined mechanisms which in turn might contribute to synaptic loss and associated memory impairment observed in AD. Integrity of neuronal networks especially in the hippocampus of APO ϵ 4 transgenic mice, APOE knockout mice, and post-mortem human brain tissue exhibit reduced neuronal spine density and length equating to fewer neuronal connections (Ji *et al.*, 2003). APO ϵ 4 was found to inhibit hippocampal neurogenesis in a transgenic APOE mouse model which is important in memory and learning (Li *et al.*, 2009; Andrews-Zwilling *et al.*, 2010).

APO ϵ 4 might also play a role in the innate immune response, triggering inflammatory processes and that can negatively affect blood-brain barrier (BBB) integrity (Lynch *et al.*, 2003; Bell *et al.*, 2012). In fact, APO ϵ 4 has been reported to trigger inflammatory cascades which contribute to increased dysfunction of brain vasculature and increase BBB permeability by causing disruption of pericytes, which are crucial in maintaining the barriers integrity (Bell *et al.*, 2012; Halliday *et al.*, 2016). Accelerated breakdown of the BBB in the hippocampus and medial temporal lobe clearly distinguishes between APO ϵ 4 carriers and

non-carriers, even in the absence of cognitive decline, but is more pronounced when cognitive dysfunction is apparent (Montagne *et al.*, 2020).

APO ϵ 4 has been linked to obesity possibly via mechanisms of increased insulin resistance and altered utilization of glucose in the brain resulting in increased cognitive deficits (Jones and Rebeck, 2019). There also appears to be an interaction between APO ϵ 4 and Type 2 Diabetes (T2D), the presence of both was shown to confer risk for developing AD to a greater extent than if each risk factor contributed in an additive way (Peila, Rodriguez and Launer, 2002; Irie *et al.*, 2008). APO ϵ 4 carriers show higher levels of low-density lipoproteins LDL and total cholesterol (Lahoz *et al.*, 2001). Due to its role in cholesterol handling, APO ϵ 4 has also been associated with an increased risk for cardiovascular conditions, such as coronary disease (Mahley and Rall, 2000; Bennet *et al.*, 2007; Mahley, Weisgraber and Huang, 2009; Zhang *et al.*, 2015), ischemic cerebrovascular disease (McCarron, Delong and Alberts, 1999) stroke (Khan *et al.*, 2013).

Modifiable risk factors for developing Alzheimer's Disease

Dementia aetiology is multifactorial with several factors contributing to the disease onset and development over the life-course. A number of epidemiological studies found a decline in age-specific dementia incidence rates (despite an increase in the absolute number of cases) in higher-income countries (Manton, Gu and Ukraintseva, 2005; Prince *et al.*, 2014; Satizabal *et al.*, 2016). This trend was attributed to better levels of education and a paralleled improvement in the management of cardiovascular health, particularly due to improved use of anti-hypertensives (Satizabal *et al.*, 2016). This is in-line with an increasing body of research which shows that the risk of developing dementia can be partially modulated by a relatively small number of factors (Livingston *et al.*, 2020). According to this life-course model of dementia risk by the Lancet Commission, improvement of lifestyle factors could reduce and/or delay dementia cases by as much as 40% (Livingston *et al.*, 2020). Worldwide

this translates to 20 million AD cases and in the UK 354,000 cases. The proposed twelve ‘modifiable lifestyle factors’ were identified to exert potentially reversible risk in different phases of life, accumulating to 40% modifiable risk, and are shown below (Livingston *et al.*, 2020).

- i) Early life (age <45 years): low-educational attainment
- ii) Midlife (age 45-65 years): hearing loss, hypertension, obesity, traumatic brain injury, alcohol consumption of 21 units or more per week
- iii) Later life (age > 65 years): smoking, depression, social isolation, physical inactivity, air pollution and diabetes.

Weighted population attributable fraction (PAF) describes the percentage reduction in new cases if a particular risk factor were eliminated. Midlife obesity and hypertension, and late life T2D were calculated to have a weighted PAF of ~ 1%, 2%, and 1%, respectively, on the development of dementia (Livingston *et al.*, 2020). Depression had a PAF of ~4%. Obesity, hypertension, and T2D portray risk factors for one another and are closely linked to diet. It is likely that shared mechanisms are underlying their pathology.

In light of these models and the failure to find effective treatments, research efforts have changed their focus to finding prevention strategies. As research moves into prevention rather than cure, the APOE gene becomes a very interesting risk factor, as it is associated with AD and, hence, investigating how this common genotype impacts on the microbiota is important for future AD risk and intervention studies.

Many of the modifiable risk factors in AD, such as hypertension, T2D, depression and many of the underlying mechanisms (inflammation, energy and lipid metabolism), are connected and modulated by another key player - the intestinal microbiota (Figure 1.7). The intestinal microbiota has received much attention recently across a broad range of conditions including

AD. Next, I will summarize the Gut-Brain axis and its potential role in AD. Of note, I was not able to investigate all modifiable risk factors within the scope of this thesis, but mainly adopted an exploratory approach.

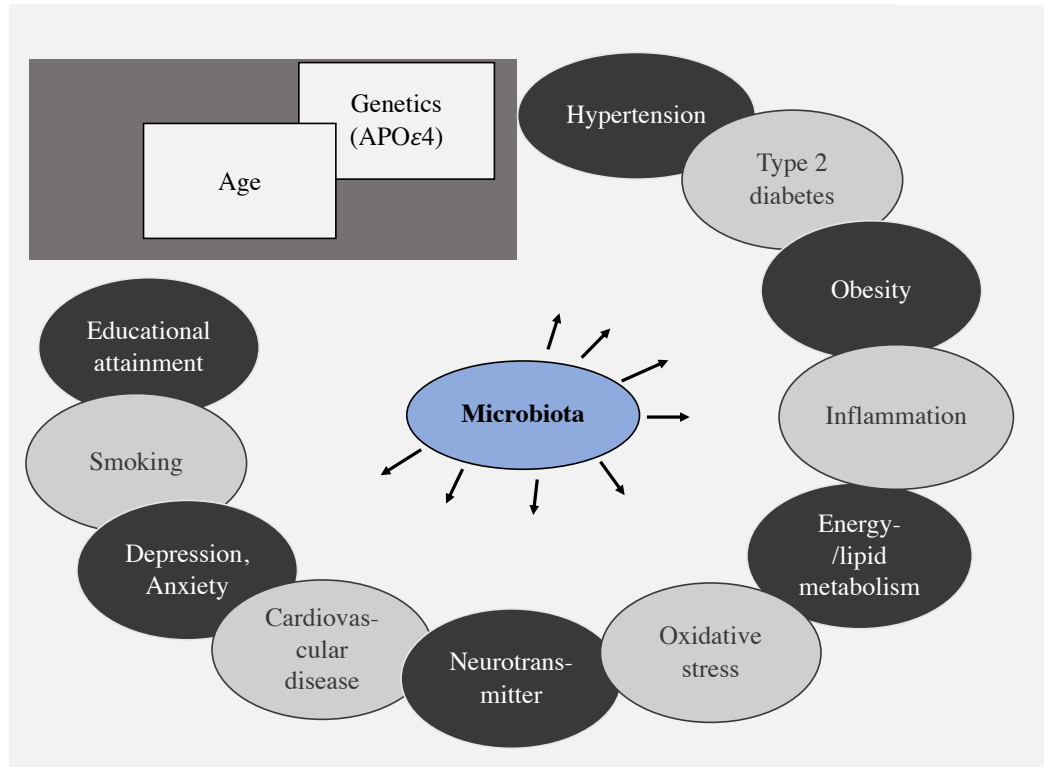


Figure 1.7 Schematic representation of suggested modifiable (circles) and non-modifiable (squares) risk factors of AD. Microbiota modulation indicated by arrows. List not exhaustive. Figure created by author

The Gut-Brain axis - an emerging key player in health and disease

Overview

The Gut-Brain axis describes a highly interactive, bi-directional communication system between the gastrointestinal (GI) tract and the brain whose key regulator is the intestinal microbiota. It integrates neural, hormonal, and immunologic signals and provides a direct route for intestinal microbes and microbiota-derived metabolites to influence brain signaling and function (Rhee, Pothoulakis and Mayer, 2009).

Microbes are found all over the body. However, there are specific body sites that host a significantly large amount of distinct microbial communities, such as the gastrointestinal tract. The human intestinal microbiome describes the collective of microbial encoded genes contained within the constituents of its members. The intestinal microbiota consists of bacteria, archaea, viruses, fungi, and protozoa. The gastrointestinal tract is colonized by 500-1,000 microbial species, amounting to a population of 10^{14} bacteria, of which the vast majority are found in the ileum and colon. Overall these species contribute to a diverse ecosystem or community consisting of trillions of microorganisms (Yatsunenko et al. 2012), with substantially more genetic diversity than the human genome (Whitman, Coleman and Wiebe, 1998). This genetic diversity exceeds that of the human genome by more than a hundredfold (Hill *et al.*, 2014), as it contains approximately four million protein-encoding genes whereas the human genetic code has only 26,600 genes. This further illustrates the importance of the symbiotic relationship between the human body and the microorganisms inhabiting it (Craig Venter *et al.*, 2001; Human Microbiome Project Consortium, 2012).

Microbial diversity

Intestinal microbial communities are particularly diverse when compared to other body habitats, as was shown by the large-scale Human Microbiome Project that found no one taxa to be present in each body habitat. Within body habitats, there appear to be certain genera

that make up 17% to 84% of communities in the respective habitat and might thus be considered ‘signature’ or core genera (Human Microbiome Project Consortium, 2012).

Besides this, microbial communities of the same individual vary over time. This temporal intra-individual variation is called alpha diversity and it is notably smaller compared to the microbial variability between two different individuals at any given time (Human Microbiome Project Consortium, 2012). This inter-individual variation is also called beta diversity. Relative community stability might be indicative of a “healthy microbiome”, whereas a reduction in alpha diversity has been associated with dysbiosis and disease. The pronounced person-specific uniqueness of the intestinal microbiota highlights the importance of longitudinal sampling to account for the dynamics of the microbiome. The complex ecosystem of microbes is thus not only widely diverse, but also highly unique to each person and very dynamic.

Host-microbiota functions

Host-microbiota interactions are predominantly mutualistic with microorganisms performing vital, non-redundant, metabolic and non-metabolic functions such as complex carbohydrate-, lipid-, protein metabolism, synthesis of vitamins, immunomodulation, a range of regulatory functions, protection against pathogen overgrowth and maintaining intestinal barrier function. The human microbiota co-evolves with human development with microbial population diversity and composition changing over the life-course. The first 3-6 years of life are a critical period in the development and maturation of the intestinal microbiota. During this time, the intestinal microbiota undergoes large-scale changes under the influence of diet and environmental factors, until it stabilizes in an adult-like configuration (Koenig *et al.*, 2011). Thereafter, the composition of the intestinal microbiota is still subject to numerous lifestyle and behavioral factors (Falony *et al.*, 2016).

The intestinal microbiota has a wide-range of imperative functions, that exceed our traditional understanding of metabolic functioning (maintenance of homeostasis or transformation of ingested food and xenobiotics). It has an immense functional spectrum and is inherently connected with host physiology on many levels, including the enteric and central nervous system and as such a growing body of literature is adding to its essential role in cognition, behaviour and immune functioning.

Via bi-directional communication along the Gut-Brain axis with its many neuroimmune, neuroendocrine, neural pathways it is now thought that the intestinal microbiota plays a role in as many as 90% of all human diseases (Clemente *et al.*, 2012), including depression (Sanada *et al.*, 2020), anxiety (Hagerty *et al.*, 2020), inflammatory bowel disease (IBS) (Zheng and Wen, 2021), PD (Romano *et al.*, 2021), autism spectrum disorder (Fu, Lee and Wang, 2021), Multiple Sclerosis (Esmaeil Amini *et al.*, 2020), obesity (Crovesy, Masterson and Rosado, 2020), T2D (Gurung *et al.*, 2020), autoimmune diseases and allergies (Okada *et al.*, 2010; Khan and Wang, 2020) and cardiovascular disease (Witkowski, Weeks and Hazen, 2020). The majority of these disease associations originally came from animal studies, most commonly transgenic mice and Germ-Free (GF) mouse models but have since been increasingly investigated also in humans. The exact mechanisms and the nature of the relationship, causality or effect, and our understanding of the complex interactions are still incomplete. Nonetheless, it has become clear that the human microbiota plays a key role in health and disease. This long-overlooked area, sometimes referred to as the ‘forgotten organ’, holds great potential and promises for understanding and improving human health.

Gut-Brain axis interaction pathways

There are four main pathways of bi-directional communication between the intestinal microbiota and the brain, namely neural pathways, endocrine pathways, immune pathways and microbial metabolites (Figure 1.8) (Strandwitz, 2018).

Neural pathways

The vagal nerve (VN) lies at the heart of the parasympathetic nervous system, innervating all of the digestive tract, and is the main afferent pathway between the abdominal cavity and the brain. It is hence an important interface between the enteric nervous system (ENS) and the CNS (Sherwin *et al.*, 2016; Bonaz, Bazin and Pellissier, 2018; Breit *et al.*, 2018). The vast majority of fibres of the VN are afferent (80%) which means that the VN is heavily involved in signalling from the GI tract to the brain, for example via the detection of metabolites in the lumen by intestinal enteroendocrine cells (Forsythe, Bienenstock and Kunze, 2014). Afferent fibres are involved in various pathways that impact behaviour and physiological effects on the brain including activation of the hypothalamic–pituitary–adrenal (HPA) axis (anxiety-like behaviour) and modulation of the immune system response through attenuation of systemic inflammatory response (Collins and Bercik, 2009).

Endocrine pathways

Enteroendocrine cells in the intestinal epithelial release multiple peptide hormones upon binding of bacterial products to one of its diverse receptors. Peptide hormones then act locally on enteric neurons or enter the circulation from where they can activate the VN or travel to other organs (Parker, Fonseca and Carding, 2020). Intestinal microbiota can also influence the neuroendocrine system via changing the activity of the HPA axis which regulates various body processes in response to psychological as well as physiological stressors (Sudo *et al.*, 2004; Farzi, Fröhlich and Holzer, 2018). Dysregulation and hypersensitivity of the HPA axis play an important part in mental health conditions, particularly depression (Liu, 2017). Studies have shown that intestinal dysbiosis causes imbalances in the HPA axis (changed levels of stress hormones) which can lead to anxiety-like behaviour in mice (Huo *et al.*, 2017). Another study demonstrated hypersensitivity of the HPA axis in GF mice that overexpressed stress hormones in response to stress: a process which was reversible through microbial re-colonization (conventionalization) (Rieder *et al.*, 2017) (Sudo *et al.*, 2004). It has further been suggested that dysregulation of the HPA stress

response can increase permeability of the intestinal epithelial barrier. Increased intestinal permeability in turn favours microbiota dysbiosis and facilitates the translocation of bacteria and their products across the intestinal lumen into the blood circulation leading to chronic low-grade inflammation (De Punder and Pruimboom, 2015; J. R. Kelly *et al.*, 2015; Slyepchenko *et al.*, 2017).

Immune pathways

The intestinal microbiota acts on many immune mediators which can signal to the brain via the VN or via secretion of cytokines or other immunomodulatory molecules into the peripheral circulation (Sherwin *et al.*, 2016; Fung, Olson and Hsiao, 2017).

The intestinal microbiota is a key regulator for the immune system from early life onwards. Postnatal colonization of microbiota is vital for the maturation of the immune system (Shapiro *et al.*, 2014). Studies using selective colonization of GF mice have greatly added to our understanding of the importance of bacteria for the development of the host immune response (Round and Mazmanian, 2009). GF mice have an immature and dysregulated immune system, reflected by numerous cellular defects and molecular deficiencies such as abnormal microglia morphology, altered levels of natural killers cells, natural killer T cells, mast cells, and cytokines, as well as abnormal immunoglobulin (Ig) A production (Hansen *et al.*, 2012; Girolamo, Coppola and Ribatti, 2017; Van Giau *et al.*, 2018) - all of which can be restored upon conventionalisation. The exact mechanisms underlying microbiota-driven microglia maturation remain incompletely understood but a role for short-chain fatty acids (SCFAs) has been suggested (Erny *et al.*, 2015).

There is mounting evidence demonstrating how the intestinal microbiota can modulate the response of the innate and adaptive immune system during infection, inflammation and autoimmunity (Round and Mazmanian, 2009; Kamada *et al.*, 2013). Lipopolysaccharides

(LPS) are primarily derived from gram-negative bacteria (particularly *Bacteroidetes*) and are a powerful pro-inflammatory endotoxin. LPS bind to toll-like receptor (TLRs), expressed on the surface of immune cells including macrophages, microglia, and monocytes, that trigger the production of proinflammatory cytokines such as interleukin (IL)-6 and IL-1 β (Sherwin *et al.*, 2016; Salguero *et al.*, 2019). A high-fat diet increases the abundance of gram-negative bacteria and consequently leads to higher levels of bacteria-derived LPS which can result in endotoxemia and the development of metabolic diseases (Cani *et al.*, 2007; Ahola *et al.*, 2017; Salguero *et al.*, 2019). Abundance of gram-negative bacteria increases with age (Zhan, Stamova and Sharp, 2018). High levels of LPS can also activate microglia and compromise the integrity of the CNS by disrupting the blood-brain barrier (Slyepchenko *et al.*, 2017). Overall, translocated LPS plays an important role in triggering systemic inflammation and possibly neuroinflammation through reducing barrier permeability of the intestinal and the brain and has been proposed to be a driving factor in the progression of AD. The important role of bacteria within this complex immunoregulatory network may have many wide-reaching effects on host health.

Microbial metabolites

Many bacteria produce or modulate host biosynthesis for a range of bioactive compounds which are central to a large number of important physiological processes (Liu *et al.*, 2020). The major groups of microbial metabolites include SCFAs, bile acids, indole, trimethylamine N-oxide (TMAO), flavonoids, n-acyl amides, protein-derived metabolites, phenols (Nicholson *et al.*, 2012) and neurotransmitters such as dopamine, noradrenaline, serotonin, GABA and histamine (Strandwitz, 2018). A large number of microbial-metabolites are either solely derived from bacterial metabolism or from processing diet-derived nutrients by bacteria. The intestinal microbiome-derived metabolites play widespread roles across cardiometabolic diseases, cancers, diabetes, obesity, hypertension and neurological disorders (Nicholson *et al.*, 2012; Descamps *et al.*, 2019).

The importance of understanding the role of microbial metabolites on human health has given rise to the field of microbial metabolomics - the study of the functional capacity of the microbial community. With advances in sequencing technology, the ability to infer the functional potential of a community, so-called predictive functional profiling, has become increasingly possible and provides a first step towards understanding the relationship between the intestinal and its function in human physiology (Mallick *et al.*, 2019). Understanding the metabolic and immunomodulatory role of specific bacteria and their microbial metabolites in turn offers a wide range of potential therapeutic targets for a range of diseases.

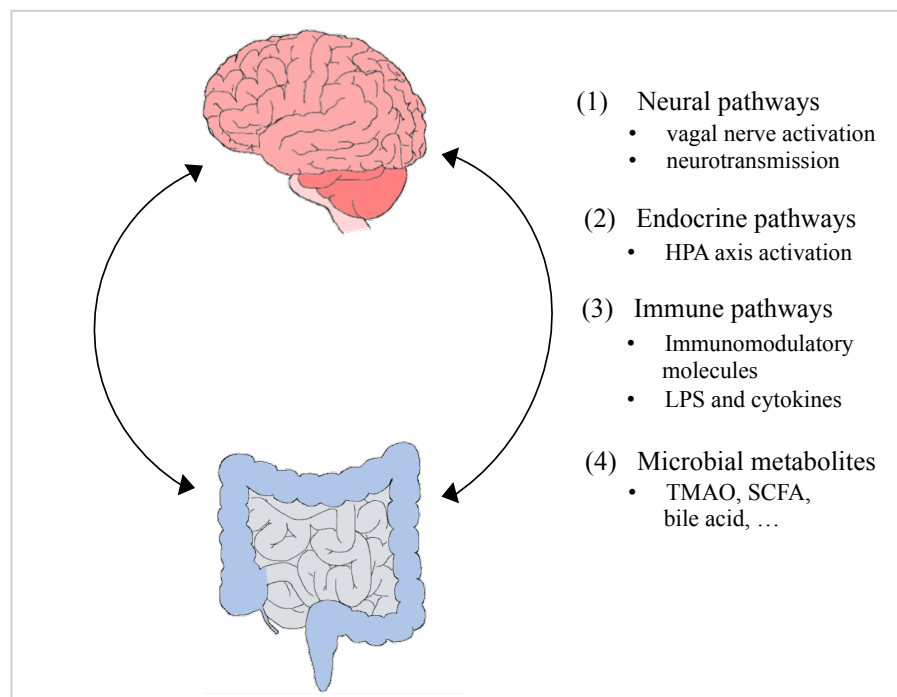


Figure 1.8 Schematic presentation of suggested Gut-Brain interaction pathways. Figure created by author

Mechanisms in Alzheimer's Disease pathophysiology and the role of the intestinal microbiota

In the following, I will discuss potential mechanisms by which the intestinal microbiota might contribute to AD pathophysiology by topics. Next, I will review evidence from observational studies in AD mouse models exploring the relationship between the intestinal microbiota and AD. Only a few studies have been undertaken investigating the role of the intestinal microbiota in AD pathology in humans, which I will review next. Finally, I will summarize the evidence for a link between APOE genotype and gut microbial alterations which might favour AD pathology.

Although interconnected in nature, the conceivable microbial-related pathways and the associated mechanistic that might be involved in AD pathophysiology can be broadly categorized as follows:

- 1) The intestinal microbiota modulates cognitive function via brain receptors and neurotransmitters
- 2) The intestinal microbiota may promote aggregation of A β in the brain
- 3) Intestinal metabolites: neuroprotective and disease-promoting mechanisms
- 4) Reduced protective barrier function at the BBB and intestinal epithelial barrier
- 5) Intestinal microbiota and the inflammation hypothesis

The intestinal microbiota modulates cognitive function

Understanding the involvement and modulation of cognition by intestinal microbiota has received an increasing amount of interest in the past decade. Exploring the link between the composition of the intestinal microbiota and cognitive functioning was first approached with various animal models (including germ-free animals) and by using various modulation strategies, including food supplements (probiotics and prebiotics), antibiotics and faecal microbial transplant (FMT).

Intestinal dysbiosis disrupts the function of brain receptors

Antibiotic-induced intestinal dysbiosis results in cognitive impairment for domains such as object recognition and working memory in mice, in the absence of neuroinflammatory processes. The impairment is partially reversible through the administration of probiotics or FMT (Cryan and Dinan, 2012). On a mechanistic level, intestinal dysbiosis leads to changes in the expression of brain-derived neurotrophic factor (BDNF), tight junction proteins, N-methyl-D-aspartate (NMDA) receptors and other brain receptors, which in turn cause cognitive impairment (Froehlich et al. 2016). BDNF plays a central role in the mechanisms that underlie learning, such as neuroplasticity (Rattiner, Davis and Ressler, 2005; Maqsood and Stone, 2016). In a rodent model, NMDA receptors were significantly less numerous in the hippocampus following antibiotic treatment (Wang *et al.*, 2015). Reduced expression of BDNF and NMDA receptor unit 2A in the cortex and hippocampus, in particular, are associated with impaired non-spatial and working memory (Sudo *et al.*, 2004; Maqsood and Stone, 2016) and were first established in a GF mouse model (Cryan and Dinan, 2012). Evidence from human-based studies show that BDNF levels in the serum and brain (post-mortem) of AD patients are significantly lower compared to healthy controls (Carlino, De Vanna and Tongiorgi, 2013). This reduction in BDNF further correlates with increased burden of amyloid and may also negatively impact on NMDA receptors of the glutamatergic system which play an important role in synaptic plasticity and cognition (Francis *et al.*, 2012).

Microbials species modulate several key neurotransmitters

Healthy brain function and cognition depends on a delicate balance of neurotransmitter levels, such as GABA, serotonin and dopamine. Several microbial species might act on cognition through their direct or indirect involvement in the functioning and production of neurotransmitters (Dinan *et al.*, 2015). *Lactobacillus rhamnosus* modulates mRNA expression of GABA receptors (Bravo *et al.*, 2011). *Bifidobacterium* is also reported to be involved in the production of GABA (Pokusaeva *et al.*, 2017). Impaired neuronal signalling

mediated by GABA is associated with depression, anxiety, impaired synaptogenesis and cognitive impairment (Paula-Lima, Brito-Moreira and Ferreira, 2013; Schmidt-Wilcke *et al.*, 2018). GABA levels were found to be significantly reduced in severe cases of AD (Solas, Puerta and Ramirez, 2015). In ageing mice, symptoms of heightened anxiety and spatial navigation cognition deficits were found to positively correlate with increased activation of pro-inflammatory cytokines and increased intestinal permeability. Besides these changes, mice also showed a shift in bacterial taxa including greater abundance of *Porphyromonadaceae*, *Odoribacter*, *Clostridium*, *Oxalobacter* and *Butyricimonas* towards a profile typically found in inflammatory bowel disease (Scott *et al.*, 2017). These findings highlight that bacteria are an integral part of healthy brain functioning.

The intestinal microbiota may promote aggregation of Amyloid beta in the brain

A key event in AD pathology is the accumulation and deposition of A β in the brain, which is caused either by increased production of amyloid into the CNS or decreased clearance of A β from the CNS, or a combination of the two. The intestinal microbiota might contribute to this hallmark feature of AD pathology by, i) increasing systemic availability of microbial-produced A β and by, ii) increasing the transit of A β into the CNS due to loss in barrier function. This might co-occur together with impaired clearing mechanisms of A β out of the CNS. Collectively, these mechanisms would favour the accumulation of amyloid peptides in the brain and might hence represent mechanistic links between the intestinal microbiota and amyloid pathology in AD (Marques *et al.*, 2013; Pistollato *et al.*, 2016).

i) Many bacterial species and fungi produce A β in the intestine which can lead to an increase in systemic levels of A β (Hufnagel, Tükel and Chapman, 2013; Hill and Lukiw, 2015; Zhao, Dua and Lukiw, 2015). Bacteria species producing amyloid include *Escherichia coli*, *Mycobacterium tuberculosis*, *Salmonella enterica*, *Salmonella typhimurium*, *Staphylococcus aureus*, and *Bacillus subtilis* (Pistollato *et al.*, 2016).

ii) Barrier permeability increases with advancing age but is also modulated by microbes (described in detail on pages 59 – 63). As a result, the protective barrier function of the intestinal epithelial barrier and BBB is reduced. This allows A β to leak paracellularly from the intestine into the circulatory system. From there A β can travel to the brain and pass through the BBB, which may lead to increased accumulation and deposition of A β in the brain (Hufnagel, Tükel and Chapman, 2013; Hill and Lukiw, 2015; Zhao, Dua and Lukiw, 2015).

Intestinal metabolites: neuroprotective and disease-promoting mechanisms

Several microbiota-derived metabolites might be of particular importance in the context of AD pathophysiology. Here I highlight the role of SCFAs, TMAO, and bile acids.

Microbiota-derived short-chain fatty acids have neuroprotective effects and maintain barrier function

SCFAs, especially valeric, propionic and butyric acid, are suggested to have modulatory functions that might be protective against AD pathophysiology. This is supported by evidence from a mouse model in AD, which shows that selected SCFAs, including valeric and butyric acid, are able to partially inhibit or disrupt self-assembly of A β peptides (Ho *et al.*, 2018). This process works by interfering with initial A β 1-40 and A β 1-42 protein-protein interactions of the assembly process, which in turn reduces the formation of AD-characteristic A β plaques (Ho *et al.*, 2018). A potential role of SCFAs in the context of AD is also supported by research findings from Zhang and colleagues (2017) who found significant reduced levels of butyric acid in the faecal matter of APP/presenilin 1 (PS1) AD mice as well as reduced levels of propionic, butyric, isobutyric, valeric acid in the brain of AD mice compared control mice (Zhang *et al.*, 2017).

As mentioned before, SCFAs also play a vital role in maintaining the intestinal epithelial and BBB integrity. A lack in butyrate is associated with increased BBB permeability (Ma *et al.*, 2018), whilst colonization with the butyrate-producing bacterium *Clostridium tyrobutyricum* or oral administration of butyrate are reported to lead to better BBB integrity via upregulation of tight junction proteins (Braniste *et al.*, 2014; Parker, Fonseca and Carding, 2020). Reduced levels of the species *Akkermanisa muciniphila*, a producer of acetate and propionate, on the other hand, are associated with disruption of the mucus layer and dysfunction of the epithelial barrier (Belzer and De Vos, 2012).

Prebiotics aimed at increasing production of SCFAs are capable to restore BBB integrity in an APO ϵ 4-FAD mouse model of AD (Hoffman *et al.*, 2019). Administration of a well-studied prebiotic compound called ‘inulin’ (a high indigestible fibre diet) was found to increase levels of *Prevotella* and *Lactobacillus*. This in turn was significantly associated with elevated levels of SCFAs in the cecum and blood, as well as changes in the levels of bile acids and other microbial metabolites. The inulin-fed APO ϵ 4 mice further showed reduced expression of inflammatory compounds in the hippocampus compared to APO ϵ 4-FAD control mice (Hoffman *et al.*, 2019).

Evidence from dietary intervention studies in individuals with MCI and biomarkers of AD show that a short-term dietary intervention had significant effects on SCFA levels. Six-week long adherence to a Mediterranean-ketogenic diet led to an increase in butyrate and propionate levels and a decrease in acetate levels compared to controls, whilst adherence to the American Heart Association Diet increased acetate and propionate levels and decreased butyrate levels compared to controls. The levels of propionate and butyrate in the faecal matter of MCI patients were negatively correlated with CSF A β -42 load (Nagpal *et al.*, 2019).

SCFAs are not only involved in important AD-related neurotoxic processes and barrier integrity, but they also play a major role in glucose homeostasis and mitochondrial function. Especially butyrate, but also propionate and acetate, can exert positive effects on mitochondrial functioning by restoring morphology and expression, by increasing glucose sensitivity in the brain (rescue hypometabolism), and by decreasing colonic inflammation and modulating lipid metabolism (Erny *et al.*, 2015; Kobayashi *et al.*, 2017; Zilberter and Zilberter, 2017; Hoffman *et al.*, 2019).

Trimethylamine-N-oxide (TMAO)

TMAO is an intestinal metabolite. Its precursor, trimethylamine (TMA), is metabolized from dietary choline and β -L-carnitine by *Archaea* (Gaci *et al.*, 2014). Levels of TMAO in the CSF were found to be significantly elevated in AD patients and positively correlated with markers of tau pathology and A β 42 load (Vogt *et al.*, 2018). The literature also suggests an age-dependent increase of circulating TMAO levels, which is associated with AD-like behaviour in an APP/PS1 mouse model and could be reduced by blocking TMAO (Gao *et al.*, 2019). Due to its role in cholesterol metabolism, insulin secretion and glucose tolerance, TMAO has been proposed as a biomarker for cardiometabolic risk (Roy *et al.*, 2020). Besides its role in glucose and cholesterol metabolisms, the possible mechanisms underlying a relationship between TMAO and neurodegenerative diseases is multi-faceted, including stabilizing properties of amyloid aggregations, promotion of tau pathology, promotion of endoplasmic reticulum stress and increased inflammation through NLR family pyrin domain containing 3 (NLRP3) inflammasome activation (Janeiro *et al.*, 2018).

Bile acids

Bile acids, the end products of cholesterol catabolism, have an important role in regulating lipid, energy and glucose homeostasis (Ramírez-Pérez *et al.*, 2017). Increased levels of bile acids might have a range of effects, including compositional microbiota changes in favour of a less diverse and *Firmicutes*-dominated community (Islam *et al.*, 2011) and disruption

of tight junctions (Liu *et al.*, 2020). The bile acid ‘tauroursodeoxycholic acid’ (TUDCA), on the other hand, has been suggested to have neuroprotective properties, as it was found to positively correlate with a reduction of amyloid plaques in a target replacement (TR) APP/PS1 AD mouse model (Ackerman and Gerhard, 2016). Hydrophilic bile acids, such as TUDCA, have been suggested to inhibit apoptosis through stabilization of mitochondrial membranes (Rodrigues *et al.*, 2000), whilst hydrophobic bile acids are known to have opposite effects (Rolo *et al.*, 2000). A set of blood-based biomarkers, including the bile acid glyoursodeoxycholic acid, was used to predict the onset of AD/amnesic MCI (aMCI) within 2-3 years with a 90% accuracy in an observational human study with 525 elderly participants (Mapstone *et al.*, 2014), further highlighting the important role of bile acids in AD.

Reduced protective barrier function

Structure and function of the blood-brain barrier

Formerly viewed as a static and impermeable barrier, the BBB is nowadays considered to be part of a neurovascular-endothelial unit which consists of multiple cell types (Parker, Fonseca and Carding, 2020). The BBB is comprised of a monolayer of brain microvascular endothelial cells (BMEC) supported by astrocytes, pericytes, microglia, neurons and extracellular matrix. Gaps between BMEC are interconnected and physically sealed by tight junctions (multi-protein complexes ensuring structural integrity), preventing molecules with high molecular weight and low lipid solubility from diffusing paracellularly into the brain (Banks, 2009; Abbott *et al.*, 2010; Marques *et al.*, 2013). The main purpose of the BBB is to ensure selective transport and protect the brain from pathogens and exposure to other harmful molecules (Weiss *et al.* 2009).

Ageing and loss of blood-brain barrier function

Ageing induces physiological changes at the site of the BBB which lead to dysfunction of tight junctions, loss of pericytes as well as changes of transmembrane receptors (Lin *et al.*,

2019). Healthy ageing also leads to a decrease in the phagocytotic activity of microglia and overall decline in immune surveillance, overall described as “immunosenescence” (Sochocka *et al.*, 2019). As a result, the ability of the brain to eliminate pathogens and to maintain homeostasis is reduced in the later decades of life. It has been suggested that the expression of receptors responsible for the transport of A β across the selective BBB is altered at advanced age, favoring the influx (over efflux) of A β from the CNS.

Diminished neuronal health in Alzheimer’s Disease

Neuronal health, which is highly dependent on intact BBB function, is of particular importance in the context of AD. It is reported that over 80% of AD patients have pathologically cerebral vascular changes including amyloid depositions, also known as cerebral amyloid angiopathy (CAA), which leads to BBB impairment. Breakdown of the BBB is considered early biomarkers for cognitive decline irrespective of A β and tau and independent of hippocampal or parahippocampal volumetric changes (Nation *et al.*, 2019).

Pericyte dysfunction in Apolipoproteins ϵ 4 decrease blood-brain barrier function

Increased vulnerability and breakdown of the BBB, as well as risk for CAA, is also associated with APO ϵ 4 genotype. Evidence from animal work suggests that APO ϵ 4 carriers have changes in the membrane proteins of cerebral blood vessels which lead to reduced perivascular drainage of A β from the brain (Hawkes *et al.*, 2012). Human APO ϵ 4 carriers further show increased BBB disruption in hippocampal and parahippocampal gyrus independent of amyloid or tau pathology and in the absence of inflammation (Montagne *et al.*, 2020). The observed BBB breakdown is associated with activation of the cyclophilin A (Cypa)-MMP9 pathway in pericytes and correlates with pericyte injury and elevated neuronal stress (increase in neuron-specific enolase) in APO ϵ 4 carriers (Montagne *et al.*, 2020). Blocking of Cypa-MMP9 pathway in APO ϵ 4 knock-in mice restored BBB functioning (Bell *et al.*, 2012). Dysregulation of calcineurin–nuclear factor of activated T

cells (NFAT–calcineurin) signaling pathway, another pathway in pericytes, is also associated with APOε4-mediated CAA pathology. It thus represents another potential target (calcineurin/NFAT inhibitors) to restore proper functioning of pericytes in APOε4 carriers (Blanchard *et al.*, 2020).

Several microbiota-targeted interventional approaches, including the administration of prebiotics and probiotics, are investigated for their neuroprotective effects on restoring cognition and behavior in AD mouse models.

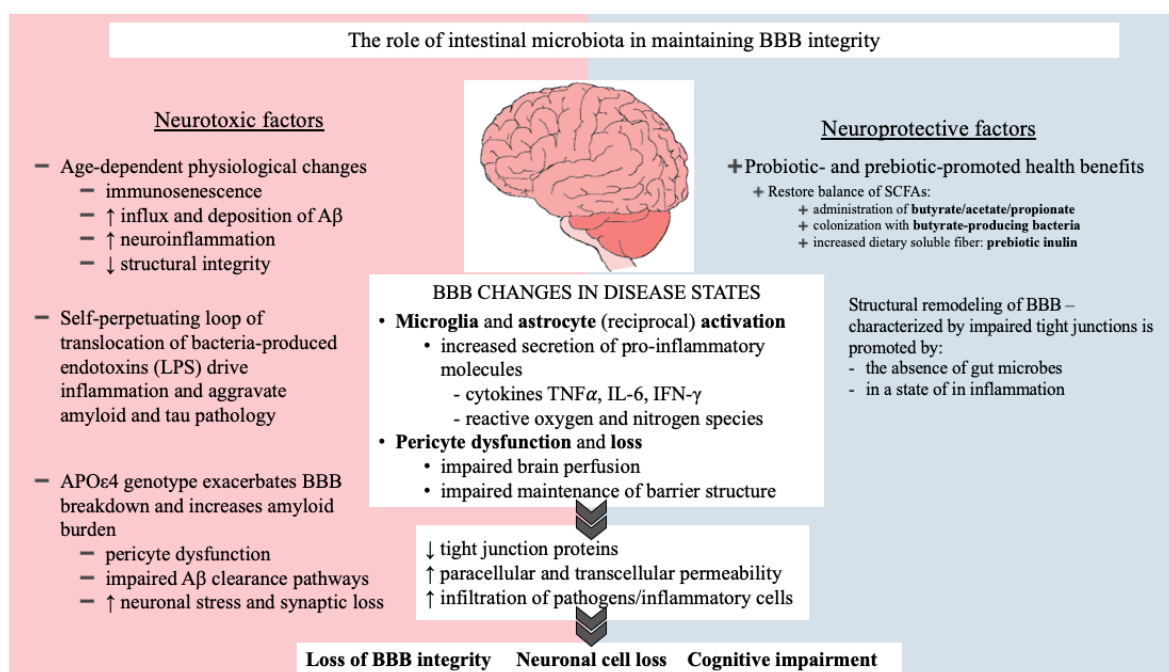


Figure 1.9 Schematic summarizing blood-brain barrier changes in disease states, neurotoxic and neuroprotective factors modulating blood-brain barrier integrity with respect to Alzheimer’s Disease pathophysiology. Figure created by author

Structure and function of the intestinal epithelial barrier

The intestinal epithelial barrier is a dynamic system consisting of a physical and an inner functional immunological barrier (Bischoff *et al.*, 2014). A single layer of epithelial cells, connected by tight junctions and other proteins, lines the intestinal lumen and forms the physical barrier between the lumen and mucosal tissue. Homeostasis is maintained by the

interplay of this physical barrier (the mucosal surface of the epithelial cell lining) and an immunological barrier (antimicrobial products, IgA and defensins) (Bischoff *et al.*, 2014). The main function of this barrier is to ensure strict regulation of molecules, which allows selective absorption of nutrient and fluids (Tran and Greenwood-Van Meerveld, 2013), but prevents the passage of pathogens, microbial organisms or toxins (Schoultz and Keita, 2020). Intact barrier integrity thus prevents pathogenic as well as commensal microorganisms from leaking paracellularly into the circulatory system. A range of major conditions including in IBS (Camilleri and Gorman, 2007), T2D (Cheru, Saylor and Lo, 2019), major depression (Maes, Kubera and Leunis, 2008), autism spectrum disorders (De Magistris *et al.*, 2010), Parkinson's disease (Forsyth *et al.*, 2011) and AD (Megur *et al.*, 2021) have all been associated with increased intestinal permeability, also termed a 'leaky gut' (Schoultz and Keita, 2020). Even though the mechanisms for increased intestinal permeability are still not fully understood, it is generally agreed that increased intestinal permeability follows age-associated intestinal dysbiosis and remodeling of epithelial tight junction proteins (Tran and Greenwood-Van Meerveld, 2013; Thevaranjan *et al.*, 2017) that may be associated with impaired innate immunity and chronic low-grade inflammation (Man *et al.*, 2015).

Consequences of increased permeability on both 'ends' of the Gut-Brain axis

Structural integrity of the barriers is also reduced as a consequence of differential expression of occludin and claudin transmembrane proteins (main constituents of tight junctions) in the absence of intestinal microbes (Braniste *et al.*, 2014), intestinal dysbiosis (Froehlich *et al.* 2016) or in response to high levels of pro-inflammatory modulators following trauma or infection (Mabbott, 2015). Conventionalizing GF mice using faecal matter from specific-pathogen free mice has shown to decrease BBB permeability which supports a fundamentally causal relationship between microbiota and BBB integrity (Braniste *et al.*, 2014).

Increased barrier permeability triggers a cascade of events, which are closely linked with inflammation, that tip the balance and may contribute to AD pathology (Arrieta, Bistritz and Meddings, 2006; Tran and Greenwood-Van Meerveld, 2013). Compromised barrier function creates a detrimental self-reinforcing loop marked by i) translocation of LPSs, commensal bacteria and pathogens, ii) activation of TLRs and iii) initiation of phagocytosis. When commensal bacteria including those containing LPS and other endotoxins leak into the blood circulation, they can upregulate the immune response through activation of TLRs - an integral part of the innate immune response. TLRs are activated upon recognition of antigens expressed by microbes (microbe-associated molecular patterns [MAMPs]). In a controlled manner, TLR-activation is a key mechanism for healthy immune function. In the context of AD, misfolded amyloid peptides are detected by TLR2 on glial cells. Recognition of amyloid by TLR2 occurs because amyloid shares structural homology with TLR2's major ligand LPS. Activated glial cells then initiate phagocytosis (Arroyo *et al.*, 2011) and activated microglia and astrocytes stimulate production of pro-inflammatory cytokines and chemokines (Boutajangout and Wisniewski, 2013; Zhao, Dua and Lukiw, 2015). Chronic neuroinflammation, which involves the overactivation and dysregulation of microglia and macrophages and associated increased secretion of pro-inflammatory molecules, is a characteristic of many neurodegenerative diseases including AD (Heppner, Ransohoff and Becher, 2015; Parker, Fonseca and Carding, 2020).

The increase in barrier permeability renders the host (in general) and the CNS (in particular) more susceptible and vulnerable to insults. The facilitated transit of amyloids, LPSs, cytokines, and other immunogenic molecules into the circulatory system and across the BBB triggers a whole cascade of neuropathological events that are likely to contribute to AD pathology.

Intestinal microbiota and the inflammation hypothesis

Neuroinflammation is a well-established and consistent feature of AD pathology (Beach, Walker and McGeer, 1989; Arends *et al.*, 2000) and strongly correlates with cognitive decline (Cagnin *et al.*, 2001). It has been suggested that the severity of neuroinflammation might regulate disease progression (Minter *et al.*, 2016). Mounting evidence featuring impairment of the vasculature, oxidative stress, microgliosis and impaired neuronal proteolysis have called for a more integrative model to describe AD disease pathogenesis. Following this, the ‘inflammation hypothesis’ emerged as an alternative to the amyloid cascade hypothesis (Liu *et al.*, 2020). In the following, I outline modulatory mechanisms of host innate immunity by intestinal microbiota in the context of AD (summarized in Figure 1.10).

Bacteria-produced endotoxins drive inflammation and exacerbate amyloid and tau pathology

Bacteroidetes are gram-negative bacteria whose relative abundance increases with advancing age (Claesson *et al.*, 2011). The major component of the outer cell wall of gram-negative bacteria is LPS. As already described in the context of losing barrier function, LPS is a bacterial endotoxin, which is known to trigger inflammation in circulatory system and the CNS and is hence associated with low-grade inflammation and decreased insulin sensitivity (Cani *et al.*, 2007; Vogt *et al.*, 2017). The mechanistic role of endotoxins implied in AD pathology might be numerous, including a key role in causing inflammation of the intestine and promoting the formation of neurotoxic plaques – the hallmark feature of AD.

Excessive production of LPS can cause intestinal inflammation, which in turn may increase the absorption of bacterial derived LPS into the blood stream. High peripheral levels of LPS cause both endotoxemia and colitis in mice (Jang *et al.*, 2018). The literature suggests that once in the brain, LPS and other microbial endotoxins, activate microglia cells and trigger a series of processes which can result in hippocampal inflammation, reduced synaptic

plasticity (suppression of BDNF) and worsening integrity of the BBB (suppression of claudin-5 expression) (Lee *et al.*, 2019).

In a transgenic mouse model for AD, administration of LPS correlated with a marked elevation of pro-inflammatory IL-1 β and was found to induce tau phosphorylation in the hippocampus and other brain areas through mediation of Cyclin-dependent kinase 5 (cdk5) enzymatic activity (a major tau kinase) (Kitazawa *et al.*, 2005). Inflammation of the CNS has since been shown to exacerbate tau pathology in another model in transgenic mice (Sy *et al.*, 2011). A model of transgenic mice that overexpress APP found that LPS-induced inflammation in the CNS led to increased level of A β 1-42 and A β 1-40 amyloidogenic species and higher total APP (precursor of A β) (Sheng *et al.*, 2003). In wild-type mice, repeated injections with LPS resulted in increased levels of IL-1 β and IL-6 (pro-inflammatory cytokines) and higher hippocampal levels of A β 1-42, as well as cognitive deficits (Kahn *et al.*, 2012).

Interestingly, the innate immune response to LPS exposure appears to be mediated differently depending on APOE status. A human study showed that APO ϵ 4 carriers were affected more negatively by an intravenous LPS challenge than APO ϵ 4 non-carriers (Gale *et al.*, 2014). Exposure to LPS in APO ϵ 4 carriers led to significantly higher hyperthermia and higher serum levels of pro-inflammatory cytokines, including TNF- α and IL-6, compared to APO ϵ 3/ ϵ 3 subjects. This markedly augmented innate immune response in APO ϵ 4 carriers is also reflected by enhanced TLR signalling. An association between APO ϵ 4 genotype and exacerbated endotoxemia and enhanced MyD88-independent TLR4 signalling has also been established in APO ϵ 4-TR mouse model (Gale *et al.*, 2014).

Apart from inflammation, bacterial endotoxins derived from gram-negative bacteria such as the abundant *Bacteroidetes fragilis* or *E. coli*, which occur at more prevalent levels in elderly

subjects (Mariat *et al.*, 2009), may also contribute directly to AD pathology. An *in vitro* study found that co-incubation of A β peptide with bacterial endotoxins promoted A β fibril formation. Post-mortem investigations of AD brains show co-localization of A β 1-40/42 with LPS and fragments of gram negative *E.coli* (Zhan *et al.*, 2016), as well as a 2- to 3-fold increased levels of LPS in hippocampus and superior temporal lobe neocortex (Zhao, Cong and Lukiw, 2017; Zhao, Jaber and Lukiw, 2017). These findings support the proposed mechanistic link between bacteria-derived endotoxins and AD pathology and suggest a key role in inflammatory-induced neurodegeneration.

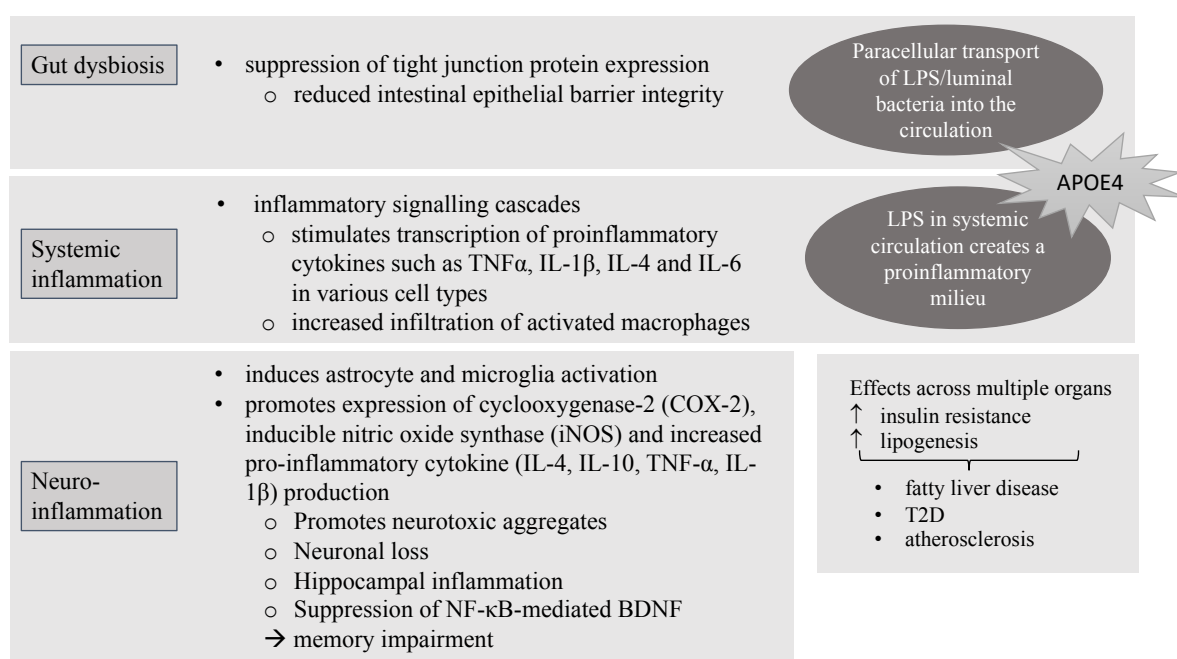


Figure 1.10 Schematic, simplified overview of suggested mechanisms underlying lipopolysaccharide-induced inflammation. LPS: lipopolysaccharide; TLR4: Toll-like receptor 4. Figure created by author

Lactobacilli and *Bifidobacterium* strains are suggested to be potent inhibitors of LPS production. Administration of *Bifidobacterium longum* has indeed been shown to reduce excessive endotoxin production and subsequent inflammation-associated processes in an AD mouse model (Lee *et al.*, 2019)

In the adult human intestine, *Bifidobacterium* is present at low but relatively stable abundance levels (Arboleya *et al.*, 2016). *Bifidobacterium* is generally ascribed a health promoting role and commonly used as a probiotic. Accumulating evidence suggests that different species of *Bifidobacterium* are associated with increased colonization resistance against pathogens, improved intestinal permeability, production of beneficial metabolites such as short-chain fatty acids and bacteriocins and able to limit inflammatory responses (Fukuda *et al.*, 2011; Underwood *et al.*, 2015; Arboleya *et al.*, 2016). Supplementation with *Bifidobacterium* was shown to promote increased intestinal barrier function and attenuate bacterial translocation (Wang *et al.*, 2006). In AD patients, 12-week long probiotic supplementation containing three strains of *Lactobacillus* and *Bifidobacterium* was found to have significant positive effects on cognitive functioning (Akbari *et al.*, 2016).

Oral administration of *Bifidobacterium* was also shown to prevent cognitive dysfunction in transgenic mouse model for AD and suppressed the expression of immune-reactive genes in hippocampal tissue (Kobayashi *et al.*, 2017). These effects might be associated with modulation of BDNF and acetate production (Kobayashi *et al.*, 2017). The literature generally agrees that probiotics can have beneficial effects, possibly mediated by enhanced intestinal epithelial barrier integrity, reduction of the inflammatory cytokine Tumour Necrosis Factor alpha (TNF- α) and other pro-inflammatory mediators and modulation of oxidative stress (Divyashri *et al.*, 2015; Musa *et al.*, 2017; Azm *et al.*, 2018; Kowalski and Mulak, 2019).

Overall, there appear to be multiple potential mechanisms underlying microbial involvement in AD pathogenesis which are summarized in Figure 1.11.

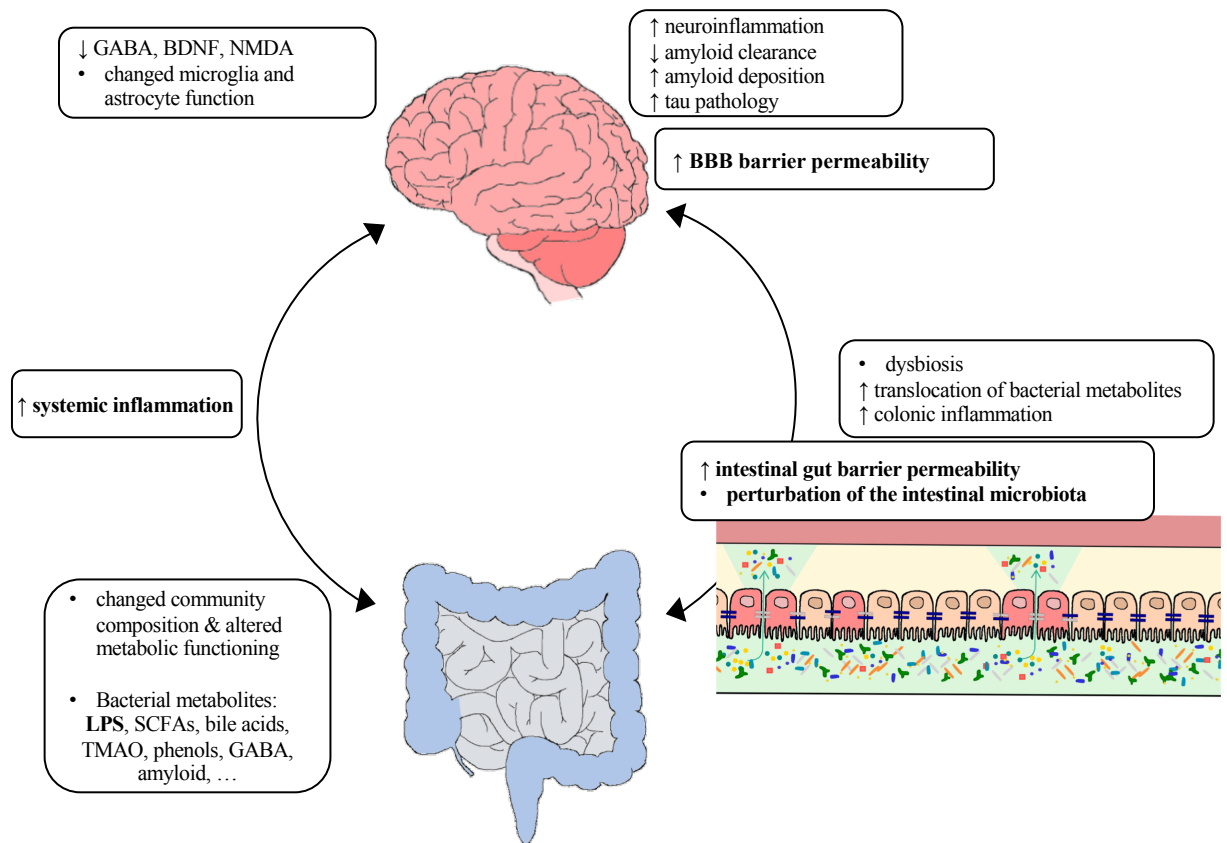


Figure 1.11 Schematic presentation of the main microbial-driven pathways suggested to be involved in Alzheimer's Disease. Figure created by author

Existing microbiota-targeted treatment for AD

The recent approval of GV-971 for the treatment of mild to moderate AD in China in November 2019 further corroborates the relevance of a microbial component in AD (Wang *et al.*, 2019; Syed, 2020). Although our understanding of the exact mechanisms is incomplete, GV-971 which is an algae-derived oligosaccharide, is thought to modify the intestinal microbiota composition and thereby reduce bacteria-related peripheral and neuronal inflammation via the downregulation of Th1 cell differentiation and microglia activity in the brain (Wang *et al.*, 2019). Its anti-neuroinflammatory properties might also inhibit the action of reactive astrocytes and lead to a reduction in pro-inflammatory TNF- α and IL-6 (Wang *et al.*, 2007). It is suggested that GV-971, which is able to cross the BBB, can also directly inhibit the formation of amyloid fibrils in the brain as well as reduce tau pathology (Hu *et al.*, 2004; Wang *et al.*, 2019). On a metabolic level, GV-971 is suggested

to decrease the peripheral and faecal levels of phenylalanine and isoleucine. A 36-week-long Phase III clinical trial of 817 participants demonstrated sustained therapeutic effects on cognitive functioning (stabilization or improvement) of GV-971 with superiority to placebo (Xiao *et al.*, 2021).

Observational studies in Alzheimer’s Disease mice models

The main observational studies that sought to explore intestinal microbiota alterations in AD using a murine model are summarized in Table 7.1 in the supplementary. Overall, the results from the here reviewed studies are heterogenous. Given the diversity in methods, seen in the mouse models, and considering the multitude of analysis methods, including immunohistochemistry, Western blotting, microscopy and 16S ribosomal RNA (16S rRNA) gene sequencing, it is difficult to directly compare the study results between each other. Even top-level results, such as assessing alpha diversity are not necessarily aligned, with some studies showing increased bacterial diversity in the AD mouse model compared to the control (Harach *et al.*, 2017; Bäuerl *et al.*, 2018), no difference between the groups (Peng *et al.*, 2018; Honarpisheh *et al.*, 2020) or a reduction in the disease model (Zhan *et al.*, 2018). Most studies reported a clustering effect by group, indicative of global compositional changes. All studies found significant differences with respect to relative taxonomic abundances of specific taxa. And some groups went on to show correlations between microbial changes and amyloid levels, epithelial barrier dysfunction and levels of proinflammatory molecules. The sample size in some of studies was low (Bäuerl *et al.*, 2018; Honarpisheh *et al.*, 2020) with just two to three mice per study/age group.

Despite widespread use of animal models, particularly mouse models, the question of translatability to humans remains. Whilst the human and mouse GI tract share some characteristics with respect to its anatomy and physiology, there is also a considerable degree of dissimilarity, which is not only true for morphology (such as the presence of a non-

glandular forestomach as seen in mice) and at the cellular level (Loan *et al.*, 2015). Whilst both the mouse and the human gut are dominated by the *Bacteroidetes* and *Firmicutes* phylum, Ley *et al.* showed that much less overlap can be found at a deeper taxonomic level, as over 85% of bacterial genera detected in the mouse intestinal microbiota were not present in humans (Ley *et al.*, 2005). Major compositional differences were further confirmed by a meta-analysis of mouse and human faecal microbiota based on published 16S data, showing that the relative abundance for the majority of dominant genera is widely different between the two organisms (Loan *et al.*, 2015). The genera *Turicibacter* for example, is one of the most abundant taxa in the murine intestinal microbiota, but is found only in very small abundances in the human intestine (Hugenholtz and de Vos, 2018). A large range of environmental factors, including housing, which has been shown to be an important confounder, but also large differences in diet and metabolic rate exert large modulating effects on the murine intestinal microbiota, which cannot be compared to the human intestinal microbiota. All of these differences, most importantly perhaps the divergence in host resident bacterial taxa, mean that findings from murine models are not necessarily translatable to humans.

Despite these limitations, animal studies provide a unique opportunity to explore how microbial-modulated mechanisms may contribute to progressive cognitive impairment and AD. There are several different AD mouse models. The most commonly seen AD models of the here reviewed literature are the double transgenic APP/PS1 mouse model for AD which overexpress APP (Bittner *et al.*, 2012; Mathias Jucker, 2020) and the senescence-accelerated mouse-prone 8 (SAMP8) model, which is a naturally occurring mouse line that exhibits a phenotype of accelerated ageing including cognitive dysfunction (learning and memory impairment) (Shimada and Hasegawa-Ishii, 2011). Whilst all of these mouse models aim to closely resemble key characteristics of the AD phenotype, there is variance between the models, which adds a further layer of variability to the results.

Human studies

To my knowledge, only nine studies to date have explored a potential relationship between the intestinal microbiota and AD in human participants. A detailed summary of all studies is shown in Table 1.1. Of note, only one study was longitudinal (Haran *et al.*, 2019) and used a shotgun metagenomic sequencing approach. All other studies are cross-sectional in nature and used predominantly 16S rRNA gene sequencing. All studies but one (Ling *et al.*, 2021) had a relatively small sample size, with a patient population between 21-43 AD patients.

The first study to investigate microbial compositional changes between patients with predominantly mild AD (n=25) and healthy controls (n=25) was conducted in 2017 using 16S rRNA gene sequencing allowing for taxonomic assessment from faecal samples (Vogt *et al.*, 2017). Vogt *et al.* observed significantly decreased richness and diversity in the AD patient cohort as well as significantly different compositional microbiomes between AD patients and controls as measured by beta diversity. They identified 82 differentially abundant taxa between patients and controls, which correlated to some extent with CSF biomarkers of AD pathology. At the phylum level, relative abundance of *Firmicutes*, one of the two main phyla of the GI tract, and *Actinobacteria* were significantly decreased in individuals with AD. Whilst *Bacteroidetes*, the second main phyla of the GI tract, was increased in the AD cohort. This was reflected by a reduction of relative abundances in 61 operational taxonomic units (OTUs) at family- and genera-level belonging to the *Firmicutes*, as well as an increase in *Bacteroidaceae* (family) and *Bacteroides* (genus). These taxonomic shifts broadly mirror findings for individuals with T2D and are associated with insulin resistance (Ott *et al.*, 1999; Larsen *et al.*, 2010; Rawlings *et al.*, 2014). Insulin resistance is a risk factor for developing AD and is also associated with impaired cerebral glucose metabolism and increased deposition of amyloid (Willette, Bendlin, *et al.*, 2015; Willette, Johnson, *et al.*, 2015). The group also used predictive functional profiling and identified several Kyoto Encyclopedia of Genes and Genomes (KEGG) pathways that were

significantly different between AD patients and controls. Enriched pathways in AD patients included energy-, carbohydrate-, amino acid metabolism, as well as an increased potential for oxidative phosphorylation, fructose and mannose metabolism, methane metabolism and many more. Whereas depleted pathways were characterized by pathways related to signal transduction, cell motility, bacterial chemotaxis, bacterial motility proteins and others.

In the following year, a study by Zhuang *et al.* (2018) investigating the role of the intestinal microbiota composition in AD disease pathology was published. This study was as a single time point analysis of 43 Chinese AD patients and 43 age- and gender-matched healthy controls. In-line with the work of Vogt and colleagues, the group found significant large-scale compositional differences (distinct β -diversity) between AD patients and healthy controls. The taxa which were identified to contribute to this separation of bacterial intestinal profiles were numerous. Zhuang and colleagues found a small but significant decrease in *Bacteroidetes* and an increase in *Actinobacteria* in the AD patient group compared to healthy controls. Whilst bacterial taxa at class-level belonging to *Firmicutes* showed both a significant increase (*Bacilli*) as well as significant decrease (*Negativicutes*) compared to healthy controls. *Christensenellaceae* and the gram-positive *Ruminococcus* were found to be increased in AD patients, whereas *Lachnospiraceae* were significantly decreased.

In 2019, Haran *et al.* were the first group to conduct a study with longitudinal design (sampling once a month for up to five months) and to use shotgun metagenomic sequencing in a cohort of 24 AD patients, 33 patients with non-AD dementias and 51 healthy controls. Analysis of β -diversity showed that the intestinal microbiota compositions separated clearly between the group of AD patients and healthy controls, whereas samples from non-AD dementia patients clustered with both other cohorts. Differential abundance analysis identified an increase in *Alistipes*, *Bacteroides*, *Barnesiella*, *Collinsella* and *Odoribacter*, as well as a reduction in *Lachnoclostridium* using the AD group as a baseline in a general linear

mixed model regression analysis. Random forest classification algorithms identified increased frailty and malnutrition as well as several microbial taxa as the best predictors for AD.

Predictive taxonomic changes were marked (amongst others) by lower abundances of *Eubacterium* and *Butyrivibrio* (butyrate-producing genera), a *Clostridium* strain, *Roseburia hominis* and *Faecalibacterium prausnitzii*. Whilst predictive taxa with higher relative proportions in AD were characterized by members of the *Odoribacter splanchius*, *Bacteroides vulgatus*, *Adlercreutzia equolifaciens*, *Klebsiella pneumonia*, *Bacteroides fragilis* and *Eggerthella lenta*. The group went on to test the ability of intestinal microbiota to modulate the P-glycoprotein/endocannabinoid(homeostasis)- Multidrug resistance-associated protein-2 (MRP2)/ hepxilin A3 (HXA3) (inflammatory) axis by incubating intestinal epithelial cells in the presence of faecal supernatants and quantifying levels of P-glycoprotein and MRP2 protein expression. This analysis was done in a small subgroup (n=9 per group) and showed lower expression of P-glycoprotein, which functionally correlated with inflammation of the GI tract in the samples of AD patients compared to the other two groups.

Li *et al.* (2019) conducted a study in patients with AD (n=30), amnesic MCI (aMCI) (n=30) and healthy controls (n=30), to characterize the microbial communities of both faecal and blood samples using 16S rRNA gene sequencing. Analysis of α -diversity of the intestinal microbiota was significantly lower only for one of the tested α -diversity indices when comparing the AD patient group to the control group. Analysis of β -diversity demonstrated significant differences between microbial communities of the AD vs control group (faecal and blood samples) but did not differ between the aMCI and AD patients.

Univariate analysis identified numerous relative abundance differences between the groups. Faecal samples of AD patients were enriched in seven genera compared to healthy controls, including *Acinetobacter*, *Dorea*, *Blautia*, *Akkermansia*, *Lactobacillus*, *Bifidobacterium* and *Streptococcus*. In comparison, relative abundances in AD patients were significantly lower for 11 genera, including *Bacteroides* (supporting Zhuang *et al.* finding), *Prevotella*, *Alistipes*, *Parabacteroides*, and *Sutterella*. Blood samples of the AD patient group vs controls were particularly enriched in *Pseudomonas*, *Escherichia*, *Acidovorax*, *Steotrophomonas* and another six genera. Whereas blood samples from healthy controls were more abundant in *Halomonas*, *Serratia*, *Acinetobacter baumannii*, *Enterobacter* and another eight genera. The decreased abundance of *Bacteroides* and increased abundance of *Escherichia* and *Lactobacillus* in the faecal samples of AD (and aMCI) group compared to the healthy control group was also confirmed by quantitative PCR. Differences in relative abundances correlated with medial temporal atrophy (MTA) (increased *Akkermansia*), cognitive performance (increased *Faecalibacterium*, *Butyricoccus*, decreased *Blautia*, *Dorea*), APOE status (increased *Anaerotruncus*, no further information given), age (increased *Anaerotruncus*, *Ruminococcus*) and disease duration (increased *Megamonas*).

In the same year, Liu *et al.* (2019) presented their work on intestinal microbiome differences between AD patients (n=33), aMCI patients (n=32) and healthy controls (n=32). In-line with previous work, they found significantly reduced microbial diversity in the AD patient cohort compared to aMCI and controls, as well as distinct microbial compositional profiles between the groups. They further found numerous associations between disease pathology and differential abundance of bacteria, including a reduction in *Firmicutes*, *Clostridia*, *Clostridiales*, *Clostridiaceae*, *Lachnospiraceae*, *Ruminococcaceae* and *Blautia*, and an increase in *Proteobacteria*, *Gammaproteobacteria*, *Enterobacteriales* and *Enterobacteriaceae* in the AD patient group. Discriminating models based on these findings, particularly those based on enriched *Enterobacteriaceae*, were able to distinguish between

AD patients and healthy controls. Liu and colleagues also performed predicted functional potential, based on KEGG functional orthologs. This showed that AD patients had an enriched potential for glycan biosynthesis and metabolism compared to controls, protein folding and contrary to Vogt *et al.* also for signal transduction. The functional potential of other pathways, including those related to immune system and biosynthesis of N-glycan, phenylalanine, tyrosine, tryptophan, histidine and amino acids were found to be reduced in the AD patient cohort compared to controls.

More insights on the relationship between AD and the gut microbiome also come from a Japanese study (Saji *et al.*, 2019, 2020). This cross-sectional study which included 25 dementia patients (classified based on cognitive scores: Mini-Mental State Examination [MMSE] <20 and/ or clinical dementia rating [CDR] ≥1) and 82 healthy controls, investigated taxonomic differences (Saji *et al.*, 2019) as well as differences between intestinal-microbiota associated metabolites (Saji *et al.*, 2020) between the two cohorts. Interestingly, contrary to previous findings, Saji and colleagues found that the patient group exhibited a higher microbial diversity compared to healthy controls. Of note, whilst using 16S rRNA gene sequencing, the group adopted a special approach for the taxonomic classification. They assigned all detected taxa to one of ten microbiota groups. Depending on the dominating bacteria, every individual was then assigned to one of three enterotypes. This approach was based on work Arumugam *et al.* 2011, who originally designated enterotype I (dominant phyla: *Bacteroides*), II (dominant phyla: *Prevotella*) and III (dominant phyla: other phyla) based on preferred community compositions. Saji *et al.* (2019) found that dementia was associated with lower prevalence of the *Bacteroides* enterotype and higher prevalence of other bacteria (enterotype III). Dementia patients were also found to have a higher *Firmicutes/Bacteroidetes* ration compared to controls.

Saji *et al.* (2020) identified a range of metabolites with significantly different levels between the cohort of dementia patients and controls including formic acid, ammonia, iso-butyric acid, iso-valeric acid, b-butyric acid, phenol and p-cresol. However, upon adjusting for age, sex, education, APO ϵ 4 genotype and enterotypes, only ammonia concentration was significant between the groups. Ammonia levels were increased in the cohort of dementia patients with an odds ratio of 1.6.

In January this year, Hou *et al.* (2021) investigated the intestinal microbiota in a Chinese cohort of AD patients, with a particular focus on genetic factors correlated with AD and associations with intestinal changes. Hou and colleagues sequenced twelve genetic loci (polymorphisms previously identified from genome-wide association studies) and confirmed that CC or CT genotype of susceptibility gene BIN1 (rs744373) as well as carriers with at least one APO ϵ 4 (rs42358/rs4512) allele had an increased risk for AD compared to non-carriers. The group then investigated the intestinal microbiota in 21 AD patients and compared this against 40 healthy controls. They found no difference in α -diversity but distinct compositional clustering (β -diversity) between AD patients and controls. Univariate analysis identified 18 significant associations with AD, including an increase in the relative abundance of *Escherichia Shigella*, *Enterobacteriales* and its associated family of *Enterobacteriaceae* (supporting Liu *et al.*' finding), *Proteobacteria* (in-line with Li and colleagues' finding), *Ruminococcaceae*, *Fingoldia*, as well as a reduction in *Megamonas*, *Enterococcaceae* and *Anaerostipes*. Targeted multivariate linear modelling of the significant taxa between AD patients (n=10) and healthy controls (n=5) with APO ϵ 4 and BIN1 showed a significant association between APO ϵ 4 carriers and increased abundances of *Proteobacteria* and *Enterococcaceae*.

The most recent work on the relationship between the intestinal microbiota and AD comes from Ling *et al.* (2021). This is the largest study of the reviewed work, with 100 AD patients

and 71 healthy controls. Cross-sectional comparison of the intestinal microbiota using 16S rRNA gene sequencing showed reduced α -diversity in the AD patient group and distinct compositional profiles. Univariate analysis of differential relative abundance identified over 30 significant associations. The AD patient group was characterized by an increase in numerous taxa, including *Actinobacteria* (replicating the result of Zhuang and colleagues), *Bacteroidetes*, *Verrucomicrobia*, *Coriobacteriaceae*, *Enterococcaceae* (contrary to Hou *et al.* finding), *Eubacterium*, *Akkermansia*, *Christensenellaceae* (supporting Zhuang *et al.* finding) and *Bifidobacterium* (replicating Li *et al.* finding) compared to controls. The AD microbiota was shown to have a significant decrease in members of *Proteobacteria* (contrary to Liu *et al.* finding), *Firmicutes*, *Clostridiaceae* (supporting Liu *et al.* finding), *Ruminococcaceae*, *Lachnospiraceae* (supporting Zhuang *et al.* finding), *Faecalibacterium* and several other taxa. Functional analysis using KEGG demonstrated various changes in the functional potential of AD patients compared to healthy controls, of which the majority showed enrichment for the AD group. These included enrichment in folate biosynthesis and reduction in bacterial chemotaxis and flagellar assembly which replicated findings of Vogt and colleagues. AD patients were also enriched in glycolysis/gluconeogenesis, galactose metabolism, fatty acid metabolism and sphingolipid metabolism, etc., but showed a reduction for biosynthesis of ansamycins and glycerolipid metabolism.

Whilst some findings, especially at higher taxonomic levels, were similar between these human studies, many of the detailed taxonomic changes were not the same. Possible reasons for discrepancies are numerous, including differences in study methodologies, geographical differences between study populations or lack of power due to small cohort sizes and noisy data. Nonetheless, overall these findings strengthen the postulated role of intestinal microbiota compositional changes in the context of AD.

Table 1.1 (Part 1) Human studies exploring the Gut-Brain axis in Alzheimer's Disease

Subjects	Sequencing	Statistical analysis method	Main findings	Ref.
25 AD, 25 HC	16S rRNA gene sequencing	α -diversity: ACE, Chao1, Shannon, Faith's PD, Inverse Simpson	Reduced alpha diversity in AD patients for all indices except for Inverse Simpson (not significant)	Vogt <i>et al.</i> , 2017
		β -diversity: Bray Curtis, UniFrac	Significant compositional differences between AD patients and HC	
		Differential abundance analysis: DESeq2	82 OTUs (14 more abundant and 68 less abundant in AD), including \downarrow <i>Firmicutes</i> , <i>Actinobacteria</i> , <i>Ruminococcaceae</i> , <i>Bifidobacteriaceae</i> , <i>Clostridiaceae</i> , <i>Mogibacteriaceae</i> \uparrow <i>Bacteroidetes</i> , <i>Bacteroidaceae</i> , <i>Rikenellaceae</i> , <i>Gemellaceae</i> , <i>Blautia</i> , <i>Bacteroides</i> , <i>Alistipes</i> , <i>Gemella</i>	
		CSF biomarkers	Differentially abundant taxa were correlated with CSF biomarkers of AD (positive and negative correlations between bacterial abundances and amyloid/tau markers)	
		Functional analysis (KEGG)	Level 2: \downarrow signal transduction, cell motility \uparrow energy/carbohydrate/amino acid metabolism, etc. Level 3: \downarrow bacterial motility proteins, bacterial chemotaxis, bacterial secretion system \uparrow oxidative phosphorylation, fructose/mannose/methane metabolism, lysine/folate biosynthesis etc.	
43 AD, 43 HC	16S rRNA gene sequencing	β -diversity: UniFrac	Significant compositional differences between AD patients and HC	Zhuang <i>et al.</i> , 2018
		Differential abundance analysis: LEfSe	64 associations with AD, including \downarrow <i>Bacteroidetes</i> , <i>Negativicutes</i> , <i>Lachnospiraceae</i> , <i>Bacteroidaceae</i> , <i>Bacteroides</i> , <i>Lachnoclostridium</i> \uparrow <i>Actinobacteria</i> , <i>Ruminococcaceae</i> , <i>Subdoligranulum</i> , <i>Christensenellaceae</i> , <i>Prevotella</i> , <i>Coprococcus</i>	
24 AD, 33 other dementias, 51 HC	shotgun metagenomic sequencing, longitudinal	β -diversity: Jaccard	Significant compositional differences between AD patients and other two groups	Haran <i>et al.</i> , 2019
		Generalized linear mixed model	AD as baseline: \downarrow <i>Lachnoclostridium</i> \uparrow <i>Alistipes</i> , <i>Bacteroides</i> , <i>Barnesiella</i> , <i>Collinsella</i> , <i>Odoribacter</i> Other dementias as baseline: \downarrow <i>Eubacterium</i> , <i>Roseburia</i> , <i>Lachnoclostridium</i> , <i>Collinsella</i> \uparrow <i>Barnesiella</i> , <i>Odoribacter</i>	
		Random forest classification	Identified increasing frailty and malnutrition and numerous microbial taxa, including <i>Odoribacter splanchnicus</i> , <i>E. eligens</i> , <i>E. rectale</i> , <i>Faecalibacterium prausnitzii</i> , etc.	
		Culture of intestinal epithelial cells in faecal supernatant	\downarrow expression of functional P-glycoprotein in AD cell cultures compared other two groups	
Sub- analysis n=9/group				

Table 1.1 (Part 2) Human studies exploring the Gut-Brain axis in Alzheimer's Disease

Subjects	Sequencing	Statistical analysis method	Main findings	Ref.	
30 AD, 30 aMCI, 30 HC	16S rRNA gene sequencing	α -diversity: Chao1, Faith's PD, observed species, Shannon	Reduced Faith's PD in AD compared to HC (other alpha indices were not significant)	Li <i>et al.</i> , 2019	
		β -diversity: UniFrac	Significant compositional differences of bacterial communities in faecal and blood samples between AD and HC (but not between AD and aMCI)		
		Differential abundance analysis: LEfSe for faecal samples (for blood samples not shown here)	↓ <i>Parabacteroides</i> , <i>Alistipes</i> , <i>Bacteroides</i> , <i>Alloprevotella</i> , <i>Haemophilus</i> , <i>Paraprevotella</i> , <i>Succinivibrio</i> , <i>Sutterella</i> , <i>Prevotella</i> , <i>Barnesiella</i> , and <i>Butyrivimonas</i> ↑ <i>Lactobacillus</i> , <i>Akkermansia</i> , <i>Dorea</i> , <i>Bifidobacterium</i> , <i>Streptococcus</i> , <i>Acinetobacter</i> , <i>Blautia</i>		
		General linear model (covariates: age, BMI, gender, constipation)	↓ <i>Alistipes</i> , <i>Bacteroides</i> , <i>Parabacteroides</i> , <i>Sutterella</i> , and <i>Paraprevotella</i> ↑ <i>Dorea</i> , <i>Lactobacillus</i> , <i>Streptococcus</i> , <i>Bifidobacterium</i> , <i>Blautia</i> , and <i>Escherichia</i>		
		qPCR for relative abundance	Kruskal-Wallis, post-hoc Dunn's test		Confirmed ↑ <i>Escherichia</i> and <i>Lactobacillus</i> and ↓ <i>Bacteroides</i> in AD and MCI faecal matter Negative relationship between A β burden and relative abundance of <i>Lactobacillus</i>
		PET scan	Spearman's rank-correlation analysis (adjusted for age and education)		Clinical characteristics associated with differential abundances: - medial temporal atrophy correlated positively with <i>Akkermansia</i> - APOE status correlated positively with <i>Anaerotruncus</i> - cognitive performance correlated positively with <i>Faecalibacterium</i> , etc.; negatively with <i>Blautia</i> , etc. - age correlated positively with <i>Anaerotruncus</i> , <i>Ruminococcus</i> ; negatively with <i>Cetobacterium</i> - disease duration correlated positively with <i>Megamonas</i>
33 AD, 32 aMCI, 32 HC	16S rRNA gene sequencing	α -diversity: Shannon, Simpson, ACE, Chao1	Reduced Shannon and Simpson in AD patients compared to aMCI&HC (other alpha indices were not significant)	Liu <i>et al.</i> , 2019	
		β -diversity: Bray Curtis, UniFrac	Significant compositional differences between AD patients and HC		
		Differential abundance analysis: LEfSe	↓ <i>Clostridiaceae</i> , <i>Ruminococcus</i> ↑ <i>Enterobacteriales</i> , <i>Enterobacteriaceae</i> , <i>Gammaproteobacteria</i> , <i>Proteobacteria</i>		
		PSL-DA	↓ <i>Firmicutes</i> , <i>Clostridia</i> , <i>Clostridiaceae</i> , <i>Lachnospiraceae</i> , <i>Ruminococcaceae</i> , <i>Blautia</i> , <i>Ruminococcus</i> ↑ <i>Proteobacteria</i> , <i>Gammaproteobacteria</i> , <i>Enterobacteriales</i> , <i>Enterobacteriaceae</i>		
		Functional analysis (KEGG)	Level 2: ↓ transcription, environmental adaptation, immune system, nervous system ↑ signal transduction, protein folding and associated processing, glycan biosynthesis and metabolism		
		Other	Significant correlation between AD clinical severity and altered abundance of taxa Model based <i>Enterobacteriaceae</i> abundance could distinguish AD from aMCI and HC		

Table 1.1 (Part 3) Human studies exploring the Gut-Brain axis in Alzheimer's Disease

Subjects	Sequencing	Statistical analysis method	Main findings	Ref.
25 dementia patients, 82 HC	16S rRNA gene sequencing (T-RFLP method)	α -diversity: Shannon, Simpson Compositional differences: enterotypes*	Increased in dementia patients vs HC (Shannon only) Dementia patients vs HC: ↓ enterotype I (<i>Bacteroides</i> > 30%) no difference for enterotype II (<i>Prevotella</i> at >15%) ↑ enterotype III ('other' bacteria) ↑ <i>Firmicutes/Bacteroidetes</i> (F/B) ratio	Saji <i>et al.</i> , 2019
*is based on classifying gut microbiota into 10 groups: <i>Prevotella</i> , <i>Bacteroides</i> , <i>Lactobacillales</i> , <i>Bifidobacterium</i> , <i>Clostridium</i> cluster IV, <i>Clostridium</i> subcluster XIVa, <i>Clostridium</i> cluster IX, <i>Clostridium</i> cluster XI, <i>Clostridium</i> cluster XVIII, and 'others'				
Sub analysis of same cohort	chromatography for metabolite levels from faecal water	Wilcoxon signed-rank test and χ^2 test Multivariable logistic regression analysis AUC	Concentrations of ammonia (↑), phenol (↑), p-cresol (↑), formic acid, iso-butyric acid (↑), n-butyric acid (↓) and iso-valeric acid (↑) in demented vs non-demented participants Every 1 SD increment in faecal ammonia concentration = ~1.6-fold increased risk for dementia (independent of age, sex, education years, Apo ϵ 4, enterotypes) Combination of a higher level of ammonia and a lower level of lactic acid = 0.69 AUC score (sensitivity 62%, specificity: 76%)*	Saji <i>et al.</i> , 2020
*compared to sensitivity, specificity, and AUC: Apo ϵ 4; 78%, 60%, 0.69; VSRAD score; 86%, 63%, 0.80				
21 AD patients, 40 HC	16S rRNA gene sequencing	α -diversity: Shannon, Sobs index β -diversity: Bray Curtis, weighted and unweighted UniFrac	No significant difference between AD and HC Significant compositional differences between AD patients and HC for all dissimilarity indices	Hou <i>et al.</i> , 2021
15 APO ϵ 4 carriers (10 AD, 5 HC)		Differential abundance analysis: LEfSe	18 taxa, significant genera AD vs HC: ↑ <i>Escherichia Shigella</i> , <i>Proteobacteria</i> , <i>Enterobacteriales</i> , <i>Enterobacteriaceae</i> , <i>Ruminococcaceae_UCG_002</i> , <i>Shuttleworthia</i> , <i>Anaerofustis</i> , <i>Morganella</i> , <i>Finegoldia</i> , <i>Anaerotruncus</i> ↓ <i>Megamonas</i> , <i>Enterococcus</i> , <i>Anaerostipes</i>	
BIN1 and APOE associates with targeted microbial taxa: MaAsLin2			APO ϵ 4 was associated ↑ in <i>Proteobacteria</i> and <i>Enterococcaceae</i>	

*AUC: Area Under the Curve

Table 1.1 (Part 4) Human studies exploring the Gut-Brain axis in Alzheimer's Disease

Subjects	Sequencing	Statistical analysis method	Main findings	Ref.
100 AD patients, 71 HC	16S rRNA gene sequencing	α -diversity: Shannon, Simpson, OTUs, ACE, Chao1 β -diversity: Bray Curtis, Jaccard, weighted and unweighted UniFrac Differential abundance analysis: LEfSe Functional analysis (KEGG)	Reduced alpha diversity in AD patients Significant compositional differences between AD patients and HC for all dissimilarity indices Over 30 significant associations, AD vs HC: ↑ <i>Actinobacteria, Bacteroidetes, Verrucomicrobia, Coriobacteriaceae, Enterococcaceae, Christensellaceae, Eggerthella, Eubacterium, Collinsella, Akkermansia, Bifidobacterium</i> ↓ <i>Proteobacteria, Firmicutes, Ruminococcaceae, Lachnospiraceae, Gemmiger, Faecalibacterium, Roseburia, Dialister</i> KEGG level 2 – AD patients vs HC: ↑ 3 pathways including carbohydrate metabolism, xenobiotics biodegradation and metabolism ↓ 4 pathways including immune system, cell motility, environmental adaptation KEGG level 3 – AD patients vs HC: ↑ 15 pathways including folate biosynthesis, glycolysis/gluconeogenesis, galactose metabolism, fatty acid metabolism, sphingolipid metabolism ↓ 15 pathways including bacterial chemotaxis, biosynthesis of ansamycins, glycerolipid metabolism	Ling <i>et al.</i> , 2021

Whilst several lines of evidence support a microbial role in AD, the exact nature of this relationship and mechanisms of intestinal microbiota changes are not yet understood. Whether microbiome changes are present in preclinical AD or at-risk groups is virtually unknown. Carriers of the APO ϵ 4 genotype are a study group with a common, well-established risk group for developing AD. Given the lack of treatment options to slow or reverse the disease trajectory once overt cognitive or behavioural impairment show, it is especially the early 'silent' preclinical phase that holds the highest potential for disease-modifying interventions. APO ϵ 4 genotyped individuals have been studied with respect to their cognition, behaviour and brain health to better understand changes prior to the manifestation of clear AD symptomology (Caselli *et al.*, 2007; Honea *et al.*, 2009; Jones and Rebeck, 2019).

In summary, albeit an emerging field in relation to neurodegenerative disease, the evidence for a microbial role in AD is becoming increasingly documented. With this the question arises whether intestinal changes are detectable prior to cognitive symptoms. Before turning to the aims and hypothesis of this work, I will next review the sparse literature for microbiome changes in APO ϵ 4 risk groups, which lays the foundation of the current knowledge to answer these important questions.

Intestinal microbiota and Apolipoprotein E genotype in Alzheimer's Disease

The relationship between the APO ϵ 4 genetic risk factor and the intestinal microbiome for developing AD is largely unknown. So far, the evidence on this relationship is restricted to findings from one study by Tran *et al.* (2019), who investigated the intestinal microbiota in individuals with four APOE genotypes (ϵ 2/ ϵ 3 n=14, ϵ 3/ ϵ 3 n=18, ϵ 3/ ϵ 4 n=18, ϵ 4/ ϵ 4 n=6) in a cross-sectional comparison using 16S rRNA gene sequencing. Besides the human work,

Tran and colleagues also explored the relationship between APO ϵ 4 and the intestinal microbiota in transgenic homozygous APO ϵ 3 and APO ϵ 4 replacement mice (Tran *et al.*, 2019). Two more observational studies using EFAD (a human APOE expressing mouse model with five familial AD mutations [5xFAD]) homozygous APO ϵ 3 and APO ϵ 4 mice models have also investigated the role of APOE genotype and the murine microbiota (Maldonado Weng *et al.*, 2019; Parikh *et al.*, 2020). Further evidence is also provided by an interventional study in which the effect of prebiotic dietary inulin on the intestinal microbiota is investigated in EFAD APO ϵ 3 and APO ϵ 4 mice (Hoffman *et al.*, 2019). The reviewed studies are summarized in Table 7.2 in the supplementary.

Tran and colleagues demonstrated that there were no large-scale taxonomic differences in community richness or structure (α - and β -diversity) between individuals with different APOE genotypes. There were, however, taxa-specific changes. APO ϵ 3/ ϵ 3 carriers had significantly higher abundance of *Prevotellaceae* compared to APO ϵ 4/ ϵ 4 (but not when compared to APO ϵ 2/ ϵ 3). Whereas APO ϵ 2/ ϵ 3 carriers had a significantly higher relative abundance of *Ruminococcaceae* than APO ϵ 3/ ϵ 3 and APO ϵ 3/ ϵ 4 (Tran *et al.*, 2019). The phylum *Firmicutes* and its associated order *Clostridiales* were also significantly higher in APO ϵ 2/ ϵ 3 carriers compared to individuals with APO ϵ 3/ ϵ 4 or APO ϵ 4/ ϵ 4.

In agreement with the human study, the murine intestinal microbiota of homozygous APO ϵ 4/ ϵ 4 and APO ϵ 3/ ϵ 3 TR mice showed no difference in α -diversity between the groups, but α -diversity was observed to decline significantly with age (18 months vs 4 months old mice). This is also supported by Weng *et al.* (2019), but not by Parikh *et al.* (2020). Compositional differences (β -diversity) were significant by genotype within age groups (Tran *et al.*, 2019). Distinct intestinal microbiota profiles by APOE genotype were also shown by the other observational studies in mice. Tran and colleagues showed that this separation of the intestinal microbiota was reflected by numerous taxa specific differences.

Whilst the APO ϵ 4/ ϵ 4 mice had significantly greater abundance of *Deferribacteres*, *Deferribacteraceae*, *Lachnospiraceae*, *Clostridium XIVa*, *Odoribacter*, *Mucispirillum*, *Enterorhabdus* and *Butyricoccus* compared to APO ϵ 3/ ϵ 3. On the other hand, their microbiota was significantly reduced in *Bacteroidaceae* and *Bacteroides* compared to APO ϵ 3/ ϵ 3 mice. Assessment of faecal metabolites also showed distinct clustering by APOE genotype and age group. Seven metabolites, including glucose, glycine, lactate, α -ketoisovaleric acid were significantly different by age-genotype interaction. Enrichment analysis further identified a large number of significantly altered pathways, including ammonia recycling, alanine metabolism and urea cycle (Tran *et al.*, 2019).

Summary

The intestinal microbiota is increasingly recognised to be a long-overlooked factor in human health and disease. The Gut-Brain axis is a contributing factor in age-related neurodegenerative diseases with wide-reaching medical implications for several reasons. Firstly, a growing body of evidence suggests that the Gut-Brain axis plays an important role in human health and is inherently connected to human well-being on many levels from the beginning of life onwards. Secondly, both the intestine and the brain are subject to age-associated physiological changes which render individuals particularly vulnerable in later life stages. Numerous potential links between the intestinal microbiota and hallmark features of AD pathology (such as impaired immune function, increased inflammation, impaired cognition, augmented amyloid aggregation, etc.) present plausible mechanisms for disease modulation. It is thus conceivable that the intestinal microbiota may play a role in the development and progression of AD. Many converging lines of evidence coming from animal work and human studies in AD found associations with changes in intestinal microbiota community and function which support this notion.

The nature of this microbiota-host interaction is both dynamic and bi-directional. Consequently, modulation of the human microbiota may offer many new and very promising

therapeutic angles. The general consensus is that detection and intervention in the early phases of AD (before cognitive symptoms and associated brain atrophy have manifested) present the best opportunity to alter the health trajectory of affected individuals. Identifying individuals who are at preclinical stages of AD is however very difficult. The above-discussed APO ϵ 4 risk gene confers a considerably increased risk for developing AD to its carriers and is well-established as the most common genetic risk factor for AD. Carriers of the APO ϵ 4 genotype, thus represent a good study population of individuals who are at increased risk of developing AD in the future, and may be regarded as a proxy for preclinical AD.

Characterizing Gut-Brain changes in healthy at-genetic-risk individuals might show significant microbiome changes in APO ϵ 4 carriers vs non-carriers, prior to AD-related cognitive, behavioral or neuroimaging changes. Such genetic-microbiome interactions could potentially be used as early marker for AD and further offer promising avenues for disease-modifying treatments from a completely novel perspective. The literature can currently not answer the question whether microbiome changes precede AD symptomology. It is unknown whether the intestinal microbiome changes over time in at-genetic-risk for AD. If changes can indeed be observed in the at-risk group, does their microbial community signature progress towards AD-like microbial phenotypes?

Overall, answering these questions, could provide further evidence to support a microbial role in the pathogenesis in AD and identify early changes in an at-risk cohort. This study aims to address these important questions.

Aims

1. Following assessment of baseline cognitive, behavioural, cardiovascular and neuroimaging measures, the intestinal microbiota will be analysed cross-sectionally in AD patients and longitudinally in APO ϵ 4 carriers and non-carriers using whole metagenome shotgun sequencing. This will allow us to define taxonomic and functional differences of the intestinal microbiota cross-sectionally and over time between the groups.
2. The functional potential of the intestinal microbiome will be assessed using *de novo* assembly of the sequenced metagenomics data.
3. This work will provide proof-of-concept data for the ‘Microbiome of the ageing gut and its effect on human gut health and cognition’ (MOTION) study enabling further work into the field of the Gut-Brain axis in AD.

Hypotheses

1. Cross-sectionally and longitudinally, the intestinal microbiota composition will change between groups and over time in APO ϵ 4 carriers at increased genetic risk for AD vs non-carriers, in the presence of normal cognitive, behavioural, cardiovascular and neuroimaging measures. Microbial profiles between the groups will show distinct changes in the abundance of specific taxa, which might indicate dysbiosis and increased vulnerability for disease-related mechanisms in the at-risk group of APO ϵ 4 carriers.
2. Cross-sectionally, the intestinal microbiota composition will differ on global and taxon-specific measures between people diagnosed with AD vs APO ϵ 4 non-carriers and vs APO ϵ 4 carriers, in the presence of clear cognitive and behavioural impairments in the AD patient group.
3. The above intestinal microbiome changes will be reflected on the level of functional pathways that are associated with potential AD disease-contributing functional changes.

CHAPTER 2: METHODS

Ethical processes and funding

The demenTia Research And Care Clinic (TRACC) study is a research study that has been running for nearly five years with the goal to become a centre of excellence in the field of dementia research. It received favourable opinion from the Research Ethics Committee (REC) on the 05.09.2016 (REC reference 16/LO/1366, London – Queen Square Research Ethics Committee). Health Research Authority (HRA) approval was given on the 7th September 2016. The study's Integrated Research Application System (IRAS) ID is 205788. Since the beginning of the study start eight amendments (one minor, two non-substantial and five substantial amendments) were added. I was involved in preparing documents for the fourth substantial amendment which was given favourable REC opinion on the 26.10.2017 and HRA approval on 03.01.2018. The documents added onto the TRACC protocol which I prepared in this process include: detailed visual instructions for stool sampling as well as the rationale for using a cardiovascular screening tool, the Norfolk Elderly and Later Life Cohort (NELLC) Health Questionnaire and General Health Questionnaire. My addition to the delegation log and the above described amendment enabled me to deliver this study under the TRACC research ethics.

The funding for this study was enabled by Norwich Research Park (NRP) Science Links Seed Corn grant of £14,779, as well as faculty funding from the Faculty of Medicine and Health Science, University of East Anglia (UEA) and the Biotechnology and Biological Sciences Research Council (BBSRC) core funding of the Quadram Institute (QI).

Study design

This study is a longitudinal, observational, multi-domain feasibility study examining the gut-brain axis in healthy elderly at differential genetic risk for developing AD and comparing them to a small group of AD patients.

Most of the study was conducted at the Bob Champion Building for Research and Education and the QI. Study visits took place in Norfolk and Suffolk, the Magnetic Resonance Imaging (MRI) was completed at the Norfolk and Norwich University Hospital (NNUH) and the metagenomics sequencing work was done by NOVOGENE UK, Ltd. in Cambridge. A flowchart of the study is shown below.

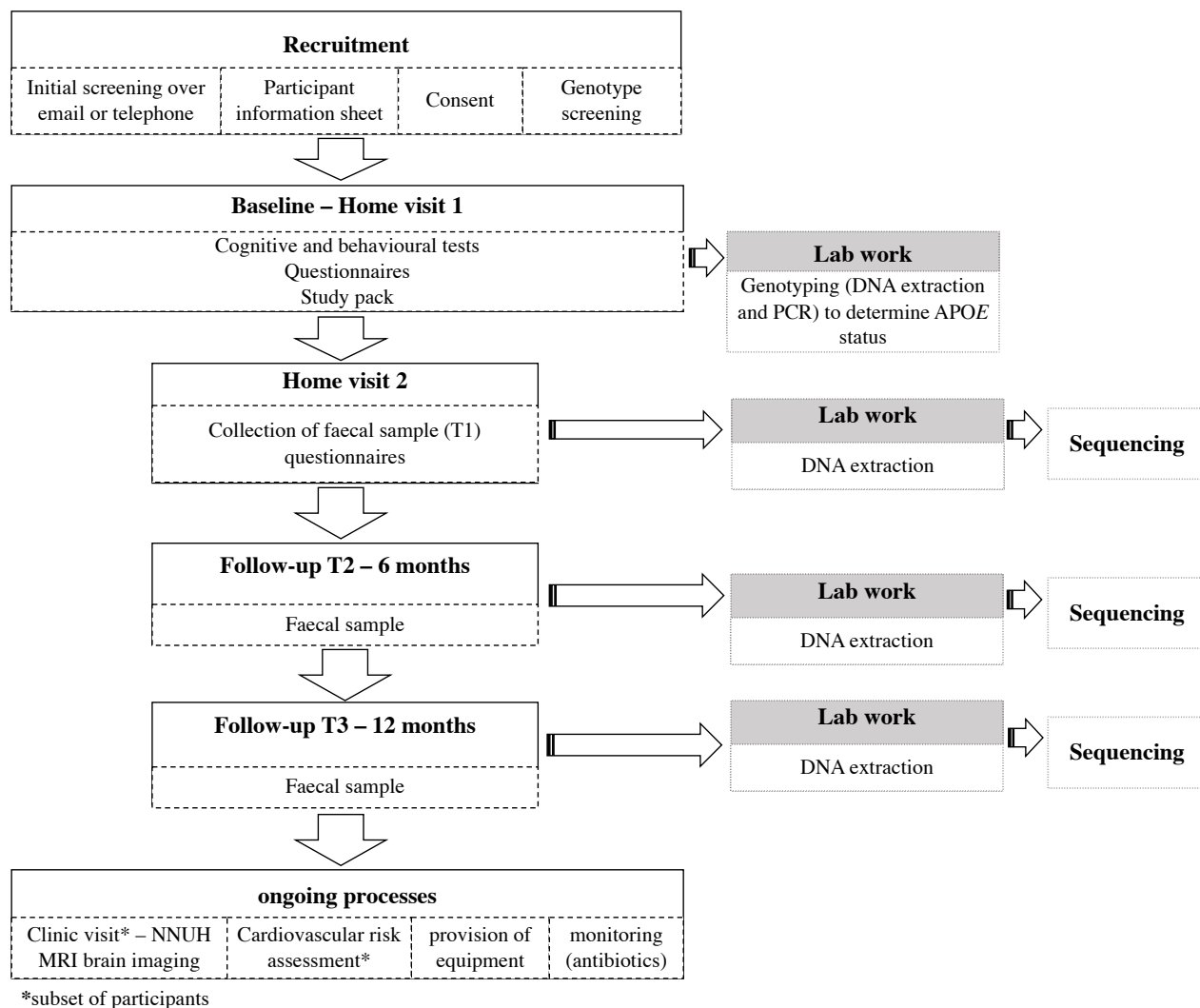


Figure 2.1 Study design flow chart

Recruitment

A major recruitment channel for this study was Join Dementia Research (JDR, www.joindementiaresearch.nihr.ac.uk), which is a national service that acts as a gateway between researchers who can register their studies and individuals from the public who register to give consent to be contacted. I also recruited from the NNET group database and used advertisement in the Eastern Daily Press and media channels (QI Facebook and homepage).

Healthy participants were screened for their APO ϵ 4 status and placed accordingly either into group of APO ϵ 4 non-carriers or carriers, with the exception of the APO ϵ 2/ ϵ 4 genotype which was excluded. The patient group was made up of AD patients. The aim was to recruit 35-40 participants per APOE group and use data from 10-15 AD patients. Given the longitudinal nature of the study, an attrition rate of 10-20% was expected for the APOE groups. The AD patient group was used for cross-sectional comparison and data was already readily available.

Power calculation

No formal power calculation was completed for this study as this study was intended to be hypothesis-generating only. With an anticipated 10-20% attrition and contemporary studies presenting around 30 participants per dataset. Given the prevalence of the APO ϵ 4 genotype, an estimated 140-160 participants would need to be screened in order to recruit the above-mentioned 35-40 for both APOE groups, with the intention of 30 per group to complete to provide sufficient data for evaluation.

Subject identification and consent

All individuals who voiced an interest to participate in the study, were pre-screened in line with the inclusion/exclusion criteria (Table 2.1) and they were sent a copy of the participant

information sheet. Following this, participants underwent genetic screening for the APOE genotype. All participants provided written consent. Because the frequency for APOε3/ε4 carriers and homozygote APOε4 carriers in the general population is 23% and 2%, respectively, the aim was to genotype approximately 140 individuals and approach individuals with known APOε4 status from an existing study. Due to the low frequency of the APOε3/ε4 and APOε4/ε4 genotype, all participants who were identified to be homozygous or heterozygous ε4 carriers completed the cognitive testing, questionnaires and repeated faecal matter sampling timepoints. I selected a subset of participants with APOε2/ε3 and APOε3/ε3 genotype to match the ε4 carriers with respect to gender and age. The AD patient group was selected from the database and consisted of patients with a diagnosis of AD, who had provided at least one faecal sample as part of the TRACC study.

Table 2.1 Study inclusion and exclusion criteria

Inclusion criteria	Exclusion criteria
<p>APOε4 non-carriers and APOε4 carriers:</p> <ul style="list-style-type: none"> - Healthy individuals aged 50-75 years at study begin. - Absence of major psychiatric or development disorder, other medical condition affecting the gut or cognition. 	<ul style="list-style-type: none"> - Presence of another major comorbid psychiatric disorder (e.g. major depression, schizophrenia, substance misuse, learning disability). - Previous history of high consumption of alcohol or other substances that in the clinician’s opinion is relevant to their disorder. - A major neurological condition not related to the conditions listed in the inclusion criteria. - Significant comorbid medical illness or visual loss likely to interfere with participation in research activities. - Placement in residential care or nursing home.
<p>AD patient group:</p> <p>A clinical diagnosis of AD with readily available faecal matter.</p>	

Apolipoprotein E genotyping

Genetic APOE status was identified for all study participants. Buccal cheek swabs (Sigma Swab 'MW941' with a foam bud and plastic shaft in sterilized tube, Medical Wire & Equipment Co Ltd, Corsham, UK) were used for the specimen collection. Deoxyribonucleic Acid (DNA) was extracted within five days of collection using the 'QIAamp DNA Blood kit' (Qiagen GmbH, Germany) in accordance with the manufacturer's protocol for 'DNA Purification from Buccal Swabs (Spin Protocol)' at the Bob Champion Research and Education Building (BCRE) laboratories.

The extracted DNA was subsequently prepared for 7500 Fast Real-Time PCR (Applied Biosystems, USA) which was completed at the BIO laboratories. I used the TaqPath ProAmp Master Mix (Thermo Fisher Scientific Ltd, UK) and two pre-designed TaqMan® single nucleotide polymorphisms (SNPs) genotyping assays (Assay ID: C_904973_10, dbSNP ID: rs7412 and Assay ID: C_3084793_20, dbSNP ID: rs429358; Applied Biosystems) to determine the specific isoform present at the two single nucleotides (rs429358 and rs7412) which are polymorphic in the APOE gene. The APOE genotype of healthy participants was determined and they were assigned into the group of APO ϵ 4 non-carriers or APO ϵ 4 carriers in line with Table 2.2. Detailed information on the DNA extraction, PCR amplification and allelic discrimination are given on p.347-350 in the supplementary.

Based on genetic risk, the APOE genotypes ' ϵ 2/ ϵ 2', ' ϵ 2/ ϵ 3', ' ϵ 2/ ϵ 4', and ' ϵ 3/ ϵ 3 were collapsed to form the APO ϵ 4 non-carriers, whereas participants with the genotype ' ϵ 3/ ϵ 4' and ' ϵ 4/ ϵ 4' formed the APO ϵ 4 carrier group.

Table 2.2 Apolipoprotein E genotype frequencies in the population of the United Kingdom and study group assignment.

APOE genotype	Frequency in the general population in the UK	Study group
$\epsilon 2/\epsilon 2$	1%	APO ϵ 4 non-carriers
$\epsilon 2/\epsilon 3$	11%	
$\epsilon 2/\epsilon 4$	2%	
$\epsilon 3/\epsilon 3$	61%	
$\epsilon 3/\epsilon 4$	23%	APO ϵ 4 carriers
$\epsilon 4/\epsilon 4$	2%	

Home visit 1

For the cognitive and behavioural testing battery five tests were administered: Addenbrooke's Cognitive Examination (ACE-III), Rey-Osterrieth Complex Figure (ROCF), Trail Making Test (TMT), Supermarket Task, Sea Hero Quest (SHQ). Participants also completed a series of questionnaires to assess their subjective cognitive change (Cognitive Change Index [CCI]), anxiety levels (Generalized Anxiety Disorder-7 [GAD-7]), depression levels (Patient Health Questionnaire-9 [PHQ-9]), behavioural changes (Cambridge-Behavioural-Inventory-Revised [CBI-R]), general lifestyle (Health Questionnaire) and diet (Food Frequency Questionnaire [FFQ]). Participants were provided a study pack with all necessary equipment and instructions to complete three faecal sample collections. The baseline cognitive and behavioural data (ACE-III, ROCF, TMT, CBI-R, GAD-7, PHQ-9) for the AD patients were administered by other members of the TRACC study and were available to me for data analysis.

Home visit 2

Participants provided their baseline faecal sample (T1) shortly after completing the first home visit. The filled-in questionnaires were collected. The baseline faecal samples of the AD patient group were already readily collected by other members of the TRACC study and

banked in the Biorepository from where I could access them for downstream processing and analysis.

Follow-up samples at 6 months (T2) and 12 months (T3)

Participants repeated faecal matter sampling two more times, with a six months interval between each sampling time point. If participants had taken antibiotics prior to their upcoming sampling time point, this date was rescheduled where possible to allow a minimum of three months without antibiotics.

Cardiovascular risk assessment

Risk factors for cardiovascular events, including mid-life hypertension and raised cholesterol levels are associated with brain atrophy, neurofibrillary tangles, and lesions in white matter which are clinical symptoms underlying Alzheimer's Disease pathology (Kivipelto *et al.*, 2001). An increasing body of research shows that risk factors for cardiovascular events and - disease can play an important role in AD aetiology (de Bruijn and Ikram, 2014; Santos *et al.*, 2017). A subgroup of participants completed the cardiovascular risk assessment. This assessment involved completing a questionnaire to establish medical history and previous cardiovascular health, taking blood pressure (M7 Intelli IT, OMRON) and determining instantaneous non-fasting lipid results.

Brain magnetic resonance imaging (MRI)

A subgroup of 40 participants (20 APO ϵ 4 group) completed a clinic visit at the Norwich and Norfolk University Hospital (NNUH) to undergo MRI of their brain, after being deemed safe to do so (safety checklist Figure 7.2 on p.351 in the supplementary). At the clinic day, participants completed a structural and functional MRI imaging scan at the NNUH/UEA 3T MRI scanner. The 45-min research scanning protocol measures both macro- (T1) structural brain changes in participants. Details of the TRACC Brain Protocol scanning sequence are

given in the supplementary on p.352. It is well-established that at-genetic-risk participants often show functional before structural brain changes. All research scans were checked by consultant radiologist, Dr Janak Saada, at NNUH. In case of an incidental finding, a report was issued, and the researcher sent it on to the participants' GP. 17 out of 40 study participants completed the MRI scanning with other members of the TRACC research team (five scans) or as part of the Spatial Navigation study (twelve scans).

Cognitive, behavioural, lifestyle and clinical measures

Addenbrooke's Cognitive Examination-III

The ACE-III is a standard screening test used to assess cognition and is well-validated for the detection of cognitive deficits as presented in AD or frontotemporal dementia (Hsieh *et al.*, 2013). The ACE-III evaluates abilities in five cognitive domains (attention, memory, verbal fluency, language and visuospatial abilities) using multiple short tasks. Participants can get a maximum score of 100, with lower scores indicating worsened cognitive functioning. Normative benchmark data and respective cut-offs are available (Mathuranath *et al.*, 2000; Mioshi *et al.*, 2006; Hsieh *et al.*, 2013, 2015; *UK ACE-III and M-ACE Administration and Scoring Guide*, 2014; So *et al.*, 2018; Bruno and Vignaga, 2019). More information on the ACE-III different domains is given in the supplementary (p.352).

The ACE-III has high reliability and construct validity. It is recommended that a cut-off score of 88 and 82 (from a total of 100) are used for suspicion of dementia. Using the lower cut-off of 82 points, the ACE-III has high specificity, meaning that those identified are very likely to have AD and reasonably high sensitivity (7% false negatives among a large majority of true positives). With the 88 cut-off the ACE-III has highest sensitivity (no one goes undetected), on the expense of slightly lower specificity (4% are false positives) (Lalkhen and McCluskey, 2008; *UK ACE-III and M-ACE Administration and Scoring Guide*, 2014).

Rey–Osterrieth Complex Figure test

The ROCF is a simple measure that is widely used in both experimental as well as clinical settings to assess visual and spatial aspects of memory (visuoconstructional abilities and nonverbal memory), including recall and recognition memory as well executive functioning and episodic memory performance (Meyers and Meyers, 1995; Spreen and Strauss, 1998; Cherrier *et al.*, 1999; Pelati *et al.*, 2011; Melrose *et al.*, 2013; Salvadori *et al.*, 2019, Frank and Landeira-Fernandez, 2008). Neural correlates for visuospatial functioning include the parietal lobe; in early AD medial and lateral areas of this brain region show disease-associated changes which might not be identifiable with other cognitive tests (Salimi *et al.*, 2018). Visual perception, construction and memory which form the basis of visuospatial function are highly complex processes. It is well-established that deficits in this domain result in spatial disorientation and that approximately 20-40% of patients manifest such deficits in early stages of AD (Mendez *et al.*, 1990; Cronin-Golomb *et al.*, 1991; Harciarek and Jodzio, 2005; Iachini *et al.*, 2009; Quental, Brucki and Bueno, 2009). The ROCF uses a complex abstract geometrical figure that implies no semantic coding and perceptually be divided into global and local elements (Figure 2.2). Global elements give a structural framework to the figure and are thus essential for the organization of local elements (Salvadori *et al.*, 2019).

The tasks consist of two parts. In the copy condition, the ROCF is placed in front of participants in landscape orientation and participants are asked to copy the figure as accurately as possible onto a blank sheet of paper with help of a pencil and eraser. The time to complete the copy is recorded. Upon completing the copy, the ROCF stimulus and copy are taken out of sight. The recall is administered after a three-minute delay. For the recall, participants draw the ROCF from memory; with no recording of time. Higher points denote better accuracy and placement More information on the scoring of the task can be found in the supplementary (p.353).

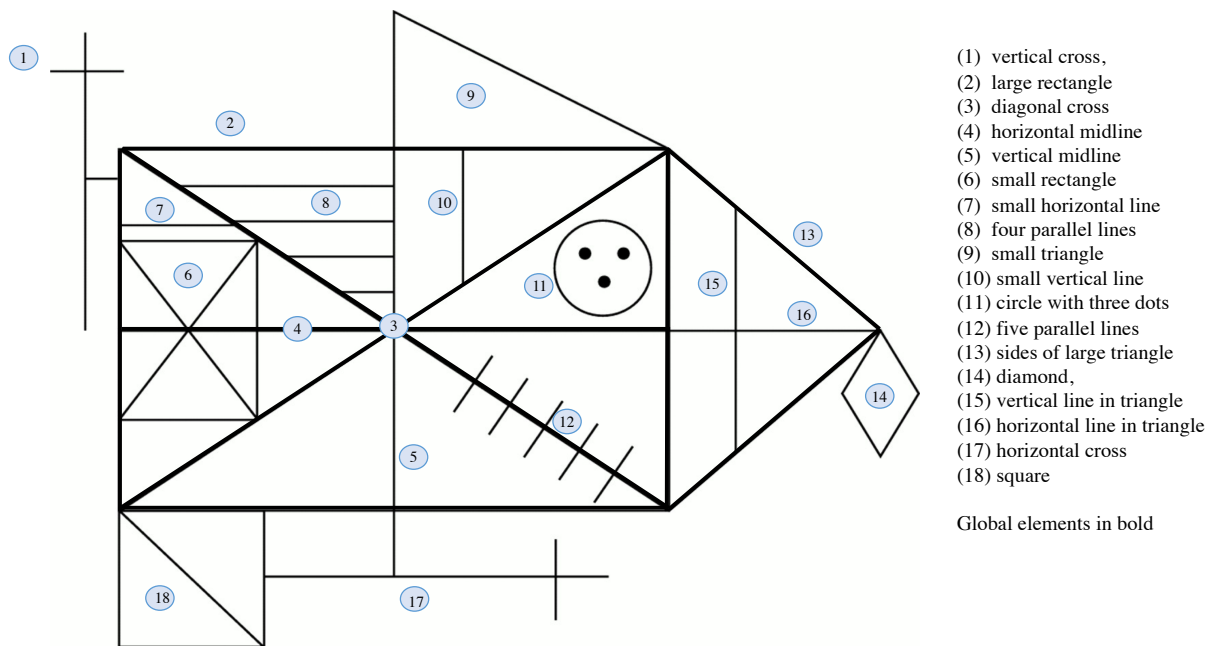


Figure 2.2 ROCF figure with 18 global and local elements

Trail Making Test

The TMT provides insight into several domains of cognition, such as executive functions (planning and switching) as well as processing speed, visual search, scanning and mental flexibility, which are thought to relate to fluid cognitive abilities and thus naturally decline with age (Tombaugh, 2004; Salthouse, 2011). The TMT, which is widely used in clinical practice, was originally used as part of the Army Individual Test Battery as a divided attention test developed by Partington and Leiter in 1939 (Llinàs-Reglà *et al.*, 2017). From a neuroanatomical perspective, the TMT was found to activate the dorsolateral prefrontal cortex, right inferior medial frontal cortex and several non-frontal brain regions including regions of the temporal gyrus and intraparietal sulcus (Zakzanis, Mraz and Graham, 2005; Llinàs-Reglà *et al.*, 2017). The test consists of two parts, henceforth denoted as TMT-A and TMT-B. In the first part, TMT-A, participants need to draw a line to connect 25 encircled numbers in continuous and increasing order. The second part, TMT-B, is similar; however, participants must now alternate between numbers and letters by starting at number “1”, then drawing a line to letter “B”, then to number “2” and so forth (“C”, “3”, “D”, etc.) (Tombaugh, 2004). A short practice trial (first 6 items of TMT-A and TMT-B) was administered to ensure

that participants understood the task before they were asked to complete the respective parts of the test.

TMT-A is considered to be a baseline measure of visual search, motor functioning and psychomotor speed. TMT-B is the more difficult part of the test, as it requires the participant to continuously perceive and retrieve the correct response whilst switching from one set of stimuli to the other (switch from counting numbers to completing the alphabet). Executive functions, particularly working memory, set-switching and inhibition control are hence abilities specifically important for TMT-B performance. Successful set-shifting is influenced by a person's ability to flexibly adapt and focus attention. Exerting such cognitive control and flexibility, allowing a person to effectively allocate cognitive resources, underpins all goal-directed behaviour (Jacobson *et al.*, 2011). Increased demands on working memory might be reflected through activation of the precentral gyrus and left-temporal-parietal lobe (Jacobson *et al.*, 2011).

Test performance is measured as the time (in seconds) taken to complete TMT-A and TMT-B respectively. Errors are also recorded but don't affect the score. The difference score, called TMT-d, is obtained by subtracting TMT-A from TMT-B. It gives a measure of executive functioning required for set-shifting. For this study, the TMT was administered as outlined by Spreen and Strauss (1998).

Spatial navigation measures

Spatial orientation is a fundamental cognitive ability which is often implicated to be impaired in early stages of AD (Weniger *et al.*, 2011; Serino *et al.*, 2015; Tu *et al.*, 2015, 2017) and shows promise to become a potential diagnostic marker for prodromal AD (Coughlan *et al.*, 2018). This notion is further supported by the fact that brain areas affected in prodromal AD are also key nodes in the spatial navigation network (Morris *et al.*, 1982;

Hartley *et al.*, 2014; Spiers and Barry, 2015; Tu *et al.*, 2017). Spatial navigation relies on the integration of egocentric, a body-based frame of orientation, and allocentric, a map-based frame of orientation (Coughlan *et al.*, 2018) (Figure 2.3).

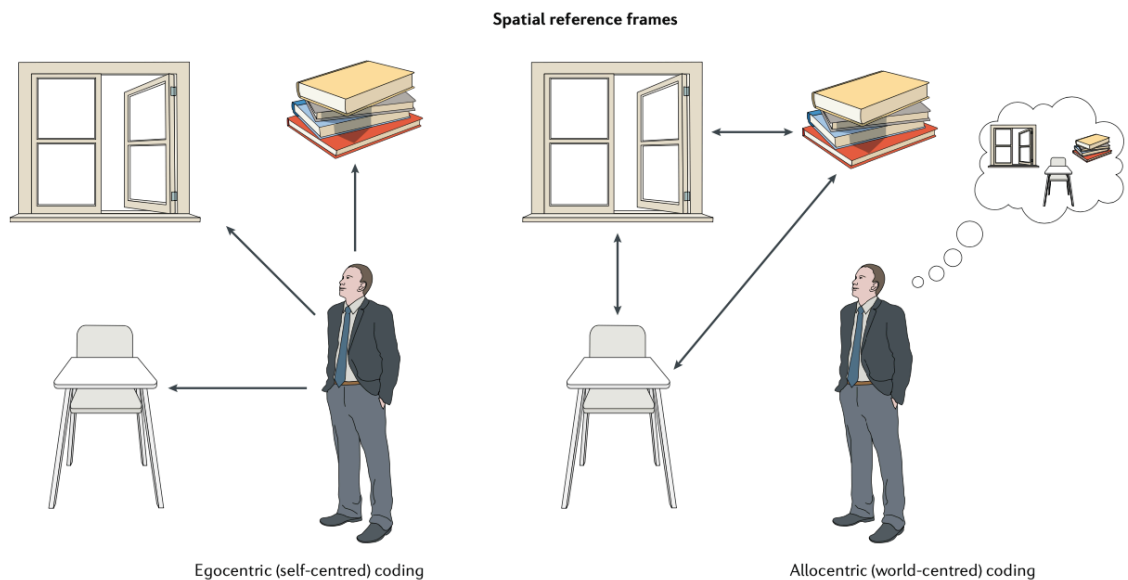


Figure 2.3 Egocentric (left) and allocentric (right) coding. Figure from Coughlan *et al.* (2018)

During everyday navigation, there is a fluid shift between both frames of orientation (McNaughton *et al.*, 2006). Localising the position of objects relative to the body is a central process in egocentric orientation, which relies on activation of the prefrontal and parietal cortex (Milner and Goodale, 1992; Arnold *et al.*, 2014). This information is then integrated together with self-motion cues in the precuneus (Wolbers and Wiener, 2014). The formation of maps, which is a fundamental process during allocentric orientation, makes use of grid, place and boundary cells of the medial temporal lobe (Lester *et al.*, 2017). The retrosplenial cortex is an important interface that integrates egocentric and allocentric orientation. Grey matter changes in the retrosplenial cortex have been associated with switching problems between egocentric and allocentric orientation strategies in AD patients (Tu *et al.*, 2015). The literature suggests that with old age people shift towards using predominantly allocentric navigation strategies and show an overall decline in spatial navigation (O’Keefe and Nadel,

1978; Lester *et al.*, 2017). I use two tasks to measure spatial navigation processes in this study cohort.

Sea Hero Quest

The SHQ app was developed by Hugo Spiers and Michael Hornberger, funded by Deutsche Telekom and Alzheimer's Research UK and supported by game developers from Glitchers Ltd. Since 2016, SHQ has been played by more than four million people worldwide across all ages and countries. SHQ primarily assesses spatial navigation and orientation performance. The app was designed to understand which factors support navigation abilities and which of these factors deteriorate over the lifespan and in disease. Age-range normative cut-offs are required to distinguish between age-related healthy decline and pathology-driven decline in spatial navigation abilities (Hartshorne and Germine, 2015; Malek-Ahmadi *et al.*, 2015; Coughlan *et al.*, 2018).

The game has two different types of levels which gather spatial navigation data on (i) goal-oriented wayfinding and (ii) path integration (Coughlan *et al.*, 2019). More details are given on p.355-356 in the supplementary. Level performance in goal-oriented wayfinding is divided into two main outcome measures: a) wayfinding distance and b) wayfinding duration. Wayfinding distance is the distance the player travelled to visit all checkpoints and can be seen as a measure of navigation efficiency. This distance will be closest to the required minimum if players succeed to retain the information retrieved from studying the level map and continuously update self-location within this 'cognitive map' based on self-motion and environmental cues in the game. The second measure, wayfinding duration, is the time in seconds taken to complete the level. Whilst inefficient navigation will inevitably result in a longer time to visit all checkpoints, wayfinding duration is mainly determined by the amount of acceleration used by the player. Acceleration can be actively used by the player through "swiping up" which will temporarily speed up the boat. Depending on how

much acceleration is used, two players could be travelling the same distance at very different speeds and thus different times. Players who travel faster might be more confident or faster at processing visual cues to inform their wayfinding (Coughlan *et al.*, 2019). Path integration levels, also referred to as flare accuracy levels, tap into the players ability to use and successfully integrate egocentric self-reference navigation over an accumulating distance travelled.

In this study, participants completed level 1 and 2 as practice levels to learn how to use the game controls and to allow us to later on normalise the data for app interaction with player proficiency. Participants also completed three wayfinding levels (level 6, 8, 11) and four flare accuracy levels (level 4, 34, 49, 54).

All SHQ data was pre-processed in MATLAB (R2017a). To account for the influence of player proficiency on digital devices, level performance was standardized against the proficiency on digital devices demonstrated in these first two levels by applying the following equation (Coughlan *et al.*, 2019): $\text{level N normalised} = \ln\left(\frac{\text{level N}}{\text{level 1} + \text{level 2}}\right)$. Subject performance on normalised levels could then be compared between subjects. I used multilevel linear mixed regression models with repeated measures (implemented with the `lmer()` package in R) for the goal-oriented way findings levels and mixed effects ordinal logistic regression (implemented with the `clm()` package in R) for the Path integration levels. Detailed information on the statistical analysis approach is given on p.355 in the supplementary.

Supermarket Task

The Supermarket Task is a computer-and tablet-based measure to evaluate spatial orientation within an ecological supermarket environment. Spatial orientation performance gained from the Supermarket Task can distinguish between AD and behavioural variant (bv)FTD patients

with 92.7% accuracy and has similarly high predictive power as memory tests (Tu *et al.*, 2015). The task has also been shown to identify important navigation differences in preclinical at-risk AD (Coughlan *et al.*, 2020). Details of the task are given in the supplementary (p.356).

The Supermarket task sets out to test spatial navigation abilities by the use of three main variables. These include (a) egocentric orientation, (b) allocentric orientation, and (c) heading direction. On top of that, I also split the map into central and peripheral areas along the half-width and half-length between the map centre point and outside border and counted the number of responses in the central area. This information was captured in a variable called (d) peripheral responses. More details on how I captured these four response variables are provided in the supplementary p.357-358.

I investigated the effect of APO ϵ 4 status on all outcome measures by running multilevel mixed regression models with age, sex and educational attainment as fixed effects. Due to the repeated nature of the task design (subjects completing 14 videos in the same supermarket environment), subject-level random effects were included in each regression model to account for the interdependence between repeated measures from playing multiple levels of the game.

Cognitive Change Index

The CCI is a questionnaire (self-report and/or informant-based) with the aim to assess a person's subjective perception of their cognitive decline compared to their ability five years ago in three domains: memory, executive and language (Rattanabannakit *et al.*, 2016). A subjective deterioration of cognition has been proposed as an early indicator for neurodegenerative disease as individuals often perceive a decline in their cognition over a decade before a diagnosis of AD or MCI (Rattanabannakit *et al.*, 2016). Subjective cognitive

decline is acknowledged as a criterion for a diagnosis of MCI (Joie *et al.*, 2016) and individuals with MCI show a higher rate of progression to dementia compared to a cognitively normal population (Roberts *et al.*, 2014). This questionnaire which focuses on subjective cognitive decline complements the measures used here for objective cognitive deficits.

The CCI is a questionnaire that consists of 20 items and asks participants (or informants) to rate the person's ability to perform certain cognitive tasks (e.g. remembering names and faces of new people, recalling conversations a few days later, organizing daily activities, etc.) to test their memory performance, executive functioning and language abilities compared to the previous five years (Rattanabannakit *et al.*, 2016). Detailed information on the CCI is given on p.358 in the supplementary. The resulting subscale scores are validated to highly correlate with scores of objective tests in same domain as well as other domains. Dementia patients scored highest but similar to a cohort of individuals with MCI. Both groups scored considerably higher compared to a cognitively healthy control group (Rattanabannakit *et al.*, 2016).

Cambridge Behavioural Inventory-Revised

The CBI-R is a self-administered or informant-rated questionnaire filled out by the participant or carer to measure changes in behaviour across a range of functional and behavioural domains. The CBI-R questionnaire is comprised of 81 items assessing a wide range of symptoms which are part of 10 functional or behavioural domains and also evaluates activities of daily living. These include memory and orientation, everyday skills, self-care, mood, abnormal behaviour, beliefs, eating habits, sleep, stereotypic behaviour, motor abilities, and motivation. In the informant-based version of the questionnaire, the participant has to rate the frequency of a particular behaviour on a scale from 0-4 (0 = never, 1= a few times per month, 2= a few times per week, 3= daily, 4=constant). On this scale a

rating of “0” denotes no impairment, whilst a score of “1” and “4” indicates an increasing degree of behavioural impairment. Particularly a score of “3” or “4” corresponding with “daily” or “constant” occurrence of the behaviour are a sign for a severe deficit.

The CBI-R is widely used in neurodegenerative disease, particularly in order to distinguish different types of dementia, Parkinson’s disease, and Huntington disease (Wedderburn *et al.*, 2007; Wear *et al.*, 2008). I used the CBI-R mainly to control for other neuropsychiatric problems which could otherwise confound of cognitive results.

Generalized Anxiety Disorder-7

The GAD is self-report measure is a validated questionnaire that is commonly used for measuring self-reported anxiety. The questionnaire consists of 7 items on a 4-point Likert scale (indicated frequency, “not at all” to “nearly every day”) related to feeling of anxiety (e.g. “Feeling nervous, anxious, or on edge”) experienced over the last 2 weeks (Spitzer RL *et al.*, 2006). Participants can score a minimum of 0 and a maximum of 21, where a score ≤ 4 indicates that the person is not anxious, whilst a score between 4-21 indicates that the person has experienced anxiety to some extent. The severity of anxiety is split into 3 stages; a score between 5-9 is considered ‘mild’, 10-14 is considered ‘moderate’, and 15-21 indicates ‘severe’ levels of anxiety.

Anxiety and depression are commonly displayed in patients with dementia but the exact nature of their relationship to dementia (causality, association or consequence) are not definitively answered. Having high trait anxiety correlates with a higher incidence for developing dementia (Mortamais *et al.*, 2018). The main rationale for the use of this test, was to control for potentially confounding neuropsychiatric problems.

Patient Health Questionnaire-9

The PHQ-9 is a self-report multipurpose instrument for screening the severity of depression symptoms in the participant (Löwe *et al.*, 2004). Participants are asked to rate how often they have been bothered by a range of problems (9 questions) using a 4-point Likert scale with increasing frequency (0= 'not at all', 1= 'several days', 2= 'more than half the days', 4= 'nearly every day') based on their experience of the last two weeks. The problems presented in the questions address pleasure in daily activities, mood, appetite, sleep, energy levels, detrimental thoughts about oneself, and lethargy. Participants can score a maximum of 27 points. The higher the total score, the stronger is the depression experienced by the individual. Depression severity falls into one of 5 categories depending on the summary score: none (≤ 4), mild (5-9), moderate (10-14), moderately severe (15-19) or severe (20-27).

A growing amount of evidence implies that depression, in particular in early life but also in late life, is associated with a greater increase in risk of dementia and is emerging as a risk factor for developing the disease. Major depressive disorder is present in a fifth of all patients with AD and half of all patients with VD (Byers and Yaffe, 2011). The mechanisms underlying the relationship between depression and dementia are complex. On a biological level, one suggested pathway is that of downregulation of the HPA-axis negative feedback loops and associated chronic elevation adrenal glucocorticoids levels and hypercortisolaemia leading to hippocampal atrophy and memory impairment that is observed in people with depression (Butters *et al.*, 2008). As with the GAD-7, I employed this test to control for the potentially confounding effect that depression might have on any of the other test measures.

Microbiome Questionnaire

A self-report questionnaire used to collect demographic and behavioural metadata collected to explain variability among healthy human-associated microbial communities (Flores *et al.*,

2014). Environmental factors heavily influence the intestinal microbiome. The collection of microbiome-associated meta data is hence highly recommendable (Wu *et al.*, 2019). 69 factors were shown to correlate significantly with overall microbiome community variation, these covariates explained 1.5 to 14.7% of variation in genus abundance as stand-alone effect. Out of which 18 factors emerged to be non-redundant, including stool consistency, age, gender, intake of specific drugs, dietary information, BMI (Falony *et al.*, 2016).

I gathered information on many environmental and lifestyle factors, including age, gender, ethnicity, handedness, dietary habits, use of probiotics and antibiotics, food supplements, allergies, medication history and many more detailed questions such as mode of birth and feeding, co-habiting with pets, smoking status, exercise, use of pool, etc. All of these factors may influence the composition of the intestinal microbiota and are thus considered important metadata to control for potentially confounding factors.

Health questionnaire

The NELLC health questionnaire is a short questionnaire, which was used to record any illnesses the participant may have experienced recently and was completed before each sampling time point (Flores *et al.*, 2014). It was employed to ensure that participants had not suffered a gastric-related illness or had taken antibiotics, that would impact their normal intestinal microbiota, shortly before providing their faecal sample.

Cardiovascular risk assessment – QRISK^{®3}

The QRISK[®] score is a well-established risk indicator for cardiovascular disease (CVD) that is used by the NHS. The QRISK^{®3} algorithm estimates the 10-year risk for a heart attack or stroke and is used across England's health service, in occupational health settings, and internationally. Risk factors for the QRISK model include age, ethnic origin, systolic blood pressure, body mass index, total cholesterol, smoking status, family history of coronary heart

disease, corticosteroid use, treated hypertension, rheumatoid arthritis, and several others (Hippisley-Cox *et al.*, 2007, 2008; Hippisley-Cox, Coupland and Brindle, 2017; Edwards *et al.*, 2018).

All lipid measurements were obtained using a handheld point-of-care device, “Mission 3-in-1 Cholesterol Meter” (*Mission*[®] Cholesterol Monitoring System, ACON Lab. Inc., San Diego, CA, USA), which gives almost instantaneous lipid levels of total cholesterol (mmol/L), high-density lipoprotein (HDL) (mmol/L), Triglycerides (mmol/L), calculated LDL (mmol/L), and a cholesterol ratio (total cholesterol/HDL). The small and portable device allows to measure cholesterol levels fast and easily, has clinical proven accuracy and is CE0123 certified. More details on the lipid measurements are given in the supplementary (p.359). I also measured participants’ blood pressure using a clinically validated blood pressure monitor device (M7 Intelli IT, OMRON). All other information was self-reported by participants (height, weight, etc.). Using this information, the QRISK[®]3 risk was determined using the online calculator at <https://qrisk.org/three>.

The QRISK[®]3 score presents the average risk of people with the same risk factors of having a heart attack or stroke within the next 10 years. The expected QRISK[®]3 score indicates the risk score a healthy individual matched for age, sex, ethnic group, who has no adverse clinical indication for cardiovascular disease (as defined by a cholesterol ratio of 4.0, stable systolic blood pressure of 125, a Body Mass Index (BMI) of 25, and no other adverse indication). The relative risk, describing the probability of an event to occur in the exposed group versus the that in the non-exposed group, is subsequently calculated through dividing the 10-year QRISK[®]3 by the matched healthy person’s QRISK[®]3 score (Poulton, 1990). A ratio of 1.0 denotes an equal risk between the groups, while a relative risk ratio <1.0 or >1.0 indicates a respectively smaller or higher risk for the individual compared to a healthy person’s risk.

Dietary assessment – Food Frequency Questionnaire

Gaining insight into participant's diet allows to investigate whether specific dietary patterns cluster with microbiome enterotypes (Wu *et al.*, 2011). Diet is considered to be a dominant force in shaping the composition of a person's intestinal microbiota (Sonnenburg and Bäckhed, 2016) (De Filippo *et al.*, 2010; Walker *et al.*, 2011; Cotillard *et al.*, 2013; David *et al.*, 2014; Kovatcheva-Datchary *et al.*, 2015; Oriach *et al.*, 2016). Thus, dietary information should be an important component for any microbiome study. Insight into this relationship has sparked efforts for developing “microbiota-derived foods” and personalized nutrition to establish bacterial community profiles that will promote health (Green *et al.*, 2017).

The FFQ is a validated tool to assess a persons' food intake in terms of frequency during the last twelve months (Kroke *et al.*, 1999). This study used a version of the European Prospective Investigation into Cancer and Nutrition (EPIC)-Norfolk FFQ which has been adapted to the UK diet and allows for a thorough breakdown of macro- and micronutrient intake (*EPIC-Norfolk: nutritional methods*; Mulligan *et al.*, 2014). Frequency ratings from a 130 food items obtained by the FFQ were analysed using a nutritional analysis software called the ‘Food Frequency Questionnaire European Prospective Investigation into Cancer and Nutrition Tool for Analysis’ (FETA) (Mulligan *et al.*, 2014). More information of the FFQ is given in the supplementary (p.359-360). In order to obtain accurate results about micro- and macronutrient intake, the food codes are mapped against the UK food composition database by McCance and Widdowson (Holland, Welch and Unwin, 1991; Chan, Brown and Church, 1996). The output created by FETA is composed of the average daily nutrient intake of 46 nutrients such as alpha carotene, carbohydrate, cholesterol, copper, folate, magnesium, Vitamin A, etc. and daily average intake from 14 food groups such as alcoholic beverages, fats and oils, meat and meat products, nuts and seeds.

The FFQ is based on self-report which means that participants can under- or overreport. It is hence difficult to establish accurateness of answers. In terms of outlier detection, I thus restricted this process to the evaluation of energy intake. Energy intake is measured by the FFQ by the variable energy in kilocalories (kcal) and kilojoule (kJ), and it is to some extent a summary variable for all reported nutrients as it incorporates the energy from all consumed nutrients. The recommended daily energy intake measured in kcal for women is 2,000 kcal and 2,500 kcal for men. To exclude extreme values, I decided to exclude FFQs from participants whose reported energy intake was below or above 1000 kcal of the recommended daily intake.

Statistical analysis of test results - generalized linear model (GLM)

Unless stated otherwise, multiple linear regression models were used to assess the cognitive and behavioural performance outcome measures presented in this thesis. All of the regression models were run in R. The results presented in Chapter 3 include sum of squares (SS), degrees of freedom (df), F-test, standardized coefficients and the squared multiple correlation (R^2). The latter describes the amount of variation explained by the model and can also be used to calculate Pearson correlation ($\sqrt{R^2}$). Beta (b) values are the regression coefficients of the predictors (X).

Regression analysis involves running a series of steps (diagnostics) that assess whether the model is a good fit to the data before one can draw inferences about the output of the analysis. All regression models were assessed with several diagnostics to check whether assumptions for regression were met (Eberly, 2007).

GLM models were used to assess the fixed effects of APOε4 status on the outcome variables of the above presented tests. Next to APOε4 status, I considered age, educational attainment

and sex as potential predictors, as all of these predictors have been shown to impact cognitive or behavioural results in the literature (Kenny *et al.*, 2013; Murman, 2015; Coutrot *et al.*, 2018). The statistical analysis was carried out using RStudio (Version 1.2.5001) (RStudio Team, 2019).

Magnetic Resonance Imaging analysis

The anonymised MRI data was first converted from DICOM to NIFTI format. Following this, all the T1-weighted structural images were processed using FMRIB Software Library (FSL) voxel-based morphometry (VBM) tool (Smith *et al.*, 2004; Douaud *et al.*, 2007) (www.fsl.fmrib.ox.ac.uk/fsl/fslwiki/FSLVBM). Support was provided by physicists Dr Donnie Cameron and Dr David Willis. In short, VBM analysis consists of 4 steps: 1) brain extraction, 2) creating the study specific grey matter (GM) template, 3) registration of native GM images to template and smoothing and 4) permutation-based non-parametric GLM testing and identification of significant clusters between groups (Good *et al.*, 2001; Andersson, Jenkinson and Smith, 2007; Winkler *et al.*, 2014).

In a first step, all structural T1 MRI images were subjected to neck removal and brain extraction step. Large amounts of non-neuronal tissues such as neck or lower head area can result in overestimation of brain volumes. Thus, before setting the field of view, removal of neck voxels was implemented using automatic ‘robustfov’ algorithm, which cropped the images below the neck area. I then used vanilla Brain Extraction Tool (BET) to separate the brain from the non-brain structures. Using FSLEyes, all brain masks were visually inspected and BET parameters were adjusted individually if required to optimise the resulting brain masks.

In the second step, all brain masks are segmented into white matter, GM and CSF. Then the study specific GM template was generated by applying affine-registration to the GM

Montreal Neurological Institute (MNI)-152 template, concatenation and averaging to all GM images. In the third step, the GM images were non-linearly registered to the study-specific template and smoothed with an isotropic Gaussian kernel (sigma 3mm). Lastly, I used the FSL randomize method with 5000 permutations to apply permutation-based voxel wise GLM and ran uncorrected as well as corrected testing for multiple comparisons to identify significant clusters between the APOE cohorts.

Experimental design of microbiome study aspects

Microbial DNA isolated from faecal matter is a powerful proxy for the distal colon microbiome. It enables us to explore the structure of microbial communities - predominantly bacteria, but fungi and viral DNA can also be obtained - and their associated function in the intestine (Gill *et al.*, 2006; Gorzelak *et al.*, 2015). The experimental design of the study can be largely divided into the following six steps as shown in Figure 2.4.

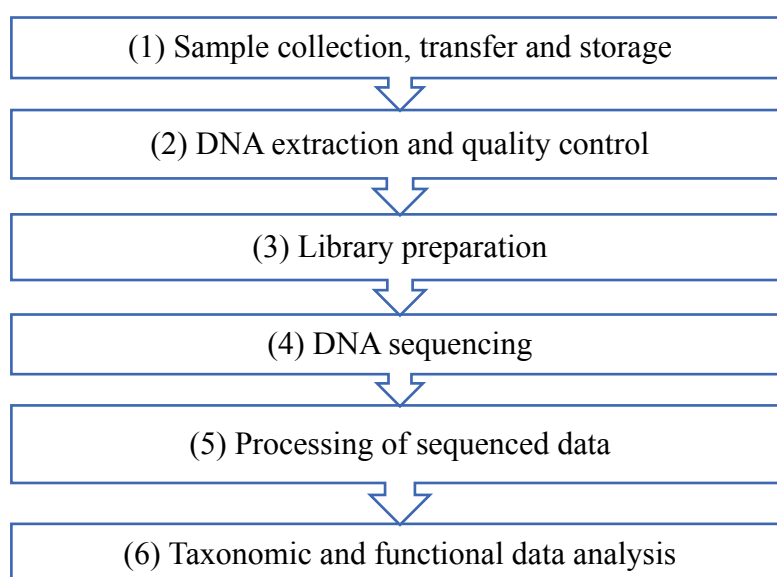


Figure 2.4 Flowchart of microbiome experimental design

Sample collection, transfer and storage

Participants collected the faecal matter from one bowel movement in a sterilized Fecotainer. They were instructed to take a small amount of faecal matter from the middle portion of their

sample and to fill this into an OMNIgene gut tube in line with the manufacturers' instructions (OM-200 DNA Genotek, Ottawa, Canada). The tubes contain a preservative that stabilises the sample at room temperature for 60 days. Samples were sent back to the research facility using Royal Mail. Special mailing equipment (including bubble wrap, biohazard bag with absorbent, cardboard envelope) was provided in accordance with International Air Transport Association (IATA) packaging regulations for exempt human specimen. At the research facility samples were stored for up to 60 days at room temperature or directly frozen before the DNA was extracted.

The NELLC questionnaire allowed us to monitor if participants were sick since their last sampling time point. If participants took antibiotics up to three months before their follow-up, this date was pushed back by three months to allow recolonization of the gut bacteria. Major and long-lasting reduction of bacteria following antibiotic treatment is well documented in the literature (Sullivan, Edlund and Nord, 2001; Palleja *et al.*, 2018).

Faecal matter from AD patients was collected as outlined by the TRACC protocol and was readily available as frozen matter in the Biorepository. Faecal matter of AD patient samples was subjected to the same processing steps and analysis as other faecal samples in this study.

DNA extraction

I used an adapted protocol of the FastDNA™ SPIN Kit for Soil (MP Biomedicals™LCC, Product code 11492400) to isolate genomic DNA from faecal samples. Much of the isolation process was conducted in a class two safety cabinet. The extraction was performed as instructed by the supplier with minor modifications which are given in detail in the supplementary material (p.361-362).

DNA quality control

The concentration and quality of the extracted nucleic acids was determined for a subset of DNA samples to minimise loss of sample but to ensure protocol efficiency and most importantly to make sure high-enough quality for downstream analysis was available. The quality of the DNA was assessed using NanoDrop Spectrophotometer and Qubit (details given in the supplementary p.362) by myself. Both methods are used widely to quantify purity and concentration of extracted DNA. An independent thorough quality control (QC) of all samples was performed as part of the library preparation by Dr David Baker and Dr Steven Rudder (Sequencing Team in the QIB) and took place before samples were sent off to the sequencing institute where samples were subjected to an external round of in-depth QC. The external QC by NOVOGENE (Cambridge, UK) included library quality control and data quality control (distribution of sequencing quality/- error rate and distribution of A/T/C/G bases, filtering) which was sent back to us as a quality report. Detailed information of the QC by NOVOGENE on p.364-367 in the supplementary and excerpts shown in supplementary Figures 7.8-7.11 and Table 7.5 in the supplementary.

Library preparation

The library preparation for this study was performed by Dr David Baker and Dr Steven Rudder at the QI. The details for creating the libraries as outlined in the supplementary (p.363) were provided by Dr David Baker.

DNA sequencing – whole metagenomic shotgun sequencing

DNA pools were sent to NOVOGENE to be sequenced on the Illumina NovaSeq 6000 platform and demultiplexed with Illumina Nextera XT v2 Set A indexes used to prepare the libraries. The number of samples submitted per run was aimed to provide an average of 10Gb per sample (deep shotgun sequencing) to ensure good enough sample coverage. Samples were submitted in batches to minimize the potential bias introduced by different sequencing

runs, even though this bias was considered small (Caporaso *et al.*, 2012). All methods related to sequencing of samples were kept consistent across the submitted batches (sequenced by NOVOGENE on the same sequencing platform).

Processing of sequenced data

The processing of the sequencing data before data was ready for analysis was performed by Dr Andrea Telatin and Dr Rebecca Ansoerge (bioinformaticians at QI). The metagenomic analysis of Illumina Paired-End libraries can be broadly divided into three steps: (i) Quality control (QC) and low-quality filtering, (ii) Read-by-read analysis, (iii) *De novo* assembly. Detailed information of (i) – (iii) are given in the supplementary (p.367-368). All samples were subjected to the same processing steps to minimize potential technical bias.

Taxonomic classification

MetaPhlAn2 (Segata *et al.*, 2012), which uses a clade-specific marker gene database, was used to assign a taxonomic identity to species level to each read in the filtered sequencing dataset and was thus used to determine taxonomic profiles from DNA. Since MetaPhlAn2 generates relative abundances (it is normalised by the length of marker gene when assigned), rather than count data, the resulting community composition can be compared against another dataset regardless of sequencing depth.

Predictive functional profiling

Whilst taxonomic analysis (the study of the composition of species in the community) offers interesting insights, metagenomic shotgun sequencing can also be subjected to a gene-centric approach that further allows characterising the functional capacity of the microbial community as a whole. We thus subjected the metagenomics data to predictive functional profiling as described below.

Homology-based functional annotation of short reads

In predictive functional analysis, each read is mapped to a database of orthologous gene groups with the aim to identify matches to genes or proteins with known or annotated functions (Carr and Borenstein, 2014). Unambiguous mapping of short sequencing reads is critical for an accurate characterization of functional profile. A key consideration for the analysis and interpretation of the data is to understand whether the data at hand represents estimated relative abundances of functions in the community or whether it represents the presence or absence of gene families and functional modules (Carr and Borenstein, 2014). The counting of reads which map to each gene family or orthology group, together with the process of annotating functions, are the starting point of every functional analysis. The taxonomic identity of the identified homologous gene is secondary to the biological function which is the true target for such an analysis. Especially in comparative studies or longitudinal studies this approach is used to detect functional shifts that might occur as a function of time or that could be associated with a disease state.

Gene orthology-based databases

In this study, predicted genes were blasted against KEGGs databases (PATHWAY, BRITE, MODULE) to identify protein-coding genes and assign them to KEGG orthology (KO) accession numbers. KOs then build the foundation for KEGG modules, pathways and metabolisms. Of note, even for well-characterized genomes of bacteria strains only a fraction of all detected protein-coding genes can be successfully mapped to KOs and the amount to which this is possible varies substantially between different bacterial strains in the database. This is one of the major intrinsic limitations of the method.

KEGG metabolism is a low-resolution overview of the global metabolic map which is broadly divided into 11 categories – ‘amino acid metabolism’, ‘energy metabolism’, ‘metabolism of cofactors and vitamins’, ‘nucleotide metabolism’, ‘biosynthesis of other secondary metabolites’, ‘glycan biosynthesis and metabolism’, ‘metabolism of other amino

acids’, ‘xenobiotics biodegradation and metabolism’, ‘carbohydrate metabolism’, ‘lipid metabolism’, and ‘metabolism of terpenoids and polyketides’. It offers an overview of the predicted functional capacity of an entire sample, which in this case, is based on the gene counts of distinct organisms.

Whereas KEGG metabolisms is a top-level approach, a greater amount information can be gained from looking at KEGG modules and pathways. KEGG modules, identified by an M number, are tighter functional units of genes or proteins which describe metabolic functions in the KEGG metabolic pathway map (Kanehisa and Sato, 2020). A module (i.e. ‘pathway modules’) consists of functionally related enzymes (K numbers), but can also involves metabolites and reactions, all of which are connected in an integrated way. As such they often correspond to a sub-pathway of the KEGG pathway map. KEGG modules are based on a logical Boolean expression of K numbers which can automatically evaluate whether the gene set is complete, so that a module is present (Kanehisa, 2013). For example, module M00141 is defined by the following expression: K00600 (K00288,(K13403 K13402)) where a space represents AND, and a comma sign represents OR.

The KEGG PATHWAY database is comprised of manually drawn maps, as well as reference pathway maps and organism-specific pathway maps, which are representative of molecular interaction diagrams (Kanehisa *et al.*, 2012, 2017) and hold information about KOs, reactions and compounds that make up a pathway.

Metagenomic data was also functionally profiled by use of the HMP Unified Metabolic Analysis Network (HUMAN3), which allowed to quantify genes and pathways and has become widely available (<http://huttenhower.sph.harvard.edu/humann>) and frequently used method to infer the functional and metabolic potential of a microbial community metagenome (Abubucker *et al.*, 2012; Abu-Ali *et al.*, 2018). In brief, the previously

described tool MetaPhlAn is used to taxonomically assign the detected organisms and determine estimated relative abundances. Next the reads are functionally annotated by mapping them to sample-specific pangenomes and organism specific-gene hits are kept, whilst the unclassified reads are further processed including alignment against a universal protein reference database (UniRef90) and a translated search. Then several steps follow for gene family and pathway quantification. In the end, the functional profile is comprised of reads that were mapped against the MetaCyc database. Four possible mapping outcomes are possible, either the reads were mapped in a i) ‘species-specific’ manner (to a specific organism of a characterized gene family involved in known pathway(s)), ii) are mapped as ‘unclassified’ (to characterized protein family, but no a specific organism), iii) remain ‘unintegrated’ (mapped to uncharacterized gene family not involved in known pathways), or iv) were ‘unmapped’, if the read failed to map to any known sequences (following the nucleotide and translated search) (Abu-Ali *et al.*, 2018). ‘UNINTEGRATED’ abundances represent the total abundance of genes of that community or species that did not contribute to a known pathway, whereas the other abundances are scaled against a constant that considers the total pathway abundance with respect to the total abundance of genes which contribute to those pathways. The community functional profiles were further differentiated between those that could be stratified by known organisms (‘STRATIFIED’) and those that were stratified by unclassified organisms (‘UNSTRATIFIED’).

Taxonomic and functional analysis of metagenomic sequencing data

The taxonomic and functional analysis of the processed sequencing data was completed by me. The choice of appropriate analysis tools and statistical tests was guided by the literature and the expert input of Dr George Savva (statistician, QI) and Dr Andrea Telatin and Dr Rebecca Ansorge.

Diversity analysis

Microbiome community structure is commonly assessed using alpha and beta diversity which are measures of within- and between sample diversity, respectively. Multiple ecological indices that fall into the category of alpha or beta diversity can be implemented using the R package *vegan*. Despite the fact that the intestinal microbiome exhibits an exceptionally high species diversity, it maintains a relatively stable state within individuals (Bäckhed *et al.*, 2005; Lozupone *et al.*, 2012; Faith *et al.*, 2013). Diversity per se, however, does not necessarily mean stability, nor does reduced diversity always indicate ill-health as was previously suggested by the literature (Manichanh *et al.*, 2006; Jiang *et al.*, 2015; Falony *et al.*, 2016). Nonetheless, it is generally agreed that diversity remains to be a fundamental concept providing important insights into the overall composition profile of complex communities. The choice of diversity index can significantly influence the results as they give different weight to different aspects of community structure (Johnson and Burnet, 2016), which I address in this study by employing a range of different indices.

Alpha diversity

The Shannon diversity index (H') and the Simpson diversity index (D_1) are two commonly used alpha diversity measures that summarize the structure of the microbial community with respect to both *species richness* (number of different taxa present) and *evenness* (equitability of taxa frequencies) in a single sample (Wagner *et al.*, 2018). The literature recommends the use of two distinct measures because richness and evenness appear to be two separate sub-constructs of alpha diversity (Hagerty *et al.*, 2020)

H' represents the uncertainty of an unknown species picked at random. The more species diversity is present in a community, the larger the uncertainty of the identity for any given species. Compared to the D_1 , H' is more strongly influenced by its richness component (abundance of rare taxa) than its evenness component (Shannon and Weaver, 1949; DeJong,

1975). In most ecological studies, H' ranges between values of 1.5 and 3.5. Whereas the Simpson index gives more weight to evenness within a community (more strongly influenced by the most abundant species in a community), but is rather insensitive to the relative contribution of rare species (Simpson, 1949; DeJong, 1975); which makes D_1 mainly an index of evenness or dominance.

I used the Inverse Simpson index ($D_2 = \text{inverse of } D_1$), which is more intuitive than D_1 since its value increases as diversity increases (Wagner *et al.*, 2018). Due to the lack of an ideal diversity index, I herein report all three aforementioned indexes to provide a more complete understanding of community structure.

Alpha diversity was calculated using the *diversity* function from the *vegan* package in R. Statistical test of between-group comparisons of alpha diversity were also implemented in R using Wilcox-rank summary test (non-normal distribution of data previously assessed).

Beta diversity

Beta diversity is a measure of variance in microbial community composition between samples, which is often calculated by comparing feature dissimilarity which creates a matrix of ecological distances between all pairs of samples. The most common beta diversity measures that quantify the difference between two communities fall into two main categories depending on whether they are based on presence/absence data or abundance data.

The Jaccard index measures the degree of community similarity and dissimilarity based on the numbers of species shared by two communities as well as the number of species unique to each community (Hao *et al.*, 2019). Because it considers only absence or presence it is a qualitative measure. It is an unweighted taxonomic metric which considers neither abundance nor phylogeny but is based purely on whether or not features (taxa in this case)

are shared. This also means that rare as well as abundant species will be given equal weight (Jaccard, 1912).

The Bray-Curtis index is a quantitative non-phylogenetic metric, which is similar to the Jaccard index, but also considers species abundance. As such, the Bray-Curtis index is more heavily influenced by the most abundant species within a community (Sørensen, 1948).

Beta diversity can be visualized using ordination plots, allowing us to identify possible data structures of the underlying compositional distance matrix. The most commonly used multivariate ordination methods in bacterial ecology are principal coordinates analysis (PCoA) and non-metric multidimensional scaling (nMDS) (Jovel *et al.*, 2016). The overall objective of any ordination is to characterize a highly complex data structure in terms of a simplified structure by representing the relationship of samples in a small number of dimensions (typically two or three axes) (Legendre and Legendre, 2012).

Permutational multivariate analysis of variance (PERMANOVA) is typically used to determine if the centroids of the cluster samples created by ordination are statistically different (Anderson, 2017). This function also estimates the amount of variance (R^2) in the distance matrix attributable to the variable of interest.

Bray-Curtis (quantitative) and Jaccard (qualitative) distance matrices were calculated using the *vegdist* function of the *vegan* package in R. Ordination methods were implemented in R by use of the *metaMDS* function from the *vegan* package and *pcoa* function of the *ape*. Statistical testing was implemented by running a PERMANOVA using the *adonis* function from the R package *vegan* with 999 permutations. A cross-sectional PERMANOVA was used to statistically determine the effect of group and also assess the effect of the covariates

(age, sex) based on between-group diversity (Bray-Curtis or Jaccard) at each taxonomic level.

Univariate differential abundance analysis

To identify the taxa which can discriminate best between the intestinal microbiota samples of participants with APOε4 non-carriers and APOε4 carriers based on differential relative abundance, univariate statistical tests was initially performed. LEfSe incorporates multiple statistical tests, including non-parametric Kruskal-Wallis sum rank test ($p < .05$), Wilcoxon rank-sum test ($p < .05$) and Linear Discriminant Analysis (LDA) with an effect size filter (Segata *et al.*, 2011). The final output is a list of the identified features (taxa) discriminative between the groups, and their estimated effect sizes. Results are plotted in a horizontal bar chart and as cladograms. Cladograms capture phylogenetic relationships and saliency. Green and red denote detected group differences of the most abundant class, whilst yellow represents non-significance. The diameter of each circle in the cladogram is proportional to the relative abundance of the taxon (Segata *et al.*, 2011). The analysis was implemented within the Galaxy framework of the Huttenhower lab (<https://huttenhower.sph.harvard.edu/galaxy/>).

Multivariate differential abundance analysis

Multivariate differential abundance analysis, which tests for difference in relative abundance of microbial taxa between groups whilst accounting for the effect of more than one covariate, was implemented using MaAsLin2 (Mallick *et al.*, 2021). MaAsLin2 is a software which conducts multivariate analysis using linear modelling or linear mixed effect modelling and is suitable for cross-sectional comparisons as well as longitudinal data. It further allows covariate adjustments, as any given number of variables (categorically- or continuously-scaled) can be used as fixed effects. This makes the method superior to non-parametric tests, such as the Wilcox rank summary test, which cannot take covariate data into account.

MaAsLin2 offers a range of options for different data pre-processing including different data normalisations and transformations. Due to the nature of metagenomic datasets (skewed, many zeros, compositionality), data pre-processing is an essential step, especially when trying to fit linear models. Zeroes become problematic, especially at the genus- and species-level where many zeros are present (Nagarajan, 2018). In particular arcsine square root transformation (AST), suitable for data given in proportions or percent, is considered a variance-stabilizing data transformation well-equipped to handle zero data (De Muth, 2007).

I ran several combinations of pre-processing options by building 4 models – ‘model 1’: a) normalisation = none, b) transformation = none; ‘model 2’: a) normalisation = none, b) transformation = AST; ‘model 3’: a) normalisation = centred log-ratio (CLR), b) transformation = none; ‘model 4’: a) normalisation = none, b) transformation = LOG. I further opted to set the minimum prevalence to 0.1 (taxa with at least 10% of non-zero values are kept in the model) and the minimum abundance threshold to 0.0001 (includes only taxa which reach a minimum relative abundance of 0.01%). I then investigated the residuals for the significant taxa (those showing an association with genotype) and report on those findings for which the models fit the distribution of each of those taxa best.

I assessed the effect of genotype whilst accounting for age and sex for each taxonomic level running linear regression models in MaAsLin2, which was implemented in R using the package *MaAsLin2*. This was performed for each sampling time point individually. Linear mixed modelling, incorporating also ‘subject ID’ as random effect and ‘batch’ as fixed effect, was used for the combined datasets (T1, T2, T3).

Functional analysis

‘MicrobiomeAnalyst’ and R were used to implement the functional aspects of the data analysis. The Shotgun Data Profiling (SDP) functionality of the MicrobiomeAnalyst offers

a set of methods for pattern discovery and comparative analysis of gene abundance tables (Chong *et al.*, 2020). MicrobiomeAnalyst (<http://www.microbiomeanalyst.ca>) is a web-based program that incorporates a comprehensive suite of analysis and visualisation tools for different types of microbiome data, including 16S rRNA gene sequencing data and SDP (Dhariwal *et al.*, 2017; Chong *et al.*, 2020). The underlying R commands are displayed during each step and together with downloadable result tables this allows users to recreate or adjust analysis locally. A major limitation of MicrobiomeAnalyst, is the lack of functionality for repeated measures or time-series. I thus performed only cross-sectional comparisons within this platform and used R (particularly MaAsLin2) to investigate the data longitudinally and for differential multivariate analysis. An overview of the steps done within the MicrobiomeAnalyst workflow (prior to data analysis) are shown in Figure 2.5 and are described in detail in the supplementary (p.367-368).

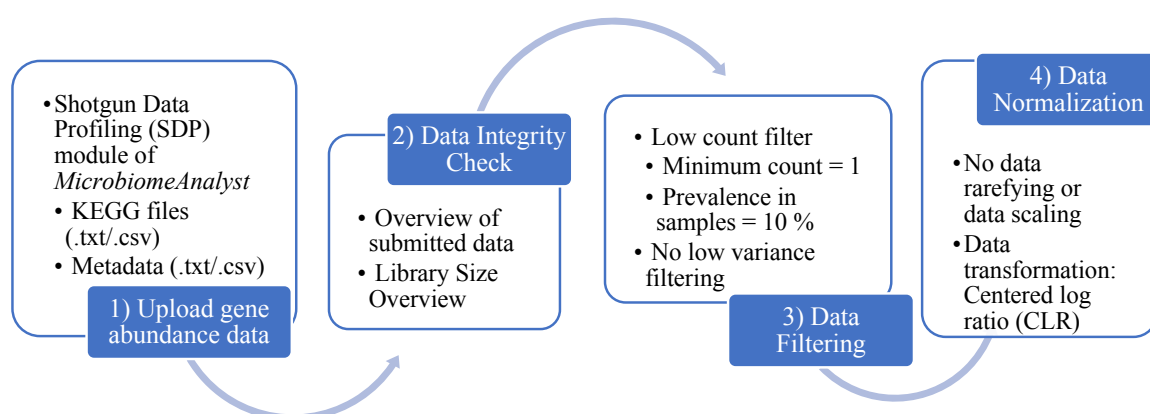


Figure 2.5 MicrobiomeAnalyst workflow of KEGG gene abundance data. Figure created by author

After data processing, the following analyses were implemented on the KEGG gene abundance and the relative abundance pathways data (Figure 2.6).

Graphical summary of Functional Diversity Profiles

An analysis overview tool was used to visualize the data with stacked area plots comparing the functional profiles between the two genetic risk groups. Multiple functional categories

visualization options are available, including KEGG metabolism, KEGG pathways, KEGG modules, which give different level of information and detail about the functional profiles. The stacked bar plots, recreated locally in R, help to visualise patterns of variation across different groups. The counts in the KEGG abundance table represent how often a KO (enzyme) was observed in a given sample, independent of how abundant the organism was that encoded for it. This data does not represent proper abundance counts. To make counts more comparable, I normalised the total hits (=counts) by the size of category (=how many enzymes/KOs are assigned to a given pathway) where possible.

Differential abundance analysis on KEGG gene abundance tables and predicted functional pathways

The normalized counts (but otherwise non-scaled or non-transformed counts) were transformed into relative values, so that they reflect the proportion of a specific KEGG metabolism/pathway/module category in a subject sample compared to the other KEGG categories in the same sample. This was done by summing the normalized counts per sample and dividing each KEGG category by this sample specific total number. Multivariate analysis was implemented using *MaAsLin2* in R (as detailed before). The aim was to explore possible significant associations between KEGG metabolism categories/pathways/modules and genetic risk whilst controlling for the effect of age and sex.

Multivariate abundance analysis on the HUMAnN3 data was carried out using *MaAsLin2* (as described before). I used unstratified and stratified relative abundance data on pathways which were generated with humann3. The stratified data shows pathway abundance per participant by the taxonomy in which a pathway was detected, whilst the unstratified data simply shows pathway abundance (in no particular order).

Beta diversity

Ordination and PERMANOVA. Ordination was performed on beta diversity (using Bray-Curtis and Euclidean distance) using NMDS and PCA. Statistical testing was carried out using PERMANOVA.

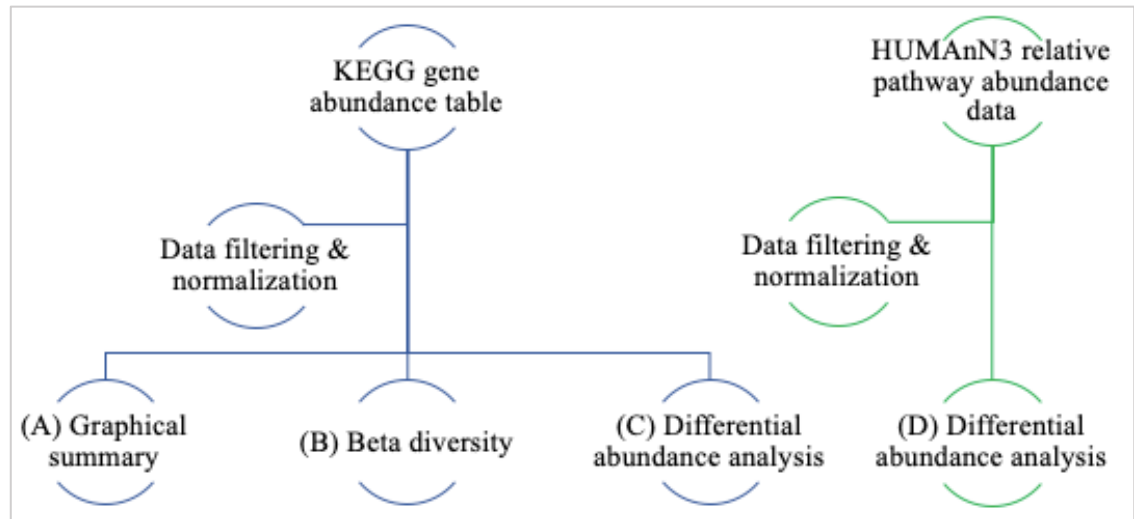


Figure 2.6 Overall workflow of predictive functional profiling and analysis of gene abundance data. Blue: KEGG-based analysis carried out using MicrobiomeAnalyst tool and R. Green: Analysis based on HUMANn3 relative abundance pathways, implemented in R. Figure created by author

CHAPTER 3: COGNITIVE, DIETARY AND HEALTH PROFILES

Participant recruitment, enrolment and study completion

A total of 306 individuals were identified between February and December 2018 via the aforementioned recruitment channels and screened for eligibility (see p.94). Of these, 241 potential participants passed the eligibility screening and were asked whether they would be interested in receiving further information about the study. Finally, 130 participants were consented for genetic screening and 82 of the consented participants were successfully enrolled into the study. The study recruitment process is schematically shown in Figure 3.1.

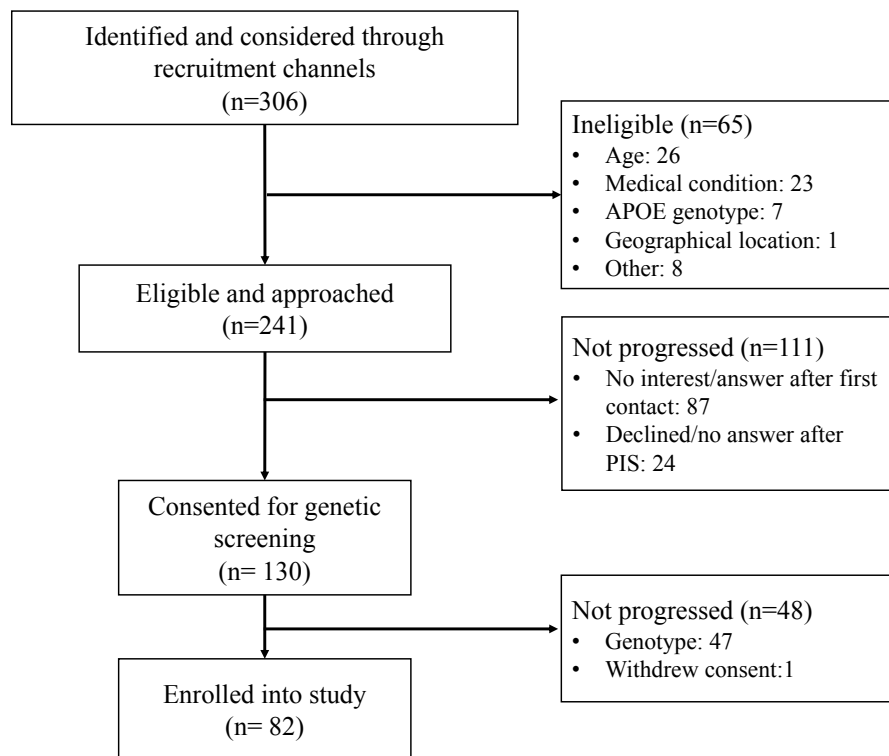


Figure 3.1 Flowchart of study recruitment process

All participants were stratified into APOE groups based on their APOε4 status – to make up the APOε4 non-carriers (n=41) and the APOε4 carriers (n=41) (Figure 3.2). Three participants withdrew from the study at this stage (due to anxiety, too much time commitment, other personal reasons). The baseline cognitive assessment and first faecal

sample collection was completed by 79 (96%) participants. One participant of the APOε4 carriers was excluded because of transient ischemic attack that occurred during the study and two APOε4 non-carriers withdrew before completing the second faecal sample, resulting in a total of 76 collected samples for T2 (93%). Two participants were unable to complete the third faecal sampling time point within the timeframe of this study due to repeated occurrence of antibiotic treatment which pushed their last sample collection past the study end date. The observed attrition of 10% is not inconsistent with other longitudinal studies.

The COVID-19 pandemic and associated lockdown of facilities led to an earlier than planned collection of the last follow-up samples of nine participants. To mitigate the closure of laboratories and to keep participants safe, I collected all outstanding samples by the 23rd of March and closed the study. A subgroup of 20 participants from each group underwent MRI imaging. The cardiovascular risk assessment was completed by 15 participants of the APOε4 non-carriers and 18 of the APOε4 carriers.

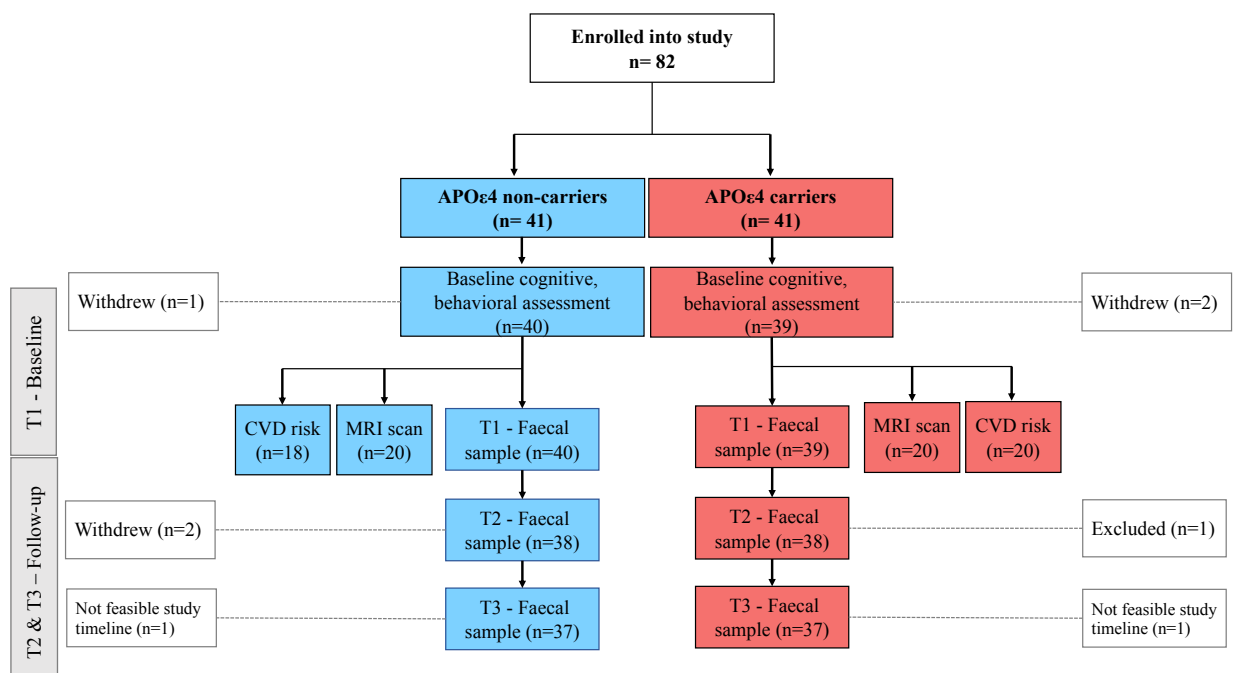


Figure 3.2 Consolidated Standards of Reporting Trials diagram showing the flow of participants through the study

Demographic characteristics of Apolipoprotein E groups

The most prevalent genotype in the APO ϵ 4 non-carrier group was ϵ 3/ ϵ 3, whilst ϵ 3/ ϵ 4 was the most common genotype among APO ϵ 4 carriers. Nine participants were ϵ 2/ ϵ 3 carriers and were assigned to the APO ϵ 4 non-carriers. Five participants of the APO ϵ 4 carriers were homozygous ϵ 4 carriers and were thus at the highest genetic risk for AD and assigned to the at-risk group. The APOE genotype frequency in the given study and assigned APO ϵ 4 status can be found in Table 3.1.

Table 3.1 Apolipoprotein E genotype frequency in participant cohort, genetic risk for developing Alzheimer’s Disease and assigned study group

Genotype	Cases (%)	Genetic risk	Study group
ϵ 2/ ϵ 2	0 (0)	low	APO ϵ 4 non-carriers
ϵ 2/ ϵ 3	9 (11)	low	APO ϵ 4 non-carriers
ϵ 3/ ϵ 3	32 (39)	low	APO ϵ 4 non-carriers
ϵ 3/ ϵ 4	36 (44)	high	APO ϵ 4 carriers
ϵ 4/ ϵ 4	5 (6)	high	APO ϵ 4 carriers

The mean age of the study participants at enrolment was 66.73 years of age (SD=5.93) in APO ϵ 4 non-carriers and 63.95 (SD=5.50) years of age in APO ϵ 4 carriers (Table 3.2). Both groups had a larger proportion of female compared to male participants. Educational attainment, defined as the highest completed level of education, was recorded as one of four categories: “no formal education”, “high school” (11 years), “college” (13 years), and “university” (16 years or more). The most frequently reported level of education in both groups was university level. Pearson's chi-squared test showed that the distribution of sex ($\chi^2=1.81$, $p>.1$) and educational attainment ($\chi^2=1.07$, $p>.1$) were not significantly different between the two groups. Three APO ϵ 4 carriers did not return information with respect to their educational attainment and are hence missing. Whilst the groups were not perfectly matched with respect to age, the age difference between the APOE groups was trending but not statistically significant (Wilcoxon rank sum test, $p=0.051$).

Table 3.2 Primary characteristics of the Apolipoprotein E groups

Measure	APOε4 non-carriers (n=40)	APOε4 carriers (n=39)	χ² (df)	p-value
Age (years)				
Mean (SD)	66.73 (5.93)	63.95 (5.50)	-	0.051
Sex				
Female (%)	25 (62.5%)	30 (78.9%)	1.81 (1)	>.1
Male (%)	15 (37.5%)	8 (21.1%)		
Educational attainment				
No formal education	0 (0%)	0 (0%)		
High school	9 (22.5%)	8 (21.1%)	1.07 (2)	>.1
College	12 (30%)	7 (18.4%)		
University	19 (47.5%)	20 (52.6%)		
missing	0 (0%)	3 (7.9%)		

Cognitive and behavioural results from administered tests

An overview of all neuropsychological test results showing the group means and standard deviations for each of the administered tests is shown in Table 3.3. Group differences were investigated by fitting a separate multiple regression model for each outcome measure and subscales using APOε4 status as predictor and controlling for age and educational attainment.

Table 3.3 Neuropsychological profile of the Apolipoprotein ε4 carriers and non-carriers

Measure	APOε4 non-carriers	APOε4 carriers
	Mean (SD) [n=39]	Mean (SD) [n=38]
ACE-III		
Summary score (/100)	95.30 (3.95)	95.34 (2.58)
Attention subscale (/18)	17.55 (0.93)	17.66 (0.85)
Memory subscale (/26)	25.03 (1.48)	25.08 (1.36)
Fluency subscale (/14)	12.35 (1.64)	12.39 (1.49)
Language subscale (/26)	24.93 (1.38)	25.21 (0.87)
Visuospatial subscale (/16)	15.45 (1.01)	15.00 (1.04)
	[n=39]	[n=38]
ROCF		
Copy score (/36)	31.39 (2.95)	31.95 (2.69)
Recall score (/36)	18.72 (5.45)	18.86 (5.29)
Copying time (/300, in sec)	162.51 (56.10)	188.34 (67.92)
	[n=38]	[n=37]
TMT		
TMT-A (sec)	34.92 (7.86)	33.62 (12.61)
TMT-B (sec)	71.16 (23.20)	62.78 (18.69)
TMT-d (TMT-B – -A, sec)	36.24 (22.39)	29.16 (16.02)

ACE=Addenbrooke's Cognitive Examination, ROCF=Rey-Osterrich-Complex-Figure test,

TMT = Trail Making Task

Addenbrooke's Cognitive Examination-III

In total, 79 study participants completed the ACE-III (for a detailed test description please see p.98). The summary ACE-III score ranged between 80-100 in the APO ϵ 4 non-carriers and 89-100 in the APO ϵ 4 carriers. In line with standard cut-offs, a score lower than 82 is used as a cut-off for dementia. One participant of the APO ϵ 4 non-carriers scored below 82 on the ACE-III and was excluded from the analysis. One participant record from the APO ϵ 4 carriers was excluded because of a transient ischemic attack. This resulted in a total of 77 neuropsychological tests. On average, participants scored high on the ACE. The APO ϵ 4 non-carriers had a mean summary score of 95.30 compared to 95.34 in the APO ϵ 4 carriers.

Effect of Apolipoprotein ϵ 4 status on Addenbrooke's Cognitive Examination-III

The ACE-III summary score ($F(4,69)=0.83$, $p>.1$, $R^2=0.17$) was not significantly predicted by APO ϵ 4 status when keeping the influence of all other predictors on the model equal (Table 7.6 in the supplementary). Our multivariate analyses, generated from running a separate model for each of the subscales of the ACE-III, showed no effect of APO ϵ 4 status on memory, fluency, or language. There was, however, a significant effect of APO ϵ 4 status ($\beta=-0.51$, $p=0.032$) on the visuospatial subscale ($F(4,69)=3.25$, $p=0.017$, $R^2=0.16$), indicating that the APO ϵ 4 carriers performed -0.51 points less well on the visuospatial aspects of the ACE-III compared to the APO ϵ 4 non-carriers. The model explained 16% of the variance observed in the data.

Rey-Osterrich-Complex-Figure test

The APOE cohorts obtained similar mean scores on the copy condition and lower but comparable mean scores on the recall condition (Table 3.3, for a detailed test description please see p.99-100). Four participants of the APO ϵ 4 carriers and two participants of the APO ϵ 4 non-carriers needed longer than the allowed maximal copying time of 300 seconds

(copying time recorded as 300 sec) for copying the ROCF. On average, the APO ϵ 4 non-carriers took 26 seconds less than the APO ϵ 4 carriers for copying the ROCF.

Effect of Apolipoprotein ϵ 4 status on Rey-Osterrich-Complex-Figure test

APO ϵ 4 status did not significantly predict ROCF copy score ($F(4,69)=1.62$, $p>.1$, $R^2=0.09$), recall score ($F(4,69)=0.86$, $p>.1$, $R^2=0.05$), or copy time ($F(4,69)=0.16$, $p>.1$, $R^2=0.01$) (Table 7.7 – 7.9 in the supplementary). Pearson product-moment correlation was calculated to explore the relationship between the three outcome variables by APO ϵ 4 status. There was a positive correlation of medium strength between copy score and recall score in the APO ϵ 4 carriers ($r=0.34$, $p=0.039$) but not in the APO ϵ 4 non-carriers. None of the other ROCF performance measures were correlated (Table 7.10 in the supplementary).

Trail Making Task

As explained in Chapter 2, scores of the TMT denote the time (in seconds) taken to complete part A (TMT-A) and part B (TMT-B) of the task (for a detailed test description please see p.100-101). The difference score, TMT-d, was calculated by subtracting the TMT-A score from the TMT-B score. Participants of the APO ϵ 4 carrier group performed similarly well on the TMT-A but were faster when completing TMT-B, compared to the APO ϵ 4 non-carriers. Whilst errors don't affect the overall score, they were also reported as per task protocol. Overall participants of both groups made errors infrequently during the TMT. The group means for errors combined from both parts are 0.42 (SD=0.76) and 0.32 (SD=0.63) in the APO ϵ 4 non-carriers and APO ϵ 4 carriers, respectively.

Effect of Apolipoprotein ϵ 4 status on Trail Making Test

There was no effect of APO ϵ 4 status on TMT-A ($F(4,67)=1.99$, $p>.1$, $R^2=0.11$) or TMT-B ($F(4,67)=3.64$, $p=0.51$, $R^2=0.01$) performance (Table 7.11 – 7.12 in the supplementary). Nor did I find an effect of APO ϵ 4 status on the difference score, TMT-d, ($F(4,67)=2.894$, $p=0.03$, $R^2=0.15$).

Supermarket Task

Descriptive performance scores of the Supermarket Task is presented in Table 3.4 (for a detailed test description please see p.104-105). The results of the multilevel mixed regression models conducted to investigate the effect of APO ϵ 4 status with age, sex, and educational attainment as covariates on egocentric orientation, allocentric orientation, heading direction and peripheral responses are summarized in the following and presented in Table 7.13 in the supplementary.

Table 3.4 Effect of Apolipoprotein ϵ 4 status on Supermarket Task performance

Measure	APO ϵ 4 non-carriers	APO ϵ 4 carriers
	Mean (SD)	Mean (SD)
	[n=37]	[n=36]
Egocentric orientation	9.22 (3.8)	10.72 (3.3)
	[n=34]	[n=35]
Allocentric orientation	30.91 (13.0)	28.77 (9.6)
	[n=34]	[n=35]
Heading direction	11.44 (3.0)	11.54 (1.9)
	[n=33]	[n=34]
Central vs peripheral navigation preference	0.67 (0.5)	1.56 (1.7)

Egocentric orientation: number of correct responses out of 14 trials, Allocentric orientation: displacement from correct location in mm, Heading direction: number of correct responses out of 14 trials, Central vs navigation preference: N(central response)/ N(peripheral response)

Effect of Apolipoprotein ϵ 4 status on the Supermarket Task

Neither egocentric orientation, allocentric orientation, nor heading direction were significantly predicted by APO ϵ 4 status. Only navigation preference (central vs peripheral navigation preference) showed a significant main effect of APO ϵ 4 status ($\beta=0.61$, $p=0.045$), indicating that APO ϵ 4 non-carriers favoured navigating closer to the boundaries of the virtual Supermarket (see Figure 3.3).

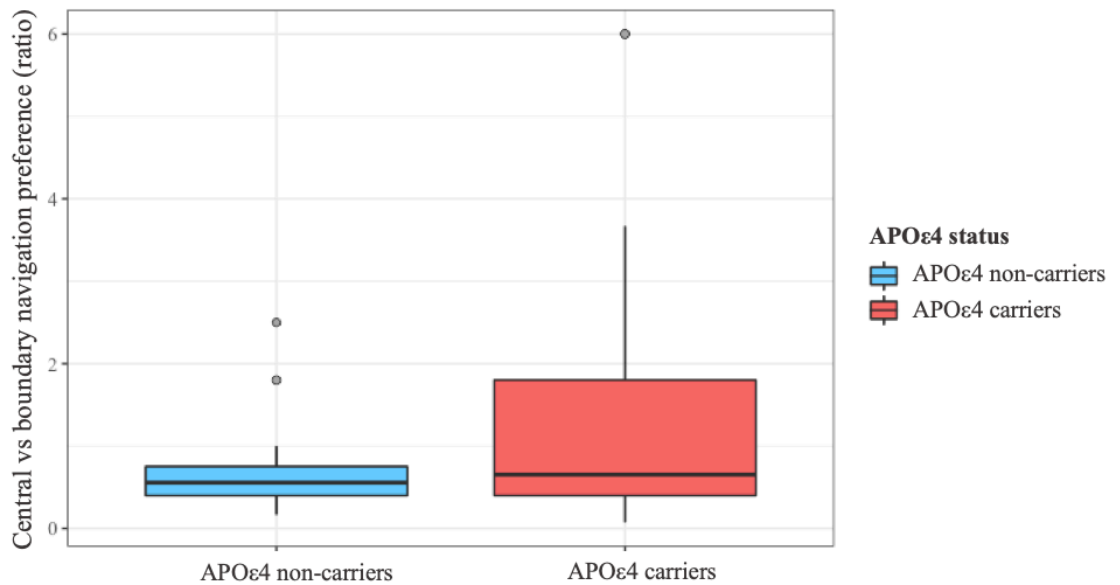


Figure 3.3 Boxplot of “Central vs boundary navigation preference” ratio by Apolipoprotein ε4 status

Sea Hero Quest

The demographics questionnaire, accompanying the SHQ task, showed that participants in the given study were comparable with respect to their handedness, daily travel time, self-perceived ability to navigate, sleep, upbringing environment, and activity level (non-significant Pearson-chi squared test). For a detailed test description please see p.103-104.

Wayfinding measures

As outlined in Chapter 2, the SHQ has two types of levels: wayfinding levels and flare levels. The three outcome variables of wayfinding levels are distance, duration and distance to border. The means for wayfinding distance (in pixels), duration (in seconds), and distance to border (in pixels) per level by APOε4 status are shown in Table 3.5. Higher values of wayfinding distance and duration indicate poorer performance, whilst higher level of distance to border indicates better performance.

I examined the relationship between these variables using Pearson correlation test, which showed a positive correlation between distance and duration ($r=0.86, p<0.001$). This means

that the further participants travel, the longer they needed to complete the level. I also found a negative correlation between distance and distance to border ($r=-0.64$, $p<0.001$), as well as duration and distance to border ($r=-0.58$, $p<0.001$). These results indicate that as participants navigated further away from the map borders (more centrally), both the distance travelled, and the time spent to complete the level was shorter.

On average, participants covered more distance and took longer with increasing level of difficulty. Interestingly, the distance to border was much smaller for both groups in level 11. This indicates that participants navigated closer to the game borders in the most difficult wayfinding level.

Table 3.5 Wayfinding performance by Apolipoprotein $\epsilon 4$ status and task level

Performance variable	APO $\epsilon 4$ non-carriers (n=38)	APO $\epsilon 4$ carriers (n=38)
Mean wayfinding distance (SD)		
Level 06	0.88 (0.46)	0.76 (0.35)
Level 08	1.53 (0.53)	1.67 (0.53)
Level 11*	2.28 (1.01)	2.53 (1.24)
Mean wayfinding duration (SD)		
Level 06	1.02 (0.74)	0.85 (0.40)
Level 08	1.73 (0.87)	1.98 (0.86)
Level 11*	2.68 (1.35)	3.38 (2.47)
Mean wayfinding distance to border (SD)		
Level 06	20.65 (4.14)	20.52 (3.73)
Level 08	18.71 (4.18)	18.96 (3.86)
Level 11*	5.79 (1.30)	5.55 (0.94)

*Level 11: missing 3 cases (APO $\epsilon 4$ non-carriers: n=36, carriers: n=37)

Effect of Apolipoprotein $\epsilon 4$ status on wayfinding distance

Our overall multilevel mixed model showed that there was no effect of APO $\epsilon 4$ status ($\beta=-0.00$, $p>.1$, Table 7.14 in the supplementary) on wayfinding distance. I further split the data

by level and ran 3 separate multilevel mixed models in order to investigate the effect of APO ϵ 4 status on wayfinding distance at each individual wayfinding level whilst controlling for age, sex and educational attainment. These models further corroborated the previous finding, as I found no effect of APO ϵ 4 status for either of the level-specific data.

Effect of other predictors on wayfinding distance

Wayfinding distance was significantly predicted by age ($\beta=-0.01$, $p=0.017$) and level ID ([level 8] $\beta=-0.76$, $p<0.001$, [level 11] $\beta=-0.95$, $p<0.001$). The fixed effects of the model accounted for 63% of the variance in the data. The results indicate that distance travelled increased by 1 pixel with every one-year age increment. When comparing the more difficult levels, level 08 and level 11, to level 06, participants travelled a further 76 and 95 pixels, respectively. The level-specific models showed that age was a mildly significant predictor of wayfinding distance at level 06 ($\beta=-0.02$, $p=0.048$). This result indicates that age has a negative effect on wayfinding performance at the easiest wayfinding level, as participants travelled longer distance to complete the level. Neither, sex, nor educational attainment significantly predicted wayfinding distance for any of the levels.

Effect of Apolipoprotein ϵ 4 status on wayfinding duration

APO ϵ 4 status did not significantly predict wayfinding duration when investigating the combined data of all levels ($\beta=0.08$, $p=0.09$, Table 7.15 in the supplementary) or when looking at each individual level separately whilst controlling for age, sex and educational attainment.

Effect of other predictors on wayfinding duration

Wayfinding duration was significantly predicted by age ($\beta=0.01$, $p=0.001$), sex ($\beta=-0.15$, $p=0.005$) and level ID ([level 08] $\beta=0.39$, $p<0.001$, [level 11] $\beta=0.71$, $p<0.001$). ($\beta=0.08$, $p=0.09$). The fixed part of the model explained 55.6% of the variance observed in the data. On average, participants required one more second per one-year increment of age to

complete the levels. Male participants were 15 seconds faster than their female counterparts during wayfinding. Participants took 39 seconds and 1 min 11 seconds longer compared to level 06 to complete levels 08 and 11, respectively.

Our analysis from the individual level data, also showed an effect of age on wayfinding duration (level 06: $\beta=0.10$, $p=0.04$, level 08: $\beta=0.01$, $p=0.04$, level 11: $\beta=0.02$, $p=0.02$). The results indicate that participants needed longer to complete the levels with every one-year age increment. And this effect was greatest at level 06, with participants taking 10 seconds longer to complete the level with every one-year age increment. An effect of sex was observed only at the more difficult two levels (level 08: $\beta=-0.16$, $p=0.04$, level 11: $\beta=-0.24$, $p=0.02$) and was most pronounced at level 11, indicating a faster level completion of male participants compared to females on the more complex levels. There was no effect of educational attainment on wayfinding duration.

Effect of Apolipoprotein $\epsilon 4$ status on wayfinding distance to border

There was no effect of APO $\epsilon 4$ status on the distance to border outcome variable when investigating all wayfinding levels ($\beta=-0.10$, $p>.1$, Table 7.16 in the supplementary) or when looking at each level individually.

Effect of other predictors on wayfinding distance to border

Only sex ($\beta=1.29$, $p=0.02$) and level ID ([level 08] $\beta=-1.67$, $p=0.001$, [level 11] $\beta=-15.01$, $p<0.001$) significantly predicted the outcome measure. This suggests that male participants navigated significantly more centrally (1.29 greater distance to border) compared to female participants, which is an indication of better navigation performance. When looking at each level individually, sex was only found to predict distance to border at level 08 ($\beta=2.15$, $p=0.04$). The distance to border further decreased as a function of increasing difficulty level. Showing that participants tended to navigate significantly closer along the level borders of the game in the more difficult levels of the game. This was particularly true for the most

difficult level, which saw the greatest reduction (-15.01 pixels) in distance to border compared to level 06. Fixed effects explained 83.5% of the variance in the data.

Path integration measured by flare accuracy levels

The frequencies of flare accuracy by APOε4 status are displayed in Table 3.6. Person-chi-squared test showed that there was only a significantly different distribution of flare accuracy between the APOε4-cohorts at level 54 ($\chi^2=7.18$, $p=0.028$).

Table 3.6 Response frequencies of flare accuracy rates by Apolipoprotein ε4 status, frequency distribution Pearson-chi-squared test (χ^2)

Performance variable	APOε4 non-carriers	APOε4 carriers	χ^2 (df)	p-value
Level 04	[n= 33]	[n = 25]		
Accuracy 1 counts (%)	0 (0)	2 (8)		
Accuracy 2 counts (%)	10 (30.3)	5 (20)	3.23 (2)	0.20
Accuracy 3 counts (%)	23 (69.7)	18 (72)		
Level 34	[n= 36]	[n= 38]		
Accuracy 1 counts (%)	8 (22.2)	7 (18.4)		
Accuracy 2 counts (%)	8 (22.2)	7 (18.4)	0.44 (2)	0.80
Accuracy 3 counts (%)	20 (55.6)	24 (63.2)		
Level 49	[n= 33]	[n= 37]		
Accuracy 1 counts (%)	9 (27.3)	18 (48.6)		
Accuracy 2 counts (%)	9 (27.3)	6 (16.2)	3.52 (2)	0.17
Accuracy 3 counts (%)	15 (45.5)	13 (35.1)		
Level 54	[n= 34]	[n= 36]		
Accuracy 1 counts (%)	13 (38.2)	7 (19.4)		
Accuracy 2 counts (%)	3 (8.8)	12 (33.3)	7.18 (2)	0.028*
Accuracy 3 counts (%)	8 (52.9)	17 (47.2)		

* $p<0.05$

Effect of Apolipoprotein ε4 status on flare accuracy

The mixed effect ordinal logistic regression showed that there was no effect of APOε4 status on flare accuracy for the overall dataset ($\beta=0.01$, $p>.1$, Table 7.17 in the supplementary), nor when evaluating individual level data

Effect of other predictors

I found that sex ($\beta=0.69, p=0.036$) was a significant predictor of flare accuracy, suggesting that male participants had a better flare accuracy rate. This was further substantiated by an odds ratio of 2.01 (males are twice as likely than women to perform well on flare accuracy). Level ID significantly contributed to explaining variance in the observed flare accuracy rate and this was true for level 49 ($\beta=-0.1.63, p<0.001$) and level 54 ($\beta=-1.23, p=0.004$) also. Both levels indicate a decreased performance on flare accuracy (which might be suggestive of higher difficulty [double “right turn”]). Fixed predictors explained 12.7% of variance in the data (Marginal R^2), whilst fixed and random effects taken together (Conditional R^2) explained 19.5% of variance. Analysis by level showed an effect for sex ($\beta=1.63, p=0.009$) at level 54 only, indicating a better performance of male participants. At level 49, the time needed to complete the level was a significant predictor of the model ($\beta=0.08, p=0.011$).

Cognitive and behavioural results from questionnaires

Mean summary scores and standard deviations of all self-reported cognitive and behavioural measures assessed in the given study are presented in Table 3.7 and explained in more detail in the following. As before, group differences with respect to APOε4 status were assessed by means of multivariate linear models, whilst accounting for the effects of age and educational attainment.

Table 3.7 Secondary neuropsychological profile of the Apolipoprotein E groups

Self-reported measure	APOε4 non-carriers (n=39)	APOε4 carriers (n=38)
CCI (missing n=5)		
Summary score	27.62 (7.87)	28.70 (7.27)
Memory subscore	1.49 (0.46)	1.61 (0.46)
Executive function subscore	1.17 (0.43)	1.17 (0.38)
Language subscore	1.31 (0.47)	1.20 (0.32)
GAD-7 (/21) (missing n=2)		
	0.87 (1.64)	0.92 (1.52)
PHQ-9 (/27)		
	1.85 (3.08)	1.94 (2.16)
CBI-R (missing n=4)		
Summary score	4.90 (5.46)	3.09 (2.67)
Memory subscore	7.15 (8.16)	6.18 (7.08)
Self-care subscore	0 (0)	0 (0)
Abnormal behaviour subscore	2.87 (5.03)	1.71 (3.26)
Everyday skills subscore	0.77 (3.54)	0.15 (0.86)
Belief subscore	0.21 (1.28)	0 (0)
Eating habits subscore	3.54 (7.72)	2.00 (5.49)
Sleep subscore	21.08 (20.56)	14.18 (16.27)
Stereotypic behaviour & motor abilities subscore	3.05 (7.56)	0.53 (1.73)
Motivation subscore	4.10 (8.50)	1.47 (3.99)

CCI = Cognitive Change Index, CBI-R = Cambridge Behaviour Inventory Revised, GAD-7 = Generalized Anxiety Disorder-7, PHQ-9=Patient Health Questionnaire-9

Cognitive Change Index

The self-reported change in cognition was low in both cohorts (for a detailed test description please see p.105). There was no effect of APOε4 status on the CCI summary score ($F(4,64)=0.14$, $p>.1$, $R^2=0.01$) (Table 7.18 in the supplementary), the memory subscale ($F(4,64)=0.29$, $p=>.1$, $R^2=0.02$), the executive function subscale ($F(4,64)=0.95$, $p>.1$, $R^2=0.06$), or the language subscale ($F(4,64)=0.43$, $p>.1$, $R^2=0.03$), which means that overall there was no subjective memory difference between the groups.

Generalized Anxiety Disorder-7

The vast majority of participants in the APOε4 non-carriers (97.4%) and in the APOε4-positive group (94.4%) had a GAD-7 score of ≤ 4 and are thus considered to experience no anxiety (for a detailed test description please see p.107). Only one participant of the APOε4 non-carriers and two participants of the APOε4 carriers experienced mild anxiety. APOε4 status did not significantly predict GAD-7 ($F(4,60)=1.24$, $p=0.09$, $R^2=0.12$) (Table 7.19 – 7.20 in the supplementary).

Patient Health Questionnaire-9

87.2% of participants in the APOε4 non-carriers and 80.6% in the APOε4 carrier group showed no signs of depression as measured by the PHQ-9 questionnaire (for a detailed test description please see p.108). Only one participant reported moderately severe depression levels. Pearson's Chi-squared test showed that the frequency distribution of the PHQ-9 scores was not statistically different between the groups (Table 7.21 in the supplementary). The multiple linear regression model ($F(4,65)=0.95$, $p>.1$, $R^2=0.06$) showed that there was no effect of APOε4 status on depression levels (Table 7.22 in the supplementary).

Cambridge Behavioural Inventory-Revised

The APOε4 non-carriers had higher mean scores in all subscales of the CBI-R than the APOε4 carriers (for a detailed test description please see p.106-107). Multiple linear regression models were used to individually assess the effect of APOε4 status, age and educational attainment on the CBI-R summary score (Table 7.23 in the supplementary) and its ten subdomain frequency scores. There was a significant main effect of APOE status ($\beta=-2.25, p=0.043$) on the summary CBI-R frequency score, which suggests that APOε4 carriers experienced behavioural and functional changes less frequently compared to the APOε4 non-carriers. This effect was likely driven by significant group difference on the motivation subdomain frequency score ($F(4,65)=2.264, p=0.07, R^2=0.21; \beta=-3.38, p=0.047$), which was found to be significantly lower in APOε4 carriers. The motivation subdomain was also significantly predicted by age ($\beta=-0.37, p=0.012$), indicating that changes in motivation also occur less frequently with increasing age. Another multiple regression model returned a significant age x APOε4 status interaction ($F(5,64)=3.342, p=0.01, R^2=0.21; \beta=0.72, p=0.011$) indicating different impact of age on CBI-R motivation between APOε4 non-carriers and APOε4 carriers. Upon visualizing this interaction, Figure 3.4, it showed that motivation changes occur less frequently with increasing age in the APOε4 non-carriers, whilst the APOε4 carriers shows a slight increase in motivation changes with increasing age (opposite trends). It is to be noted that changes in functional and behavioural domains were quantitatively small across all participants, as is reflected by the low mean scores in Table 3.7. None of the other subscales showed a significant association with APOε4 status.

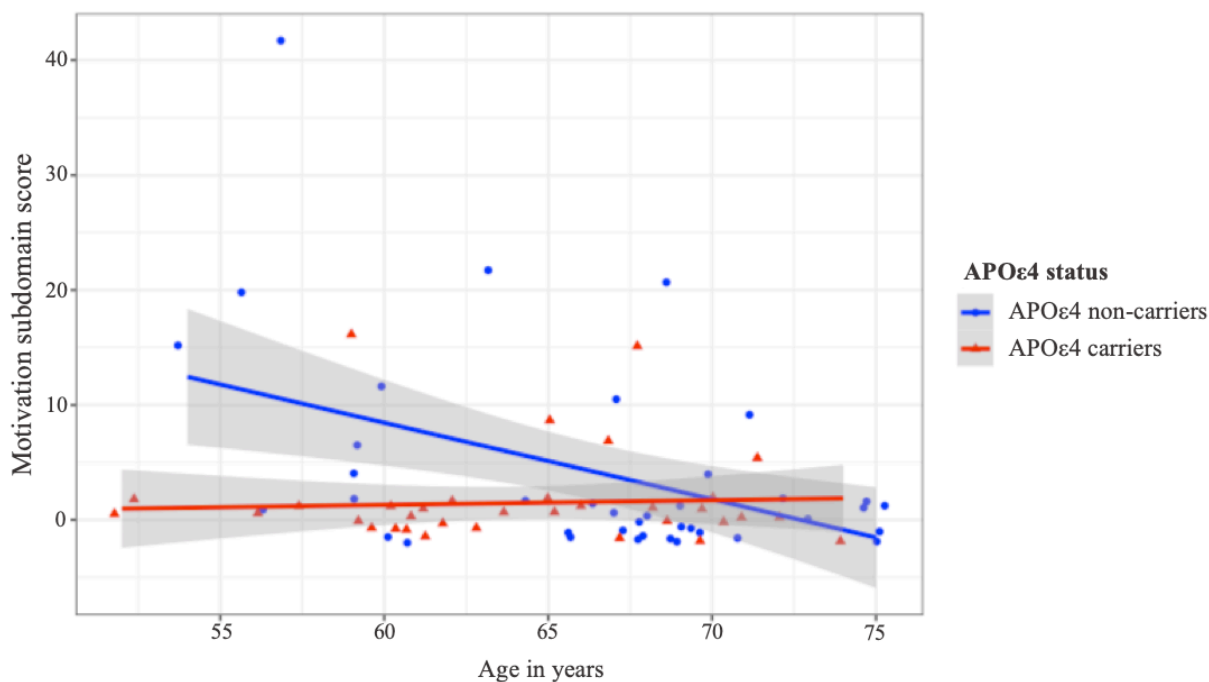


Figure 3.4 Scatterplot with line of best fit showing age*motivation subdomain score interaction

There was also an effect of age on the frequency score of the following three subdomains: mood ($F(4,65)=1.71$, $p>.1$, $R^2=0.10$; age: $\beta=-0.37$, $p=0.026$), beliefs ($F(4,65)=3.04$, $p>.1$, $R^2=0.09$; age: $\beta=-0.04$, $p=0.041$), and eating habits ($F(4,65)=2.17$, $p=.08$, $R^2=.12$; age: $\beta=-0.30$, $p=0.035$). Results indicate more functional and behavioural changes occur with respect to motivation, beliefs and eating habits with increasing age across all participants.

Dietary, cardiovascular and general health data

Food Frequency Questionnaire

As described in the methods, outlier detection was based on the self-reported mean daily energy intake (for a detailed test description please see p.111-112). Following this process, one female participant of the APOε4 non-carriers who self-reported intake was calculated to equal a daily energy intake of 4,755 kcal was excluded from the analysis.

Multiple linear regression was used to investigate the effect of APOε4 status on the different nutrients and food groups. Only one nutrient group showed a significant effect of APOε4 status ($\beta=-0.41$, $p=0.010$), namely carbohydrate galactose ($F(1,70)=7.11$, $p=0.01$, $R^2=0.09$), indicating the consumption of carbohydrate galactose among APOε4-carriers was on average -0.41g lower over the year than that of APOε4 non-carriers.

It is to be noted that standard deviations from the mean intake were large with respect to many nutrient recordings. All results for the 46 nutrients and 14 food groups are summarized in Table 3.8 and 3.9 below, respectively.

Table 3.8 Average daily intake and standard deviation of nutrients

Nutrients	APOε4 non-carriers	APOε4 carriers
	(n=38) Mean ± SD	(n =33) Mean ± SD
α-Carotene (mcg)	591.0 ± 500.0	611.1 ± 530.0
Alcohol (g)	9.1 ± 9.7	8.7 ± 12.8
β-Carotene (mcg)	3987.5 ± 2775.5	3867.1 ± 2237.0
Calcium (mg)	880.9 ± 249.8	805.1 ± 233.5
Carotene total carotene equivalents (mcg)	4490.2 ± 3063.3	4376.8 ± 2495.2
Carbohydrate (g)	194.3 ± 65.3	190.1 ± 45.8
Cholesterol (mg)	238.4 ± 95.4	226.0 ± 101.2
Chloride (mg)	3828.0 ± 1243.9	3709.1 ± 1027.5
Copper (mg)	1.2 ± 0.5	1.18 ± 0.4
Englyst Fibre Non-Starch Polysaccharides (g)	18.5 ± 7.1	18.5 ± 6.0
Iron (mg)	10.9 ± 3.1	11.0 ± 2.7
Total folate (mcg)	318.3 ± 111.6	305.1 ± 74
Carbohydrate fructose (g)	24.7 ± 11.4	23.1 ± 9.3
Carbohydrate galactose (g)	0.86 ± 0.74	0.46 ± 0.52
Carbohydrate glucose (g)	21.5 ± 9.9	20.7 ± 8.0
Iodine (mcg)	142.6 ± 51.6	134.7 ± 45.7
Potassium (mg)	3717.5 ± 1038.1	3526.6 ± 784.9
Energy (kcal)	1738.6 ± 553.0	1618.1 ± 397.3
Energy (kj)	7306.4 ± 2314.5	6809.4 ± 1663.1
Carbohydrate lactose (g)	15.8 ± 7.9	15.0 ± 8.2
Carbohydrate maltose (g)	1.8 ± 1.3	1.6 ± 1.0
Magnesium (mg)	337.5 ± 103.8	318.6 ± 75.5
Manganese (mg)	3.8 ± 1.5	3.5 ± 1.2
Sodium (mg)	2536.6 ± 826.0	2456.3 ± 694.3
Niacin (mg)	21.8 ± 6.7	21.3 ± 5.8
Phosphorus (mg)	1329.6 ± 348.4	1275.1 ± 300.9
Protein (g)	72.6 ± 18.2	71.2 ± 18.4
Vitamin A retinol (mcg)	487.5 ± 433.3	495.7 ± 503.2
Vitamin A retinol equivalents (mcg)	1250.0 ± 717.6	1235.4 ± 609.2
Vitamin B2 riboflavin (mg)	2.0 ± 0.7	1.8 ± 0.6
Selenium (mcg)	55.1 ± 19.3	57.1 ± 15.6
Carbohydrate starch (g)	83.4 ± 37.1	86.5 ± 24.1
Carbohydrate sucrose (g)	39.1 ± 17.7	36.2 ± 15.1
Vitamin B1 Thiamin (mg)	1.5 ± 0.4	1.4 ± 0.3
Nitrogen (g)	11.8 ± 2.9	11.5 ± 2.9
Carbohydrate sugars total (g)	106.2 ± 40.4	99.5 ± 30.2
Vitamin B12 Cobalamin (g)	6.0 ± 3.2	6.3 ± 3.0
Vitamin B6 Pyridoxine (mg)	2.2 ± 0.6	2.2 ± 0.6
Vitamin C Ascorbic acid (mg)	136.4 ± 63.9	128.7 ± 56.8
Vitamin D Ergocalciferol (mcg)	2.8 ± 1.7	2.7 ± 1.6
Vitamin E Alpha Tocopherol equivalents (mg)	13.5 ± 5.8	11.6 ± 3.4
Zinc (mg)	8.3 ± 2.2	8.4 ± 2.2
Fat total (g)	73.1 ± 34.0	62.4 ± 22.1
Monounsaturated-fatty-acids total (g)	27.0 ± 16.0	22.6 ± 8.6
Polyunsaturated-fatty-acids total (g)	14.5 ± 6.5	12.1 ± 4.4
Saturated fatty-acids total (g)	25.5 ± 11.9	22.3 ± 9.7

Table 3.9 Average daily intake and standard deviation of food groups

Nutrients	APOε4 non-carriers	APOε4 carriers
	n=38 Mean ± SD	n =33 Mean ± SD
Alcoholic beverages	135.1 ± 162.2	125.5 ± 198.5
Cereals and cereal products (g)	191.8 ± 108.2	195.2 ± 72.6
Eggs and egg dishes (g)	21.2 ± 17.4	20.9 ± 13.8
Fats and oils (g)	19.9 ± 13.80	14.4 ± 9.2
Fish and fish products (g)	41.8 ± 31.6	45.5 ± 26.3
Fruit (g)	282.8 ± 177.6	288.3 ± 240.9
Meat and meat products (g)	65.3 ± 44.3	75.1 ± 53.2
Milk and milk products (g)	347.0 ± 158.4	314.6 ± 153.7
Non-alcoholic beverages (g)	948.4 ± 442.5	807.1 ± 393.8
Nuts and seeds (g)	18.3 ± 31.1	11.5 ± 13.3
Potatoes (g)	73.5 ± 39.1	67.8 ± 35.3
Soups and sauces (g)	72.2 ± 53.3	83.3 ± 66.9
Sugars, preserves and snacks (g)	29.7 ± 23.1	32.9 ± 31.6
Vegetables (g)	322.8 ± 196.7	304.2 ± 130.6

Microbiome Health Questionnaire

The main purpose of this extensive self-reported questionnaire, as described in the methods chapter, was to characterize the study population and gain metadata which could explain variability in the microbiome data (for a detailed test description please see p.108-109). All the results are given in Table 7.24 in the supplementary. Pearson Chi-squared test was nonsignificant for all questions, indicating that there was no significant difference in the answer distribution between the APOE groups. The majority of participants classed their diet as omnivores, all participants are Caucasian, and two thirds live in the countryside.

Cardiovascular Risk

All participants who completed the cardiovascular risk assessment (for a detailed test description please see p.109-110) were of Caucasian ethnicity and over 60% in the APOε4 non-carriers and 66.7% in the APOε4 carrier subgroups were female. No participant had diabetes, chronic kidney disease, rheumatoid arthritis or systemic lupus erythematosus. The majority of participants were non-smokers. 20% in the low and 16.7% in the APOε4 carrier subgroup reported a family history (first degree relative) of angina or heart attack. A third

of participants in both groups were on blood pressure medication, but no participant took steroid tablets regularly.

Table 3.10 Demographic information and clinical variables of the QRISK®3 risk prediction model by Apolipoprotein ε4 status

QRisk®3 clinical variables	APOε4 non-carriers (n=15) Count (%)	APOε4 carriers (n=18) Count (%)	χ² (df)	p-value
Sex				
Female	9 (60%)	12 (66.7%)	0.00 (1)	0.97
Male	6 (40%)	6 (33.3%)		
Ethnicity				
Caucasian	15 (100%)	18 (100%)	0.27 (1)	0.60
Smoking status				
non-smoker	11(73.3%)	16 (88.9%)	0.49 (1)	0.48
ex-smoker	4 (26.7%)	2 (11.1%)		
Diabetes	0 (0%)	0 (0%)	0.27 (1)	0.60
Angina or heart attack in first degree relative	3 (20%)	3 (16.7%)	0.00 (1)	1
Chronic kidney disease	0 (0%)	0 (0%)	0.27 (1)	0.60
Atrial fibrillation	0 (0%)	1 (6%)	0.00 (1)	1
On blood pressure medication	5 (33.3%)	6 (33.3%)	0.00 (1)	1
Migraines	1 (7%)	4 (22.2%)	0.57 (1)	0.45
Rheumatoid arthritis	0 (0%)	0 (0%)	0.27 (1)	0.60
Systemic lupus erythematosus	0 (0%)	0 (0%)	0.27 (1)	0.60
Severe mental illness	0 (0%)	0 (0%)	0.00 (1)	1
Atypical antipsychotic medication	0 (0%)	0 (0%)	0.27 (1)	0.60
On regular steroid tablets	0 (0%)	0 (0%)	0.27 (1)	0.60
Erectile dysfunction				
present	0 (0%)	1 (6%)		
not present	6 (40%)	5 (27.8%)	1.26 (1)	0.53
not applicable	9 (60%)	12 (66.7%)		
Clinical measures	APOε4 non-carriers (n=15) Mean (SD)	APOε4 carriers (n=18) Mean (SD)		
BMI (kg/m ²)	25.93 (3.9)	26.02 (5.8)		
Total Cholesterol (mmol/L)	5.79 (1.27)	7.04 (1.44)		
HDL (mmol/L)	1.89 (0.49)	1.89 (0.44)		
LDL (mmol/L)	2.50 (1.06)	4.04 (1.42)		
Cholesterol/HDL	3.30 (0.83)	4.17 (1.30)		
Triglycerides (mmol/L)	3.26 (1.02)	2.51 (1.10)		
Systolic blood pressure	136.47 (13.88)	139.22 (17.78)		

Effect of Apolipoprotein $\epsilon 4$ status on clinical measures of the QRisk®3

I ran several multiple regression models to investigate the effect of APO $\epsilon 4$ status on the clinical measures that were obtained including BMI, total cholesterol, HDL, LDL, Triglycerides, whilst accounting for the effect of age and sex. Our analyses showed that there was a significant effect of APO $\epsilon 4$ status ($\beta=1.93, p=0.005$) on LDL levels ($F(3,21)=3.365, p=0.038, R^2=0.325$) with the model explaining 32.5% of the variance in the data. APO $\epsilon 4$ status ($\beta=1.42, p=0.019$) also significantly predicted total cholesterol levels ($F(3,28)=2.395, p=0.089, R^2=0.204$). The model suggests that APO $\epsilon 4$ carriers had a 1.93 mmol/L significantly increased average LDL (Figure 3.5 [A]) and a 1.42 mmol/L significantly higher total cholesterol (Figure 3.5 [B]) compared to the APO $\epsilon 4$ non-carriers. There was no effect of APO $\epsilon 4$ status on HDL levels ($\beta=-0.07, p>.1$) or on Triglycerides ($\beta=-0.85, p=0.08$) (Tables 7.25 – 7.26 in the supplementary).

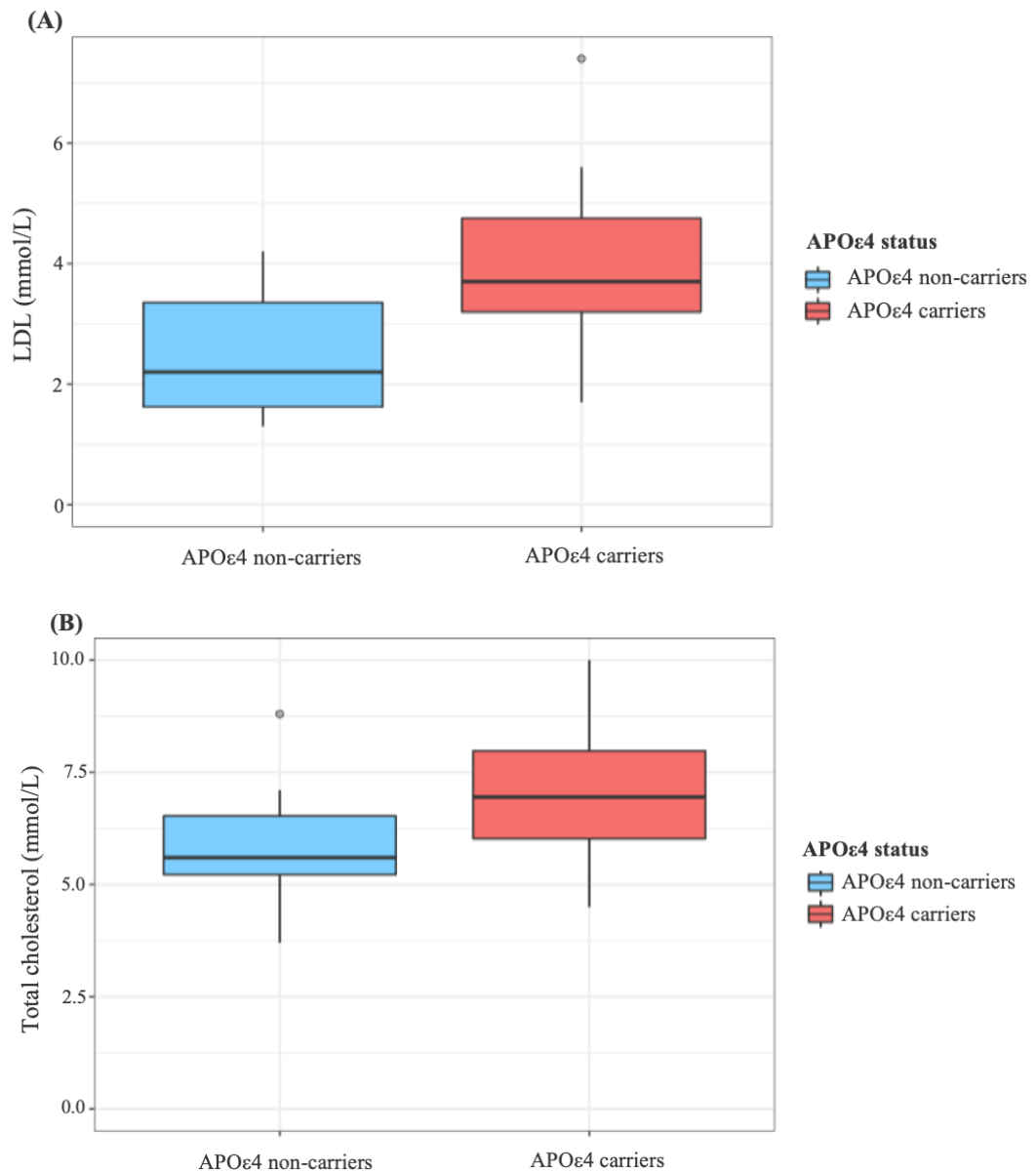


Figure 3.5 Boxplot of (A) low-density lipoprotein levels and (B) total cholesterol levels by Apolipoprotein ε4 status

In this subsample, the 10-year QRISK[®]3 score was 16.51 (SD=5.7) and 14.58 (SD=10.35) in the APOε4 non-carrier and carriers, respectively. The relative risk in the APOε4 non-carriers was 1.07 (SD=0.25) and 1.35 (SD=0.49) in the APOε4 carriers. 40% of non-carriers had a relative risk smaller than 1, indicating that they were less likely to experience a cardiovascular event in the next 10 years compared to a group of matched healthy individuals. In the APOε4 carriers only 11% had a relative risk below 1. 53% and 78% in the APOε4 non-carriers and APOε4 carriers, respectively, were however at a greater risk (relative risk>1) to have a cardiovascular event compared against matched healthy

individuals. A similar picture emerged after closer investigation of heart age, with 60% in the APOε4 non-carriers and 78% in APOε4 carriers having a heart age that is greater than their actual age.

Table 3.11 QRISK[®]3 risk scores by Apolipoprotein ε4 status

Calculated cardiovascular risk scores	APOε4 non-carriers (n=15)	APOε4 carriers (n=18)
	Mean (SD)	Mean (SD)
10-year QRISK [®] 3 score (%)	16.51 (5.7)	14.58 (10.35)
Expected QRISK [®] 3 score (%) ¹	15.33 (4.1)	10.33 (4.3)
Relative risk ²	1.07 (0.25)	1.35 (0.49)
Relative risk <1.0 (count, [%])	6 (40%)	2 (11%)
Relative risk =1.0 (count, [%])	1 (7%)	2 (11%)
Relative risk >1.0 (count, [%])	8 (53%)	14 (78%)
Age (years)	70.93 (3.3)	65.77 (5.4)
Heart age according to QRISK [®] 3 score (years)	72.13 (4.87)	69.39 (7.79)
Heart health age older than actual age (count, [%])	9 (60%)	14 (78%)
Heart health age equal to than actual age (count, [%])	0 (0%)	2 (11%)
Heart health age younger than actual age (count, [%])	6 (40%)	2 (11%)

¹10-year QRISK[®]3 score of a healthy person of the same age, sex and ethnic group (meaning no adverse clinical indicators, cholesterol ratio of 4.0, a stable systolic blood pressure of 125, a BMI of 25). ²The relative risk is the 10-year QRISK[®]3 risk score divided by the healthy person's risk (=expected QRISK[®]3 score)

As the QRISK[®]3 model already accounts for the effect of many variables including age and sex, no covariates were added to the multiple linear regression model, when investigating the effect of genetic risk on relative risk. There was no significant effect of APOE status on 10-year QRISK[®]3 score ($F(1,31)=0.41$, $p>.1$, $R^2=0.01$), relative risk ($F(1,31)=3.98$, $p=0.055$, $R^2=0.11$) or heart age ($F(1,31)=1.40$, $p>.1$, $R^2=0.04$).

Neuroimaging

Voxel based morphometry

Having thoroughly investigated the cognitive, behavioural, dietary and cardiovascular profiles of the APO ϵ 4 carrier and non-carrier cohort, I next sought to explore potential volumetric differences in a subgroup of the two APOE cohorts.

To this purpose, whole-brain characterization of differences in cerebral volume and brain-matter tissue in structural MRI brain images was applied to the T1-weighted scans of 41 participants, of which 20 were APO ϵ 4 carriers and 21 were APO ϵ 4 non-carriers from the larger study cohort (for a detailed description of the method please see p.113-114). The APO ϵ 4 carrier subgroup consisted of fourteen female and six male participants, whereas the APO ϵ 4 non-carrier subgroup was comprised of eleven female and ten male participants. With a mean age of 63.5 (SD = 4.7) in the carriers and 68.4 (SD= 5.0) in the non-carriers, the APO ϵ 4 carriers were significantly younger ($p=0.003$) than the APO ϵ 4 non-carriers. Given the role of age in brain health, I thus incorporated age as a covariate into the GLM model. An example of T1-weighted image processing steps showing (A) removal of large non-neuronal tissue (neck area) and (B) masking the brain area are shown in Figure 3.6.

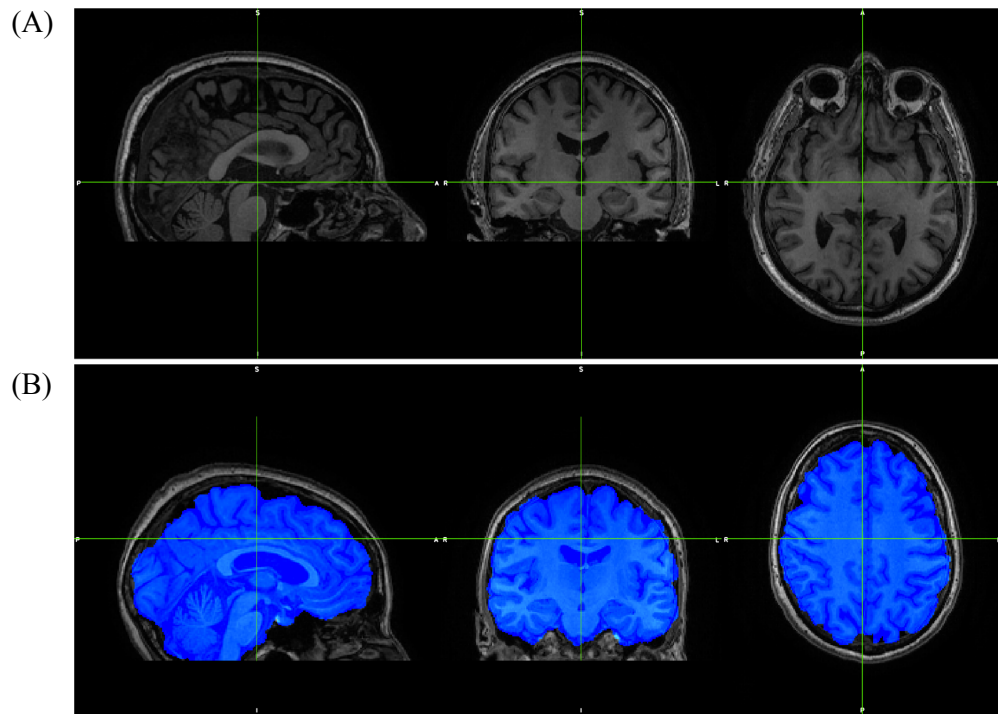


Figure 3.6 Example of image-processing: (A) removal of neck voxels and (B) brain mask

Multiple comparison corrected maps showed no clusters that would indicate a greater level of atrophy when contrasting the GM images of the APO ϵ 4 non-carriers against the APO ϵ 4-positive subgroup. When investigating uncorrected maps at $p < .001$, however, several significant clusters were present. According to the Harvard probabilistic atlas significant clusters of uncorrected maps highlighted the following cortical areas: (A) lingual gyrus, (B) subcallosal cortex, (C) supramarginal gyrus (anterior division), (D) frontal operculum cortex, (E) frontal orbital cortex.

Chapter Discussion

Relationship between Apolipoprotein ϵ 4 and cognition/behaviour

The APOE cohorts presented here are overall well-matched for educational attainment, sex, age, and lifestyle factors, and had no obvious medical conditions. Consistent with the hypothesis, I found that the APOE genotyped cohorts did not differ significantly with respect to the vast majority of cognitive and behavioural domains.

Some empirical evidence has shown that APOε4 carriers show a decline for ‘global cognitive ability’ (Small *et al.*, 2004; Wisdom, Callahan and Hawkins, 2011). I did not observe differences in the global cognitive functioning between the APOε4 carriers and non-carriers, apart from visuospatial ability subdomain (ACE-III), where APOε4 carriers had a small but significantly lowered performance compared to APOε4 non-carriers.

A national survey of 1762 healthy individuals aged 68-69 years of age, using ACE-III as their primary outcome measure, found a small but negative association between APOε4 carriers and the ACE-III score - driven largely by lowered performance in two subdomains: attention and memory (Richards *et al.*, 2019). In light of the small effect sizes observed by other studies, it is possible that a significantly larger sample size would have been required to detect potential subtle differences.

The next measure of the study, ROCF, showed that there was no difference with respect to visuospatial functioning or nonverbal memory between the groups. This is in line with results from a small longitudinal study, which showed no performance differences on visuospatial skills (ROCF copy) and visual memory (ROCF delay) between 20 cognitively healthy APOε4 carriers and 29 non-carriers at baseline (Lavretsky *et al.*, 2003). The group did however see a decline over time as indicated by significantly worsened visuospatial skills in both groups at the two-year follow-up. Interestingly, the age-related decrease in visual memory was only observed in the group of APOε4 non-carriers.

I found no differences between APOε4 carriers or non-carriers with respect to their executive functions, motor functions, or psychomotor speed, as assessed by the TMT. Age, on the other hand, was significantly associated with both parts of the TMT regardless of APOε4 status. These results are largely congruent with the current literature. In a large-scale cohort

study with 7,526 participants (aged 40-79 years), performance on the TMT-B was negatively associated with smoking, less physical activity and lower occupational attainment but showed no association with APOE status (Rodriguez *et al.*, 2018). The work of Reas and colleagues (2019) in 1,393 older adults who were followed for 27 years (tested seven times) further supports these research findings. Participants' performance on a range of neuropsychological measures, including the TMT-B, could not be distinguished by APOE4 status in a cross-sectional comparison, but significantly declined as a function of age (Reas *et al.*, 2019). Their analysis further showed that performance on the TMT-B declined fastest in APOE4 carriers and slowest in APOE2 carriers compared to APOE3/E3 participants. This is corroborated by further cohort studies (Wilson *et al.*, 2002; Mielke *et al.*, 2016). Evidence from neuroimaging studies (Caselli *et al.*, 2011; Fennema-Notestine *et al.*, 2011) also shown that executive functioning and processing speed are particularly susceptible to decline in normal ageing and this vulnerability might be exacerbated in APOE4 carriers.

Contrary to expectations, I did not replicate findings that would support changes in navigation strategies or spatial navigation deficits in APOE4 carriers (Coughlan *et al.*, 2018). Our spatial navigation measures, the Supermarket task and SHQ, showed that spatial navigation performance was similarly good in both APOE groups, with no obvious differences in their egocentric or allocentric navigation strategies.

Self-reported interoception, which is emerging in frontotemporal dementia research as a new way of understanding reduced emotional reactivity (García-Cordero *et al.*, 2016; Marshall *et al.*, 2017), self-awareness and empathy, was similar between the APOE groups.

I also found no differences between the two APOE cohorts with respect to their self-reported subjective cognitive decline as was measured by the CCI. Subjective cognitive decline (SCD) is a common condition amongst elderly with no clear prognosis and as such it has

lately gained increasing interest in the context of dementia research (Reisberg *et al.*, 2010). Self-perceived worsening in cognition, in the absence of measurable, objective decline in cognitive functions, might present a risk factor for developing dementia and it has even been proposed to represent a preclinical stage of MCI and dementia, making it an interesting target for early detection of cognitive impairment (Reisberg *et al.*, 2010). A meta-analysis of 36 studies concluded that there is little evidence to support that APO ϵ 4 carriers are more likely to experience SCD (Ali, Smart and Gawryluk, 2018), which is in line with my findings. And yet, the same meta-analysis concluded that APO ϵ 4 status and SCD confer both an individual risk but also a multiplicative risk to individuals for future objective cognitive decline (Ali, Smart and Gawryluk, 2018), which is an interesting finding that requires further exploration.

Whilst the literature supports an increased prevalence for neuropsychiatric symptoms in AD, such as anxiety and depression (Lyketsos *et al.*, 2000; Porter *et al.*, 2003; Bergh and Selbæk, 2012), the relationship between APO ϵ 4 status and neuropsychiatric symptoms remains unclear. I found no neuropsychiatric differences with respect to anxiety (GAD-7) or depression (PHQ-9), between the APOE groups, apart from the fact that the APO ϵ 4 non-carriers reported a lower motivation score (subdomain of the CBI-R). This reduced motivation, was a stand-alone finding, which was further negatively affected by increasing age in the APO ϵ 4 non-carriers. Other domains, such as memory, self-care, abnormal behaviour and other subdomains of the CBI-R were not associated with APO ϵ 4 status.

All in all, the study population investigated here showed no salient signs of cognitive decline or impairment in behavioural or functional areas. Domain-specific group differences in cognition between the APO ϵ 4 carriers and non-carriers were largely non-existent, further adding to the mixed literature on the relationship between APO ϵ 4 status and cognition.

Relationship between Apolipoprotein ε4 status dietary, cardiovascular and general health profiles

The APOε4 carriers showed a significantly lower consumption of galactose, which is a simple sugar gained from metabolising carbohydrates. This dietary finding cannot be explained. All other nutrients and food groups were the same across the two groups, indicating that the groups' overall diet was very similar in nutritional content.

The extensive health and demographic data captured by the microbiome health questionnaire showed that the here studied cohorts were very well matched across a wide range of lifestyle and behavioural criteria, such as eating habits and alcohol consumption, allergies, travelling habits, handedness, exercise, sleep behaviour, and medications.

Sub-group analysis of cardiovascular risk showed that both subgroups, whilst considered overweight (BMI>25.0), were generally of good health, with low occurrences of diseases or other clinical conditions. The only medication that was taken by a relatively high percentage of participants (a third in both groups) was blood pressure lowering medication, which is representative for the observed prevalence of anti-hypertensive treatment within a population with comparable demographics (Joffres *et al.*, 2013). The APOε4 carriers had significantly higher levels of LDL and total cholesterol compared to the APOε4 non-carriers. APOE plays a key role in lipid transport as a major ligand for LDL receptors with differential binding affinity depending on allelic expression (Mahley, 2012) which is reflected by altered lipoprotein metabolism in APOε4 carriers (Li *et al.*, 2013) and leads to 3-15% increase of LDL and total cholesterol levels when comparing APOε4 carriers to non-carriers. This finding is thus congruent with my hypothesis that APOε4 carriers show a distinctly different lipid profile.

Relationship between Apolipoprotein ε4 status and brain health

The literature regarding the role of APOE status is not only mixed with respect to cognitive and behavioural changes, but there is also conflicting evidence coming from neuroimaging studies (Reiman *et al.*, 1996; Tohgi *et al.*, 1997; Moffat *et al.*, 2000; Lemaître *et al.*, 2005; Lind *et al.*, 2006; Wishart *et al.*, 2006; Jak *et al.*, 2007; Burggren *et al.*, 2008; Cherbuin *et al.*, 2008; Honea *et al.*, 2009) which have tried to elucidate potential pre-clinical brain changes in APOε4 carriers.

I found no volumetric differences after applying a correction for multiple comparisons. This finding is in line with the hypothesis that APOε4 carriers do not exhibit any gross structural brain changes. Although brain changes can precede overt cognitive decline by a decade or more, such changes, if present, are expected to be subtle.

Uncorrected maps showed decreased volumes in five brain areas. Given the lack of correction for multiple comparisons, it is important to be cautious interpreting the findings from the uncorrected maps, as these are likely to be false positives. Nonetheless, it is possible these findings, particularly those showing large clusters as opposed to single clusters, are indeed an indication of an effect and that a study with a larger sample size might replicate findings of the relevant brain areas presented in the given study. In light of the fact that APOε4 carriers in this study do not represent with obvious cognitive or behaviour changes, failing to find significant volumetric differences is in line with my expectation.

In summary, the literature suggests that volumetric brain changes in APOε4 carriers are, if present, subtle and associated with hippocampal differences and show faster rates of decline over time in APOε4 carriers (Tohgi *et al.*, 1997; Moffat *et al.*, 2000; Lind *et al.*, 2006). Due to the effect exerted by inter-subject variability, which further increases with age, it might be difficult to reliably detect differences associated with APOε4 status, which is supported

by my findings. In fact, a large-scale experimental design like that of Lemaître *et al.* (2005) including over 700 participants, showed to be insufficiently powered to detect any volumetric differences smaller than 2% (at a 0.05 threshold for type I errors) between APOε4 heterozygotes and non-carriers (Lemaître *et al.*, 2005).

More work in this area is required to investigate whether neural pathological changes on a macroscopic level, such as the here investigated volumetric differences, are modulated by APOε4 and whether such global changes can be identified and distinguished from age-associated changes before the onset of overt cognitive changes, thus potentially offering great diagnostic value.

The findings demonstrate that the here studied participants performed equally well on a range of measures assessing their cognition, behaviour and neuropsychiatric functioning regardless of APOε4 status, with no signs of global or domain-specific impairment. This was further supported by the neuroimaging analysis, which did not identify noticeable macroscopic differences in volumes after applying multiple corrections. Sub-cohort evaluation of cardiovascular health corroborates the notion that APOε4 is associated with an altered lipid metabolism, which favours LDL and total cholesterol levels. This was the most striking difference between APOε4 carriers and non-carriers. The importance of these findings is that the two study groups are very well-matched, therefore, any microbiome changes observed between the two APOE groups is highly unlikely to be due to cognitive, clinical or behavioural differences between the groups, but instead represent a difference in microbial signature based on APOE genotype.

CHAPTER 4: CROSS-SECTIONAL AND LONGITUDINAL ASSESSMENT OF THE INTESTINAL MICROBIOTA PROFILES IN APOE4 CARRIERS AND NON-CARRIERS

Faecal sample collection

As outlined in the methods, participants provided a faecal sample at baseline (T1), as well as at approximately six months (T2) and at 12 months (T3) after baseline. The cross-sectional comparison with the AD patient cohort was based on readily collected and previously banked faecal samples.

To characterize the intestinal microbiota of individuals over time, I collected faecal samples as described above between March 2018 and March 2020 (Figure 4.1). Samples were aimed to be provided within 183 days (\pm 15 days) after the last sample. The sampling time point had to be moved to an earlier or (most commonly) later time point for 16 samples for the following reasons: use of antibiotics (n=5), holidays abroad (n=2), or coronavirus disease of 2019 (COVID-19) (n=9).

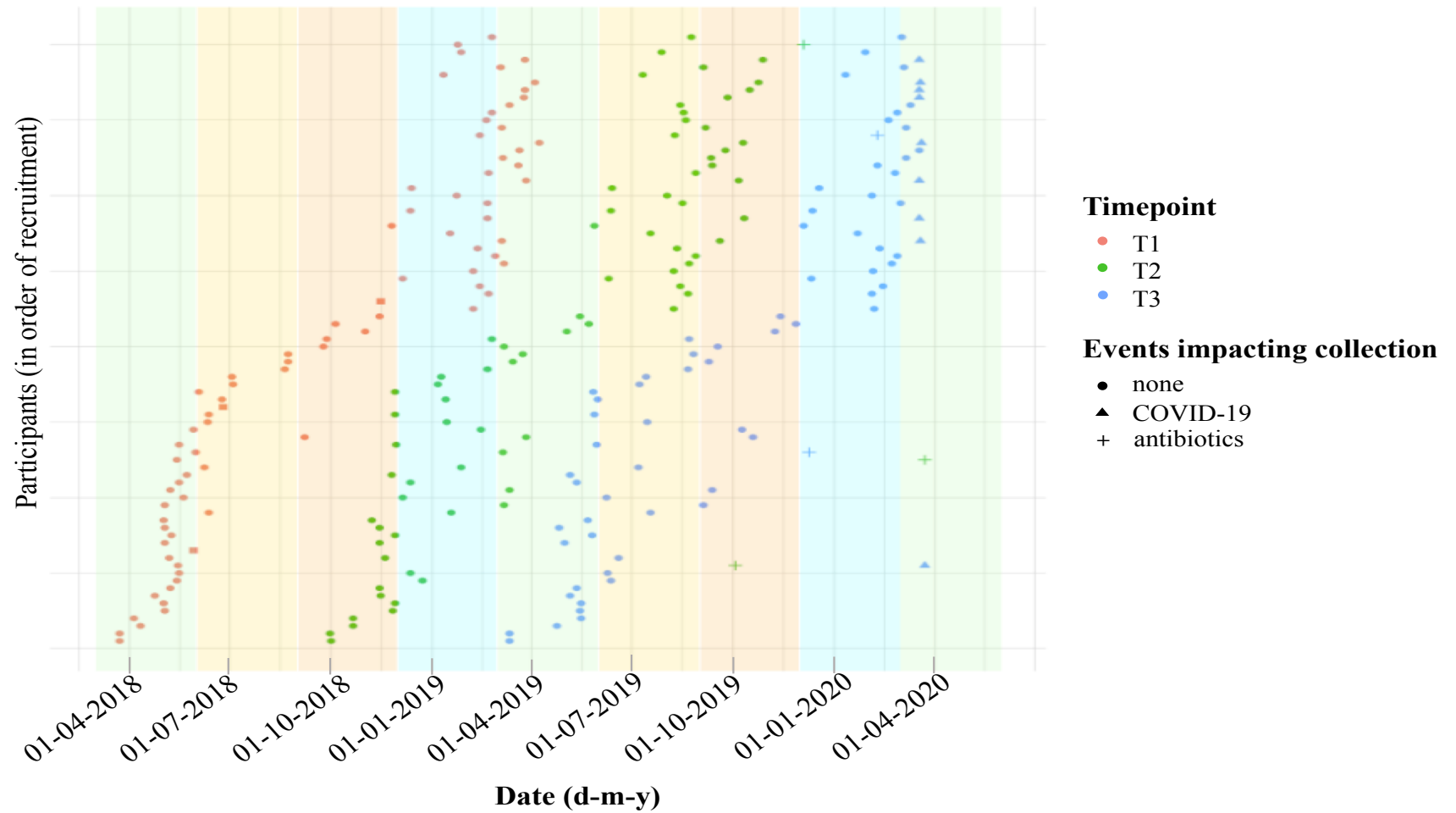


Figure 4.1 Scatterplot showing faecal sample collection throughout the study. Coloured dots denote sampling timepoints - red: T1, green: T2, blue: T3. Shapes denote events impacting sample collection – circle: none, triangle: sample collection affected by COVID-19, cross: antibiotics. Shaded areas denote the seasons; green = spring, yellow = summer, orange = autumn, blue = winter. Every subject keeps the same position along the y-axis

There were 79 faecal samples at baseline, 75 samples at T2 and 72 samples at T3 (Figure 4.2), summing up to an overall total of 226 samples.

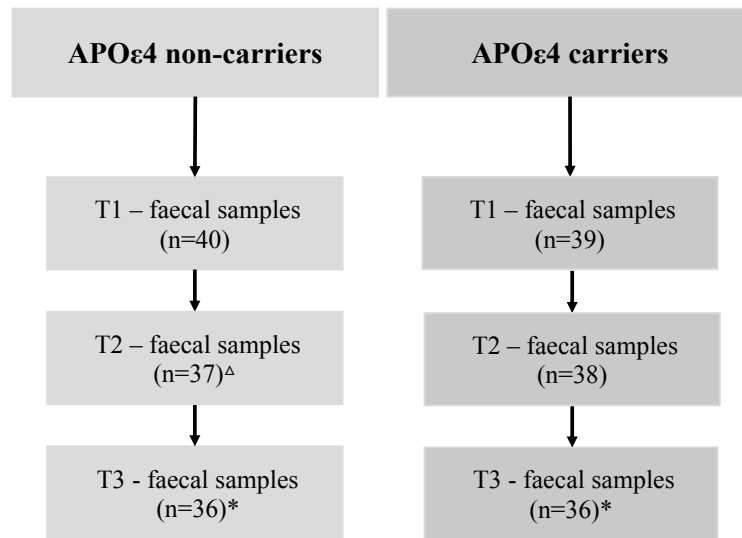


Figure 4.2 Faecal samples analyzed at T1, T2, and T3

^Δ Sequencing for the T2 sample of subject 28 failed.

*Due to repeated antibiotics subjects 26 and 123 provided no T3 sample

Taxonomic analysis

Descriptive summary of taxonomic profiles

Phylum - Baseline (T1)

A total of 10 phyla, including *Actinobacteria*, *Euryarchaeota*, and *Verrucomicrobia* were detected in the microbial profiles of the APOE groups and were dominated by *Firmicutes* and *Bacteroidetes*. *Firmicutes* accounted for 60.4% (SD=12.7) in the APOε4 non-carriers and 61.3% (SD=10.5) in the carriers on average, whereas *Bacteroidetes* made up 27.1% (SD=12.7) and 27.0% (SD=12.9) of the relative abundance in the community profile in the APOε4 non-carriers and carriers, respectively (Figure 4.3). These phyla dominate the human gastrointestinal tract (Human Microbiome Project Consortium, 2012; Ling *et al.*, 2013). The third most abundant phylum was *Actinobacteria*, followed by *Proteobacteria*, *Verrucomicrobia* and *Euryarchaeota*. A graphical representation of the relative abundances per group are shown in Figure 4.3.

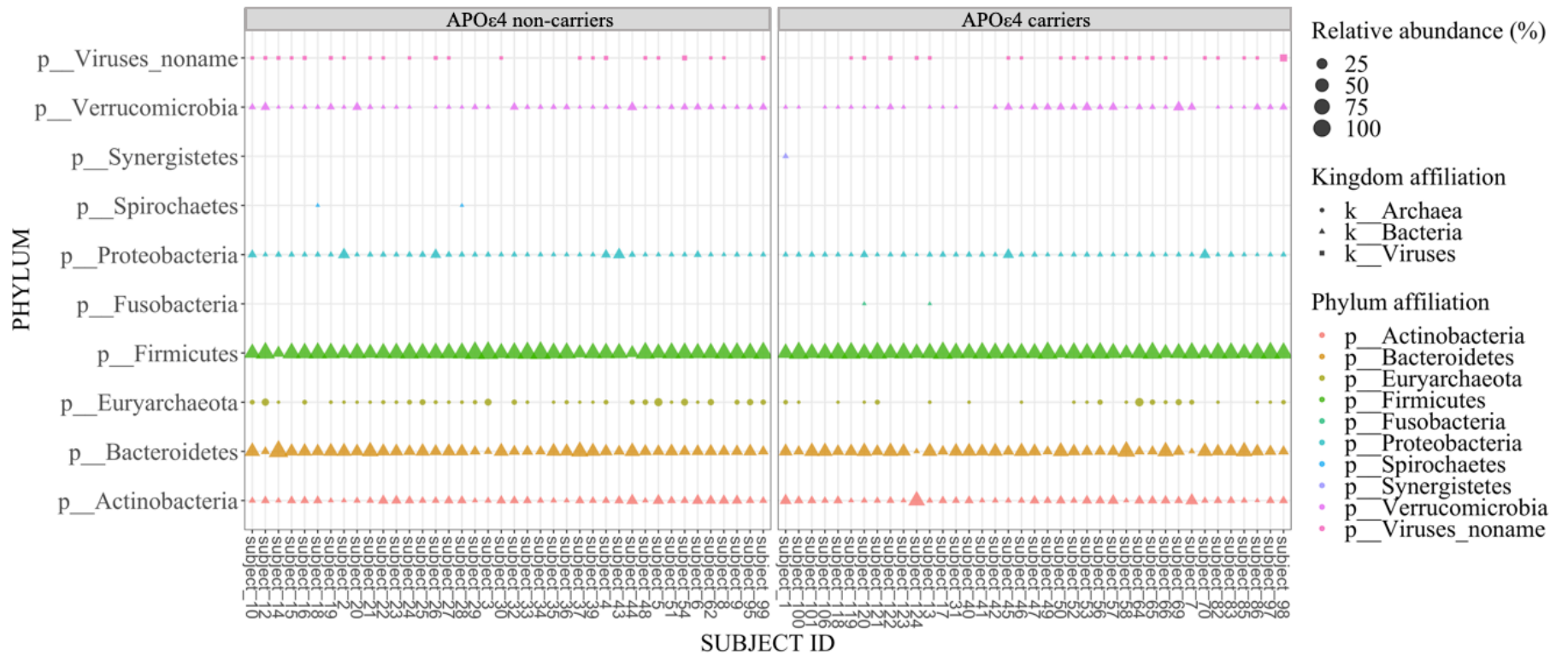


Figure 4.3 Relative abundances of phyla at baseline, Apolipoprotein ε4 non-carriers (left panel), Apolipoprotein ε4-carriers (right panel), shape showing kingdom affiliation, size represents relative abundances

Phylum - 6-months follow-up (T2)

I identified 12 phyla in the samples of the first follow-up. The 6-months follow-up intestinal microbiota composition at phylum-level was similar to that at baseline and was dominated by members of the *Firmicutes* (non-carriers: M=60.1%, SD=15.5; carriers: M=59.8%, SD=11.6) and *Bacteroidetes* (non-carriers: M=19.8%, SD=11.2; carriers: M=25.6%, SD=11.0) phyla with similar mean relative abundances compared to group means at T1. For an illustrative comparison see Figure 4.4 and associated Table 4.1. Compared to T1, *Actinobacteria* were almost twice as abundant at T2 in the group of APOε4 non-carriers (M=13.4, SD=13.9) but only slightly increased in the APOε4 carriers (M=7.7, SD=5.6). As already seen at baseline, the ‘core’ phyla present in the vast majority of subjects also included *Verrucomicrobia*, *Proteobacteria*, *Euryarchaeota*, and *Viruses*. However, different to T1, at T2 I saw the addition of three new phyla, namely *Candidatus Saccharibacteria*, *Ascomycota* and *Cyanobacteria*, but also the loss of the *Fusobacteria* phylum. All of these “dynamic” phyla were only present in up to five subjects and accounted for less than 0.01% of the total relative abundance.

Phylum - 12-months follow-up (T3)

The community profiles at T3 were comprised of 13 phyla and were dominated by the *Firmicutes* (non-carriers: M=60.0%, SD=10.5; carriers: M=60.0%, SD=12.0) and *Bacteroidetes* (non-carriers: M=27.5%, SD=9.6; carriers: M=28.1%, SD=12.7) with comparable relative abundances between the groups and similar to the other two timepoints. As already observed at T1 and T2, only five other phyla apart from the *Firmicutes* and *Bacteroidetes* inhabited the intestinal microbiota of all participants. Besides these core phyla, only a few community profiles were also inhabited by members belonging to rare phyla such as that of *Spirochaetes*, with very low relative mean abundances (M<0.001%).

Table 4.1 Relative abundances (%) of most abundant phyla across all timepoints

Mean (SD)	APOε4 non-carriers			APOε4 carriers		
	T1	T2	T3	T1	T2	T3
<i>Firmicutes</i>	60.39 (12.66)	60.06 (15.46)	59.98 (10.26)	61.27 (10.48)	59.81 (11.62)	60.00 (11.99)
<i>Bacteroidetes</i>	27.14 (12.69)	19.79 (11.15)	27.54 (9.61)	26.99 (12.89)	25.63 (10.95)	28.08 (12.67)
<i>Actinobacteria</i>	6.14 (4.52)	13.44 (13.92)	6.01 (4.83)	6.86 (8.40)	7.65 (5.61)	5.53 (4.42)
<i>Verrucomicrobia</i>	1.79 (2.57)	2.04 (3.27)	1.27 (1.61)	2.14 (3.30)	1.70 (2.51)	1.57 (2.35)
<i>Proteobacteria</i>	2.69 (4.67)	2.54 (4.15)	2.05 (3.86)	1.71 (3.20)	2.84 (5.35)	2.05 (4.64)
<i>Euryarchaeota</i>	1.76 (2.96)	2.01 (4.29)	3.10 (4.43)	0.76 (2.46)	1.58 (4.82)	2.69 (7.76)
<i>Viruses</i>	0.09 (0.24)	0.13 (0.34)	0.04 (0.15)	0.24 (1.27)	0.77 (4.51)	0.08 (0.15)
Others	0.00	0.03	0.00	0.02	0.01	0.00

Overall, the intestinal community profiles are largely characterized by seven phyla (Figure 4.4), which I found to stay relatively stable over time and showed similar relative abundances also between the two groups.

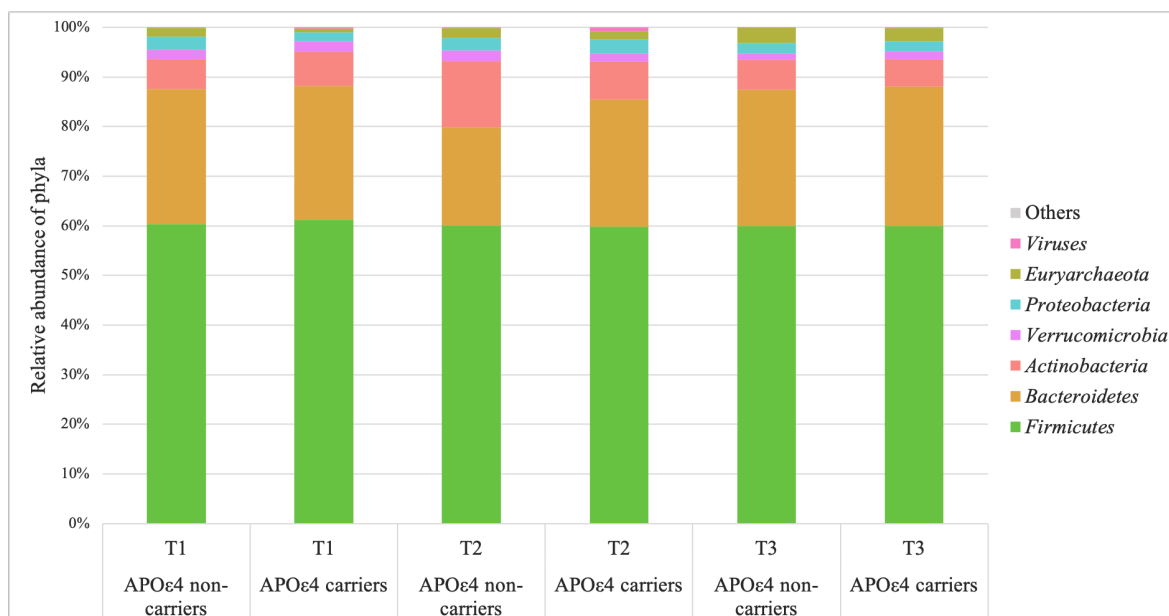


Figure 4.4 Relative abundances (%) of phyla between Apolipoprotein E groups over time

Family - Baseline (T1)

I identified 49 taxa at the family-level, of which the 15 most abundant families make up over 95% of the overall community profile (Table 4.2). All of these families belong to the kingdom of *Bacteria* at the highest taxonomic level. A cross-sectional visualisation of the ten most abundant families (~90% coverage) showed dominance of the following taxa in decreasing order (Figure 4.5): *Ruminococcaceae* which was by far the most abundant family (non-carriers: M=24.2%, SD=8.6; carriers: M=25.6%, SD=8.5), *Bacteroidaceae* (non-carriers: M=16.0%, SD=10.0; carriers: M=15.1%, SD=11.1), *Lachnospiraceae* (non-carriers: M=14.3%, SD=9.0; carriers: M=14.5%, SD=6.8) and *Eubacteriaceae* (non-carriers: M=14.2%, SD=11.2; carriers: M=13.2%, SD=9.1). All following family have an abundance of below 5% *Bifidobacteriaceae*, *Prevotellaceae*, *Rikenellaceae*, *Porphyromonadaceae*, *Verrucomicrobiaceae*, and *Veillonellaceae*. The 10 most abundant families belonged to one of four phyla; *Actinobacteria*, *Verrucomicrobia*, *Bacteroidetes* or *Firmicutes*, with all but two families belonging to the latter two phyla (Figure 4.5). The family *Coriobacteriaceae*, *Clostridiaceae*, *Enterobacteriaceae*, *Methanobacteriaceae* and *Streptococcaceae* were the next five most abundant families.

Mean relative abundances for the other 34 families make up the remaining 5%, indicating that the majority of the families are present in very small abundances and that the human intestinal microbiota community profile was diverse at this taxonomic rank. The large standard deviations further highlight the variability of intestinal microbiota composition between individuals.

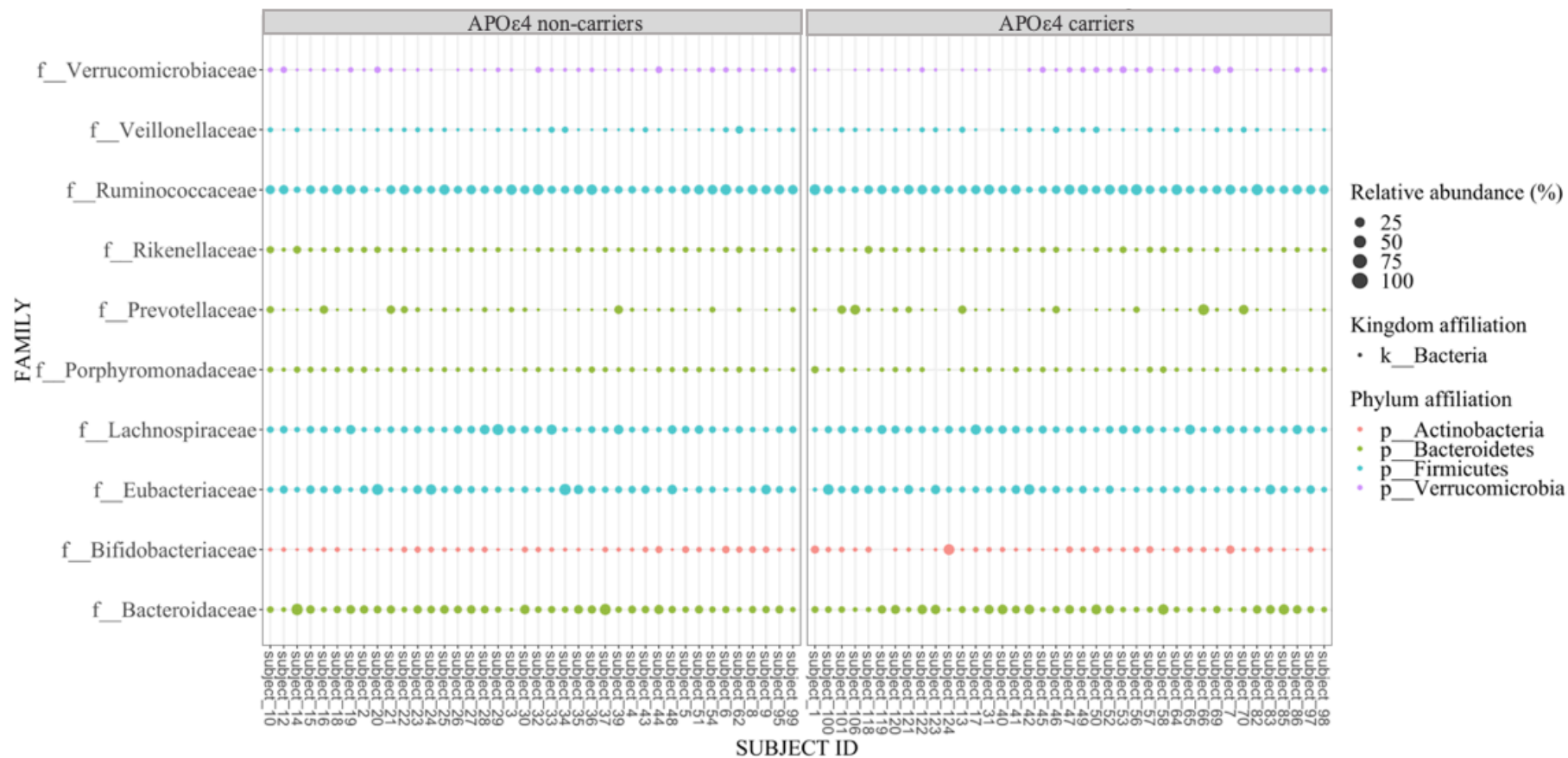


Figure 4.5 Relative abundance of top 10 taxa at family-level at baseline, Apolipoprotein ε4 non-carriers (left panel), Apolipoprotein ε4-carriers (right panel), shape showing kingdom affiliation, size represents relative abundances

Family - 6-months follow-up (T2)

At family-level, I observed a total of 57 taxa. Whilst the majority of the ten most abundant families were present at similar relative abundances as before, the ranking changed for two taxa. The taxa *Coriobacteriaceae* and *Methanobacteriaceae* replaced *Verrucomicrobiaceae* and *Veillonellaceae* in the list of the ten most abundant species. Relative abundance of the *Coriobacteriaceae* family at T2 (non-carriers: M= 4.0% SD= 3.5; carriers: M= 2.7% SD= 2.8) almost doubled compared to baseline for the group of APOε4 non-carriers (non-carriers: M= 2.1% SD= 1.3; carriers: M= 1.8% SD= 1.7). Whereas the relative abundance of *Methanobacteriaceae* increased most noticeably in the group of APOε4 carriers – now present at 1.58% (SD=4.8) compared to 0.8% (SD=2.5) at baseline (Table 4.2). Albeit still one of the top ten abundant families, there was a nominally large decrease in *Bacteroidaceae* in the group of APOε4 non-carriers (M= 9.5% SD= 5.4) and a small decrease in the carrier group (M= 12.1% SD= 7.8) at T2. The relative abundance of *Bifidobacteriaceae*, on the other hand, more than doubled in the APOε4 non-carriers (M= 9.4% SD= 12.2) but remained at similar abundance levels in the APOε4 carriers (M= 4.9% SD= 4.7) compared to baseline (Figure 4.6).

Family - 12-months follow-up (T3)

There were 43 distinct families identified at T3. Looking more closely at the ten most abundant families, there was a large overlap with previously seen taxa. As before, the family *Ruminococcaceae* was the most abundant family (non-carriers: M=23.5%, SD=8.5; carriers: M=23.9%, SD=9.3), followed by *Bacteroidaceae* which recovered to T1-like levels (non-carriers: M=16.7%, SD=8.8; carriers: M=15.8%, SD=10.0) and *Lachnospiraceae* (non-carriers: M=16.3%, SD=8.7; carriers: M=15.2%, SD=6.9). The family of *Methanobacteriaceae* remained in the list of ten most abundant families.

Considering the intestinal profiles at family-level, I observed a reasonably small number of families which made up the majority of the community profiles of both cohorts (Figure 4.6).

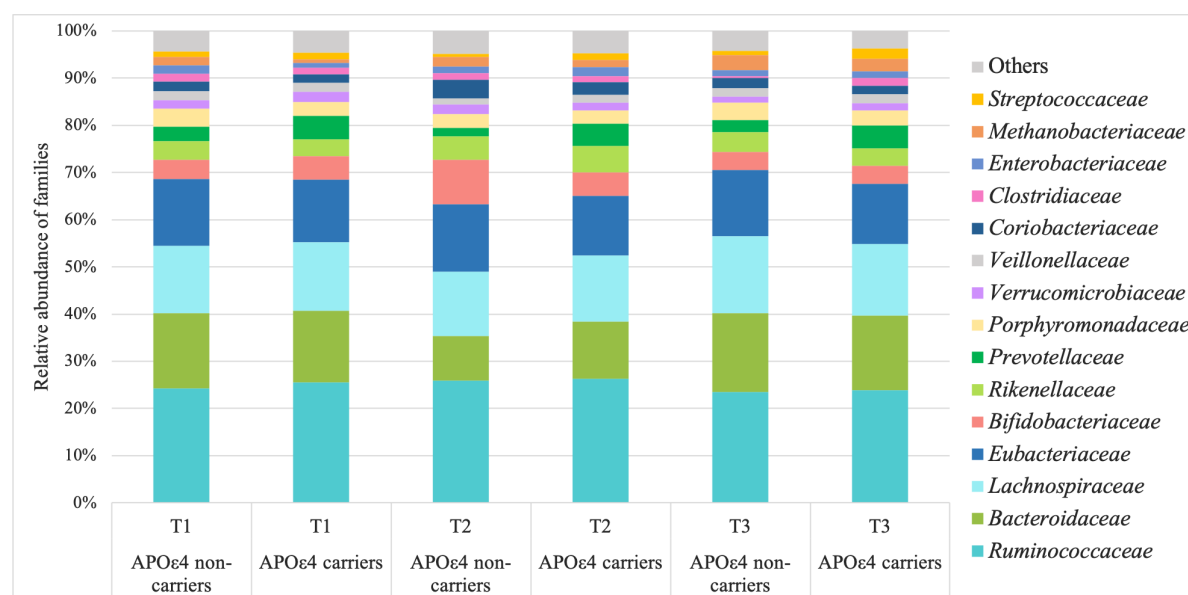


Figure 4.6: Relative abundances (%) of families between Apolipoprotein E groups over time

Table 4.2 Relative abundances (%) of most abundant families across all timepoints

Mean (SD)	APOε4 non-carriers			APOε4 carriers		
	T1	T2	T3	T1	T2	T3
<i>Ruminococcaceae</i>	24.22 (8.61)	25.90 (9.81)	23.46 (8.51)	25.59 (8.53)	26.32 (9.25)	23.91 (9.28)
<i>Bacteroidaceae</i>	15.95 (10.04)	9.46 (5.42)	16.74 (8.79)	15.14 (11.14)	12.12 (7.81)	15.79 (10.02)
<i>Lachnospiraceae</i>	14.25 (9.03)	13.66 (6.01)	16.32 (8.66)	14.54 (6.83)	14.03 (6.99)	15.16 (6.88)
<i>Eubacteriaceae</i>	14.21 (11.24)	14.28 (12.81)	13.99 (8.77)	13.21 (9.08)	12.60 (9.69)	12.76 (7.96)
<i>Bifidobacteriaceae</i>	4.06 (3.79)	9.43 (12.23)	3.90 (4.20)	5.05 (7.64)	4.94 (4.67)	3.80 (3.59)
<i>Rikenellaceae</i>	4.02 (3.35)	5.00 (5.34)	4.18 (4.11)	3.58 (3.11)	5.61 (5.34)	3.71 (3.64)
<i>Prevotellaceae</i>	3.06 (6.03)	1.77 (4.11)	2.48 (4.58)	4.94 (10.58)	4.80 (10.53)	4.91 (10.88)
<i>Porphyromonadaceae</i>	3.73 (2.07)	2.87 (2.98)	3.73 (2.35)	2.94 (2.65)	2.74 (1.55)	3.12 (2.67)
<i>Verrucomicrobiaceae</i>	1.79 (2.57)	2.04 (3.27)	1.27 (1.61)	2.14 (3.30)	1.70 (2.51)	1.57 (2.35)
<i>Veillonellaceae</i>	1.93 (3.00)	1.32 (2.30)	1.86 (3.74)	1.94 (2.47)	1.63 (2.88)	1.95 (2.69)
<i>Coriobacteriaceae</i>	2.07 (1.28)	3.95 (3.48)	2.10 (1.11)	1.78 (1.74)	2.68 (2.83)	1.72 (1.51)
<i>Clostridiaceae</i>	1.64 (3.27)	1.46 (3.50)	0.37 (0.90)	1.35 (2.55)	1.28 (2.95)	1.71 (3.64)
<i>Enterobacteriaceae</i>	1.83 (4.74)	1.35 (3.73)	1.37 (3.87)	1.03 (3.25)	1.90 (5.23)	1.38 (4.66)
<i>Methanobacteriaceae</i>	1.76 (2.96)	2.01 (4.29)	3.10 (4.43)	0.76 (2.46)	1.58 (4.82)	2.69 (7.76)

<i>Streptococcaceae</i>	1.09 (1.39)	0.66 (1.20)	0.97 (2.23)	1.39 (1.97)	1.42 (2.89)	2.14 (6.63)
-------------------------	----------------	----------------	----------------	----------------	----------------	----------------

Genera/Species - Baseline (T1)

At baseline, I identified a total of 108 genera. On average, the ten most abundant genera made up 63% of the community profiles. In-line with my observations made at higher taxonomic level, the community profiles of both APOE cohorts were dominated by genera belonging to the *Firmicutes* and *Bacteroidetes* phyla. Within the *Firmicutes* phylum, *Eubacterium* (non-carriers: M=14.2%, SD=11.2; carriers: M=13.2%, SD=9.1), *Ruminococcus* (non-carriers: M=9.2%, SD=6.4; carriers: M=10.2%, SD=5.8) and *Subdoligranulum* (non-carriers: M=8.4%, SD=6.43 carriers: M=8.2%, SD=7.9) were the most abundant genera. Whereas within the *Bacteroidetes* phylum, *Bacteroides* (non-carriers: M=16.0%, SD=10.0; carriers: M=15.1%, SD=11.1) and *Alistipes* (non-carriers: M=4.0%, SD=3.4; carriers: M=3.6%, SD=3.1) were the most abundant genera (Figure 4.7). The less frequently represented *Actinobacteria* phylum was mainly characterized by members of the *Bifidobacterium* (non-carriers: M=4.1%, SD=3.8; carriers: M=5.1%, SD=7.6) and *Collinsella* (non-carriers: M=1.9%, SD=1.2; carriers: M=1.5%, SD=1.7) genera. There was only one genus per phylum within the 20 most abundant genera which belonged to *Proteobacteria* or *Verrucomicrobia*, namely the genera *Escherichia* and *Akkermansia*, respectively, with relative abundances around 2%.

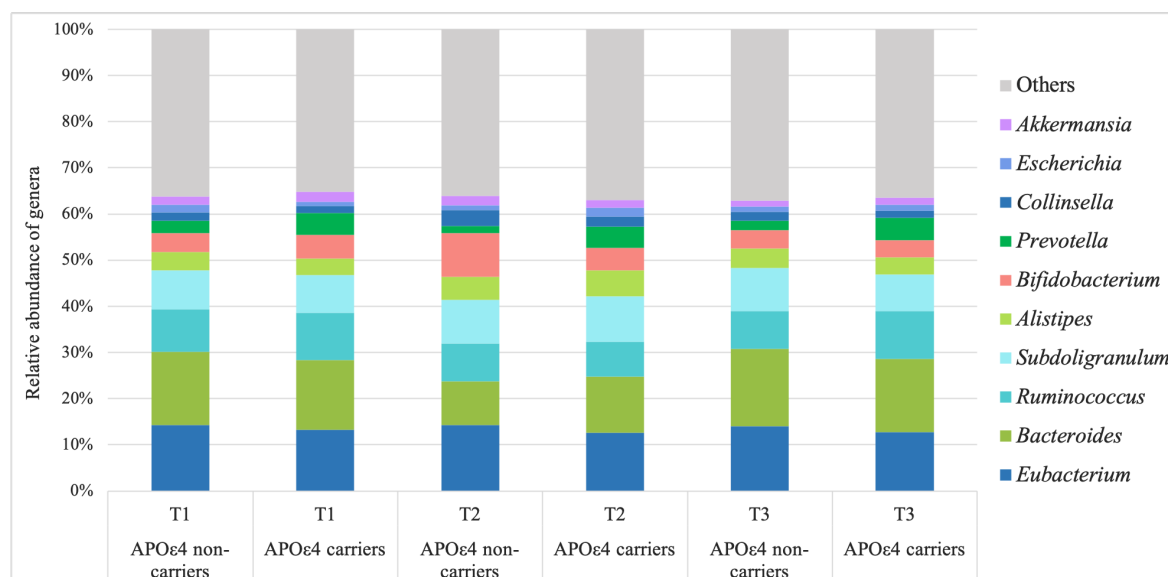


Figure 4.7 Relative abundances (%) of genera between Apolipoprotein E groups over time

Table 4.3 Relative abundances (%) of most abundant genera across all timepoints

Mean (SD)	APOε4 non-carriers			APOε4 carriers		
	T1	T2	T3	T1	T2	T3
<i>Eubacterium</i>	14.21 (11.24)	14.28 (12.81)	13.99 (8.77)	13.21 (9.08)	12.60 (9.69)	12.76 (7.96)
<i>Ruminococcus</i>	9.18 (6.35)	8.21 (6.25)	8.30 (6.00)	10.17 (5.82)	7.54 (5.65)	10.47 (7.03)
<i>Bacteroides</i>	15.95 (10.04)	9.46 (5.42)	16.74 (8.79)	15.14 (11.14)	12.12 (7.81)	15.79 (10.02)
<i>Alistipes</i>	4.02 (3.35)	5.00 (5.34)	4.18 (4.11)	3.58 (3.11)	5.61 (5.34)	3.71 (3.64)
<i>Bifidobacterium</i>	4.05 (3.79)	9.42 (12.23)	3.90 (4.20)	5.05 (7.64)	4.94 (4.67)	3.79 (3.59)
<i>Collinsella</i>	1.87 (1.20)	3.54 (3.33)	1.90 (1.17)	1.51 (1.65)	2.29 (2.56)	1.50 (1.44)
<i>Escherichia</i>	1.59 (4.51)	0.99 (3.31)	1.19 (3.69)	0.92 (2.89)	1.83 (5.17)	1.35 (4.62)
<i>Akkermansia</i>	1.79 (2.57)	2.04 (3.27)	1.27 (1.61)	2.14 (3.30)	1.70 (2.51)	1.57 (2.35)
<i>Subdoligranulum</i>	8.41 (6.28)	9.48 (6.85)	9.33 (5.59)	8.29 (7.92)	9.87 (8.89)	7.85 (6.93)
<i>Prevotella</i>	2.70 (6.10)	1.51 (4.01)	2.09 (4.61)	4.76 (10.62)	4.53 (10.62)	4.79 (10.92)

The microbial profiles at baseline consisted of 322 species, of which the 25 most abundant species are shown in Figure 4.8. The five most abundant species were *Subdoligranulum unclassified* (non-carriers: M=8.4%, SD=6.2; carriers: M=8.3%, SD=5.6), *Eubacterium rectale* (non-carriers: M=8.3%, SD=10.5; carriers: M=7.9%, SD=8.6), *Faecalibacterium prausnitzii* (non-carriers: M=6.6%, SD=4.0; carriers: M=7.1%, SD=4.3), *Ruminococcus*

bromii (non-carriers: M=5.7%, SD=5.9; carriers: M=4.9%, SD=5.7) and *Prevotella copri* (non-carriers: M=2.6%, SD=6.1; carriers: M=4.7%, SD=10.6). With the exception of *P. copri*, which is a gram-negative bacterium of the *Bacteroidetes* phylum, the top five species are all gram-positive bacteria belonging to the *Clostridia* class (phylum: *Firmicutes*). Due to high inter-subject variability, the standard deviations were particularly high at species-level. Even the most abundant species were not present in all subjects. *P. copri*, for example, was absent in 12 samples, but occurred at a mean relative abundance of 30% in the community profiles of three participants.

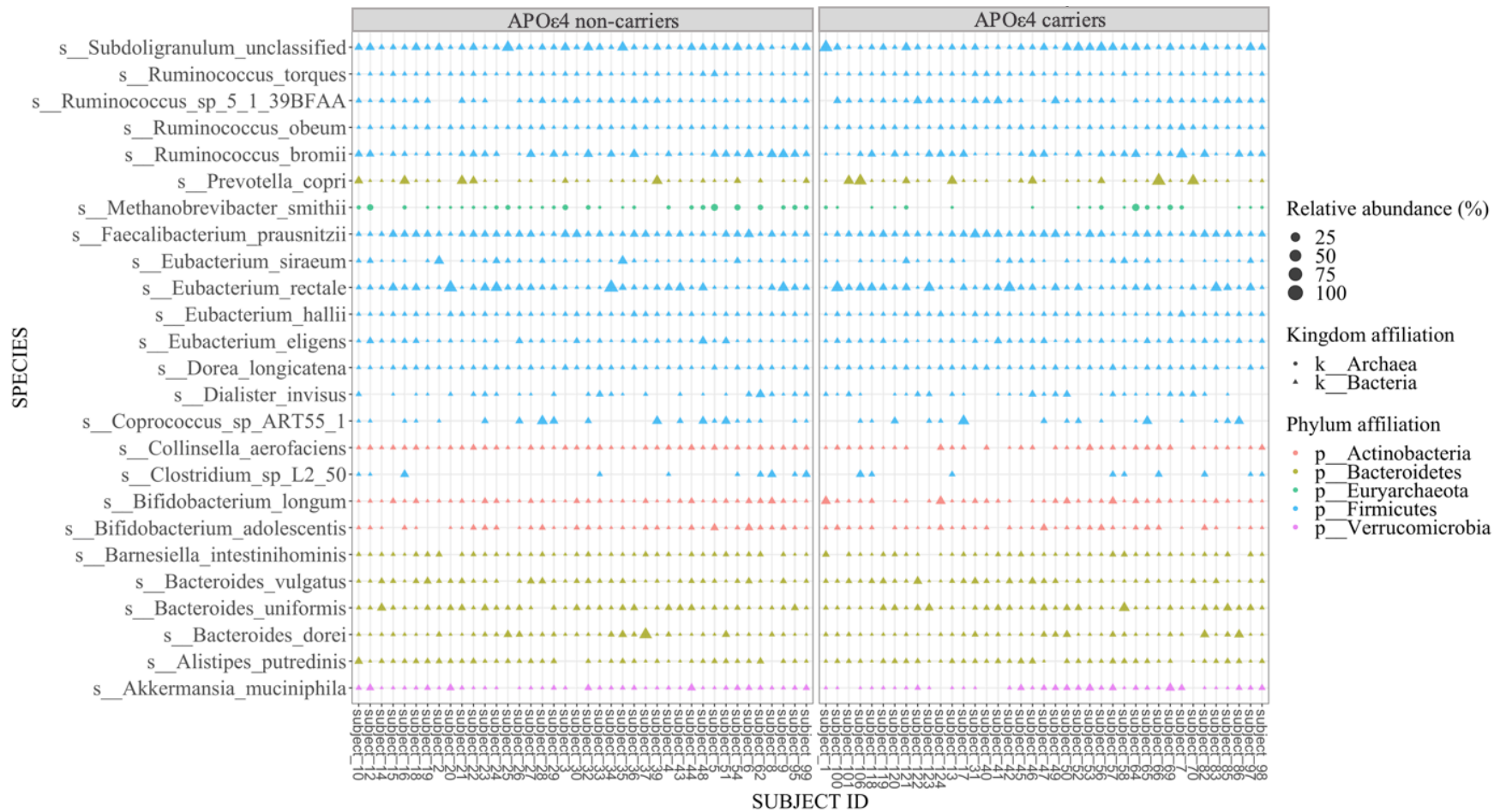


Figure 4.8 Top 25 most abundant species at baseline, Apolipoprotein ε4 non-carriers (left panel), Apolipoprotein ε4-carriers (right panel), shape showing kingdom affiliation, size represents relative abundance

Genera/Species - 6-months follow-up (T2)

Relative abundances of the most abundant genera at T2 showed only a few differences compared to baseline. The group of APO ϵ 4 non-carriers saw an increase in genera of the *Actinobacteria* clade - *Bifidobacterium* (M=9.5, SD=5.4) and *Collinsella* (M=3.5, SD=3.3) compared to T1, but a considerable decrease in *Bacteroides* (M=9.5, SD=5.4). The taxa making up the 25 most abundant species, from a total of 395 identified species, were largely comparable to baseline. As before, an unclassified species of the genus *Subdoligranulum* was the most abundant species, followed closely by *E. rectale* and *F. prausnitzii* (Figure 4.9, Table 4.4). In comparison to baseline, the community profiles at T2 were nominally higher in *Alistipes onderdonkii*, *Escherichia coli* and *Bacteroidetes stercoris*, but had decreases abundances of *Bacteroides dorei*, *Dialister invisus* and *Clostridium sp L2 50*.

Genera/Species - 12-months follow-up (T3)

The taxonomic profile at genera and species-level at T3 was comparable to the two previous time points. The community profiles at T3, were dominated by the same species as already observed before. Interestingly, *Methanobrevibacter smithii*'s relative abundance increased in a stepwise manner over the three timepoints (Table 4.4). The relative abundance for *P. copri* was almost twice as high in the group of APO ϵ 4 carriers compared to the non-carriers across all timepoints, whereas the community profiles of APO ϵ 4 non-carriers were consistently more abundant in *B. stercoris* than those of the APO ϵ 4 carrier group. Despite the large number of species detected, about 50% of the community profiles can be described by the 16 most abundant species (Figure 4.9).

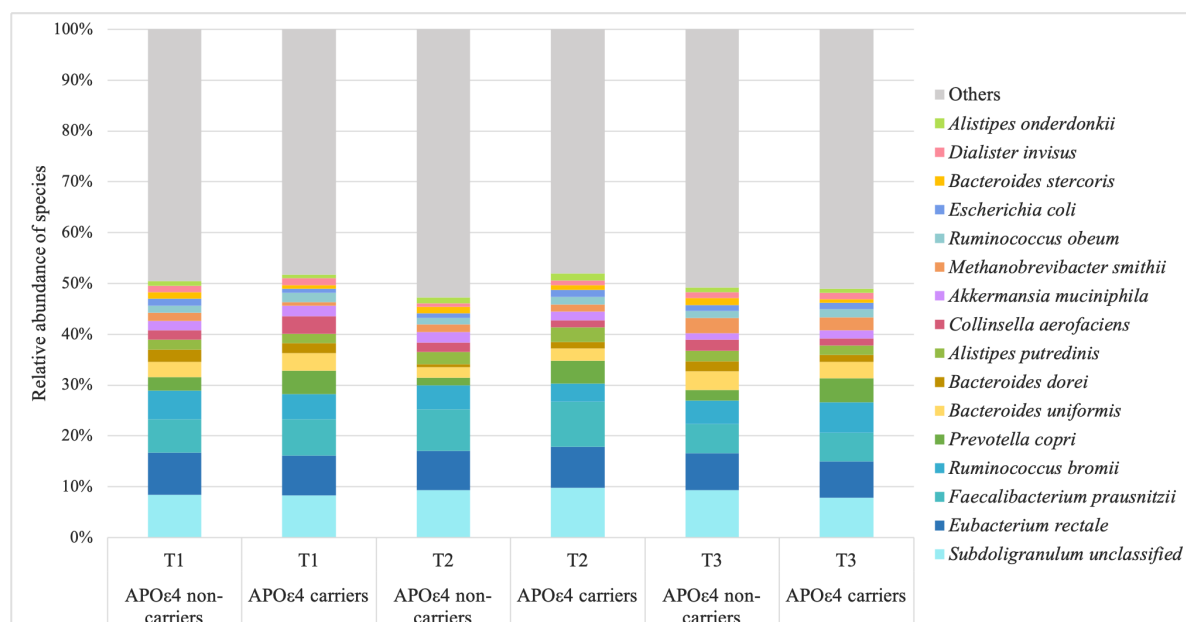


Figure 4.9 Relative abundances (%) of families between Apolipoprotein E groups over time

Table 4.4 Relative abundances (%) of most abundant species across all timepoints

Mean (SD)	APOε4 non-carriers			APOε4 carriers		
	T1	T2	T3	T1	T2	T3
<i>Subdoligranulum unclassified</i>	8.38 (6.27)	9.35 (6.85)	9.31 (5.59)	8.27 (7.81)	9.82 (8.87)	7.82 (6.93)
<i>Eubacterium rectale</i>	8.28 (10.52)	7.76 (10.26)	7.25 (7.30)	7.87 (8.55)	8.02 (7.91)	7.19 (7.38)
<i>Faecalibacterium prausnitzii</i>	6.60 (3.95)	8.13 (5.67)	5.78 (3.81)	7.11 (4.26)	8.89 (5.43)	5.59 (3.40)
<i>Ruminococcus bromii</i>	5.69 (5.92)	4.73 (5.05)	4.65 (4.78)	4.94 (5.68)	3.60 (5.53)	6.07 (7.00)
<i>Ruminococcus obeum</i>	1.37 (0.94)	1.26 (1.11)	1.44 (1.17)	1.85 (1.29)	1.59 (0.90)	1.66 (0.98)
<i>Prevotella copri</i>	2.64 (6.12)	1.49 (4.01)	2.03 (4.63)	4.70 (10.64)	4.51 (10.63)	4.72 (10.94)
<i>Alistipes onderdonkii</i>	0.86 (1.89)	1.11 (2.87)	0.92 (2.22)	0.69 (2.02)	1.38 (3.78)	0.84 (2.22)
<i>Alistipes putredinis</i>	1.96 (1.95)	2.41 (2.51)	2.05 (2.13)	1.89 (1.45)	2.84 (2.08)	1.86 (1.67)
<i>Escherichia coli</i>	1.38 (3.90)	0.85 (3.04)	1.13 (3.55)	0.78 (2.44)	1.30 (3.80)	1.16 (3.89)
<i>Bacteroides stercoris</i>	1.31 (2.61)	1.36 (2.31)	1.31 (2.56)	0.69 (1.44)	0.95 (2.01)	0.70 (1.51)
<i>Bacteroides dorei</i>	2.47 (5.79)	0.61 (0.78)	1.98 (4.88)	1.90 (3.54)	1.30 (1.90)	1.46 (2.17)
<i>Dialister invisus</i>	1.27 (2.78)	0.65 (1.41)	1.18 (3.17)	1.30 (2.20)	0.98 (2.58)	1.33 (2.41)
<i>Bacteroides uniformis</i>	2.97 (2.99)	2.03 (2.37)	3.70 (4.54)	3.41 (4.48)	2.35 (2.12)	3.13 (3.42)
<i>Akkermansia muciniphila</i>	1.79 (2.57)	2.04 (3.27)	1.27 (1.61)	2.14 (3.30)	1.70 (2.51)	1.57 (2.35)

<i>Methanobrevibacter smithii</i>	1.64 (2.84)	1.56 (3.32)	3.00 (4.32)	0.73 (2.46)	1.37 (4.12)	2.54 (7.09)
<i>Collinsella aerofaciens</i>	1.85 (1.23)	3.41 (3.16)	1.87 (1.20)	1.41 (1.64)	2.17 (2.61)	1.38 (1.42)
<i>Bifidobacterium longum</i>	1.62 (1.84)	3.20 (5.05)	1.31 (1.48)	2.21 (4.00)	2.48 (2.69)	1.68 (2.42)
<i>Bifidobacterium adolescentis</i>	1.60 (2.28)	4.23 (8.03)	2.07 (3.77)	1.33 (1.93)	1.69 (2.66)	1.15 (1.51)
<i>Eubacterium siraeum</i>	1.85 (4.08)	3.80 (8.20)	2.25 (4.64)	1.10 (1.92)	1.39 (2.81)	1.09 (2.34)
<i>Dorea longicatena</i>	1.67 (1.19)	1.64 (1.35)	2.21 (1.98)	1.85 (1.27)	1.78 (1.06)	2.01 (1.43)
<i>Ruminococcus torques</i>	1.22 (1.23)	1.49 (1.59)	1.58 (1.70)	1.26 (0.98)	1.19 (1.17)	1.44 (1.55)
<i>Ruminococcus sp5_1_39BFAA</i>	2.36 (1.77)	2.21 (1.86)	2.58 (2.64)	3.78 (3.49)	2.58 (2.12)	3.16 (2.65)
<i>Coproccoccus sp ART55_1</i>	2.79 (5.50)	2.77 (4.37)	2.36 (5.23)	2.31 (5.51)	2.69 (5.49)	3.37 (5.65)

Overall, the taxonomic profiles were comparable across the three timepoints and between the two groups, with some changes in the abundance of species. There was however marked individual variability as indicated by the large standard deviations. I next subjected the data to global measures of alpha and beta diversity to better understand the variability or stability of the taxonomic profiles of the APOE groups.

Alpha diversity: Between-group and intra-subject variability

Between-group variability

Baseline (T1)

There was no significant difference in alpha diversity between the two APOE cohorts at any taxonomic level, except at the kingdom-level. At kingdom-level, APOε4 carriers had significantly lower Shannon ($p=0.005$) and Inverse Simpson ($p=0.004$) diversity indices compared to the APOε4 non-carriers.

6-months follow-up (T2)

The between-group comparison of species richness and evenness at the 6-months follow-up was non-significant for all taxonomic levels.

12-months follow-up (T3)

In agreement with the baseline results, I found a significant difference in community differences at kingdom-level, as indicated by significantly reduced Shannon ($p=0.011$) and Inverse Simpson ($p=0.012$) diversity indices in the APOε4 carriers compared to the non-carriers. Community richness was also significantly lower in the APOε4 carriers at species level, but only when assessed with the Shannon diversity index ($p=0.044$).

Longitudinal comparison of alpha diversity indices (T1-T3)

At group-level, alpha diversity remained largely constant over time and between the groups apart from at T3. At the species level, the APOε4 non-carriers saw a reduction from 3.15 at baseline to 3.05 at T2, which then increased to 3.19 at T3. The mean alpha diversity of the APOε4 carriers remained stable (3.08-3.09) across all three sampling time points. All results of alpha diversity by APOE group are found in the Table 7.27 in the supplementary.

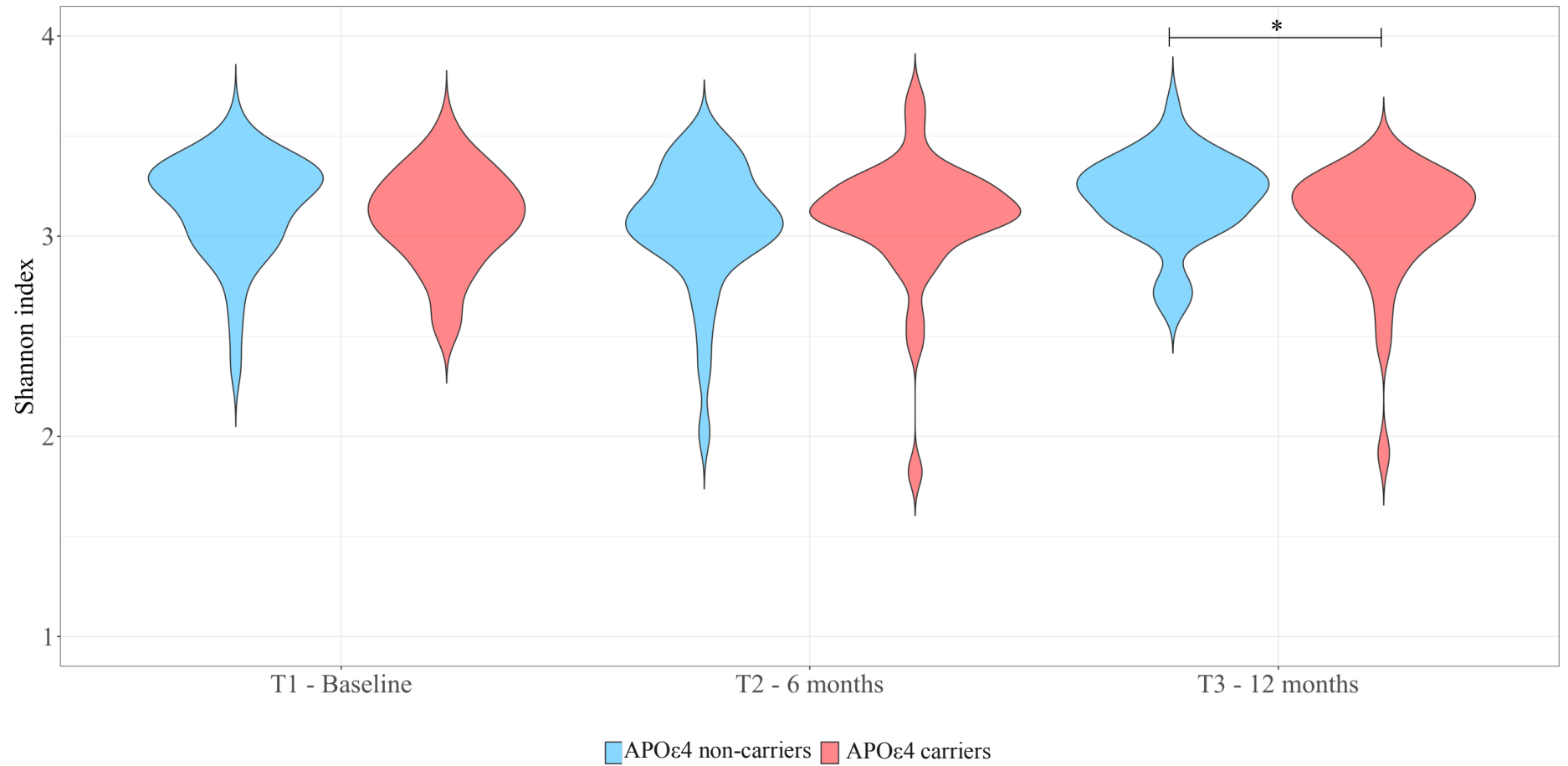


Figure 4.10 Alpha diversity (measured as Shannon diversity at species-level) between the groups at T1, T2 and T3. Blue: Apolipoprotein ε4 non-carriers, red: Apolipoprotein ε4 carriers. Statistical significance $* < 0.05$

Intra-subject variability

Alpha diversity varied to different degrees within subjects over time, with some exhibiting dynamic changes and others remaining stable over time (Figure 4.11).

Within the group of APO ϵ 4 non-carriers, the community profiles of three subjects (20, 37, 03) were among the ten least diverse at each time point. Another four samples of the APO ϵ 4 non-carriers (subjects 35, 39, 29, 95) were also among the least diverse at two out of three sampling time points.

Within the APO ϵ 4 carriers, subject 01 and 106 exhibited a low alpha diversity at all three time points. Subjects 123, 70, 13, 118 and 64 were amongst the ten least diverse at two of the three time points.

Examining the most diverse communities within the APO ϵ 4 non-carriers, four subjects (4, 10, 18 and 44) were seen amongst the top at three timepoints, whilst an additional four subjects (99, 27, 54, and 16) were amongst the most diverse at two time points. Within the APO ϵ 4 carriers, subjects 120, 69, 53 and 65 were amongst those with the most diverse communities at all three timepoints, and three subjects (101, 7 and 42) were amongst the top ten most diverse profiles at two time points.

Eight APO ϵ 4 carriers (subjects 42, 7, 124, 98, 13, 40, 101, 45) and three APO ϵ 4 non-carriers (5, 2, 12) were part of the most diverse samples, as well as part of the least diverse samples at different time points, showing a substantial degree of intra-subject variability over time.

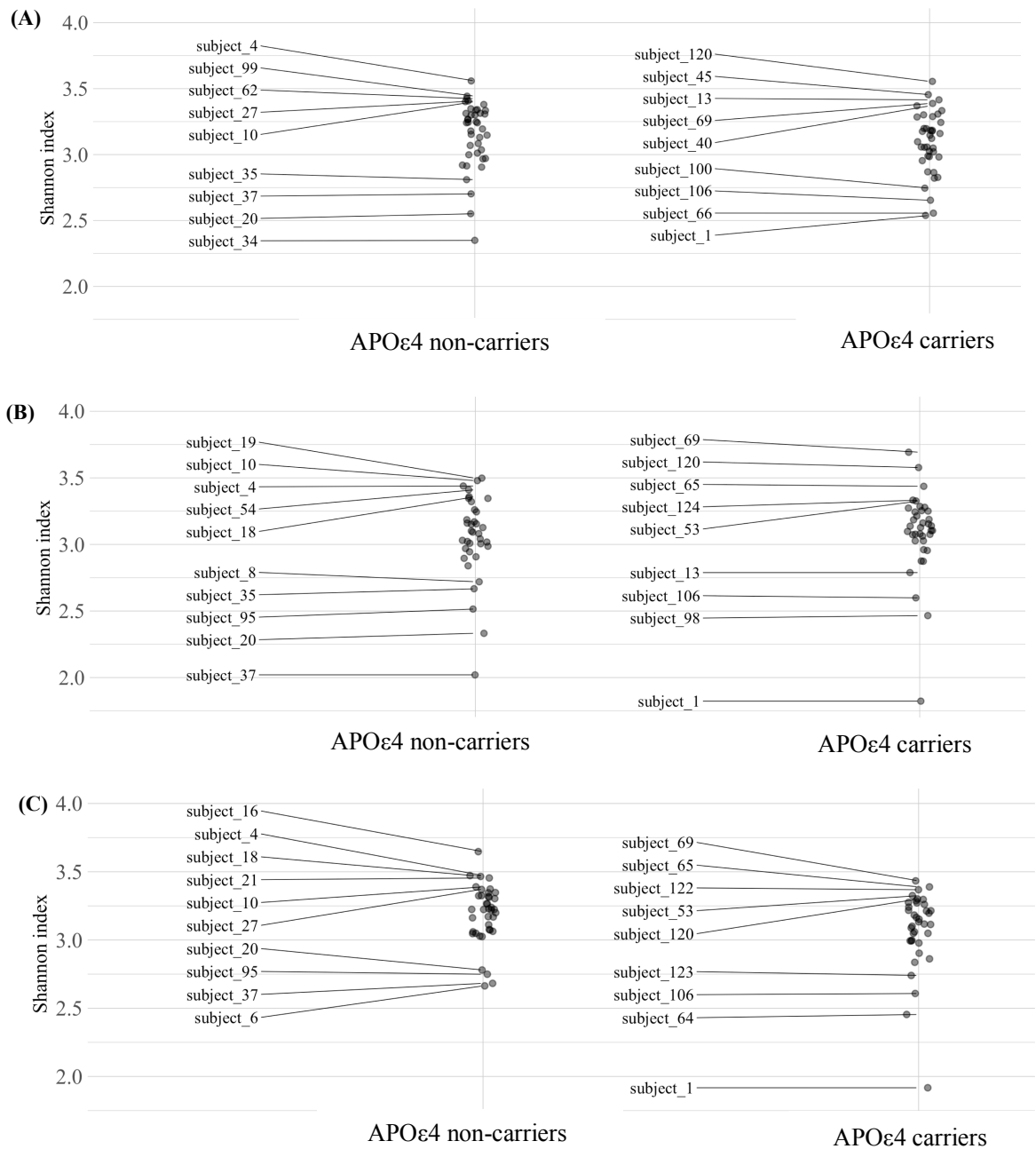
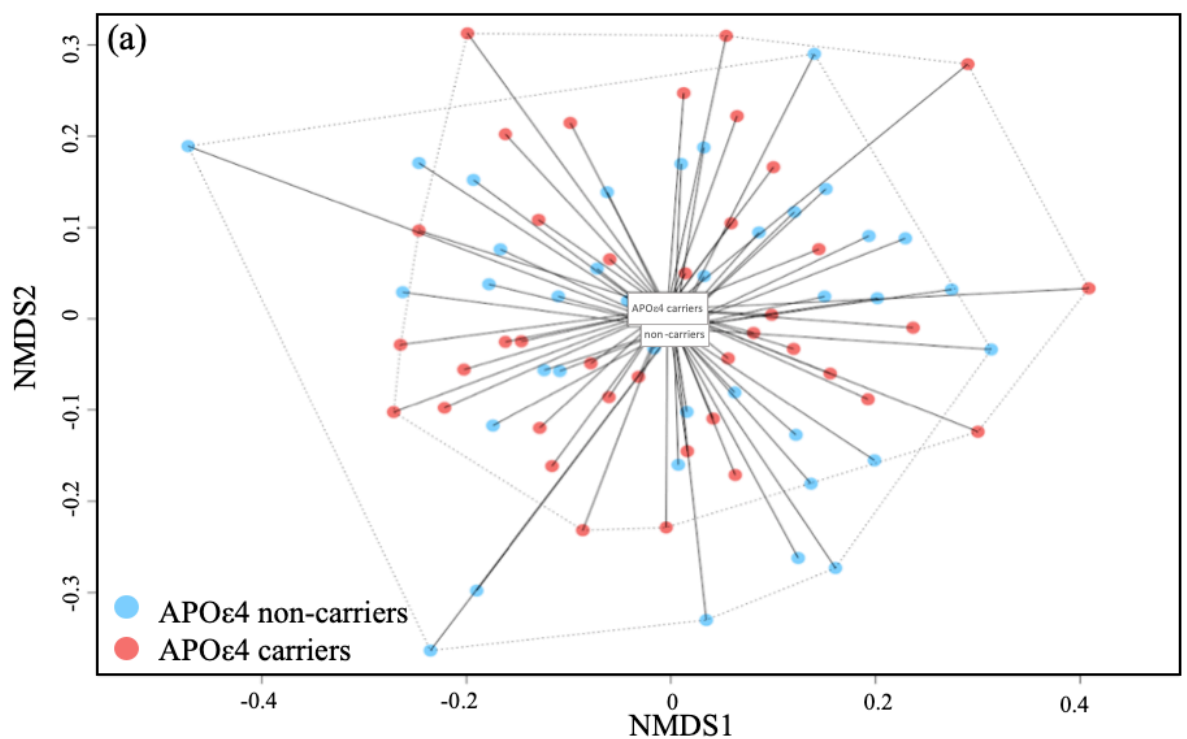


Figure 4.11 Scatterplot of Shannon diversity index, labelling of the most and least diverse samples of individual subjects at T1 (A), T2 (B), and T3 (C) by Apolipoprotein ε4 status

Beta diversity: Between-group diversity comparison

Beta diversity – Baseline (T1)

To examine the effect of APO ϵ 4 status, as well as the effect of the covariates sex (female [n=56], male [n=23]) and age (groups: 52-60 [N=20], 61-69 [N=38], 70-75 [n=21]) on the composition of the intestinal microbiota profiles, I performed a PERMANOVA on the between-sample Bray-Curtis dissimilarity and Jaccard index at all taxonomic levels (Table 7.28 in the supplementary). The PERMANOVA on the ordination at baseline showed that neither APO ϵ 4 status, or any of the covariates made a statistically significant contribution to the model, meaning that none of these factors significantly affected the overall composition of the intestinal microbiome (Figure 4.12).



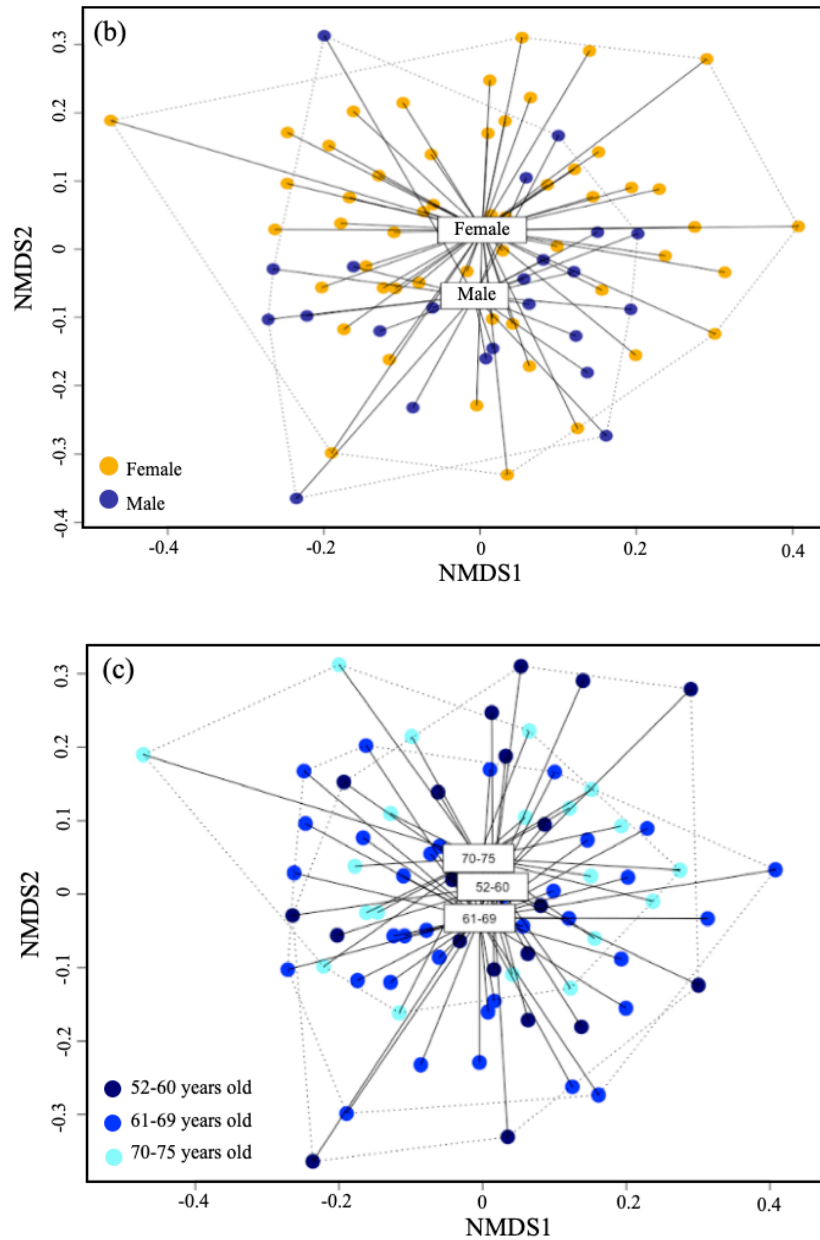


Figure 4.12 Non-metric multidimensional scaling on Bray-Curtis dissimilarity between the species relative-abundance intestinal microbiota profiles at baseline by (a) Apolipoprotein $\epsilon 4$ status, (b) sex, (c) age group. With labels denoting the centroid of points

Metric multidimensional scaling by PCoA of the same data (Figure 4.13) showed no graphical separation by genotype. On the contrary, the clusters were seen to be overlapping and further supported the finding that there were no large-scale compositional changes between the two APOE groups.

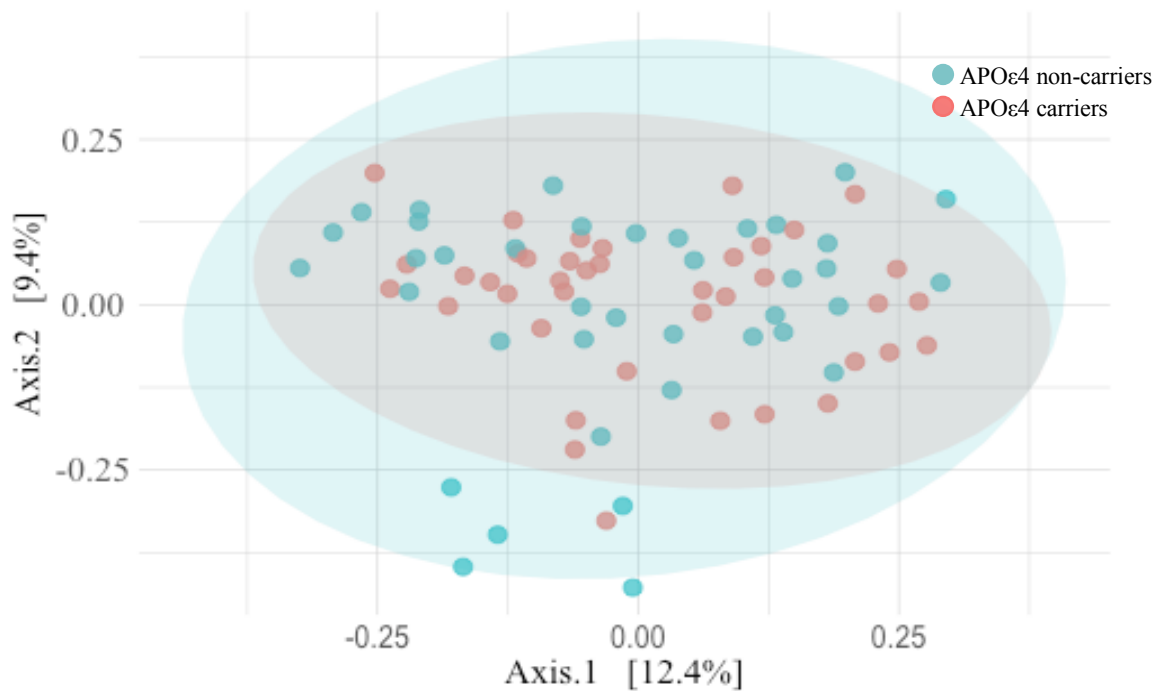


Figure 4.13 Principal component analysis on Bray-Curtis dissimilarity between the species relative-abundance intestinal microbiota profiles at baseline by Apolipoprotein ε4 status. Ellipse showing 95% confidence interval

Beta diversity – 6-months follow-up (T2)

APOε4 status and sex were the only factors able to explain significant differences in the intestinal microbiota profiles of participants at T2. APOε4 status was significant at phylum- ($p=0.024$), class- ($p=0.023$) and order-level ($p=0.03$, Figure 4.4), whereas sex was significant at the lower taxonomic level (family to species-level). APOε4 status was able to explain approximately 4% and sex 3% of the variation observed (Table 7.29 in the supplementary).

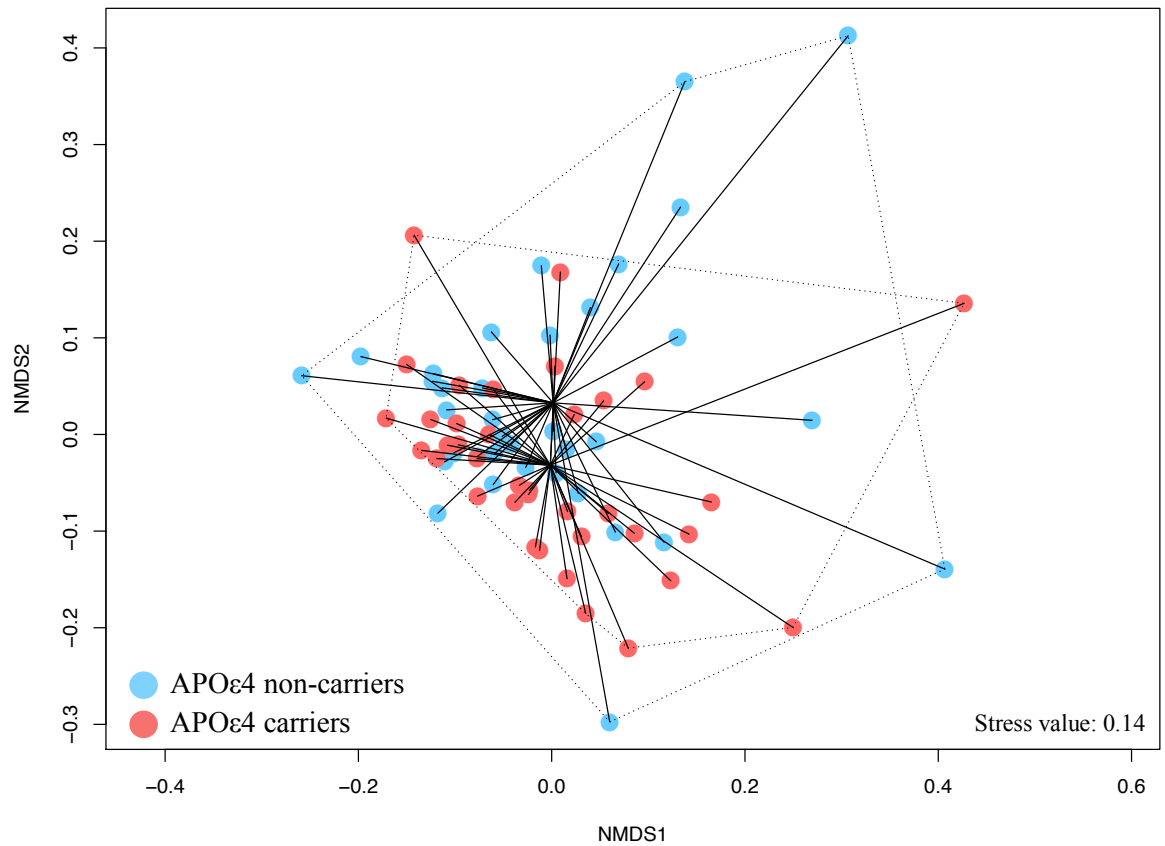


Figure 4.14 NMDS on Bray-Curtis dissimilarity on intestinal microbiota profiles at order-level by Apolipoprotein $\epsilon 4$ status (light blue = Apolipoprotein $\epsilon 4$ non-carriers, red = Apolipoprotein $\epsilon 4$ carriers) at T2. Each point denotes a sample in a reduced dimensional space and is connected with a line to the group centroid

I obtained similar results using Jaccard (rather than Bray-Curtis) as a dissimilarity index, with significant results for APO $\epsilon 4$ status at phylum-level ($p=0.018$), class-level ($p=0.027$), and at order-level ($p=0.030$). Sex was significant at family-level ($p=0.034$), genus-level ($p=0.021$), and at species-level ($p=0.007$). Age groups did not cluster separately.

Beta diversity – 12-months follow-up (T3)

APO $\epsilon 4$ status did not explain variation in the intestinal microbiota profiles at any of the taxonomic levels at T3 (Table 7.30 in the supplementary), which was also visually reflected by overlapping centroids (Figure 4.15). Age groups explained 7.9% of the variance at kingdom-level ($p=0.038$). In-line with the T2 results, sex explained approximately 3% of the variation at family- ($p=0.013$) and genus-level ($p=0.023$).

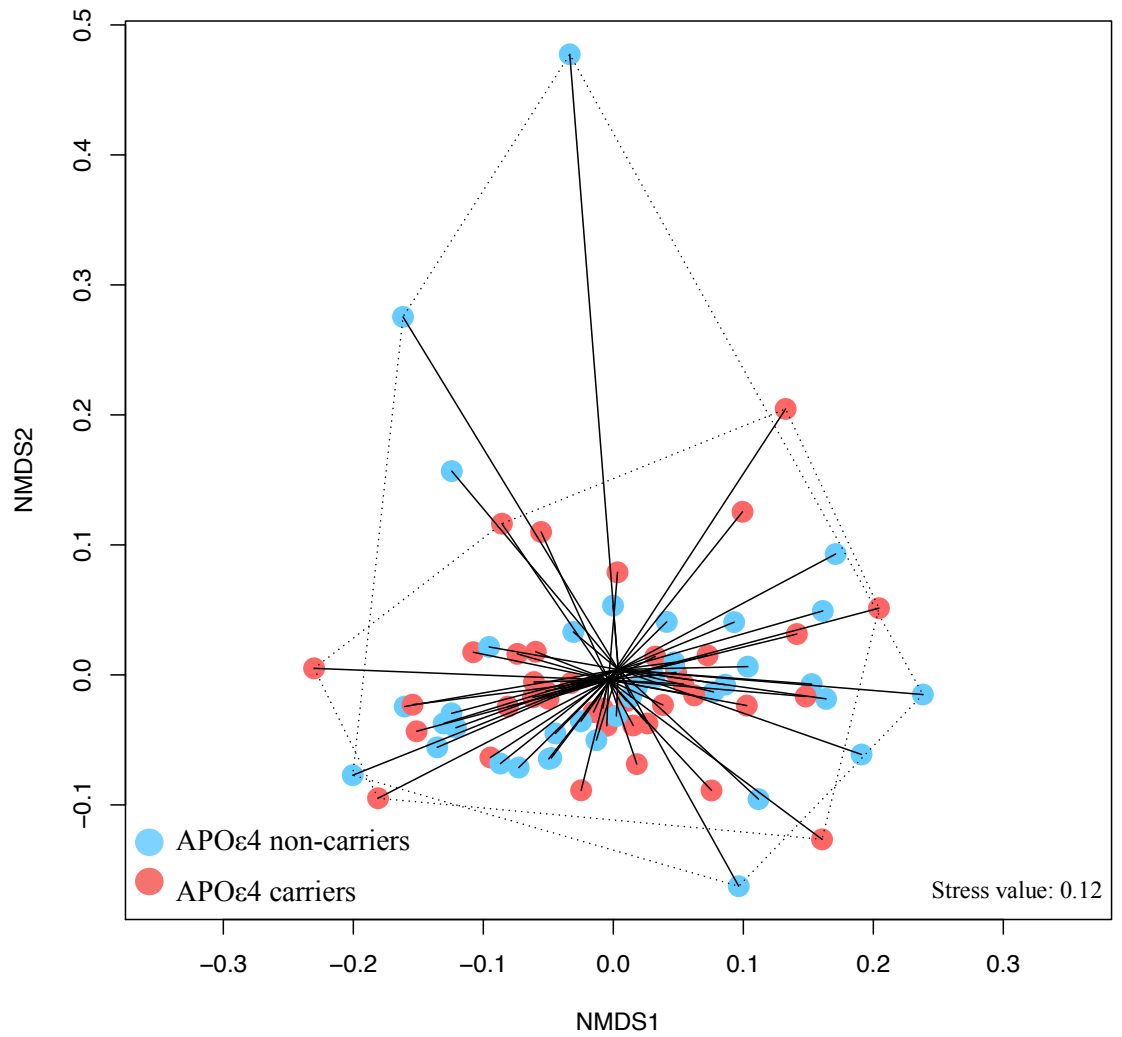


Figure 4.15 Non-metric multidimensional scaling on Bray-Curtis dissimilarity on intestinal microbiota profiles at order-level by Apolipoprotein $\epsilon 4$ status (light blue = Apolipoprotein $\epsilon 4$ non-carriers, red = Apolipoprotein $\epsilon 4$ carriers) at T3. Each point denotes a sample in a reduced dimensional space and is connected with a line to the group centroid

Differential abundance analysis

Univariate differential abundance analysis (LEfSe)

I next used univariate statistical tests to determine if specific bacterial taxa would be present at significantly different abundance levels between the two APOE groups at each of the timepoints.

LEfSe – baseline (T1)

In the absence of global differences at baseline, LEfSe identified a total of 24 taxa with LDA scores of 2.0 or above that were significantly enriched at $p < .05$ in the intestinal microbiota of the APOE4 non-carriers. By contrast, samples from the APOE4 carriers were significantly enriched for 12 taxa at $p < .05$ (Figure 4.16). Overall, 21 of the 36 discriminate features found by LEfSe were at species- or strain-level. A phylogenetic overview of the univariate analysis results is shown in Figure 4.17 (Table 7.31 – 7.32 in the supplementary).

In the APOE4 non-carriers, one clade (with eight taxa belonging to it) in particular, was found to be significantly higher in relative abundance compared to the APOE4 carriers. This clade had associations at each taxonomic level, starting at the *Archaea* kingdom down to strain-level of the species *Methanobrevibacter smithii*, accounting for a third of all discriminative taxa detected within the APOE4 non-carriers (Figure 4.17 - (D)).

Samples from APOE4 non-carriers were also enriched in several members down to strain-level belonging to the genus *Bacteroides* which is part of the order *Bacteroidales* (phylum *Bacteroidetes*) (Figure 4.17 - (A)). Besides the *Bacteroides*, I also saw increased levels of bacteria belonging to the *Alistipes* genus and the *Porphyomonadaceae* family.

The intestinal microbiota of APOE4 non-carriers was also more abundant in members of the *Actinobacteria* phylum, particularly a strain belonging to the species *Collinsella aerofaciens*

and an unclassified genus of the *Propionbacteriaceae* family (Figure 4.16 - (B)). APOε4 non-carriers also had a significantly higher abundance of members of the *Holdermania filiformis* species (phylum *Firmicutes*) and was enriched with members of an unclassified genus belonging to the *Sutterellaceae* family (phylum *Proteobacteria*).

The APOε4 carriers were characterized by higher abundance of the *Firmicutes* and *Bacteroidetes* phyla, with several members of the *Lachnospiraceae* family and *Bacteroidaceae* family being enriched (Figure 4.17 - (C)). Interestingly, different species of the *Bacteroides* genus were more abundant in both groups. Whilst *B. eggerthii*, *B. uniformis* and *B. stercoris*, were enriched in APOε4 non-carriers, APOε4 carriers had higher relative abundances of *B. intestinalis* and *B. cellulosilyticus* (Figure 4.17 - (A)).

To reduce the alpha error (as indicated by permutation analysis) and obtain a more conservative identification of discriminating features I adjusted the p-value of the Kruskal Wallis and the Wilcoxon rank sum test for subclass comparison to $p < 0.01$ (rather than 0.05). Following this adjustment, fewer discriminating taxa were significantly enriched in either APOε4 cohort. In the APOε4 non-carriers, only the eight members of the previously identified clade including the *Methanobacteria* class, *Methanobrevibacter* genus and *M. smithii* species survived the analysis. In the APOε4 carriers, only three significantly enriched taxa were identified. Beyond the kingdom level only the species *B. intestinalis* and its associated strain (*GCF_000172175*) were significantly enriched compared to the APOε4 non-carriers.

Collectively, these results highlight that whilst APOε4 status is not associated with global differences in the intestinal microbiota at baseline (as indicated by alpha and beta diversity measures), I am able to detect significant differences at the level of individual taxa and clades between the APOε4 non-carriers and carriers.

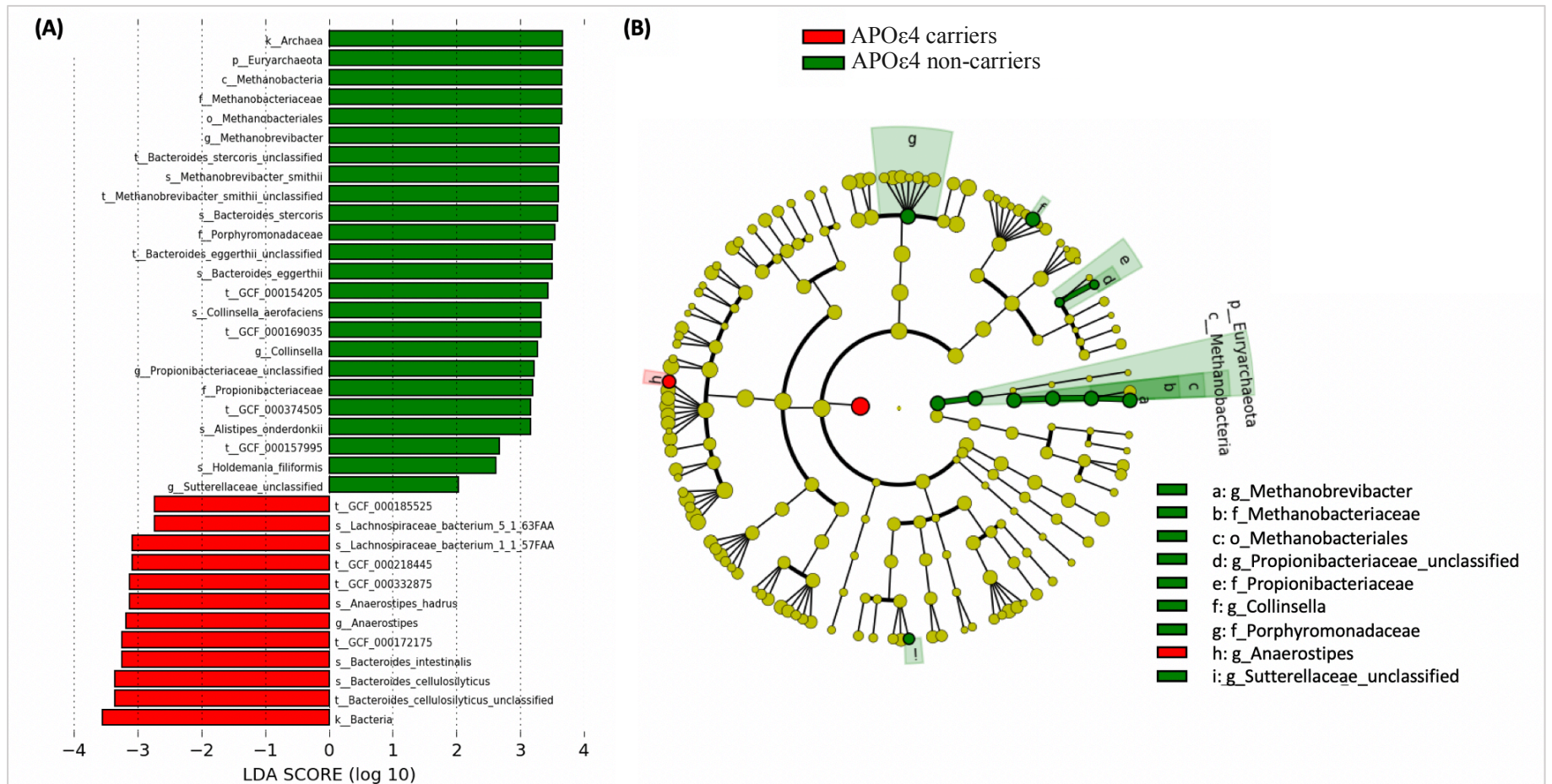


Figure 4.16 (A) Linear Discriminant Analysis effect size of discriminative taxa between Apolipoprotein ε4 non-carriers (green) and carriers (red) at baseline. Length of bar chart represents increasing abundance and associated Linear Discriminant Analysis scores are on a log₁₀ scale. (B) Cladogram showing results using saliency and phylogenetic relatedness for a clearer visualisation. Figures generated by LEfSe

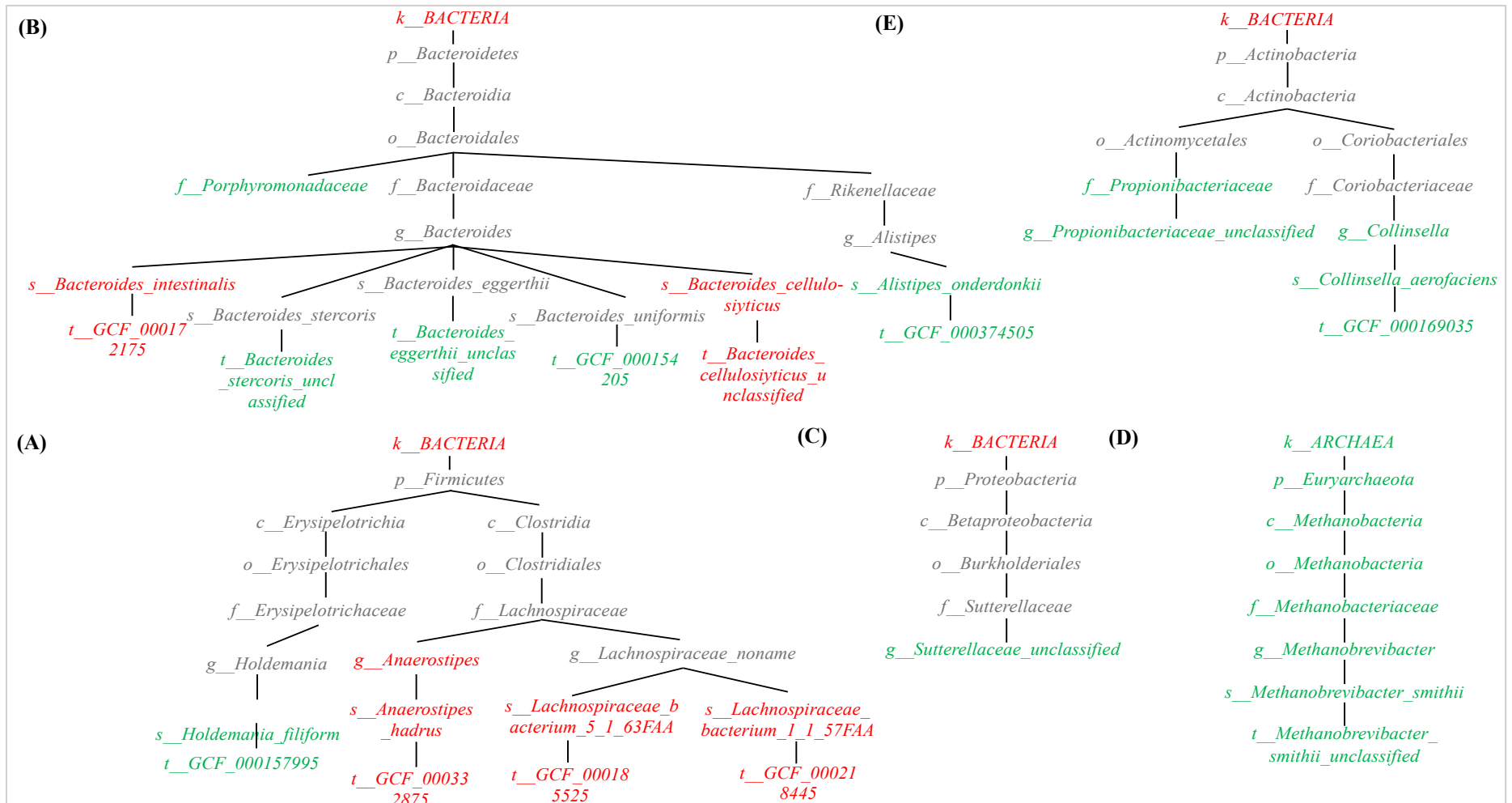


Figure 4.17 Phylogenetic overview of univariate analysis findings. (A) – (E) distinct clades. Green = significant enrichment of taxa in Apolipoprotein ε4 non-carriers, red = significant enrichment of taxa in Apolipoprotein ε4 carriers, grey = no significant association for taxa with Apolipoprotein ε4 status

LEfSe – 6-months follow-up (T2)

LEfSe identified two clades per group that characterized the differences between APOε4 non-carriers (16 associations) and APOε4 carriers (four associations) at T2 (Figure 4.18).

APOε4 non-carriers had a higher abundance of the *Actinobacteria* phylum and class, with enriched abundance for members of the *Atinomycetaceae* and *Coriobacteriaceae* families, including the species *C. aerofaciens* (non-carriers: M=3.41, SD=3.2; carriers: M=2.17, SD=2.6), *Atopobium parvulum* (average abundance <0.01%), *Actinomyces graevenitzii* (average abundance <0.01%) and associated strains.

There were two associations with members of the class *Clostridia* (phylum *Firmicutes*) with opposite direction for the two APOE groups. Whilst samples of the APOε4 non-carriers were enriched in members of the species *Clostridium methylpentosum*, the APOε4 carrier cohort was characterized by increased relative abundance for members of the *Ruminococcus obeum* species. It is however noteworthy, that *C. methylpentosum* was only present in very small abundances (<0.001% on average) and was absent in all but three participants. Mean relative abundance for *R. obeum* species was 1.26% (SD=1.1) in the APOε4 non-carriers and 1.59% (SD=0.9) in the APOε4 carriers. I further observed an association between APOε4 carrier status and *Bacteroides plebeius* and its associated strain which belongs to the genus *Bacteroides* and was significantly more abundant (albeit occurring at very low abundances) in samples of the APOε4 carriers (non-carriers: M=0.060, SD=0.2; carriers: M=0.064, SD=1.7).

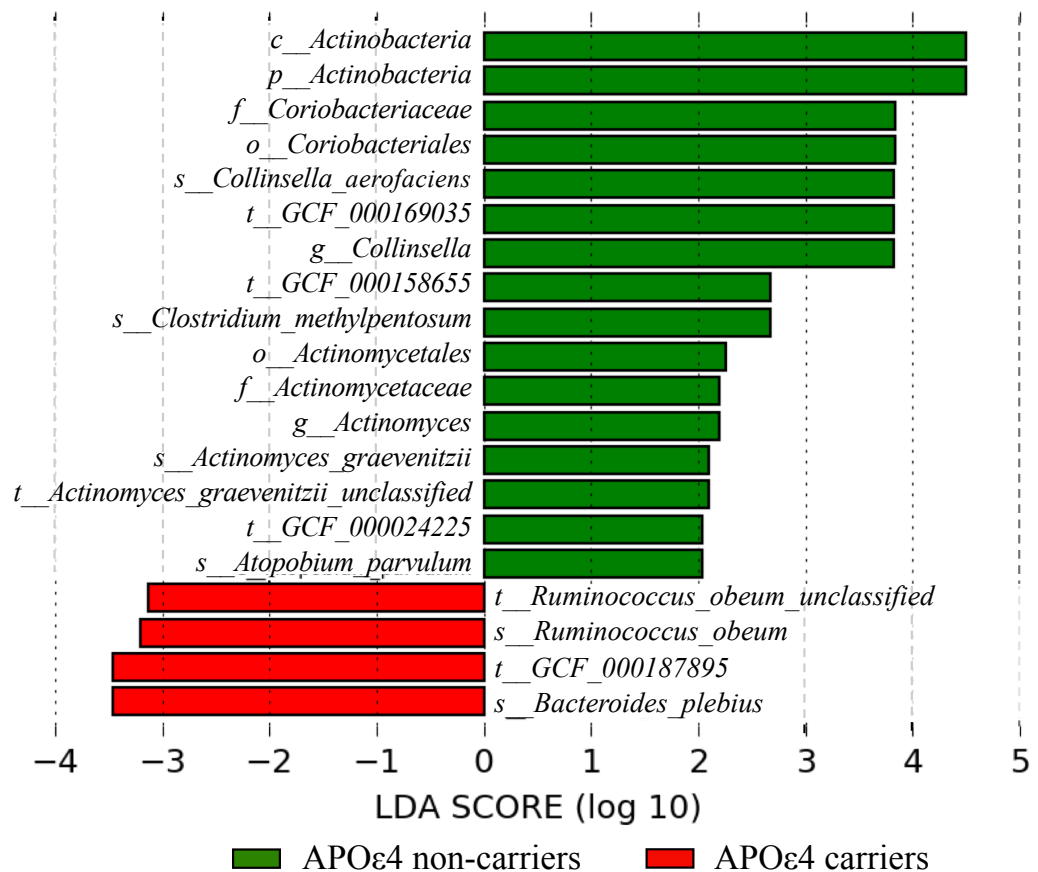


Figure 4.18 Linear Discriminant Analysis effect size of discriminative taxa Apolipoprotein ε4 non-carriers (green) and carriers (red) at the 6-months follow-up. Length of bar chart represent increasing abundance and associated Linear Discriminant Analysis scores are on a log10 scale

Upon further lowering the alpha value to $p < 0.01$ for the Kruskal Wallis (and the Wilcoxon rank sum test) and re-running LEfSe analysis, six associations of the previously identified discriminating taxa remained statistically significant. All six taxa were enriched in the APOε4 non-carriers and were taxonomically related to the *Actinobacteria* clade. Five of the six associations were members belonging to the order of *Coriobacteriales* including the previously identified *Coriobacteriaceae* family, *Collinsella* genus, *C. aerofaciens* species and its associated strain. The only other association surviving the alpha value adjustment, was the genus *Actinomyces*.

LEfSe – 12-months follow-up (T3)

LEfSe found a total of 52 associations with APOε4 status, 33 for the APOε4 non-carriers and 19 for the APOε4 carriers at T3. Of these 42% and 64% of associations in the APOε4 non-carriers and carriers, respectively, were at species- or strain-level (Figure 4.19). APOε4 carriers were significantly more abundant in members of the kingdom *Bacteria* and *Viruses*, whilst APOε4 non-carriers were enriched in *Archaea*. APOε4 carriers had higher abundance in *Streptococcus vestibularis* and *Streptococcus australis* and associated strains and were further enriched in the *Clostridiaceae* family and *Clostridium* genus of the *Firmicutes* phylum.

Within the *Actinobacteria* phyla, APOε4 carriers had higher abundances of the genus *Eggerthella* and an unclassified related species. The APOε4 carriers were also enriched in the *Escherichia* genus (phylum *Proteobacteria*), as well as for members of the *B. plebeius* species (phylum *Bacteroidetes*). Interestingly, APOε4 carriers were significantly associated with an unspecified *Virus* phylum, identifying seven associations with this particular clade related to an unclassified species (non-carriers: M=0.02, SD=0.4; carriers: M=0.69, SD=1.5) of the *C2likevirus* genus (family *Siphoviridae*, order *Caudovirales*) at a lower taxonomic level.

APOε4 non-carriers had significantly higher abundances of the *Archaea* clade, with enriched abundance at every taxonomic level down to the strain-level, including the class *Methanobacteria*, *M. smithii* species and an unclassified associated strain. APOε4 non-carriers also had several associations with members belonging to the order of *Coriobacteriales* of the phylum *Actinobacteria*. Whilst APOε4 carriers were enriched in the *Eggerthella* genus related to this order, APOε4 non-carriers were enriched in the order *Collinsella* and *Slackia*, including the species *C. aerofaciens* and *S. piriformis* and associated strains. Similar to APOε4 carriers, APOε4 non-carriers also showed associations at species-

level with the *Bacteroides* genus. Members of *B. intestinalis* and *B. stercoris* were enriched in APOε4 non-carriers.

APOε4 non-carriers were also characterized by increased abundance of several species and strains belonging to the family of *Lachnospiraceae*, *Eubacteriaceae* and *Clostridiales Family XI Incertae Sedis*, which in turn are all part of the *Clostridiales* order. The species *Dialister succinatiphilus* and an unclassified *Acidaminococcus* species, which are also part of the *Firmicutes* phylum, but belong to the order of *Selenomonadales*, were also enriched.

Upon further lowering the alpha value to $p < 0.01$ for the Kruskal Wallis and the Wilcoxon rank sum test, only 12 associations of the previously identified discriminating taxa remained statistically significant. For APOε4 carriers, these associations included the species *Bacteroides plebeius* and *Streptococcus vestibularis* and their associated strains. For APOε4 non-carriers, the entire *Archaea* clade, down to an unclassified strain of the *Methanobrevibacter smithii* species remained significant.

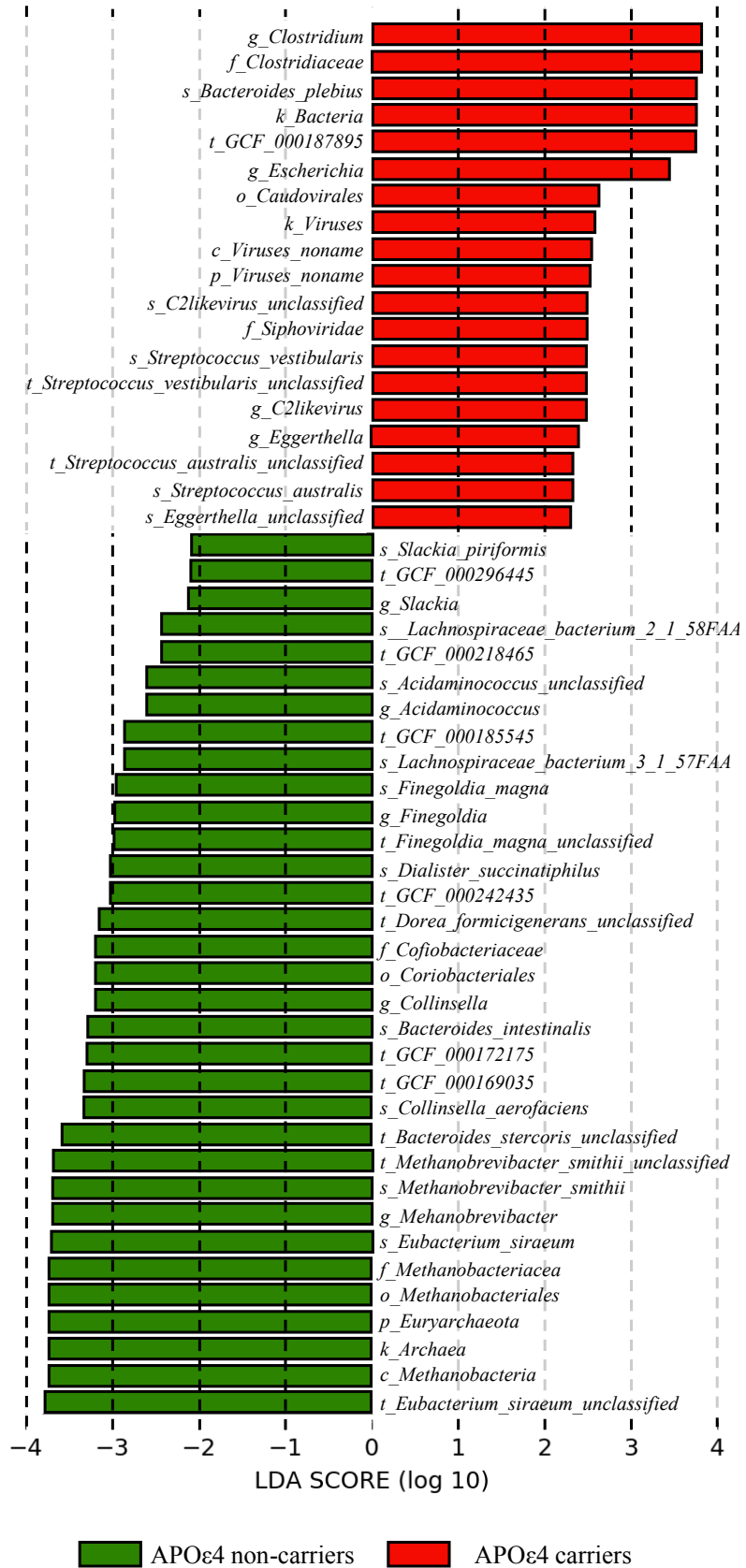


Figure 4.19 Linear Discriminant Analysis effect size of discriminative taxa between Apolipoprotein ε4 non-carriers (green) and carriers (red) at T3. Length of bar chart represent increasing abundance and associated Linear Discriminant Analysis scores are on a log10 scale

Comparison of LEfSe results across all three timepoints

Overall, there were considerably fewer discriminating taxa for APOε4 genotype (LDA score 2.0 or more) identified at T2 (20 associations) compared to baseline (35 associations) and the T3 (52 associations). Across all three timepoints, the number of associations for taxa enriched in APOε4 non-carriers was greater than in APOε4 carriers. More specifically, over two thirds of all associations at baseline, 80% of all associations at T2, and 63% of associations at T3 represented significant enrichment of taxa for the APOε4 non-carriers.

Increased abundance of *Archaea*, which includes the phylum *Euryarchaeota* and *M. smithii* species, characterised the intestinal microbiota of the APOε4 non-carriers at both T1 and T3. Within the *Bacteria* kingdom, I predominately found associations with APOε4 non-carriers and taxa from the *Actinobacteria*, *Bacteroidetes*, and *Firmicutes* phyla. At all three timepoints APOε4 non-carriers were also enriched in members belonging to the genus of *Collinsella*, *C. aerofaciens* species, and *GCF_000169035* strain – all of which belong to the *Actinobacteria* phylum. I also identified an unclassified strain of the *B. stercoris* species at both T1 and T3 for APOε4 non-carriers.

There were few replications of identical taxa identified at more than one time point in APOε4 carriers. All associations for T1 and T2 belonged to *Bacteroidaceae* or *Lachnospiraceae* families, whereas T3 had associations with taxa also belonging to the *Actinobacteria* and *Proteobacteria* phyla, as well as several associations with an unnamed *Virus* phylum. APOε4 carriers were significant enriched in the *Bacteria* kingdom at both T1 and T3. I also identified significantly increased relative abundances in member of the species *B. plebeius* and the *GCF_00187895* strain in samples at T2 and T3.

I found no differentially abundant taxa when running the univariate analysis on the combined dataset including all timepoints.

Multivariate differential abundance analysis (MaAsLin2)

Next, I attempted to gain an even better understanding for the role of APO ϵ 4 and to identify taxa associated with APO ϵ 4 status by accounting for the role of potentially confounding variables using multivariate linear modelling and adjusting the p-value for false positives.

MaAsLin2 – Baseline (T1)

After accounting for age and sex there were three taxa showing a significant difference in relative abundance between the two APOE cohorts (Table 7.33 in the supplementary). APO ϵ 4 carriers were significantly depleted in members of the *Verrucomicrobia* phylum ($\beta=-0.30$, false discovery rate [FDR]-corrected p-value=0.009) compared to APO ϵ 4 non-carriers (Figure 4.20). Out of the ten phyla that I identified and commonly occur in the human gastrointestinal tract, *Verrucomicrobia* was one of the less abundant phyla, with a mean relative abundance below 5%.

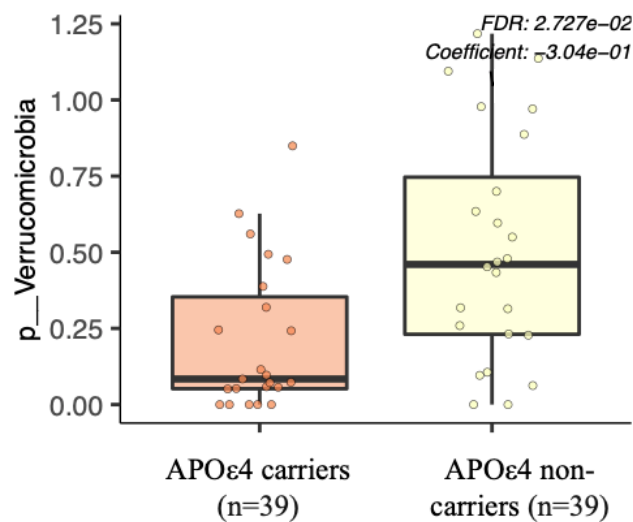


Figure 4.20 Boxplot of *Verrucomicrobia* between the Apolipoprotein E cohorts

The association between APO ϵ 4 genotype and *Verrucomicrobia* was also found to be significant at class level ($\beta=-0.30$, FDR-corrected p-value=0.018), and order level ($\beta=-0.30$, FDR-corrected p-value=0.025).

Comparison of differential analysis results (LEfSe vs MaAsLin2) for T1

Our univariate analysis identified associations between differences in relative abundance of taxa and APOε4 status, spanning many of the large phyla with the majority related to members of the *Bacteroidetes*, *Firmicutes* or *Actinobacteria* phyla. Multivariate analysis detected three associations belonging to members of the *Verrucomicrobia* phyla, which was not identified by the univariate analysis.

MaAsLin2 – 6-months follow-up (T2)

At T2, the multivariate differential abundance analysis identified two taxa that were significantly associated with APOε4 status, after accounting for the effect of sex and age and FDR-adjustment (Table 7.34 in the supplementary, Figure 4.21).

The relative abundance of the *Bacteroidetes* phylum ($\beta=3.42$, FDR-corrected p-value=0.046), was significantly increased in APOε4 carriers, which was also reflected by its mean relative abundance of 25.6% (SD=10.9) in the APOε4 carriers to 19.8% (SD=11.2) in the non-carrier group. I also observed reduction in relative abundance of the phylum *Actinobacteria* ($\beta=-0.76$, FDR-corrected p-value=0.033) in APOε4 carriers (M=7.65% SD=5.61) compared to the APOε4 non-carriers (M=13.44% SD=13.9).

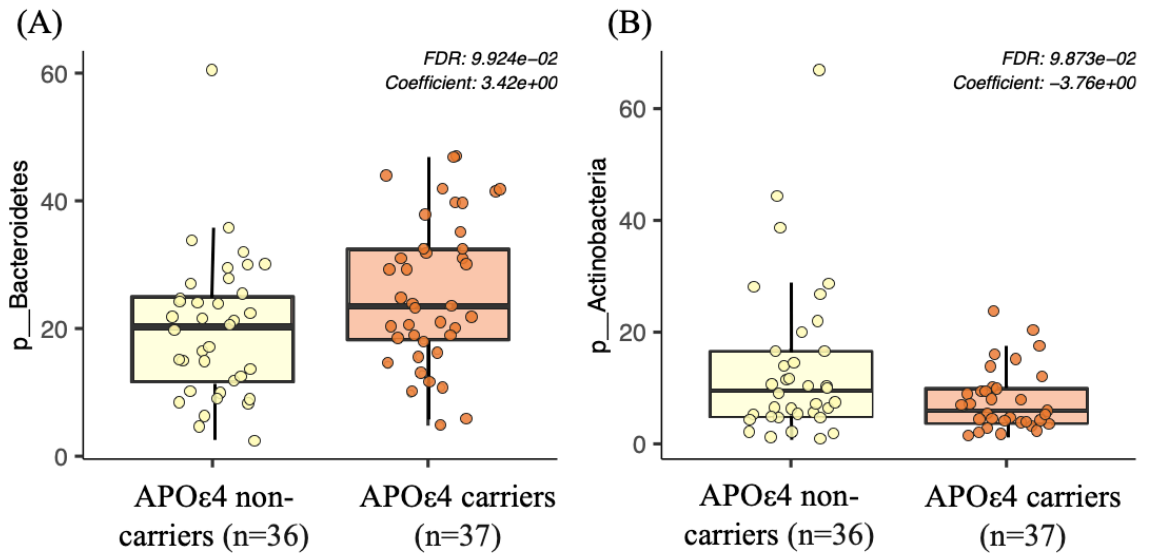


Figure 4.21 Boxplot of (A) *Bacteroidetes* and (B) *Actinobacteria* between Apolipoprotein E cohorts

Comparison of differential analysis results (LEfSe vs MaAsLin2) for T2

The univariate differential abundance analysis identified 20 significant associations between APOε4 status and taxa abundance. After further accounting for the effect of age and sex (multivariate analysis) only two taxa were associated with APOε4 status, after p-value FDR-adjustment. Overall, LEfSe found associations at all taxonomic levels, with the majority of associations at genus-level or higher resolution, whilst MaAsLin2 found no associations between APOε4 status and relative abundance for any taxa below the phylum-level.

Both analyses were consistent in identifying members of the *Actinobacteria* phylum being enriched in the APOε4 non-carriers compared to the APOε4 carriers. The *Bacteroidetes* phylum, which was depleted in the APOε4 non-carriers, was not identified by the univariate model. It did, however, identify *B. plebeius* species belonging to the *Bacteroidetes* phylum.

MaAsLin2 – 12-months follow-up (T3)

Participants were significantly distinct with respect to five phylogenetically related taxa following multivariate analysis at T3. APOε4 non-carriers had significantly higher relative abundances for the kingdom *Archaea* ($\beta=0.15$, FDR-corrected p-value=0.002), the phylum

Euryarchaeota ($\beta=0.15$, FDR-corrected p-value=0.005), its related class of *Methanobacteria* ($\beta=0.15$, FDR-corrected p-value=0.01), *Methanobacteriales* order ($\beta=0.15$, FDR-corrected p-value=0.014) and *Methanobacteriaceae* family ($\beta=0.15$, FDR-corrected p-value=0.03) compared to the APO ϵ 4 carriers (Table 7.35 in the supplementary, Figure 4.22). The overall group mean for *Methanobacteriaceae* at T3 was 3.10% (SD=4.43) in the APO ϵ 4 non-carriers and 2.69% (SD=7.76) in the APO ϵ 4 carriers, respectively.

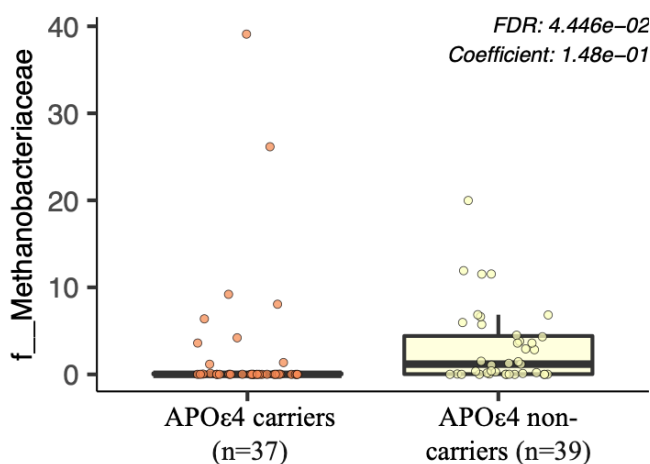


Figure 4.22 Boxplot of *Methanobacteriaceae* between Apolipoprotein E cohorts

Comparison of differential analysis results (LEfSe vs MaAsLin2) for T3

Whilst the number of taxa associated with APO ϵ 4 genotype was substantially smaller in the multivariate analysis (as seen for T1 and T2), the latter replicated the findings with respect to the *Archaea* clade. In the univariate analyses members of this clade were the only ones to survive further alpha error adjustment. The univariate analysis, did however, also identify members at genus-, species-, and strain-level.

MaAsLin2 – Longitudinal mixed effect model analysis of T1-T3

Using the combined datasets from all sampling timepoints, three taxa showed significant associations with APO ϵ 4 status at three taxonomic levels (Table 7.36 in the supplementary, Figure 4.23), belonging to two distinct bacterial clades. The family *Prevotellaceae* ($\beta=-6.08$, FDR-corrected p-value=0.031) and its associated genus *Prevotella* ($\beta=-6.33$, FDR-corrected

p-value=0.044), which both belong to the *Bacteroidetes* phylum, were significantly more abundant in APOε4 carriers compared to APOε4 non-carriers across all three timepoints. APOε4 status was also significantly associated with the species *R. obeum* ($\beta=-0.32$, FDR-corrected p-value=0.013), showing significant enrichment across all sampling timepoints in APOε4 carriers.

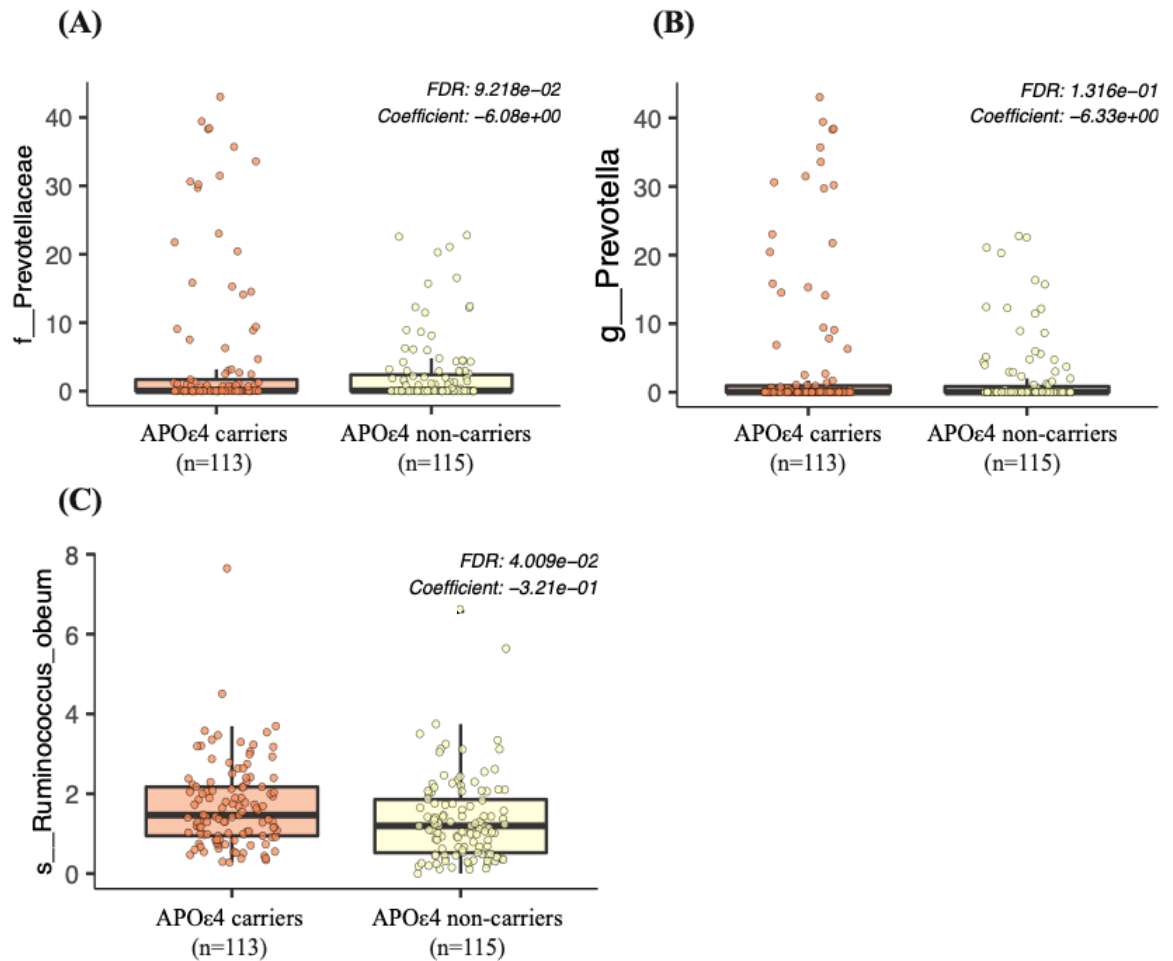


Figure 4.23 Boxplot of (A) *Prevotellaceae*, (B) *Prevotella*, and (C) *R. obeum* between the Apolipoprotein E groups across T1-T3

Interestingly, neither *Prevotellaceae*, nor *Prevotella* were identified by the univariate or multivariate models at any of the timepoints. *R. obeum* and an associated strain were detected to be significantly increased in the APOε4 carriers by the univariate analysis at T2.

Predictive Functional Profiling

I next sought to gain a better understanding of the intestinal community profiles of the two APOE groups with respect to their functional capability.

KEGG gene abundance data

The KEGG gene abundance table of the 219 submitted samples showed an average read count of 413,488 counts per sample, with a minimum of 111,798 and a maximum of 790,733 reads per sample. Data filtering (minimum count =1 in at least 10% of samples) removed a total of 2,661 low abundance features. This left 8,394 features for the ordination and multivariate analysis.

Beta diversity of KEGG data

The PERMANOVA on the beta diversity distance matrix for the KEGG metabolism, -modules, and -pathways was not significant for APOε4 status ($p > 0.05$ for all), whilst accounting for the effect of age and sex (Table 7.41 in the supplementary). Visualisation of the NMDS ordination for each of the levels further supported the lack of global functional differences as shown for the KEGG metabolism (KEGG module: Figure 4.24, KEGG modules and -pathways Figure 7.12 in the supplementary).

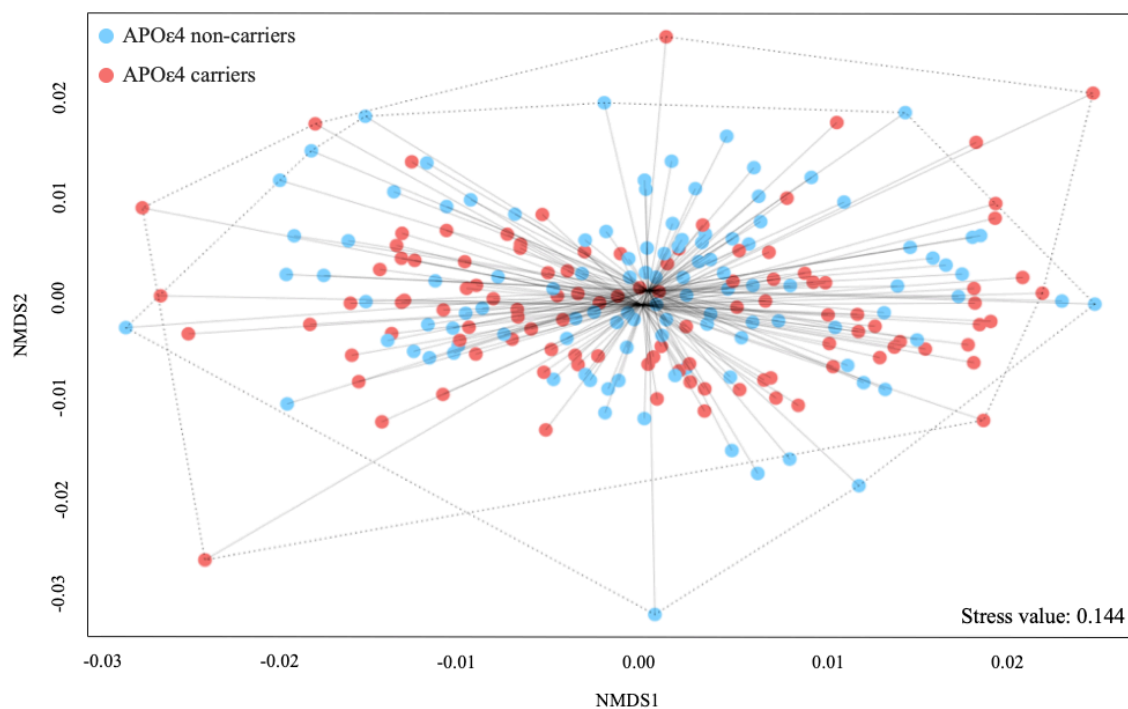


Figure 4.24 Non-metric multidimensional scaling of beta diversity (Jaccard index) between the predicted KEGG metabolism by group (light blue = Apolipoprotein ϵ 4 non-carriers, red = Apolipoprotein ϵ 4 carriers). Each point denotes a sample in a reduced dimensional space and is connected with a line to the group centroid

Multivariate analysis of normalized KEGG data

The multilinear mixed modelling of the KEGG data showed no significant association with APO ϵ 4 status at the level of KEGG metabolism. At the level of KEGG modules, I identified 14 significant features, whereas analysis of the KEGG pathways revealed a total of six significant associations for APO ϵ 4 status. After subjecting the significant results to FDR adjustment for multiple testing, none survived. Here, I present all findings with a significant p-value before FDR adjustment (Table 7.37 – 7.38 in the supplementary).

The predicted functional potential of the intestinal microbiota of the APO ϵ 4 carriers was significantly decreased for seven KEGG modules, comprising three KEGG modules involved in glycan metabolism including N-glycosylation by oligosaccharyltransferase (p=0.03) and N-glycan biosynthesis, complex type (p=0.039). Two modules involved lipid metabolism, namely acylglycerol degradation (p=0.003) and the biosynthesis of

phosphatidylethanolamine ($p=0.044$). Microbiota of APO ϵ 4 carriers also had a decreased functional potential for formaldehyde assimilation ($p=0.006$), as well as reduced capability for uridine monophosphate (UMP) biosynthesis ($p=0.038$) and for one-carbon C1-unit interconversion ($p=0.01$).

The microbial functional potential of the APO ϵ 4 carrier cohort was increased in seven KEGG modules compared to APO ϵ 4 non-carriers, of which five are related to energy metabolism. More specifically, one module involved sulphur metabolism (assimilatory sulphate reduction, $p=0.002$) and three modules involved in nitrogen metabolism and the reduction of nitrate to ammonia via the dissimilatory ($p=0.0001$) and via the assimilatory ($p=0.027$) pathway, as well as denitrification of nitrate to nitrogen ($p=0.044$). APO ϵ 4 carriers were also characterized by increased microbial functional ability of the pentose phosphate pathway (PPP) ($p=0.001$), the biosynthesis of monolignol ($p=0.039$) and the biosynthesis of capsaicin via L-Phenylalanine ($p=0.039$).

At the level of KEGG pathways, the intestinal microbiota of APO ϵ 4 carriers had a significantly decreased functional potential for glycine, serine and threonine metabolism ($p=0.014$) and for the biosynthesis of ansamycins ($p=0.028$) compared to APO ϵ 4 non-carriers. On the other hand, APO ϵ 4 carriers' microbial functional capability was significantly enriched for four distinct KEGG pathways compared to the non-carrier group which included an increased potential for fructose and mannose metabolism ($p=0.039$), aflatoxin biosynthesis ($p=0.040$), linoleic acid metabolism ($p=0.037$), and sulphur metabolism ($p=0.035$).

HUMAN3 functional profiles

All of the results reported here from the HUMAN3 analysis were significant after Bonferroni correction for multiple comparison (Table 7.39 – 7.40 in the supplementary).

The stratified output of the HUMAnN3 analysis showed that microbial communities of APOε4 carriers were significantly enriched in the relative abundance of the *P. copri* species (FDR-corrected p-value=0.011) and an associated strain (*P. copri* CAG:164, FDR-corrected p-value=0.002) compared to the microbiota of APOε4 non-carriers. Whereas the species *B. adolescentis* (FDR-corrected p-value=0.029) was significantly reduced in relative abundance in APOε4 carrier group compared to the non-carriers. All of the identified taxa were ‘unintegrated’, meaning that they did not contribute to a known pathway.

The unstratified pathways analysis showed 15 features that were significantly associated with APOε4 status. The microbial functional profiles of APOε4 carriers was characterized by significantly increased relative abundances of genes involved in the biosynthesis of 6-hydroxymethyl-dihydropterin diphosphate (FDR-corrected p-value=0.012), which is important in folate biosynthesis. I further found enrichment in the superpathway of phospholipid biosynthesis (FDR-corrected p-value=0.045), as well as for two associated pathways, the plastidic and non-plastidic biosynthesis pathways of phosphatidylglycerol (PG) (FDR-corrected p-value=0.045). Apart from this, APOε4 carriers also showed increased microbial functional potential for the CMP-3-deoxy-D-mannose-octulosonate biosynthesis I pathway (FDR-corrected p-value=0.045) and for the superpathway of L-aspartate and L-asparagine biosynthesis (FDR-corrected p-value=0.045).

The intestinal microbiota of APOε4 carriers showed decreased functional expression for seven pathways compared to APOε4 non-carriers. The intestinal community of APOε4 carriers were marked by a reduction in anaerobic energy metabolism (FDR-corrected p-value=0.012), as well as gluconeogenesis (FDR-corrected p-value=0.031). APOε4 carriers were further shown to have decreased expression of two pathways responsible for the biosynthesis of inosine monophosphate (IMP) (FDR-corrected p-value=0.045). The data also showed a decrease in the functional potential of APOε4 carriers for L-proline

biosynthesis (FDR-corrected p-value=0.046), L-histidine degradation (FDR-corrected p-value=0.046) and for a pathway involved in folate transformations (FDR-corrected p-value=0.046).

Chapter discussion

Key findings

Neither alpha- nor beta diversity measures indicated the presence of consistent large-scale differences between APOε4 non-carriers and carriers. Differential abundance analysis identified numerous taxa significantly associated with APOε4 status. Members of *Bacteroidetes*, the *Prevotella* genus and the species *R. obeum* were enriched in the APOε4 carriers compared to the non-carriers. Whereas the community profiles of APOε4 non-carriers showed higher relative abundances for *Verrucomicrobiales*, *Actinobacteria* and several members of *Archaea* including *Methanobrevibacter smithii*. Functional profiling of the intestinal microbiota identified several interesting pathways associated with APOε4 genotype, including a shift in energy metabolism, with a notable reduction of gluconeogenesis and an upregulation of the PPP and fructose and mannose metabolism in the APOε4 carriers' microbiota compared to that of non-carriers. The intestinal microbiota of APOε4 carriers further showed an upregulation in nitrogen metabolism, indicative of increased production of neurotoxic ammonia.

Detailed discussion

Besides this study, there is only the aforementioned study by Tran *et al.* (2019) that has investigated the impact of APOE genotypes on the intestinal microbiota. Comparing their study methodology to the methodology of this work, there are multiple important differences in the overall study design (cross-sectional vs repeated sampling), in the group assignment of subjects based on APOE genotype (four APOE genotypes vs presence or absence of the APOε4 allele), sequencing approaches (16S rRNA gene sequencing vs whole-genome

shotgun metagenomics sequencing) and other differences which make a direct comparison of results difficult.

Apart from Tran *et al.* (2019), I am only aware of two observational and one interventional study in mice which have investigated the relationship between APOE genotype and the murine intestinal microbiota. An overview of the main findings coming from these studies is summarized in Table 7.2 in the supplementary. Given the multitude of physiological differences between the human and murine intestinal tract, which are important determinants of microbiome constitution and function, any findings coming from mouse models have to be interpreted with caution and may not translate to humans.

To assess the stability and community diversity of the intestinal microbiota, I evaluated between-group differences in alpha diversity. Our APOE groups exhibited little variation in community richness/evenness over time or between the groups. Nonetheless, I observed a small but significant shift in the taxonomic community composition of APOE4 carriers at kingdom- (at T1, T3) and species-level (at T3) - indicating a loss in species richness compared to APOE4 non-carriers. Tran and colleagues (2019) found no significant difference in alpha diversity between the groups. A lack of consistent altered alpha diversity by APOE genotype is further supported by animal work (Maldonado Weng *et al.*, 2019; Parikh *et al.*, 2020).

Descriptive analysis showed some perceptible differences in the compositional profiles over time. Whilst there was a certain level of similarity, especially at the low-resolution taxonomic levels, I also observed the presence of new taxa and small shifts among the most abundant taxa at higher taxonomic levels. This is in-line with the literature which suggests that each body habitat (such as the intestinal microbiota) is characterized by a small set of relatively stable 'core' taxa. Apart from these core taxa, the literature suggests that

communities exhibit marked variation between people (Huttenhower *et al.*, 2012). Congruent with this, I observed large standard deviations with respect to relative abundances of taxa, which further supports the notion of large between-subject-variation.

Statistical investigation of the compositional profiles (beta diversity) between the APOE cohorts at the three sampling time points showed mixed results. At baseline and at the 12-months follow-up, APOε4 status did not affect the overall composition of the intestinal microbiota. At 6-months, however, APOε4 status was significantly associated with global differences in community structure at the phylum-, class- and order-level (3.7 % explanatory power). Thus, even when considering the combined effects of general demographic information (age and sex) and APOε4 status, I was unable to explain the majority of variation observed in the compositional profiles of the two APOE groups. Tran *et al.* (2019) showed no compositional differences by APOE genotype between their human subjects but show distinct clustering by APOE genotype in the murine intestinal microbiota. This is congruent with the work by Weng *et al* (2019) and Parikh *et al.* (2020) who reported significant compositional differences by APOE status between the two EFAD mice models.

I conclude that a significant association between APOε4 status and large global differences in the human intestinal microbiota structure cannot be supported by this study. Given that the intestinal microbiota is influenced by numerous factors and changes dynamically over time, it is difficult to detect a signal on a global measure (such as alpha and beta diversity). It is thus possible that large compositional differences are indeed present but are overpowered by the effect of other factors and can hence not be shown consistently.

Despite the absence of large-scale differences in the overall community structure by APOE genotype, there are numerous individual taxa whose relative abundances differed significantly between the two APOE cohorts. Our longitudinal multivariate assessment

identified the genus *Prevotella* and its associated family *Prevotellaceae*, which both belong to the phylum of the *Bacteroidetes*, to be increased in the APO ϵ 4 carriers compared to the APO ϵ 4 non-carriers. Tran *et al.* (2019) showed that their APO ϵ 3/ ϵ 4 carriers as well as their APO ϵ 3/ ϵ 3 had a greater abundance in *Prevotellaceae* compared to APO ϵ 2/ ϵ 3 carriers. A significant association of *Prevotellaceae* with APOE genotype is also supported by animal studies. However, whilst Parikh and colleagues did not report directionality of the association, Weng *et al.*' observation is contrary to this study's and Tran's results as they reported depletion of *Prevotella* in APO ϵ 4 homozygous mice. Although *Prevotella* has been ascribed largely health-promoting properties, some evidence supports a potential pathological role (Iljazovic *et al.*, 2021). Overabundance of members belonging to this genus has been associated with insulin resistance, T2D, intestinal inflammation, and rheumatoid arthritis (Pedersen *et al.*, 2016; Leite *et al.*, 2017; Stoll, 2020; Iljazovic *et al.*, 2021). And whilst the immunomodulatory action of *Prevotella* is incompletely understood, *Prevotella* overabundance may cause a decrease in colonic IL-18 levels and stimulate the release of inflammatory mediators, which in turn may promote intestinal inflammation and dysbiosis, and lead to a reduction of acetate-producing bacteria (Larsen, 2017; Iljazovic *et al.*, 2021). Increased *Prevotella* abundance may thereby shift the intestinal microbiota towards a pro-inflammatory state, which in turn could trigger a series of events that might contribute to developing AD.

APO ϵ 4 carriers were also enriched in *R. obeum* (longitudinal multivariate analysis, univariate analysis at T2). Despite its name, this species belongs to the genus *Blautia* and not *Ruminococcus* (Lawson and Finegold, 2015). The *Blautia* genus (family *Lachnospiraceae*, order *Clostridia*) is comprised of over 20 species of strict anaerobes which are generally considered to have probiotic properties. In the human intestinal microbiota, *Blautia* species are the main producers of the SCFA propionate via succinate and propanediol pathways from fructose and rhamnose (Vacca *et al.*, 2020). *R. obeum* has been

suggested to produce acetate from hydrogen gas and carbon dioxide. Members of the genus *Blautia* are associated with lower levels of indole-propionic acid, which plays an important role in host gut barrier function and antioxidant activity (Menni *et al.*, 2019). *Blautia* overabundance is however also associated with IBS (Rajilić-Stojanović *et al.*, 2011; Nishino *et al.*, 2018). Collectively, this suggests pleiotropic effects of *Blautia* on host health.

The intestinal microbiota of APOε4 non-carriers at T1 and T3 was characterized by increased relative abundance of an *Archaea* clade down to strain-level, including the *Methanobacteriaceae* family and *M. smithii* species. This is the most robust finding generated by the univariate analysis as it also survived strict filtering for type I errors. An association between APOε4 status and this clade is also supported by the multivariate analysis, which identified five members of this clade at T2. Members of this clade are methanogenic archaea which play a key role in host metabolism by converting dihydrogen (H₂), an end-product of bacterial fermentation, and carbon dioxide to methane (Camara *et al.*, 2021). *M. smithii* is a common colonic commensal, which protects against oxidative stress by reducing carbon dioxide to methane (Garcez, Jacobs and Guillemin, 2019). Build-up of H₂, on the other hand, inhibits fermentation of polysaccharides. Methane production is thus associated with altered SCFA metabolism and increased abundance of methanogenic archaea favours increased production of acetate (Fernandes *et al.*, 2013). In the context of ageing, methanogenesis may represent a protective mechanism to counteract oxidative stress, which is a major contributor to AD pathogenesis (Emerit, Edeas and Bricaire, 2004; Sharma *et al.*, 2019). As such the reduction of this species in APOε4 carriers might compromise the protective action of methanogenic archaea, and impact on the production of acetate and other SCFAs.

B. plebeius, *B. intestinalis* and *B. cellulosilyticus* were enriched in APOε4 carriers whereas the group of non-carriers had increased abundances of *B. eggerthii*, *A. onderdonkii* and strains of the *Bacteroidetes* phylum. Tran *et al.* also support modulation of the *Bacteroides*

by APOE genotype – the murine community profiles of APOε4 homozygous mice were marked by increased relative abundances of *Bacteroides* and *Bacteroidaceae* compared to controls. As the second most abundant phylum in the human intestinal microbiota, *Bacteroidetes* are obligate anaerobes with a wide range of beneficial and health promoting functions (Zafar and Saier, 2021). However, if translocated outside of the gastrointestinal tract *Bacteroidetes* can contribute to systemic infections. Future work is needed to better understand the specific role and potential relevance of *Bacteroidetes* and its many different species.

The intestinal microbiota of APOε4 non-carriers showed increased relative abundances for several families of the *Actinobacteria* compared to APOε4 carriers across all three sampling time points. This enrichment included the family of *Coriobacteriaceae*, its associated genus *Collinsella* and the species *C. aerofaciens* (and a related strain). A corresponding decrease in the phylum *Actinobacteria* in APOε4 carriers was also supported by the multivariate analysis. *Collinsella* ferment a large range of carbohydrates producing H₂, lactate, ethanol and SCFAs, and can modulate bile acid metabolism and peripheral cholesterol levels (Rajilić-Stojanović and de Vos, 2014). Several strains, including the here found *C. aerofaciens*, are considered pathobionts, whose increased abundance is linked with IBS (Kassinen *et al.*, 2007) and rheumatoid arthritis (Chen *et al.*, 2016). This association is inconsistent with the health promoting properties and functions ascribed to *C. aerofaciens*, which is also a producer of butyric acid (Qin *et al.*, 2019). A potential mechanistic role for *C. aerofaciens* and other *Actinobacteria* members in APOε4 carriers should be addressed in future work.

Our multivariate abundance analysis at baseline showed that APOε4 carriers are significantly depleted in members of the order *Verrucomicrobiales*, its' associated class and phylum. The evidence regarding *Verrucomicrobiales* is limited. The best-studied member

of this clade is the species *A. muciniphilia*, a mucin-degrading bacterium, which plays a role in maintaining the mucus layer of the intestinal epithelial barrier (Hoffman *et al.*, 2019). *A. muciniphilia* is also suggested to mediate glucose tolerance (Haikal, Chen and Li, 2019). Decreased abundances of *A. muciniphilia* have been identified in a range of metabolic conditions, such as obesity, dyslipidaemia and T2D. In the context of PD, however, an increase in abundance for members of the *Akkermansia* genus is considered a defining feature of the PD microbial signature (Baldini *et al.*, 2019; Haikal, Chen and Li, 2019). Future work is needed to investigate what potential role members of these taxa may have in the context of APO ϵ 4 genotype.

The functional potential of the intestinal microbiota in Apolipoprotein ϵ 4 carriers and non-carriers

The functional potential of the intestinal microbiota in APO ϵ 4 carriers was reduced with respect to several modules relating to lipid-, glycan-, methane- and pyrimidine metabolism. Regarding lipid metabolism, I observed a decreased potential for the breakdown of the acylglycerol (esters of glycerol and fatty acids) as well as reduced potential for the biosynthesis of ethanolamine (EA) to phosphatidylethanolamine (PE) (Weete, 1980). Little is known about acylglycerol apart from its fundamental role in lipid membranes (Blanco and Blanco, 2017). PE synthesis deficiency is suggested to have negative effects on intestinal membrane barrier integrity and is associated with metabolic and inflammatory diseases, including IBD (Brown *et al.*, 2019; Zhou *et al.*, 2020). The synthesis of sphingolipids, such as EA and PE, is restricted to members of *Bacteroidetes*.

The functional potential of the intestinal microbiota of APO ϵ 4 carriers was also significantly decreased with respect to N-glycan biosynthesis and N-glycosylation. N-linked glycosylation is mediated by oligosaccharyltransferase and may play a role in AD development, negatively affecting tau protein and APP (Schedin-Weiss, Winblad and

Tjernberg, 2014; Kizuka, Kitazume and Taniguchi, 2017). In the brain, protein phosphorylation and glycosylation may be an early biomarker for AD (Lassen *et al.*, 2017). The notion that glycan metabolism is impaired in AD is supported by the work of Liu and colleagues (2019), who showed that N-glycan biosynthesis in the intestinal microbiota was decreased in a cohort of AD patients compared to healthy controls and patients with aMCI (Liu *et al.*, 2019). The intestinal epithelial glycome also plays a role in IBD aetiology, where alterations to glycosylation processes contribute to inflammation and compromising the mucus barrier (Kudelka *et al.*, 2020). Although there is no data available on glycan metabolism in APO ϵ 4 besides this research, this pathway might represent an interesting target for future research.

Knowledge of the uridine monophosphate biosynthesis, which was reduced in the intestinal microbiota community of APO ϵ 4 carriers, is incomplete. It has been suggested that UMP maintains intestinal health and is important in the development and apoptosis of enterocytes (Sato *et al.*, 1999). Supplementation with oral UMP in an animal model of pigs had positive effects on the permeability of the intestinal epithelial barrier (G. Li *et al.*, 2019).

There was also a reduction in the microbial functional ability of APO ϵ 4 carriers for ansamycin biosynthesis. This pathway describes the production of small compounds with potent anti-bacterial and anti-inflammatory properties and is inherent to *Actinomyces* strains (Vardanyan and Hruby, 2016). This is in line with the observation of a decrease in *Actinomycetales* in APO ϵ 4 carriers compared to non-carriers. Even though ansamycins might be a potentially promising target with suggested inhibitory action against LPS-induced nitric oxide (NO) production (Tang *et al.*, 2018), I found no evidence of their use as an anti-inflammatory therapeutic.

An accumulating body of evidence suggests that APO ϵ 4 genotype is connected with impaired glucose and insulin pathways (Janak *et al.*, 2020; Koren-Iton *et al.*, 2020), which is strengthened by the fact that glucose hypometabolism in the brain is a hallmark feature of AD (Hammond *et al.*, 2020; Janak *et al.*, 2020). In this study, the intestinal microbiota of APO ϵ 4 carriers showed a decrease in gluconeogenesis. Community profiles of APO ϵ 4 carriers also showed a downregulation in anaerobic energy metabolism pathways but an increased potential for the PPP compared to the intestinal microbiota of APO ϵ 4 non-carriers. The latter pathway counteracts oxidative stress and is an alternative pathway for glucose metabolism (Riganti *et al.*, 2012) as is explained in detail later p. 280.

In a study investigating the metabolome of hippocampal tissue from APO ϵ 3 and APO ϵ 4 homozygous mice, fed a high-fat or low-fat diet, the PPP was shown to be significantly associated with APO ϵ 4 status regardless of diet (Johnson *et al.*, 2017). This supports a relationship between PPP and APO ϵ 4 albeit in eukaryotic rather than microbial cells.

The microbiota of APO ϵ 4 carriers was characterized by enrichment of several microbial pathways related to nitrogen metabolism, including denitrification and nitrate reduction to ammonia via the dissimilatory and assimilatory pathway. Ammonia, with its powerful neurotoxic effects, may play a role in the disease progression of AD, giving rise to the ammonia hypothesis of AD in 1993 (Seiler, 2002; Adlimoghaddam, Sabbir and Albeni, 2016). This hypothesis is supported by the evidence discussed on p.279 suggesting a strong link between intestinal-related production of ammonia and AD pathology. In the context of APO ϵ 4 carriers, the relationship between APOE genotype and ammonia agrees with Tran and colleagues' (2019) animal work showing an association with ammonia recycling.

The intestinal microbiota of APO ϵ 4 carriers showed an increased sulphur metabolism and reduction in assimilatory sulphate function, a process by which sulphate is converted to

hydrogen sulphide (H₂S) by sulphate-reducing bacteria. H₂S is linked to IBS via mechanisms of perturbing the intestinal mucosa and lowering luminal pH (Dordević *et al.*, 2021). In the context of AD, H₂S metabolism is dysregulated (Vandini *et al.*, 2019). It has however been shown that H₂S can counteract pathological processes in AD by preventing hyperphosphorylation of Tau by inhibiting Tau kinase activity and exerting anti-inflammatory effects (Vandini *et al.*, 2019; Giovinazzo *et al.*, 2021).

I also observed an enrichment in linoleic acid (LA) metabolism when comparing the intestinal microbial functional potential of APOε4 carriers against that of APOε4 non-carriers. The polyunsaturated omega fatty-acid, LA, has negative effects on many bacteria and is able to inhibit bacterial growth and induce metabolic stress (Senizza *et al.*, 2020). Excessive intake of LA via the diet is associated with metabolic disease (Miyamoto *et al.*, 2019) and whilst certain polyunsaturated fatty acids, such as Docosahexaenoic acid (DHA) and Eicosapentaenoic acid (EPA), are considered protective for AD, the metabolites related to LA are associated with increased risk for AD pathology (Snowden *et al.*, 2017; Gustafson *et al.*, 2020).

The fructose and mannose metabolism were increased in the microbiota community of APOε4 carriers. As explained in detail later, upregulation of this pathway is closely connected with glycolysis and the PPP and may hence represent an interesting functional target for future research and intervention strategies.

The microbiota of APOε4 carriers showed increased relative abundances for three pathways related to the biosynthesis of phospholipids, particularly phospholipid PG. Phospholipids are a large class of diverse lipids, with key roles in membrane structures. Elevated levels of PGs are also associated with many metabolic diseases (Kayser *et al.*, 2019). Although the exact mechanisms are yet to be elucidated, the literature suggests a strong relationship between

circulating phospholipids, gut dysbiosis and low-grade inflammation. There further appears to be a positive correlation between the levels of LPS and PGs and subsequent upregulation of inflammatory pathways (Kayser *et al.*, 2019). PGs might promote low-grade inflammation in APO ϵ 4 carriers.

Taken together, this work shows that APO ϵ 4 status is associated with various taxonomic and functional changes of the microbiota, which require further exploration but may play a role in promoting AD disease-mediated mechanisms.

In light of the altered microbiota composition in the two studied APOE groups, the next logical assessment was to see if changes observed in the at-genetic risk group related to the microbiome changes in patients diagnosed with AD. If there was a link between the microbial community in the APO ϵ 4 carrier group and the AD group, this may enable the identification of an ‘at risk’ microbial signature. Particularly novel and largely underexplored are also functional changes in AD patients, which can be predicted with shotgun metagenomics sequencing data, and may provide more insights into disease associated mechanisms that may link microbial changes to AD pathophysiology.

CHAPTER 5: AD PATIENT GROUP COMPARISON

Demographic profile of Alzheimer's Disease patient cohort

The small group of clinically diagnosed AD patients was comprised of nine individuals with a mean age of 73 years. All AD patients had undergone extensive cognitive and behavioural testing as part of the TRACC testing protocol and had readily banked faecal samples, were included in this study. This patient cohort was made up of two females and seven males. The majority of patients attained a high school or college level of education. The average time since symptom onset was approximately six years (Table 5.1).

Table 5.1 Primary characteristics of the Alzheimer's Disease patient group compared against the two Apolipoprotein E cohorts

Measure	AD patient group (n=9)	APOε4 non-carriers (n=40)	APOε4 carriers (n=39)	AD vs APOε4 non-carriers ¹ AD vs APOε4 carriers ² <i>p</i> -value
Age (years)				
Mean (SD)	73.1 (5.9)	66.73 (5.9)	63.95 (5.5)	<0.001 ^{1,2}
Sex				
Female (%)	2 (22.2%)	25 (62.5%)	30 (78.9%)	<0.001 ^{1,2}
Male (%)	7 (77.8%)	15 (37.5%)	8 (21.1%)	
Educational attainment				
No formal education	0 (0%)	0 (0%)	0 (0%)	
High school	4 (44.4%)	9 (22.5%)	8 (21.1%)	>.1 ^{1,2}
College	4 (44.4%)	12 (30%)	7 (18.4%)	
University	1 (11.2%)	19 (47.5%)	20 (52.6%)	
missing	0 (0%)	0 (0%)	3 (7.9%)	

¹Group comparison between AD patient group and APOε4 non-carriers, ²Group comparison between AD patient group and APOε4 carriers

In comparison to the demographics of the two the APOE groups, the AD patient cohort had a significantly higher mean age ($p < 0.001$) and a significantly different sex distribution ($p < 0.001$) with a higher ratio of males to females. All three groups were matched for educational attainment ($p = 0.167$).

Cognitive test performance of Alzheimer's Disease patient cohort

The cognitive results from the ACE-III, ROCF and TMT of the AD patient cohort are summarized in Table 5.2 and are described in the following. I used multiple regression models to investigate the effect of 'group' (AD patients, APOε4 carriers or non-carriers) on the measures' performance outcomes whilst accounting for the effect of age and educational attainment.

Table 5.2 Neuropsychological profile of the Alzheimer's Disease patient group compared against the two Apolipoprotein E cohorts

Measure	AD patient group Mean (SD) [n=9]	APOε4 non-carriers Mean (SD) [n=39]	APOε4 carriers Mean (SD) [n=38]	AD vs APOε4 non-carriers ¹ AD vs APOε4 carriers ² <i>p</i> -value
ACE-III				
Summary score (/100)	70.33 (11.86)	95.30 (3.95)	95.34 (2.58)	p<0.001 ^{1,2}
Attention sub. (/18)	13.33 (4.15)	17.55 (0.93)	17.66 (0.85)	p<0.001 ^{1,2}
Memory sub. (/26)	14.44 (3.64)	25.03 (1.48)	25.08 (1.36)	p<0.001 ^{1,2}
Fluency sub. (/14)	7.11 (1.83)	12.35 (1.64)	12.39 (1.49)	p<0.001 ^{1,2}
Language sub. (/26)	22.78 (3.7)	24.93 (1.38)	25.21 (0.87)	p<0.001 ^{1,2}
Visuospatial sub. (/16)	12.67 (4.36)	15.45 (1.01)	15.00 (1.04)	p<0.001 ^{1,2}
ROCF				
Copy score (/36)	25.22 (10.10)	31.39 (2.95)	31.95 (2.69)	p<0.001 ^{1,2}
Recall score (/36)	6.17 (6.49)	18.72 (5.45)	18.86 (5.29)	p<0.001 ^{1,2}
Copying time (sec)	288.33 (141.80)	162.51 (56.10)	188.34 (67.92)	p<0.01 ^{1,2}
TMT				
TMT-A (sec)	56.71 (31.62)	34.92 (7.86)	33.62 (12.61)	p<0.001 ^{1,2}
TMT-B (sec)	209.43 (105.68)	71.16 (23.20)	62.78 (18.69)	p<0.001 ^{1,2}
TMT-d (TMT-B - -A, sec)	152.71 (94.33)	36.24 (22.39)	29.16 (16.02)	p<0.001 ^{1,2}

¹Group comparison between AD patient group and APOε4 non-carriers, ²Group comparison between AD patient group and APOε4 carriers, ACE=Addenbrooke's Cognitive Examination, ROCF=Rey-Osterrich-Complex-Figure test, TMT = Trail Making Test

Addenbrooke's Cognitive Examination-III

The AD patients performed significantly lower on the ACE-III, indicating an overall impairment in cognition, compared to the APO ϵ 4 carriers ($\beta=-23.98$, $p<0.001$) and non-carriers ($\beta=-23.59$, $p<0.001$) (Table 7.42 in the supplementary). As outlined in the methods, the threshold for a diagnosis of suspicion for AD is 82 (with high specificity). These results indicate that the AD patient group scored ~24 points less than the APOE cohorts (Figure 5.1). Our regression model accounted for 74% of the observed variance in the data.

This was also reflected by a significant decline in all five cognitive domains evaluated by the ACE-III, namely attention, memory, verbal fluency, language and visuospatial abilities.

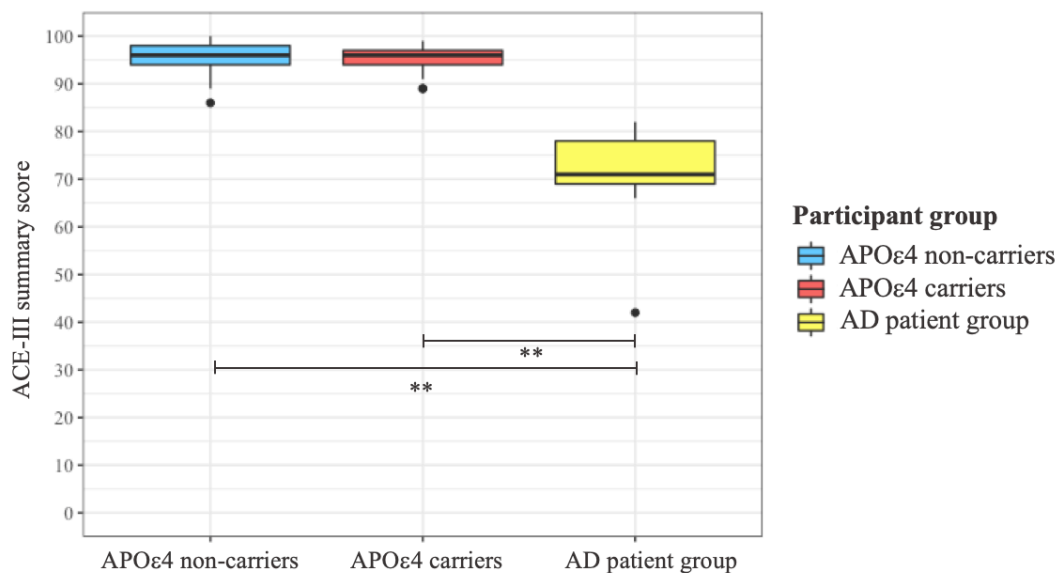


Figure 5.1 Boxplot of summary Addenbrooke's Cognitive Examination-III score between the three groups, ** $p<0.001$

Rey-Osterrich-Complex-Figure test

AD patients performed significantly less well on visuoconstructional abilities and non-verbal abilities such as executive functioning, as measured by ROCF copy score. AD patients took significantly longer to complete the copy drawing, compared to the APO ϵ 4 carriers ($\beta= 6.74$, $p<0.001$) and non-carriers ($\beta= 6.34$, $p<0.001$) (Table 7.42 and Figure 7.43 in the supplementary).

Nonverbal (recall and recognition) memory, which I further evaluated using the three-minute delayed recall of the ROCF, was also significantly impaired in AD patients compared to the both APOE cohorts (Figure 5.2). AD status explained 36.4% of the observed data variance, whereas neither age nor educational attainment added significantly to the performance prediction. On average participants of the AD group scored 11.58 ($p<0.001$) and 11.22 ($p<0.001$) less well on the recall drawing, compared to the APO ϵ 4 non-carriers and carriers, respectively (Table 7.44 in the supplementary).

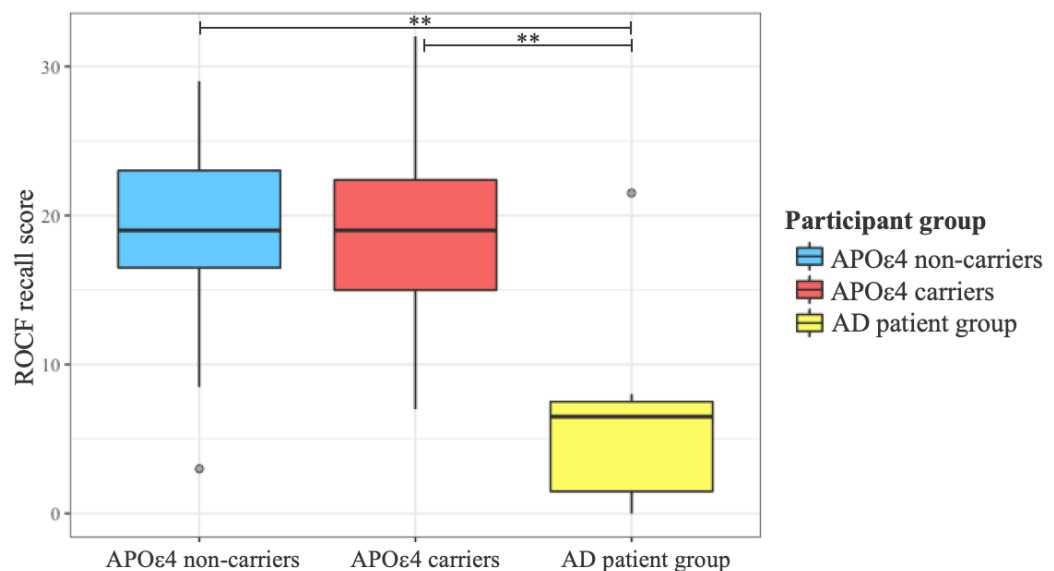


Figure 5.2 Boxplot of Rey-Osterrich-Complex-Figure recall score by participant group, ** $p<0.001$

The model for ROCF copy time significantly predicted 13.6% of variance in the data, with a significant effect of group, but no effect for age or educational attainment. Results indicate that the AD patient group took 1 min 42 sec and 1 min 26 sec longer compared to the APO ϵ 4 non-carriers ($p<0.01$) and APO ϵ 4 carriers ($p<0.01$), respectively, to complete the ROCF copy drawing (Table 7.46 in supplementary).

Trail Making Test

Analyses of the TMT results showed that AD patients had a significantly reduced ability for visual scanning and psychomotor speed (TMT-A) compared the APO ϵ 4 non-carriers (β =-20.29, p <0.001) and the APO ϵ 4 carriers (β =-21.28, p <0.001) (Table 7.47 in supplementary). This was also reflected by the mean TMT-A scores.

The AD patient group performed also significantly less well in important domains of executive functioning (working memory), including stimuli-shifting and inhibition control as indicated by significantly lowered performance on the TMT-B (Figure 5.3), compared to the APO ϵ 4 groups (non-carriers: β =-129.75, p <0.001, carriers: β =-135.60, p <0.001) (Table 7.48 in supplementary). Increasing age was also found to be positively associated with worsened performance on the TMT-B (β =1.65, p =0.019). This association reflects the well-established decrease in fluid cognitive abilities that occurs in healthy ageing. The results suggest that when keeping the influence of all other predictors constant, participants needed an extra 1.65 seconds with every one-year increment of age. Furthermore, AD patients took 2 min 9 seconds or 2 min 15 sec more than the APO ϵ 4 non-carriers and APO ϵ 4 carriers respectively, to complete part B of the TMT.

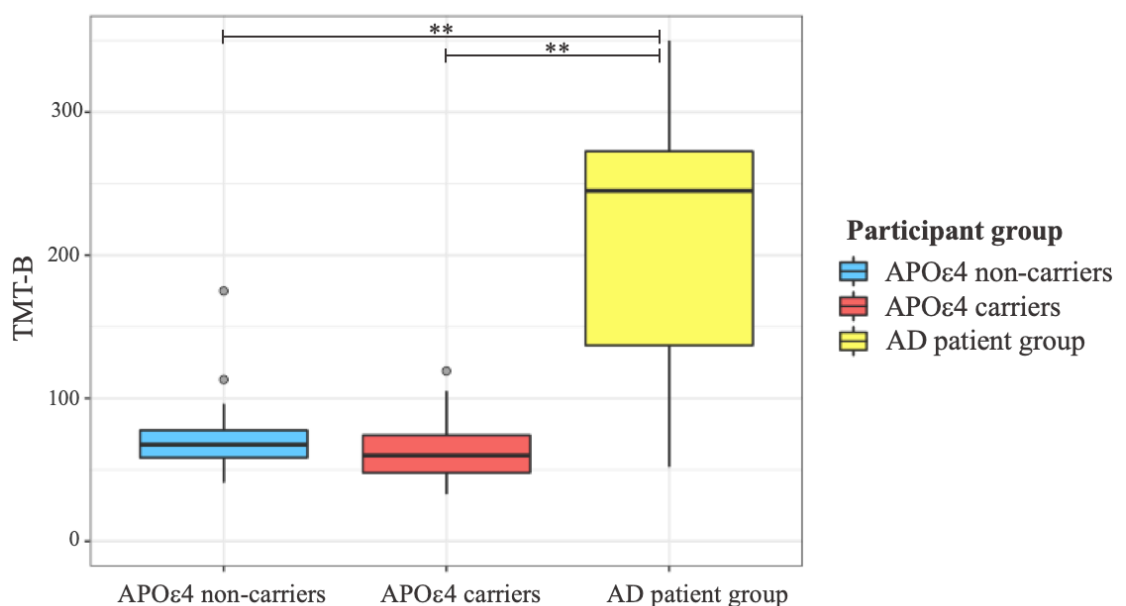


Figure 5.3 Boxplot of Trail Making Test-B performance by participant group, ** p <0.001

Cognitive and behavioural results of Alzheimer’s Disease patients from questionnaires

The patients’ self-reported anxiety (GAD-7) and depression (PHQ-9) levels, as well as the frequency of behavioural changes (CBI-R) were compared against the APOE groups. The data from these questionnaires is given in Table 6.3.

Table 5.3 Secondary neuropsychological profile of the Alzheimer’s Disease patient group compared against the two Apolipoprotein E cohorts

Self-reported measure	AD patient group (n=9) Mean (SD)	APOε4 non-carriers (n=39) Mean (SD)	APOε4 carriers (n=38) Mean (SD)	AD vs APOε4 non-carriers ¹ AD vs APOε4 carriers ² p-value
GAD-7 (/21)	4 (4.61)	0.87 (1.64)	0.92 (1.52)	p<0.001^{1,2}
PHQ-9 (/27)	4.89 (4.01)	1.85 (3.08)	1.94 (2.16)	p<0.001¹ p=0.001²
CBI-R (/180)				
Summary score	26.33 (17.72)	4.90 (5.46)	3.09 (2.67)	p<0.001^{1,2}
Memory subscore	52.22 (17.33)	7.15 (8.16)	6.18 (7.08)	p<0.001^{1,2}
Self-care subscore	17.44 (22.74)	0 (0)	0 (0)	p<0.001^{1,2}
Abnormal beh. subscore	15 (17.66)	2.87 (5.03)	1.71 (3.26)	p<0.001^{1,2}
Everyday skills subscore	30.56 (21.75)	0.77 (3.54)	0.15 (0.86)	p<0.001^{1,2}
Belief subscore	6 (12.49)	0.21 (1.28)	0 (0)	p<0.001^{1,2}
Eating habits subscore	18.11 (21.46)	3.54 (7.72)	2.00 (5.49)	p<0.001^{1,2}
Sleep subscore	36.33 (32.25)	21.08 (20.56)	14.18 (16.27)	p =0.055 ¹ , p<0.01²
Stereotypic beh. & motor abilities subscore	27.78 (34.07)	3.05 (7.56)	0.53 (1.73)	p<0.001^{1,2}
Motivation subscore	38.89 (24.47)	4.10 (8.50)	1.47 (3.99)	p<0.001^{1,2}

¹Group comparison between AD patient group and APOε4 non-carriers, ²Group comparison between AD patient group and APOε4 carriers, CBI-R = Cambridge Behaviour Inventory Revised (all scores are given as frequency scores), GAD-7 = Generalized Anxiety Disorder-7, PHQ-9=Patient Health Questionnaire-9

Generalized Anxiety Disorder-7

Anxiety was not prevalent in either of the three groups. On average, the AD patient group reported a GAD-7 score of 4.00, indicating that they experienced no anxiety with anything below a score of “5.00” denoting no anxiety. The mean GAD-7 scores in the APOE cohorts were even lower, with a mean of 0.87 in the APOε4 non-carrier and 0.92 in the APOε4 carrier group. The difference between the numerical scores of the AD patient group and APOε4 groups, albeit below the threshold to signify the presence of anxiety, were statistically significant. The AD patient group had significantly higher scores compared to the two APOE cohorts (APOε4 non-carriers: $\beta=-3.21$, $p<0.001$, APOε4 carriers: $\beta=-3.18$, $p=0.001$) (Table 7.49 in the supplementary).

Patient Health Questionnaire-9

The number of participants who were identified to be mildly or moderately depressed was small across all three groups. The group mean score of the AD patients indicated mild levels of depression, whilst the APOE cohorts showed no levels of depression with PHQ-9 scores of 1.85 (APOε4 non-carriers) and 1.94 (APOε4 carriers). The AD patient group had significantly higher PHQ-9 scores than the APOε4 non-carriers ($\beta=-3.21$, $p<0.001$) and carriers ($\beta=-3.18$, $p=0.001$) (Table 7.50 in the supplementary).

Cambridge Behaviour Inventory-Revised

There were evident changes when comparing AD patients to the APOE cohorts on the outcome measures of the CBI-R. With a group average of 26.33 for the CBI-R summary score, the AD patient group scored 22.13 and 24.19 points higher compared to the APOε4 non-carriers ($p<0.001$) and APOε4-carriers ($p<0.001$), respectively (Figure 5.4). This indicates noticeable changes in the overall behaviour and functioning of AD patients. The regression model was able to explain 51.6% of the variance in the data (Table 7.51 in the supplementary).

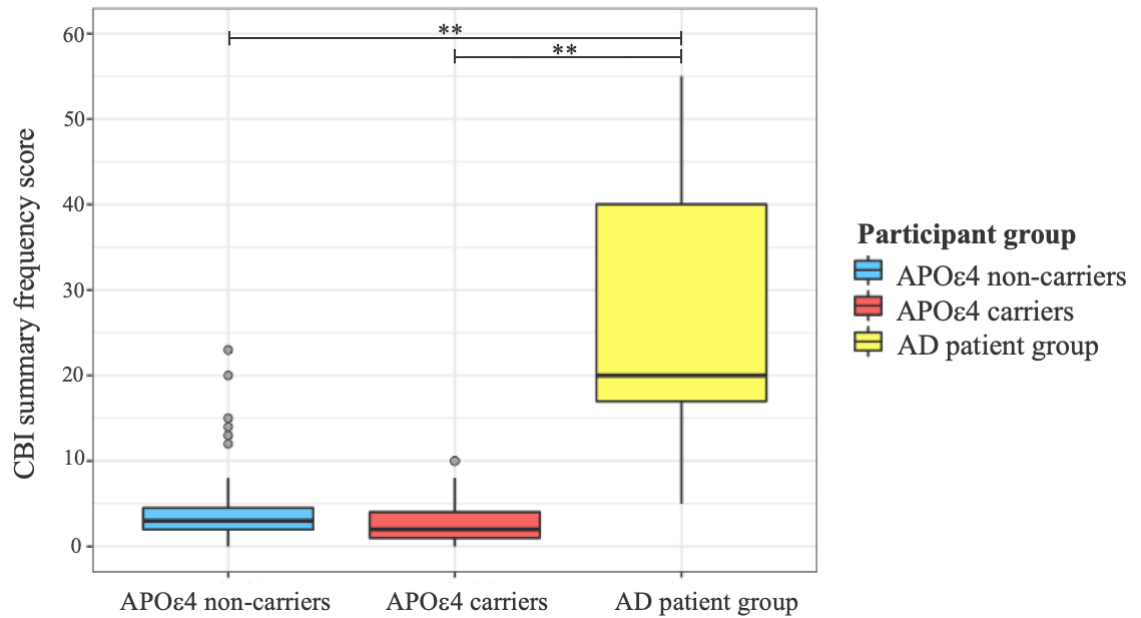


Figure 5.4 Boxplot of Cambridge Behaviour Inventory-Revised summary frequency mean by group, ** p<0.001

The AD patient cohort scored significantly worse in nine out of the ten functional and behavioural domains measured by the CBI-R. This was marked by a significant decline in memory, everyday skills, self-care, abnormal behaviour, mood, beliefs, eating habits, stereotypic and motor behaviour, and motivation in the AD patient cohort. The variation in the data that could be explained by group (APOε4 carriers, APOε4 non-carriers, AD patient group) in the regression models was high. In particular for the memory, everyday skills and motivation frequency domains, for which group explained 72.4%, 62.8% and 57.5% of the data, respectively. The only exception was the sleep subscale, for which only the group contrast of AD vs APOε4 carriers was significant ($\beta=-23.29$, $p<0.008$), whilst comparing the AD patients to the APOε4 non-carriers did not reach significance ($\beta=-15.60$, $p=0.055$).

Taxonomic profile

Descriptive summary

In order to mitigate against the introduction of potential bias inherent to different sequencing runs, which can be a source of technical noise, and thus to maximise the ability to detect a true signal, the below presented cross-sectional comparison is based on sequencing data from the same sequencing run. The AD patient data was not collected prospectively and was not available longitudinally. I extracted the genomic DNA from the banked samples using the same methods as for the samples of the APOE groups. Next, the AD patient samples were pooled and sequenced together with the APOE group data gathered at T2. Thus, to avoid adding further variability from the sequencing run, this means that I herein compare AD patient data against the T2 time point of the APOE groups.

The intestinal microbiota of the AD patient group was made up of nine phyla and was characterized predominantly by *Firmicutes* (M=51.43%, SD=21.3) and *Actinobacteria* (M=23.90%, SD=19.2). The mean relative abundances of the phyla *Euryarchaeota* and *Bacteroidetes* were also high compared to other phyla, contributing to a further 11.44% (SD=24.8) and 9.11% (SD=10.1), respectively. The remaining 4.12% of the total relative abundances, were mainly accounted for by *Verrucomicrobia*, *Proteobacteria*, and *Viruses*. I also observed the occurrence of *Candidatus Saccariabacteria* in three patient samples with very low relative abundance (<0.01%), as well as one occurrence of *Ascomycota* (Figure 5.5).

There were several pronounced numerical differences when comparing the intestinal composition of AD patients to those of the APOE cohorts (Figure 5.5 and 5.6, Table 5.4).

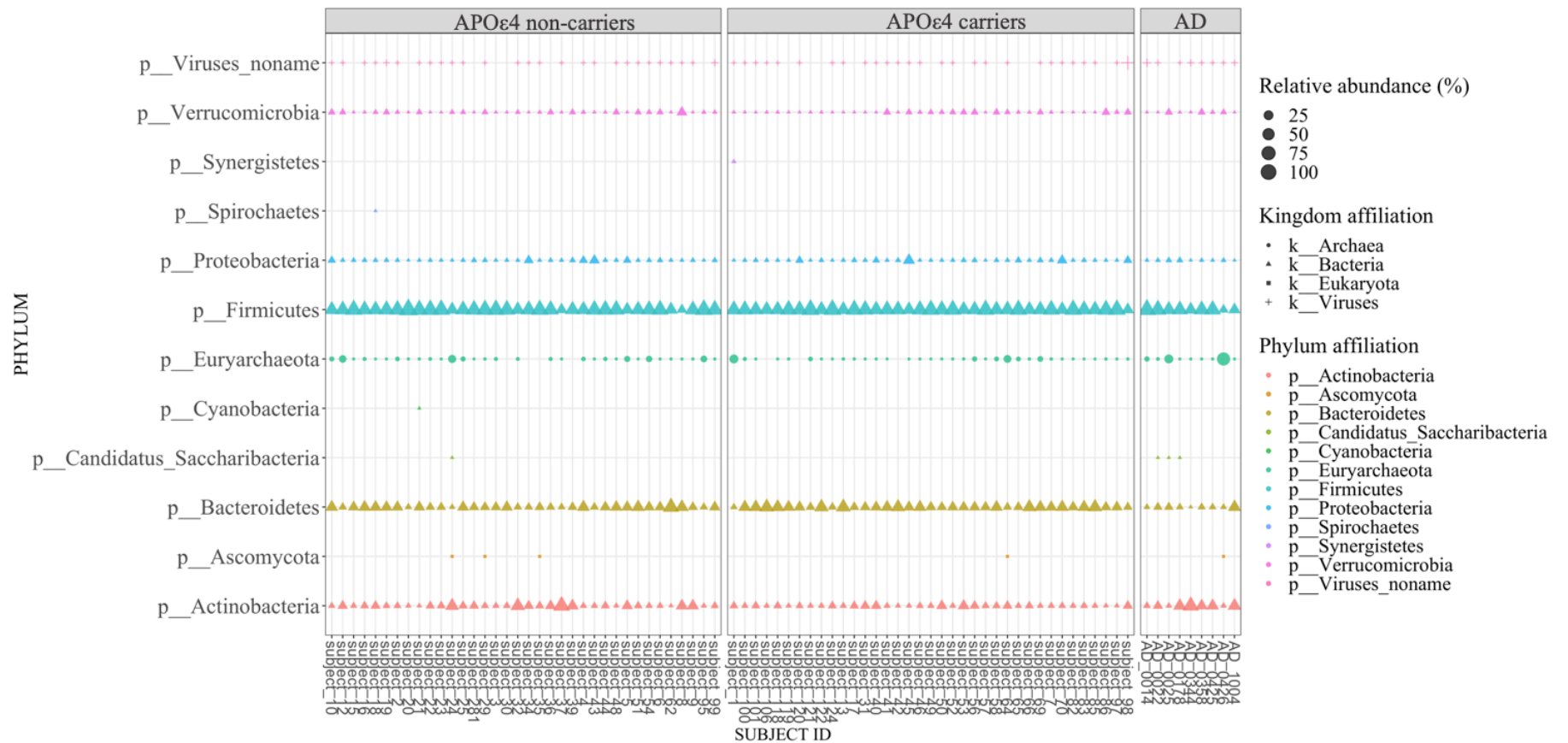


Figure 5.5 Relative abundances of phyla by group: Apolipoprotein ε4 non-carriers (left panel), Apolipoprotein ε4 carriers (middle panel), Alzheimer's Disease patient group (right panel), shape showing kingdom affiliation, size represents relative abundances

Firstly, whilst *Firmicutes* were the most abundant phylum in all three groups, the relative abundance in the AD patient group was about 10% smaller compared to the relative abundance of *Firmicutes* observed in the two APOE cohorts (both approximately 60%). Next, whereas *Bacteroidetes* was the second most abundant phylum in the microbial profiles of the APOE groups, this phylum ranked only fourth in the AD patient group. On the other hand, microbiota communities of AD patients showed comparatively much greater abundance of *Actinobacteria* and *Euryarchaeota* (the latter phylum belonging to the kingdom of *Archaea*) compared to those of the APOE groups. Whilst only present at overall low abundances, *Proteobacteria* were observed to be more than twice as abundant in the profiles of APOE groups than AD patients, whereas *Verrucomicrobia* occurred at similar relative abundances between the three groups. The relative abundance of *Viruses* was smallest in the APOE4 non-carriers and increased in a stepwise manner, via the APOE4 carriers to the AD patient group, which had the highest relative mean abundance.

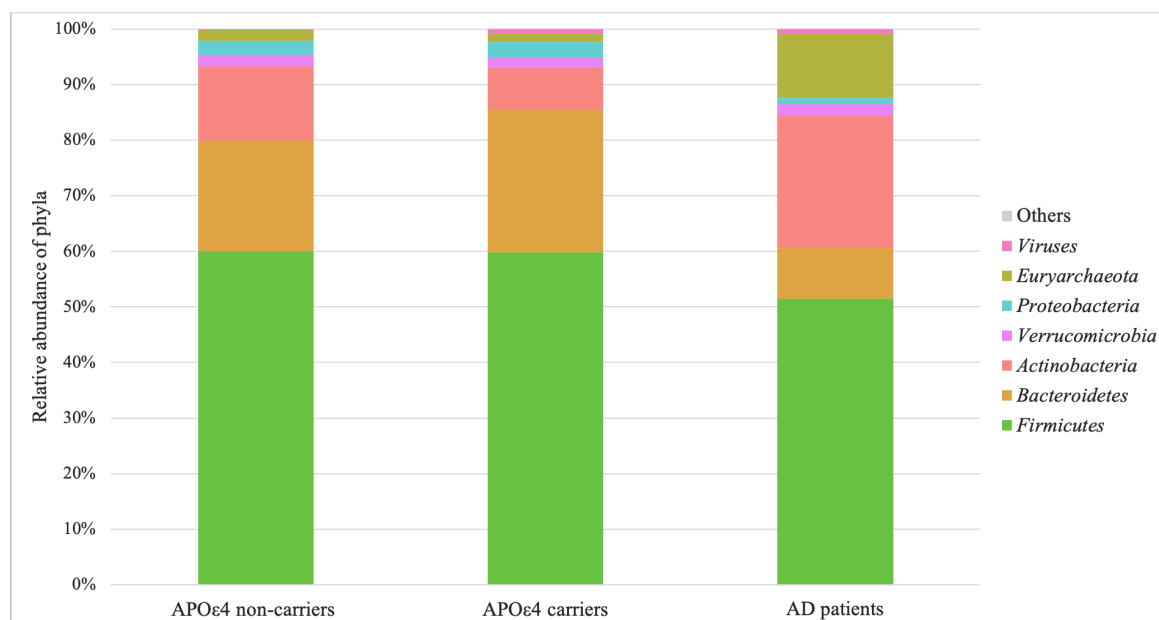


Figure 5.6 Relative abundance of phyla by group (2): Apolipoprotein ε4 non-carriers (left), Apolipoprotein ε4 carriers (middle), Alzheimer’s Disease patient group (right)

Table 5.4 Relative abundances (%) of most abundant phyla by group

Mean (SD)	APOε4 non-carriers	APOε4 carriers	AD
	T2	T2	
<i>Firmicutes</i>	60.06 (15.46)	59.81 (11.62)	51.43 (21.34)
<i>Bacteroidetes</i>	19.79 (11.15)	25.63 (10.95)	9.11 (10.11)
<i>Actinobacteria</i>	13.44 (13.92)	7.65 (5.61)	23.90 (19.24)
<i>Verrucomicrobia</i>	2.04 (3.27)	1.70 (2.51)	2.06 (2.99)
<i>Proteobacteria</i>	2.54 (4.15)	2.84 (5.35)	1.14 (1.24)
<i>Euryarchaeota</i>	2.01 (4.29)	1.58 (4.82)	11.44 (24.77)
<i>Viruses</i>	0.13 (0.34)	0.77 (4.51)	0.91 (1.47)
Others	0.03	0.01	0.01

Overall, the intestinal microbiota composition at phylum-level was very similar between the two APOE groups. The intestinal microbiota composition of the AD patient cohort, however, showed some clear numerical differences in the group means of relative abundances, with notable increases in *Actinobacteria* and *Euryarchaeota*, coupled with decreases in the relative abundance of *Firmicutes* and *Bacteroidetes*. Nonetheless, *Firmicutes* remained the dominant phyla in all three compositional profiles (Figure 5.6, Table 5.4).

There were 45 distinct taxa at family-level within the AD patient cohort. The 15 most abundant families made up 91.5% of the total compositional profile. With a mean relative abundance of 19.84% (SD=15.65) and 19.41% (SD=18.0), the families of *Ruminococcaceae* and *Bifidobacteriaceae*, respectively, were by far the most abundant families in the AD patient group. The ten most abundant families besides the already mentioned also included the following: *Methanobacteriaceae* and *Lachnospiraceae* (with relative abundance above 10%), *Eubacteriaceae* and *Bacteroidaceae* (with relative abundances above 5%), and lastly the families *Coriobacteriaceae*, *Streptococcaceae*, *Lactobacillaceae* and *Verrucomicrobia* (with relative abundances below 5% but above 2%) (Figure 5.7).

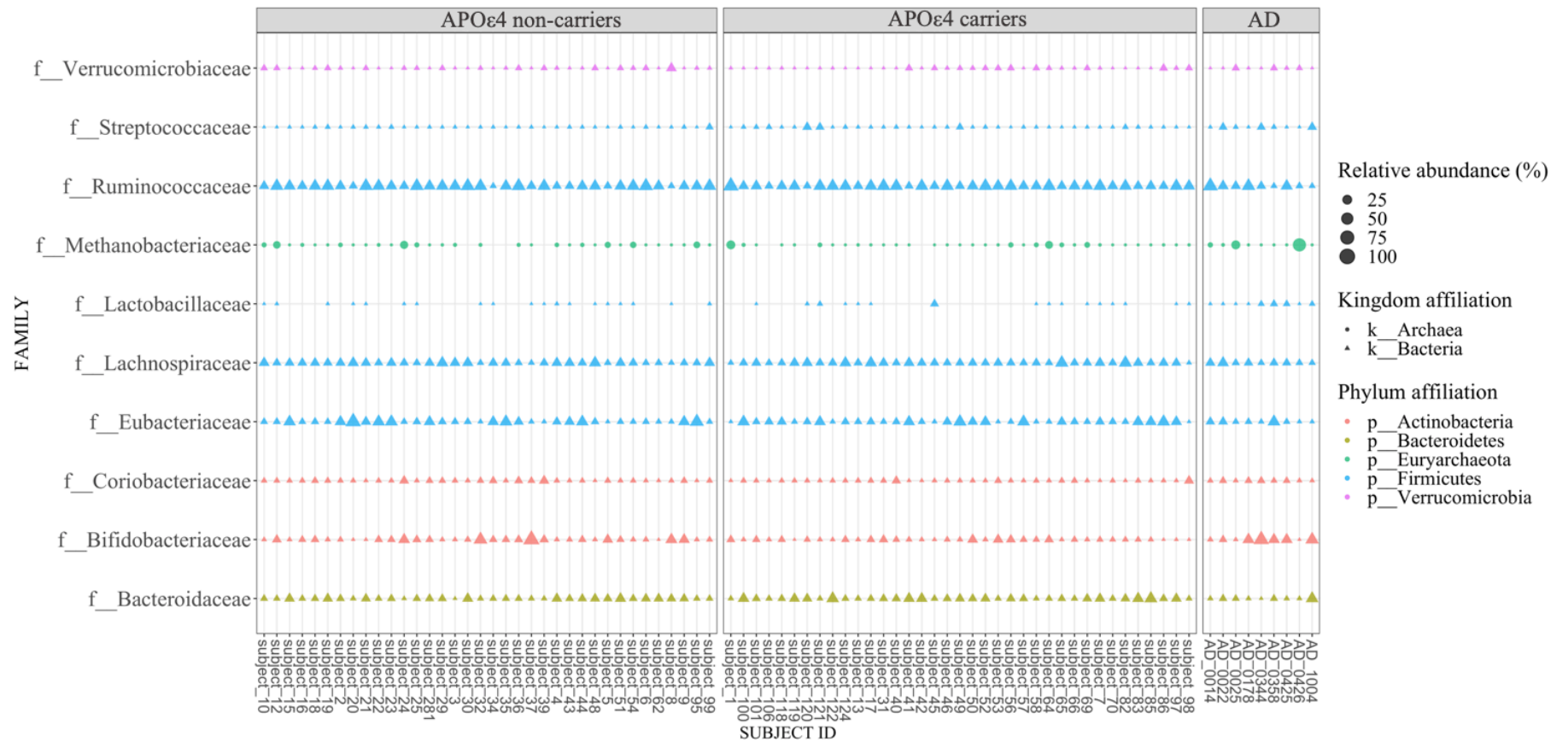


Figure 5.7 Relative abundances of top ten families within Alzheimer's Disease patient group. Apolipoprotein ε4 non-carriers (left panel), Apolipoprotein ε4 carriers (middle panel), Alzheimer's Disease patient group (right panel), shape showing kingdom affiliation, size represents relative abundances

There was a relatively large overlap with respect to the ten most abundant families between the APOE groups and the AD patient group. However, neither members of the *Porphyromonadaceae*, *Prevotellaceae*, or *Rikenellaceae* which belonged to the ten most abundant families in the APOE groups, were part of the top ten most abundant families within the AD intestinal profiles. In their place, the AD patient group saw high abundances in members of *Bifidobacteriaceae*, *Methanobacteriaceae*, *Streptococcaceae*, and *Verrucomicrobiaceae* compared to the APOE groups. Whilst *Ruminococcaceae*, *Eubacteriaceae*, and *Bacteroidaceae* occurred at lower abundances in the AD patient group (Figure 5.8, Table 5.5).

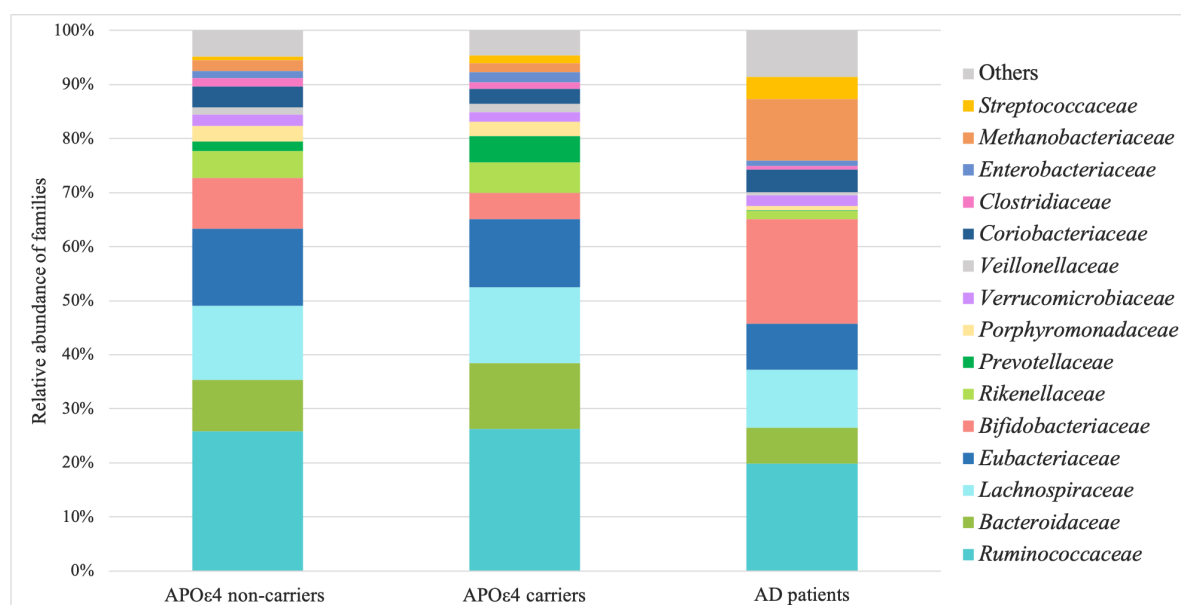


Figure 5.8 Relative abundance of families by group (2), Apolipoprotein ε4 non-carriers (left), Apolipoprotein ε4 carriers (middle), Alzheimer’s Disease patient group (right)

Table 5.5 Relative abundances (%) of most abundant families by group

Mean (SD)	APOε4 non-carriers	APOε4 carriers	AD
	T2	T2	
<i>Ruminococcaceae</i>	25.90 (9.81)	26.32 (9.25)	19.84 (15.65)
<i>Bacteroidaceae</i>	9.46 (5.42)	12.12 (7.81)	6.68 (9.33)
<i>Lachnospiraceae</i>	13.66 (6.01)	14.03 (6.99)	10.71 (5.94)
<i>Eubacteriaceae</i>	14.28 (12.81)	12.60 (9.69)	8.50 (9.34)
<i>Bifidobacteriaceae</i>	9.43 (12.23)	4.94 (4.67)	19.41 (17.99)
<i>Rikenellaceae</i>	5.00 (5.34)	5.61 (5.34)	1.49 (1.42)
<i>Prevotellaceae</i>	1.77 (4.11)	4.80 (10.53)	0.18 (0.25)
<i>Porphyromonadaceae</i>	2.87 (2.98)	2.74 (1.55)	0.67 (0.80)
<i>Verrucomicrobiaceae</i>	2.04 (3.27)	1.70 (2.51)	2.06 (2.99)
<i>Veillonellaceae</i>	1.32 (2.30)	1.63 (2.88)	0.54 (0.90)
<i>Coriobacteriaceae</i>	3.95 (3.48)	2.68 (2.83)	4.20 (2.61)
<i>Clostridiaceae</i>	1.46 (3.50)	1.28 (2.95)	0.64 (1.28)
<i>Enterobacteriaceae</i>	1.35 (3.73)	1.90 (5.23)	0.97 (1.22)
<i>Methanobacteriaceae</i>	2.01 (4.29)	1.58 (4.82)	11.44 (24.77)
<i>Streptococcaceae</i>	0.66 (1.20)	1.42 (2.89)	4.12 (5.20)

At the species-level, there were 395 taxa. However, 67% of the compositional profile in the AD patient group was made up by the 20 most abundant species (Figure 5.9). Taking a closer look at these top 20 species across all groups, showed that half of the species belonged to the *Firmicutes* phylum, thus well reflecting the compositional picture already seen at a higher taxonomic level, and overall spanned across five main phyla (Figures 5.9 and 5.10, Table 5.6).

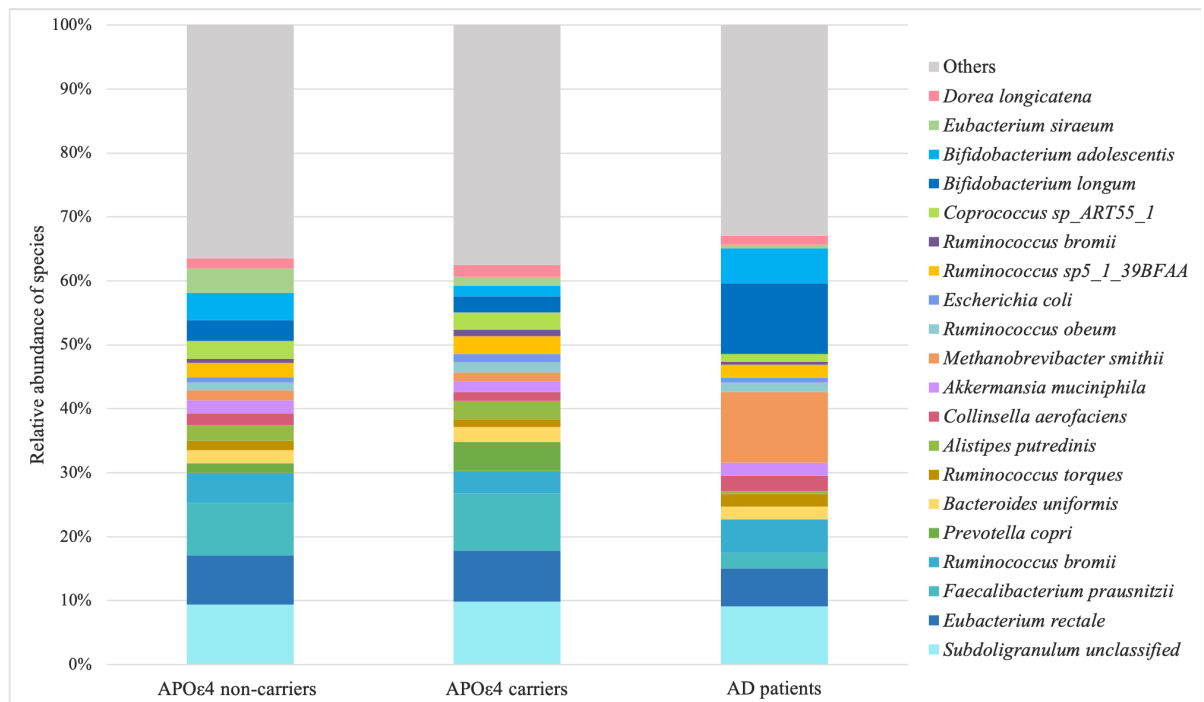


Figure 5.9 Relative abundance of species by group (2), Apolipoprotein ε4 non-carriers (left), Apolipoprotein ε4 carriers (middle), Alzheimer’s Disease patient group (right)

Table 5.6 Relative abundances (%) of most abundant species by group

Mean (SD)	APOε4 non-carriers	APOε4 carriers	AD
	T2	T2	
<i>Subdoligranulum unclassified</i>	9.35 (6.85)	9.82 (8.87)	9.15 (9.96)
<i>Eubacterium rectale</i>	7.76 (10.26)	8.02 (7.91)	5.92 (8.41)
<i>Faecalibacterium prausnitzii</i>	8.13 (5.67)	8.89 (5.43)	2.43 (2.48)
<i>Ruminococcus bromii</i>	4.73 (5.05)	3.60 (5.53)	5.18 (6.35)
<i>Ruminococcus obeum</i>	1.26 (1.11)	1.59 (0.90)	1.46 (1.69)
<i>Prevotella copri</i>	1.49 (4.01)	4.51 (10.63)	0.10 (0.18)
<i>Alistipes onderdonkii</i>	1.11 (2.87)	1.38 (3.78)	0.10 (0.19)
<i>Alistipes putredinis</i>	2.41 (2.51)	2.84 (2.08)	0.47 (0.72)
<i>Escherichia coli</i>	0.85 (3.04)	1.30 (3.80)	0.80 (0.95)
<i>Bacteroides stercoris</i>	1.36 (2.31)	0.95 (2.01)	0.17 (0.51)
<i>Bacteroides dorei</i>	0.61 (0.78)	1.30 (1.90)	0.27 (0.44)
<i>Dialister invisus</i>	0.65 (1.41)	0.98 (2.58)	0.48 (0.89)
<i>Bacteroides uniformis</i>	2.03 (2.37)	2.35 (2.12)	1.91 (4.23)
<i>Akkermansia muciniphila</i>	2.04 (3.27)	1.70 (2.51)	2.06 (2.99)
<i>Methanobrevibacter smithii</i>	1.56 (3.32)	1.37 (4.12)	11.07 (24.59)
<i>Collinsella aerofaciens</i>	3.41 (3.16)	2.17 (2.61)	2.34 (2.53)
<i>Bifidobacterium longum</i>	3.20 (5.05)	2.48 (2.69)	11.06 (9.49)
<i>Bifidobacterium adolescentis</i>	4.23 (8.03)	1.69 (2.66)	5.36 (8.90)
<i>Eubacterium siraeum</i>	3.80 (8.20)	1.39 (2.81)	0.58 (1.45)
<i>Dorea longicatena</i>	1.64 (1.35)	1.78 (1.06)	1.36 (1.50)
<i>Ruminococcus torques</i>	1.49 (1.59)	1.19 (1.17)	2.03 (2.07)
<i>Ruminococcus sp5_1_39BFAA</i>	2.21 (1.86)	2.58 (2.12)	2.01 (2.00)
<i>Coprococcus sp ART55_1</i>	2.77 (4.37)	2.69 (5.49)	1.19 (2.36)

The ten species belonging to the phylum of *Firmicutes* were all found to be part of the order *Clostridiales*. Within this order classification, they can further be sub-classified to belong to one of three families – *Lachnospiraceae*, *Ruminococcaceae*, *Eubacteriaceae* – which are part of the ten most abundant families. Abundance of the species *E. siraeum* was reduced in

a stepwise fashion from APO ϵ 4 non-carriers (M=3.8%, SD=8.2), over APO ϵ 4 carriers (M=1.4%, SD=2.8), to AD patients (M=0.6%, SD=1.5). *E. rectale* was similarly abundant between the APOE groups (M=8-8.3%, SD=7.9-10.5), but nominally less abundant in the AD patient group (M=5.9%, SD=8.4). Another striking difference between the APOE groups and the AD patient group, was the 3- to 4-fold reduction in the mean relative abundance of *F. prausnitzii* (non-carriers: M=8.1%, SD=5.7; carriers: M=8.9%, SD=5.4; AD patients: M=2.4%, SD=2.5).

The five species belonging to the *Bacteroidetes* phylum, are part of five different families, of which only the *Bacteroidaceae* (M=10.7%, SD=5.9) is represented in the top ten families. These five species were *P. copri* (M=0.1%, SD=0.2), *Barnesiella intestinihominis* (M=0.2%, SD=0.3), *B. vulgatus* (M=0.4%, SD=0.8), *B. uniformis* (M=1.9%, SD=4.2), and *Alistipes putredinis* (M=0.5%, SD=0.7). Particularly *P. copri* was nominally distinctly different, with a 15- to 45- fold reduction in AD patients compared to the APO ϵ 4 non-carriers (M=1.5%, SD=4.0) and APO ϵ 4 carriers (M=4.5%, SD=10.6), respectively.

Three species belonging to the *Actinobacteria* clade were also found to rank among the 20 most abundant species, namely *C. aerofaciens* (non-carriers: M=3.4%, SD=3.2; carriers: M=2.2%, SD=2.6; AD patients: M=2.3%, SD=2.5), *B. longum* (non-carriers: M=3.2%, SD=5.0; carriers: M=2.5%, SD=2.7; AD patients: M=11.1%, SD=9.5) and *B. adolescentis* (non-carriers: M=4.3%, SD=8.0; carriers: M=1.7%, SD=2.7; AD patients: M=5.4%, SD=8.9). On a higher taxonomic level, these species belong to the families *Coriobacteriaceae* and *Bifidobacteriaceae*. Both *Bifidobacterium* species had considerably higher relative abundances in AD patients than the APOE groups. This was especially true for *B. longum* which was over three times more abundant in the AD patient group compared to the APOE cohorts.

The two-remaining species of the 20 most abundant species, belong to the phyla *Verrucomicrobia* (*Verrucomicrobiaceae* family) and the *Euryarchaeota* (family *Methanobacteriaceae*). Within the *Euryarchaeota*, the archaea species *M. smithii* was considerably more abundant in the AD patient group with at mean relative abundance of 11.07% (SD=24.59), compared to the below 2% average abundance of the APOE groups.

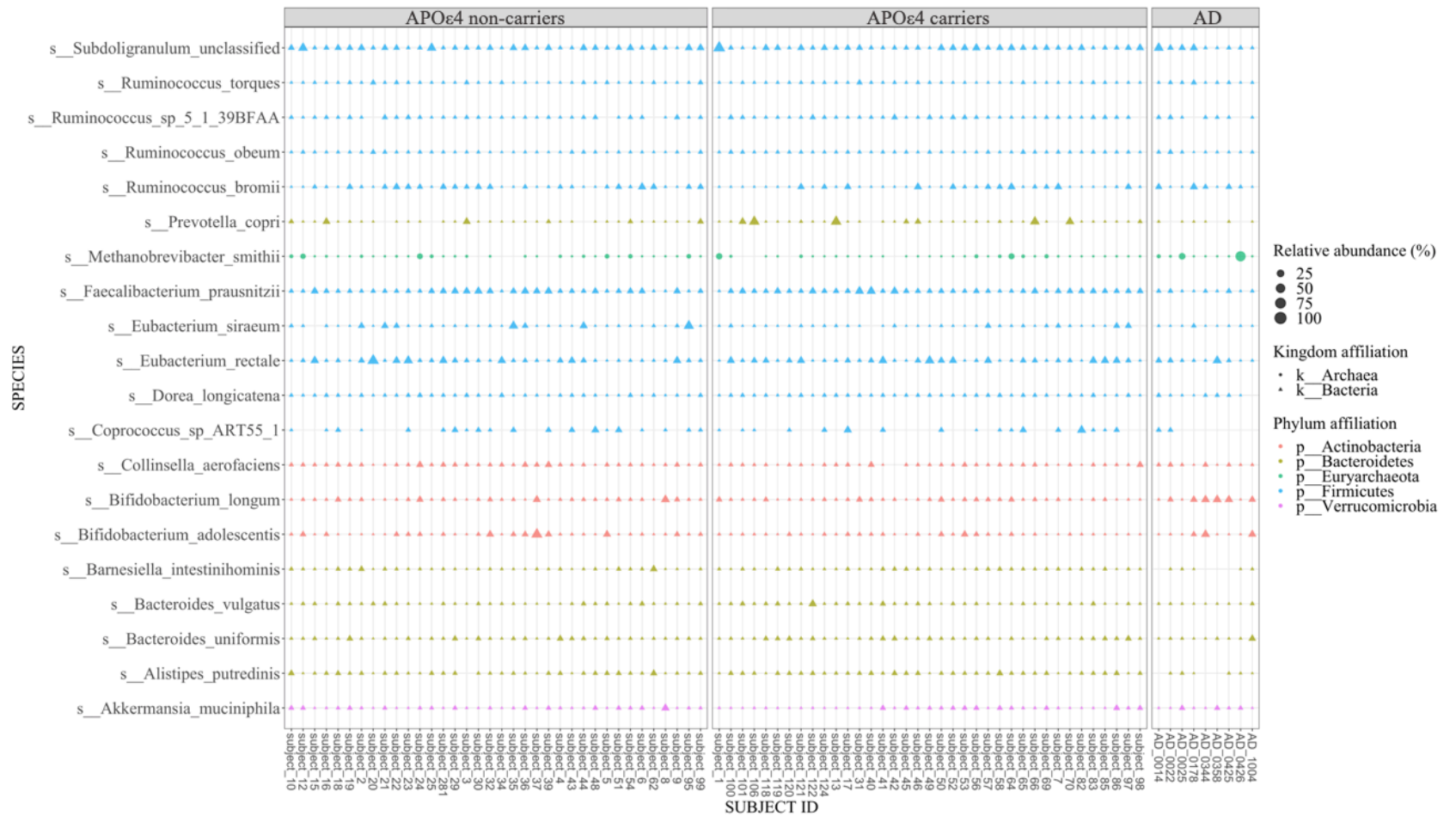


Figure 5.10 Relative abundances of top 20 species. Apolipoprotein ϵ 4 non-carriers (left panel), Apolipoprotein ϵ 4 carriers (middle panel), Alzheimer's Disease patient group (right panel), shape showing kingdom affiliation, size represents relative abundances

Overall, the descriptive summary indicates that there are some noticeable numerical differences in the intestinal taxonomic composition between the groups. These differences were observed to be particularly perceptible when making the comparison between the AD patient group and the APOE cohorts. Whether the observed differences in relative abundances are indeed able to distinguish between the groups, will be addressed in the following by subjecting the compositional profiles to diversity and differential abundance analysis.

Alpha diversity

The between-group comparison of alpha diversity indices, comparing the AD patient group to the APOE4 carriers, was significant at kingdom-level (Shannon $p=0.017$, Inverse Simpson $p=0.017$), at genus-level (Shannon $p=0.039$, Inverse Simpson $p=0.042$) and at species-level (Shannon $p=0.012$, Inverse Simpson $p=0.029$). At the kingdom-level, the AD group exhibited a larger species richness and diversity than the APOE4 carriers. At genus- and at species-level community diversity was reduced in the AD patient group (Figure 5.11, Table 7.52 in the supplementary).

When comparing the AD patient group to the APOE4 non-carriers, I observed a significant difference only at species-level. Here, the AD group had a mean Shannon diversity index of 2.72 and an Inverse Simpson index of 9.97 which was significantly smaller compared to that of the APOE4 non-carriers (Shannon=3.05, $p=0.028$; Inverse Simpson=12.73, $p=0.033$) (Figure 5.11, Table 7.52 in the supplementary).

There was no statistically significant difference in alpha diversity at any of the taxonomic levels between the APOE groups.

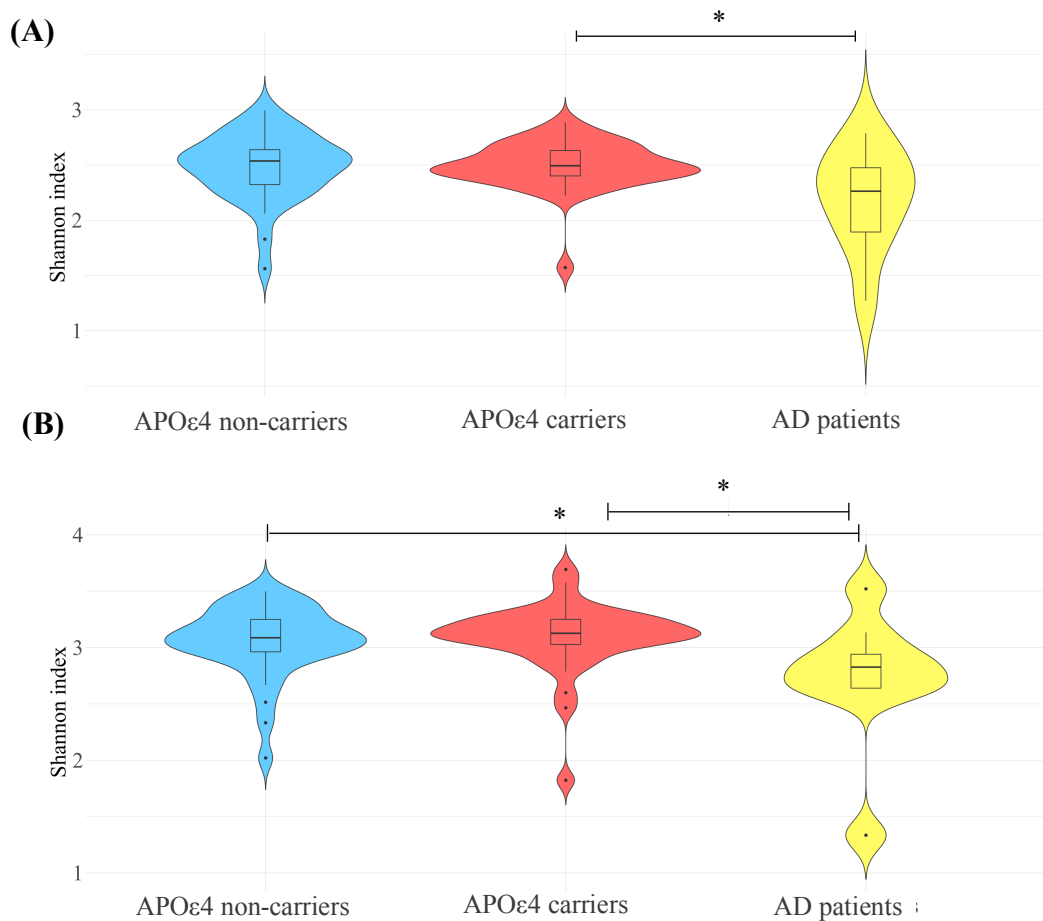


Figure 5.11 Alpha diversity (measured as Shannon diversity index) at (A) genus-level and (B) species-level between the groups; * $p < 0.05$. Blue: Apolipoprotein $\epsilon 4$ non-carriers, red: Apolipoprotein $\epsilon 4$ carriers, yellow: Alzheimer's Disease patient group

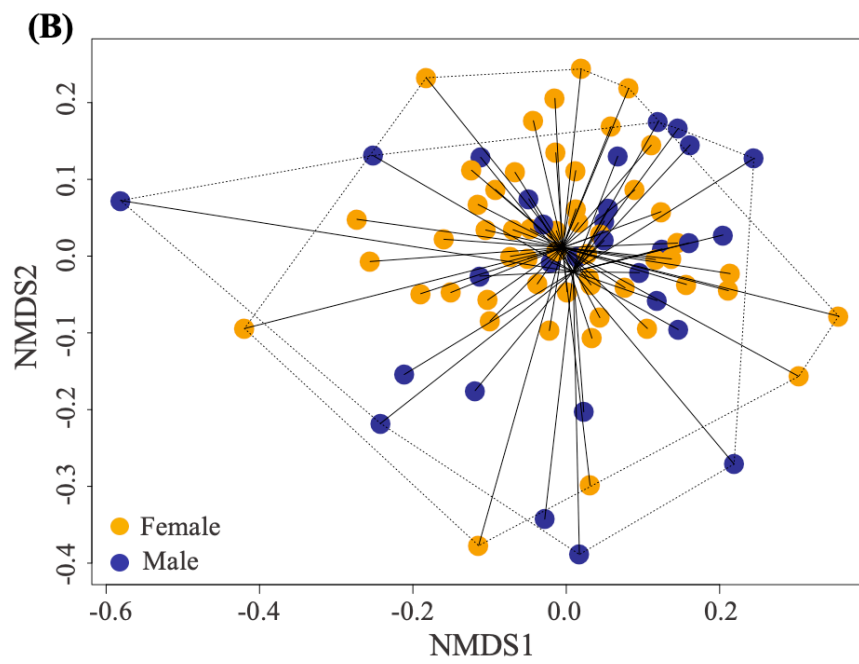
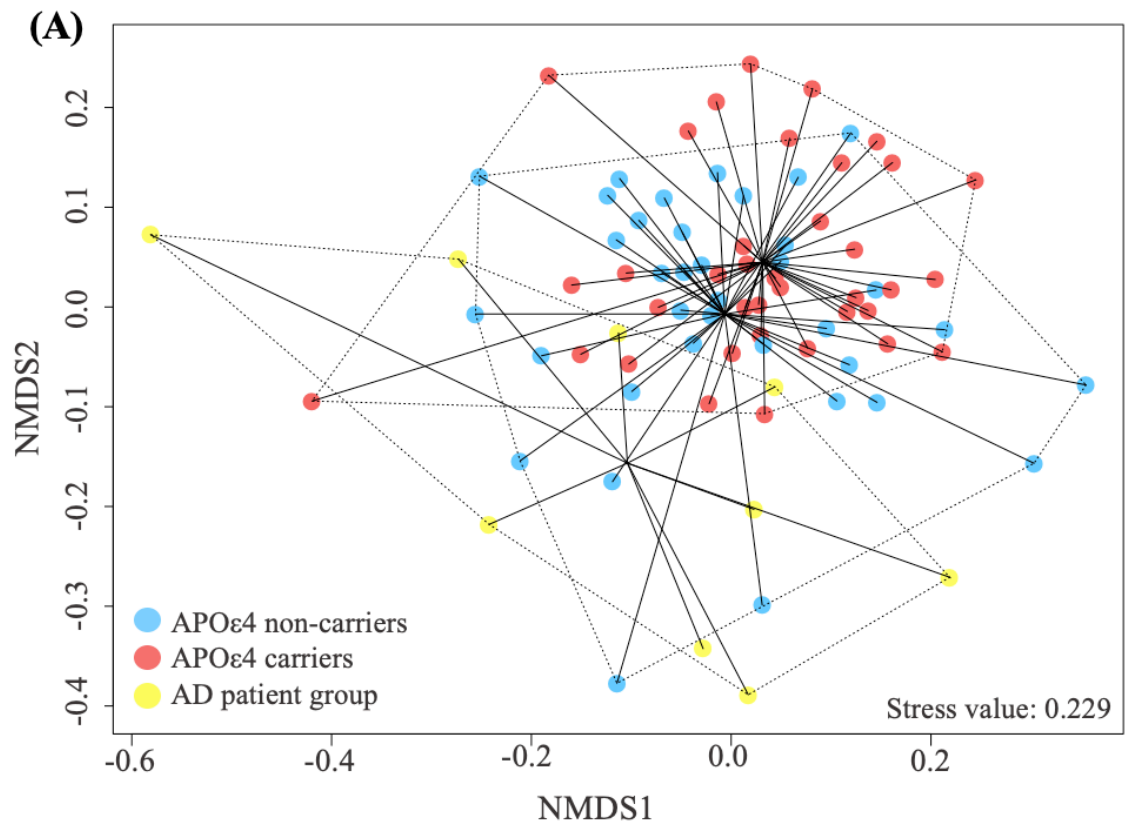
The significantly lower alpha diversity in the AD patient group compared to both APOE cohorts at species-levels indicates that the intestinal microbiota community of AD patients is characterized by a lower species richness and evenness.

Beta diversity

Large-scale compositional differences were further assessed by determining beta diversity indices and assessing them for statistical significance between the three groups with a PERMANOVA, using age and sex as covariates. The stratification of participants was implemented as follows. Participants were classified to belong to either of three groups depending on their health and APOε4 status: the APOε4 non-

carriers (n=36), the APOε4 carriers (n=37), or the AD patient group (n=9). They were further stratified into three age groups: 52-60 years old (n=14), 61-69 years old (n=42), and 70+ years old (n=26). Sex was used as a second covariate (female: n=53, male: n=29).

Participant group was the most significant factor to drive variation in the intestinal microbiota, showing a significant effect at every taxonomic level ($p < 0.001$, Table 7.53 in the supplementary), except for at kingdom-level, and contributing to 5.3%-12.3% of the variance observed in the data (Figure 5.12 (A)). The largest effect of group was observed at class-level, explaining 12.3% of the variation in beta diversity. The different age groups did not explain variation in the community distance profiles (Figure 5.12 (C)). The effect of sex was not significant, except for at genus- ($p = 0.029$) and at species-level ($p = 0.023$, Figure 5.12 (B)). Here, sex could explain 2.2% of variance in the beta diversity profiles.



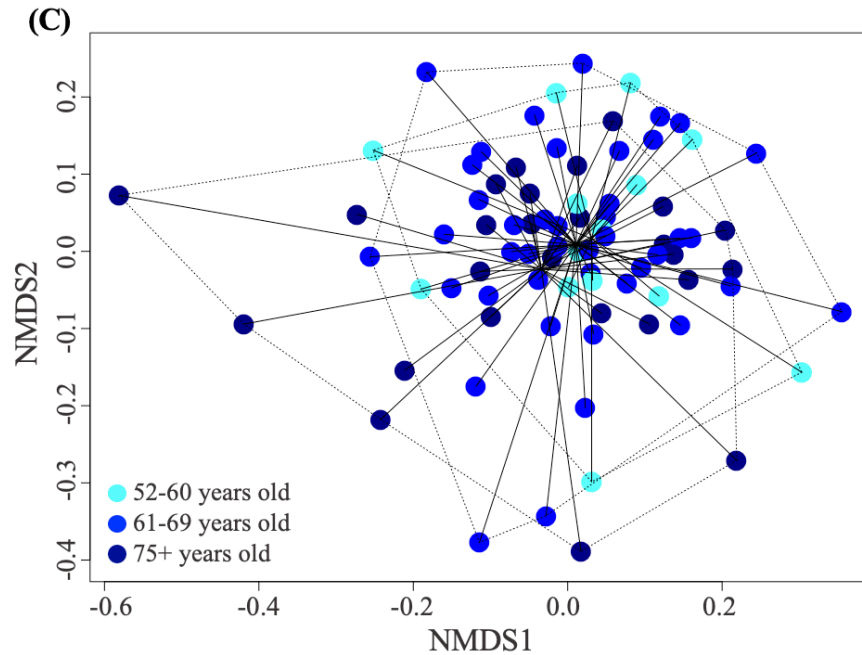


Figure 5.12 Non-metric Multidimensional Scaling on Bray-Curtis dissimilarity between the species relative-abundance intestinal microbiota profiles by (A) group (light blue = Apolipoprotein ϵ 4 non-carriers, red = Apolipoprotein ϵ 4 carriers, yellow = Alzheimer's Disease patients), (B) sex (orange = female, blue = male), (C) age group (light blue = 52-60 years old, middle blue = 61-69 years old, dark blue = 75+ years old). Each point denotes a sample in a reduced dimensional space and is connected with a line to the group centroid

Pairwise comparison for all pairs of groups with FDR-correction (AD vs APO ϵ 4 carriers, AD vs APO ϵ 4 non-carriers, APO ϵ 4 carriers vs non-carriers) showed that group differences were significant when comparing the AD patient group to either the APO ϵ 4 non-carriers or carriers. However, beta diversity was not different when comparing the two APOE cohorts to each other (Table 7.54 in the supplementary).

Similar results were obtained when repeating the analysis using Jaccard distance instead of Bray-Curtis dissimilarity index to build the distance matrices.

Differential abundance analysis

Univariate abundance analysis (LEfSe)

LEfSe analysis identified a total of 42 significant ($p < .05$) associations (Figure 5.13; Table 7.55 in the supplementary). All three groups were enriched in members of several taxa. The APO ϵ 4 non-carriers was the group with the smallest number of discriminating taxa.

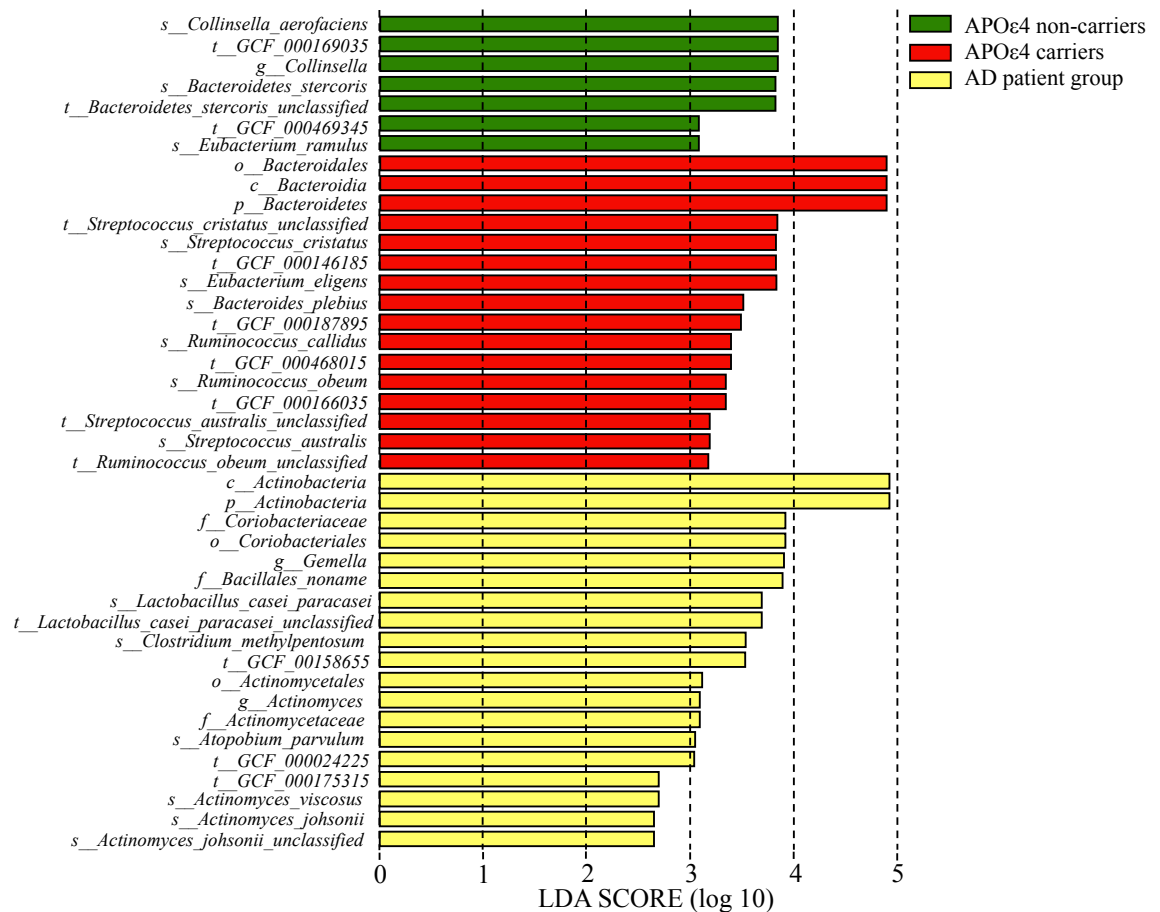


Figure 5.13 Linear Discriminant Analysis effect size of discriminative taxa between Apolipoprotein ϵ 4 non-carriers (green), Apolipoprotein ϵ 4 carriers (red) and the Alzheimer's Disease patient group (yellow). The length of bar charts represents increasing abundance. Associated Linear Discriminant Analysis scores are on a log₁₀ scale

The AD patient group was broadly characterized by increased abundances for bacteria belonging to two clades – the *Actinobacteria* and *Firmicutes* phyla. Within the *Firmicutes* phylum, the intestinal microbiota of the AD patient group was enriched in members belonging to either of three orders - *Bacillales*, *Lactobacillales*, or *Clostridiales*. Only the AD patient group showed any associations for the *Bacillales* order, which at a higher taxonomic level included members of the genus *Gemella*. Distinct members of the *Lactobacillales* order were found to be enriched in the AD group, as well as in the APOε4 carriers. The AD cohort showed an increased relative abundance in *L. casei paracasei* with a mean abundance of 1.97% compared to 0.03% and 0.04% in the APOε4 non-carriers and carriers, respectively. The APOε4 carriers, on the other hand, had a higher abundance in *Streptococcus cristatus* and *Streptococcus australis*. The latter two species overall occurred at very low abundances (<0.02%).

All three groups showed enrichment in members of the *Clostridiales* order, with the majority of associations found for the APOε4 carriers. The AD patient group had only two associations within this order, namely for the species *Clostridium methylpentosum* and an associated strain. It is, however, noteworthy that this species was very rare, showing a mean relative abundance of 0.01% in the AD patient group and was completely absent from the two APOE cohorts. Altogether LEfSe detected seven discriminating taxa within the APOε4 carriers for the *Clostridiales* order, which at a higher taxonomic resolution belonged to the *Ruminococcaceae*, *Lachnospiraceae*, *Eubacterium* families – including *Ruminococcus callidus*, a strain of the *F. prausnitzii* species, *Ruminococcus obeum* and *Eubacterium eligens*. All of these taxa were significantly more abundant in the APOε4 carriers compared to the other two groups. Of the detected species, *E. eligens*, was most prevalent (mean relative abundance APOε4 carriers: 1.57%, APOε4 non-carriers: 0.92%, AD patients: 0.10%). The

APOε4 non-carriers were also enriched in members of the *Eubacterium* family - namely for the species *E. ramulus* and an associated strain.

The intestinal microbiota of the AD patient group was also characterized by increased abundance of several members of the *Actinobacteria* clade. Broadly, the associations belonged to members of two families – *Coriobacteriaceae* or *Actinomycetaceae*. Within the latter family, there were two associated species *Actinomyces viscosus* and *Actinomyces johnsonii* species and associated strains. Whereas the *Coriobacteriaceae* family was enriched in members of the *Atopobium parvulum* species. The APOε4 non-carriers also had an association with a species of the *Coriobacteriaceae*, however, this increase was related to the *C. aerofaciens* species.

LEfSe analysis also found discriminating features within the *Bacteroidetes* phylum. The APOε4 carriers were enriched in *Bacteroidetes*, *Bacteroidia* and *Bacteroidales*, and the species *B. plebeius*. The APOε4 non-carriers, on the other hand, showed increased abundance in members of *B. stercoris* and an associated strain, but not other taxa of the *Bacteroidetes*.

Upon lowering the alpha value to <0.01, LEfSe analysis only returned three significant associations. All of these were for the AD patient group, namely for three closely related members of the already described *Actinobacteria* clade – the order *Actinomycetales*, the family *Actinomycetaceae*, and the *Actinomyces* genus.

Multivariate analysis (MaAsLin2)

Per-feature testing in MaAsLin2 was used to identify taxa associated with ‘group’, whilst adjusting for potential confounders (age and sex). There were 52 significant associations with group (Table 7.56 in the supplementary). The identified features spanned over two kingdoms and five phyla and included 14 associations at species-level. Within the model, the AD patient group was used as a baseline contrast against which the APOε4 carriers and APOε4 non-carriers were compared against.

Of the 52 distinct taxa identified by MaAsLin2, 47 were found for both comparisons (Figure 5.14, taxa in black). One association was only significant in the AD vs APOε4 non-carrier comparison (Figure 5.14, taxa in blue), whereas four associations were found to be present only between the AD patient and APOε4 carrier comparison (Figure 5.14, taxa in red).

The vast majority of taxa associations were found for the kingdom of *Bacteria* and belonged to four phyla, namely *Actinobacteria*, *Bacteroidetes*, *Firmicutes* and *Proteobacteria*. Overall, about a third of all associations were related to the *Bacteroidetes* phylum, approximately 27% were related to the phylum *Firmicutes*, one in four were related to the *Actinobacteria* phylum, and 11.5% belonged to phylum of *Proteobacteria*. The remaining associations were linked to members of an unnamed phylum of the *Virus* kingdom.

All associations within the *Actinobacteria* clade (Figure 5.14, [A]) showed a significantly reduced abundance of taxa in the two APOE cohorts compared to the AD patient group. More specifically, this significant reduction in abundance was found for members belonging to three distinct orders: *Actinomycetales*, *Bifidobacteriales*, and members of the *Coriobacteriales*. At the highest taxonomic resolution four species,

Actinomyces viscosus, *Actinomyces oris*, *B. longum* and an unclassified *Eggerthella* species, were significantly enriched in AD. *B. longum* was 10.02% and 8.90% less abundant in the APOε4 carriers and non-carriers, respectively, compared to the AD patient group (Figure 5.14, [B]). Whereas *A. oris* and *A. viscosus* mean relative abundances were approximately 2% higher in the AD patient group. The unclassified *Eggerthella* species was only half as abundant in the APOE cohorts compared to the AD patient group (Figure 5.14, [A]).

The *Bacteroidetes* clade, had the largest number of significant associations. On the contrary to the *Actinobacteria* clade, I found that all identified taxa were present at significantly higher relative abundances in the APOE cohorts compared to the AD patient group. This was reflected by increased mean relative abundances for the *Bacteroidales* order (AD: M= 9.11%, SD = ±10.11; non-carriers: M=19.79%, SD = ±11.15; carriers: 25.63%, SD = 10.95) as well as for three associated families and their members- *Bacteroidaceae*, *Porphyromonadaceae* and *Rikenellaceae*. At even higher taxonomic resolution, I found six species enriched within these three families - *B. stercoris*, *Parabacteroides merdae*, *Barnisiella intestinhominis*, *Odoribacter splanchnicus*, and two species of the *Alistipes* genus (Figure 5.14 [B]).

The third clade, which had several associations with group was that of the *Firmicutes* phylum (which in itself was not significant). In contrast to the *Actinobacteria* clade for which all significant members were significantly enriched in AD patients, and the *Bacteroidetes* clade for which all significant members were depleted in the AD group, I observed both reduction and enrichment in taxa within the *Firmicutes* compared to the APOE groups (Figure 5.14 (C)).

The class of *Bacilli* and its associated order *Lactobacillales*, as well as several members belonging to this order, were all significantly reduced compared to the AD group. With mean relative abundances for *Lactobacillales* increasing in a stepwise manner from 0.97% (SD = 1.91) in the APOε4 non-carriers, 1.79% (SD = 3.49) to in APOε4 carriers, and 7.53% (SD = 6.17) in the AD group.

Whereas the class of *Clostridia*, its order *Clostridiales* and six related members were significantly enriched compared to the AD group. Here I observed a stepwise reduction from the APOε4 non-carriers, over the APOε4 carriers, to the AD patient group for the *Clostridia* order. Within the *Clostridia* order, I found four associated families: *Clostridiales Family XIII Incertae Sedis* (enriched in AD), *Eubacteriaceae* (depleted in AD), *Ruminococcaceae* (depleted in AD) and *Lachnospiraceae* (depleted in AD). The species *F. prausnitzii* of the *Ruminococcaceae* was over three times as abundant in both APOE cohorts (non-carriers: 8.13%, SD=5.67; carriers: 8.89%, SD=5.43) compared to the AD patient group (2.43%, SD=2.48).

There were also several associations with a fourth bacterial clade, namely with members of the *Proteobacteria* phylum, which included associations for the order of *Burkholderiales* and *Pasteurellales*. Within the *Pasteurellales*, the species *Haemophilus parainfluenza* was significantly more abundant in the APOε4 non-carriers (0.07%, SD=0.13) and APOε4 carriers (0.06%, SD=0.10) compared to the AD patient group (0.002%, SD=0.003).

Lastly, I also observed significant associations with an unnamed phylum of the *Virus* kingdom, that belonged to the order of *Caudovirales* at lower taxonomic levels.

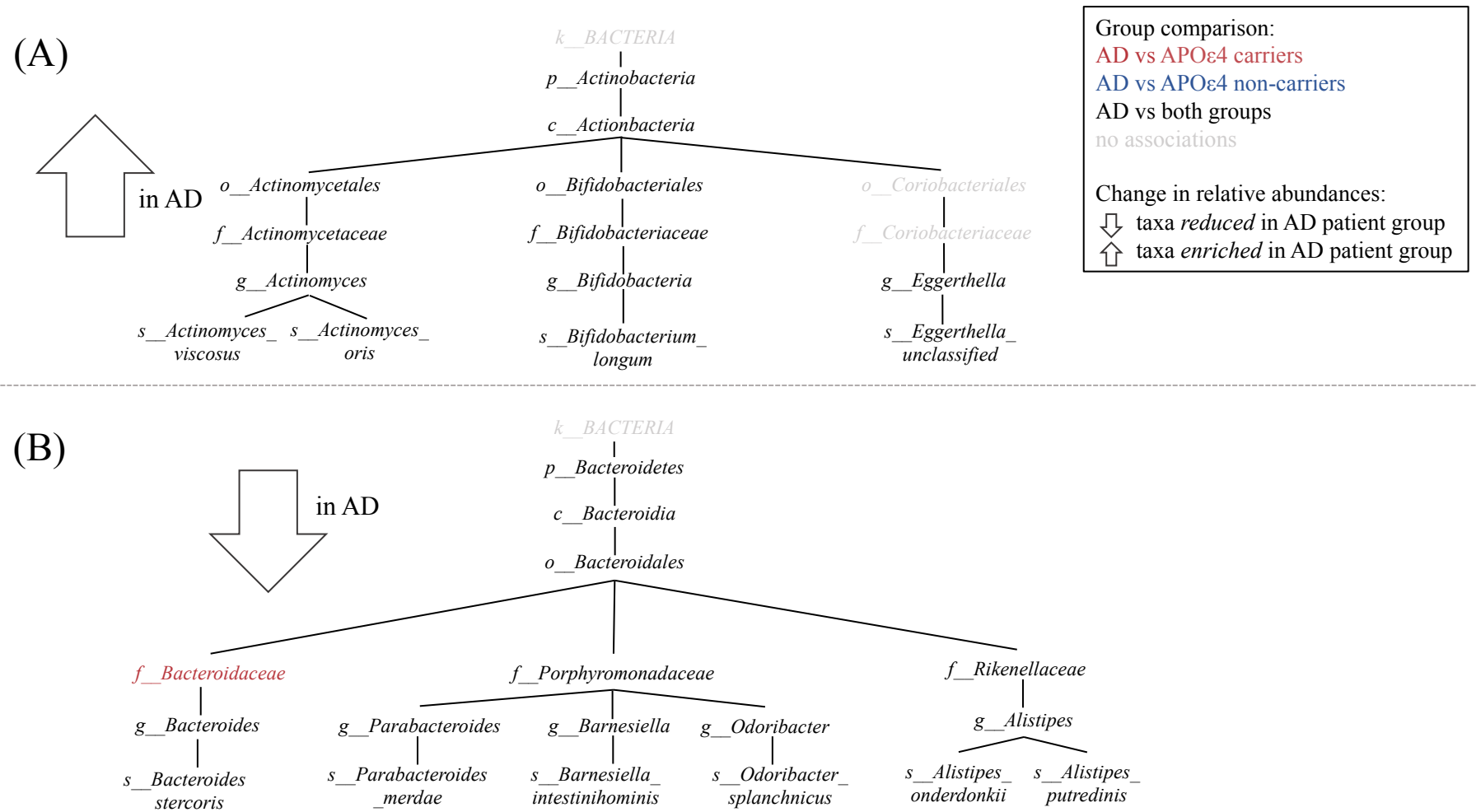
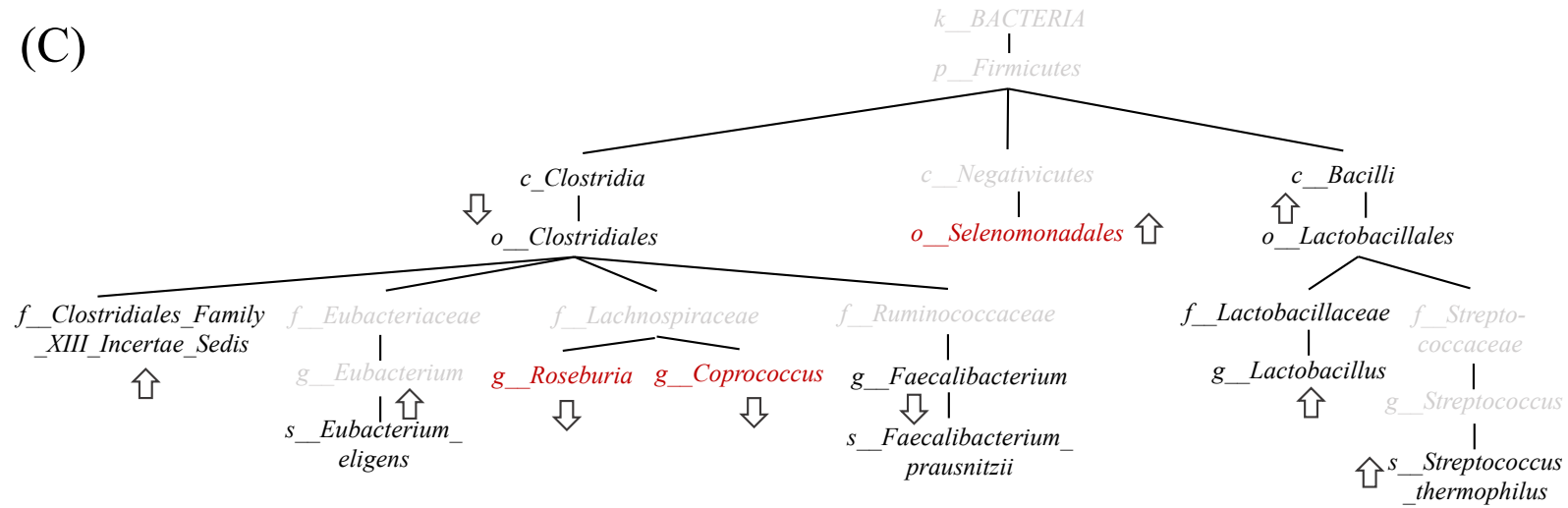
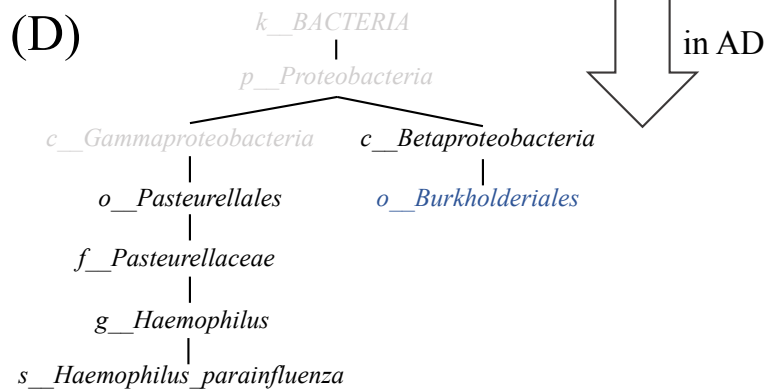


Figure 5.14 Significant associations identified by MaAsLin2 analysis grouped by phylogeny, Clades: (A) *Actinobacteria*, (B) *Bacteroidetes*, (C) *Firmicutes*, (D) *Proteobacteria*, (E) *Viruses*. Black: associations with Alzheimer’s Disease group and both Apolipoprotein E cohorts, blue: Alzheimer’s Disease only with Apolipoprotein ε4 non-carriers, red: AD only with Apolipoprotein ε4 carriers, grey: no associations. Upward (increased) and downward arrow (decreased) indicate relative abundance in Alzheimer’s Disease patient group compared to the APOE groups.

(C)



(D)



(E)

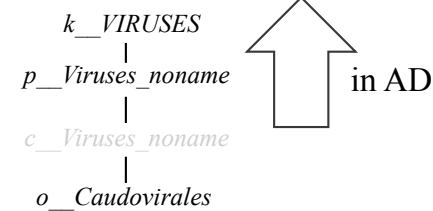


Figure 5.14 (continued) Significant associations identified by MaAsLin2 analysis grouped by phylogeny, Clades: (A) *Actinobacteria*, (B) *Bacteroidetes*, (C) *Firmicutes*, (D) *Proteobacteria*, (E) *Viruses*. Black: associations with Alzheimer's Disease group and both Apolipoprotein E cohorts, blue: Alzheimer's Disease only with Apolipoprotein $\epsilon 4$ non-carriers, red: AD only with Apolipoprotein $\epsilon 4$ carriers, grey: no associations. Upward (increased) and downward arrow (decreased) indicate relative abundance in Alzheimer's Disease patient group compared to the APOE groups.

Comparison of differential analysis results (LEfSe vs MaAsLin2)

Both analyses identified numerous associations at different taxonomic levels. However, whilst the majority of discriminating taxa identified with LEfSe analysis were at species-level or strain-level, MaAsLin2 analysis identified associations that more equally distributed across all taxonomic levels.

In both analyses numerous significantly associated taxa belonged to the *Actinobacteria*, *Bacteroidetes* and *Firmicutes* (dominating in LEfSe analysis) clade. I found that eight taxa were identified by both analyses: the phylum and class of *Actinobacteria*, one associated order, family, genus (*Actinomyces*), and the species *A. viscosus*. Both analyses also identified the phylum *Bacteroidetes*, the *Bacteroidia*, *Bacteroidales* order, and the species *B. stercoris* and *E. eligens*.

Whilst the number of exact taxa detected by both analyses was limited, there was a striking overlap in phylogenetic lineages that were identified. Besides the already mentioned, both analyses also returned significant associations for members belonging the *Streptococcaceae*, *Lactobacillaceae*, *Ruminococcaceae*, and *Lachnospiraceae* families belonging to the *Firmicutes* phylum.

Predictive Functional profiling

In a next step, I used predictive functional profiling in order to gain a better insight into changes of the functional potential that might be associated with AD pathology.

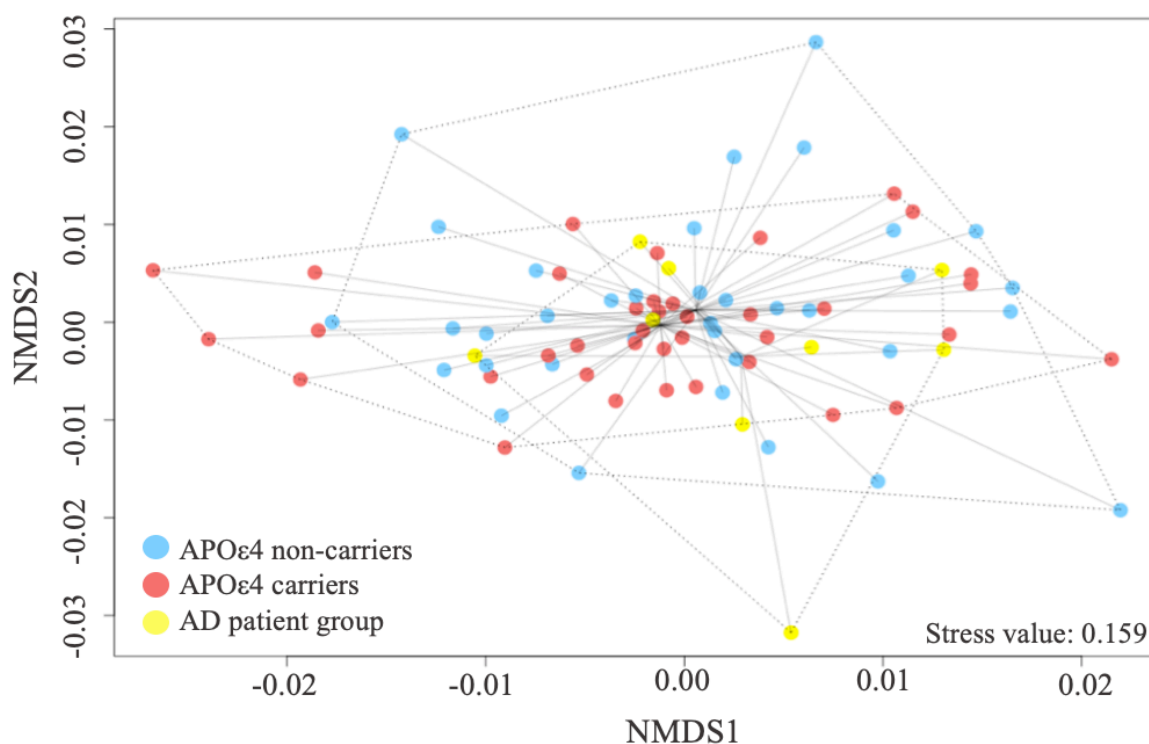
The KEGG gene abundance table had an average read count of 479,229 reads per sample, ranging between a minimum of 111,787 reads per sample to a maximum of 790,719 reads per sample. A total of 1,962 low abundance features were removed based on prevalence (minimum count =1 in at least 10% of samples) during data filtering, leaving an overall of 8,544 features.

The functional potential was defined by 11 KEGG metabolisms, 210 KEGG modules and 148 KEGG pathways. Of note, the here investigated KEGG data represents the predicted functional potential of distinct organisms or genes encoding for enzymes or KOs involved in a certain metabolism, module or pathway, irrespective of the abundance for these organisms. Whereas the HUMAnN3 data also shows relative abundances.

Beta diversity

Beta diversity (Jaccard diversity index) of the predictive functional potential of the microbial communities was significant for the effect of group for KEGG metabolism ($p=0.027$), KEGG module ($p=0.026$) and KEGG pathway ($p=0.028$), whilst accounting for the effect of age and sex (Table 7.66 in the supplementary). Pairwise PERMANOVA showed that the comparison between the groups driving the group effect was only significant when comparing the APO ϵ 4 non-carriers against the AD patient group (FDR-corrected p -value = 0.018) and explained approximately 12% of the observed variance in the data (Table 7.67 in supplementary). Importantly, the microbial functional potential of the APO ϵ 4 carriers and AD group was not statistically different, implying a greater degree of similarity between these two groups.

A visualisation of the NMDS ordination on the level of KEGG metabolism is shown below. The NMDS plots of KEGG modules and pathways can be found in the supplementary Figure 7.14.



5.15 Non-metric Multidimensional Scaling on Jaccard index between the predicted KEGG metabolism by participant group (light blue = Apolipoprotein ε4 non-carriers, red = Apolipoprotein ε4 carriers, yellow = Alzheimer’s Disease patients). Each point denotes a sample in a reduced dimensional space and is connected with a line to the group centroid

Multivariate analysis of normalized Kyoto Encyclopedia of Genes and Genomes count data

Kyoto Encyclopedia of Genes and Genomes - metabolism

Our multivariate general linear model showed that the intestinal microbiota of the AD group had a significantly larger number of distinct genes involved in ‘carbohydrate metabolism’ compared to the APOε4 carriers ($\beta=-0.0039$, corrected p-value=0.009) and APOε4 non-carriers ($\beta=-0.0039$, corrected p-value=0.007). The predictive functional potential of distinct organisms involved in ‘metabolism of cofactors and vitamins’ was reduced in the microbial community of AD patients compared to that of APOε4 carriers ($\beta=0.0040$, corrected p-

value=0.04), but was increased in comparison to that of APOε4 non-carriers (β =-0.0017, corrected p-value=0.014). For a full overview of the KEGG results please refer to Table 7.57-7.61 in the supplementary.

Kyoto Encyclopedia of Genes and Genomes - modules

I then investigated the KEGG modules, which are small functional unit of organisms that encode for KOs that correspond to conserved sub-pathways in the KEGG pathway network, to assess the intestinal metabolic potential on a more granular level. There were 21 modules with a significantly larger and an equal number of modules with a significantly lower microbial functional potential in the AD patient group compared to the APOE cohorts.

Of the modules enriched in the microbial community of AD patients, nine modules belong to the ‘carbohydrate metabolism’ on a higher functional level, five modules are part of ‘energy metabolism’, and three modules belong to ‘lysine biosynthesis’. The ‘metabolisms of cofactors and vitamins’, ‘nucleotide metabolism’, and ‘xenobiotics biodegradation and metabolism’ were each increased for one module.

The enriched modules involved in carbohydrate metabolism were glycolysis (M00001), the PPP (M00004, M00006, M00007), Entner-Doudoroff pathway (M00008) and the glucuronate pathway (uronate pathway) (M00014). Via their central biochemical role in carbon metabolisms, these modules were also closely linked with two modules belonging to KEGG energy metabolism (carbon fixation), namely reductive pentose phosphate cycle (Calvin cycle, M00165) and reductive pentose phosphate cycle (glyceraldehyde-3P => ribulose-5P, M00167). Within the bracket of KEGG energy metabolism, I also found an increased microbial functional potential for formaldehyde assimilation via the xylulose (M00344) and via the ribulose (M00345) monophosphate pathway, as well as increased metabolic potential for nitrogen fixation (nitrogen => ammonia, M00175).

The intestinal microbiota of AD patients also had a significantly larger predicted functional potential for three pathways of lysine biosynthesis, namely the succinyl- diaminopimelic acid (DAP) pathway (M00016), DAP aminotransferase pathway (M00027) and the acetyl-DAP pathway (M00525). Modules of lysine biosynthesis belong to the KEGG amino acid metabolism on a higher level, just like GABA biosynthesis (eukaryotes, M00135), which was also increased in AD.

Besides these associations, I also found an increased microbial potential for guanine ribonucleotide biosynthesis (M00050), tocopherol/tocotrienol biosynthesis (M00112), and carbazole degradation (M00544).

As outlined, there were also several modules for which the predicted functional potential of distinct organisms in the microbial community in the AD group was reduced compared to the APOE cohorts. A third (seven modules) of the reduced modules belong to the ‘metabolism of cofactors and vitamins’, whereas all other KEGG metabolisms had a maximum of four associated modules (glycan biosynthesis and metabolism) or less. The only KEGG metabolism for which I found no related modules was the ‘metabolism of other amino acids’. The modules related to the ‘metabolism of cofactors and vitamins’ were all associated with synthesis of vitamins of the B family and included pyridoxal phosphate (vitamin B₆) biosynthesis (M00124), riboflavin (vitamin B₂) biosynthesis (M00125), three modules involved in the biosynthesis of biotin (vitamin B₇) including biotin biosynthesis, pimeloyl-ACP/CoA (M00123), biotin biosynthesis, BioI pathway (M00573), biotin biosynthesis, BioW pathway (M00577), as well as pantothenate (vitamin B₅) biosynthesis (M00119) and the closely linked coenzyme A (CoA) biosynthesis (M00120). The latter module is also linked to the sub-pathway of β -oxidation, acyl-CoA synthesis (M00086), which belong to ‘fatty acid metabolism’. Four modules (M00060, M00063, M00064,

M00080) who are all involved lipopolysaccharide metabolism and belong to ‘glycan biosynthesis and metabolism’ were also found to be decreased in AD.

Kyoto Encyclopedia of Genes and Genomes - pathways

Several of the findings at the level of KEGG modules, were also reflected on the level of KEGG pathways (including glycolysis/gluconeogenesis, pentose phosphate pathway, fructose and mannose metabolism as well as lipopolysaccharide biosynthesis, riboflavin metabolism and biotin metabolism). I identified a total of 21 metabolic pathways after FDR-correction for multiple testing comparison, of which 16 were significantly increased and five were significantly decreased in AD compared to the APOE cohorts.

The majority of KEGG pathways with a predicted increased microbial functional potential, included pathways related to ‘carbohydrate metabolism’ such as glycolysis/gluconeogenesis (ko00010), pentose phosphate pathway (ko00030), fructose and mannose metabolism (ko00051), galactose metabolism (ko00052) and ascorbate and aldarate metabolism (ko00053). Pathways belonging to ‘xenobiotics (aromatics) biodegradation and metabolism’ included chloroalkane and chloroalkene degradation (ko00625), naphthalene degradation (ko00626), metabolism of xenobiotics by cytochrome P450 (ko00980), drug metabolism – cytochrome P450 (ko00982) and steroid degradation (ko00984). For a full list of all associated KEGG pathways please see Table 7.60-7.61 in the supplementary.

There were overall fewer KEGG pathways with a reduced microbial functional potential in AD compared to the APOE cohorts. Three of those pathways belong to the ‘metabolism of cofactors and vitamins’, namely one carbon pool by folate (ko00670), riboflavin metabolism (ko00740), and biotin metabolism (ko00780). Apart from this, there was also a decreased functional potential of lipopolysaccharide biosynthesis (ko00540) and terpenoid backbone biosynthesis (ko00900) in the AD group.

HUMAN3 functional profiles

The HUMAN3 analysed data returned functional community profiles that were either stratified by known organisms or unstratified pathways. The stratified output showed increased relative abundances in the AD patient group for four species, namely *Actinomyces naeslundii*, *Bifidobacterium dentium*, *Streptococcus thermophilus* and *Bifidobacterium bifidum*, and decreased relative abundance for *Roseburia intestinalis* (Table 7.62 – 7.63 in the supplementary). Unfortunately, the here listed species were all assigned “UNINTEGRATED” abundances, which means that they did not contribute to a known pathway and are hence not further discussed.

The unstratified functional profiles returned 45 pathways with significantly increased relative abundance and two pathways with significantly reduced relative abundances when comparing the microbial profiles of the AD against the APOE groups (Table 7.64 – 7.65 in the supplementary). All differences are based on relative abundances for genes in the described pathway.

Congruent with the KEGG analyses, many of the pathways shown here were already identified previously. This overlap in results between the KEGG and HUMAN3 data analysis includes: the succinylase variant of the L-lysine DAP pathway (DAPLYSINESYN-PWY), as well as the dehydrogenase variant (PWY-2942) and the related superpathway which integrated the biosynthesis of L-lysine but also of L-aspartate, L-threonine and L-methionine (P4-PWY). I also found an overlap with respect to four pathways describing glycolysis from glucose and sucrose (PWY-5484, GLYCOLYSIS, ANAGLYCOLYSIS-PWY, PWY66-400). Albeit not identified in the KEGG analysis, glucose fermentation is also closely linked to the here found ‘Bifidobacterium shunt’ pathway (P124-PWY), which is also known as the ‘fructose-6-phosphate pathway’, that produces acetate and lactate from glucose (whilst discovered in *Bifidobacterium* this pathway is also found in other

organisms), the sucrose degradation pathway (PWY-5384) and starch biosynthesis (PQY-622). Glycolysis is closely connected to the glycogen degradation (GLYCOCAT-PWY), which provides glucose-6-phosphate for glycolysis, and was statistically the most significant pathway in this analysis.

In keeping with the KEGG analyses, the microbiota of AD patients was enriched in the ribulose monophosphate (RuMP) pathway of formaldehyde assimilation (PWY-1861). The analysis further identified several pathways that were not seen with the KEGG count data, including five pathways that are involved in the biosynthesis of pyrimidine deoxyribonucleotides (PWY-7198, PWY-7211, PWY0-166, PWY-7187) and the related superpathway of pyrimidine ribonucleotides biosynthesis (PWY0-162). Notably, the second most significant increase was observed for a superpathway that synthesises O-antigen. Besides lipid A and the core oligosaccharides, O-antigen (a polysaccharide) is a fundamental component of lipopolysaccharides.

In-line with the KEGG pathway findings, the intestinal microbiota of AD patients was reduced in the relative abundance of pathways related to vitamins of the B family. This was supported by a decrease in the pathway of riboflavin biosynthesis in the microbial functional potential of the AD patient group (RIBOSYN2-PWY: flavin biosynthesis I [bacteria and plants]) and by a reduction of a pathway (THISYN-PWY: superpathway of thiamine diphosphate biosynthesis I) that synthesizes thiamine diphosphate (vitamin B₁).

Chapter Discussion

Key findings

The intestinal microbiota in the AD patients studied here was characterized by global and specific differences in taxonomy and function compared to healthy individuals, with and without APOE genetic risk for AD. This work identified significant differences in the overall community composition, and a significant reduction in community richness and evenness in the AD patient group compared to the two APOE cohorts. Taxa-specific changes in the AD patient group were numerous and included increased abundance of members belonging to the *Actinobacteria* (*Coriobacteriaceae*, *Actinomyces*, *Bifidobacterium*), an increased abundance in *Lactobacillus* and *Streptococcus* species, as well as decreased abundance of *Bacteroidetes* members (*Bacteroides*, *Barnesiella*, *Odoribacter*, *Alistipes*) and decreased abundance of SCFA-producers of the *Clostridiales* order (*E. eligens*, *F. prausnitzii*, *Lachnospiraceae*) in the AD patient group compared to the APOE groups. The functional analysis revealed various differences in the predicted potential of the microbial community function. Notable differences included that in the AD group, there was upregulation in glucose and alternative glucose pathways (notably the PPP), methane metabolism, pathways of ammonia production and methionine biosynthesis and was downregulated for the synthesis of B-vitamins (incl. riboflavin). Overall, the findings from this study support the notion of a microbial component in AD pathology.

Neuropsychological and behavioural analysis

Neuropsychological testing was used to validate cognitive and behavioural impairment in the AD patient cohort. As expected AD patients showed clear, objectively measurable, cognitive impairment as they performed consistently less well on all of the measures compared to the cognitively healthy APOE groups. AD patients scored significantly lower on the ACE-III, reflected by a significant decline in all five cognitive domains evaluated by the ACE-III, namely attention, memory, verbal fluency, language and visuospatial abilities

(Bruno and Vignaga, 2019). In-line with the literature, the AD patient cohort is significantly impaired on measures for visuoconstructional abilities, executive functioning and non-verbal abilities (recall and recognition memory) (Melrose *et al.*, 2013) as was shown by significantly worse performance on the ROCF compared to the APOE cohorts. Reduced ability in visual scanning, psychomotor speed and executive functioning, known to be impaired in AD (Ashendorf *et al.*, 2008), were also evidently impaired in the AD patient group as was shown by their poor TMT performance. Anxiety and depression, both prevalent in AD pathology (Kuring, Mathias and Ward, 2018), albeit low in all study participants, were significantly elevated in the AD group. The functional and behavioural domains that affect AD patients (Wear *et al.*, 2008) and that can be reliably measured by the CBI-R, such as memory, everyday skills, self-care, mood, beliefs and motivation, were all noticeably impaired in the AD patient cohort.

Diversity analysis

The community structure of the AD patient cohort was marked by significantly fewer distinct kinds of species (richness) and by less evenly distributed species (evenness) at the lower taxonomic levels, as measured by Shannon and Inverse Simpson indices, compared to the APOE groups. This decrease in alpha diversity broadly parallels results by Vogt *et al.* (2017) who report decreased alpha diversity on several measures in AD patients, including a significantly lower Shannon diversity index (but no significant difference with respect to their Inverse Simpson index). This also agrees with Liu *et al.* (2019), who found a significantly reduced Shannon and Simpson index, but no difference on the Chao1 or ACE diversity indices. Li *et al.* report a reduction on the Faith's PD, but no difference when measuring alpha diversity with the Chao1 or Shannon index. A decrease in diversity is also supported by the work of Ling *et al.* (2021), who show a significant reduction across several alpha diversity metrics in the AD cohort. Contrary to these findings, Saji *et al.* (2019) are the only group to report increased community richness (Shannon diversity) in their AD

patient cohort but show no difference for the Simpson index. Hou *et al.* (2021) show no difference between their groups as measured by the Shannon and Sobs metric. At large, the majority of studies advocate the notion of reduced community diversity in AD. The majority of evidence from animal work also supports the notion of reduced microbial diversity in AD mice (D. Chen *et al.*, 2017; Zhang *et al.*, 2017; Lee, Hwang and Kim, 2018; Xin *et al.*, 2018; Lee *et al.*, 2019). Importantly, when comparing the APOE groups against each other (T2 data), there were no differences between the group of APOE4 carriers and non-carriers, indicating a comparable richness and evenness in their compositional microbiota profiles. At T1 and T3, however, alpha diversity of the APOE4 carriers was reduced at the kingdom and species-level, which indicates a shift towards a lower diversity, as also observed for the AD patient group.

Reduced diversity is widely associated with intestinal dysbiosis, and it is hypothesized that reduced diversity might indicate an unstable microbial ecosystem, that is at greater risk for opportunistic pathogens and vulnerable to a loss of equilibrium between species (Mosca, Leclerc and Hugot, 2016). Dysbiosis is also linked to intestinal and systemic inflammation (Mosca, Leclerc and Hugot, 2016). Congruent with this, many diseases that are associated with reduced diversity, share an inflammatory disease component. Although understanding the cause and effect of reduced microbial diversity in the context of AD requires further investigation, mounting evidence indicates that changes in alpha diversity may indeed be associated with AD pathology.

Microbial community profiles, assessed using beta diversity measures, were distinctly different between the AD patients and the APOE groups. AD disease status was a significant driver of community structure at each taxonomic level. Among all factors considered in the analysis, AD status accounted for the largest proportion of variation in the community profiles. There was however no difference between the compositional profiles of the APOE4

carriers and non-carriers, which indicates that the compositional profiles are undistinguishable between APOE cohorts at this top-level view.

These large-scale compositional differences are in-keeping with previous findings showing community structure differences between AD patients and controls (saji *et al.*, no date; Vogt *et al.*, 2017; Zhuang *et al.*, 2018; B. Li *et al.*, 2019; Haran *et al.*, 2019; Liu *et al.*, 2019; Hou *et al.*, 2021; Ling *et al.*, 2021). Although the studies used a variety of dissimilarity metrics, which in turn use different approaches to determine the ecological distance between all pairs of samples, they largely show significant community variation between AD patients and controls. All studies using Bray Curtis dissimilarity (used also in the present study) and all but two accounts using weighted and unweighted UniFrac found compositional differences. Taken together, these studies show that AD status explains between 9-12% of the observed variation in the data, depending on the dissimilarity metric used and taxonomic level presented. Comparable to this, I found a mean explanatory power of 8.2% (range: 5.3%-12.3%) across all taxonomic levels.

These global changes in taxonomic structure are indicative for a microbial role in AD pathology but it requires more well-conducted, longitudinal and large-cohort studies to explore this potential two-way relationship of the Gut-Brain axis in AD further.

Descriptive community analysis

On a descriptive level, I observed noticeable numerical differences in the intestinal microbiota abundance profiles of AD patients compared to the APOE cohorts. Whilst the human intestinal microbiota in healthy individuals were dominated by bacteria of the *Firmicutes* and *Bacteroidetes* phyla, as was the case for the APOE groups, the intestinal community of the AD patient cohort was dominated by *Firmicutes* and *Actinobacteria*. In fact, *Bacteroidetes* was only the fourth most abundant phylum (*Euryarchaeota* is the third)

in the given AD patient group. This observation is consistent with Saji *et al.* (2019) and Hou *et al.* (2021) who report an inverse relationship in the ratio of *Bacteroidetes* (Hou *et al.*: 18%, this work: 9%) to *Firmicutes* (Hou *et al.*: 52%, this work: 51%) in AD patients. This top-level shift in the distribution of phyla was seen throughout the community structure at all taxonomic levels and is supported by numerous significant taxa-specific differences between the AD group and the APOE groups but not when comparing the APOE groups against each other.

Differential abundance analysis

Univariate analysis of different relative taxonomic abundances

The lack of a gold standard with respect to the data collection, DNA extraction process, downstream processing and analysis method, particularly in light of the wealth of an ever-growing number of new methods in a fast-moving field, leads to a huge amount of heterogeneity between studies on any given number of methodological or study design aspects. This heterogeneity may represent a source of bias. Microbiome studies, which are subject to a large degree of inherent noise (inter- and intra-subject variability), are potentially at even greater risk of confounding factors due to inconsistent methodology.

There are currently nine human research studies that have investigated the role of the intestinal microbiota in AD patients (Table 1.1). A range of statistical models and methods can be chosen to implement differential abundance analysis. Given the technical bias, it is recommendable to make comparisons across studies that have used a similar methodology. Thus, I will compare the differential abundance results gained from LEfSe against those studies employing the same statistical approach.

LEfSe determined 19 significantly enriched taxa for the AD patient group, compared to 32 enriched taxa in AD by Ling *et al.* (2021), 21 taxa by Zhuang *et al.* (2018), 14 taxa by Hou

et al. (2021), seven taxa by Li *et al.* (2019) and four taxa by Liu *et al.* (2019). The majority of results from LEfSe analysis are at high taxonomic resolution, with the exception of Li *et al.* who identified taxa that were all above genus-level. In this study 64% of associations are at genus-level or below, which is comparable to the results by Zhuang *et al.* (67%), Hou *et al.* (63%) and Ling *et al.* (64%). Liu *et al.* only report associations at genus-level. Importantly, this study was the only study to employ shotgun metagenomic sequencing (apart from Haran *et al.* [2019] who did not use LEfSe), which allows us to investigate taxa abundances down to strain-level.

Here, I reported increased abundances for several members of the *Actinobacteria* and *Firmicutes* phyla in AD patients. On a phylum-level, this finding is congruent with Ling *et al.* and is broadly mirrored by Zhuang *et al.* and Li *et al.*, whose majority of associations were members belonging to these two phyla. Most notably, this study and the study of Zhuang *et al.* as well as that by Ling *et al.* showed that faecal samples of the AD patient group are significantly enriched in members of *Actinobacteria*. Within the *Actinobacteria*, I identified members of the *Coriobacteriaceae* and *Actinomycetaceae* families. This replicates Ling *et al.*' finding, who also find enrichment for *Coriobacteriaceae* and is further supported by Zhang and colleagues who identified members of the *Coriobacteriaceae* family. At species-level, I found increased prevalence of *A. parvulum* and an associated strain.

Members of the *Coriobacteriaceae*, which is a family of 'pathobionts' (defined as potentially pathological organisms), can metabolize cholesterol-derived substances such as bile acids and are hence important in bile acid metabolism (Just, 2017). *Coriobacteriaceae* are also regulators of lipid metabolism and have been suggested to mediate insulin resistance (Clavel *et al.*, 2014). The latter has long been associated with AD pathophysiology and is still investigated by many studies that are trying to disentangle the links between metabolic disease and AD (Janak and Jenner, 2020).

A. parvulum, previously classified *Streptococcus parvulum*, is a gram-positive obligate anaerobic bacterium. It is considered a common pathobiont in the oral microbiota which is closely linked to periodontal disease (Mizutani, Yamada and Yachida, 2020). In the intestine, *A. parvulum* metabolizes glucose to lactose, formic and acetic acid, and is a key producer of toxic H₂S. Excessive H₂S has been shown to activate autocrine T-cells, thereby triggering inflammation (Miller *et al.*, 2012; Mottawea *et al.*, 2016). *A. parvulum* has also been shown to promote degradation of the mucus layer of the intestinal barrier and is associated with a range of diseases, including Crohn's disease, IBS, colorectal cancer and cirrhosis (Mizutani, Yamada and Yachida, 2020).

Increased abundance of *Coriobacteriaceae*, particularly *A. parvulum*, might contribute to AD pathology, which is characterized by increased systemic inflammation, which in turn is likely to be (at least in part) the result of impaired intestinal barrier function that allows for the of translocation of inflammation-inducing components from the lumen to the peripheral system. Similar to the proposed mechanism of action in Crohn's disease, the host defense in AD patients appears to be weakened, which may be influenced by a reduction of SCFA-producing bacteria, as I will discuss in more detail later.

The data also showed enrichment for several members belonging to the *Actinomyces* genus (*Actinobacteria*) in AD samples. Like the *Atopium* genus, the *Actionmyces* genus also classes as a genus of gram-positive, obligate, anaerobic bacteria, which are considered pathogenic commensals. In the oral cavity, certain species of *Actinomyces* participate in the formation of biofilm and dental plaques and have been linked to periodontal disease (Li *et al.*, 2018). This is interesting in the context of AD because it was recently shown that certain microbes are good clinical markers of periodontitis and that presence of these bacteria is strongly associated with incident for AD and for all-cause dementia (Beydoun *et al.*, 2020). Another large cohort study supporting a microbial role in periodontitis, identified a series of bacteria

that are involved in periodontitis, including a species of *Actinomyces*, which also correlated with elevated serum IgG levels (Noble *et al.*, 2014).

On a species-level, *A. viscosus* and *A. johnsonii* were enriched in the faecal samples of the AD patient cohort. Pathogenicity of *A. viscosus* is mediated by its lipoproteins (lipophilic fraction of the bacterium) which act as ligands of TLR2 and are thus responsible for inducing an inflammatory response via the production of cytokines (Shimada *et al.*, 2012), further adding to potential mechanisms of increased inflammation in AD. Of note, members of the family *Actinomycetales* and *Porphyromonas gingivalis* (order *Bacteroidales*) have been repeatedly found in AD brain tissue (Emery *et al.*, 2017; Siddiqui *et al.*, 2019). This evidence further supports a potential role for *Actinobacteria* and periodontitis-related bacterial pathogens in AD. Interestingly, an antimicrobial agent that acts against an enzyme secreted by *P. gingivalis* is being tested in a Phase II/III clinical trial in AD patients (NCT03823404, expected completion in 2022), further supporting a potential association. Whilst the picture is still incomplete, there is mounting evidence that implicates *Actinomyces* as a potential driver of pathogenic processes which may be of relevance in the context of AD.

Within the *Firmicutes* phylum, I observed enrichment for the genus *Gemella*, the species *Lactobacillus casei paracasei* (genus *Lactobacillus*) and *C. methylpentosum* (genus *Clostridium*) in the AD patient group. This is broadly mirrored by Liu *et al.* who report enrichment of *Lactobacillus* and by Ling *et al.* who demonstrate increased abundance for several members of the *Clostridium* genera. *Gemella* are gram-positive cocci (opportunistic pathogens), that inhabit mucosal membranes and can cause serious infections, but are otherwise sparsely documented in the literature (Jayananda, Gollol-Raju and Fadul, 2017). Interestingly, *L. casei* and *L. paracasei* are some of the most studied species, that are commonly used as probiotics due to their wide-reaching health promoting properties (Hill

et al., 2018). Increased prevalence of *Lactobacillus* bacteria in AD patient samples cannot be explained.

Albeit not directly comparable, certain taxa emerged to be significantly different in the comparison of APOE cohorts against the AD group as well as in the APOE groups-only comparison over time. The APOE4 carriers were repeatedly enriched in the species *R. obeum* and an associated unclassified strain when compared to the APOE4 non-carriers. They also showed increased abundance for *B. plebeius* and a strain belonging to this species. The APOE4 non-carriers on the other hand were repeatedly enriched in *Collinsella*, *C. aerofaciens* and an unclassified strain of the species *B. stercoris*. The group of APOE4 non-carriers was enriched in many members of the *Actinobacteria* clade, including the *Coriobacteriales* and *Actinomyces*, which were also enriched but to a much larger degree in the AD patient group.

Overall, the degree of overlap between LEfSe results from this study and the other AD studies results is small. The discrepancy between the findings might partly reflect the level of noise introduced by environmental factors, such as diet, lifestyle or medication, between the AD patient groups in the different studies. Notably, the majority of studies compared against were all conducted in Chinese populations who are likely to be differentially influenced with respect to a large number of environmental factors (such as diet) from this UK cohort. Univariate analyses cannot account for the effect of covariate factors. This presents an inherent and considerable limitation of the method and is of particular importance for microbiota studies. Thus, I also employed a multivariate approach, using linear mixed modelling, allowing for covariate adjustment. Multivariate models are generally more flexible than univariate approaches, as they also offer a large number of possibilities to transform or normalize the data, which given the compositionality problem of microbiome data is another noteworthy strength.

Multivariate analysis of different relative taxonomic abundances

Only three of the nine previous studies subjected their taxonomic data to GLM modelling. Haran *et al.* performed GLM modelling adjusting for age, malnutrition, frailty, medication (PPIs and antipsychotics), and dementia status (no dementia, AD, or other dementia). Li *et al.* on the other hand, adjusted for the effect of age, sex, BMI, and constipation in their GLM. Hou *et al.* used GLM modelling to explore the relationship of selected microbial taxa with genetic risk variants (APOE genotype and *BNII*), adjusting for age and sex, in a small subgroup of AD patients. Of note, Hou *et al.* report abundance changes only for genus-level but did not consider changes on other taxonomic levels.

I performed GLM modelling adjusting for the possible effects of age and sex, as these were the two covariates that were most consistently adjusted for in other studies. Given the small sample size, I further recognized that adding additional covariates would reduce power.

In-line with the univariate findings and congruent with the results from Li *et al.*, AD samples were enriched in members belonging to the phylum *Actinobacteria*. The genus *Bifidobacteria* is identified by us as well as by Li and colleagues. I also observed enrichment for the *Actinomyces* (hereby further supporting the univariate findings from this study) and *Eggerthella* genera. On a species-level this corresponds to increased abundance of *B. longum*, *A. viscosus* (as also identified by LEfSe), *A. oris*, and an unclassified *Eggerthella* species. Members of the *Eggerthella* genus have potential pathogenic properties and are associated with bacteraemia (due to translocation of the bacteria into the circulatory system). Increased abundances of this genus have also been reported to predict rheumatoid arthritis status (Chen *et al.*, 2016).

In this study, all discriminant taxa identified within the *Bacteroidetes* phylum were decreased in relative abundance when comparing the AD patient group to the APOE groups.

This loss in *Bacteroidetes* has to be interpreted with caution as it may have been influenced by the presence or absence of a cryoprotectant and is discussed in more detail in the limitations section. The observation mirrors the findings of Li *et al.* who report a decrease in members of this phylum in AD patients compared to healthy controls. Especially a decrease in the genera of *Alistipes*, *Bacteroides* and for members of the *Porphyromonadaceae* family marked intestinal changes in both this work and that of Li and colleagues. Whilst Li and colleagues only report changes at genus-level, I demonstrated associations on all taxonomic levels, including the identification of seven discriminant species, namely *B. stercoris*, *P. merdae*, *B. instestinihominis*, *O. splanchnicus*, *A. onderdonkii* and *A. putredinis*. Contradictory to this, Haran and colleagues showed increased abundances for *Bacteroides*, *Alistipes*, *Odoribacter* and a *Barnesiella* species. Contrary to Haran *et al.* but congruent with this study's results, Saji *et al.* (2019) demonstrated that a lower prevalence of *Bacteroides* is strongly associated with dementia. This in turn is contrary to the findings by Vogt *et al.* who report increased prevalence for *Bacteroides* in dementia patients. This inconsistency with respect to members of the *Bacteroidetes* phylum may be a testament to the variable nature of the intestinal microbiota.

Several *Bacteroides* species correlated with increased expression of membrane protein ZO-1 and are thus thought to improve intestinal barrier integrity. The literature further suggests that several species of the *Bacteroides* genus, including *B. stercoris*, occur at significantly lower abundances in patients with Multiple Sclerosis (Miyake *et al.*, 2015) and suggest that a reduction of this phylum is linked with inflammation-induced colorectal cancer (Polimeno *et al.*, 2019). *B. instestinihominis* is an important regulator of immunomodulatory cells and confers resistance against the colonization of antibiotic-resistant pathogens (Ubeda *et al.*, 2013). The species has sparked interest as an 'oncomicrobiotic' due to its essential role in cyclophosphamide cancer treatment, whose efficacy is dependent on modulatory functions of certain intestinal microbiota (Daillère *et al.*, 2016). Despite its important

immunomodulatory role (on regulatory T (Treg) cells and T helper cell type 1 [Th1] cells) very little is known about this species. I can thus only speculate about its role in the context of AD. A reduction in the relative abundance of *B. intestinhominis* could potentially lead to altered immunomodulation and a weakened response against the potential domination of opportunistic pathogens. More research is required to test this hypothesis. *B. stercoris* has not been studied as extensively as some of the other *Bacteroides* species (e.g. *B. fragilis*, -*uniformis*). Therefore, more research is needed to gain insights into these species' role in human health.

O. splanchnicus, a common member of the intestinal microbiota, is a producer of SCFAs and as such lower abundance of this bacterium are associated with cystic fibrosis, IBD, Crohn's disease and other diseases (Hiippala *et al.*, 2020). A decrease in *Bacteroides* species and *O. splanchnicus* in AD may contribute to reduced barrier protection and decreased anti-inflammatory ability.

The *Alistipes* genus, comprised of thirteen species, may have both detrimental or beneficial effects on human health. Bacteria of this genus are capable to produce acetate and propionate (Parker *et al.*, 2020). In the context of liver disease (non-alcoholic fatty liver disease and liver cirrhosis), *Alistipes* may play a protective role via its anti-inflammatory properties (Parker *et al.*, 2020). Reduction in the abundance of this genus significantly correlates with disease state and worsening of the liver disease. Using a functional approach, *Alistipes* were also reported to have the highest number of putrefaction pathways (fermentation of undigested proteins) compared to other commensal bacteria. Products of these pathways are considered deleterious and include products such as ammonia, H₂S, cresol, indole and phenol (Windey, De Preter and Verbeke, 2012; Yao, Muir and Gibson, 2016). The contradictory evidence for *Alistipes*' role in host health highlights the need for future research.

In this study, taxa belonging to the *Firmicutes* phylum, such as several members of the *Clostridiales* order, including *F. prausnitzii* and its associated order, *E. eligens*, the genera *Roseburia* and *Coprococcus* (*Lachnospiraceae*) were significantly depleted in the AD patient group. Whilst I observed no direct overlap with the findings of Haran and colleagues with respect to the Firmicutes phylum, they also reported a decrease in a genus that belongs to the *Lachnospiraceae* family. The *Lachnospiraceae* and the closely related *Ruminococcaceae* families consist of several butyrate-producing bacteria. There is ample evidence for a health promoting role of *F. prausnitzii*, as this anaerobic bacterium is a common inhabitant of the human colon and the key producer of the SCFA butyrate and salicylic acid (Louis and Flint, 2009; Ferreira-Halder, Faria and Andrade, 2017). Species of the *Roseburia* genus are also important SCFAs producers (Tamanai-Shacoori *et al.*, 2017) and *E. eligens* might contribute to the production of SCFAs via fermentation of non-digestible fibre (particularly pectin) (Chung *et al.*, 2016). Butyrate is essential to the maintenance of intestinal barrier integrity (used by colonocytes) as it is required for epithelial proliferation as well as for the production of mucin. Butyrate has also been shown to suppress inflammatory responses (induces differentiation and expression of Treg which suppresses inflammation). As such *F. prausnitzii* and the *Roseburia* species are important modulators of inflammatory processes, able to inhibit the pro-inflammatory actions of NFκB and IL-8. They are further able to induce the production of anti-inflammatory IL-10 (Hakansson and Molin, 2011). The depletion of *F. prausnitzii* and/or *Roseburia* species is associated with a range of pathological processes and conditions, including ulcerative colitis (Machiels *et al.*, 2014), T2D (Karlsson *et al.*, 2013), colorectal cancer (Balamurugan *et al.*, 2008) and others. In the context of AD, it is possible that the depletion of these SCFA producers contributes to chronic intestinal inflammation, which may lead to decreased integrity of the intestinal barrier. Overall, this may feed into a perpetuating loop of inflammatory responses resulting in increased systemic inflammation in AD. Future work is

required to understand these complicated dynamics. Particularly, evidence from human studies and interventional studies aimed at increasing the levels of SCFAs could provide valuable insights into the complex relationship between SCFAs, barrier permeability and inflammation in AD. This line of work is already investigated in animal models with promising results (Bonfili *et al.*, 2017; Kobayashi *et al.*, 2017; Hoffman *et al.*, 2019).

Not all members of the Firmicutes phyla were reduced in AD. Taxa belonging to the order *Selenomonadales* and *Lactobacillales* were enriched in AD compared to compared to the APOε4 carriers. In agreement with previous work by Li and colleagues, I report increased abundance in members of the *Lactobacillus* and *Streptococcus* genera (*Streptococcus thermophilus*). Lactic-producing bacteria from the *Lactobacillales* genus or *Streptococcus thermophilus* are generally ascribed health-promoting properties and are widely considered and used as probiotics to improve health (Turroni *et al.*, 2014; Vitetta, Llewellyn and Oldfield, 2019) with reduced abundance reported in patients with obesity, T2D, cancer (Heeney, Gareau and Marco, 2018) and in Crohn's disease (Wang *et al.*, 2014; Lewis *et al.*, 2015). Of note, the abundance of *Firmicutes* in the AD patient samples may have been affected by the absence of using a cryoprotectant prior to DNA extraction for the AD patient samples. Due to this possible technical bias, results need to be interpreted with caution (more details are given in the limitations).

The phylum of *Proteobacteria* showed significant changes for members belonging to the classes of *Betaproteobacteria* and *Gammaproteobacteria*, which was marked by decreased abundances of *Haemophilus parainfluenza* and *Burkholderiales* in this AD patient cohort. This finding broadly mirrors the work by Li and colleagues, who demonstrate a decrease in the relative abundance of *Sutterella*, which on a higher taxonomic level belongs to the here detected *Burkholderiales*. The literature generally suggests that an increase in *Proteobacteria*, which occur at low abundances in the human intestine, is associated with

high-fat diets, obesity and might play a negative role (cause gut dysbiosis) in human health (Shin, Whon and Bae, 2015; Méndez-Salazar *et al.*, 2018). Evidence regarding members of the *Proteobacteria* is sparse and more work is required to gain a better understanding of this bacteria's relationship with the host and its potential involvement in the context of AD.

Another important finding in the given work, which has not been replicated by other work, was the increase in the abundance of *Caudovirales* of the *Viruses* kingdom. The order of *Caudovirales* is considered the most abundant and heterogenous group of viruses, with remarkable diversity that call for a major reclassification. This is testament of our poor understanding of these viruses and their potential role in human health (Barylski *et al.*, 2020).

When comparing the multivariate results in the APOε4 group-only models to those comparing the AD patient group against the APOE groups, the most striking difference was the large number of significantly different taxa that were identified by the latter comparison. All but five of the detected taxa were significantly different for both the AD vs APOε4 carrier and the AD vs APOε4 non-carrier comparison. This also implies a large degree of similarity between the APOE groups, which is supported by the comparatively small number of differentially abundant taxa identified in the APOε4 group-only comparisons. Besides the number of differences, there was also a noticeable difference in the magnitude of effect size, quantifying the abundance differences. Effect sizes were small for significant taxa between the APOε4 carriers and non-carriers, but large in the AD patient to APOE groups comparisons. Collectively, these two observations provide further evidence that the intestinal microbiota profiles of the APOE groups can only be distinguished by a few small changes in taxa but are not clearly separable by large-scale measures. When compared to the AD patient group, the compositional profiles of the APOE cohorts appear almost

undistinguishable. Whereas microbiota changes clearly separated the AD patient from the other participants regardless of APOε4 genotype.

In summary, the taxonomic findings from this work strengthen the notion of a bacterial component in AD pathology. The relative abundance changes in the intestinal microbiota of AD patients largely relate back to mechanisms of inflammation.

Microbiota functional potential

Of the previously reviewed human work investigating the role of the Gut-Brain axis in AD, only Liu *et al.*, Vogt *et al.* and Ling *et al.* used predictive functional profiling to gain insights into the functional capability of the AD microbiome, whereas Saji *et al.* performed metabolic analysis from faecal water. Given the limitations of the data and methods as well as the lack of power, all presented findings should be considered as hypothesis-generating.

A series of KEGG modules and pathways were significantly associated with AD, with the majority demonstrating enrichment rather than reduction of metabolic potential in the AD patient group. This is congruent with the work by Vogt *et al.* and by Liu *et al.*.

On KEGG level 2 (low resolution), I observed an increased functional potential of carbohydrate metabolism in the microbiota of the AD group, which is consistent with the work of Vogt *et al.* and Ling *et al.*. Whilst I did not replicate any of the findings by Liu *et al.* for an increased potential for glycan biosynthesis and metabolism. The microbiota of AD patients was however enriched in four modules that relate back to this metabolism. The predicted functional differences of Liu and colleagues do not go beyond the resolution of KEGG level 2, and I can thus not confirm an overlap with respect to more specific pathways.

KEGG level 3 and 4 data shows the functional capabilities at the level of KEGG modules and pathways. This study replicated the findings by Vogt and colleagues of a greater functional potential for fructose and mannose metabolism and for lysine biosynthesis in the microbiota of the AD patient group. Congruent with Ling *et al.*, the AD patients' microbiota was further characterized by increased glycolysis/gluconeogenesis, galactose metabolism and a decrease in riboflavin metabolism. The findings are discussed in more detail below.

Increased fructose metabolism might drive Alzheimer's Disease pathogenesis

High-fructose consumption is associated with negative health outcomes, including obesity, non-alcoholic fatty liver disease and metabolic syndrome. Fructose is fermented by *Lactobacilli* either via the Embden-Meyerhof pathway or the 6-phosphogluconate/phosphoketolase (6-PG/PK) pathway and is particularly prevalent in Western diets. Excessive fructose intake is associated with a decrease in *Bacteroidetes* and increase in *Firmicutes* and causes reduced mucus thickness and epithelial barrier dysfunction, thereby favouring bacterial translocation and endotoxemia (Volynets *et al.*, 2017; Kawabata *et al.*, 2019; Beisner *et al.*, 2020). In the context of AD, high consumption of fructose is linked with worsened memory performance and hippocampal reduction (Johnson *et al.*, 2020). It has been hypothesized that chronically elevated fructose metabolism in the brain might be a key driver in AD aetiology. According to this hypothesis, increased availability and metabolism of fructose initiates a cascade of events including the upregulation of fructose metabolism in the brain, mitochondrial oxidative stress, increased glycolysis (a compensatory mechanism meant to counteract decreased ATP) and upregulation of the PPP to counteract oxidative stress that result in neurodegenerative processes (Johnson *et al.*, 2020).

Lysine an underexplored pathway with links to Herpes Simplex Virus-1 infection

There were significant functional changes related to L-lysine biosynthesis in the microbiota of the here studied AD patients. Lysine metabolism comprises nine L-lysine biosynthesis pathways. Two distinct L-lysine pathways have evolved separately - the DAP pathway and aminoadipic acid (AAA) pathway. The former synthesizes lysine from aspartate and pyruvate and has four variations. It is mostly used by bacteria. Our AD patient groups' microbiota had a greater functional potential and increased abundance for several variations of this pathway. The AAA pathway, on the other hand, produces lysine from alpha-ketoglutarate and acetyl-CoA and is largely restricted to fungi (Rodionov *et al.*, 2003; Liu,

White and Whitman, 2010). The AD group had a decreased functional capability for the AAA pathway.

In the context of AD lysine supplementation has been suggested as a potential treatment for herpes simplex type 1 virus (HSV-1) infection (Rubey, 2010). HSV-1 is associated with AD via several mechanisms such as inflammation and formation of amyloid and it has further been suggested to confer a particular high risk for developing AD to APO ϵ 4 carriers (Itzhaki *et al.*, 2004). Given the evidence for a potential role of HSV-1 infection in AD, an antiviral therapy using *Valacyclovir* is currently being tested in an ongoing interventional Phase II trial in patients with AD (NCT03282916, estimated completion in 2022).

Neurotoxic effects of increased formaldehyde production in Alzheimer's Disease

Vogt *et al.* showed enrichment for methane metabolism. This finding is broadly mirrored by this study's findings, which identified two important KEGG modules belonging to methane metabolism. The microbiota of the AD patient group had a greater functional potential and significantly increased relative abundances for formaldehyde assimilation- a process by which methanotrophs and methylotrophs oxidize methane to produce formaldehyde. Within the large and complex pathway of methane metabolism this last conversion step can be performed via three pathways, of which I see two significantly associated with AD. Elevated levels of formaldehyde are associated with changes in energy metabolism and cognitive impairment (Lu *et al.*, 2013; Tulpule and Dringen, 2013). Increased expression of formaldehyde-generating enzymes has been associated with AD, MS, diabetes and a range of other diseases. In the brain, formaldehyde has a range of negative effects (e.g., stimulating the rate of glycolysis in astrocytes and increased efflux of the antioxidant glutathione from the brain) that may lead to cerebral acidosis, impaired energy metabolism, increased oxidative stress and excitotoxicity. Animal work shows that formaldehyde can induce hyperphosphorylation of tau protein in N2a brain cells, which provides another mechanistic

link with AD (Lu *et al.*, 2013). Notably, the polyphenol anti-oxidant Resveratrol, which has shown promising effects in the phase II clinical trials for AD (Sawda, Moussa and Turner, 2017), may in part exert its neuroprotective effects by acting on formaldehyde as Resveratrol was shown to effectively decrease formaldehyde-induced cytotoxicity and tau hyperphosphorylation in N2a cells (Li *et al.*, 2012; He *et al.*, 2017).

Microbiota of Alzheimer's Disease patients shows increased functional capability to produce ammonia

Our AD patient cohort was further characterized by increased metabolic capability for nitrogen fixation and the reduction of nitrogen to ammonia. This agrees with the metabolic insights gained from Saji *et al.* (2020) who demonstrated that ammonia levels were significantly elevated in their AD patient cohort. Saji and colleagues further reported a strong relationship between faecal ammonia concentration and the risk for developing AD (with every 1 SD increment in faecal ammonia concentration, the risk for AD is increased 1.6-fold). This finding is in-line with the assumption that ammonia is neurotoxic and linked to AD aetiology and progression (Adlimoghaddam, Sabbir and Albeni, 2016). It has been suggested that the health-promoting effect of dietary interventions such as the Mediterranean Diet or that of certain probiotics, containing large amounts of *Lactobacilli*, are mediated by lowering systemic levels of ammonia (Jin *et al.*, 2018). In addition, the antibiotic *Rifaximin*, may reduce peripheral levels of ammonia by altering the intestinal microbiota and is currently tested in an ongoing clinical Phase II trial in patients with mild-to-moderate AD (NCT03856359, completion of study expected in 2021).

Methionine and Alzheimer's Disease

Increased biosynthesis of methionine is congruent with reported increases in methionine levels in AD (Kaddurah-Daouk *et al.*, 2013). Methionine is a precursor of homocysteine. The latter is associated with neurofibril pathology and was found at elevated levels in CSF and the serum of AD patients (Popp *et al.*, 2009; Vogel *et al.*, 2009). The reduced functional

potential of the microbial community for pyridoxal phosphate synthesis that I also observed in this AD patient cohort might aggravate this even further, as a decline in pyridoxal phosphate is associated with elevated homocysteine levels.

Increased glucose metabolism - compensatory action in Alzheimer's Disease

Notably, I observed an increase in relative abundances of the microbial functional potential for glycolysis and alternative central carbon pathways, particularly the PPP, which are involved in the metabolism of glucose. This finding of a change in energy metabolism is supported by Ling and colleagues. Functional differences for two of the six identified pathways involved in the metabolism of glucose were only distinctly different in the microbial community of AD patient vs APO ϵ 4 non-carrier comparison, indicating a more similar microbial functional potential between APO ϵ 4 carriers and AD patients.

The majority of evidence regarding the role of the PPP in cell metabolism comes from research in eukaryotic cells. It is however suggested that the pathway is ubiquitous and present also in most prokaryotic cells (Bräsen *et al.*, 2014; Masi, Mach and Mach-Aigner, 2021). As in eukaryotes, the PPP represents a main pathway for central carbon metabolism in bacteria. Importantly, in bacteria the PPP provides the necessary precursor to initiate LPS biosynthesis and is thus essential to its production. It is additionally the only pathway in bacteria that is able to breakdown sugars including D-ribose and D-xylose (Stincone *et al.*, 2015).

Research from eukaryotic cells identifies the PPP as a very dynamic pathway, which adapts flexibly to varying nutrient supply and stress conditions. Changes in the hosts' PPP have been linked to several diseases, including AD, cardiovascular disease, T2D, cancer and metabolic syndrome (Orešič *et al.*, 2011; Riganti *et al.*, 2012; Ge *et al.*, 2020). In addition to the biosynthesis of nucleic acids and amino acid sugar phosphate precursors, the PPP has several regulatory processes such as the maintenance of redox homeostasis through the

production of NADPH and interactions with oncogenic signalling pathways (Stincone *et al.*, 2015). Through its involvement in reducing glutathione (via NADPH), PPP is a first-line defense response for cells to oxidative stress (Janak and Jenner, 2020). Limited evidence exists regarding the role of PPP of the intestinal microbiota and oxidative stress in human disease. In patients with Crohn's Disease with ileal involvement it was observed that microbial PPP was increased in the presence of increased oxidative stress in the intestine (Morgan *et al.*, 2012).

Oxidative stress, particularly in the brain, is well-established as a contributor in AD pathology, but to what extent the microbiota might mediate or react to the increase in reactive oxygen species (ROS) levels requires future work. The evidence suggests that in a state of oxidative stress, involvement of PPP may reflect an increase in antioxidant activity (Palmer, 1999). Increased production of enzymes crucial to the PPP's activity (glucose-6-phosphate dehydrogenase and 6-phosphonogluconate dehydrogenase) was found in neocortex tissue of AD patients (Palmer, 1999). Several studies have since documented an upregulation of glucose-6-phosphate dehydrogenase of the PPP in the context of AD pathology, which is suggested to represent a compensatory response mechanism to maintain redox homeostasis (Yan *et al.*, 2020). Metabolic impairment of pentose and glucuronate pathway-dependent conversions of glucose were also shown to be involved in an APP/PS1 mouse model of AD (Yu *et al.*, 2017). Whilst a decline in the cerebral glucose metabolism is a well-established early feature of AD (Cunnane *et al.*, 2011; Croteau *et al.*, 2018), it is unclear if changes in the metabolic functioning of the intestinal microbiota, such as the here observed upregulation of glucose metabolism, are linked to AD pathology. There is however increasing evidence to support interrelated functioning of the intestinal microbiota and host health. Whilst speculative, increased PPP activity of the intestinal microbiota in AD remains an intriguing observation which may indicate the presence of increased oxidative stress.

Reduced synthesis of B-vitamins might lead to loss of protective functioning in Alzheimer's Disease

The predicted functional potential of several modules and pathways related to the synthesis of B-vitamins were decreased in the microbiota of the AD patient cohort. Vitamin B6, B2 and other vitamins are ascribed a protective role against cognitive decline and AD (Morris, Schneider and Tangney, 2006; Tao *et al.*, 2019). A reduced ability to produce these vitamins has potentially wide-reaching effects on many metabolic processes that could contribute to AD pathology.

Here I report a downregulation in the predicted functional potential of CoA, its precursor Vitamin B₅ and the aerobic mitochondrial synthesis pathway via acyl-CoA. Interestingly, this was only observed when comparing the AD patients' microbiota against the microbiota of APOε4 carriers. Changes in the levels of CoA are associated with neurodegenerative diseases, cancers, diabetes and other conditions (Czumaj *et al.*, 2020). CoA biosynthesis is an essential cofactor that is important in a large number of metabolic reactions, including the synthesis of phospholipids which are fundamental components of structural barrier function, synthesis of bile acids and for the synthesis and degradation of fatty acids. Notably, it is also required for the formation of acetyl-CoA which is in turn a key substrate in many other metabolic processes. Importantly, acetyl-CoA is involved in the synthesis of cholesterol and it also constitutes the most prevalent pathway of butyrate production. Due to its important role in lipid biosynthesis and butyrate synthesis, CoA and related substrates provide a myriad of possible mechanistic link to AD. CoA was suggested as a therapeutic target for AD to ensure proper mitochondrial homeostasis (Currais *et al.*, 2019).

The predicted functional profile of AD microbiota was also characterized by reduced potential of biotin synthesis (Vitamin B₇), also only significantly different between AD patients' and APOε4 carriers' microbiota. Studies investigating the role of biotin in animal models of AD have shown that biotin may contribute to tau pathology in the AD brain (via

reduced carboxylase biotinylation levels) and lead to impaired mitochondrial functioning (Lohr *et al.*, 2021). Conversely, high-dose supplementation of biotin has been shown to have neuroprotective effects in MS (McCarty and DiNicolantonio, 2017). Biotin is considered to have good tolerability and might present a feasible pharmacological target for AD that remains to be further explored.

The functional potential for the biosynthesis of riboflavin (vitamin B₂) and pyridoxal phosphate (vitamin B₆) was reduced in the microbiota of the AD patient cohort. The former is supported by the work of Ling *et al.*. Both coenzymes play important roles in numerous metabolic pathways and are considered neuroprotective agents. The wide-reaching antioxidant properties of riboflavin are well-established and include counteracting of oxidative stress, neurogenic inflammation, mitochondrial dysfunction, homocysteine neurotoxicity, and glutamate excitotoxicity (Marashly and Bohlega, 2017). Treatment with riboflavin in a mouse model of AD protected against cognitive and behavioural decline and led to a significant reduction in the level of ROS and malondialdehyde (MDA) (indicators of free radicals) (Zhao *et al.*, 2018). Riboflavin is also the major cofactor of the oxidase which synthesises pyridoxal phosphate. Pyridoxal phosphate is important in the tryptophan-kynurenine pathway and homocysteine metabolism. Deficiency in pyridoxal phosphate is linked to increased homocysteine levels, which is considered a risk factor in cerebrovascular disease and has also been implicated as a possible mechanism in the development of AD (Malouf and Grimley Evans, 2003).

Comparing the functional potential of the microbiota of AD patients to that of the APOE cohorts showed a large number of distinctly different pathways. The beta diversity analysis on the KEGG metabolism, modules and pathways was only significant between the AD patients and the APOE4 non-carriers, indicating a greater similarity in the functional potential of APOE4 carriers and AD patients. However, when only comparing the APOE4

carriers against the APO ϵ 4 non-carriers, none of the identified KEGG pathways were significant after BH-correction. This observation supports the notion that intestinal functional potential of APOE participants could not be distinguished reliably by APO ϵ 4 genotype. Whereas that of AD patients clearly separated them from the APOE groups. The analysis of the microbial functional potential of the AD patients highlighted different possible mechanistic links with AD pathophysiology.

CHAPTER 6: GENERAL DISCUSSION, LIMITATIONS AND FUTURE DIRECTIONS

General discussion

Key outcome: APO ϵ 4 carriers cannot be distinguished from non-carriers using neuropsychological, cardiovascular or brain imaging measures, but can be distinguished by an altered lipid metabolism.

APO ϵ 4 carriers showed no salient signs of cognitive or behavioural dysfunction or volumetric differences in brain structures compared to the APO ϵ 4 non-carriers. These findings add to the body of mixed literature (Jorm *et al.*, 2007; Wisdom, Callahan and Hawkins, 2011; Alfred *et al.*, 2014; Bunce *et al.*, 2014). The evidence suggests that if neuropsychological performance differences can be detected between APO ϵ 4 carriers and non-carriers, that these differences have small to middle effect sizes, which become less with increasing age and are modulated by APO ϵ 4 genotype (no ϵ 4 > ϵ 4 > ϵ 4/ ϵ 4) (Caselli *et al.*, 2007; Wisdom, Callahan and Hawkins, 2011). Considering these points, it is likely that a larger sample size is required to reliably detect differences with only small or medium effect sizes (discussed more in the limitations). This also highlights the fact that traditional markers of cognitive decline are poor markers to detect preclinical stages of AD. APO ϵ 4 carriers had significantly increased levels of LDL and total cholesterol, in the absence of an overall increased cardiovascular risk. This finding adds to the existing body of evidence (Chen *et al.*, 2021).

Key outcome: APO ϵ 4 status is not associated with large-scale compositional changes of the intestinal microbiota, but significantly differs with respect to specific taxa abundances and microbiota function.

There were no consistent large-scale changes in the microbial community between the APOE groups. When considering individual taxa however, rather than the whole community, it was noted that numerous taxa that were differentially abundant by APOE4 status. In particular, changes in microbiota with immunomodulatory properties (such as *Prevotella*), bacteria involved in the production of SCFAs and other key metabolites (*R. obeum*, *Coriobacteriales*) or microbiota regulating oxidative stress (*Methanobrevibacter*) emerged as key findings. Metabolic differences, particularly increased functional reliance on alternative pathways to the traditional glucose metabolism in APOE4 carriers (such as the PPP), may be indicative of heightened levels of oxidative stress as the PPP is known as a first-line defense pathway of oxidative stress. Upregulation in nitrogen metabolism and associated ammonia production in APOE4 carriers represent increased production of neurotoxic compounds. Although hypothesis-generating in nature, these APOE-associated changes in the microbiota community composition and its function are indicative of intestinal dysbiosis that may promote a community profile more vulnerable to AD-related mechanism.

Key outcome: The Gut-Brain axis, with the intestinal microbiota as its main modulator, appears to be involved in AD pathology. Insights from this work point towards mechanisms of inflammation and reduced homeostasis.

The number of studies investigating the role of the intestinal microbiota in AD patients is limited to nine studies (Vogt *et al.*, 2017; Zhuang *et al.*, 2018; F. Li *et al.*, 2019; Haran *et al.*, 2019; Liu *et al.*, 2019; Saji *et al.*, 2019, 2020; Hou *et al.*, 2021; Ling *et al.*, 2021), the general consensus is that AD pathology is associated with microbial dysbiosis.

This work showed large-scale changes in microbiota community composition and a decrease in community richness which clearly distinguished the AD patients from the non-patient APOE groups, thereby further adding to the literature (Vogt *et al.*, 2017; F. Li *et al.*, 2019;

Liu *et al.*, 2019; Ling *et al.*, 2021). The intestinal microbiota of these here studied AD patients is characterized by a decrease in several bacteria that typically inhibit inflammation in a state of homeostasis (*Clostridiales* members: *Lachnospiraceae*, *F. prausnitzii*, *Roseburia*, *Coprococcus*, *E. eligens*; *Bacteroidetes* members: *Barnesiella*, *Odoribacter*, *Alistipes*, *Bacteroides*). These inflammation-suppressing mechanisms act via the production of microbial metabolites (such as SCFAs), via direct stimulation of anti-inflammatory components of the immune system, or via modulation of the GI barrier. Of note, abundance changes in members belonging to the Bacteroidetes and Firmicutes may have been influenced by the absence of cryoprotectant for the preservation of the AD patient samples. In particular the loss of Bacteroidetes in the microbiota of AD patients, observed in this study, should thus be interpreted with caution. A reduction of these bacteria might shift the host to an inflammation-prone state. Functional changes of the intestinal microbiota in AD indicate an increased activation of first-line defense responses to oxidative stress (upregulation of glucose and alternative glucose pathways, notably the PPP), increased availability of pro-inflammatory compounds (increased production of formaldehyde and ammonia) and a reduced potential for vitamins with anti-inflammatory action (downregulation of B-vitamins synthesis, including riboflavin). Many of these findings are functionally interrelated calling for a systems approach to gain a deeper understanding of the role of taxonomic and functional microbiota changes in AD pathophysiology.

Key outcome: Existing literature highlights the role of certain microbiota including *Actinobacteria*, *Clostridiaceae*, *Bifidobacterium*, *Akkermansia* and *Lactobacillus*, which could potentially serve as diagnostic aid for AD. Inflammation emerges as a common theme across the studies.

Only considering findings that have been replicated by at least one other study using the same statistical method, the intestinal microbiota of AD patients is enriched in

Actinobacteria, *Proteobacteria*, *Enterobacteriales*, *Coriobacteriales*, *Enterobacteriaceae*, *Christensenellaceae*, *Akkermansia*, *Bifidobacterium* and *Lactobacillus*. A decrease of relative abundances in the AD group is observed for *Bacteroidetes*, *Lachnospiraceae*, *Clostridiaceae*, *Parabacteroides*, *Bacteroides*, and *B. plebeius* (Figure 6.1). These abundance changes are particularly interesting as Ling *et al.* (2021) showed that combining information of six abundant genera could support AD diagnosis. These genera include three of the above-mentioned taxa *Bifidobacterium*, *Akkermansia* and *Lactobacillus*, as well as *Faecalibacterium*, *Roseburia*, and *Enterococcus*. Overall, these data suggest that intestinal microbiota of AD patients is characterized by an increase in lactate-producing and mucin-degrading bacteria, as well as a reduction of anti-inflammatory and butyrate-producing bacteria. It also shows that differential relative abundance of microbiota genera could be used to distinguish AD patients from healthy individuals which offers exciting and novel targets for therapeutic interventions. The intestinal microbiota of the AD patient cohort is further characterized by several metabolic differences, which include an increase in the microbial functional potential for carbohydrate metabolism, folate biosynthesis, glycolysis/gluconeogenesis, galactose metabolism and fructose and mannose metabolism, and downregulation of the immune system, cell motility, bacterial chemotaxis and riboflavin metabolism (Figure 6.1). Taken together, the upregulation of these pathways may also be involved in increased oxidative stress and inflammatory processes and a dysregulation of the intestinal epithelial barrier function. At the same time, I observe a downregulation in the intestinal microbiota of pathways involved in anti-inflammatory processes, such as the biosynthesis of anti-inflammatory agents (riboflavin), indicating that there is an overall shift of metabolic pathways which might increase vulnerability to AD and promote disease-associated processes.

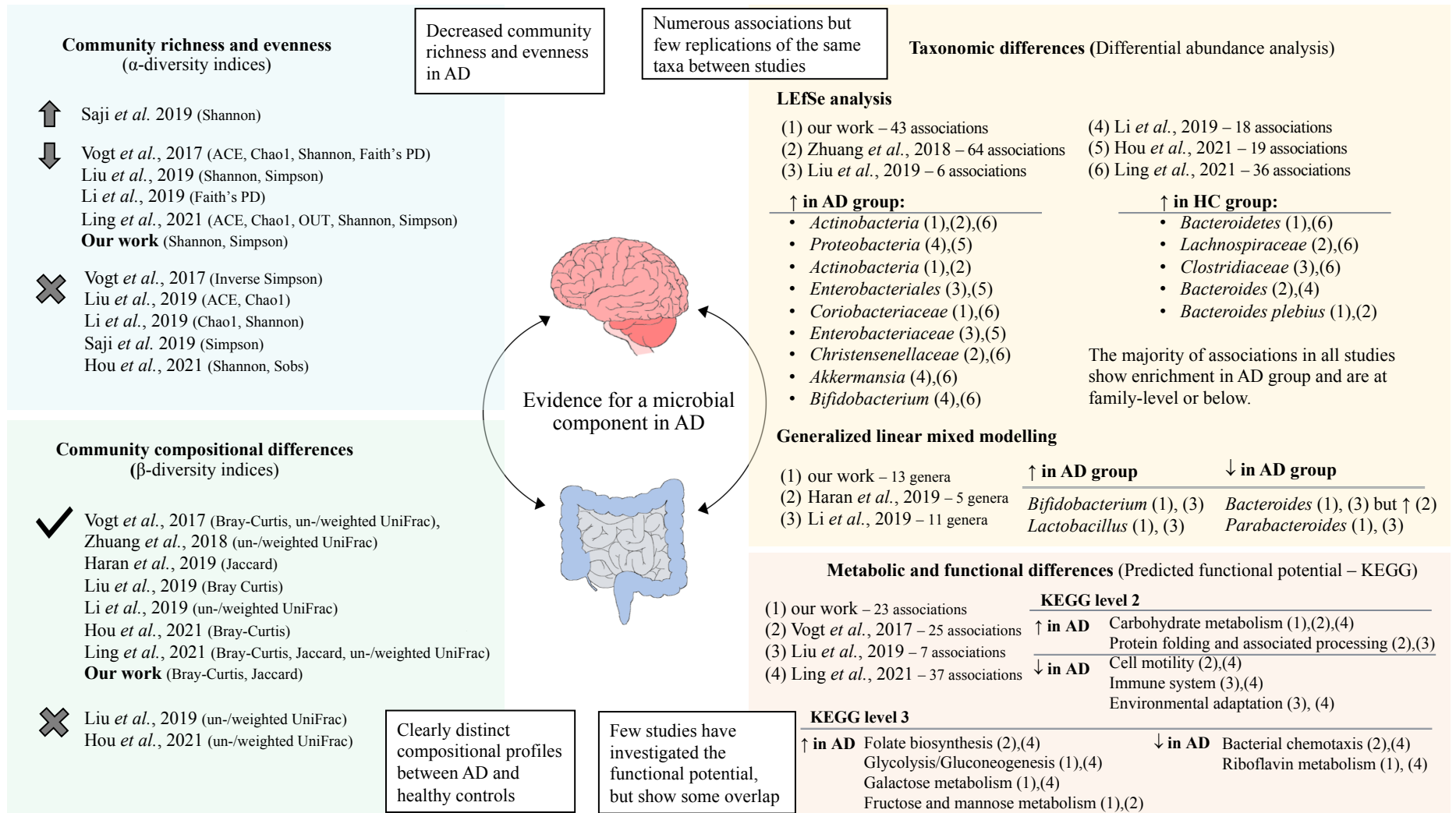


Figure 6.1 Graphical summary of the evidence for a microbial component in Alzheimer's Disease based on the current literature, findings for taxonomy and function only shown if replicated by at least one other study, ↑ = increase, ↓ = decrease, X = no association, ✓ = differences exist

Conclusion

AD pathological changes often precede disease symptomology by a decade or more. By the time that cognitive decline presents itself, brain changes are irreversible. Thus, it is thought that the preclinical stages of AD offer the greatest opportunity for intervention, prevention, and disease-course modification. The APO ϵ 4 gene confers a three- to 12-fold increased to its carriers for developing AD in the future and they thus represent a good study population. Although our understanding of APOE has been growing over four decades of research, the exact relationship between isoform structure and function, as well as the exact nature of associated mechanisms in the context of AD, are still incompletely understood (especially *in vivo*). In this work, I performed a comprehensive baseline assessment of several health areas related to AD in APO ϵ 4 carriers and non-carriers. The hallmark cognitive and behavioural symptoms associated with AD present later in the disease progression and are thus likely to be preceded by other physiological changes and are poor markers for preclinical stages of AD.

In light of inconclusive amyloid- and tau-centric clinical trials, investigating the Gut-Brain axis in AD pathogenesis is an exciting new perspective with the potential to offer novel insights and treatment avenues. How exactly microbiota changes affect host health or whether they precede AD symptomology and could be used as potential biomarkers to identify early stages of the disease is virtually unknown. Yet, given the shift in the AD research community to focus more on preventative and early approaches, these questions are particularly relevant and have here been explored further via longitudinal characterisation of the intestinal microbiota in APO ϵ 4 carriers and non-carriers. This work identified numerous taxonomic and functional findings. This is the second study to investigate the relationship of APOE on the Gut-Brain axis in humans and because of the limitations discussed later, the findings presented here should be considered hypothesis-generating.

Although causality cannot be determined on the basis of the current observational evidence, this work supports the hypothesis for a microbial component in AD and provides further evidence for a role of the Gut-Brain axis in AD. The findings from this work strengthen the notion that relative abundance changes and up-/downregulation of pathways favour a state of dysbiosis and mechanisms that underlie inflammation. I propose that the lowered abundances of the above described bacteria may downregulate inflammation-suppressing actions of the intestinal microbiota and thereby shift the host to an inflammation-prone state. Future work is essential to gain a better understanding of bacteria-related mechanisms in AD and interventional study designs will be necessary to test cause-effect relationships.

Despite consolidated efforts, the lack of treatment options for AD persists. Particularly in light of the over 200 of clinical trials that have failed to modulate the disease trajectory by targeting the A β cascade, a new perspective is needed. The approval of GV-971 is particularly exciting as it is the first therapeutic intervention in AD which works via modulation of the microbiome, which in turn strengthens the notion that targeting the Gut-Brain axis is a promising avenue with great potential.

Limitations

Study-specific limitations

This study has several limitations. Firstly, I did not assess the subjects' cognitive or behavioural performance in the long-term and can thus not infer rates of decline over time. As outlined above, the literature strongly suggests that APO ϵ 4 carriers exhibit accelerated rates of decline in some cognitive domains in midlife to early old age compared to non-carriers in the absence of clinical cognitive impairment (Whitehair *et al.*, 2010; Rawle *et al.*, 2018). Given the accelerated decline in APO ϵ 4 carriers, a longitudinal design might have also been better equipped to detect volumetric changes with small effect sizes that cannot be uncovered in cross-sectional studies. Also, although a genetic risk, this was not an event

driven study and I do not know which participants from the APO ϵ 4 carriers will develop AD. Vice versa, I also do not know which participants from the non-carrier group might develop AD. This is a major limitation, which is difficult to overcome given that preclinical AD is ill-defined and remains difficult to detect.

Secondly, the study population is relatively homogenous with respect to their socioeconomic background, ethnicity, access to healthcare, and has an above-average level of education. Whilst this limits the generalisability to the general public, it also minimizes the amount of bias introduced by confounding variables.

And lastly, the small effect sizes of differences between APO ϵ 4 carriers and non-carriers, raises the question of using different measures for similar cognitive functions and pooling effects across several measures that tap into the same cognitive domain (Mielke *et al.*, 2016). Administering multiple standardized measures, that have a high correlation, has indeed been suggested as a means to avoid any potential losses in validity (Wisdom, Callahan and Hawkins, 2011).

With respect to the AD patient group, I recognise that the sample size is very small and that the patient group was not matched with respect to age or sex against the APOE groups. Whilst I am going to address the topic of sample size in the following, I acknowledge that any findings coming from the AD patient group should be considered hypothesis-generating and need to be validated in a study with a larger cohort.

In the following, I am going to describe limitations that concern all microbiome studies and need to be considered carefully when deciding on an experimental design and procedures. A significant challenge for every microbiome study is the amount of variability in the data, which is intrinsic to the nature of intestinal microbiota communities but is further increased

by a large range of external factors. Ultimately this leads to a low signal-to-noise ratio that makes it difficult to detect differences between groups and to reliably discern a true signal from noise. Each step, from sample size, participant selection, gathering of metadata, sample collection, sample transport and storage, over to DNA extraction, sequencing technology and subsequent data processing and analysis, are crucial steps in the experimental design. Each step can introduce variation in the final results, which may easily overpower true differences in intestinal microbiota communities, particularly in study settings where the signal of interest (effect size) is considered small to medium. The heterogeneity of study designs adds a further level of complexity with respect to comparing and interpreting findings between studies and remains a pervasive challenge (Vujkovic-Cvijin *et al.*, 2020). After reviewing the major challenges of microbiome studies, I will discuss how this study addressed each of the limitations.

Sample size

An important limiting factor which applies to the majority of microbiota studies, is that of insufficient samples size. Statistical power calculations and the associated estimates for a sample size sufficient to detect an effect and derive meaningful conclusions which are generalizable beyond the study population, are dependent on the level of specificity and sensitivity (type I and II errors) considered acceptable (Casals-Pascual *et al.*, 2020). This in turn is dependent on the effect size, that the variable of interest exerts on the dependent variable. In microbiome studies, this question often takes the shape of differences within the microbial communities which are associated with a certain disease phenotype. Unfortunately, it is often unknown how large a change in community needs to be in order to be considered relevant. To perform power calculations, one must also quantify the expected within-group variance (B. Kelly *et al.*, 2015). Both effect size and the distribution of microbial diversity are difficult to estimate and will further depend on the statistical test used to determine a difference in community profiles (e.g. alpha or beta diversity measures),

which makes power calculations difficult, particularly without preliminary data to inform estimates on effect size (Casals-Pascual *et al.*, 2020). In the study by Vujikovic-Cvijin *et al.* (2020), beta diversity was strongly associated with sample size with most variables showing a performance plateau in the Random Forest model around n=400-500 participants. Another paper suggests that even after matching participants for numerous factors, the sample size of each group should be no less than 100 subjects for a reliable detection of differences which are small in magnitude (McDonald *et al.*, 2015). The calculation of a sufficient sample size for repeated-measures or longitudinal studies is further complicated by the fact that variances (mean and standard deviation of the response variable) and correlations between the measures must be determined for each measurement time point (Guo and Pandis, 2015).

With a sample size of 82 participants at enrolment, this study is comparable to a large number of other microbiome research studies. With a prevalence of approximately 22% for the APOε4 genotype, identifying 100 APOε4 carriers requires the screening of over 450 people who are eligible and willing to participate. Although the AD patient group is very small, the other human studies report patient numbers in the range of 21-43 participants (with one exception 100 AD patients in Ling *et al.* [2021] study).

Given the lack of preliminary data, I was not able to perform a power calculation and I thus cannot not assume to have statistical power. Consequently, results coming from this study should be interpreted with caution and are hypothesis-generating. This study was able to test feasibility of protocols, determine estimates for effect size and prevalence of features, evaluate temporal variation and collect considerable amount of preliminary data which can be utilized to design trial protocols, generate hypotheses and guide future work.

Intersubject-, intrasubject- and temporal variability of the human intestinal microbiome

Research has repeatedly shown that the human intestinal microbiota forms a dynamic and diverse community, which is unique to an individual, and can differ considerably between people (Eckburg *et al.*, 2005; Turnbaugh *et al.*, 2009; Qin *et al.*, 2010; Human Microbiome Project Consortium, 2012). This breadth in compositional differences among individuals, and the absence of a reference set of taxa shared by all healthy people, add to the difficulty to reliably discern intestinal microbiota differences associated with a phenotype from those of spurious correlations caused by chance. Intersubject variability is markedly more pronounced than intrasubject variability (Human Microbiome Project Consortium, 2012).

Temporal dynamics add another dimension to the existing variation of an individual's intestinal microbiota. Our understanding of the temporal variation within the taxonomic or functional composition of the human intestinal microbiota is still limited (Faust *et al.*, 2015). Only a few longitudinal studies have tried to address this gap, and findings have been inconsistent, with some evidence arguing for considerable variability within body sites among a small core of stable microbial taxa (Caporaso *et al.*, 2011) and others suggesting long-term stability of the intestinal microbiota at strain-level (Faith *et al.*, 2013). Temporal variation within the intestinal microbiota of adults is considered relatively stable (Costello *et al.*, 2009).

Cross-sectional studies are inherently subject to between-subject variability and are only able to provide a snapshot picture of the intestinal community at a particular time. Longitudinal studies are able to reduce variability by using repeated measures of the same individuals. Most importantly, longitudinal designs allow the assessment of shifts in community profiles over time (Guo and Pandis, 2015), which adds valuable insights into the temporal dynamics of intestinal microbiota changes. When trying to establish causality, longitudinal studies are considered superior to a cross-sectional studies (Allaband *et al.*,

2019). Extensive metadata collection, to allow controlling for confounding variables, remains of utmost importance in any study design.

Confounding variables

Confounding variables spuriously increase variation in intestinal microbiota profiles and can thus erroneously lead to interpreting differences between controls and patients as disease-associated microbiota differences, when in reality they are independent of disease. The amount of noise introduced by confounding variables can be considerable. Vujkovic-Cvijin *et al.* (2020) applied a machine-learning framework to the largest known publicly available human intestinal microbiota dataset to identify sources of variability and to assess their impact and found that confounder-matched analyses significantly reduced the number of apparent ‘disease-associated’ intestinal microbiota differences in 13 out of 19 diseases (Vujkovic-Cvijin *et al.*, 2020). Age, sex, BMI, alcohol consumption and bowel movement quality (BMQ) in particular were determined to exert a large confounding impact on study results in a range of conditions. The impact of microbiota covariates, especially sex, age, and BMI has become well-established in the field (Yun *et al.*, 2017; de la Cuesta-Zuluaga *et al.*, 2019; Van Soest *et al.*, 2020). In this study, I accounted for the effect of age and sex in the multivariate differential abundance analysis. Other studies that employed multivariate approaches were found to use a range of covariates, but consistently controlled for age and sex. I thus decided to use sex and age as the main covariates. Of note, exhaustive testing and gathering large amounts of metadata, as well as in-depth information on lifestyle and dietary self-reported questionnaires, demonstrated that APOE groups showed no significant differences across any of the assessed areas. This allowed us to minimize the risk of false-positive associations. I suggest that future study designs need to carefully consider which confounding factors are likely to have an effect and gather a large amount of metadata. Careful participant selecting, and matching are very important in microbiome studies. If matching cannot be achieved, statistical adjustment for confounding covariates can reduce the number of spurious observations.

Technical source of variation

Another key source of variation and potential bias can be introduced by faecal matter collection, storage and processing, as well as sequencing. The sampling procedure is arguably one of the most important steps in any microbiome study because of its critical impact on all downstream analyses. Sample collection methods and storage of the sample have big effects on the quality and accuracy on metagenomics results, as their effect size on the microbial community can exceed the effect size of the biological variables of interest (Quince *et al.*, 2017).

Being able to stabilize faecal matter for extended periods of time at room temperature and mailing samples back to the research facility is practical and advantageous in particular for longitudinal studies. I thus decided to use OMNIgene Gut tubes OM-200, which are storage- and mailer-friendly. OMNIgene Gut tubes are designed to collect a small and fixed amount of faecal matter, which is subsequently homogenized through shaking of the tube and preserved in the stabilizing buffer. OMNIgene tubes are well-validated alternatives, yielding comparable DNA quality to fresh samples, where rapid freezing of faecal matter or DNA isolation from fresh samples is not possible (Choo, Leong and Rogers, 2015; Anderson *et al.*, 2016; Song *et al.*, 2016; Abrahamson *et al.*, 2017; Kim *et al.*, 2017). One key limitation of OMNIgene Gut tubes and an important factor in any study is cost. The tubes used in this study are considerably more expensive than collection devices for fresh faecal matter.

Faecal matter samples of the AD patient group were readily banked at -80 degrees Celsius and contrary to the OMNIgene tubes, the DNA of these samples was not preserved by use of a cryoprotectant prior to the DNA extraction. It has been shown that certain bacteria, such as members of the gram-negative *Bacteroidetes* show considerable loss in non-cryoprotected samples, which conversely leads to a proportional increase of other microbial species such as that of the *Firmicutes* and overall results in a higher *Firmicutes* to *Bacteroidetes* ratio

(Bahl, Bergström and Licht, 2012; McKain *et al.*, 2013). Whether a change in the abundance profiles also results in a statistically meaningful distortion of the community composition is not unequivocally supported (Fouhy *et al.*, 2015).

I acknowledge that the lack of using a cryoprotectant to equally preserve microbiota of the AD patients' samples may have had a negative effect on the inferred community composition. The results thus need to be considered with caution, which is further compounded by the fact that the samples of the APO E cohorts were collected and preserved with a different method, which decreases comparability.

DNA processing and isolation

The yield and quality of extracted DNA from faecal matter using different kits can vary (McOrist, Jackson and Bird, 2002; Kennedy *et al.*, 2014). Commercial kits for isolation of microbial DNA have become increasingly popular. They allow for the extraction of numerous samples at once, are less time consuming than traditional methods, internally reliable and easy-to-use. They are also useful for standardizing methods and comparing results of different research studies. The here used MP Biomedicals™ FastDNA™ SPIN Kit for Soil showed to be superior in yield and purity compared to 14 manual and four automated commercial kits (Burbach *et al.*, 2016) and demonstrated high DNA quantity and quality (Panek *et al.*, 2018). Of note, commercial kits are predominately able to capture bacterial genomic information but are less good at extracting the DNA of fungi or viruses. Another limitation is cost. A third limitation is “kitomes”, which describes the contamination introduced by the reagents of a DNA extraction kit (Stinson, Keelan and Payne, 2019).

The focus of this work is to characterize the bacteria in the intestinal microbiota, however, I acknowledge that archaea and viruses are also present. The study of the intestinal microbiota is still evolving, and the tools currently available are best suited to characterize the role of

bacteria (e.g. technical limitations in extracting non-bacterial DNA). However, future work should also examine the role of fungi, viruses and archaea more closely.

Library preparation and metagenomics sequencing platforms

There are many different platforms for sequencing. Whole shotgun metagenomic sequencing has considerably better resolution and is able to identify more species, particular those at low prevalence, compared to 16S rRNA gene sequencing (Durazzi *et al.*, 2021). The high-throughput more expensive Illumina NovaSeq sequencing platform by NOVOGENE showed superior performance to MiSeq (Besser *et al.*, 2018; Singer *et al.*, 2019) and was chosen for this study.

Statistical methods

A systematic literature review of the statistical methods used by studies using 16S rRNA gene sequencing or metagenomic shotgun sequencing on human samples published between June 2018 and June 2019, resulted in the review of 419 studies (Bardenhorst *et al.*, 2021). Besides the biological and technical variability outlined above (noisy data), microbiome data presents several other challenges to statistical analyses methods. Microbiome data is highly-dimensional, sparse (zero-inflated), skewed and compositional in nature, with many hundreds of taxa occurring at small abundances and sometimes only in a few participants (low prevalence). Phylogenetic relatedness and taxonomic levels mean that taxa are correlated (Moreno-Indias *et al.*, 2021). There is a breadth of statistical methods available, spanning alpha diversity, beta diversity analysis and dimension reduction, as well as a considerable number of approaches for differential abundance analysis and an increasing number of predictive models – which leads to substantial heterogeneity in the field (Bardenhorst *et al.*, 2021). Predicted functional profiling is further limited by a lack of sufficient available classification and annotation in reference databases which means that genes and organisms can often not be assigned a function (Thomas and Segata, 2019).

Even after applying carefully considered methods for the analysis, the interpretability of findings particularly for single taxonomic units or functional pathways is not straightforward. Whether the presence or specific relative abundances of a certain bacteria is 'good' or 'bad' for host health is often unknown. The complexity of microbial communities, which form a dynamic ecosystem, makes it even more difficult to identify individual species which are causally linked to disease states or have health-promoting effects. We thus need to be particularly cautious when interpolating the results from a study investigating microbial signatures in one disease-setting to another disease setting. The interconnectedness of the intestinal microbiota further calls into question whether considering a bacteria's role in host health in isolation (rather than its contribution towards homeostasis in the overall network) is the best approach. I carefully evaluated existing approaches for diversity measures, differential abundance analysis and the functional analysis as outlined in the methods chapter. I adopted both a univariate and multivariate approach to explore differential taxa abundances, because the former was most commonly reported in studies (thus allowing to make direct comparisons to results). The latter was employed because of the aforementioned importance of controlling for covariates and because newer studies were frequently choosing GLM modelling. I recognise that there is not one best way to analyse microbiome data and that all currently existing methods have their strengths and weaknesses.

Future directions

Despite the arguably many challenges, the microbiome field is rapidly evolving and offers novel and exciting avenues for research and future diagnoses and treatment options, especially as most diseases are now assumed to have some microbiome component to it (Rackaityte and Lynch, 2020).

Further detailed characterization is needed to improve our understanding of the role the Gut-Brain axis plays in the context of AD and in at-risk cohorts such as APO ϵ 4 carriers. Given that AD lies on a continuum, it is particularly the ‘silent’ (potentially decades long) preclinical phase in which pathological processes are underway but individuals appear cognitively unimpaired and are hence often not identified, which offers the best opportunity to alter the disease trajectory. APO ϵ 4 carriers have an established genetic risk for developing AD and are thus a good study population, with a clearly defined and non-modifiable risk.

Having tested and validated the methods used here, future work should firstly focus on scaling. A statistically powered multi-omics study (combining for example genomics, microbiomics and metabolomics) with repeated measures in APO ϵ 4 genotyped individuals and AD patients matched for age and sex would be the logical next step in better understanding the role of the intestinal microbiota in preclinical and clinical AD and in identifying therapeutic targets for future intervention studies.

The intestinal microbiota is closely linked to many mechanisms of inflammation. As such I suggest that future studies in AD gather insights on the inflammatory status on a systemic and intestinal level by assessing the levels of serum inflammatory cytokines as well as faecal markers such as calprotectin, lactoferrin and alpha-1-antitrypsin (Schwiertz *et al.*, 2018). In-line with this, a clear understanding of the metabolites produced by the microbiota (metabolomics) would not only compliment predicted functional profiling but give

important mechanistic insights on health-mediating metabolites (SCFAs, neurotransmitter, immunomodulators). Although more difficult to evaluate in humans, another key question is to what extent the intestinal epithelial barrier (for example via probe-based confocal laser endomicroscopy) and BBB (dynamic contrast-enhanced magnetic resonance imaging [DCE-MRI]) promote disease-associated processes through increased permeability (Wallace *et al.*, 2014; Varatharaj *et al.*, 2019). ‘Leaky’ barriers might be fundamental drivers in many disease settings and as such they offer great promise as therapeutic targets. Several of the above-mentioned microbiome-related targets are already being investigated in interventional studies using mice.

In a next step, I suggest a placebo-controlled, double-blinded, event-driven intervention study in APO ϵ 4 carriers, powered for AD diagnosis as primary endpoint, that builds on the insights from the large cohort-study by targeting one of the identified disease mechanisms (e.g. administration of SCFAs producing bacteria to decrease intestinal barrier permeability). The suggested microbiota-intervention should aim to test the efficacy of a prebiotic/probiotic (previously shown to be safe for use in humans, otherwise safety would need to be shown first) on the incidence for AD in the intervention group vs placebo. Particularly interventions using oligosaccharides, like the aforementioned GV-971, have shown promising results in animal studies and in Chinese AD patients and might offer new treatment options for AD.

Studying the interplay of the intestinal microbiota and the brain, the Gut-Brain axis, is an underexplored but an exciting area of research and part of new conceptual era in which we approach human health from a truly holistic perspective, with the promise for novel therapeutic interventions for AD and many other diseases.

BIBLIOGRAPHY

- Abbott, N. J. *et al.* (2010) 'Structure and function of the blood–brain barrier', *Neurobiology of Disease*, 37(1), pp. 13–25. doi: 10.1016/j.nbd.2009.07.030.
- Abrahamson, M. *et al.* (2017) 'Successful collection of stool samples for microbiome analyses from a large community-based population of elderly men'. doi: 10.1016/j.conctc.2017.07.002.
- Abu-Ali, G. S. *et al.* (2018) 'Metatranscriptome of human faecal microbial communities in a cohort of adult men', *Nature Microbiology*. Nature Publishing Group, 3(3), pp. 356–366. doi: 10.1038/s41564-017-0084-4.
- Abubucker, S. *et al.* (2012) 'Metabolic Reconstruction for Metagenomic Data and Its Application to the Human Microbiome', *PLoS Computational Biology*. Edited by J. A. Eisen. Public Library of Science, 8(6), p. e1002358. doi: 10.1371/journal.pcbi.1002358.
- Ackerman, H. D. and Gerhard, G. S. (2016) 'Bile acids in neurodegenerative disorders', *Frontiers in Aging Neuroscience*. Frontiers Media S.A., p. 263. doi: 10.3389/fnagi.2016.00263.
- Adlimoghaddam, A., Sabbir, M. G. and Albensi, B. C. (2016) 'Ammonia as a potential neurotoxic factor in alzheimer's disease', *Frontiers in Molecular Neuroscience*. Frontiers Research Foundation, p. 57. doi: 10.3389/fnmol.2016.00057.
- Ahola, A. J. *et al.* (2017) 'Dietary patterns reflecting healthy food choices are associated with lower serum LPS activity', *Scientific Reports*. Nature Publishing Group, 7(1). doi: 10.1038/s41598-017-06885-7.
- Akbari, E. *et al.* (2016) 'Effect of probiotic supplementation on cognitive function and metabolic status in Alzheimer's disease: A randomized, double-blind and controlled trial', *Frontiers in Aging Neuroscience*. Frontiers Media S.A., 8(NOV). doi: 10.3389/fnagi.2016.00256.
- Albert, M. S. *et al.* (2011) 'The diagnosis of mild cognitive impairment due to Alzheimer's disease: Recommendations from the National Institute on Aging-Alzheimer's Association workgroups on diagnostic guidelines for Alzheimer's disease', *Alzheimer's and Dementia*. Elsevier Inc., 7(3), pp. 270–279. doi: 10.1016/j.jalz.2011.03.008.
- Alfred, T. *et al.* (2014) 'Associations between APOE and low-density lipoprotein cholesterol genotypes and cognitive and physical capability: The HALCYon programme', *Age*. Kluwer Academic Publishers, 36(4). doi: 10.1007/s11357-014-9673-9.
- Ali, J. I., Smart, C. M. and Gawryluk, J. R. (2018) 'Subjective cognitive decline and APOE ϵ 4: A systematic review', *Journal of Alzheimer's Disease*. IOS Press, pp. 303–320. doi: 10.3233/JAD-180248.
- Allaband, C. *et al.* (2019) 'Microbiome 101: Studying, Analyzing, and Interpreting Gut Microbiome Data for Clinicians', *Clinical Gastroenterology and Hepatology*. W.B. Saunders, pp. 218–230. doi: 10.1016/j.cgh.2018.09.017.
- Alzheimer's Society (2009) *Counting the cost Caring for people with dementia on hospital wards*.
- Alzheimer Association (2016) '2016 Alzheimer's Disease Facts and Figures', *Alzheimer's & Dementia 2016*, 12(4), pp. 1–80. doi: 10.1016/j.jalz.2016.03.001.
- Anderson, E. L. *et al.* (2016) 'A robust ambient temperature collection and stabilization strategy: Enabling worldwide functional studies of the human microbiome', *Scientific Reports*. Nature Publishing Group, 6(1), pp. 1–10. doi: 10.1038/srep31731.
- Anderson, M. J. (2017) 'Permutational Multivariate Analysis of Variance

(PERMANOVA)', in *Wiley StatsRef: Statistics Reference Online*. John Wiley & Sons, Ltd, pp. 1–15. doi: 10.1002/9781118445112.stat07841.

Andersson, J. L. R., Jenkinson, M. and Smith, S. (2007) *Non-linear registration aka Spatial normalisation FMRIB Technical Report TR07JA2*.

Andrews-Zwilling, Y. *et al.* (2010) 'Apolipoprotein E4 causes age- and Tau-dependent impairment of GABAergic interneurons, leading to learning and memory deficits in mice', *Journal of Neuroscience*. Society for Neuroscience, 30(41), pp. 13707–13717. doi: 10.1523/JNEUROSCI.4040-10.2010.

Arboleya, S. *et al.* (2016) 'Gut bifidobacteria populations in human health and aging', *Frontiers in Microbiology*. Frontiers Media S.A. doi: 10.3389/fmicb.2016.01204.

Arends, Y. M. *et al.* (2000) 'Microglia, amyloid and dementia in Alzheimer disease: A correlative study', *Neurobiology of Aging*, 21(1), pp. 39–47. doi: 10.1016/S0197-4580(00)00094-4.

Areosa, S. A., Sherriff, F. and McShane, R. (2005) 'Memantine for dementia', in *The Cochrane Database of Systematic Reviews*. John Wiley & Sons, Ltd. doi: 10.1002/14651858.cd003154.pub3.

Arnold, A. E. G. F. *et al.* (2014) 'Differential neural network configuration during human path integration', *Frontiers in Human Neuroscience*. Frontiers Media S. A., 8(1 APR), p. 263. doi: 10.3389/fnhum.2014.00263.

Arrieta, M. C., Bistriz, L. and Meddings, J. B. (2006) 'Alterations in intestinal permeability.', *Gut*. BMJ Group, 55(10), pp. 1512–20. doi: 10.1136/gut.2005.085373.

Arroyo, D. S. *et al.* (2011) 'Toll-like receptors are key players in neurodegeneration.', *International immunopharmacology*. NIH Public Access, 11(10), pp. 1415–21. doi: 10.1016/j.intimp.2011.05.006.

Ashendorf, L. *et al.* (2008) 'Trail Making Test errors in normal aging, mild cognitive impairment, and dementia', *Archives of Clinical Neuropsychology*. Arch Clin Neuropsychol, 23(2), pp. 129–137. doi: 10.1016/j.acn.2007.11.005.

Azm, S. A. N. *et al.* (2018) 'Lactobacilli and bifidobacteria ameliorate memory and learning deficits and oxidative stress in β -amyloid (1–42) injected rats', *Applied Physiology, Nutrition and Metabolism*. Canadian Science Publishing, 43(7), pp. 718–726. doi: 10.1139/apnm-2017-0648.

Bäckhed, F. *et al.* (2005) 'Host-bacterial mutualism in the human intestine', *Science*. Science, pp. 1915–1920. doi: 10.1126/science.1104816.

Bahl, M. I., Bergström, A. and Licht, T. R. (2012) 'Freezing fecal samples prior to DNA extraction affects the Firmicutes to Bacteroidetes ratio determined by downstream quantitative PCR analysis', *FEMS Microbiology Letters*, 329(2), pp. 193–197. doi: 10.1111/j.1574-6968.2012.02523.x.

Balamurugan, R. *et al.* (2008) 'Real-time polymerase chain reaction quantification of specific butyrate-producing bacteria, *Desulfovibrio* and *Enterococcus faecalis* in the feces of patients with colorectal cancer', *Journal of Gastroenterology and Hepatology (Australia)*. Blackwell Publishing, 23(8 PART1), pp. 1298–1303. doi: 10.1111/j.1440-1746.2008.05490.x.

Baldini, F. *et al.* (2019) 'Parkinson's disease-associated alterations of the gut microbiome can invoke disease-relevant metabolic changes', *bioRxiv*. bioRxiv, p. 691030. doi: 10.1101/691030.

Banks, W. A. (2009) 'Characteristics of compounds that cross the blood-brain barrier.', *BMC neurology*. BioMed Central, 9 Suppl 1(Suppl 1), p. S3. doi: 10.1186/1471-2377-9-

S1-S3.

Bardenhorst, S. K. *et al.* (2021) 'Data Analysis Strategies for Microbiome Studies in Human Populations-a Systematic Review of Current Practice'. doi: 10.1128/mSystems.01154-20.

Barylski, J. *et al.* (2020) 'Analysis of Spounaviruses as a Case Study for the Overdue Reclassification of Tailed Phages', *Systematic Biology*. Edited by L. Jarmin. Oxford University Press, 69(1), pp. 110–123. doi: 10.1093/sysbio/syz036.

Bäuerl, C. *et al.* (2018) 'Shifts in gut microbiota composition in an APP/PSS1 transgenic mouse model of Alzheimer's disease during lifespan', *Letters in Applied Microbiology*, 66(6), pp. 464–471. doi: 10.1111/lam.12882.

Beach, T. G., Walker, R. and McGeer, E. G. (1989) 'Patterns of gliosis in alzheimer's disease and aging cerebrum', *Glia*, 2(6), pp. 420–436. doi: 10.1002/glia.440020605.

Beisner, J. *et al.* (2020) 'Fructose-induced intestinal microbiota shift following two types of short-term high-fructose dietary phases', *Nutrients*. MDPI AG, 12(11), pp. 1–21. doi: 10.3390/nu12113444.

Bekris, L. M. *et al.* (2010) 'Review article: Genetics of Alzheimer disease', *Journal of Geriatric Psychiatry and Neurology*. NIH Public Access, pp. 213–227. doi: 10.1177/0891988710383571.

Bell, R. D. *et al.* (2012) 'Apolipoprotein e controls cerebrovascular integrity via cyclophilin A', *Nature*. Nature Publishing Group, 485(7399), pp. 512–516. doi: 10.1038/nature11087.

Belzer, C. and De Vos, W. M. (2012) 'Microbes inside from diversity to function: The case of Akkermansia', *ISME Journal*. Nature Publishing Group, 6(8), pp. 1449–1458. doi: 10.1038/ismej.2012.6.

Bennet, A. M. *et al.* (2007) 'Association of apolipoprotein e genotypes with lipid levels and coronary risk', *Journal of the American Medical Association*. JAMA, pp. 1300–1311. doi: 10.1001/jama.298.11.1300.

Bennett-Levy, J. (1984) 'Determinants of performance on the Rey-Osterrieth Complex Figure Test: an analysis, and a new technique for single-case assessment.', *The British journal of clinical psychology*, 23 (Pt 2), pp. 109–19. Available at: <http://www.ncbi.nlm.nih.gov/pubmed/6722375> (Accessed: 8 September 2019).

Bergh, S. and Selbæk, G. (2012) 'The prevalence and the course of neuropsychiatric symptoms in patients with dementia', *Norsk Epidemiologi*. Norwegian Epidemiological Society, 22(2), pp. 225–232. doi: 10.5324/nje.v22i2.1570.

Bergström, P. *et al.* (2016) 'Amyloid precursor protein expression and processing are differentially regulated during cortical neuron differentiation', *Scientific Reports 2016 6:1*. Nature Publishing Group, 6(1), pp. 1–14. doi: 10.1038/srep29200.

Besser, J. *et al.* (2018) 'Next-generation sequencing technologies and their application to the study and control of bacterial infections', *Clinical Microbiology and Infection*. Elsevier B.V., pp. 335–341. doi: 10.1016/j.cmi.2017.10.013.

Beydoun, M. A. *et al.* (2020) 'Clinical and Bacterial Markers of Periodontitis and Their Association with Incident All-Cause and Alzheimer's Disease Dementia in a Large National Survey', *Journal of Alzheimer's Disease*. IOS Press, 75(1), pp. 157–172. doi: 10.3233/jad-200064.

Birks, J. (2006) 'Cholinesterase inhibitors for Alzheimer's disease', *Cochrane Database of Systematic Reviews*. John Wiley and Sons Ltd. doi: 10.1002/14651858.CD005593.

Bischoff, S. C. *et al.* (2014) 'Intestinal permeability - a new target for disease prevention

- and therapy', *BMC Gastroenterology*. BioMed Central Ltd. doi: 10.1186/s12876-014-0189-7.
- Bittner, T. *et al.* (2012) 'Amyloid plaque formation precedes dendritic spine loss', *Acta Neuropathologica*, 124(6), pp. 797–807. doi: 10.1007/s00401-012-1047-8.
- Blanchard, J. W. *et al.* (2020) 'Reconstruction of the human blood–brain barrier in vitro reveals a pathogenic mechanism of APOE4 in pericytes', *Nature Medicine*. Springer US, 26(6), pp. 952–963. doi: 10.1038/s41591-020-0886-4.
- Blanco, A. and Blanco, G. (2017) 'Lipids', in *Medical Biochemistry*. Elsevier, pp. 99–119. doi: 10.1016/B978-0-12-803550-4.00005-7.
- de Boer, R. *et al.* (2010) 'Improved detection of microbial DNA after bead-beating before DNA isolation.', *Journal of microbiological methods*, 80(2), pp. 209–11. doi: 10.1016/j.mimet.2009.11.009.
- Bonaz, B., Bazin, T. and Pellissier, S. (2018) 'The vagus nerve at the interface of the microbiota-gut-brain axis', *Frontiers in Neuroscience*. Frontiers Media S.A. doi: 10.3389/fnins.2018.00049.
- Bonfili, L. *et al.* (2017) 'Microbiota modulation counteracts Alzheimer's disease progression influencing neuronal proteolysis and gut hormones plasma levels', *Scientific Reports*. Springer US, 7(1), pp. 1–21. doi: 10.1038/s41598-017-02587-2.
- Boutajangout, A. and Wisniewski, T. (2013) 'The innate immune system in Alzheimer's disease.', *International journal of cell biology*. Hindawi, 2013, p. 576383. doi: 10.1155/2013/576383.
- Braak, H. *et al.* (2006) 'Staging of Alzheimer disease-associated neurofibrillary pathology using paraffin sections and immunocytochemistry.', *Acta neuropathologica*. Springer, 112(4), pp. 389–404. doi: 10.1007/s00401-006-0127-z.
- Braniste, V. *et al.* (2014) 'The gut microbiota influences blood-brain barrier permeability in mice', *Science Translational Medicine*, 6(263). Available at: <http://stm.sciencemag.org/content/6/263/263ra158> (Accessed: 1 August 2017).
- Bräsen, C. *et al.* (2014) 'Carbohydrate Metabolism in Archaea: Current Insights into Unusual Enzymes and Pathways and Their Regulation', *Microbiology and Molecular Biology Reviews : MMBR*. American Society for Microbiology (ASM), 78(1), p. 89. doi: 10.1128/MMBR.00041-13.
- Bravo, J. A. *et al.* (2011) 'Ingestion of Lactobacillus strain regulates emotional behavior and central GABA receptor expression in a mouse via the vagus nerve', *Proceedings of the National Academy of Sciences*, 108(38), pp. 16050–16055. doi: 10.1073/pnas.1102999108.
- Breit, S. *et al.* (2018) 'Vagus nerve as modulator of the brain-gut axis in psychiatric and inflammatory disorders', *Frontiers in Psychiatry*. Frontiers Media S.A. doi: 10.3389/fpsy.2018.00044.
- Brodbeck, J. *et al.* (2008) 'Rosiglitazone increases dendritic spine density and rescues spine loss caused by apolipoprotein E4 in primary cortical neurons', *Proceedings of the National Academy of Sciences of the United States of America*. National Academy of Sciences, 105(4), pp. 1343–1346. doi: 10.1073/pnas.0709906104.
- Brown, E. M. *et al.* (2019) 'Bacteroides-Derived Sphingolipids Are Critical for Maintaining Intestinal Homeostasis and Symbiosis', *Cell Host and Microbe*. Cell Press, 25(5), pp. 668-680.e7. doi: 10.1016/j.chom.2019.04.002.
- de Bruijn, R. F. A. G. and Ikram, M. A. (2014) 'Cardiovascular risk factors and future risk of Alzheimer's disease', *BMC Medicine*, 12:1 Artic, pp. 1–9. doi: Artn 130rDoi 10.1186/S12916-014-0130-5.

- Brunnström, H. R. and Englund, E. M. (2009) 'Cause of death in patients with dementia disorders', *European Journal of Neurology*. Eur J Neurol, 16(4), pp. 488–492. doi: 10.1111/j.1468-1331.2008.02503.x.
- Bruno, D. and Vignaga, S. S. (2019) 'Addenbrooke's cognitive examination III in the diagnosis of dementia: A critical review', *Neuropsychiatric Disease and Treatment*. Dove Medical Press Ltd., pp. 441–447. doi: 10.2147/NDT.S151253.
- Bunce, D. *et al.* (2014) 'APOE genotype and cognitive change in young, middle-aged, and older adults living in the community', *Journals of Gerontology - Series A Biological Sciences and Medical Sciences*. Oxford University Press, 69(4), pp. 379–386. doi: 10.1093/gerona/glt103.
- Burbach, K. *et al.* (2016) 'Evaluation of DNA extraction kits and phylogenetic diversity of the porcine gastrointestinal tract based on Illumina sequencing of two hypervariable regions.', *MicrobiologyOpen*. Wiley-Blackwell, 5(1), pp. 70–82. doi: 10.1002/mbo3.312.
- Burggren, A. C. *et al.* (2008) 'Reduced cortical thickness in hippocampal subregions among cognitively normal apolipoprotein E e4 carriers', *NeuroImage*. Academic Press, 41(4), pp. 1177–1183. doi: 10.1016/j.neuroimage.2008.03.039.
- Butters, M. A. *et al.* (2008) 'Pathways linking late-life depression to persistent cognitive impairment and dementia', *Dialogues in Clinical Neuroscience*. Les Laboratoires Servier, 10(3), p. 345.
- Byers, A. L. and Yaffe, K. (2011) 'Depression and risk of developing dementia', *Nature Reviews Neurology*, pp. 323–331. doi: 10.1038/nrneurol.2011.60.
- Cagnin, A. *et al.* (2001) 'In-vivo measurement of activated microglia in dementia', *Lancet*. Lancet Publishing Group, 358(9280), pp. 461–467. doi: 10.1016/S0140-6736(01)05625-2.
- Cai, Z., Hussain, M. D. and Yan, L. J. (2014) 'Microglia, neuroinflammation, and beta-amyloid protein in Alzheimer's disease', *International Journal of Neuroscience*. Informa Healthcare, pp. 307–321. doi: 10.3109/00207454.2013.833510.
- Camara, A. *et al.* (2021) 'Clinical evidence of the role of Methanobrevibacter smithii in severe acute malnutrition', *Scientific reports*. NLM (Medline), 11(1), p. 5426. doi: 10.1038/s41598-021-84641-8.
- Camilleri, M. and Gorman, H. (2007) 'Intestinal permeability and irritable bowel syndrome', *Neurogastroenterology and Motility*. Neurogastroenterol Motil, pp. 545–552. doi: 10.1111/j.1365-2982.2007.00925.x.
- Cani, P. D. *et al.* (2007) 'Metabolic Endotoxemia Initiates Obesity and Insulin Resistance', *Diabetes*, 56(7), pp. 1761–1772. doi: 10.2337/db06-1491.
- Caporaso, J. G. *et al.* (2011) 'Moving pictures of the human microbiome', *Genome Biology*. BioMed Central Ltd., 12(5), p. R50. doi: 10.1186/gb-2011-12-5-r50.
- Caporaso, J. G. *et al.* (2012) 'Ultra-high-throughput microbial community analysis on the Illumina HiSeq and MiSeq platforms', *ISME Journal*. Nature Publishing Group, 6(8), pp. 1621–1624. doi: 10.1038/ismej.2012.8.
- Carlino, D., De Vanna, M. and Tongiorgi, E. (2013) 'Is altered BDNF biosynthesis a general feature in patients with cognitive dysfunctions?', *Neuroscientist*, 19(4), pp. 345–353. doi: 10.1177/1073858412469444.
- Carone, M., Asgharian, M. and Jewell, N. P. (2014) 'Estimating the lifetime risk of dementia in the Canadian elderly population using cross-sectional cohort survival data.', *Journal of the American Statistical Association*. NIH Public Access, 109(505), pp. 24–35. doi: 10.1080/01621459.2013.859076.
- Carr, R. and Borenstein, E. (2014) 'Comparative analysis of functional metagenomic

- annotation and the mappability of short reads', *PLoS ONE*. Public Library of Science, 9(8), p. 105776. doi: 10.1371/journal.pone.0105776.
- Casals-Pascual, C. *et al.* (2020) 'Microbial Diversity in Clinical Microbiome Studies: Sample Size and Statistical Power Considerations', *Gastroenterology*. W.B. Saunders, pp. 1524–1528. doi: 10.1053/j.gastro.2019.11.305.
- Caselli, R. J. *et al.* (2007) 'Cognitive domain decline in healthy apolipoprotein E ϵ 4 homozygotes before the diagnosis of mild cognitive impairment', *Archives of Neurology*. American Medical Association, 64(9), pp. 1306–1311. doi: 10.1001/archneur.64.9.1306.
- Caselli, R. J. *et al.* (2011) 'Longitudinal modeling of frontal cognition in APOE ϵ 4 homozygotes, heterozygotes, and noncarriers', *Neurology*. Neurology, 76(16), pp. 1383–1388. doi: 10.1212/WNL.0b013e3182167147.
- Castellano, J. M. *et al.* (2011) 'Human apoE Isoforms Differentially Regulate Brain Amyloid- Peptide Clearance', *Science Translational Medicine*, 3(89), pp. 89ra57-89ra57. doi: 10.1126/scitranslmed.3002156.
- Chan, W., Brown, J. and Church, S. (1996) 'Meat products and dishes. The sixth supplement to McCance and Widdowson's the composition of foods. 5th edn.', *Cambridge: Royal Society of Chemistry*.
- Chen, D. *et al.* (2017) 'Prebiotic effect of Fructooligosaccharides from *Morinda officinalis* on Alzheimer's disease in rodent models by targeting the microbiota-gut-brain axis', *Frontiers in Aging Neuroscience*, 9(DEC), pp. 1–28. doi: 10.3389/fnagi.2017.00403.
- Chen, G. F. *et al.* (2017) 'Amyloid beta: Structure, biology and structure-based therapeutic development', *Acta Pharmacologica Sinica*. Nature Publishing Group, 38(9), pp. 1205–1235. doi: 10.1038/aps.2017.28.
- Chen, J. *et al.* (2016) 'An expansion of rare lineage intestinal microbes characterizes rheumatoid arthritis', *Genome Medicine*. BioMed Central Ltd., 8(1), p. 43. doi: 10.1186/s13073-016-0299-7.
- Chen, Y. *et al.* (2021) 'Apolipoprotein E: Structural Insights and Links to Alzheimer Disease Pathogenesis', *Neuron*. Cell Press, pp. 205–221. doi: 10.1016/j.neuron.2020.10.008.
- Cherbuin, N. *et al.* (2008) 'Total and Regional Gray Matter Volume Is Not Related to APOE*E4 Status in a Community Sample of Middle-Aged Individuals', *The Journals of Gerontology Series A: Biological Sciences and Medical Sciences*. Gerontological Society of America, 63(5), pp. 501–504. doi: 10.1093/gerona/63.5.501.
- Cherrier, M. M. *et al.* (1999) 'Performance on the Rey-Osterrieth Complex Figure Test in Alzheimer disease and vascular dementia.', *Neuropsychiatry, neuropsychology, and behavioral neurology*, 12(2), pp. 95–101. Available at: <http://www.ncbi.nlm.nih.gov/pubmed/10223256> (Accessed: 7 September 2019).
- Cheru, L., Saylor, C. F. and Lo, J. (2019) 'Gastrointestinal Barrier Breakdown and Adipose Tissue Inflammation', *Current Obesity Reports*. Springer Science and Business Media LLC, 8(2), pp. 165–174. doi: 10.1007/s13679-019-00332-6.
- Chong, J. *et al.* (2020) 'Using MicrobiomeAnalyst for comprehensive statistical, functional, and meta-analysis of microbiome data', *Nature Protocols*. Nature Research, 15(3), pp. 799–821. doi: 10.1038/s41596-019-0264-1.
- Choo, J. M., Leong, L. E. X. and Rogers, G. B. (2015) 'Sample storage conditions significantly influence faecal microbiome profiles', *Scientific Reports*. Nature Publishing Group, 5. doi: 10.1038/srep16350.
- Chung, W. S. F. *et al.* (2016) 'Modulation of the human gut microbiota by dietary fibres

- occurs at the species level', *BMC Biology*. BioMed Central Ltd., 14(1), p. 3. doi: 10.1186/s12915-015-0224-3.
- Claesson, M. J. *et al.* (2011) 'Composition, variability, and temporal stability of the intestinal microbiota of the elderly.', *Proceedings of the National Academy of Sciences of the United States of America*. National Academy of Sciences, (Suppl 1), pp. 4586–91. doi: 10.1073/pnas.1000097107.
- Clavel, T. *et al.* (2014) 'Intestinal microbiota in metabolic diseases', *Gut Microbes*. Landes Bioscience, 5(4), pp. 544–551. doi: 10.4161/gmic.29331.
- Clemente, J. C. *et al.* (2012) 'The impact of the gut microbiota on human health: An integrative view', *Cell*. Elsevier Inc., 148(6), pp. 1258–1270. doi: 10.1016/j.cell.2012.01.035.
- Collins, S. M. and Bercik, P. (2009) 'The Relationship Between Intestinal Microbiota and the Central Nervous System in Normal Gastrointestinal Function and Disease', *Gastroenterology*. W.B. Saunders, 136(6), pp. 2003–2014. doi: 10.1053/j.gastro.2009.01.075.
- Corrada, M. M. *et al.* (2010) 'Dementia incidence continues to increase with age in the oldest old the 90+ study', *Annals of Neurology*. NIH Public Access, 67(1), pp. 114–121. doi: 10.1002/ana.21915.
- Costello, E. K. *et al.* (2009) 'Bacterial community variation in human body habitats across space and time', *Science*, 326(5960), pp. 1694–1697. doi: 10.1126/science.1177486.
- Cotillard, A. *et al.* (2013) 'Dietary intervention impact on gut microbial gene richness.[Erratum appears in Nature. 2013 Oct 24;502(7472)580]', *Nature*, 500(7464), pp. 585–588. doi: <http://dx.doi.org/10.1038/nature12480>.
- Coughlan, G. *et al.* (2018) 'Spatial navigation deficits — Overlooked cognitive marker for preclinical Alzheimer disease?', *Nature Reviews Neurology*. Nature Publishing Group, pp. 496–506. doi: 10.1038/s41582-018-0031-x.
- Coughlan, G. *et al.* (2019) 'Toward personalized cognitive diagnostics of at-genetic-risk Alzheimer's disease', *Proceedings of the National Academy of Sciences of the United States of America*. National Academy of Sciences, 116(19), pp. 9285–9292. doi: 10.1073/pnas.1901600116.
- Coughlan, G. *et al.* (2020) 'Functional connectivity between the entorhinal and posterior cingulate cortices underpins navigation discrepancies in at-risk Alzheimer's disease', *Neurobiology of Aging*. Elsevier Inc., 90, pp. 110–118. doi: 10.1016/j.neurobiolaging.2020.02.007.
- Coutrot, A. *et al.* (2018) 'Global Determinants of Navigation Ability'. doi: 10.1016/j.cub.2018.06.009.
- Craig Venter, J. *et al.* (2001) 'The sequence of the human genome', *Science*, 291(5507), pp. 1304–1351. doi: 10.1126/science.1058040.
- Cronin-Golomb, A. *et al.* (1991) 'Visual dysfunction in Alzheimer's disease: relation to normal aging.', *Annals of neurology*, 29(1), pp. 41–52. doi: 10.1002/ana.410290110.
- Croteau, E. *et al.* (2018) 'A cross-sectional comparison of brain glucose and ketone metabolism in cognitively healthy older adults, mild cognitive impairment and early Alzheimer's disease', *Experimental Gerontology*. Elsevier Inc., 107, pp. 18–26. doi: 10.1016/j.exger.2017.07.004.
- Crovesy, L., Masterson, D. and Rosado, E. L. (2020) 'Profile of the gut microbiota of adults with obesity: a systematic review', *European Journal of Clinical Nutrition*. Springer Nature, pp. 1251–1262. doi: 10.1038/s41430-020-0607-6.

- Cryan, J. F. and Dinan, T. G. (2012) 'Mind-altering microorganisms: the impact of the gut microbiota on brain and behaviour', *Nature Reviews Neuroscience*. Nature Publishing Group, 13(10), pp. 701–712. doi: 10.1038/nrn3346.
- Cunnane, S. *et al.* (2011) 'Brain fuel metabolism, aging, and Alzheimer's disease', *Nutrition*. Elsevier Inc., pp. 3–20. doi: 10.1016/j.nut.2010.07.021.
- Cunningham, E. L. *et al.* (2015) 'Dementia.', *The Ulster medical journal*, 84(2), pp. 79–87. Available at: <http://www.ncbi.nlm.nih.gov/pubmed/26170481> (Accessed: 4 December 2019).
- Currais, A. *et al.* (2019) 'Elevating acetyl-CoA levels reduces aspects of brain aging', *eLife*. eLife Sciences Publications Ltd, 8. doi: 10.7554/eLife.47866.
- Czumaj, A. *et al.* (2020) 'The pathophysiological role of CoA', *International Journal of Molecular Sciences*, 21(23), pp. 1–30. doi: 10.3390/ijms21239057.
- Daillère, R. *et al.* (2016) 'Enterococcus hirae and Barnesiella intestinihominis Facilitate Cyclophosphamide-Induced Therapeutic Immunomodulatory Effects', *Immunity*. Cell Press, 45(4), pp. 931–943. doi: 10.1016/j.immuni.2016.09.009.
- David, L. A. *et al.* (2014) 'Diet rapidly and reproducibly alters the human gut microbiome.', *Nature*. NIH Public Access, 505(7484), pp. 559–63. doi: 10.1038/nature12820.
- DeJong, T. M. (1975) 'A Comparison of Three Diversity Indices Based on Their Components of Richness and Evenness', *Oikos*. JSTOR, 26(2), p. 222. doi: 10.2307/3543712.
- Demuro, A., Parker, I. and Stutzmann, G. E. (2010) 'Calcium Signaling and Amyloid Toxicity in Alzheimer Disease *'. doi: 10.1074/jbc.R109.080895.
- Descamps, H. C. *et al.* (2019) 'The path toward using microbial metabolites as therapies', *EBioMedicine*. Elsevier B.V., pp. 747–754. doi: 10.1016/j.ebiom.2019.05.063.
- Dhariwal, A. *et al.* (2017) 'MicrobiomeAnalyst: A web-based tool for comprehensive statistical, visual and meta-analysis of microbiome data', *Nucleic Acids Research*. Oxford University Press, 45(W1), pp. W180–W188. doi: 10.1093/nar/gkx295.
- Dinan, T. G. *et al.* (2015) 'Collective unconscious: How gut microbes shape human behavior', *Journal of Psychiatric Research*, 63, pp. 1–9. doi: 10.1016/j.jpsychires.2015.02.021.
- Divyashri, G. *et al.* (2015) 'Probiotic attributes, antioxidant, anti-inflammatory and neuromodulatory effects of Enterococcus faecium CFR 3003: In vitro and in vivo evidence', *Journal of Medical Microbiology*. Microbiology Society, 64(12), pp. 1527–1540. doi: 10.1099/jmm.0.000184.
- Dominy, S. S. *et al.* (2019) 'Porphyromonas gingivalis in Alzheimer's disease brains: Evidence for disease causation and treatment with small-molecule inhibitors', *Science Advances*. American Association for the Advancement of Science, 5(1), p. eaau3333. doi: 10.1126/sciadv.aau3333.
- Dordević, D. *et al.* (2021) 'Hydrogen sulfide toxicity in the gut environment: Meta-analysis of sulfate-reducing and lactic acid bacteria in inflammatory processes', *Journal of Advanced Research*. Elsevier B.V., pp. 55–69. doi: 10.1016/j.jare.2020.03.003.
- Douaud, G. *et al.* (2007) 'Anatomically related grey and white matter abnormalities in adolescent-onset schizophrenia', *Brain*. Brain, 130(9), pp. 2375–2386. doi: 10.1093/brain/awm184.
- Durazzi, F. *et al.* (2021) 'Comparison between 16S rRNA and shotgun sequencing data for the taxonomic characterization of the gut microbiota', *Scientific Reports*. Nature Research,

- 11(1), p. 3030. doi: 10.1038/s41598-021-82726-y.
- Eberly, L. E. (2007) 'Multiple Linear Regression.', in *Topics in Biostatistics*. Humana Press Inc. doi: 10.1136/bmj.b167.
- Eckburg, P. B. *et al.* (2005) 'Microbiology: Diversity of the human intestinal microbial flora', *Science*. NIH Public Access, 308(5728), pp. 1635–1638. doi: 10.1126/science.1110591.
- Edwards, N. *et al.* (2018) 'QRISK3 improves detection of cardiovascular disease risk in patients with systemic lupus erythematosus', *Lupus Science and Medicine*. BMJ Publishing Group, 5(1). doi: 10.1136/lupus-2018-000272.
- Eisenberg, D. and Jucker, M. (2012) 'The amyloid state of proteins in human diseases', *Cell*. NIH Public Access, 148(6), p. 1188. doi: 10.1016/J.CELL.2012.02.022.
- Ellis, J. M. (2005) 'Cholinesterase Inhibitors in the Treatment of Dementia', *The Journal of the American Osteopathic Association*. American Osteopathic Association, 105(3), pp. 145–158. doi: 10.7556/JAOA.2005.105.3.145.
- Emerit, J., Edeas, M. and Bricaire, F. (2004) 'Neurodegenerative diseases and oxidative stress', *Biomedicine & Pharmacotherapy*, 58(1), pp. 39–46. doi: 10.1016/j.biopha.2003.11.004.
- Emery, D. C. *et al.* (2017) '16S rRNA next generation sequencing analysis shows bacteria in Alzheimer's Post-Mortem Brain', *Frontiers in Aging Neuroscience*. Frontiers Media S.A., 9(JUN), p. 195. doi: 10.3389/fnagi.2017.00195.
- England and Wales: Mortality Statistics* (2019). Available at: <https://www.dementiastatistics.org/statistics/deaths-due-to-dementia/>.
- EPIC-Norfolk: nutritional methods* (no date) *University of Cambridge*.
- Erny, D. *et al.* (2015) 'Host microbiota constantly control maturation and function of microglia in the CNS', *Nature Neuroscience*. Nature Publishing Group, 18(7), pp. 965–977. doi: 10.1038/nn.4030.
- Esmaeil Amini, M. *et al.* (2020) 'Gut microbiome and multiple sclerosis: New insights and perspective', *International Immunopharmacology*. Elsevier B.V. doi: 10.1016/j.intimp.2020.107024.
- Faith, J. J. *et al.* (2013) 'The long-term stability of the human gut microbiota', *Science*, 341(6141). doi: 10.1126/science.1237439.
- Falony, G. *et al.* (2016) 'Population-level analysis of gut microbiome variation', *Science*. American Association for the Advancement of Science, 352(6285), pp. 560–564. doi: 10.1126/science.aad3503.
- Farrer, L. A. *et al.* (1997) 'Effects of Age, Sex, and Ethnicity on the Association Between Apolipoprotein E Genotype and Alzheimer Disease', *JAMA*. American Medical Association, 278(16), p. 1349. doi: 10.1001/jama.1997.03550160069041.
- Farzi, A., Fröhlich, E. E. and Holzer, P. (2018) 'Gut Microbiota and the Neuroendocrine System', *Neurotherapeutics*, 15(1), pp. 5–22. doi: 10.1007/s13311-017-0600-5.
- Faust, K. *et al.* (2015) 'Metagenomics meets time series analysis: Unraveling microbial community dynamics', *Current Opinion in Microbiology*. Elsevier Ltd, pp. 56–66. doi: 10.1016/j.mib.2015.04.004.
- Fennema-Notestine, C. *et al.* (2011) 'Presence of ApoE ϵ 4 allele associated with thinner frontal cortex in middle age', *Journal of Alzheimer's Disease*. IOS Press, 26(SUPPL. 3), pp. 49–60. doi: 10.3233/JAD-2011-0002.
- Fernandes, J. *et al.* (2013) 'Age, Dietary Fiber, Breath Methane, and Fecal Short Chain

- Fatty Acids Are Interrelated in Archaea-Positive Humans', *The Journal of Nutrition*. Oxford Academic, 143(8), pp. 1269–1275. doi: 10.3945/jn.112.170894.
- Ferreira-Halder, C. V., Faria, A. V. de S. and Andrade, S. S. (2017) 'Action and function of *Faecalibacterium prausnitzii* in health and disease', *Best Practice and Research: Clinical Gastroenterology*. Bailliere Tindall Ltd, pp. 643–648. doi: 10.1016/j.bpg.2017.09.011.
- De Filippo, C. *et al.* (2010) 'Impact of diet in shaping gut microbiota revealed by a comparative study in children from Europe and rural Africa', *Proceedings of the National Academy of Sciences*, 107(33), pp. 14691–14696. doi: 10.1073/pnas.1005963107.
- Flores, G. E. *et al.* (2014) 'Temporal variability is a personalized feature of the human microbiome', *Genome biology*, 15(12), p. 531. doi: 10.1186/s13059-014-0531-y.
- Folch, J. *et al.* (2018) 'Memantine for the treatment of dementia: A review on its current and future applications', *Journal of Alzheimer's Disease*. IOS Press, pp. 1223–1240. doi: 10.3233/JAD-170672.
- Forsyth, C. B. *et al.* (2011) 'Increased Intestinal Permeability Correlates with Sigmoid Mucosa alpha-Synuclein Staining and Endotoxin Exposure Markers in Early Parkinson's Disease', *PLoS ONE*. Edited by C. Oreja-Guevara. Public Library of Science, 6(12), p. e28032. doi: 10.1371/journal.pone.0028032.
- Forsythe, P., Bienenstock, J. and Kunze, W. A. (2014) 'Vagal pathways for microbiome-brain-gut axis communication', *Advances in Experimental Medicine and Biology*. Springer New York LLC, 817, pp. 115–133. doi: 10.1007/978-1-4939-0897-4_5.
- Fouhy, F. *et al.* (2015) 'The effects of freezing on faecal microbiota as determined using miseq sequencing and culture-based investigations', *PLoS ONE*. Public Library of Science, 10(3). doi: 10.1371/journal.pone.0119355.
- Francis, B. M. *et al.* (2012) 'Object recognition memory and BDNF expression are reduced in young TgCRND8 mice.', *Neurobiology of aging*. PMC Canada manuscript submission, 33(3), pp. 555–63. doi: 10.1016/j.neurobiolaging.2010.04.003.
- Frank, J. and Landeira-Fernandez, J. (2008) 'Comparison between two scoring systems of the Rey–Osterrieth Complex Figure in left and right temporal lobe epileptic patients', *Archives of Clinical Neuropsychology*, 23(7–8), pp. 839–845. doi: 10.1016/j.acn.2008.06.001.
- Fröhlich, E. E. *et al.* (2016) 'Cognitive impairment by antibiotic-induced gut dysbiosis: Analysis of gut microbiota-brain communication', *Brain, Behavior, and Immunity*, 56, pp. 140–155. doi: 10.1016/j.bbi.2016.02.020.
- Fu, S. C., Lee, C. H. and Wang, H. (2021) 'Exploring the association of autism spectrum disorders and constipation through analysis of the gut microbiome', *International Journal of Environmental Research and Public Health*. MDPI AG, 18(2), pp. 1–13. doi: 10.3390/ijerph18020667.
- Fukuda, S. *et al.* (2011) 'Bifidobacteria can protect from enteropathogenic infection through production of acetate', *Nature*, 469(7331), pp. 543–549. doi: 10.1038/nature09646.
- Fung, T. C., Olson, C. A. and Hsiao, E. Y. (2017) 'Interactions between the microbiota, immune and nervous systems in health and disease', *Nature Neuroscience*. Nature Publishing Group, pp. 145–155. doi: 10.1038/nn.4476.
- Gaci, N. *et al.* (2014) 'Archaea and the human gut: New beginning of an old story', *World Journal of Gastroenterology*. WJG Press, pp. 16062–16078. doi: 10.3748/wjg.v20.i43.16062.

- Gale, S. C. *et al.* (2014) 'APOε4 is associated with enhanced in vivo innate immune responses in human subjects', *Journal of Allergy and Clinical Immunology*. Mosby Inc., 134(1), p. 127. doi: 10.1016/j.jaci.2014.01.032.
- Gao, Q. *et al.* (2019) 'Decreased levels of circulating trimethylamine N-oxide alleviate cognitive and pathological deterioration in transgenic mice: A potential therapeutic approach for Alzheimer's disease', *Aging*. Impact Journals LLC, 11(19), pp. 8642–8663. doi: 10.18632/aging.102352.
- Garcez, M. L., Jacobs, K. R. and Guillemin, G. J. (2019) 'Microbiota Alterations in Alzheimer's Disease: Involvement of the Kynurenine Pathway and Inflammation', *Neurotoxicity Research*, 36(2), pp. 424–436. doi: 10.1007/s12640-019-00057-3.
- García-Cordero, I. *et al.* (2016) 'Feeling, learning from and being aware of inner states: Interoceptive dimensions in neurodegeneration and stroke', *Philosophical Transactions of the Royal Society B: Biological Sciences*. Royal Society of London, 371(1708). doi: 10.1098/rstb.2016.0006.
- Ge, T. *et al.* (2020) 'The Role of the Pentose Phosphate Pathway in Diabetes and Cancer', *Frontiers in Endocrinology*. Frontiers Media S.A., p. 365. doi: 10.3389/fendo.2020.00365.
- Ghosh, K., Agarwal, P. and Haggerty, G. (2011) 'Alzheimer's disease - not an exaggeration of healthy aging.', *Indian journal of psychological medicine*. Medknow Publications, 33(2), pp. 106–114. doi: 10.4103/0253-7176.92047.
- Van Giau, V. *et al.* (2018) 'Gut microbiota and their neuroinflammatory implications in alzheimer's disease', *Nutrients*. MDPI AG, p. 1765. doi: 10.3390/nu10111765.
- Gill, S. R. *et al.* (2006) 'Metagenomic analysis of the human distal gut microbiome', *Science*, 312(5778), pp. 1355–1359. doi: 10.1126/science.1124234.
- Giovinazzo, D. *et al.* (2021) 'Hydrogen sulfide is neuroprotective in Alzheimer's disease by sulfhydrating GSK3β and inhibiting Tau hyperphosphorylation', *Proceedings of the National Academy of Sciences of the United States of America*. National Academy of Sciences, 118(4). doi: 10.1073/pnas.2017225118.
- Girolamo, F., Coppola, C. and Ribatti, D. (2017) 'Immunoregulatory effect of mast cells influenced by microbes in neurodegenerative diseases', *Brain, Behavior, and Immunity*. Academic Press Inc., 65, pp. 68–89. doi: 10.1016/j.bbi.2017.06.017.
- Good, C. D. *et al.* (2001) 'A voxel-based morphometric study of ageing in 465 normal adult human brains', *NeuroImage*. Neuroimage, 14(1 I), pp. 21–36. doi: 10.1006/nimg.2001.0786.
- Gorzalak, M. A. *et al.* (2015) 'Methods for improving human gut microbiome data by reducing variability through sample processing and storage of stool', *PLoS ONE*. Public Library of Science, 10(8). doi: 10.1371/journal.pone.0134802.
- Green, J. M. *et al.* (2017) 'Food and microbiota in the FDA regulatory framework', *Science*. American Association for the Advancement of Science, pp. 39–40. doi: 10.1126/science.aan0836.
- Gregg, R. E. *et al.* (1986) 'Abnormal in vivo metabolism of apolipoprotein E4 in humans', *Journal of Clinical Investigation*. American Society for Clinical Investigation, 78(3), pp. 815–821. doi: 10.1172/JCI112645.
- Guo, Y. and Pandis, N. (2015) 'Sample-size calculation for repeated-measures and longitudinal studies', *American Journal of Orthodontics and Dentofacial Orthopedics*. Mosby Inc., pp. 146–149. doi: 10.1016/j.ajodo.2014.10.009.
- Gurung, M. *et al.* (2020) 'Role of gut microbiota in type 2 diabetes pathophysiology', *EBioMedicine*. Elsevier B.V. doi: 10.1016/j.ebiom.2019.11.051.

- Gustafson, D. R. *et al.* (2020) 'Dietary fatty acids and risk of Alzheimer's disease and related dementias: Observations from the Washington Heights-Hamilton Heights-Inwood Columbia Aging Project (WHICAP)', *Alzheimer's & Dementia*. John Wiley and Sons Inc, 16(12), pp. 1638–1649. doi: 10.1002/alz.12154.
- Hagerty, S. L. *et al.* (2020) 'An empirically derived method for measuring human gut microbiome alpha diversity: Demonstrated utility in predicting health-related outcomes among a human clinical sample', *PLOS ONE*. Edited by P. V. Nerurkar. Public Library of Science, 15(3), p. e0229204. doi: 10.1371/journal.pone.0229204.
- Haikal, C., Chen, Q. Q. and Li, J. Y. (2019) 'Microbiome changes: An indicator of Parkinson's disease?', *Translational Neurodegeneration*. BioMed Central Ltd., pp. 1–9. doi: 10.1186/s40035-019-0175-7.
- Hakansson, A. and Molin, G. (2011) 'Gut microbiota and inflammation', *Nutrients*. MDPI AG, pp. 637–687. doi: 10.3390/nu3060637.
- Halliday, M. R. *et al.* (2016) 'Accelerated pericyte degeneration and blood-brain barrier breakdown in apolipoprotein E4 carriers with Alzheimer's disease', *Journal of Cerebral Blood Flow and Metabolism*. Nature Publishing Group, 36(1), pp. 216–227. doi: 10.1038/jcbfm.2015.44.
- Hammond, T. C. *et al.* (2020) 'β-amyloid and tau drive early Alzheimer's disease decline while glucose hypometabolism drives late decline', *Communications Biology*. Nature Research, 3(1), pp. 1–13. doi: 10.1038/s42003-020-1079-x.
- Hansen, C. H. F. *et al.* (2012) 'Patterns of early gut colonization shape future immune responses of the host', *PLoS ONE*, 7(3), p. e34043. doi: 10.1371/journal.pone.0034043.
- Hao, M. *et al.* (2019) 'Assessing biological dissimilarities between five forest communities', *Forest Ecosystems*. SpringerOpen, 6(1), p. 30. doi: 10.1186/s40663-019-0188-9.
- Harach, T. *et al.* (2017) 'Reduction of Abeta amyloid pathology in APPPS1 transgenic mice in the absence of gut microbiota', *Nature Publishing Group*. doi: 10.1038/srep41802.
- Haran, J. P. *et al.* (2019) 'Alzheimer's disease microbiome is associated with dysregulation of the anti-inflammatory P-glycoprotein pathway', *mBio*, 10(3), pp. 1–14. doi: 10.1128/mBio.00632-19.
- Harciarek, M. and Jodzio, K. (2005) 'Neuropsychological differences between frontotemporal dementia and Alzheimer's disease: a review.', *Neuropsychology review*, 15(3), pp. 131–45. doi: 10.1007/s11065-005-7093-4.
- Hardy, J. A. and Higgins, G. A. (1992) 'Alzheimer's disease: The amyloid cascade hypothesis', *Science*. American Association for the Advancement of Science, pp. 184–185. doi: 10.1126/science.1566067.
- Hartley, T. *et al.* (2014) 'Space in the brain: How the hippocampal formation supports spatial cognition', *Philosophical Transactions of the Royal Society B: Biological Sciences*. Royal Society. doi: 10.1098/rstb.2012.0510.
- Hartshorne, J. K. and Germine, L. T. (2015) 'When does cognitive functioning peak? The asynchronous rise and fall of different cognitive abilities across the life span.', *Psychological science*, 26(4), pp. 433–43. doi: 10.1177/0956797614567339.
- Hawkes, C. A. *et al.* (2012) 'Disruption of arterial perivascular drainage of amyloid-β from the brains of mice expressing the human APOE ε4 allele', *PLoS ONE*. Public Library of Science, 7(7). doi: 10.1371/journal.pone.0041636.
- He, X. *et al.* (2017) 'Resveratrol attenuates formaldehyde induced hyperphosphorylation of tau protein and cytotoxicity in N2a cells', *Frontiers in Neuroscience*. Frontiers Media S.A.,

- 10(JAN), p. 598. doi: 10.3389/fnins.2016.00598.
- Heeney, D. D., Gareau, M. G. and Marco, M. L. (2018) 'Intestinal Lactobacillus in health and disease, a driver or just along for the ride?', *Current Opinion in Biotechnology*. Elsevier Ltd, pp. 140–147. doi: 10.1016/j.copbio.2017.08.004.
- Heppner, F. L., Ransohoff, R. M. and Becher, B. (2015) 'Immune attack: the role of inflammation in Alzheimer disease', *Nature Publishing Group*, 16. doi: 10.1038/nrn3880.
- Hiippala, K. *et al.* (2020) 'Novel Odoribacter splanchnicus Strain and Its Outer Membrane Vesicles Exert Immunoregulatory Effects in vitro', *Frontiers in Microbiology*. Frontiers Media S.A., 11, p. 2906. doi: 10.3389/fmicb.2020.575455.
- Hill, D. *et al.* (2018) 'The Lactobacillus casei group: History and health related applications', *Frontiers in Microbiology*. Frontiers Media S.A. doi: 10.3389/fmicb.2018.02107.
- Hill, J. M. *et al.* (2014) 'The gastrointestinal tract microbiome and potential link to Alzheimer's disease', *Frontiers in Neurology*, 5 APR(April), pp. 23–26. doi: 10.3389/fneur.2014.00043.
- Hill, J. M. and Lukiw, W. (2015) 'Microbial-generated amyloids and Alzheimer's disease (AD)', *Frontiers in Aging Neuroscience*, 7(JAN), pp. 1–5. doi: 10.3389/fnagi.2015.00009.
- Hippisley-Cox, J. *et al.* (2007) 'Derivation and validation of QRISK, a new cardiovascular disease risk score for the United Kingdom: prospective open cohort study', *BMJ*, 335(7611), pp. 136–136. doi: 10.1136/bmj.39261.471806.55.
- Hippisley-Cox, J. *et al.* (2008) 'Predicting cardiovascular risk in England and Wales: prospective derivation and validation of QRISK2', *BMJ*, 336(7659), pp. 1475–1482. doi: 10.1136/bmj.39609.449676.25.
- Hippisley-Cox, J., Coupland, C. and Brindle, P. (2017) 'Development and validation of QRISK3 risk prediction algorithms to estimate future risk of cardiovascular disease: Prospective cohort study', *BMJ (Online)*. BMJ Publishing Group, 357. doi: 10.1136/bmj.j2099.
- Ho, L. *et al.* (2018) 'Protective roles of intestinal microbiota derived short chain fatty acids in Alzheimer's disease-type beta-amyloid neuropathological mechanisms', *Expert Review of Neurotherapeutics*. Taylor and Francis Ltd, 18(1), pp. 83–90. doi: 10.1080/14737175.2018.1400909.
- Hoffman, J. D. *et al.* (2019) 'Dietary inulin alters the gut microbiome, enhances systemic metabolism and reduces neuroinflammation in an APOE4 mouse model', *PLoS ONE*, 14(8), pp. 1–22. doi: 10.1371/journal.pone.0221828.
- Holland, B., Welch, A. and Unwin, I. (1991) 'McCance and Widdowson's the composition of foods.', *Cambridge: Royal Society of Chemistry*.
- Honarpisheh, P. *et al.* (2020) 'Dysregulated gut homeostasis observed prior to the accumulation of the brain amyloid- β in Tg2576 mice', *International Journal of Molecular Sciences*, 21(5). doi: 10.3390/ijms21051711.
- Honea, R. A. *et al.* (2009) 'Impact of APOE on the healthy aging brain: A voxel-based MRI and DTI study', *Journal of Alzheimer's Disease*. IOS Press, 18(3), pp. 553–564. doi: 10.3233/JAD-2009-1163.
- Hou, M. *et al.* (2021) 'APOE- ϵ 4 Carrier Status and Gut Microbiota Dysbiosis in Patients With Alzheimer Disease', *Frontiers in Neuroscience*, 15(February), pp. 1–11. doi: 10.3389/fnins.2021.619051.
- Hsieh, S. *et al.* (2013) 'Validation of the Addenbrooke's Cognitive Examination III in frontotemporal dementia and Alzheimer's disease.', *Dementia and geriatric cognitive*

- disorders*. Karger Publishers, 36(3–4), pp. 242–50. doi: 10.1159/000351671.
- Hsieh, S. *et al.* (2015) ‘The Mini-Addenbrooke’s Cognitive Examination: a new assessment tool for dementia.’, *Dementia and geriatric cognitive disorders*, 39(1–2), pp. 1–11. doi: 10.1159/000366040.
- Hu, J. *et al.* (2004) ‘Acidic oligosaccharide sugar chain, a marine-derived acidic oligosaccharide, inhibits the cytotoxicity and aggregation of amyloid beta protein’, *Journal of Pharmacological Sciences*. Japanese Pharmacological Society, 95(2), pp. 248–255. doi: 10.1254/jphs.FPJ04004X.
- Huang, Y. and Mahley, R. W. (2014) ‘Apolipoprotein E: Structure and function in lipid metabolism, neurobiology, and Alzheimer’s diseases’, *Neurobiology of Disease*. Academic Press Inc., pp. 3–12. doi: 10.1016/j.nbd.2014.08.025.
- Hufnagel, D. A., Tükel, Ç. and Chapman, M. R. (2013) ‘Disease to Dirt: The Biology of Microbial Amyloids’, *PLoS Pathogens*. Edited by H. L. True. Public Library of Science, 9(11), p. e1003740. doi: 10.1371/journal.ppat.1003740.
- Hugenholtz, F. and de Vos, W. M. (2018) ‘Mouse models for human intestinal microbiota research: a critical evaluation’, *Cellular and Molecular Life Sciences*. Birkhauser Verlag AG, pp. 149–160. doi: 10.1007/s00018-017-2693-8.
- Human Microbiome Project Consortium, T. (2012) ‘Structure, function and diversity of the healthy human microbiome The Human Microbiome Project Consortium*’, *Nature*, 486. doi: 10.1038/nature11234.
- Huo, R. *et al.* (2017) ‘Microbiota Modulate Anxiety-Like Behavior and Endocrine Abnormalities in Hypothalamic-Pituitary-Adrenal Axis’, *Frontiers in Cellular and Infection Microbiology*, 7. doi: 10.3389/fcimb.2017.00489.
- Huttenhower, C. *et al.* (2012) ‘Structure, function and diversity of the healthy human microbiome’, *Nature*. Nature Publishing Group, 486(7402), pp. 207–214. doi: 10.1038/nature11234.
- Iachini, T. *et al.* (2009) ‘Visuospatial Memory in Healthy Elderly, AD and MCI: A Review’, *Current Aging Science*, 2(1), pp. 43–59. doi: 10.2174/1874609810902010043.
- Iljazovic, A. *et al.* (2021) ‘Perturbation of the gut microbiome by *Prevotella* spp. enhances host susceptibility to mucosal inflammation’, *Mucosal Immunology*. Springer Nature, 14(1), pp. 113–124. doi: 10.1038/s41385-020-0296-4.
- Iqbal, K. *et al.* (2005) ‘Tau pathology in Alzheimer disease and other tauopathies’, *Biochimica et Biophysica Acta - Molecular Basis of Disease*. Elsevier, pp. 198–210. doi: 10.1016/j.bbadis.2004.09.008.
- Irie, F. *et al.* (2008) ‘Enhanced risk for Alzheimer disease in persons with type 2 diabetes and APOE ε4: The cardiovascular health study cognition study’, *Archives of Neurology*. Arch Neurol, 65(1), pp. 89–93. doi: 10.1001/archneurol.2007.29.
- Irvine, M. A. *et al.* (2018) ‘The Cognitive Ageing, Nutrition and Neurogenesis (CANN) trial: Design and progress’, *Alzheimer’s and Dementia: Translational Research and Clinical Interventions*. Elsevier Inc, 4, pp. 591–601. doi: 10.1016/j.trci.2018.08.001.
- Islam, K. B. M. S. *et al.* (2011) ‘Bile acid is a host factor that regulates the composition of the cecal microbiota in rats’, *Gastroenterology*. W.B. Saunders, 141(5), pp. 1773–1781. doi: 10.1053/j.gastro.2011.07.046.
- Itzhaki, R. F. *et al.* (2004) ‘Infiltration of the brain by pathogens causes Alzheimer’s disease’, *Neurobiology of Aging*. Elsevier Inc., 25(5), pp. 619–627. doi: 10.1016/j.neurobiolaging.2003.12.021.
- Jaccard, P. (1912) ‘THE DISTRIBUTION OF THE FLORA IN THE ALPINE ZONE.’,

New Phytologist. John Wiley & Sons, Ltd, 11(2), pp. 37–50. doi: 10.1111/j.1469-8137.1912.tb05611.x.

Jack, C. R. *et al.* (2010) ‘Hypothetical model of dynamic biomarkers of the Alzheimer’s pathological cascade’, *The Lancet Neurology*. Lancet Publishing Group, pp. 119–128. doi: 10.1016/S1474-4422(09)70299-6.

Jacobson, S. C. *et al.* (2011) ‘An fMRI investigation of a novel analogue to the Trail-Making Test’, *Brain and Cognition*. Academic Press, 77(1), pp. 60–70. doi: 10.1016/j.bandc.2011.06.001.

Jak, A. J. *et al.* (2007) ‘Differential cross-sectional and longitudinal impact of APOE genotype on hippocampal volumes in nondemented older adults’, *Dementia and Geriatric Cognitive Disorders*. NIH Public Access, 23(6), pp. 382–389. doi: 10.1159/000101340.

Janak, P. *et al.* (2020) *Metabolic and Bioenergetic Drivers of Neurodegenerative Disease: Neurodegenerative Disease Research and Commonalities with Metabolic Diseases*. Edited by Z. Kruze. Academic Press. Available at: <https://www.elsevier.com/books/metabolic-and-bioenergetic-drivers-of-neurodegenerative-disease-neurodegenerative-disease-research-and-commonalities-with-metabolic-diseases/soderbom/978-0-12-820076-6> (Accessed: 20 April 2021).

Janak, P. and Jenner, P. (2020) *International Review of Neurobiology, Metabolic and Bioenergetic Drivers of Neurodegenerate Disease, Educational Management Administration & Leadership*. doi: 10.1177/174114328501300311.

Janeiro, M. H. *et al.* (2018) ‘Implication of trimethylamine n-oxide (TMAO) in disease: Potential biomarker or new therapeutic target’, *Nutrients*. MDPI AG. doi: 10.3390/nu10101398.

Jang, H. M. *et al.* (2018) ‘Evidence for interplay among antibacterial-induced gut microbiota disturbance, neuro-inflammation, and anxiety in mice’, *Mucosal Immunology*. Nature Publishing Group, 11(5), pp. 1386–1397. doi: 10.1038/s41385-018-0042-3.

Jayananda, S., Gollol-Raju, N. S. and Fadul, N. (2017) ‘Gemella Species Bacteremia and Stroke in an Elderly Patient with Respiratory Tract Infection’, in *Case Reports in Medicine*. Hindawi Limited. doi: 10.1155/2017/1098527.

Jessen, F. *et al.* (2014) ‘AD dementia risk in late MCI, in early MCI, and in subjective memory impairment’, *Alzheimer’s and Dementia*, 10(1), pp. 76–83. doi: 10.1016/j.jalz.2012.09.017.

Ji, Y. *et al.* (2003) ‘Apolipoprotein E isoform-specific regulation of dendritic spine morphology in apolipoprotein E transgenic mice and Alzheimer’s disease patients’, *Neuroscience*, 122(2), pp. 305–315. doi: 10.1016/j.neuroscience.2003.08.007.

Jiang, H. *et al.* (2015) ‘Altered fecal microbiota composition in patients with major depressive disorder’, *Brain, Behavior, and Immunity*. Academic Press Inc., 48, pp. 186–194. doi: 10.1016/j.bbi.2015.03.016.

Jin, Y. Y. *et al.* (2018) ‘Blood ammonia as a possible etiological agent for Alzheimer’s disease’, *Nutrients*. MDPI AG, p. 564. doi: 10.3390/nu10050564.

Joffres, M. *et al.* (2013) ‘Hypertension prevalence, awareness, treatment and control in national surveys from England, the USA and Canada, and correlation with stroke and ischaemic heart disease mortality: A cross-sectional study’, *BMJ Open*. British Medical Journal Publishing Group, 3(8), p. e003423. doi: 10.1136/bmjopen-2013-003423.

Johnson, K. V. A. and Burnet, P. W. J. (2016) ‘Microbiome: Should we diversify from diversity?’, *Gut Microbes*. Taylor and Francis Inc., pp. 455–458. doi: 10.1080/19490976.2016.1241933.

- Johnson, L. A. *et al.* (2017) ‘Apolipoprotein E4 and Insulin Resistance Interact to Impair Cognition and Alter the Epigenome and Metabolome’, *Scientific Reports*. Nature Publishing Group, 7(September 2016), pp. 1–12. doi: 10.1038/srep43701.
- Johnson, R. J. *et al.* (2020) ‘Cerebral Fructose Metabolism as a Potential Mechanism Driving Alzheimer’s Disease’, *Frontiers in Aging Neuroscience*. Frontiers Media S.A., 12, p. 11. doi: 10.3389/fnagi.2020.560865.
- Joie, R. La *et al.* (2016) ‘Neuroimaging Qualitative and quantitative assessment of self-reported cognitive difficulties in nondemented elders: Association with medical help seeking, cognitive deficits, and b-amyloid imaging’, *Alzheimer’s & Dementia: Diagnosis, Assessment & Disease Monitoring*, 5, pp. 23–34. doi: 10.1016/j.dadm.2016.12.005.
- Jones, N. S. and Rebeck, G. W. (2019) ‘The synergistic effects of APOE genotype and obesity on Alzheimer’s Disease risk’, *International Journal of Molecular Sciences*. MDPI AG. doi: 10.3390/ijms20010063.
- Jones, P. B. *et al.* (2011) ‘Apolipoprotein E: Isoform specific differences in tertiary structure and interaction with amyloid- β in human Alzheimer brain’, *PLoS ONE*. PLoS One, 6(1). doi: 10.1371/journal.pone.0014586.
- Jorm, A. F. *et al.* (2007) ‘APOE genotype and cognitive functioning in a large age-stratified population sample’, *Neuropsychology*. Neuropsychology, 21(1), pp. 1–8. doi: 10.1037/0894-4105.21.1.1.
- Jovel, J. *et al.* (2016) ‘Characterization of the gut microbiome using 16S or shotgun metagenomics’, *Frontiers in Microbiology*. Frontiers Media S.A., 7(APR), p. 459. doi: 10.3389/fmicb.2016.00459.
- Just, S. (2017) *Impact of the interplay between bile acids , lipids , intestinal Coriobacteriaceae and diet on host metabolism*, Thesis.
- Kaddurah-Daouk, R. *et al.* (2013) ‘Alterations in metabolic pathways and networks in Alzheimer’s disease’, *Translational Psychiatry*. Nature Publishing Group, 3(4), p. 3. doi: 10.1038/tp.2013.18.
- Kahn, M. S. *et al.* (2012) ‘Prolonged elevation in hippocampal A β and cognitive deficits following repeated endotoxin exposure in the mouse’, *Behavioural Brain Research*, 229(1), pp. 176–184. doi: 10.1016/j.bbr.2012.01.010.
- Kamada, N. *et al.* (2013) ‘Role of the gut microbiota in immunity and inflammatory disease’, *Nature Reviews Immunology*, 13(5), pp. 321–335. doi: 10.1038/nri3430.
- Kametani, F. and Hasegawa, M. (2018) ‘Reconsideration of amyloid hypothesis and tau hypothesis in Alzheimer’s disease’, *Frontiers in Neuroscience*. Frontiers Media S.A. doi: 10.3389/fnins.2018.00025.
- Kanehisa, M. *et al.* (2012) ‘KEGG for integration and interpretation of large-scale molecular data sets’, *Nucleic Acids Research*. Oxford University Press, 40(D1), p. D109. doi: 10.1093/nar/gkr988.
- Kanehisa, M. (2013) ‘Automated interpretation of metabolic capacity from genome and metagenome sequences’, *Quantitative Biology*. Higher Education Press, pp. 192–200. doi: 10.1007/s40484-013-0019-x.
- Kanehisa, M. *et al.* (2017) ‘KEGG: New perspectives on genomes, pathways, diseases and drugs’, *Nucleic Acids Research*. Oxford University Press, 45(D1), pp. D353–D361. doi: 10.1093/nar/gkw1092.
- Kanehisa, M. and Sato, Y. (2020) ‘KEGG Mapper for inferring cellular functions from protein sequences’, *Protein Science*. Blackwell Publishing Ltd, 29(1), pp. 28–35. doi: 10.1002/pro.3711.

- Kanekiyo, T., Xu, H. and Bu, G. (2014) 'ApoE and A β in Alzheimer's disease: Accidental encounters or partners?', *Neuron*, pp. 740–754. doi: 10.1016/j.neuron.2014.01.045.
- Karlsson, F. H. *et al.* (2013) 'Gut metagenome in European women with normal, impaired and diabetic glucose control', *Nature*, 498(7452), pp. 99–103. doi: 10.1038/nature12198.
- Kassinen, A. *et al.* (2007) 'The Fecal Microbiota of Irritable Bowel Syndrome Patients Differs Significantly From That of Healthy Subjects', *Gastroenterology*. W.B. Saunders, 133(1), pp. 24–33. doi: 10.1053/j.gastro.2007.04.005.
- Kawabata, K. *et al.* (2019) 'A high-fructose diet induces epithelial barrier dysfunction and exacerbates the severity of dextran sulfate sodium-induced colitis', *International Journal of Molecular Medicine*. Spandidos Publications, 43(3), pp. 1487–1496. doi: 10.3892/ijmm.2018.4040.
- Kayser, B. D. *et al.* (2019) 'Phosphatidylglycerols are induced by gut dysbiosis and inflammation, and favorably modulate adipose tissue remodeling in obesity', *FASEB Journal*. FASEB, 33(4), pp. 4741–4754. doi: 10.1096/fj.201801897R.
- Kelly, B. *et al.* (2015) 'Power and sample-size estimation for microbiome studies using pairwise distances and PERMANOVA', *Bioinformatics*. Oxford University Press, 31(15), pp. 2461–2468. doi: 10.1093/bioinformatics/btv183.
- Kelly, J. R. *et al.* (2015) 'Breaking down the barriers: The gut microbiome, intestinal permeability and stress-related psychiatric disorders', *Frontiers in Cellular Neuroscience*. Frontiers Media S.A. doi: 10.3389/fncel.2015.00392.
- Kennedy, N. A. *et al.* (2014) 'The impact of different DNA extraction kits and laboratories upon the assessment of human gut microbiota composition by 16S rRNA gene sequencing', *PLoS ONE*. Public Library of Science, 9(2). doi: 10.1371/journal.pone.0088982.
- Kenny, R. A. *et al.* (2013) 'Normative values of cognitive and physical function in older adults: Findings from the Irish Longitudinal Study on Ageing', *Journal of the American Geriatrics Society*. J Am Geriatr Soc, 61(SUPPL2). doi: 10.1111/jgs.12195.
- Khan, M. F. and Wang, H. (2020) 'Environmental Exposures and Autoimmune Diseases: Contribution of Gut Microbiome', *Frontiers in Immunology*. Frontiers Media S.A., p. 3094. doi: 10.3389/fimmu.2019.03094.
- Khan, T. A. *et al.* (2013) 'Apolipoprotein E genotype, cardiovascular biomarkers and risk of stroke: Systematic review and meta-analysis of 14 015 stroke cases and pooled analysis of primary biomarker data from up to 60 883 individuals', *International Journal of Epidemiology*. Int J Epidemiol, 42(2), pp. 475–492. doi: 10.1093/ije/dyt034.
- Kim, D. *et al.* (2017) 'Optimizing methods and dodging pitfalls in microbiome research', *Microbiome*. BioMed Central Ltd. doi: 10.1186/s40168-017-0267-5.
- Kitazawa, M. *et al.* (2005) 'Lipopolysaccharide-induced inflammation exacerbates tau pathology by a cyclin-dependent kinase 5-mediated pathway in a transgenic model of Alzheimer's disease', *Journal of Neuroscience*, 25(39), pp. 8843–8853. doi: 10.1523/JNEUROSCI.2868-05.2005.
- Kivipelto, M. *et al.* (2001) 'Midlife vascular risk factors and Alzheimer's Disease in later life: Longitudinal, population based study', *Bmj*, 322(June), pp. 1447–1451. doi: 10.1136/bmj.322.7300.1447.
- Kizuka, Y., Kitazume, S. and Taniguchi, N. (2017) 'N-glycan and Alzheimer's disease', *Biochimica et Biophysica Acta - General Subjects*. Elsevier B.V., pp. 2447–2454. doi: 10.1016/j.bbagen.2017.04.012.
- Kobayashi, Y. *et al.* (2017) 'Therapeutic potential of Bifidobacterium breve strain A1 for

- preventing cognitive impairment in Alzheimer's disease', *Scientific Reports*. Nature Publishing Group, 7(1). doi: 10.1038/s41598-017-13368-2.
- Koenig, J. E. *et al.* (2011) 'Succession of microbial consortia in the developing infant gut microbiome.', *Proceedings of the National Academy of Sciences of the United States of America*. National Academy of Sciences, (Suppl 1), pp. 4578–85. doi: 10.1073/pnas.1000081107.
- Kok, E. *et al.* (2009) 'Apolipoprotein E-dependent accumulation of alzheimer disease-related lesions begins in middle age', *Annals of Neurology*, 65(6), pp. 650–657. doi: 10.1002/ana.21696.
- Koren-Iton, A. *et al.* (2020) 'Central and peripheral mechanisms in apoE4-driven diabetic pathology', *International Journal of Molecular Sciences*. MDPI AG, 21(4). doi: 10.3390/ijms21041289.
- Kovatcheva-Datchary, P. *et al.* (2015) 'Dietary Fiber-Induced Improvement in Glucose Metabolism Is Associated with Increased Abundance of Prevotella.', *Cell metabolism*, 22(6), pp. 971–82. doi: 10.1016/j.cmet.2015.10.001.
- Kowalski, K. and Mulak, A. (2019) 'Brain-gut-microbiota axis in Alzheimer's disease', *Journal of Neurogastroenterology and Motility*. Korean Society of Neurogastroenterology and Motility, 25(1), pp. 48–60. doi: 10.5056/jnm18087.
- Kroke, A. *et al.* (1999) *Validation of a self-administered food-frequency questionnaire administered in the European Prospective Investigation into Cancer and Nutrition (EPIC) Study: Comparison of energy, protein, and macronutrient intakes estimated with the doubly labeled water*, *American Journal of Clinical Nutrition*. doi: 10.1093/ajcn/70.4.439.
- Kudelka, M. R. *et al.* (2020) 'Intestinal epithelial glycosylation in homeostasis and gut microbiota interactions in IBD', *Nature Reviews Gastroenterology and Hepatology*. Nature Research, pp. 597–617. doi: 10.1038/s41575-020-0331-7.
- Kuring, J. K., Mathias, J. L. and Ward, L. (2018) 'Prevalence of Depression, Anxiety and PTSD in People with Dementia: a Systematic Review and Meta-Analysis', *Neuropsychology Review*. Springer New York LLC, pp. 393–416. doi: 10.1007/s11065-018-9396-2.
- de la Cuesta-Zuluaga, J. *et al.* (2019) 'Age- and Sex-Dependent Patterns of Gut Microbial Diversity in Human Adults', *mSystems*. American Society for Microbiology, 4(4). doi: 10.1128/msystems.00261-19.
- LaDu, M. J. *et al.* (1994) 'Isoform-specific binding of apolipoprotein E to beta-amyloid.', *The Journal of biological chemistry*, 269(38), pp. 23403–6. Available at: <http://www.ncbi.nlm.nih.gov/pubmed/8089103> (Accessed: 17 July 2017).
- Lahoz, C. *et al.* (2001) 'Apolipoprotein E genotype and cardiovascular disease in the Framingham Heart Study', *Atherosclerosis*. Elsevier, 154(3), pp. 529–537. doi: 10.1016/S0021-9150(00)00570-0.
- Lalkhen, A. G. and McCluskey, A. (2008) 'Clinical tests: Sensitivity and specificity', *Continuing Education in Anaesthesia, Critical Care and Pain*. Oxford University Press, 8(6), pp. 221–223. doi: 10.1093/bjaceaccp/mkn041.
- Larsen, J. M. (2017) 'The immune response to Prevotella bacteria in chronic inflammatory disease', *Immunology*. Blackwell Publishing Ltd, pp. 363–374. doi: 10.1111/imm.12760.
- Larsen, N. *et al.* (2010) 'Gut Microbiota in Human Adults with Type 2 Diabetes Differs from Non-Diabetic Adults', *PLoS ONE*. Edited by S. Bereswill. Public Library of Science, 5(2), p. e9085. doi: 10.1371/journal.pone.0009085.
- Lassen, P. S. *et al.* (2017) 'Understanding Alzheimer's disease by global quantification of

- protein phosphorylation and sialylated N-linked glycosylation profiles: A chance for new biomarkers in neuroproteomics?', *Journal of Proteomics*. Elsevier B.V., 161, pp. 11–25. doi: 10.1016/j.jprot.2017.04.003.
- Lavretsky, H. *et al.* (2003) 'Apolipoprotein ϵ 4 Allele Status, Depressive Symptoms, and Cognitive Decline in Middle-Aged and Elderly Persons without Dementia', *American Journal of Geriatric Psychiatry*. Elsevier B.V., 11(6), pp. 667–673. doi: 10.1097/00019442-200311000-00011.
- Lawson, P. A. and Finegold, S. M. (2015) 'Reclassification of *Ruminococcus obeum* as *Blautia obeum* comb. nov', *International Journal of Systematic and Evolutionary Microbiology*, 65(3), pp. 789–793. doi: 10.1099/ijs.0.000015.
- Lee, H. J. *et al.* (2019) 'Suppression of gut dysbiosis by *Bifidobacterium longum* alleviates cognitive decline in 5XFAD transgenic and aged mice', *Scientific Reports*. Springer US, 9(1), pp. 1–12. doi: 10.1038/s41598-019-48342-7.
- Lee, H. J., Hwang, Y. H. and Kim, D. H. (2018) 'Lactobacillus plantarum C29-Fermented Soybean (DW2009) Alleviates Memory Impairment in 5XFAD Transgenic Mice by Regulating Microglia Activation and Gut Microbiota Composition', *Molecular Nutrition and Food Research*, 62(20), pp. 5–11. doi: 10.1002/mnfr.201800359.
- Legendre, P. and Legendre, L. (2012) *Numerical Ecology*. 3rd edn. Elsevier.
- Leite, A. Z. *et al.* (2017) 'Detection of increased plasma interleukin-6 levels and prevalence of *Prevotella copri* and *Bacteroides vulgatus* in the feces of type 2 diabetes patients', *Frontiers in Immunology*. Frontiers Media S.A., 8(SEP). doi: 10.3389/fimmu.2017.01107.
- Lemaître, H. *et al.* (2005) 'No ϵ 4 gene dose effect on hippocampal atrophy in a large MRI database of healthy elderly subjects', *NeuroImage*. Academic Press, 24(4), pp. 1205–1213. doi: 10.1016/j.neuroimage.2004.10.016.
- Lester, A. W. *et al.* (2017) 'The Aging Navigational System', *Neuron*. Cell Press, pp. 1019–1035. doi: 10.1016/j.neuron.2017.06.037.
- Lewis, J. D. *et al.* (2015) 'Inflammation, Antibiotics, and Diet as Environmental Stressors of the Gut Microbiome in Pediatric Crohn's Disease', *Cell Host and Microbe*. Cell Press, 18(4), pp. 489–500. doi: 10.1016/j.chom.2015.09.008.
- Ley, R. E. *et al.* (2005) 'Obesity alters gut microbial ecology', *Proceedings of the National Academy of Sciences*, 102(31), pp. 11070–11075. doi: 10.1073/pnas.0504978102.
- Li, B. *et al.* (2019) 'Mild cognitive impairment has similar alterations as Alzheimer's disease in gut microbiota', *Alzheimer's and Dementia*. Elsevier Inc., 15(10), pp. 1357–1366. doi: 10.1016/j.jalz.2019.07.002.
- Li, F. *et al.* (2012) 'Resveratrol, A Neuroprotective Supplement for Alzheimer's Disease', *Current Pharmaceutical Design*. Bentham Science Publishers Ltd., 18(1), pp. 27–33. doi: 10.2174/138161212798919075.
- Li, F. *et al.* (2019) 'Alteration of the fecal microbiota in North-Eastern Han Chinese population with sporadic Parkinson's disease', *Neuroscience Letters*. Elsevier Ireland Ltd. doi: 10.1016/j.neulet.2019.134297.
- Li, G. *et al.* (2009) 'GABAergic Interneuron Dysfunction Impairs Hippocampal Neurogenesis in Adult Apolipoprotein E4 Knockin Mice', *Cell Stem Cell*, 5(6), pp. 634–645. doi: 10.1016/j.stem.2009.10.015.
- Li, G. *et al.* (2019) 'Uridine/UMP metabolism and their function on the gut in segregated early weaned piglets', *Food and Function*. Royal Society of Chemistry, 10(7), pp. 4081–4089. doi: 10.1039/c9fo00360f.

- Li, H. *et al.* (2013) ‘Molecular mechanisms responsible for the differential effects of ApoE3 and ApoE4 on plasma lipoprotein-cholesterol levels’, *Arteriosclerosis, Thrombosis, and Vascular Biology*. NIH Public Access, 33(4), pp. 687–693. doi: 10.1161/ATVBAHA.112.301193.
- Li, J. *et al.* (2018) ‘Actinomyces and Alimentary Tract Diseases: A Review of Its Biological Functions and Pathology’, *BioMed Research International*. Hindawi Limited. doi: 10.1155/2018/3820215.
- Lin, C. *et al.* (2019) ‘Microbiota-gut-brain axis and toll-like receptors in Alzheimer’s disease’, *Computational and Structural Biotechnology Journal*. Elsevier B.V., pp. 1309–1317. doi: 10.1016/j.csbj.2019.09.008.
- Lind, J. *et al.* (2006) ‘Reduced hippocampal volume in non-demented carriers of the apolipoprotein E ε4: Relation to chronological age and recognition memory’, *Neuroscience Letters*. Elsevier, 396(1), pp. 23–27. doi: 10.1016/j.neulet.2005.11.070.
- Ling, Z. *et al.* (2013) ‘Pyrosequencing analysis of the human microbiota of healthy Chinese undergraduates’, *BMC Genomics*. BioMed Central, 14(1), p. 390. doi: 10.1186/1471-2164-14-390.
- Ling, Z. *et al.* (2021) ‘Structural and Functional Dysbiosis of Fecal Microbiota in Chinese Patients With Alzheimer’s Disease’, *Frontiers in Cell and Developmental Biology*, 8(February), pp. 1–16. doi: 10.3389/fcell.2020.634069.
- Liu, Chia-Chen *et al.* (2013) ‘Apolipoprotein E and Alzheimer disease: risk, mechanisms and therapy.’, *Nature reviews. Neurology*. NIH Public Access, 9(2), pp. 106–18. doi: 10.1038/nrneuro.2012.263.
- Liu, P. *et al.* (2019) ‘Altered microbiomes distinguish Alzheimer’s disease from amnesic mild cognitive impairment and health in a Chinese cohort’, *Brain, Behavior, and Immunity*. Academic Press Inc., 80, pp. 633–643. doi: 10.1016/j.bbi.2019.05.008.
- Liu, R. T. (2017) ‘The microbiome as a novel paradigm in studying stress and mental health’, *American Psychologist*. American Psychological Association Inc., 72(7), pp. 655–667. doi: 10.1037/amp0000058.
- Liu, S. *et al.* (2020) ‘Gut Microbiota and Dysbiosis in Alzheimer’s Disease: Implications for Pathogenesis and Treatment’, *Molecular Neurobiology*. Springer, 57(12), p. 5026. doi: 10.1007/S12035-020-02073-3.
- Liu, Y., White, R. H. and Whitman, W. B. (2010) ‘Methanococci use the diaminopimelate aminotransferase (DapL) pathway for lysine biosynthesis’, *Journal of Bacteriology*. American Society for Microbiology (ASM), 192(13), pp. 3304–3310. doi: 10.1128/JB.00172-10.
- Livingston, G. *et al.* (2020) ‘Dementia prevention, intervention, and care: 2020 report of the Lancet Commission’, *The Lancet*. Lancet Publishing Group, pp. 413–446. doi: 10.1016/S0140-6736(20)30367-6.
- Llinàs-Reglà, J. *et al.* (2017) ‘The Trail Making Test: Association With Other Neuropsychological Measures and Normative Values for Adults Aged 55 Years and Older From a Spanish-Speaking Population-Based Sample’, *Assessment*. SAGE Publications Inc., 24(2), pp. 183–196. doi: 10.1177/1073191115602552.
- Loan, T. *et al.* (2015) ‘How informative is the mouse for human gut microbiota research?’, pp. 1–16. doi: 10.1242/dmm.017400.
- Lohr, K. M. *et al.* (2021) ‘Biotin rescues mitochondrial dysfunction and neurotoxicity in a tauopathy model’, *Proceedings of the National Academy of Sciences of the United States of America*. National Academy of Sciences, 117(52), pp. 33608–33618. doi: 10.1073/PNAS.1922392117.

- Louis, P. and Flint, H. J. (2009) 'Diversity, metabolism and microbial ecology of butyrate-producing bacteria from the human large intestine', *FEMS Microbiology Letters*. Oxford Academic, 294(1), pp. 1–8. doi: 10.1111/j.1574-6968.2009.01514.x.
- Löwe, B. *et al.* (2004) 'Monitoring depression treatment outcomes with the patient health questionnaire-9. Responsiveness and reliability', *Medical Care*, 42(12), pp. 1194–1201. doi: 10.1097/00005650-200412000-00006.
- Lozupone, C. A. *et al.* (2012) 'Diversity, stability and resilience of the human gut microbiota', *Nature*. Nature, pp. 220–230. doi: 10.1038/nature11550.
- Lu, J. *et al.* (2013) 'Formaldehyde induces hyperphosphorylation and polymerization of Tau protein both in vitro and in vivo', *Biochimica et Biophysica Acta - General Subjects*. Elsevier, 1830(8), pp. 4102–4116. doi: 10.1016/j.bbagen.2013.04.028.
- Lyketsos, C. G. *et al.* (2000) 'Mental and behavioral disturbances in dementia: Findings from the cache county study on memory in aging', *American Journal of Psychiatry*, 157(5), pp. 708–714. doi: 10.1176/appi.ajp.157.5.708.
- Lynch, C. (2020) *World Alzheimer Report 2019: Attitudes to dementia, a global survey, Alzheimer's & Dementia*. doi: 10.1002/alz.038255.
- Lynch, J. R. *et al.* (2003) 'APOE genotype and an ApoE-mimetic peptide modify the systemic and central nervous system inflammatory response', *Journal of Biological Chemistry*, 278(49), pp. 48529–48533. doi: 10.1074/jbc.M306923200.
- Ma, D. *et al.* (2018) 'Ketogenic diet enhances neurovascular function with altered gut microbiome in young healthy mice', *Scientific Reports*, 8(1), pp. 1–10. doi: 10.1038/s41598-018-25190-5.
- Mabbott, N. A. (2015) 'A breakdown in communication? Understanding the effects of aging on the human small intestine epithelium.', *Clinical science (London, England : 1979)*. Portland Press Ltd, 129(7), pp. 529–31. doi: 10.1042/CS20150364.
- Machiels, K. *et al.* (2014) 'A decrease of the butyrate-producing species *roseburia hominis* and *faecalibacterium prausnitzii* defines dysbiosis in patients with ulcerative colitis', *Gut*. BMJ Publishing Group, 63(8), pp. 1275–1283. doi: 10.1136/gutjnl-2013-304833.
- Maes, M., Kubera, M. and Leunis, J.-C. (2008) 'The gut-brain barrier in major depression: Intestinal mucosal dysfunction with an increased translocation of LPS from gram negative enterobacteria (leaky gut) plays a role in the inflammatory pathophysiology of depression (PDF Download Available)', *Neuroendocrinology Letter*. Available at: https://www.researchgate.net/publication/5569445_The_gut-brain_barrier_in_major_depression_Intestinal_mucosal_dysfunction_with_an_increased_translocation_of_LPS_from_gram_negative_enterobacteria_leaky_gut_plays_a_role_in_the_inflammatory_pathophysio (Accessed: 10 February 2017).
- De Magistris, L. *et al.* (2010) 'Alterations of the intestinal barrier in patients with autism spectrum disorders and in their first-degree relatives', *Journal of Pediatric Gastroenterology and Nutrition*. J Pediatr Gastroenterol Nutr, 51(4), pp. 418–424. doi: 10.1097/MPG.0b013e3181dcc4a5.
- Mahley, R. W. (2012) 'Apolipoprotein E: from cardiovascular disease to neurodegenerative disorders'. doi: 10.1007/s00109-016-1427-y.
- Mahley, R. W. and Rall, S. C. (2000) 'Apolipoprotein E: Far more than a lipid transport protein', *Annual Review of Genomics and Human Genetics*. Annual Reviews Inc., 1(2000), pp. 507–537. doi: 10.1146/annurev.genom.1.1.507.
- Mahley, R. W., Weisgraber, K. H. and Huang, Y. (2009) 'Apolipoprotein E: Structure determines function, from atherosclerosis to Alzheimer's disease to AIDS', *Journal of Lipid Research*. J Lipid Res. doi: 10.1194/jlr.R800069-JLR200.

- Maldonado Weng, J. *et al.* (2019) ‘Synergistic effects of APOE and sex on the gut microbiome of young EFAD transgenic mice’, *Molecular Neurodegeneration*. *Molecular Neurodegeneration*, 14(1), pp. 1–9. doi: 10.1186/s13024-019-0352-2.
- Malek-Ahmadi, M. *et al.* (2015) ‘Age-and education-adjusted normative data for the Montreal Cognitive Assessment (MoCA) in older adults age 70-99’, *Aging, Neuropsychology, and Cognition*. Routledge, 22(6), pp. 755–761. doi: 10.1080/13825585.2015.1041449.
- Mallick, H. *et al.* (2019) ‘Predictive metabolomic profiling of microbial communities using amplicon or metagenomic sequences’, *Nature Communications*. Nature Publishing Group, 10(1), pp. 1–11. doi: 10.1038/s41467-019-10927-1.
- Mallick, H. *et al.* (2021) ‘Multivariable Association Discovery in Population-scale Metagenomics Studies 3’, *bioRxiv*. Cold Spring Harbor Laboratory, p. 2021.01.20.427420. doi: 10.1101/2021.01.20.427420.
- Malouf, R. and Grimley Evans, J. (2003) ‘Vitamin B6 for cognition’, *Cochrane Database of Systematic Reviews*. Wiley, (4). doi: 10.1002/14651858.cd004393.
- Man, A. L. *et al.* (2015) ‘Age-associated modifications of intestinal permeability and innate immunity in human small intestine’, *Clinical Science*. Portland Press Ltd, 129(7), pp. 515–527. doi: 10.1042/CS20150046.
- Manichanh, C. *et al.* (2006) ‘Reduced diversity of faecal microbiota in Crohn’s disease revealed by a metagenomic approach’, *Gut*. *Gut*, 55(2), pp. 205–211. doi: 10.1136/gut.2005.073817.
- Manton, K. C., Gu, X. L. and Ukraintseva, S. V. (2005) ‘Declining prevalence of dementia in the U.S. elderly population.’, *Advances in gerontology = Uspekhi gerontologii / Rossiiskaia akademiia nauk, Gerontologicheskoe obshchestvo*, 16, pp. 30–37.
- Mapstone, M. *et al.* (2014) ‘Plasma phospholipids identify antecedent memory impairment in older adults’, *Nature Medicine*. Nature Publishing Group, 20(4), pp. 415–418. doi: 10.1038/nm.3466.
- Maqsood, R. and Stone, T. W. (2016) ‘The Gut-Brain Axis, BDNF, NMDA and CNS Disorders’, *Neurochemical Research*. Springer US, 41(11), pp. 2819–2835. doi: 10.1007/s11064-016-2039-1.
- Marashly, E. T. and Bohlega, S. A. (2017) ‘Riboflavin has neuroprotective potential: Focus on Parkinson’s disease and migraine’, *Frontiers in Neurology*. Frontiers Media S.A., p. 1. doi: 10.3389/fneur.2017.00333.
- Mariat, D. *et al.* (2009) ‘The Firmicutes/Bacteroidetes ratio of the human microbiota changes with age’, *BMC Microbiology*, 9(1), p. 123. doi: 10.1186/1471-2180-9-123.
- Marques, F. *et al.* (2013) ‘Blood-brain-barriers in aging and in Alzheimer’s disease.’, *Molecular neurodegeneration*. BioMed Central, 8, p. 38. doi: 10.1186/1750-1326-8-38.
- Marshall, C. R. *et al.* (2017) ‘Impaired interoceptive accuracy in semantic variant primary progressive aphasia’, *Frontiers in Neurology*. Frontiers Media S.A., 8(NOV), p. 610. doi: 10.3389/fneur.2017.00610.
- Masi, A., Mach, R. L. and Mach-Aigner, A. R. (2021) ‘The pentose phosphate pathway in industrially relevant fungi: crucial insights for bioprocessing’, *Applied Microbiology and Biotechnology*. Springer, 105(10), p. 4017. doi: 10.1007/S00253-021-11314-X.
- Mathias Jucker, P. . (2020) *APPPSI | ALZFORUM*. Available at: <https://www.alzforum.org/research-models/appps1> (Accessed: 6 February 2020).
- Mathuranath, P. S. *et al.* (2000) ‘A brief cognitive test battery to differentiate Alzheimer’s disease and frontotemporal dementia.’, *Neurology*, 55(11), pp. 1613–20. doi:

10.1212/01.wnl.0000434309.85312.19.

Mattson, M. P. and Magnus, T. (2006) 'Ageing and neuronal vulnerability.', *Nature reviews. Neuroscience*, 7(4), pp. 278–94. doi: 10.1038/nrn1886.

Maukonen, J., Simões, C. and Saarela, M. (2012) 'The currently used commercial DNA-extraction methods give different results of clostridial and actinobacterial populations derived from human fecal samples', *FEMS Microbiology Ecology*, 79(3), pp. 697–708. doi: 10.1111/j.1574-6941.2011.01257.x.

McCarron, M. O., DeLong, D. and Alberts, M. J. (1999) 'APOE genotype as a risk factor for ischemic cerebrovascular disease: A meta-analysis', *Neurology*. Lippincott Williams and Wilkins, 53(6), pp. 1308–1311. doi: 10.1212/wnl.53.6.1308.

McCarty, M. F. and DiNicolantonio, J. J. (2017) 'Neuroprotective potential of high-dose biotin', *Medical Hypotheses*. Churchill Livingstone, 109, pp. 145–149. doi: 10.1016/j.mehy.2017.10.012.

McDonald, D. *et al.* (2015) 'Towards large-cohort comparative studies to define the factors influencing the gut microbial community structure of ASD patients', *Microbial Ecology in Health & Disease*. Co-Action Publishing, 26(0). doi: 10.3402/mehd.v26.26555.

McGeer, P. L., Rogers, J. and McGeer, E. G. (2016) 'Inflammation, Antiinflammatory Agents, and Alzheimer's Disease: The Last 22 Years', *Journal of Alzheimer's Disease*. IOS Press, pp. 853–857. doi: 10.3233/JAD-160488.

McGeer, P. L., Schulzer, M. and McGeer, E. G. (1996) 'Arthritis and anti-inflammatory agents as possible protective factors for Alzheimer's disease: a review of 17 epidemiologic studies.', *Neurology*, 47(2), pp. 425–32. doi: 10.1212/wnl.47.2.425.

McKain, N. *et al.* (2013) 'Differential recovery of bacterial and archaeal 16S rRNA genes from ruminal digesta in response to glycerol as cryoprotectant', *Journal of Microbiological Methods*. Elsevier, 95(3), pp. 381–383. doi: 10.1016/J.MIMET.2013.10.009.

McKhann, G. M. *et al.* (2011) 'The diagnosis of dementia due to Alzheimer's disease: Recommendations from the National Institute on Aging-Alzheimer's Association workgroups on diagnostic guidelines for Alzheimer's disease', *Alzheimer's and Dementia*. Elsevier Inc., 7(3), pp. 263–269. doi: 10.1016/j.jalz.2011.03.005.

Mclaren, E. (2015) *Office for National Statistics Deaths Registered in England and Wales 2014*, Office for National Statistics. Available at: <https://www.ons.gov.uk/peoplepopulationandcommunity/birthsdeathsandmarriages/deaths/bulletins/deathsregisteredinenglandandwalesseriesdr/2015> (Accessed: 19 July 2017).

McNaughton, B. L. *et al.* (2006) 'Path integration and the neural basis of the "cognitive map"', *Nature Reviews Neuroscience*. Nat Rev Neurosci, pp. 663–678. doi: 10.1038/nrn1932.

McOrist, A. L., Jackson, M. and Bird, A. R. (2002) 'A comparison of five methods for extraction of bacterial DNA from human faecal samples', *Journal of Microbiological Methods*, 50(2), pp. 131–139. doi: 10.1016/S0167-7012(02)00018-0.

Megur, A. *et al.* (2021) 'The microbiota–gut–brain axis and Alzheimer's disease: Neuroinflammation is to blame?', *Nutrients*. MDPI AG, pp. 1–24. doi: 10.3390/nu13010037.

Melrose, R. J. *et al.* (2013) 'Association between cerebral metabolism and Rey-Osterrieth Complex Figure Test performance in Alzheimer's disease', *Journal of Clinical and Experimental Neuropsychology*, 35(3), pp. 246–258. doi: 10.1080/13803395.2012.763113.

Méndez-Salazar, E. O. *et al.* (2018) 'Altered Gut Microbiota and Compositional Changes in Firmicutes and Proteobacteria in Mexican Undernourished and Obese Children',

- Frontiers in Microbiology*. Frontiers Media S.A., 9(OCT), p. 2494. doi: 10.3389/fmicb.2018.02494.
- Mendez, M. F. *et al.* (1990) 'Complex visual disturbances in Alzheimer's disease.', *Neurology*, 40(3 Pt 1), pp. 439–43. doi: 10.1212/wnl.40.3_part_1.439.
- Menni, C. *et al.* (2019) 'Circulating levels of the anti-oxidant indolepropionic acid are associated with higher gut microbiome diversity', *Gut Microbes*. Taylor and Francis Inc., 10(6), pp. 688–695. doi: 10.1080/19490976.2019.1586038.
- Mesulam, -Marsel and Geula, C. (1994) 'Butyrylcholinesterase reactivity differentiates the amyloid plaques of aging from those of dementia', *Annals of Neurology*, 36(5), pp. 722–727. doi: 10.1002/ana.410360506.
- Meyers, J. E. and Meyers, K. R. (1995) *Rey Complex Figure Test and Recognition Trial: Professional Manual*. Psychological Assessment Resources, Odessa.
- Miao, Y. *et al.* (2009) 'Deletion of tau attenuates heat shock-induced injury in cultured cortical neurons', *Journal of Neuroscience Research*. 2009/07/31. doi: 10.1002/jnr.22188 [doi].
- Mielke, M. M. *et al.* (2016) 'Influence of amyloid and APOE on cognitive performance in a late middle-aged cohort', *Alzheimer's and Dementia*. Elsevier Inc., 12(3), pp. 281–291. doi: 10.1016/j.jalz.2015.09.010.
- Miller, T. W. *et al.* (2012) 'Hydrogen sulfide is an endogenous potentiator of T cell activation', *Journal of Biological Chemistry*. American Society for Biochemistry and Molecular Biology, 287(6), pp. 4211–4221. doi: 10.1074/jbc.M111.307819.
- Milner, A. D. and Goodale, M. A. (1992) *Separate visual pathways for perception and action*.
- Minter, M. R. *et al.* (2016) 'Antibiotic-induced perturbations in gut microbial diversity influences neuro-inflammation and amyloidosis in a murine model of Alzheimer's disease', *Scientific Reports*. Nature Publishing Group, 6. doi: 10.1038/srep30028.
- Mioshi, E. *et al.* (2006) 'The Addenbrooke's Cognitive Examination revised (ACE-R): A brief cognitive test battery for dementia screening', *International Journal of Geriatric Psychiatry*, 21(11), pp. 1078–1085. doi: 10.1002/gps.1610.
- Miyake, S. *et al.* (2015) 'Dysbiosis in the gut microbiota of patients with multiple sclerosis, with a striking depletion of species belonging to clostridia XIVa and IV clusters', *PLoS ONE*. Public Library of Science, 10(9). doi: 10.1371/journal.pone.0137429.
- Miyamoto, J. *et al.* (2019) 'Gut microbiota confers host resistance to obesity by metabolizing dietary polyunsaturated fatty acids', *Nature Communications*. Nature Publishing Group, 10(1), pp. 1–15. doi: 10.1038/s41467-019-11978-0.
- Mizutani, S., Yamada, T. and Yachida, S. (2020) 'Significance of the gut microbiome in multistep colorectal carcinogenesis', *Cancer Science*. Blackwell Publishing Ltd, 111(3), pp. 766–773. doi: 10.1111/cas.14298.
- Moffat, S. D. *et al.* (2000) 'Longitudinal change in hippocampal volume as a function of apolipoprotein E genotype', *Neurology*. Lippincott Williams and Wilkins, 55(1), pp. 134–136. doi: 10.1212/WNL.55.1.134.
- Montagne, A. *et al.* (2020) 'APOE4 leads to blood–brain barrier dysfunction predicting cognitive decline', *Nature*. Springer US, 581(7806), pp. 71–76. doi: 10.1038/s41586-020-2247-3.
- Moreno-Indias, I. *et al.* (2021) 'Statistical and Machine Learning Techniques in Human Microbiome Studies: Contemporary Challenges and Solutions', *Frontiers in Microbiology*. Frontiers Media S.A., 12, p. 635781. doi: 10.3389/fmicb.2021.635781.

- Morgan, X. C. *et al.* (2012) ‘Dysfunction of the intestinal microbiome in inflammatory bowel disease and treatment’, *Genome Biology*, 13(9), p. R79. doi: 10.1186/gb-2012-13-9-r79.
- Morris, M. C., Schneider, J. A. and Tangney, C. C. (2006) ‘Thoughts on B-vitamins and dementia’, *Journal of Alzheimer’s Disease*. IOS Press, pp. 429–433. doi: 10.3233/JAD-2006-9409.
- Morris, R. G. M. *et al.* (1982) ‘Place navigation impaired in rats with hippocampal lesions’, *Nature*, 297(5868), pp. 681–683. doi: 10.1038/297681a0.
- Mortamais, M. *et al.* (2018) ‘Anxiety and 10-year risk of incident Dementia-An association shaped by depressive symptoms: Results of the prospective Three-City study’, *Frontiers in Neuroscience*. Frontiers Media S.A., 12(APR). doi: 10.3389/fnins.2018.00248.
- Mosca, A., Leclerc, M. and Hugot, J. P. (2016) ‘Gut microbiota diversity and human diseases: Should we reintroduce key predators in our ecosystem?’, *Frontiers in Microbiology*. Frontiers Media S.A., 7(MAR), p. 455. doi: 10.3389/fmicb.2016.00455.
- Mottawea, W. *et al.* (2016) ‘Altered intestinal microbiota-host mitochondria crosstalk in new onset Crohn’s disease’, *Nature Communications*. Nature Publishing Group, 7. doi: 10.1038/ncomms13419.
- Mulligan, A. A. *et al.* (2014) ‘A new tool for converting food frequency questionnaire data into nutrient and food group values: FETA research methods and availability.’, *BMJ open*. British Medical Journal Publishing Group, 4(3), p. e004503. doi: 10.1136/bmjopen-2013-004503.
- Murman, D. L. (2015) ‘The Impact of Age on Cognition’, *Seminars in Hearing*. Thieme Medical Publishers, Inc., 36(3), pp. 111–121. doi: 10.1055/s-0035-1555115.
- Musa, N. H. *et al.* (2017) ‘Lactobacilli-fermented cow’s milk attenuated lipopolysaccharide-induced neuroinflammation and memory impairment in vitro and in vivo’, *Journal of Dairy Research*. Cambridge University Press, 84(4), pp. 488–495. doi: 10.1017/S0022029917000620.
- De Muth, J. E. (2007) *Basic Statistics and Pharmaceutical Statistical Applications*, *Biometrics*. doi: 10.1111/j.1541-0420.2006.00787_9.x.
- Nagarajan, M. (2018) *Metagenomics: Perspectives, Methods, and Applications - Google Books*, Academic Press, Elsevier. Available at: https://books.google.co.uk/books?id=28gpDwAAQBAJ&pg=PA68&lpg=PA68&dq=log+or+square+root+transformation+metagenomic+data&source=bl&ots=j8z9yBluUn&sig=A CfU3U1_d2cNz5NCp52OvJUEy5sNO70jgA&hl=en&sa=X&ved=2ahUKEwib8JiI8abqA hXTh1wKHYEPCJQQ6AEwCXoECAgQAQ#v=onepag (Accessed: 29 June 2020).
- Nagpal, R. *et al.* (2019) ‘Modified Mediterranean-ketogenic diet modulates gut microbiome and short-chain fatty acids in association with Alzheimer’s disease markers in subjects with mild cognitive impairment’, *EBioMedicine*. The Authors, 47, pp. 529–542. doi: 10.1016/j.ebiom.2019.08.032.
- Nation, D. A. *et al.* (2019) ‘Blood–brain barrier breakdown is an early biomarker of human cognitive dysfunction’, *Nature Medicine*. Nature Publishing Group, 25(2), pp. 270–276. doi: 10.1038/s41591-018-0297-y.
- NICE (2018) *Donepezil, galantamine, rivastigmine and memantine for the treatment of Alzheimer’s disease*. Available at: <https://www.nice.org.uk/guidance/TA217/chapter/1-Guidance> (Accessed: 8 May 2021).
- Nicholson, J. K. *et al.* (2012) ‘Host-Gut Microbiota Metabolic Interactions’, *Science*, 336(6086), pp. 1262–1267. doi: 10.1126/science.1223813.

- Nishino, K. *et al.* (2018) ‘Analysis of endoscopic brush samples identified mucosa-associated dysbiosis in inflammatory bowel disease’, *Journal of Gastroenterology*. Springer Tokyo, 53(1), pp. 95–106. doi: 10.1007/s00535-017-1384-4.
- Noble, J. M. *et al.* (2014) ‘Serum IgG antibody levels to periodontal microbiota are associated with incident Alzheimer disease’, *PLoS ONE*. Public Library of Science, 9(12). doi: 10.1371/journal.pone.0114959.
- O’Donoghue, M. C. *et al.* (2018) ‘APOE genotype and cognition in healthy individuals at risk of Alzheimer’s disease: A review’, *Cortex*. Masson SpA, pp. 103–123. doi: 10.1016/j.cortex.2018.03.025.
- O’Keefe, J. and Nadel, L. (1978) *The hippocampus as a cognitive map*. Oxford University Press.
- Office for National Statistics (2015) *How has life expectancy changed over time?* Available at: <https://www.ons.gov.uk/peoplepopulationandcommunity/birthsdeathsandmarriages/lifeexpectancies/articles/howhaslifeexpectancychangedovertime/2015-09-09> (Accessed: 4 December 2019).
- Office for National Statistics (2019) *Living longer: is age 70 the new age 65? - Office for National Statistics*, Office for National Statistics. Available at: <https://www.ons.gov.uk/peoplepopulationandcommunity/birthsdeathsandmarriages/ageing/articles/livinglongerisage70thenewage65/2019-11-19> (Accessed: 8 May 2021).
- Office for National Statistics (2020) *Leading causes of death, UK*, Office for National Statistics. Available at: <https://www.ons.gov.uk/peoplepopulationandcommunity/healthandsocialcare/causesofdeath/articles/leadingcausesofdeathuk/latest%0Ahttps://www.ons.gov.uk/peoplepopulationandcommunity/healthandsocialcare/causesofdeath/articles/leadingcausesofdeathuk/2001to2018> (Accessed: 8 May 2021).
- Okada, H. *et al.* (2010) ‘The “hygiene hypothesis” for autoimmune and allergic diseases: an update.’, *Clinical and experimental immunology*. Wiley-Blackwell, 160(1), pp. 1–9. doi: 10.1111/j.1365-2249.2010.04139.x.
- Olin, J. and Schneider, L. (2001) ‘Galantamine for Alzheimer’s disease.’, *The Cochrane database of systematic reviews*, (4), p. CD001747. doi: 10.1002/14651858.CD001747.
- Opara, J. A. (2012) ‘Activities of daily living and quality of life in Alzheimer disease.’, *Journal of medicine and life*. Carol Davila - University Press, 5(2), pp. 162–7. Available at: <http://www.ncbi.nlm.nih.gov/pubmed/22802883> (Accessed: 3 November 2017).
- Orešič, M. *et al.* (2011) ‘Metabolome in progression to Alzheimer’s disease’, *Translational Psychiatry*. Transl Psychiatry, 1(12). doi: 10.1038/tp.2011.55.
- Oriach, C. S. *et al.* (2016) ‘Food for thought: The role of nutrition in the microbiota-gut-brain axis’, *Clinical Nutrition Experimental*. Elsevier Ltd, 6, pp. 25–38. doi: 10.1016/j.yclnex.2016.01.003.
- Ott, A. *et al.* (1999) ‘Diabetes mellitus and the risk of dementia: The Rotterdam Study’, *Neurology*, 53(9), pp. 1937–1942. doi: 10.1212/wnl.53.9.1937.
- Palleja, A. *et al.* (2018) ‘Recovery of gut microbiota of healthy adults following antibiotic exposure’, *Nature Microbiology*. Nature Publishing Group. doi: 10.1038/s41564-018-0257-9.
- Palmer, A. M. (1999) *The activity of the pentose phosphate pathway is increased in response to oxidative stress in Alzheimer’s disease*, *J Neural Transm.*
- Panek, M. *et al.* (2018) ‘Methodology challenges in studying human gut microbiota-

- Effects of collection, storage, DNA extraction and next generation sequencing technologies', *Scientific Reports*. Nature Publishing Group, 8(1), pp. 1–13. doi: 10.1038/s41598-018-23296-4.
- Parikh, I. J. *et al.* (2020) 'Murine Gut Microbiome Association With APOE Alleles', *Frontiers in Immunology*, 11(February), pp. 1–11. doi: 10.3389/fimmu.2020.00200.
- Parker, A., Fonseca, S. and Carding, S. R. (2020) 'Gut microbes and metabolites as modulators of blood-brain barrier integrity and brain health', *Gut Microbes*. Taylor & Francis, 11(2), pp. 135–157. doi: 10.1080/19490976.2019.1638722.
- Parker, B. J. *et al.* (2020) 'The Genus *Alistipes*: Gut Bacteria With Emerging Implications to Inflammation, Cancer, and Mental Health', *Frontiers in Immunology*. Frontiers Media S.A. doi: 10.3389/fimmu.2020.00906.
- Paula-Lima, A. C., Brito-Moreira, J. and Ferreira, S. T. (2013) 'Deregulation of excitatory neurotransmission underlying synapse failure in Alzheimer's disease', *Journal of Neurochemistry*, pp. 191–202. doi: 10.1111/jnc.12304.
- Pedersen, H. K. *et al.* (2016) 'Human gut microbes impact host serum metabolome and insulin sensitivity', *Nature*. Nature Research, 535(7612), pp. 376–381. doi: 10.1038/nature18646.
- Peila, R., Rodriguez, B. L. and Launer, L. J. (2002) 'Type 2 diabetes, APOE gene, and the risk for dementia and related pathologies: The Honolulu-Asia Aging Study', *Diabetes*. American Diabetes Association Inc., 51(4), pp. 1256–1262. doi: 10.2337/diabetes.51.4.1256.
- Pelati, O. *et al.* (2011) 'When Rey-Osterrieth's Complex Figure Becomes a Church: Prevalence and Correlates of Graphic Confabulations in Dementia', *Dementia and Geriatric Cognitive Disorders Extra*. S. Karger AG, 1(1), pp. 372–380. doi: 10.1159/000332019.
- Peng, W. *et al.* (2018) 'Association of gut microbiota composition and function with a senescence-accelerated mouse model of Alzheimer's Disease using 16S rRNA gene and metagenomic sequencing analysis', *Aging*. Impact Journals LLC, 10(12), pp. 4054–4065. doi: 10.18632/aging.101693.
- Pistollato, F. *et al.* (2016) 'Role of gut microbiota and nutrients in amyloid formation and pathogenesis of Alzheimer disease', 74(10), pp. 624–634. doi: 10.1093/nutrit/nuw023.
- Pokusaeva, K. *et al.* (2017) 'GABA-producing *Bifidobacterium dentium* modulates visceral sensitivity in the intestine.', *Neurogastroenterology and motility: the official journal of the European Gastrointestinal Motility Society*. Wiley-Blackwell, 29(1). doi: 10.1111/nmo.12904.
- Polimeno, L. *et al.* (2019) 'Gut Microbiota Imbalance is Related to Sporadic Colorectal Neoplasms. A Pilot Study', *Applied Sciences*. MDPI AG, 9(24), p. 5491. doi: 10.3390/app9245491.
- Polvikoski, T. *et al.* (1995) 'Apolipoprotein e, dementia, and cortical deposition of β -amyloid protein', *New England Journal of Medicine*, 333(19), pp. 1242–1248. doi: 10.1056/NEJM199511093331902.
- Popp, J. *et al.* (2009) 'Homocysteine metabolism and cerebrospinal fluid markers for Alzheimer's disease', *Journal of Alzheimer's Disease*. IOS Press, 18(4), pp. 819–828. doi: 10.3233/JAD-2009-1187.
- Porter, V. R. *et al.* (2003) 'Frequency and characteristics of anxiety among patients with Alzheimer's disease and related dementias', *Journal of Neuropsychiatry and Clinical Neurosciences*. American Psychiatric Publishing Inc., 15(2), pp. 180–186. doi: 10.1176/jnp.15.2.180.

- Poulton, B. (1990) 'Relative risks.', *Nursing standard (Royal College of Nursing (Great Britain) : 1987)*. StatPearls Publishing, 4(33), pp. 44–46. doi: 10.7748/ns.4.33.44.s44.
- Prince, M. *et al.* (2014) *Dementia UK: Second Edition*, https://www.alzheimers.org.uk/sites/default/files/migrate/downloads/dementia_uk_update.pdf. doi: 10.1007/s007690000247.
- Public Health England (2017) *Health Profile for England: 2017*, gov.uk. Available at: <https://www.gov.uk/government/publications/health-profile-for-england-2019> (Accessed: 4 December 2019).
- De Punder, K. and Pruimboom, L. (2015) 'Stress induces endotoxemia and low-grade inflammation by increasing barrier permeability', *Frontiers in Immunology*. Frontiers Media S.A., 6(MAY). doi: 10.3389/fimmu.2015.00223.
- Qin, J. *et al.* (2010) 'A human gut microbial gene catalogue established by metagenomic sequencing', *Nature*. Nature Publishing Group, 464(7285), pp. 59–65. doi: 10.1038/nature08821.
- Qin, P. *et al.* (2019) 'Characterization a novel butyric acid-producing bacterium collinsella aerofaciens subsp. Shenzhenensis subsp. nov.', *Microorganisms*. MDPI AG, 7(3). doi: 10.3390/microorganisms7030078.
- Quental, N. B. M., Brucki, S. M. D. and Bueno, O. F. A. (2009) 'Visuospatial function in early Alzheimer's disease: Preliminary study', *Dementia & Neuropsychologia*. FapUNIFESP (SciELO), 3(3), pp. 234–240. doi: 10.1590/s1980-57642009dn30300010.
- Quince, C. *et al.* (2017) 'Shotgun metagenomics, from sampling to sequencing and analysis', *Nature Biotechnology*, 35(9), pp. 833–844. doi: 10.1038/nbt.3935.
- Rackaityte, E. and Lynch, S. V. (2020) 'The human microbiome in the 21st century', *Nature Communications*. Nature Research, pp. 1–3. doi: 10.1038/s41467-020-18983-8.
- Rajilić-Stojanović, M. *et al.* (2011) 'Global and deep molecular analysis of microbiota signatures in fecal samples from patients with irritable bowel syndrome', *Gastroenterology*. W.B. Saunders, 141(5), pp. 1792–1801. doi: 10.1053/j.gastro.2011.07.043.
- Rajilić-Stojanović, M. and de Vos, W. M. (2014) 'The first 1000 cultured species of the human gastrointestinal microbiota', *FEMS Microbiology Reviews*. Blackwell Publishing Ltd, 38(5), pp. 996–1047. doi: 10.1111/1574-6976.12075.
- Ramírez-Pérez, O. *et al.* (2017) 'The role of the gut microbiota in bile acid metabolism', *Annals of Hepatology*. Fundacion Clinica Medica Sur, 16, pp. S21-s26. doi: 10.5604/01.3001.0010.5494.
- Rattanabannakit, C. *et al.* (2016) 'The cognitive change index as a measure of self and informant perception of cognitive decline: Relation to neuropsychological tests', *Journal of Alzheimer's Disease*, 51(4), pp. 1145–1155. doi: 10.3233/JAD-150729.
- Rattiner, L. M., Davis, M. and Ressler, K. J. (2005) 'Brain-Derived Neurotrophic Factor in Amygdala-Dependent Learning', *The Neuroscientist*, 11(4), pp. 323–333. doi: 10.1177/1073858404272255.
- Rawle, M. J. *et al.* (2018) 'Apolipoprotein-E (ApoE) ϵ 4 and cognitive decline over the adult life course', *Translational Psychiatry*. Nature Publishing Group, 8(1), p. 18. doi: 10.1038/s41398-017-0064-8.
- Rawlings, A. M. *et al.* (2014) 'Diabetes in midlife and cognitive change over 20 years: A cohort study', *Annals of Internal Medicine*. American College of Physicians, 161(11), pp. 785–793. doi: 10.7326/M14-0737.
- Readhead, B. *et al.* (2018) 'Multiscale Analysis of Independent Alzheimer's Cohorts Finds

- Disruption of Molecular, Genetic, and Clinical Networks by Human Herpesvirus', *Neuron*. Cell Press, 99(1), pp. 64–82.e7. doi: 10.1016/j.neuron.2018.05.023.
- Reas, E. T. *et al.* (2019) 'Effects of APOE on cognitive aging in community-dwelling older adults', *Neuropsychology*. American Psychological Association Inc., 33(3), pp. 406–416. doi: 10.1037/neu0000501.
- Reiman, E. M. *et al.* (1996) 'Preclinical Evidence of Alzheimer's Disease in Persons Homozygous for the $\epsilon 4$ Allele for Apolipoprotein E', *New England Journal of Medicine*. New England Journal of Medicine (NEJM/MMS), 334(12), pp. 752–758. doi: 10.1056/NEJM199603213341202.
- Reiman, E. M. *et al.* (2009) 'Fibrillar amyloid- burden in cognitively normal people at 3 levels of genetic risk for Alzheimer's disease', *Proceedings of the National Academy of Sciences*, 106(16), pp. 6820–6825. doi: 10.1073/pnas.0900345106.
- Reiman, E. M. *et al.* (2020) 'Exceptionally low likelihood of Alzheimer's dementia in APOE2 homozygotes from a 5,000-person neuropathological study', *Nature Communications*. Nature Research, 11(1), pp. 1–11. doi: 10.1038/s41467-019-14279-8.
- Reisberg, B. *et al.* (2010) 'Outcome over seven years of healthy adults with and without subjective cognitive impairment', *Alzheimer's and Dementia*. No longer published by Elsevier, 6(1), pp. 11–24. doi: 10.1016/j.jalz.2009.10.002.
- Rhee, S. H., Pothoulakis, C. and Mayer, E. A. (2009) 'Principles and clinical implications of the brain-gut-enteric microbiota axis.', *Nature reviews. Gastroenterology & hepatology*. NIH Public Access, 6(5), pp. 306–14. doi: 10.1038/nrgastro.2009.35.
- Richards, M. *et al.* (2019) 'Identifying the lifetime cognitive and socioeconomic antecedents of cognitive state: seven decades of follow-up in a British birth cohort study', *BMJ Open*, 9, p. 24404. doi: 10.1136/bmjopen-2018-024404.
- Rieder, R. *et al.* (2017) 'Microbes and mental health: A review'. doi: 10.1016/j.bbi.2017.01.016.
- Riganti, C. *et al.* (2012) 'The pentose phosphate pathway: An antioxidant defense and a crossroad in tumor cell fate', *Free Radical Biology and Medicine*. Free Radic Biol Med, pp. 421–436. doi: 10.1016/j.freeradbiomed.2012.05.006.
- Roberson, E. D. *et al.* (2007) 'Reducing endogenous tau ameliorates amyloid ??-induced deficits in an Alzheimer's disease mouse model', *Science*, 316(5825), pp. 750–754. doi: 10.1126/science.1141736.
- Roberts, R. O. *et al.* (2014) 'Higher risk of progression to dementia in mild cognitive impairment cases who revert to normal', *Neurology*. Lippincott Williams and Wilkins, 82(4), pp. 317–325. doi: 10.1212/WNL.0000000000000055.
- Rodionov, D. A. *et al.* (2003) 'Regulation of lysine biosynthesis and transport genes in bacteria: Yet another RNA riboswitch?', *Nucleic Acids Research*. Oxford University Press, 31(23), pp. 6748–6757. doi: 10.1093/nar/gkg900.
- Rodrigues, C. M. P. *et al.* (2000) 'Tauroursodeoxycholic acid partially prevents apoptosis induced by 3-nitropropionic acid: Evidence for a mitochondrial pathway independent of the permeability transition', *Journal of Neurochemistry*. J Neurochem, 75(6), pp. 2368–2379. doi: 10.1046/j.1471-4159.2000.0752368.x.
- Rodriguez, F. S. *et al.* (2018) 'APOE $\epsilon 4$ -genotype and lifestyle interaction on cognitive performance: Results of the LIFE-adult-study', *Health Psychology*. American Psychological Association Inc., 37(2), pp. 194–205. doi: 10.1037/hea0000515.
- Rolo, A. P. *et al.* (2000) 'Bile acids affect liver mitochondrial bioenergetics: Possible relevance for cholestasis therapy', *Toxicological Sciences*. Oxford University Press, 57(1),

pp. 177–185. doi: 10.1093/toxsci/57.1.177.

Romano, S. *et al.* (2021) ‘Meta-analysis of the Parkinson’s disease gut microbiome suggests alterations linked to intestinal inflammation’, *npj Parkinson’s Disease*. Nature Research, 7(1), pp. 1–13. doi: 10.1038/s41531-021-00156-z.

Round, J. L. and Mazmanian, S. K. (2009) ‘The gut microbiota shapes intestinal immune responses during health and disease’, *Nature Reviews Immunology*. NIH Public Access, pp. 313–323. doi: 10.1038/nri2515.

Roy, S. *et al.* (2020) ‘Plasma Trimethylamine-N-oxide and impaired glucose regulation: Results from the Oral infections, Glucose Intolerance and Insulin Resistance Study (ORIGINS)’, *PLoS ONE*. Public Library of Science, 15(1). doi: 10.1371/journal.pone.0227482.

Rubey (2010) ‘Could lysine supplementation prevent Alzheimer’s dementia? A novel hypothesis’, *Neuropsychiatric Disease and Treatment*. Dove Medical Press Ltd., 6, p. 707. doi: 10.2147/ndt.s14338.

saji, N. *et al.* (no date) ‘Analysis of the relationship between the gut microbiome and dementia: a cross-sectional study conducted in Japan’. doi: 10.1038/s41598-018-38218-7.

Saji, N. *et al.* (2019) ‘Analysis of the relationship between the gut microbiome and dementia: a cross-sectional study conducted in Japan’, *Scientific Reports*. Nature Publishing Group, 9(1). doi: 10.1038/s41598-018-38218-7.

Saji, N. *et al.* (2020) ‘Relationship between dementia and gut microbiome-associated metabolites: a cross-sectional study in Japan’, *Scientific Reports*. Nature Research, 10(1), pp. 1–11. doi: 10.1038/s41598-020-65196-6.

Salguero, M. *et al.* (2019) ‘Dysbiosis of Gram-negative gut microbiota and the associated serum lipopolysaccharide exacerbates inflammation in type 2 diabetic patients with chronic kidney disease’, *Experimental and Therapeutic Medicine*. Spandidos Publications. doi: 10.3892/etm.2019.7943.

Salimi, S. *et al.* (2018) ‘Can visuospatial measures improve the diagnosis of Alzheimer’s disease?’, *Alzheimer’s and Dementia: Diagnosis, Assessment and Disease Monitoring*. Elsevier Inc, pp. 66–74. doi: 10.1016/j.dadm.2017.10.004.

Salonen, A. *et al.* (2010) ‘Comparative analysis of fecal DNA extraction methods with phylogenetic microarray: effective recovery of bacterial and archaeal DNA using mechanical cell lysis.’, *Journal of microbiological methods*, 81(2), pp. 127–34. doi: 10.1016/j.mimet.2010.02.007.

Salthouse, T. A. (2011) ‘What cognitive abilities are involved in trail-making performance?’, *Intelligence*. NIH Public Access, 39(4), pp. 222–232. doi: 10.1016/j.intell.2011.03.001.

Salvadori, E. *et al.* (2019) ‘Qualitative Evaluation of the Immediate Copy of the Rey-Osterrieth Complex Figure: Comparison Between Vascular and Degenerative MCI Patients’, *Archives of clinical neuropsychology : the official journal of the National Academy of Neuropsychologists*. NLM (Medline), 34(1), pp. 14–23. doi: 10.1093/arclin/acy010.

Sanada, K. *et al.* (2020) ‘Gut microbiota and major depressive disorder: A systematic review and meta-analysis’, *Journal of Affective Disorders*. Elsevier B.V., pp. 1–13. doi: 10.1016/j.jad.2020.01.102.

Santos, C. Y. *et al.* (2017) ‘Pathophysiologic relationship between Alzheimer’s disease, cerebrovascular disease, and cardiovascular risk: A review and synthesis’, *Alzheimer’s & Dementia: Diagnosis, Assessment & Disease Monitoring*. Elsevier, 7, pp. 69–87. doi: 10.1016/j.dadm.2017.01.005.

- Satizabal, C. L. *et al.* (2016) 'Incidence of dementia over three decades in the Framingham heart study', *New England Journal of Medicine*. Massachusetts Medical Society, 374(6), pp. 523–532. doi: 10.1056/NEJMoa1504327.
- Sato, N. *et al.* (1999) 'In vitro and in vivo effects of exogenous nucleotides on the proliferation and maturation of intestinal epithelial cells', *Journal of Nutritional Science and Vitaminology*. Center for Academic Publications Japan, 45(1), pp. 107–118. doi: 10.3177/jnsv.45.107.
- Sawda, C., Moussa, C. and Turner, R. S. (2017) 'Resveratrol for alzheimer's disease', *Annals of the New York Academy of Sciences*. Blackwell Publishing Inc., pp. 142–149. doi: 10.1111/nyas.13431.
- Saxena, S. and Caroni, P. (2011) 'Selective Neuronal Vulnerability in Neurodegenerative Diseases: from Stressor Thresholds to Degeneration', *Neuron*, 71(1), pp. 35–48. doi: 10.1016/j.neuron.2011.06.031.
- Schedin-Weiss, S., Winblad, B. and Tjernberg, L. O. (2014) 'The role of protein glycosylation in Alzheimer disease', *FEBS Journal*. FEBS J, 281(1), pp. 46–62. doi: 10.1111/febs.12590.
- Schmechel, D. E. *et al.* (1993) 'Increased amyloid β -peptide deposition in cerebral cortex as a consequence of apolipoprotein E genotype in late-onset Alzheimer disease', *Proceedings of the National Academy of Sciences of the United States of America*. National Academy of Sciences, 90(20), pp. 9649–9653. doi: 10.1073/pnas.90.20.9649.
- Schmidt-Wilcke, T. *et al.* (2018) 'GABA—from Inhibition to Cognition: Emerging Concepts', *Neuroscientist*. SAGE Publications Inc., pp. 501–515. doi: 10.1177/1073858417734530.
- Scholey, A. (2017) 'Nutrients for neurocognition in health and disease: measures, methodologies and mechanisms'. doi: 10.1017/S0029665117004025.
- Schultz, I. and Keita, A. V. (2020) 'The Intestinal Barrier and Current Techniques for the Assessment of Gut Permeability', *Cells*. NLM (Medline). doi: 10.3390/cells9081909.
- Schwartz, A. *et al.* (2018) 'Fecal markers of intestinal inflammation and intestinal permeability are elevated in Parkinson's disease', *Parkinsonism and Related Disorders*. Elsevier Ltd, 50, pp. 104–107. doi: 10.1016/j.parkreldis.2018.02.022.
- Scott, K. A. *et al.* (2017) 'Revisiting Metchnikoff: Age-related alterations in microbiota-gut-brain axis in the mouse', *Brain, Behavior, and Immunity*. Academic Press Inc., 65, pp. 20–32. doi: 10.1016/j.bbi.2017.02.004.
- Segata, N. *et al.* (2011) 'Metagenomic biomarker discovery and explanation', *Genome Biology*. BioMed Central Ltd, 12(6), p. R60. doi: 10.1186/gb-2011-12-6-r60.
- Segata, N. *et al.* (2012) 'Metagenomic microbial community profiling using unique clade-specific marker genes', *Nature Methods*. NIH Public Access, 9(8), pp. 811–814. doi: 10.1038/nmeth.2066.
- Seiler, N. (2002) 'Ammonia and Alzheimer's disease', *Neurochemistry International*. Pergamon, pp. 189–207. doi: 10.1016/S0197-0186(02)00041-4.
- Selkoe, D. J. and Hardy, J. (2016) 'The amyloid hypothesis of Alzheimer's disease at 25 years', *EMBO Molecular Medicine*, 8(6), pp. 595–608. doi: 10.15252/emmm.201606210.
- Senizza, A. *et al.* (2020) 'Linoleic acid induces metabolic stress in the intestinal microorganism *Bifidobacterium breve* DSM 20213', *Scientific Reports*. Nature Research, 10(1), pp. 1–10. doi: 10.1038/s41598-020-62897-w.
- Serino, S. *et al.* (2015) 'Detecting early egocentric and allocentric impairments deficits in

- Alzheimer's disease: An experimental study with virtual reality', *Frontiers in Aging Neuroscience*. Frontiers Media S.A., 7(MAY). doi: 10.3389/fnagi.2015.00088.
- Serrano-Pozo, A. *et al.* (2011) 'Neuropathological alterations in Alzheimer disease.', *Cold Spring Harbor perspectives in medicine*. Cold Spring Harbor Laboratory Press, 1(1), p. a006189. doi: 10.1101/cshperspect.a006189.
- Shannon, C. E. and Weaver, W. (1949) 'On the mathematical theory of communication', *University of Illinois Press*. doi: 10.4992/jjpsy.25.110.
- Shapiro, H. *et al.* (2014) 'The cross talk between microbiota and the immune system: metabolites take center stage This review comes from a themed issue on Effects of endogenous immune stimulants', *Current Opinion in Immunology*, 30, pp. 54–62. doi: 10.1016/j.coi.2014.07.003.
- Sharma, P. *et al.* (2019) 'Comprehensive review of mechanisms of pathogenesis involved in Alzheimer's disease and potential therapeutic strategies', *Progress in Neurobiology*. Elsevier, 174(December 2018), pp. 53–89. doi: 10.1016/j.pneurobio.2018.12.006.
- Sheng, J. G. *et al.* (2003) 'Lipopolysaccharide-induced-neuroinflammation increases intracellular accumulation of amyloid precursor protein and amyloid β peptide in APPswe transgenic mice', *Neurobiology of Disease*. Academic Press Inc., 14(1), pp. 133–145. doi: 10.1016/S0969-9961(03)00069-X.
- Sherwin, E. *et al.* (2016) 'May the Force Be With You: The Light and Dark Sides of the Microbiota???Gut???Brain Axis in Neuropsychiatry', *CNS Drugs*. Springer International Publishing, 30(11), pp. 1019–1041. doi: 10.1007/s40263-016-0370-3.
- Shimada, A. and Hasegawa-Ishii, S. (2011) 'Senescence-accelerated Mice (SAMs) as a Model for Brain Aging and Immunosenescence.', *Aging and disease*. JKL International LLC, 2(5), pp. 414–35. Available at: <http://www.ncbi.nlm.nih.gov/pubmed/22396891> (Accessed: 6 February 2021).
- Shimada, E. *et al.* (2012) 'Lipoproteins of *Actinomyces viscosus* induce inflammatory responses through TLR2 in human gingival epithelial cells and macrophages', *Microbes and Infection*. Elsevier Masson, 14(11), pp. 916–921. doi: 10.1016/j.micinf.2012.04.015.
- Shin, N. R., Whon, T. W. and Bae, J. W. (2015) 'Proteobacteria: Microbial signature of dysbiosis in gut microbiota', *Trends in Biotechnology*. Elsevier Ltd, pp. 496–503. doi: 10.1016/j.tibtech.2015.06.011.
- Siddiqui, H. *et al.* (2019) 'High Throughput Sequencing Detect Gingivitis And Periodontal Oral Bacteria In Alzheimer's Disease Autopsy Brains', *Neuro Research*, 1(1), p. 3. doi: 10.35702/nrj.10003.
- Simpson, E. H. (1949) 'Measurement of diversity', *Nature*. Nature Publishing Group, 163(4148), p. 688. doi: 10.1038/163688a0.
- Singer, G. A. C. *et al.* (2019) 'Comprehensive biodiversity analysis via ultra-deep patterned flow cell technology: a case study of eDNA metabarcoding seawater', *Scientific Reports*. Nature Publishing Group, 9(1), pp. 1–12. doi: 10.1038/s41598-019-42455-9.
- Singh, P. P., Singh, M. and Mastana, S. S. (2006) 'APOE distribution in world populations with new data from India and the UK', *Annals of Human Biology*, 33(3), pp. 279–308. doi: 10.1080/03014460600594513.
- Slyepchenko, A. *et al.* (2017) 'Gut Microbiota, Bacterial Translocation, and Interactions with Diet: Pathophysiological Links between Major Depressive Disorder and Non-Communicable Medical Comorbidities', *Psychotherapy and Psychosomatics*, 86(1), pp. 31–46. doi: 10.1159/000448957.
- Small, B. J. *et al.* (2004) 'Apolipoprotein E and cognitive performance: A meta-analysis',

- Psychology and Aging*, 19(4), pp. 592–600. doi: 10.1037/0882-7974.19.4.592.
- Smith, S. M. *et al.* (2004) ‘Advances in functional and structural MR image analysis and implementation as FSL’, in *NeuroImage*. Neuroimage. doi: 10.1016/j.neuroimage.2004.07.051.
- Snowden, S. G. *et al.* (2017) ‘Association between fatty acid metabolism in the brain and Alzheimer disease neuropathology and cognitive performance: A nontargeted metabolomic study’, *PLoS Medicine*. Public Library of Science, 14(3). doi: 10.1371/journal.pmed.1002266.
- So, M. *et al.* (2018) ‘Addenbrooke’s Cognitive Examination III: Psychometric Characteristics and Relations to Functional Ability in Dementia’, *Journal of the International Neuropsychological Society*. Cambridge University Press, 24(8), pp. 854–863. doi: 10.1017/S1355617718000541.
- Sochocka, M. *et al.* (2019) ‘The Gut Microbiome Alterations and Inflammation-Driven Pathogenesis of Alzheimer’s Disease—a Critical Review’, *Molecular Neurobiology*. Humana Press Inc., pp. 1841–1851. doi: 10.1007/s12035-018-1188-4.
- Van Soest, A. P. M. *et al.* (2020) ‘Associations between Pro-and Anti-Inflammatory Gastro-Intestinal Microbiota, Diet, and Cognitive Functioning in Dutch Healthy Older Adults: The NU-AGE Study’, *Nutrients*, 12, p. 3471. doi: 10.3390/nu12113471.
- Solas, M., Puerta, E. and Ramirez, M. (2015) ‘Treatment Options in Alzheimer’s Disease: The GABA Story’, *Current Pharmaceutical Design*. Bentham Science Publishers Ltd., 21(34), pp. 4960–4971. doi: 10.2174/1381612821666150914121149.
- Song, S. J. *et al.* (2016) ‘Preservation Methods Differ in Fecal Microbiome Stability, Affecting Suitability for Field Studies’, *mSystems*. American Society for Microbiology, 1(3). doi: 10.1128/msystems.00021-16.
- Sonnenburg, J. L. and Bäckhed, F. (2016) ‘Diet-microbiota interactions as moderators of human metabolism’, *Nature*. Nature Publishing Group, pp. 56–64. doi: 10.1038/nature18846.
- Sørensen, T. (1948) ‘A method of establishing groups of equal amplitude in plant sociology based on similarity’, *Kong. Dansk. vidensk. Selsk. Biol. Skr.* KÅ, benhavn: I kommission hos E. Munksgaard, 5(4), pp. 1–34.
- Spiers, H. J. and Barry, C. (2015) ‘Neural systems supporting navigation’, *Current Opinion in Behavioral Sciences*. Elsevier Ltd, pp. 47–55. doi: 10.1016/j.cobeha.2014.08.005.
- Spitzer RL *et al.* (2006) ‘A Brief Measure for Assessing Generalized Anxiety Disorder.’, *Archives of Internal Medicine*, 166(10), pp. 1092–1097. doi: 10.1001/archinte.166.10.1092.
- Spreen, O. and Strauss, E. (1998) *A compendium of neuropsychological tests: Administration, norms and commentary (2nd ed.)*. New York: Oxford University Press.
- Stincone, A. *et al.* (2015) ‘The return of metabolism: biochemistry and physiology of the pentose phosphate pathway’, *Biological Reviews*. Blackwell Publishing Ltd, 90(3), pp. 927–963. doi: 10.1111/brv.12140.
- Stinson, L. F., Keelan, J. A. and Payne, M. S. (2019) ‘Identification and removal of contaminating microbial DNA from PCR reagents: impact on low-biomass microbiome analyses’, *Letters in Applied Microbiology*. Blackwell Publishing Ltd, 68(1), pp. 2–8. doi: 10.1111/lam.13091.
- Stoll, M. L. (2020) ‘Genetics, Prevotella, and the pathogenesis of rheumatoid arthritis’, *The Lancet Rheumatology*. Lancet Publishing Group, pp. e375–e376. doi: 10.1016/S2665-

9913(20)30090-4.

Strandwitz, P. (2018) 'Neurotransmitter modulation by the gut microbiota', *Brain Research*. Elsevier B.V., pp. 128–133. doi: 10.1016/j.brainres.2018.03.015.

Sudo, N. *et al.* (2004) 'Postnatal microbial colonization programs the hypothalamic-pituitary-adrenal system for stress response in mice', *Journal of Physiology*, 558(1), pp. 263–275. doi: 10.1113/jphysiol.2004.063388.

Sullivan, Å., Edlund, C. and Nord, C. E. (2001) 'Effect of antimicrobial agents on the ecological balance of human microflora', *The Lancet Infectious Diseases*, 1(2), pp. 101–114. doi: 10.1016/S1473-3099(01)00066-4.

Sy, M. *et al.* (2011) 'Inflammation induced by infection potentiates tau pathological features in transgenic mice', *American Journal of Pathology*. Elsevier Inc., 178(6), pp. 2811–2822. doi: 10.1016/j.ajpath.2011.02.012.

Syed, Y. Y. (2020) 'Sodium Oligomannate: First Approval', *Drugs*. Springer International Publishing, 80(4), pp. 441–444. doi: 10.1007/s40265-020-01268-1.

Takashima, A. *et al.* (1993) 'tau Protein kinase I is essential for amyloid β -protein-induced neurotoxicity', *Proceedings of the National Academy of Sciences of the United States of America*, 90(16), pp. 7789–7793. doi: 10.1073/pnas.90.16.7789.

Takeda, S., Sato, N. and Morishita, R. (2014) 'Systemic inflammation, blood-brain barrier vulnerability and cognitive/non-cognitive symptoms in Alzheimer disease: relevance to pathogenesis and therapy', *Frontiers in Aging Neuroscience*. Frontiers, 6, p. 171. doi: 10.3389/fnagi.2014.00171.

Tamanai-Shacoori, Z. *et al.* (2017) 'Roseburia spp.: A marker of health?', *Future Microbiology*. Future Medicine Ltd., pp. 157–170. doi: 10.2217/fmb-2016-0130.

Tang, D. *et al.* (2018) 'Ansamycins with Antiproliferative and Antineuroinflammatory Activity from Moss-Soil-Derived *Streptomyces cacaoi* subsp. *asoensis* H2S5', *Journal of Natural Products*. American Chemical Society, 81(9), pp. 1984–1991. doi: 10.1021/acs.jnatprod.8b00203.

Tao, L. *et al.* (2019) 'Dietary Intake of Riboflavin and Unsaturated Fatty Acid Can Improve the Multi-Domain Cognitive Function in Middle-Aged and Elderly Populations: A 2-Year Prospective Cohort Study', *Frontiers in Aging Neuroscience*. Frontiers Media S.A., 11(AUG), p. 226. doi: 10.3389/fnagi.2019.00226.

Taylor, E. M. (1995) *Psychological appraisal of children with cerebral deficits*. MA: Harvard University Press, Cambridge.

Thevaranjan, N. *et al.* (2017) 'Age-Associated Microbial Dysbiosis Promotes Intestinal Permeability, Systemic Inflammation, and Macrophage Dysfunction', *Cell Host and Microbe*. Cell Press, 21(4), pp. 455–466.e4. doi: 10.1016/j.chom.2017.03.002.

Thomas, A. M. and Segata, N. (2019) 'Multiple levels of the unknown in microbiome research', *BMC Biology*. BioMed Central Ltd., p. 48. doi: 10.1186/s12915-019-0667-z.

Tohgi, H. *et al.* (1996) 'Cerebrospinal fluid acetylcholine and choline in vascular dementia of Binswanger and multiple small infarct types as compared with Alzheimer-type dementia', *Journal of Neural Transmission*, 103(10), pp. 1211–1220. doi: 10.1007/BF01271206.

Tohgi, H. *et al.* (1997) 'Reduced size of right hippocampus in 39- to 80-year-old normal subjects carrying the apolipoprotein E ϵ 4 allele', *Neuroscience Letters*. Elsevier, 236(1), pp. 21–24. doi: 10.1016/S0304-3940(97)00743-X.

Tombaugh, T. N. (2004) 'Trail Making Test A and B: Normative data stratified by age and education', *Archives of Clinical Neuropsychology*, 19(2), pp. 203–214. doi:

10.1016/S0887-6177(03)00039-8.

Tran, L. and Greenwood-Van Meerveld, B. (2013) 'Age-associated remodeling of the intestinal epithelial barrier.', *The journals of gerontology. Series A, Biological sciences and medical sciences*. Oxford University Press, 68(9), pp. 1045–56. doi: 10.1093/gerona/glt106.

Tran, T. T. T. *et al.* (2019) 'APOE genotype influences the gut microbiome structure and function in humans and mice: relevance for Alzheimer's disease pathophysiology', *FASEB Journal*, 33(7), pp. 8221–8231. doi: 10.1096/fj.201900071R.

Tremblay, M. P. *et al.* (2015) 'Normative data for the rey-osterrieth and the taylor complex figure tests in Quebec-French people', *Archives of Clinical Neuropsychology*. Oxford University Press, 30(1), pp. 78–87. doi: 10.1093/arclin/acu069.

Tu, S. *et al.* (2015) 'Lost in spatial translation - A novel tool to objectively assess spatial disorientation in Alzheimer's disease and frontotemporal dementia', *Cortex*. Masson SpA, 67, pp. 83–94. doi: 10.1016/j.cortex.2015.03.016.

Tu, S. *et al.* (2017) 'Egocentric versus Allocentric Spatial Memory in Behavioral Variant Frontotemporal Dementia and Alzheimer's Disease.', *Journal of Alzheimer's disease : JAD*, 59(3), pp. 883–892. doi: 10.3233/JAD-160592.

Tulpule, K. and Dringen, R. (2013) 'Formaldehyde in brain: an overlooked player in neurodegeneration?', *Journal of Neurochemistry*. John Wiley & Sons, Ltd, 127(1), pp. 7–21. doi: 10.1111/jnc.12356.

Turnbaugh, P. J. *et al.* (2009) 'A core gut microbiome in obese and lean twins', *Nature*, 457(7228), pp. 480–484. doi: 10.1038/nature07540.

Turroni, F. *et al.* (2014) 'Molecular dialogue between the human gut microbiota and the host: A Lactobacillus and Bifidobacterium perspective', *Cellular and Molecular Life Sciences*. Springer, pp. 183–203. doi: 10.1007/s00018-013-1318-0.

Ubeda, C. *et al.* (2013) 'Intestinal microbiota containing *Barnesiella* species cures vancomycin-resistant *Enterococcus faecium* colonization', *Infection and Immunity*. Infect Immun, 81(3), pp. 965–973. doi: 10.1128/IAI.01197-12.

UK ACE-III and M-ACE Administration and Scoring Guide (2014).

Underwood, M. A. *et al.* (2015) 'Bifidobacterium longum subspecies infantis: Champion colonizer of the infant gut', *Pediatric Research*. Nature Publishing Group, pp. 229–235. doi: 10.1038/pr.2014.156.

Vacca, M. *et al.* (2020) 'The controversial role of human gut lachnospiraceae', *Microorganisms*. MDPI AG. doi: 10.3390/microorganisms8040573.

Vandini, E. *et al.* (2019) 'Mechanisms of hydrogen sulfide against the progression of severe Alzheimer's disease in transgenic mice at different ages', *Pharmacology*. S. Karger AG, 103(1–2), pp. 93–100. doi: 10.1159/000494113.

Varatharaj, A. *et al.* (2019) 'Blood–brain barrier permeability measured using dynamic contrast-enhanced magnetic resonance imaging: a validation study', *Journal of Physiology*. Blackwell Publishing Ltd, 597(3), pp. 699–709. doi: 10.1113/JP276887.

Vardanyan, R. and Hruby, V. (2016) 'Antibiotics', in *Synthesis of Best-Seller Drugs*. Elsevier, pp. 573–643. doi: 10.1016/B978-0-12-411492-0.00030-4.

Verghese, P. B., Castellano, J. M. and Holtzman, D. M. (2011) 'Apolipoprotein E in Alzheimer's disease and other neurological disorders.', *The Lancet. Neurology*. NIH Public Access, 10(3), pp. 241–52. doi: 10.1016/S1474-4422(10)70325-2.

Vitetta, L., Llewellyn, H. and Oldfield, D. (2019) 'Gut dysbiosis and the intestinal

- microbiome: *Streptococcus thermophilus* a key probiotic for reducing uremia', *Microorganisms*. MDPI AG. doi: 10.3390/microorganisms7080228.
- Vogel, T. *et al.* (2009) 'Homocysteine, vitamin B₁₂, folate and cognitive functions: a systematic and critical review of the literature', *International Journal of Clinical Practice*. John Wiley & Sons, Ltd, 63(7), pp. 1061–1067. doi: 10.1111/j.1742-1241.2009.02026.x.
- Vogt, N. M. *et al.* (2017) 'Gut microbiome alterations in Alzheimer's disease', *Scientific Reports*. Nature Publishing Group, 7(1). doi: 10.1038/s41598-017-13601-y.
- Vogt, N. M. *et al.* (2018) 'The gut microbiota-derived metabolite trimethylamine N-oxide is elevated in Alzheimer's disease', *Alzheimer's Research & Therapy*. BioMed Central Ltd., 10(1), p. 124. doi: 10.1186/s13195-018-0451-2.
- Volynets, V. *et al.* (2017) 'Intestinal barrier function and the gut microbiome are differentially affected in mice fed a western-style diet or drinking water supplemented with fructose', *Journal of Nutrition*. American Society for Nutrition, 147(5), pp. 770–780. doi: 10.3945/jn.116.242859.
- Vujkovic-Cvijin, I. *et al.* (2020) 'Host variables confound gut microbiota studies of human disease', *Nature*. Nature Research, 587(7834), pp. 448–454. doi: 10.1038/s41586-020-2881-9.
- Wagner, B. D. *et al.* (2018) 'On the Use of Diversity Measures in Longitudinal Sequencing Studies of Microbial Communities', *Frontiers in Microbiology*. Frontiers Media S.A., 9(MAY), p. 1037. doi: 10.3389/fmicb.2018.01037.
- Walker, A. W. *et al.* (2011) 'Dominant and diet-responsive groups of bacteria within the human colonic microbiota', *The ISME Journal*, 5(2), pp. 220–230. doi: 10.1038/ismej.2010.118.
- Wallace, M. B. *et al.* (2014) 'Imaging the leaky gut', *Gastroenterology*. W.B. Saunders, pp. 952–954. doi: 10.1053/j.gastro.2014.09.027.
- Wang, S. *et al.* (2007) 'A marine-derived acidic oligosaccharide sugar chain specifically inhibits neuronal cell injury mediated by β -amyloid-induced astrocyte activation in vitro', *Neurological Research*. Taylor & Francis, 29(1), pp. 96–102. doi: 10.1179/174313206X152483.
- Wang, T. *et al.* (2015) 'Lactobacillus fermentum NS9 restores the antibiotic induced physiological and psychological abnormalities in rats', *Beneficial Microbes*. Wageningen Academic Publishers, 6(5), pp. 707–717. doi: 10.3920/BM2014.0177.
- Wang, W. *et al.* (2014) 'Increased proportions of Bifidobacterium and the Lactobacillus group and loss of butyrate-producing bacteria in inflammatory bowel disease', *Journal of Clinical Microbiology*. American Society for Microbiology Journals, 52(2), pp. 398–406. doi: 10.1128/JCM.01500-13.
- Wang, X. *et al.* (2019) 'Sodium oligomannate therapeutically remodels gut microbiota and suppresses gut bacterial amino acids-shaped neuroinflammation to inhibit Alzheimer's disease progression', *Cell Research*. Springer US, 29(10), pp. 787–803. doi: 10.1038/s41422-019-0216-x.
- Wang, Z. *et al.* (2006) 'The role of bifidobacteria in gut barrier function after thermal injury in rats', *Journal of Trauma - Injury, Infection and Critical Care*, 61(3), pp. 650–657. doi: 10.1097/01.ta.0000196574.70614.27.
- Ward, A. *et al.* (2013) 'Rate of Conversion from Prodromal Alzheimer's Disease to Alzheimer's Dementia: A Systematic Review of the Literature', *Dementia and Geriatric Cognitive Disorders Extra*. S. Karger AG, 3(1), pp. 320–332. doi: 10.1159/000354370.
- Wear, H. J. *et al.* (2008) 'The Cambridge Behavioural Inventory revised', *Dementia &*

- Neuropsychologia*, 2(2), pp. 102–107. Available at: <http://www.scielo.br/pdf/dn/v2n2/1980-5764-dn-2-02-00102.pdf> (Accessed: 25 April 2017).
- Wedderburn, C. *et al.* (2007) ‘The utility of the Cambridge Behavioural Inventory in neurodegenerative disease’. doi: 10.1136/jnnp.2007.122028.
- Weete, J. D. (1980) ‘Acylglycerols and Related Lipids’, in *Lipid Biochemistry of Fungi and Other Organisms*. Springer US, pp. 130–156. doi: 10.1007/978-1-4757-0064-0_5.
- Weniger, G. *et al.* (2011) ‘Egocentric and allocentric memory as assessed by virtual reality in individuals with amnesic mild cognitive impairment.’, *Neuropsychologia*, 49(3), pp. 518–27. doi: 10.1016/j.neuropsychologia.2010.12.031.
- Whitehair, D. C. *et al.* (2010) ‘Influence of apolipoprotein e ϵ 4 on rates of cognitive and functional decline in mild cognitive impairment’, *Alzheimer’s and Dementia*. NIH Public Access, 6(5), pp. 412–419. doi: 10.1016/j.jalz.2009.12.003.
- Whitman, W. B., Coleman, D. C. and Wiebe, W. J. (1998) ‘Perspective Prokaryotes: The unseen majority’, 95, pp. 6578–6583. Available at: <http://www.pnas.org/content/95/12/6578.full.pdf> (Accessed: 27 June 2017).
- WHO (2012) *Dementia: a public health priority*. Available at: https://apps.who.int/iris/bitstream/handle/10665/75263/9789241564458_eng.pdf;jsessionid=2173FB3249A4C9C5E692631BEAF5A1EE?sequence=1 (Accessed: 4 December 2019).
- WHO (2017) *WHO | Dementia*, WHO. World Health Organization. Available at: <http://www.who.int/mediacentre/factsheets/fs362/en/> (Accessed: 14 September 2017).
- Willette, A. A., Bendlin, B. B., *et al.* (2015) ‘Association of insulin resistance with cerebral glucose uptake in late middle-aged adults at risk for Alzheimer disease’, *JAMA Neurology*. American Medical Association, 72(9), pp. 1013–1020. doi: 10.1001/jamaneurol.2015.0613.
- Willette, A. A., Johnson, S. C., *et al.* (2015) ‘Insulin resistance predicts brain amyloid deposition in late middle-aged adults’, *Alzheimer’s and Dementia*. Elsevier Inc., 11(5), pp. 504–510.e1. doi: 10.1016/j.jalz.2014.03.011.
- Wilson, R. S. *et al.* (2002) ‘The apolipoprotein E ϵ 2 allele and decline in episodic memory’, *Journal of Neurology Neurosurgery and Psychiatry*. J Neurol Neurosurg Psychiatry, 73(6), pp. 672–677. doi: 10.1136/jnnp.73.6.672.
- Windey, K., De Preter, V. and Verbeke, K. (2012) ‘Relevance of protein fermentation to gut health’, *Molecular Nutrition & Food Research*. John Wiley & Sons, Ltd, 56(1), pp. 184–196. doi: 10.1002/mnfr.201100542.
- Winkler, A. M. *et al.* (2014) ‘Permutation inference for the general linear model’, *NeuroImage*. Academic Press Inc., 92(100), pp. 381–397. doi: 10.1016/j.neuroimage.2014.01.060.
- Wisdom, N. M., Callahan, J. L. and Hawkins, K. A. (2011) ‘The effects of apolipoprotein E on non-impaired cognitive functioning: A meta-analysis’, *Neurobiology of Aging*. Elsevier, 32(1), pp. 63–74. doi: 10.1016/j.neurobiolaging.2009.02.003.
- Wishart, H. A. *et al.* (2006) ‘Regional brain atrophy in cognitively intact adults with a single APOE ϵ 4 allele’, *Neurology*. Wolters Kluwer Health, Inc. on behalf of the American Academy of Neurology, 67(7), pp. 1221–1224. doi: 10.1212/01.wnl.0000238079.00472.3a.
- Wisniewski, T. *et al.* (1994) ‘Acceleration of Alzheimer’s fibril formation by apolipoprotein E in vitro’, *American Journal of Pathology*. American Society for Investigative Pathology, 145(5), pp. 1030–1035. Available at:

/pmc/articles/PMC1887417/?report=abstract (Accessed: 10 March 2021).

Witkowski, M., Weeks, T. L. and Hazen, S. L. (2020) 'Gut Microbiota and Cardiovascular Disease', *Circulation Research*. Lippincott Williams and Wilkins, pp. 553–570. doi: 10.1161/CIRCRESAHA.120.316242.

Wittenberg, R. *et al.* (2019) *Projections of older people with dementia and costs of dementia care in the United Kingdom, 2019-2040*. 5. Available at: https://www.alzheimers.org.uk/sites/default/files/2019-11/cpec_report_november_2019.pdf (Accessed: 8 May 2021).

Wolbers, T. and Wiener, J. M. (2014) 'Challenges for identifying the neural mechanisms that support spatial navigation: The impact of spatial scale', *Frontiers in Human Neuroscience*. Frontiers Media S. A. doi: 10.3389/fnhum.2014.00571.

Wong, C. H., Siah, K. W. and Lo, A. W. (2019) 'Estimation of clinical trial success rates and related parameters', *Biostatistics*. Oxford University Press, 20(2), pp. 273–286. doi: 10.1093/biostatistics/kxx069.

World Health Organization (2019a) *Global health estimates: Leading causes of death*. Available at: <https://www.who.int/data/gho/data/themes/mortality-and-global-health-estimates/ghe-leading-causes-of-death> (Accessed: 8 May 2021).

World Health Organization (2019b) *The top 10 causes of death*. Available at: <https://www.who.int/news-room/fact-sheets/detail/the-top-10-causes-of-death> (Accessed: 8 May 2021).

Wu, G. D. *et al.* (2011) 'Linking Long-Term Dietary Patterns with Gut Microbial Enterotypes', *Science*, 334(6052), pp. 105–108. doi: 10.1126/science.1208344.

Wu, W. K. *et al.* (2019) 'Optimization of fecal sample processing for microbiome study — The journey from bathroom to bench', *Journal of the Formosan Medical Association*. Elsevier B.V., pp. 545–555. doi: 10.1016/j.jfma.2018.02.005.

Xiao, S. *et al.* (2021) 'Trial of Sodium Oligomannate for Mild-to-Moderate Alzheimer ' s Dementia', 7, pp. 1–21.

Xin, Y. *et al.* (2018) 'Effects of oligosaccharides from morinda officinalis on gut microbiota and metabolome of APP/PS1 transgenic mice', *Frontiers in Neurology*, 9(JUN), pp. 1–14. doi: 10.3389/fneur.2018.00412.

Xing, Y. and Higuchi, K. (2002) 'Amyloid fibril proteins', *Mechanisms of Ageing and Development*. Elsevier, 123(12), pp. 1625–1636. doi: 10.1016/S0047-6374(02)00098-2.

Yao, C. K., Muir, J. G. and Gibson, P. R. (2016) 'Review article: insights into colonic protein fermentation, its modulation and potential health implications', *Alimentary Pharmacology & Therapeutics*. Blackwell Publishing Ltd, 43(2), pp. 181–196. doi: 10.1111/apt.13456.

Yu, J. *et al.* (2017) 'High-Throughput Metabolomics for Discovering Potential Metabolite Biomarkers and Metabolic Mechanism from the APP^{swe}/PS1^{dE9} Transgenic Model of Alzheimer's Disease', *Journal of Proteome Research*. American Chemical Society, 16(9), pp. 3219–3228. doi: 10.1021/acs.jproteome.7b00206.

Yun, Y. *et al.* (2017) 'Comparative analysis of gut microbiota associated with body mass index in a large Korean cohort', *BMC Microbiology*. BioMed Central Ltd., 17(1). doi: 10.1186/s12866-017-1052-0.

Zafar, H. and Saier, M. H. (2021) 'Gut Bacteroides species in health and disease', *Gut Microbes*. Bellwether Publishing, Ltd., pp. 1–20. doi: 10.1080/19490976.2020.1848158.

Zakzanis, K. K., Mraz, R. and Graham, S. J. (2005) 'An fMRI study of the Trail Making Test', *Neuropsychologia*. Pergamon, 43(13), pp. 1878–1886. doi:

10.1016/j.neuropsychologia.2005.03.013.

Zhan, G. *et al.* (2018) 'Abnormal gut microbiota composition contributes to cognitive dysfunction in SAMP8 mice', *Aging*. Impact Journals LLC, 10(6), pp. 1257–1267. doi: 10.18632/aging.101464.

Zhan, X. *et al.* (2016) 'Gram-negative bacterial molecules associate with Alzheimer disease pathology', *Neurology*. Lippincott Williams and Wilkins, 87(22), pp. 2324–2332. doi: 10.1212/WNL.0000000000003391.

Zhan, X., Stamova, B. and Sharp, F. R. (2018) 'Lipopolysaccharide associates with amyloid plaques, neurons and oligodendrocytes in Alzheimer's disease brain: A review', *Frontiers in Aging Neuroscience*. Frontiers Media S.A. doi: 10.3389/fnagi.2018.00042.

Zhang, L. *et al.* (2017) 'Altered Gut Microbiota in a Mouse Model of Alzheimer's Disease', *Journal of Alzheimer's Disease*, 60(4), pp. 1241–1257. doi: 10.3233/JAD-170020.

Zhang, X. and Song, W. (2013) 'The role of APP and BACE1 trafficking in APP processing and amyloid- β generation', *Alzheimer's Research and Therapy*. BioMed Central, 5(5), pp. 1–8. doi: 10.1186/ALZRT211/FIGURES/3.

Zhang, Y. *et al.* (2015) 'Meta-analysis for the association of apolipoprotein e ϵ 2/ ϵ 3/ ϵ 4 polymorphism with coronary heart disease', *Chinese Medical Journal*. Chinese Medical Association, 128(10), pp. 1391–1398. doi: 10.4103/0366-6999.156803.

Zhao, R. *et al.* (2018) 'Vitamin B2 blocks development of Alzheimer's disease in APP/PS1 transgenic mice via anti-oxidative mechanism', *Tropical Journal of Pharmaceutical Research*. University of Benin, 17(6), pp. 1049–1054. doi: 10.4314/tjpr.v17i6.10.

Zhao, Y., Cong, L. and Lukiw, W. J. (2017) 'Lipopolysaccharide (LPS) accumulates in neocortical neurons of Alzheimer's disease (AD) brain and impairs transcription in human neuronal-glia primary co-cultures', *Frontiers in Aging Neuroscience*. Frontiers Media S.A., 9(DEC). doi: 10.3389/fnagi.2017.00407.

Zhao, Y., Dua, P. and Lukiw, W. J. (2015) 'Microbial Sources of Amyloid and Relevance to Amyloidogenesis and Alzheimer's Disease (AD).', *Journal of Alzheimer's disease & Parkinsonism*. NIH Public Access, 5(1), p. 177. doi: 10.4172/2161-0460.1000177.

Zhao, Y., Jaber, V. and Lukiw, W. J. (2017) 'Secretory products of the human GI tract microbiome and their potential impact on Alzheimer's disease (AD): Detection of lipopolysaccharide (LPS) in AD hippocampus', *Frontiers in Cellular and Infection Microbiology*. Frontiers Media S.A., 7(JUL). doi: 10.3389/fcimb.2017.00318.

Zheng, L. and Wen, X. L. (2021) 'Gut microbiota and inflammatory bowel disease: The current status and perspectives', *World Journal of Clinical Cases*. Baishideng Publishing Group Co, 9(2), pp. 321–333. doi: 10.12998/wjcc.v9.i2.321.

Zhou, J. *et al.* (2020) 'Ethanolamine improves colonic barrier functions and inflammatory immunoreactions via shifting microbiome dysbiosis', *bioRxiv*. Cold Spring Harbor Laboratory, p. 2020.07.09.196592. doi: 10.1101/2020.07.09.196592.

Zhuang, Z. Q. *et al.* (2018) 'Gut Microbiota is Altered in Patients with Alzheimer's Disease', *Journal of Alzheimer's Disease*. IOS Press, 63(4), pp. 1337–1346. doi: 10.3233/JAD-180176.

Zilberter, Y. and Zilberter, M. (2017) 'The vicious circle of hypometabolism in neurodegenerative diseases: Ways and mechanisms of metabolic correction', *Journal of Neuroscience Research*. John Wiley and Sons Inc., pp. 2217–2235. doi: 10.1002/jnr.24064.

SUPPLEMENTARY INFORMATION

Table 7.1 (Part 1) Observational mice studies investigating the relationship of Alzheimer's Disease on the intestinal microbiota

Mouse model	Age	Sequencing	Analysis method	Main findings	Reference
APP/PS1, WT (n≥6/group)	1, 3, 5 and 8 months	16S rRNA gene sequencing	α-diversity: Rarefaction curves β-diversity: un/weighted UniFrac Differential abundance analysis: ANOVA	↑ in 8M APP/PS1 compared to 8M WT mice Significant clustering between groups at 8 months 8M APP/PS1 vs 8M WT: ↑ <i>Bacteroidetes</i> , <i>Tenericutes</i> , <i>Rikenellaceae</i> ↓ <i>Firmicutes</i> , <i>Verrucomicrobia</i> , <i>Proteobacteria</i> , <i>Actinobacteria</i> , <i>Allobaculum</i> , <i>Akkermansia</i>	Harach <i>et al.</i> , 2016
GF-APP/PS1, APP/PS1 (n≥5/group)	1, 3, 5 and 8 months		immunohistochemistry, western blotting microscopy ELISAs	At 8 months, rel. abundance of several bacterial genera was correlated with levels of Aβ42 in the brain in APP/PS1 Reduction of cerebral Aβ load in young and aged GF-APP/PS1 compared to APP/PS1 No age-related increase in pro-inflammatory cytokine (IL-1β) in GF-APP/PS1 mice, contrary to APP/PS1 IFN-γ, IL-2 and IL-5 also significantly lower in GF-APP/PS1 mice	
4M GF-APP/PS1 mice faecal transplant from 1) aged WT (COLOWT-APP/PS1) 2) aged APP/PS1 (COLOAD-APP/PS1) (n= 6/group)			amyloid pathology α-diversity: Rarefaction curves Differential abundance analysis: ANOVA	Colonization of GF-APP/PS1 mice with microbiota increases Aβ pathology COLOWT-APP/PS1 vs COLOAD-APP/PS1: ↑ diversity at day 1, 4 and week 2,4,6 of colonization Day 1: ↓ <i>Rikenellaceae</i> , <i>Ruminococcus</i> , <i>Dorea</i> in COLOAD-APP/PS1 mice Day 4: ↓ <i>Bacteroides</i> in COLOAD-APP/PS1 mice	
5xFAD, WT (n≥6/group)	6, 9 and 18 weeks	PCR of selected bacterial taxa	Differential abundance analysis: unpaired Student t-test enzyme activity	Few group differences of quantified bacterial taxa 5xFAD at 9 weeks vs WT (but not at 6 or 18 weeks): ↑ <i>Firmicutes</i> and <i>Clostridium leptum</i> , ↓ <i>Bacteroidetes</i> ↓ trypsin activity in 5xFAD mice (especially in young mice)	Brandscheid <i>et al.</i> , 2017
APP/PS1, WT (n = 6/group)	3,6, and 8 months	16S rRNA gene sequencing	α-diversity: Shannon, Simpson Differential abundance analysis	No difference between the groups ↓ in α-diversity with increasing age in APP/PS1 mice (not in WT) APP/PS1 vs WT: ↑ <i>Helicobacteraceae</i> , <i>Desulfovibrionaceae</i> , <i>Odoribacter</i> , <i>Helicobacter</i> , <i>Coriobacteriaceae</i> ↓ <i>Prevotella</i> , <i>Ruminococcus</i> Changes in APP/PS1 over time: ↑ <i>Prevotellaceae</i> (no investigated in WT group)	Shen <i>et al.</i> , 2017

Table 7.1 (Part 2) Observational mice studies investigating the relationship of Alzheimer's Disease on the intestinal microbiota

Mouse model	Age	Sequencing	Analysis method	Main findings	Reference
APP/PS1 (PAP), WT (n=6/group)	1,3,5 and 8 months	16S rRNA gene sequencing	<p>α-diversity: observed species (OTUs), Chao1, Shannon, Simpson, ACE</p> <p>β-diversity: weighted and unweighted UniFrac</p> <p>Differential abundance analysis: LEfSe</p> <p>Student T-test</p> <p>Functional: KEGG SCFAs</p>	<p>Changes over time (all indices apart from Simpson): \uparrow PAP8M vs PAP3M, \uparrow WT8M vs all WT groups Group comparison: \uparrow PAP5M vs WT5M (Chao1), \downarrow PAP8M vs WT8M (Shannon)</p> <p>Significant clustering into 6 groups by age, PAP and WT distinct from 5 months onwards: (1) PAP8M; (2) WT8M; (3) PAP5M; (4) WT5M; (5) PAP3M&WT3M; (6) PAP1M&WT1M Variability explained PC1: 48.43%, PC2: 17.16%</p> <p>PAP8M vs WT8M: \uparrow <i>Erysipelotrichaceae</i>, <i>Erysipelotrichales</i>, <i>Erysipelotrichales</i> Several taxa differences within groups at different ages</p> <p>PAP8M vs WT8M: \downarrow <i>Ruminococcus</i>, <i>Butyricoccus</i>, <i>B. pullicaecorum</i> PAP5M vs WT5M: \uparrow <i>Desulfovibrio C21 c20</i></p> <p>Upregulation of several pathways in PAP5M and PAP8M compared to WT</p> <p>Faecal matter: \downarrow butyric acid in PAP5/8M vs WT brain: \downarrow butyric acid (5/8M), isobutyric acid (5,8M), valeric (3M) and isovaleric (5M) in PAP vs WT</p>	Zhang <i>et al.</i> , 2017
APP/PS1 (n=3 at 3/6M, n=2 at 24M) WT (n=3 at 3/6/24m)	3, 6 and 24 months	16S rRNA gene sequencing	<p>α-diversity: Shannon, Chao1</p> <p>β-diversity: un/weighted UniFrac</p> <p>Differential abundance analysis: ANOVA and Student t-test</p>	<p>Diversity increased as a function of age and group (greatest in 24M-/6M-old APP/PS1, then 24M-/6M-old WT; lowest in younger mice)</p> <p>3M-old and 6/24M-old mice cluster together regardless of group, PC1: 18%, PC2:12%</p> <p>Changes over time: \uparrow <i>Rikenellaceae</i>, <i>Proteobacteria</i> Group comparison: \downarrow <i>Rikenellaceae</i> compared to WT 24m, <i>Clostridiales</i> in TG 3m vs WT 3m, <i>Bacteroidales</i>, <i>Ruminococcus</i>, <i>Oscillospira</i> in TG 24m vs WT 24m \uparrow <i>Proteobacteria</i>, particularly <i>Betaproteobacteria</i> and associated <i>Sutterella</i> in TG 6m vs WT 3/6/24m, <i>Erysipelotrichaceae</i> in TG 24m vs WT</p>	Bäuerl <i>et al.</i> , 2018
SAMP8, SAMR1 (n=13/group)	male 6 months	16S rRNA gene sequencing shotgun	<p>α-diversity: Shannon, Chao1, Ace</p> <p>β-diversity: un/weighted UniFrac</p> <p>Differential abundance analysis: LEfSe</p> <p>Functional analysis: COG and KEGG (LEfSe)</p>	<p>no difference in alpha diversity</p> <p>Significant compositional differences</p> <p>SAMP8: \uparrow <i>Lachnospiraceae</i>, <i>Alistipes</i>, <i>Akkermansia</i>, <i>Odoribacter</i> SAMR1: \uparrow <i>Bacteroidales</i> (S24_7_group), <i>Prevotella_9</i>, <i>Parasutterella</i>, <i>Butyrivibrio</i></p> <p>11 functional COG categories differed significantly Over 20 different functional groups at KEGG level 1-3</p>	Peng <i>et al.</i> , 2018

Table 7.1 (Part 3) Observational mice studies investigating the relationship of Alzheimer's Disease on the intestinal microbiota

Mouse model	Age	Sequencing	Analysis method	Main findings	Reference
SAMP8, SAMR1	7 months	16S rRNA gene sequencing	α -diversity: Shannon, Chao1, Simpson β -diversity: Bray-Curtis dissimilarity Differential abundance analysis: Student t-test	significantly reduced Shannon and Chao1 in SAMP8 mice No statistical testing performed. Visual assessment: samples clustered within groups but were separate from each other 27 taxa significantly different (all but one taxon was reduced in SAMP8) \downarrow <i>Deltaproteobacteria</i> , <i>Deferribacterales</i> , <i>Desulfovibrionales</i> , <i>Ruminococcaceae</i> , and many more \uparrow uncultured <i>Bacteroidales</i> bacterium	Zhan <i>et al.</i> , 2018
Control WT, GF-WT, GF-SAMR1, GF-SAMP8	faecal transplant into pseudo GF mice		α -diversity: Shannon, Chao1, PD whole tree Differential abundance analysis: One-way ANOVA and Fisher's exact test	Intestinal microbiota transplant from SAMR1 mice, but not from SAMP8 mice, significantly improved abnormality in α -diversity Several taxa changed abundance levels after faecal matter transplant GF-SAMP8 vs all other groups: \uparrow <i>Betaproteobacteria</i> , <i>Burkholderiales</i> , <i>Alcaligenaceae</i> , <i>Parasutterella</i> Change as a function of group: Control, GF-Control, GF-SAMR1, -SAMP8 \downarrow <i>Firmicutes</i> , <i>Clostridiales</i> , <i>Lachnospiraceae</i> \uparrow <i>Bacteroidales</i>	
Tg2576, WT n=3.5 per group	6 (Yg-Tg:pre-symptomatic) and 15 (Ag-Tg) months	16S rRNA gene sequencing	α -diversity: Shannon, OTUs β -diversity: weighted UniFrac Differential abundance analysis: Two-way ANOVA Immunohistochemical staining Brain immunohistochemistry Inflammatory markers A β visualization	no difference in alpha diversity Ag-Tg vs WT: significant clustering, PC1: 54% <i>Firmicutes</i> to <i>Bacteroides</i> ratio significantly higher in Ag-Tg \downarrow <i>Ruminiclostridium</i> in Yg-Tg and Ag-Tg vs Yg-WT \uparrow <i>Lactobacillus</i> in Ag-Tg vs Ag-WT Intestinal epithelial barrier dysfunction before development of cerebral A β pathology in Yg-Tg (significant reduction of E-cadherin) Significant reduction in the expression levels of claudin 11 in Ag-Tg Plasma levels of IL-9, VEGF- α , and IP-10 elevated in the plasma in Yg-Tg but not in Ag-Tg, MCP-1 elevated in Ag-Tg only intestinal (ileum and cecum) A β deposits in Yg-Tg and Ag-Tg	Honarpish <i>et al.</i> , 2020

Table 7.2 (Part 1) Human and animal studies investigating the role of Apolipoprotein E genotype and the intestinal microbiota

Subjects	Sequencing	Analysis method	Main findings	Reference
APOE human study N= 14 ε2/ε3 carriers N= 18 ε3/ε3 carriers N= 18 ε3/ε4 carriers N= 6 ε4/ε4 carriers	16S rRNA gene sequencing	α-diversity: Shannon, Chao1, phylogenetic diversity	no difference in α-diversity	Tran <i>et al.</i> , 2019
		β-diversity: weighted and unweighted UniFrac	no difference in β-diversity	
APOE4 TR-mouse model young (4 months old, N=10/genotype) mice old (18 months old, N=6/genotype) mice • APO ε3/ε3-TR mice • APO ε4/ε4-TR mice	Metabolomic NMR analysis	Differential abundance analysis: LEfSe	APOε2/ε3 vs APOε3/ε4 and APO ε4/ε4: ↑ <i>Firmicutes</i> , <i>Clostridiales</i> APOε2/ε3 vs APOε3/ε3 and APOε3/ε4: ↑ <i>Ruminococcaceae</i> , <i>Clostridium IV</i> APOε2/ε3 vs APOε3/ε3 and APOε4/ε4: ↓ <i>Prevotellaceae</i> APOε2/ε3 vs APOε4/ε4: ↑ <i>Gemmiger</i>	
		α-diversity: Shannon, Chao1, phylogenetic diversity	no difference in α-diversity	
		β-diversity: weighted and unweighted UniFrac	distinct clustering by genotype within each age group	
		Differential abundance analysis: Mann-Whitney U test and BH correction	APOε3/ε3 vs APOε4/ε4: (across both age groups): ↑ <i>Lachnospiraceae</i> , <i>Deferribacteraceae</i> , <i>Clostridium XIVa</i> , <i>Odoribacter</i> , <i>Mucispirillum</i> , <i>Enterorhabdus</i> , <i>Butyricoccus</i> ↓ <i>Bacteroidaceae</i> , <i>Bacteroides</i>	
		Metabolites	39 metabolites distinct between APOE genotypes, including Alanine, Glycine, Lactate, Propionate, Xylose, Urocanate	
		Enrichment analysis	Distinct pathways between APOE genotypes: ammonia recycling, urea cycle, and alanine metabolism	

Table 7.2 (Part 2) Human and animal studies investigating the role of Apolipoprotein E genotype and the intestinal microbiota

Subjects	Sequencing	Analysis	Main findings	Reference
EFAD APOE4 mouse model (homozygous APOE, 5x familial AD mutations, 4 months-old) <ul style="list-style-type: none"> • APOE3-FAD mice (N=28) • APOE4-FAD mice (N=20) 	16S rRNA gene sequencing	α -diversity: Shannon β -diversity: Bray-Curtis dissimilarity Differential abundance analysis: Mann-Whitney U test and BH correction	no difference in α -diversity significant clustering at OTU level, family- and genus-level APOE3-FAD vs APOE4-FAD mice: ↑ <i>Prevotella</i> , <i>Ruminococcus</i> , <i>Sutterella</i> ↓ <i>Anaeroplasma</i>	Weng <i>et al.</i> , 2019
EFAD mice 4 months-old <ul style="list-style-type: none"> • APOE2-FAD mice (N=33) • APOE3-FAD mice (N=55) • APOE4-FAD mice (N=51) 6 months-old <ul style="list-style-type: none"> • APOE2-FAD mice (N=24) • APOE3-FAD mice (N=16) • APOE4-FAD mice (N=51) 		α -diversity: Shannon β -diversity: Bray-Curtis dissimilarity, weighted and unweighted UniFrac Differential abundance analysis: LEfSe Random Forest analysis	no difference in α -diversity consistent and robust association with APOE genotype with all three measures, explaining 8.9% - 22.2% Taxa associated with APOE: <i>Prevotellaceae</i> , <i>Rikenellaceae</i> , <i>Gastranaerophilales</i> , <i>Lactobacillaceae</i> , <i>Peptococcaceae</i> , <i>Turibacter</i> , <i>Desulfovibrionales</i> , <i>Mollicutes</i> , <i>Ruminococcaceae</i> Identified same bacterial families as LEfSe, best predictor: <i>Muribaculaceae</i> (only present in the murine microbiome)	Parikh <i>et al.</i> , 2020
EFAD APOE4 mouse model Intervention study: Dietary inulin E4FAD-Control E3FAD-Control E4FAD-Inulin (N = 15/group)	16S rRNA gene sequencing mass spectrometry	α -diversity: Shannon β -diversity: Bray-Curtis dissimilarity Differential abundance analysis: ANOVA Cecum: SCFAs Periphery: microbial metabolites Hippocampus: metabolites and inflammation	E4FAD-Inulin significantly lower than E4FAD-Control distinct clustering between E4FAD-Inulin and control groups E4FAD-Inulin vs E4FAD-Control mice: ↑ <i>Prevotella</i> , <i>Lactobacillus</i> ↓ <i>Escherichia</i> , <i>Turicibacter</i> , <i>Akkermansia</i> ↑ acetate, butyrate and propionate in E4FAD-Inulin vs E4FAD-Control E4FAD-Inulin vs E4FAD-Control mice: ↑ acetate ↑ tryptophan metabolites (indolepropionate and indoleacrylate), ↑ bile acids (cholate, deoxycholate) E4FAD-Inulin vs E3FAD-Control: ↑ metabolites involved in TCA cycle (mitochondrial dysfunction), PPP associated metabolites (reduced oxidative stress) Metabolites: E4FAD-Inulin vs E4FAD-Control mice: ↑ scyllo-inositol (inhibitor of A β) ↓ myo-inositol (decreased inflammation) Inflammation: Enriched inflammatory gene expression in the hippocampus of APOE4 mice with FAD mutation. E4FAD-Inulin decreased expression of 2 pro-inflammatory genes	Hoffman <i>et al.</i> , 2019

Genomic DNA extraction from saliva samples

The buccal samples were processed using the QIAamp Blood DNA Mini Kit (Qiagen) in accordance with the manufacturer's protocol for 'DNA Purification from Buccal Swabs (Spin Protocol)' as follows. First the foam tip was cut off from its shaft with sterilized scissors and placed into a 2ml microcentrifuge. 400 μ L of PBS were added, followed by 20 μ l of QIAGEN Protease stock solution and 400 μ L of Buffer AL (contains chaotropic salt). The mixture was then mixed by vortexing for 15s. All samples were transferred into a heat block and incubated at 56 °C for 10min. Following this, all samples were centrifuged for 5s and 400 μ L of ethanol (96-100%) were added. The samples were vortexed and centrifuged again as described before. Next, 700 μ L of the mixture were transferred to the QIAamp Mini spin column and centrifuged at 8000rpm for one minute. The filtrate was discarded, the remaining mixture was added to the spin column and subjected to another round of centrifugation. For the washing steps, 500 μ L of Buffer AW1 was added and the samples were centrifuged at 8000rpm for 1 min. After discarding the filtrate, 500 μ L of Buffer AW2 were added and the samples were centrifuged at 14000rpm for 3 min. The collection tube containing the filtrate was discarded and another round of dry spinning was performed (centrifuge at 14000rpm for 2min) to eliminate possible carryover from Buffer AW2. Lastly, the purified DNA bound in the spin column was eluted with AE buffer by adding 150 μ L of the buffer to the sample and incubating at room temperature for 1 min. Following this, the sample was centrifuged at 8000rpm for 1min. The eluate at the bottom of the collection tube was added to the spin filter again and centrifugation was repeated. Repeating the elution step without adding further buffer was performed to increase the yield of DNA.

DNA quality control

According to the manufacturer's instructions the resultant DNA should have a total concentration of 0.5-3.5ug of DNA in 150uL of buffer (3-23ng/ μ L) with purity measurement (absorbance ratio at A_{260}/A_{280}) between 1.7-1.9. Following the extraction, the purified

genomic DNA samples were quantified using NanoDrop™ spectrophotometer (Thermo Fisher) and diluted with RNase/DNase free water to be in a range of 1-20ng. All samples were subsequently stored at -80°C until further processing.

DNA amplification

The APOE genotype was determined using two RT-PCR SNP Genotyping Assays, which determine the 112 T/C (rs429358) APOE4 polymorphism and 158 C/T (rs7412) APOE2 polymorphism. The two SNP genotyping assays were diluted to a 20x working stock with 1x TE buffer and aliquoted into many smaller volumes to prevent deleterious freeze-thaw cycles. These assays featured into either of the two master mixes (“MM112” for the APOE4 polymorphism, and “MM158” for the APOE2 polymorphism). Each of the Master Mixes contained TaqPath ProAmp MasterMix (5µL per sample), RNase and DNase free water (2.5µL per sample) and the respective primer (0.5µL per sample) for master mixes. The primers were kept on ice and wrapped up in aluminium foil to protect from light.

96-well PCR reaction plates (MicroAmp Fast 96-well reaction plate, 0.1mL, Applied Biosystems) were prepared as follows: add 8µL of the prepared mastermix and 2µL of DNA (containing 1-20 ng purified genomic DNA either for the external/ internal controls or samples of interest) or 2µL of RNase/DNase free water for the negative template controls (NTC’s) to each well resulting in a total volume of 10µL per well. Each reaction plate had 3 NTC’s, four external controls with known APOE genotype (see Table 3) from the ‘Cognitive Ageing, Nutrition and Neurogenesis’ (CANN) trial (Irvine *et al.*, 2018) and two internal controls from previously genotyped samples.

Table 7.3 External controls to determine Apolipoprotein E allelic discrimination

SAMPLE	GENOTYPE	112	158
S025	ε3/ε3	2/2 (TT)	1/1 (CC)
S013	ε2/ε4	1/2 (CT)	1/2 (CT)
COB349	ε2/ε2	2/2 (TT)	2/2 (TT)
S112	ε4/ε4	1/1 (CC)	1/1 (CC)

After the reaction plate set-up was completed, an adhesive optical cover (MicroAmp Optical Adhesive Film, Applied Biosystems) was applied to the top of the plate. The plate was vortexed to mix the plates and centrifuged for 2 min at 1,000rpm to spin down the contents and eliminate any air bubbles. Then the reaction plate was loaded in the Applied Biosystems 7500 Fast Real-Time PCR system (Thermo Fisher Scientific, Ashford, UK). In between steps the reaction plate was kept on ice. The PCR plate experimental design was set-up on the computer to reflect “unknowns”, “positive controls”, “negative control” properties before running the plate for 90 min.

The PCR cycling conditions on the 7500 Fast Real-Time PCR machine system were as follows: one cycle of denaturation at 95°C for 10 min, 50 cycles of denaturation at 92°C for 15 s and annealing at 60°C for 60 s, and soak at 4°C until use. The fluorescence signals were detected during the annealing/extension step. After the PCR step was completed, the data was visually inspecting with help of allelic discrimination plots (Figure 1) and analysed in reference to the information presented in Table 4. Each PCR run produced two allelic discrimination plots, one for 112 T/C APO ϵ 4 polymorphism and 158 C/T APO ϵ 2 polymorphism. After automatic calling and comparison against controls, the samples were automatically divided into one of four different clusters as shown in Figure 1: (1) Blue is homozygote allele 2 (TT), (2) Green is heterozygote allele 2 (CT), (3) Red homozygote allele 1 (CC), (4) Black: no template control (note that negative control samples without any DNA in it will also fall into this cluster).

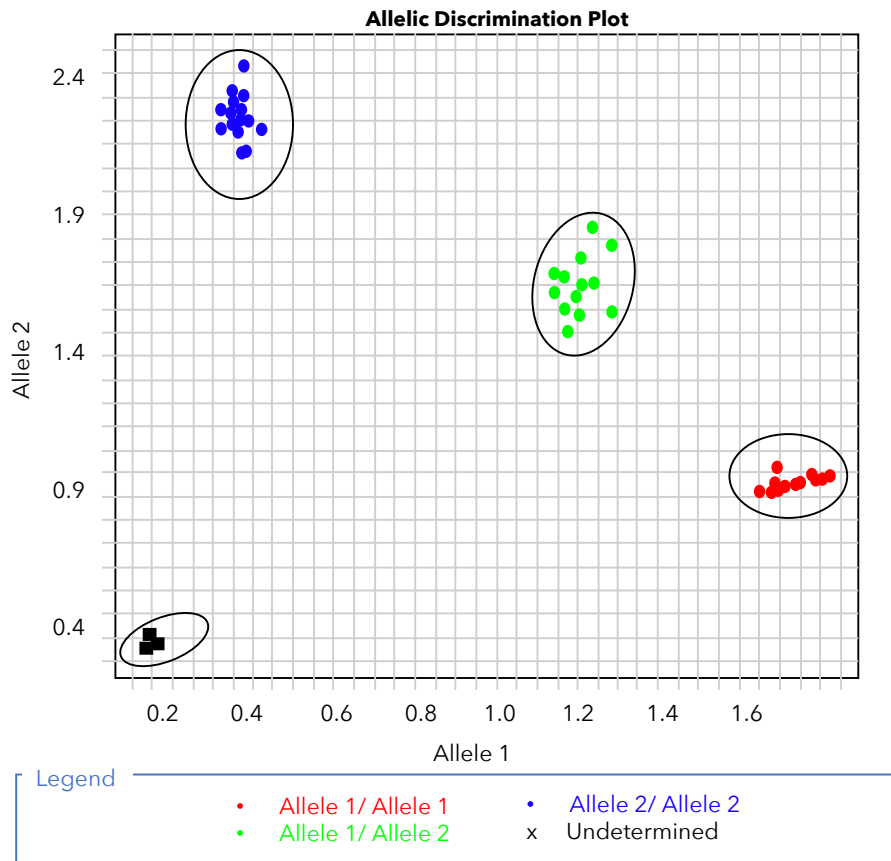


Figure 7.1 Representative printout of allelic discrimination plot

Table 7.4 Reference table to determine Apolipoprotein E genotype

APOE Genotype	112	158
E3/E4	CT (1/2)	CC (1/1)
E2/E2	TT (2/2)	TT (2/2)
E2/E3	TT (2/2)	CT (1/2)
E2/E4	CT (1/2)	CT (1/2)
E3/E3	TT (2/2)	CC (1/1)
E4/E4	CC (1/1)	CC (1/1)

Magnetic Resonance Imaging (MRI): Patient and Escort Safety Questionnaire

To assess whether it is safe for you to have an MRI scan we need to know about any metal objects you may have in or on your body, therefore **please complete and sign** the following questionnaire.

Name:	Hospital ID: (If known)	Date of birth:	
Address:		Weight:	Height:
		Yes	No
1. Do you have or have you EVER had a cardiac pacemaker?			
2. Have you EVER had heart surgery?			
3. Do you have any aneurysm clip(s) in your head?			
4. Do you have a hydrocephalus shunt?			
If YES , is it a programmable shunt?			
5. Have you had any operations on your head, brain, eye(s) or spine?			
6. Have you EVER had metal dust/fragments go into your eye(s)?			
7. Have you EVER sustained any metal injuries to any other part of your body (e.g. shrapnel, bullets, pellets)?			
8. Have you EVER had any other type of electronic, mechanical or magnetic implants? (e.g. cochlear implant, neurostimulators, drug infusion pump)?			
9. Have you EVER had any operations involving the use of metal implants, plates, pins, clips or stents including gastric bands or breast tissue expanders?			
10. Have you had any operations on your body in the last 8 weeks?			
11. Do you have any kidney problems?			
12. Have you had or are you waiting for a liver transplant?			
13. Have you ever had a previous reaction to an MRI contrast agent?			
14. Do you suffer from fits, blackouts or epilepsy?			
15. Do you have ANY piercing, hearing aids or dentures? If Yes, please remove them.			
16. Do you have any medication patches, tattoos or permanent eyeliner?			
Female patients only:			
17. Are you, or is there any chance you might be, pregnant?			
18. Are you breast-feeding?			
19. Do you have an Intrauterine Contraceptive Device (IUD)?			

Important Note: If you answer **YES** to questions 1 to 10 or 17 to 19 you **MUST** provide the details in the box below **AND** call the MRI Department on 01603 286107 to discuss. If you fail to do this your scan may be delayed or cancelled when you attend.

Details:

DECLARATION: I take full responsibility for the information above and confirm that it is correct.

Signature..... Date.....
(Patient/Guardian/Escort/Representative)

MR Operator's signature..... Date.....

Figure 7.2 Safety Checklist for Magnetic Resonance Imaging scanning

Brain Protocol Magnetic Resonance Imaging Sequence

The structural MRI data was obtained by using the TRACC Brain Protocol on a 3 tesla Discovery 750w wide bore system (GE Healthcare, Milwaukee, WI, USA) with a 12-channel phased-array head coil for signal reception. Structural T1-weighted images were obtained using a whole-head three-dimensional inversion-recovery fast spoiled gradient recalled echo (IR-FSPGR) sequence. The parameters for this sequence were as follows: field-of-view (FOV) = 256mm, acquired matrix = 256 x 256, 196 sagittal sections of 1mm thickness, repetition time (TR) = 7.7ms, echo time (TE) = 3.1ms, inversion time (TI) = 400ms, flip angle = 11 degrees, ASSET acceleration with a factor of 2 in phase-encoding direction.

Details on neuropsychological testing battery

Addenbrooke's Cognitive Examination-III – detailed test description

The first subdomain, attention, can score up to 18 points. Participants need to give information about the date, season and current location. They also need to repeat back 3 words and do a serial subtraction. Memory is tested by delayed recall, memorizing a name and address as well as recalling names and facts. A maximal subdomain score of 26 points can be achieved. For the fluency subdomain, with a maximum score of 14 points, participants are asked to generate as many words as possible starting with a specific letter in 1 minute and naming as many animals as they can in 1 min. The language subdomain consists of several smaller tasks, including repetition of polysyllabic words and two proverbs, reading out words which have a mismatch between their spelling and sound and naming 12 objects. Just like the memory domain, participants can score a maximum of 26 points in the language domain. Visuospatial ability, with a domain score of 16 points, is assessed by asking participants to copy an infinity look and a wire cube diagram as well as asking them to draw a clock face. They also need to count dots and recognize fragmented letters of the alphabet (Bruno and Vignaga, 2019).

Rey-Osterrich-Complex Figure test - scoring of the task

Many scoring systems have been developed; in this study we adopted a widely used 36-point system by Lezak (1976, 1983, 1995) adapted by E. M. Taylor (1995) which breaks the figure down into 18 elements. Each element is awarded a score between 0 and 2 points depending on accuracy and placement. Age-stratified normative data is available and important for the correct interpretation of performance. The literature suggests that a longer copying time is associated with a poorer recall score (Tremblay *et al.*, 2015). Longer copying time might indicate a poor organized strategy if accuracy of the copy is low, on the other hand, if the accuracy is high, it might reflect ‘effort’ and ‘care’ taken to complete the copy (Bennett-Levy, 1984). Understanding copying strategy has been suggested to be a major determinant for copy and recall performance and it might help to differentiate between the type of recall deficit (organization vs forgetting) (Bennett-Levy, 1984).

Sea Hero Quest – two types of level to assess spatial navigation

(i) Goal-oriented wayfinding levels. In goal-oriented wayfinding levels, the player is at first presented with a map of the level which showing the starting location and checkpoints that need be found in a set order (Figure S.3). The checkpoints are buoys with flags which upon getting closer also show their checkpoint number. Participants can study the level map for as long as they wish but this time is being recorded. Upon leaving the map view, participants need to navigate the boat (third-person perspective) to the checkpoints under timed conditions. If a given time is exceeded, an arrow appears which helps the player navigation by pointing along the Euclidean line to the next checkpoint (Coughlan *et al.*, 2019).

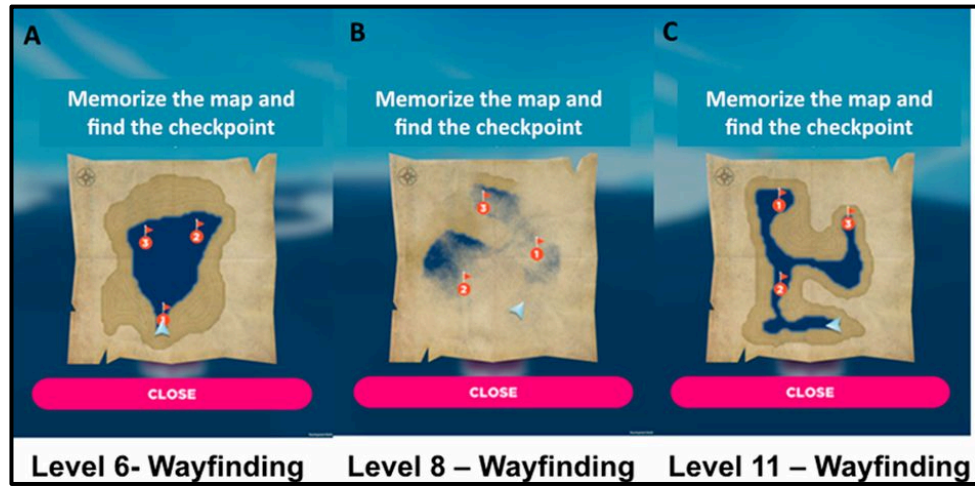


Figure 7.3 Maps presented in wayfinding levels 6 (A), 8 (B), 11 (C) adapted from Coughlan (2019)

(ii) Flare accuracy levels. Contrary to wayfinding levels, the player is not presented with a map and hence has no information about the level's size or shape which could inform a cognitive map. Instead, the player is immediately navigating along a river with the instruction to find a red flare gun located somewhere in the level and to shoot this flare back to the starting position. Upon successfully finding the flare gun, the boat rotates by 180° and the player is asked to shoot the flare back to their initial starting point by choosing one of three options (A-left, B-front, C- right).

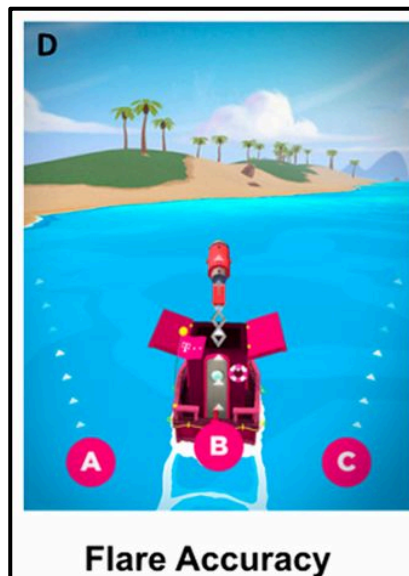


Figure 7.4 Flare accuracy level modified from Coughlan (2019)

In order to find the flare gun, players need to keep track of where they have been whilst navigating through and searching this novel environment. As they travel through the level, players also need to keep an accurate representation of their current location with respect to their starting location as well as integrate this information during self-motion and after a 180° rotation.

Sea Hero Quest - Statistical analysis method

(i) Goal-oriented wayfinding levels. Given the design of the experiment, with each participant repeatedly being tested on navigation performance by completing multiple levels of the SHQ game, we used “subject ID” as a random effect in our models to allow varying the intercept for subject. We then assessed the explanatory effect of various variables including sex, age, educational attainment and subjective navigation abilities on the SHQ outcome variables to identify and retain those predictors in the final model that would significantly contribute to the model/ increase the model fit. This decision was mainly guided by our research aim which was to investigate the effect of genotype whilst controlling for potential confounders (as suggested by the literature). Inclusion vs exclusion of fixed effects was further informed by Bayesian information criterion (BIC), Akaike information criterion (AIC), and Log-likelihood (logLik).

Following this, multilevel mixed regression models were run to evaluate the effect of genetic risk on the three outcome measures: wayfinding distance, wayfinding duration, and flare accuracy. For wayfinding levels, we implemented multilevel linear mixed regression models with the lmer() package in R.

(ii) Flare accuracy levels. For SHQ flare levels, we used mixed effects ordinal logistic regression, which is appropriate for ordinally-scaled observations with a finite set of categories, to model flare accuracy of “1”, “2”, or “3”. Where “3” denotes a correct answer,

shooting the flare back to the starting location. A flare accuracy of “2” and “1” however, indicate an increasing distance between the correct location and the chosen location, with “1” being furthest away from the target location. Flare accuracy can thus be order in terms of test performance (3 = best, 2= second best, 1 = worst) and are hence ordinally scaled. We implemented mixed effects ordinal logistic regression with genetic risk, age, sex, education and completion time as fixed effects and subject ID as random effects in R by using the “clmm” command from the “ordinal” package. We also investigated the individual level data, where each player has a single observation, thus excluding subject ID as random effect. This was implemented by running standard ordinal logistic regression (without random effects) with same fixed effects as before, using the `clm()` package in R.

Supermarket Task – detailed test description

In the Supermarket Task, participants watch 14 short clips on an iPad. These clips show how a person is navigating through a virtual supermarket environment making several 90° turns from a first-person perspective (Tu *et al.*, 2015). Every clip starts from the same location, the entrance of the supermarket, and finishes at set locations in the supermarket. The number of turns taken, and distance travelled through the supermarket is longer for videos 8-14 (40 sec, 5 turns) than for videos 1-7 (20 sec, 3 turns). After every clip, participants have to answer three questions. First, the participant is asked to indicate the direction of their starting point (=the entrance) whilst imagining that they are themselves in the supermarket at the position where the clip ended. This question taps into egocentric orientation as participants need to use an egocentric frame of reference to make the right answer. Next, participants are shown a map of the supermarket layout from birds-eye perspective and are asked to indicate their finish location on the map. This question taps into allocentric orientation. Lastly, participants are asked which direction they were facing when the video stopped which assesses heading orientation. A practice trial is completed to make sure that all instructions are understood. No feedback on task performance is provided. All trials were administered in sequence.

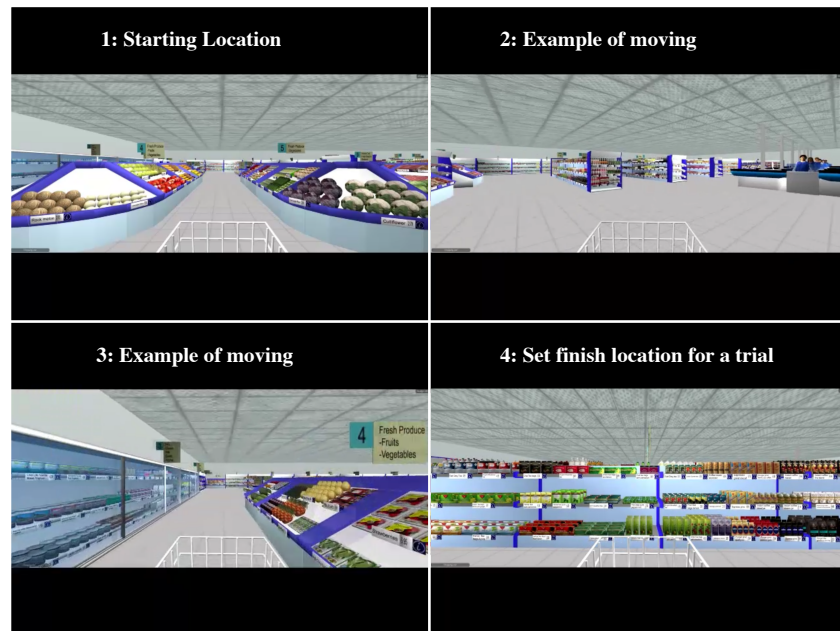


Figure 7.5 Example screenshots from the Supermarket Task

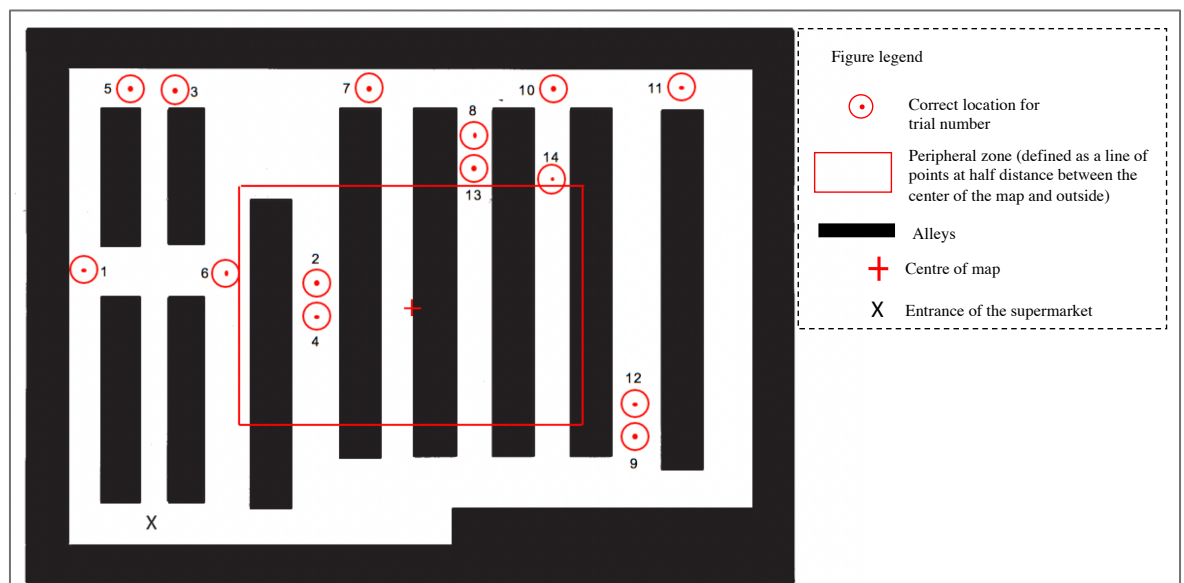


Figure 7.6 Spatial layout of supermarket response sheet modified from (Tu *et al.*, 2015)

- (a) Egocentric orientation gives the sum of correct answers to the question “Which way is the starting point?” (answer options are: front left, front right, back right and back left) with a minimum score of 0 and a maximum of 14.
- (b) Allocentric orientation is the displacement (distance in mm) between the participant’s location as indicated by them after each trial and the correct location;

here the smaller the distance, the better the performance. Displacement is also measured between the participants response and the centre of the map.

- (c) For heading direction, all correct heading questions for the 14 trials are summed up to form a final score with a minimum of 0 and a maximum of 14.
- (d) Central navigation preference was calculated as the number of central responses divided by the number of peripheral responses. With only 2 locations inside the central zone, a ratio of 0.17 is correct. A ratio higher than 0.17 indicates a preference towards central map areas whilst a ratio smaller than 0.17 indicates a preference towards peripheral map locations. A series of multiple regression models was fitted to explore the effect of genetic risk and other variables on the four outcome variables: egocentric orientation, allocentric orientation, heading direction, and central navigation preference.

Cognitive Change Index – detailed information on the questionnaire

The CCI is a questionnaire that consists of 20 items and asks participants (or informants) to rate the participant's ability to perform certain cognitive tasks (e.g. remembering names and faces of new people, recalling conversations a few days later, organizing daily activities, etc.) compared to the previous five years (Rattanabannakit *et al.*, 2016). Performance is rated on a 1 to 5-point Likert scale with higher scores indicating greater perceived decline (1=no change, 2= minimal change, 3= some change, 4= clearly noticeable change, 5= much worse). If no change is perceived a total minimum score of 20 is obtained, whilst the biggest self-perceived change in cognition would result in a maximum of 100 points. Before answering all the questions, participants are also asked to give a general indication to whether they "feel like [their] memory is becoming worse". The three options to choose from are "No", "Yes, but this does not worry me", and "Yes and this worries me". The 20 questions are tapping into three domains, with 12 questions evaluating memory performance, five questions assessing executive functioning and three questions focusing on language.

QRISK[®]3 – lipid measurements

After sterilizing the fingertip with an alcohol swab, a safety lancet was used to prick the participants finger, then a small sample of venous blood (35µl) was transferred onto the cholesterol test strip (inserted into the device) with help of a capillary tube, and all the measurements given by the Mission-3-in-1 Cholesterol Meter were recorded. Participants were also asked to self-report their height and weight as well as fill in a questionnaire to provide information about risk factors important for the QRISK model.

Food Frequency Questionnaire – detailed description

The FFQ is eleven pages long and asks participants to give frequency ratings for food and drinks in nine categories: “Meat and Fish” (Figure S.7), “Bread and Savoury biscuits”, “Cereals”, “Potatoes, Rice and Pasta”, “Dairy Products and Fats”, “Sweets and Snacks”, “Soups, Sauces and Spreads”, “Drinks”, “Fruit” and “Vegetables”. The FFQ also gathers further information linking back to nutritionally important food items (e.g. milk type, cereal type, fat type for cooking and baking, etc.). All frequency ratings were coded as numerical values from 1 to 9 (1 for ‘never or less than once a month’, all the way to 9 for ‘6+ times per day; and ‘-9’ for missing answers) and more detailed information were assigned food codes using flowcharts and look-up lists. The resulting codes are saved in a comma-separated file and processed by the FETA programme. More details regarding how FFQ data is processed with FETA are published by Mulligan *et al.* (2014).

Please estimate your average food use as best you can, and please answer every question - do not leave ANY lines blank. PLEASE PUT A TICK (✓) ON EVERY LINE

FOODS AND AMOUNTS	AVERAGE USE LAST YEAR									
	Never or less than once/month	1-3 per month	Once a week	2-4 per week	5-6 per week	Once a day	2-3 per day	4-5 per day	6+ per day	
MEAT AND FISH (medium serving)										
Beef: roast, steak, mince, stew or casserole										
Beefburgers										
Pork: roast, chops, stew or slices										
Lamb: roast, chops or stew										
Chicken or other poultry eg. turkey										
Bacon										
Ham										
Corned beef, Spam, luncheon meats										
Sausages										
Savoury pies, eg. meat pie, pork pie, pasties, steak & kidney pie, sausage rolls										
Liver, liver paté, liver sausage										
Fried fish in batter, as in fish and chips										
Fish fingers, fish cakes										
Other white fish, fresh or frozen, eg. cod, haddock, plaice, sole, halibut										
Oily fish, fresh or canned, eg. mackerel, kippers, tuna, salmon, sardines, herring										
Shellfish, eg. crab, prawns, mussels										
Fish roe, taramasalata										
	Never or less than once/month	1-3 per month	Once a week	2-4 per week	5-6 per week	Once a day	2-3 per day	4-5 per day	6+ per day	

Please check that you have a tick (✓) on EVERY line

Figure 7.7 Example page from the Food Frequency Questionnaire

Shotgun metagenomic sequencing and analysis

Genomic DNA extraction from faecal matter

200-280µl of the faecal sample (either from frozen or preserved in liquid) was transferred to Lysing Matrix tube E (provided with kit). Lysing Matrix E consist of 1.4 ceramic spheres, 0.1 mm silica spheres, and one 4 mm glass bead – this mixture of ceramic and silica particles is designed to efficiently lyse all organisms including gram positive bacteria, and fungi. First 980µl Sodium Phosphate Buffer and then 120 µl of MT buffer were added to bead beating tubes containing the faecal sample. These two reagents were developed to protect and solubilize nucleic acids and proteins during the cell lysis step that followed.

The mixture was homogenized, and cells were mechanically disrupted through extremely quick and vigorous mixing in the FastPrep instrument for 3 mins at a speed setting of 6.0. Mechanical lysis results in higher DNA yields than enzymatic lysis (Maukonen, Simões and Saarela, 2012). The bead-beating step improves the cell lysis step as it helps to recover DNA not only from gram-negative but also gram-positive bacteria. The latter of the two have a thick cell wall that requires rigorous mechanical disruption to free contained DNA (de Boer *et al.*, 2010; Salonen *et al.*, 2010). After homogenization, samples were centrifuged at maximum speed (14,000 rpm) for 15 min to pellet debris. Following centrifugation, 1 ml of the supernatant was transferred to a catch tube (=clean 2.0mL microcentrifuge tube) containing 250µl of Protein Precipitation Solution (PPS). Samples were mixed by inverting the tube 10 times by hand and centrifuged for 10 minutes at full speed to pellet the precipitate (a step to separate the solubilized nucleic acids from lysing matrix and cellular debris). 1ml of the sample supernatant was transferred to 5mL Eppendorf tubes that contained 1mL of resuspended Binding Matrix. In this step, nucleic acids bind to the silica matrix in the presence of chaotropic salts which allows to purify DNA.

Samples were inverted for 2 minutes allowing DNA to bind and placed aside for a minimum of 3min (and a maximum of one hour) to allow matrix to settle. Then 500µl of the supernatant were discarded and the remaining binding matrix now bound to the DNA was resuspended. 700µl of the resuspended solution were transferred into SPIN filter tubes and centrifuged at 14,000 rpm for 2 min. The catch tube was emptied, and the step was repeated until all of the mixture had been added to the SPIN filter which was binding the DNA. Then next step was washing; 500µl SEWS-M solution were used to resuspend the pellet that had formed in the SPIN filter. This step uses desalting ethanol and other detergents to remove impurities. The tubes were centrifuged at full speed for 5 min, the catch tubes were emptied, and this was followed by another dry spin centrifugation step of 5 min to get rid of residual ethanol. The SPIN filters were incubated at room temperature for 10 min and eluted in 80µl of DNase/Pyrogen-Free water (DES buffer) which is a low salt elution that leads to the collapse cation bridges and thus rehydrates the silica and DNA. During centrifugation (at 14,000rpm for 5 min) the DNA passes through the filter bucket and is collected in a clean tube. The eluted DNA was transferred to cryovial tubes and stored at -20°C.

Quality control of DNA from faecal matter

Qubit working solution was prepared by diluting 1µL (x n sample) of Qubit® dsDNA BR Reagent with 199µL (x n sample). Then the two standards (Standard 1 and 2) were prepared as follows. First, we added 190µL of the working solution to each thin-walled 500µL Eppendorf. Then we added 10µL of Qubit® dsDNA BR Standard #1 solution to “Standard 1” and 10µL of Qubit® dsDNA BR Standard #2 solution to “Standard 2”, resulting in a final volume of 200µL. The samples that were to be tested were set up similarly, however, for the test samples we added 198uL of the working solution to individual assay tube and then added 2µL of the respective test sample. All tubes were mixed by vortexing for 2-3 seconds and then briefly centrifuged to bring any liquid down. Next, all samples were incubated at room temperature and away from light for 2 minutes. We then proceeded to the Qubit 3.0

Fluorometer machine calibrated to BR assay with a total volume of 100µL and set up the machine to read first Standard 1 and then 2. Following this all samples were run one by one. Concentration results on the Qubit® 3.0 Fluorometer are automatically calculated and given in µg/mL.

Library preparation

The genomic DNA of all baseline samples (N=80) was normalised to 0.5ng/µl with EB (10mM Tris-HCl). 0.9 µl of TD Tagment DNA Buffer (Illumina Catalogue No. 15027866) was mixed with 0.09 µl TDE1, Tagment DNA Enzyme (Illumina Catalogue No. 15027865) and 2.01 µl PCR grade water in a master mix and 3µl added to a chilled 96 well plate. 2 µl of normalised DNA (1ng total) was pipette mixed with the 3 µl of the Tagmentation mix and heated to 55 °C for 10 minutes in a PCR block. A PCR master mix was made up using 4 µl kapa2G buffer, 0.4 µl dNTP's, 0.08 µl Polymerase and 6.52 µl PCR grade water, contained in the Kap2G Robust PCR kit (Sigma Catalogue No. KK5005) per sample and 11 µl were added to each well. 2 µl of each P7 and P5 of Nextera XT Index Kit v2 index primers (Illumina Catalogue No. FC-131-2001 to 2004) were added to each well. Finally, the 5 µl of Tagmentation mix was added and mixed. The PCR was run with 72°C for 3 minutes, 95°C for 1 minute, 14 cycles of 95°C for 10s, 55°C for 20s and 72°C for 3 minutes. Following the PCR reaction, the libraries were quantified using the Quant-iT dsDNA Assay Kit, high sensitivity kit (Catalogue No. 10164582) and run on a FLUOstar Optima plate reader. Libraries were pooled following quantification in equal quantities. The final pool was double-SPRI size selected between 0.5 and 0.7X bead volumes using KAPA Pure Beads (Roche Catalogue No. 07983298001). The final pool was also run MiSeq Nano V2 kit. The index distribution was checked, and samples were re-pooled on those values. The final pool was subjected to a second MiSeq Nano run. The final pool was quantified on a Qubit 3.0 instrument and run on a High Sensitivity D1000 ScreenTape (Agilent Catalogue No. 5067-5579) using the Agilent Taestation 4200 to calculate the final library pool molarity.

The pool was run at a final concentration of 1.8 pM on an Illumina Nextseq500 instrument using a Mid Output Flowcell (NSQ® 500 Mid Output KT v2(300 CYS) Illumina Catalogue FC-404-2003) following the Illumina recommended denaturation and loading recommendations which included a 1% PhiX spike in (PhiX Control v3 Illumina Catalogue FC-110-3001). Data was uploaded to Basespace (www.basespace.illumina.com) where the raw data for each sample was converted to 8 FASTQ files.

Library quality control by NOVOGENE

(1) Distribution of Sequencing Quality

This shows the probability that the right base quality value was given during the sequencing. A quality score (Q-score) of 10 means has a probability of 90% for the right base, whilst Q-20, Q-30 and Q-40 have a probability of 99%, 99.9% and 99.99% for right base, respectively.

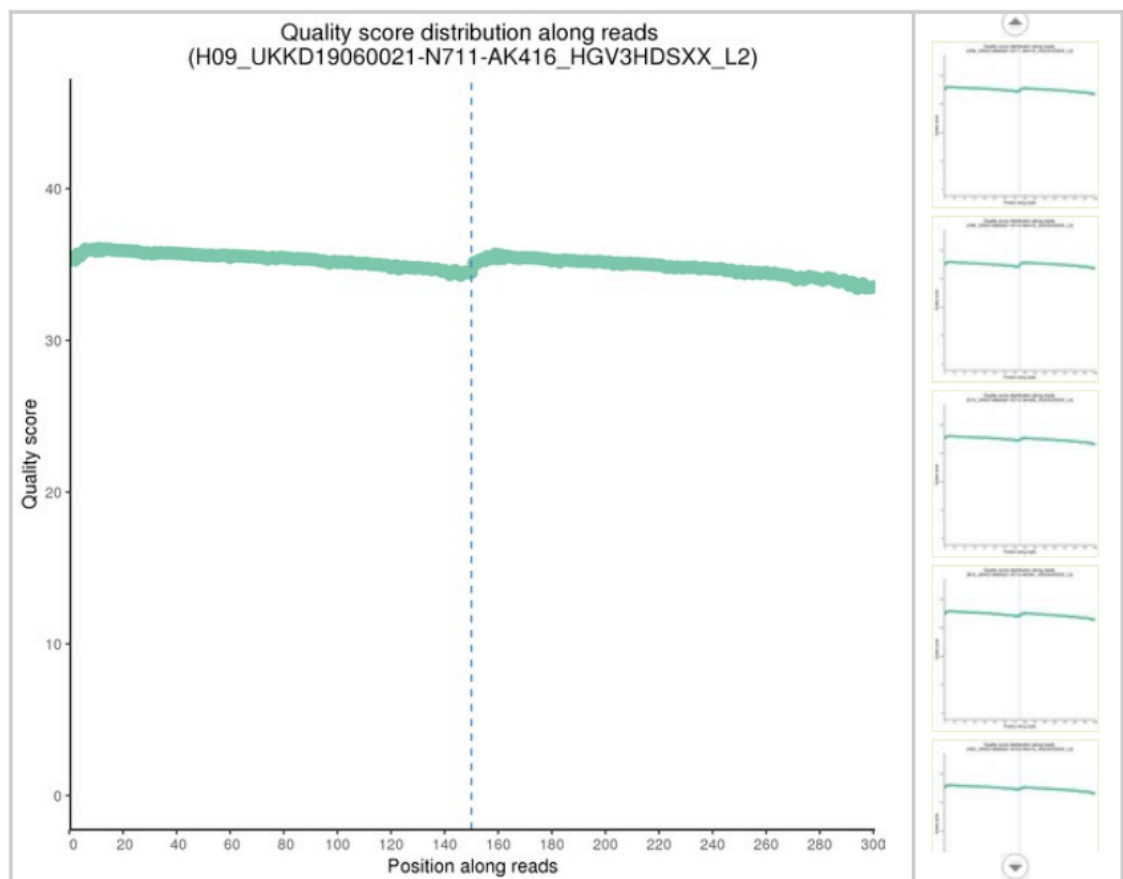


Figure 7.8 Example distribution of Sequencing Quality for submitted sample H09

(2) Distribution of Sequencing Error Rate

Illumina SBS technology is subject to two sources of error. Error rates increase as more sequencing reagent is consumed and the first several bases have a higher probability for sequencing errors than others. The error rate for single bases along the read should be lower than 1%.

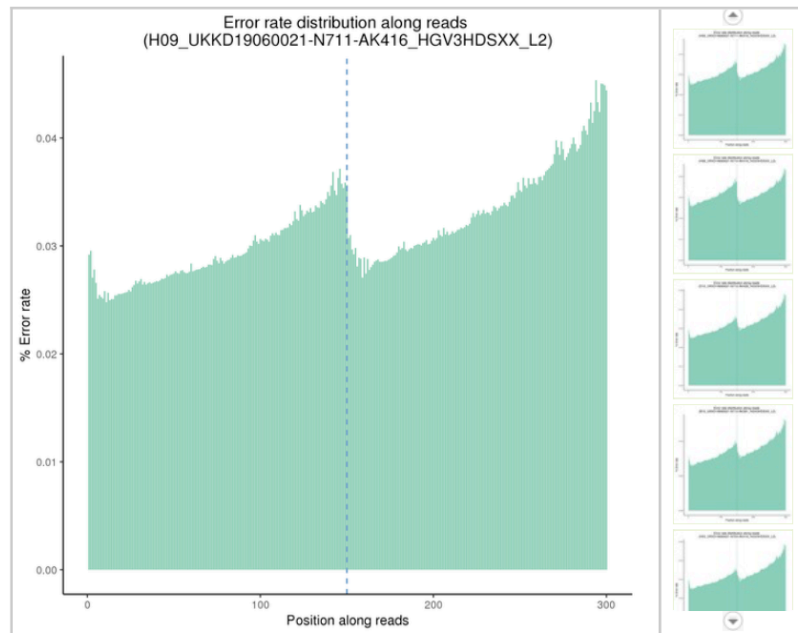


Figure 7.9 Example error rate distribution along reads for submitted sample H09

(3) Distribution of A/T/G/C Base

Following the principle of complementary bases, the content of AT and GC bases should be constant during the sequencing. In reality, the distribution will vary for the first several nucleotides.

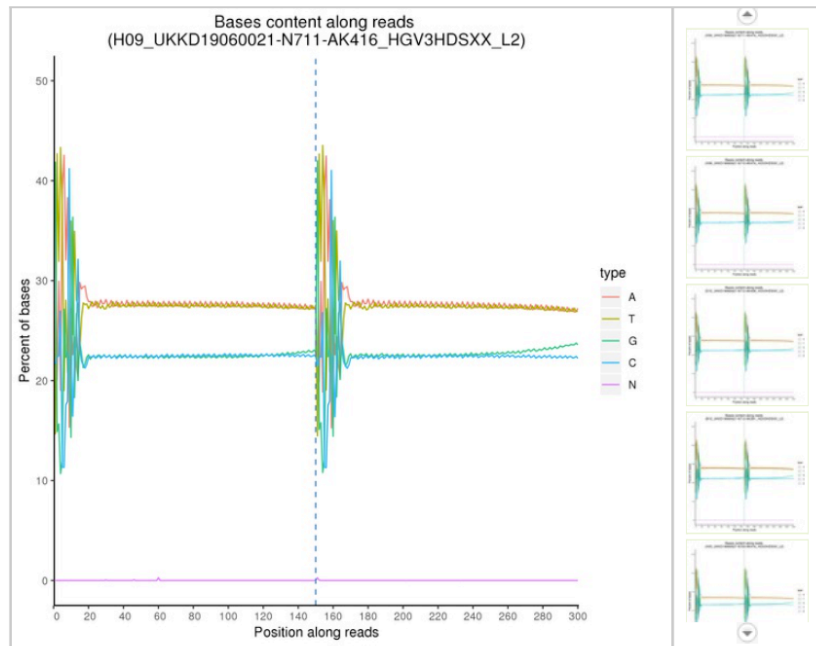


Figure 7.10 Example distribution of A/T/G/C content for submitted sample H09

Data quality control by NOVOGENE

(1) Raw Data Filtering

The sequenced raw reads contain low quality reads (containing N = base cannot be determined with enough accuracy, Q-score below 5) and adapter sequences that need to be filtered out.

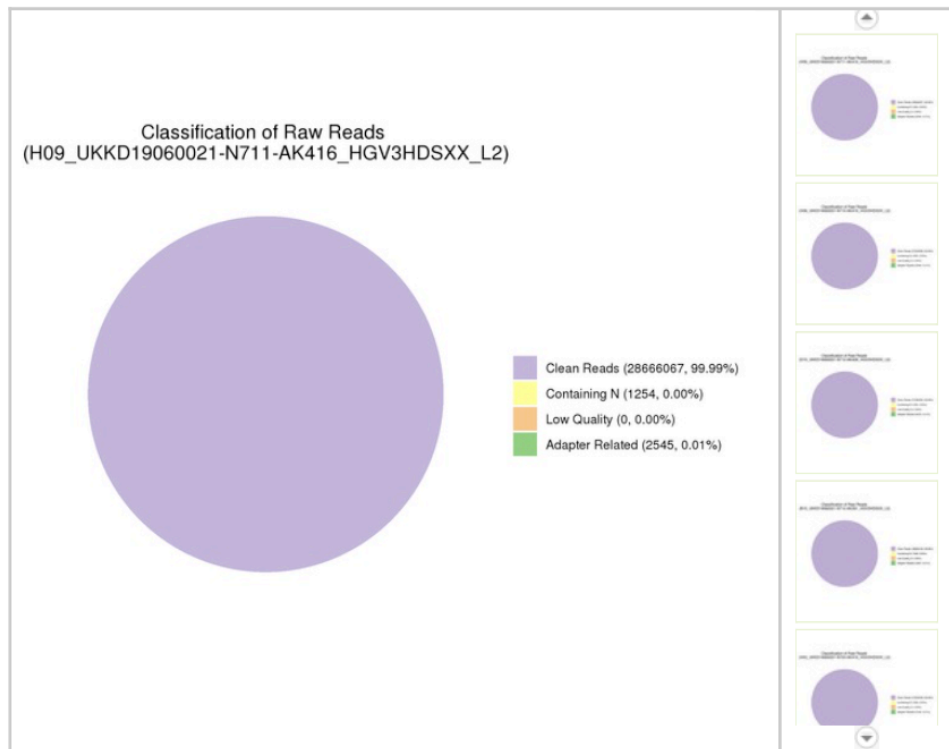


Figure 7.11 Example composition of Raw Reads for submitted sample H09

Table 7.5 Excerpt of Summary of Sequencing Data information provided by NOVOGENE for three T2 samples

Sample	Raw Reads	Clean Reads	Raw Base (G)	Clean Base (G)	Effective Rate (%)	Error Rate (%)	Q20 (%)	Q30 (%)	GC content (%) ¹⁰
S7	84.866.496	84.848.308	25.5	25.5	99.98	0.03	96.28	90.75	47.59
S45	109.735.347	109.712.030	32.9	32.9	99.98	0.03	96.78	91.72	49.23
S53	65.154.518	65.141.296	19.5	19.5	99.98	0.03	96.05	89.97	49.38

Processing of sequenced metagenomics data

(i) QC involves to removing all human reads, which was performed using bbmap (Version 28.76) and cleaning of the paired-end reads. For this Illumina adapters and phiX internal Illumina standards were removed and quality trimming with a minimum Phred quality score of 30 (=99.9% correct base calling) was carried out using *fastp* (version 0.21.0).

(ii) Taxonomic classification and ‘read-by-read analysis’ were obtained using MetaPhlan2 (version 2.7.8, database: mpa_v20_m200). The resultant read, and relative abundance information were used in downstream taxonomic statistical analysis.

(iii) The *de novo* assembly was performed using MEGAHIT (version 1.1.3). Functional gene prediction and annotation of the contigs was done with Metaprokka (v1.14.6c). Finally, a count matrix for KEGG was produced using eggnoG mapper (v2.0.1; emapper database: v2.0) and custom scripts. Humann3 (v. 3.0.0.alpha.1; nucleotide database: uniref90; protein database: full_chocophlan. v296_201901) was used to create pathway abundance files presenting relative abundance of pathways in the community.

Microbiome Analyst workflow – detailed description

In a first step, the pre-processed KEGG gene abundance table and associated metadata file were uploaded using the SDP module of the Microbiome Analyst (this was done separately for each time point). The next step is data inspection. In this step, a summary of the submitted

gene abundance table, including the total gene number and average counts per sample, and a Library Size Overview which is a graphical summary of the read counts per sample are generated. The third step is data filtering. The low count filter parameters were set to include all features with a minimum count of “1” and a prevalence in samples of “10%”. The low variance filter for feature removal was set to 0%, as we are more concerned with losing data unnecessarily rather than with noise in this type of data. The final step before data can be analysed, is data normalization. Here, we opted to apply centred-log-ratio (CLR) for data transformation (as this is commonly used and recommended to overcome compositionality issues) but applied no other scaling or data rarefying steps.

Results neuropsychological assessment of Apolipoprotein E groups

Addenbrooke’s Cognitive Examination-III

Table 7.6 Multivariate regression analysis results, Addenbrooke’s Cognitive Examination-III summary score

ACE III summary score				
Observations: 74, R^2 : 0.17 F(4,69)=0.83, p=0.51				
Predictors	β coefficient	CI	Standardized beta values	p-value
(Intercept)	92.28	89.42 – 104.29		<0.001
age	-0.02	-0.13 – 0.09	-0.04	0.726
educational attainment [college]	-1.62	-3.42 – 0.18	-0.25	0.078
educational attainment [university]	1.17	-0.39 – 2.72	0.21	0.139
APO ϵ 4 status [carriers]	-0.63	-1.91 – 0.65	-0.11	0.327

Rey-Osterrich-Complex Figure test

Table 7.7 Multivariate regression analysis results, Rey-Osterrich-Complex Figure: Copy score

Rey-Osterrich-Complex Figure: Copy score				
Observations: 74, R^2 : 0.086 F(4,69)=1.62, p=0.179				
Predictors	β coefficient	CI	Standardized beta values	p-value
(Intercept)	32.86	25.10 – 40.62	0.00	<0.001
age	-0.00	-0.11 – 0.11	0.00	0.994
educational attainment [college]	-1.40	-3.26 – 0.46	-0.22	0.137
educational attainment [university]	-1.97	-3.60 – -0.35	-0.35	0.018
APO ϵ 4 status [carriers]	0.55	-0.79 – 1.89	0.10	0.415

Table 7.8 Multivariate regression analysis results, Rey-Osterrich-Complex Figure: Recall score

Observations: 74, R ² : 0.048 F(4,69)=0.86, p=0.489				
Predictors	β coefficient	CI	Standardized beta values	p-value
(Intercept)	30.50	15.70 – 45.30	0.00	< 0.001
age	-0.17	-0.39 – 0.04	-0.19	0.118
educational attainment [college]	-1.22	-4.76 – 2.33	-0.10	0.496
educational attainment [university]	-0.01	-3.12 – 3.10	-0.00	0.994
APO ϵ 4 status [carriers]	-0.53	-3.08 – 2.02	-0.05	0.678

Table 7.9 Multivariate regression analysis results, Rey-Osterrich-Complex Figure: Copy time

Observations: 74, R ² : 0.009 F(4,69)=0.16, p=0.955				
Predictors	β coefficient	CI	Standardized beta values	p-value
(Intercept)	117.79	-130.25 - 365.82	0.00	0.347
age	0.87	-2.75 – 4.48	0.06	0.633
educational attainment [college]	-6.05	-65.46 – 53.36	-0.03	0.840
educational attainment [university]	-0.66	-52.76 – 51.45	-0.00	0.980
APO ϵ 4 status [carriers]	14.64	-28.08 – 57.37	0.08	0.496

Table 7.10 Person Product-moment correlation coefficient (r) between Rey-Osterrich-Complex Figure variables by group

	(1) COPY SCORE	(2) RECALL SCORE
Apo ϵ 4 non-carriers		
(1) copy score		
(2) copying time	r=0.23, p=0.154	
(3) recall score	r=0.13, p=0.420	r=0.05, p=0.755
Apo ϵ 4 carriers		
(1) copy score		
(2) copying time	r=0.28, p=0.089	
(3) recall score	r=0.34, p=0.039*	r=-0.20, p=0.220

* denotes p<0.05

Trail Making Test

Table 7.11 Multivariate regression analysis results, Trail Making Test-A

Observations: 72, R ² : 0.106 F(4,67)=1.99, p=0.105				
Predictors	β coefficient	CI	Standardized beta values	p-value
(Intercept)	1.65	-27.08 – 30.38	0.00	0.909
age	0.45	0.03 – 0.86	0.26	0.034
educational attainment [college]	6.34	-0.63 – 13.31	0.27	0.074
educational attainment [university]	3.79	-2.31 – 9.89	0.18	0.219
APO ϵ 4 status [carriers]	-1.14	-6.04 – 3.75	-0.06	0.643

Table 7.12 Multivariate regression analysis results, Trail Making Test-B

Observations: 72, R ² : 0.009 F(4,67)=3.64, p=0.51				
Predictors	β coefficient	CI	Standardized beta values	p-value
(Intercept)	1.32	-54.36 – 56.99	0.00	0.962
age	1.11	0.30 – 1.91	0.32	0.008
educational attainment [college]	-4.66	-18.17 – 8.84	-0.10	0.493
educational attainment [university]	-5.53	-17.35 – 6.29	-0.13	0.354
APO ϵ 4 status [carriers]	-6.60	-16.09 – 2.89	-0.16	0.170

Supermarket task

Table 7.13 Multivariate regression analysis results, Supermarket test

Egocentric orientation				
Observations: 70				
Predictors	β coefficient	CI	SE	p-value
(Intercept)	18.70	9.17 – 28.23	4.99	<0.001
age	-0.12	-0.27 – 0.02	0.07	0.103
APO ϵ 4 status [carriers]	0.89	-0.77 – 2.54	0.86	0.310
sex	0.41	-1.36 – 2.19	0.93	0.659
educational attainment [college]	-3.06	-5.37 – -0.75	1.21	0.014
educational attainment [university]	-1.04	-3.08 – 1.00	1.07	0.332
Allocentric orientation (log transformed)				
Observations: 66				
Predictors	β coefficient	CI	SE	p-value
(Intercept)	2.51	1.55 – 3.48	0.51	<0.001
age	0.01	-0.00 – 0.03	0.01	0.144
APO ϵ 4 status [carriers]	-0.04	-0.21 – 0.13	0.09	0.646
sex	-0.09	-0.27 – 0.09	0.09	0.341
educational attainment [college]	0.23	-0.00 – 0.46	0.21	0.064
educational attainment [university]	0.23	-0.02 – 0.44	0.11	0.037
Heading direction				
Observations: 66				
Predictors	β coefficient		SE	p-value
(Intercept)	12.66		3.82	0.002
age	-0.02		0.06	0.673
APO ϵ 4 status [carriers]	-0.03		0.67	0.962
sex	1.00		0.71	0.164
educational attainment [college]	-0.05		0.90	0.574
educational attainment [university]	0.38		0.81	0.644
Central vs peripheral navigation preference				
Observations: 64				
Predictors	β coefficient		SE	p-value
(Intercept)	2.22		1.67	0.190
age	-0.02		0.03	0.410
APO ϵ 4 status [carriers]	0.61		0.30	0.045
sex	-0.20		0.32	0.535
educational attainment [college]	-0.54		0.41	0.199
educational attainment [university]	0.17		0.37	0.647

Table 7.14 Multilevel mixed model results, Sea Hero Quest: wayfinding distance

Wayfinding distance					
Marginal R ² : 0.630					
Fixed effects	β coefficient	CI	SE	t-value	p-value
(Intercept)	2.04	1.51 – 2.57	0.26	7.56	<0.001
age	-0.01	-0.02 – -0.00	0.00	-2.38	0.017
sex [male]	-0.07	-0.03 – 0.17	0.05	1.36	0.174
APO ϵ 4 status [carriers]	-0.00	-0.09 – 0.09	0.05	-0.00	0.993
educational attainment [College]	-0.07	-0.20 – 0.05	0.06	-1.11	0.269
educational attainment [University]	0.03	-0.08 – 0.14	0.06	0.49	0.625
level [8]	-0.76	0.86 – -0.65	0.05	-14.18	<0.001
level [11]	-0.95	-1.06 – -0.84	0.05	-17.63	<0.001
Random effects					
σ^2	0.10				
τ_{00} subject_id	0.00				
N subject_id	73				
N level ID	3				

Marginal R² = variance explained by fixed effects. Due to the inverse data transformation of the data, all coefficients have opposite signs.

Table 7.15 Multilevel mixed model results, Sea Hero Quest: wayfinding duration

Wayfinding duration					
Marginal R ² : 0.514					
Fixed effect	β coefficient	CI	SE	t-value	p-value
(Intercept)	-0.38	-0.95 – 0.18	0.29	-1.33	0.183
age	0.01	0.01 – 0.02	0.00	3.43	0.001
sex [male]	-0.15	-0.15 – -0.04	0.05	-2.79	0.005
APO ϵ 4 status [carriers]	0.08	-0.01 – 0.18	0.05	1.71	0.088
educational attainment [College]	0.09	-0.04 – 0.23	0.07	1.37	0.170
educational attainment [Univer.]	0.07	-0.04 – 0.19	0.06	1.21	0.227
level [8]	0.39	0.30 – 0.48	0.05	8.43	<0.001
level [11]	0.71	0.61 – 0.80	0.05	15.16	<0.001
Random effects					
σ^2	0.08				
τ_{00} subject id	0.01				
N subject_id	73				

Marginal R² = variance explained by fixed effects

Table 7.16 Multilevel mixed model results, Sea Hero Quest: wayfinding distance to border

Wayfinding distance to border					
Marginal R ² : 81.7					
Fixed effect	β coefficient	CI	SE	t-value	p-value
(Intercept)	24.34	18.43– 30.26	3.02	8.07	<0.001
age	-0.06	-0.15–0.03	0.04	-1.39	0.165
sex [male]	1.29	0.21 – 2.38	0.55	2.34	0.019
APO ϵ 4 status [carriers]	-0.10	-1.10– 0.89	0.51	-0.20	0.840
educational attainment [College]	-0.38	-1.76–1.00	0.70	-0.54	0.591
educational attainment [Univer.]	0.19	-1.02–1.39	0.61	0.30	0.762
level [8]	-1.67	-2.66–0.69	0.50	-3.34	0.001
level [11]	-15.01	-16.00–14.02	0.51	-29.69	<0.001
Random effects					
σ^2	8.89				
τ_{00} subject_id	1.22				
N subject_id	73				

Marginal R² = variance explained by fixed effects

Table 7.17 Mixed effects ordinal logistic regression results, Sea Hero Quest: flare accuracy

Flare accuracy					
Marginal R ² =0.116					
Conditional R ² =0.195					
Predictors	β coefficient	Std. Error	Odds Ratio	95% CIs	p-value
age	0.01	0.02	1.01	0.97 – 1.07	0.551
sex [male]	0.69	0.33	2.01	1.05 – 3.84	0.034*
APO ϵ 4 status [carriers]	0.04	0.29	0.96	0.55 – 1.68	0.885
educational attainment [College]	-0.24	0.41	0.79	0.35 – 1.76	0.562
educational attainment [University]	-0.45	0.36	0.64	0.32 – 1.28	0.207
level ID [34]	-0.72	0.38	0.49	0.23 – 1.04	0.062
level ID [49]	-1.64	0.39	0.19	0.09 – 0.42	<0.001**
level ID [54]	-1.24	0.39	0.29	0.14 – 0.62	0.001**
Random Effects					
σ^2	3.29				
τ_{00} subject_id	0.28				
ICC	0.08				
N subject_id	71				

* p<0.05, **p<0.01, ***p<0.001

Cognitive Change Index

Table 7.18 Multiple regression analysis results, Cognitive Change Index: summary score

Observations: 69, R^2 : 0.009
 $F(4,64)=0.14$, $p=0.967$

Predictors	β coefficient	CI	Standardized beta values	p-value
(Intercept)	23.85	1.07 – 46.64	0.00	0.040
age	0.05	-0.28 – 0.39	0.41	0.750
educational attainment [college]	-0.31	-5.63 – 5.01	-0.02	0.908
educational attainment [university]	0.62	-4.14 – 5.37	0.04	0.797
APO ϵ 4 status [carriers]	1.14	-2.78 – 5.06	0.07	0.565

Generalized Anxiety Disorder-7

Table 7.19 Percentage of participants experiencing anxiety by severity categories and by Apolipoprotein ϵ 4 status

GAD-7 anxiety severity	APO ϵ 4 non-carriers (%) n=39	APO ϵ 4 carriers (%) n=36	χ^2 (df)	p-value
none (≤ 4)	97.4	94.4	12.50 (6)	0.051
mild (5-9)	2.6	5.6		
moderate (10-14)	0	0		
severe (15-21)	0	0		

Table 7.20 Multivariate regression results, Generalized Anxiety Disorder-7

Observations: 65, R^2 : 0.124
 $F(4,60)=2.13$, $p=0.089$

Predictors	β coefficient	CI	Standardized beta values	p-value
(Intercept)	7.02	2.61 – 11.44	0.00	0.002
age	-0.09	-0.15 – -0.02	-0.34	0.008
educational attainment [college]	-0.00	-1.07 – 1.06	-0.00	0.993
educational attainment [university]	-0.55	-1.52 – 0.41	-0.17	0.994
APO ϵ 4 status [carriers]	0.00	-0.80 – 0.81	0.00	0.255

Patient Health Questionnaire-9

Table 7.21 Frequency distribution of depression severity by Apolipoprotein E genotype

Depression severity	APO ϵ 4 non-carriers (%), n=39	APO ϵ 4 carriers risk (%), n=36	χ^2 (df)	p-value
none (≤ 4)	87.2	80.6	13.70 (10)	0.19
mild (5-9)	10.2	19.4		
moderate (10-14)	0	0		
moderately severe (15-19)	2.6	0		
severe (20-27)	0	0		

Table 7.22 Multivariate regression results, Patient Health Questionnaire-9

Observations: 65, R ² : 0.060 F(4,60)=0.95, p=0.440				
Predictors	β coefficient	CI	Standardized beta values	p-value
(Intercept)	7.27	-0.32 – 14.85	0.00	0.060
age	-0.09	-0.20 – 0.03	-0.20	0.133
educational attainment [college]	0.15	-1.68 – 1.99	0.03	0.869
educational attainment [university]	0.71	-0.94 – 2.36	0.13	0.392
APO ϵ 4 status [carriers]	-0.32	-1.69 – 1.06	-0.06	0.648

Cambridge Behavioural Inventory-Revised

Table 7.23 Multivariate regression results, Cambridge Behavioural Inventory-Revised: summary score

Observations: 70, R ² : 0.090 F(4,65)=1.61, p=0.182				
Predictors	β coefficient	CI	Standardized beta values	p-value
(Intercept)	15.82	3.16 – 28.49	0.00	0.015
age	-0.17	-0.35 – 0.02	-0.22	0.076
educational attainment [college]	0.21	-2.74 – 3.16	0.02	0.887
educational attainment [university]	0.30	-2.34 – 2.93	0.03	0.882
APO ϵ 4 status [carriers]	-2.25	-4.43 – -0.07	-0.25	0.043

Microbiome health questionnaire

Table 7.24 Response frequencies of microbiome questionnaire by Apolipoprotein ϵ 4 status, Pearson Chi-squared (χ^2) and p-value

Question Item	APO ϵ 4 non-carriers n=39	APO ϵ 4 carriers, n=35	χ^2 (df)	p-value
1. How would you classify your diet?				
Omnivore	87.2%	88.6%	5.98 (4)	0.20
Vegetarian	12.8%	8.5%		
Vegan	0%	2.9%		
2. Taking a daily multivitamin?	20.5%	25.7%	0.06 (1)	0.80
3. Taking any other nutritional/herbal supplements?	42.1%	45.7%	0.01(1)	0.94
4. Lactose intolerant	5.1%	2.9%	0.00 (1)	1.00
5. Gluten intolerant	5.1%	2.9%	0.00 (1)	1.00
6. I am allergic to (<i>missing n=1</i>)				
Peanuts	5.1%	0%	2.25 (3)	0.52
Shellfish	5.1%	5.9%		
Other	2.6%	5.9%		
No allergies	87.2%	88.2%		
7. Diabetes	0%	0%	0.22 (1)	0.64
8. Do you follow any other special diet restrictions other than those indicated above? (<i>missing n=2</i>)				
Yes	13.2%	9.1%	0.03 (1)	0.87
9. What is your race/ethnicity? (<i>missing n=1</i>)				
Caucasian	100%	100%	0.34 (1)	0.56
10. When did you move to East Anglia (Norfolk, Suffolk)? (<i>missing n=3</i>)	100%	100%	0.22 (1)	0.64

I have lived in East Anglia for more than a year.					
11. I have travelled outside of the UK in the past ...					
I have not been outside the UK in the past year					
1 month	30.8%	31.4%	7.74 (4)	0.10	
3 months	10.3%	8.6%			
6 months	12.8%	31.4%			
1 year	7.7%	14.3%			
	38.5%	14.3%			
12. Where do you live?					
In the city	35.9%	34.3%	0.00 (1)	1.00	
In the countryside	64.1%	65.7%			
13. Do you live in your own home?					
Yes	100%	100%	0.22 (1)	0.64	
14. Do you lived in a shared community housing such as a nursing home?					
No	100%	100%	0.22 (1)	0.64	
15. Do you eat the majority of your meals in your place of residence?					
Yes	100%	100%	0.22 (1)	0.64	
16. How many other people do you live with?					
None	28.2%	22.9%	2.29 (3)	0.52	
One	56.4%	65.7%			
Two	10.3%	11.4%			
Three	5.1%	0%			
17. Has dog(s)?					
	28.2%	28.6%	0 (1)	1.00	
18. Has cat(s)?					
	12.2%	20%	0.27 (1)	0.60	
19. Which is your dominant hand?					
Right-handed	87.8%	80%	1.70 (2)	0.43	
Left-handed	7.7%	17.1%			
Ambidextrous	5.1%	2.9%			
20. How often do you exercise?					
Never	2.6%	5.7%	2.64 (4)	0.60	
Rarely (few times/months)	5.1%	14.3%			
Occasionally (1-2 times/week)	20.5%	14.3%			
Regularly (3-5 times/week)	33.3%	28.6%			
Daily	38.5%	37.1%			
21. Do you regularly exercise indoors or outdoors?					
Indoors	10.3%	2.9%	4.55 (4)	0.34	
Outdoors	33.3%	48.6%			
Both	43.6%	40%			
None	2.6%	5.7%			
22. Do you bite your fingernails?					
Yes	10.3%	2.9%	0.64 (1)	0.42	
23. How often do you use a swimming pool/sauna?					
Never	46.2%	60%	4.65 (3)	0.20	
Rarely (few times/months)	25.6%	31.4%			
Occasionally (1-2 times/week)	17.9%	5.7%			
Regularly (3-5 times/week)	10.3%	2.9%			
Daily	0%	0%			
24. How often do you smoke cigarettes?					
Never	100%	91.4%	1.63 (1)	0.20	
Rarely (few times/months)	0%	8.6%			
25. How often do you drink alcohol?					
Never	17.9%	2.9%	6.01 (4)	0.19	
Rarely (few times/months)	10.3%	22.9%			
Occasionally (1-2 times/week)	23.1%	28.6%			
Regularly (3-5 times/week)	33.3%	28.6%			
Daily	15.4%	17.1%			
26. How often do you brush your teeth?					
Regularly (3-5 times/week)	5.1%	5.7%	0.00 (1)	1.00	
Daily	94.9%	94.3%			
27. How often do you floss your teeth?					
Never	7.7%	25.7%			
Rarely (few times/months)	5.1%	8.6%			

	Occasionally (1-2 times/week)	12.8%	11.4%	5.39 (4)	0.25
	Regularly (3-5 times/week)	28.2%	17.1%		
	Daily	46.2%	37.1%		
28. How often do you wear facial cosmetics?				4.29 (4)	0.37
	Never	46.2%	37.1%		
	Rarely (few times/months)	12.8%	17.1%		
	Occasionally (1-2 times/week)	0%	8.6%		
	Regularly (3-5 times/week)	23.1%	17.1%		
	Daily	17.9%	20%		
29. Do you use deodorant or antiperspirant? (<i>missing n=1</i>)				5.22 (3)	0.16
	Antiperspirant	39.5%	28.6%		
	Deodorant	42.1%	45.7%		
	Not sure but I use some form of antiperspirant/deo	18.4%	14.3%		
	Neither	0%	11.4%		
30. Approximately how many hours of sleep do you get in an average night?				2.46 (4)	0.65
	Less than 5 hours	7.7%	5.7%		
	5-6 hours	12.8%	14.3%		
	6-7 hours	51.3%	45.7%		
	7-8 hours	25.6%	22.9%		
	8 hours or more	2.6%	11.4%		
31. Do you use fabric softener when drying your clothes? (<i>missing n=1</i>)				1.04 (1)	0.31
	Yes	36.8%	51.4%		
32. I have taken antibiotics in the last...				3.49 (3)	0.32
	month	2.4%	0%		
	6 months	5.1%	14.3%		
	year	20.5%	11.4%		
	I have taken no antibiotics in the past year	71.8%	74.3%		
33. I have gotten a flu vaccine in the last...				3.70 (4)	0.45
	week	5.1%	0%		
	month	2.6%	2.9%		
	6 months	35.9%	37.1%		
	year	17.9%	8.6%		
	I didn't get the flu vaccine in the past year	38.5%	51.4%		
34. Are you currently taking any of the following medications?				4.25 (4)	0.37
	Yes, to control blood pressure.	20.5%	25.7%		
	Yes, to control cholesterol.	10.3%	5.7%		
	Yes, for gut symptoms such as constipation/diarrhoea or irritable bowel syndrome.	7.6%	2.9%		
	Yes, for other disorders or conditions.	33.3%	20%		
	No.	28.2%	45.7%		
36. In the last 6 months, my weight has...				2.35 (2)	0.31
	increased more than 4kg	7.7%	5.7%		
	decreased more than 4kg	2.6%	11.4%		
	remained stable	89.7%	82.9%		
37. Have you had your tonsils removed?				0.15 (1)	0.70
	Yes	38.5%	31.4%		
38. Have you had your appendix removed?				0.03 (1)	0.86
	Yes	10.3%	14.3%		
39. Have you had food poisoning?				0.11 (1)	0.74
	Yes	30.7%	37.1%		
40. Do you currently take prescription medication for any gut related symptoms?				0.01 (1)	0.91
	Yes	17.9%	14.3%		
41. Do you consume any probiotic based food products such as yoghurts? (<i>missing n=1</i>)				2.30 (1)	0.13
	Yes	60.5%	40%		
42. Do you currently take any over the counter or prescription medicine for other conditions? (<i>missing n=2</i>)				0.00 (1)	0.97
	Yes	47.4%	44.1%		

43. Were you born via caesarean section (C-section) (missing n=1)					
	Yes	5.1%	2.9%	0.46 (2)	0.79
	No	89.7%	94.1%		
	Not sure	5.1%	2.9%		
44. As an infant were you breastfed? (missing n=4)					
	Yes	75%	70.6%	1.12 (2)	0.57
	No	25%	26.5%		
	Not sure	0%	2.9%		
45. Do you have asthma?					
	Yes	15.4%	11.4%	0.25 (2)	0.88
	No	82.1%	85.7%		
	Not sure	2.6%	2.9%		
46. Do you have seasonal allergies?					
	Yes	23.1%	22.9%	1.13 (2)	0.57
	No	76.9%	74.3%		
	Not sure	0%	2.9%		

Cardiovascular Risk

Table 7.25 Multivariate regression results, Low-density lipoprotein and total cholesterol

LDL				
Observations: 25, R^2 : 0.325 F(3,21)=3.365				
Predictors	β coefficient	Confidence Intervals	Standardized β coefficient	p-value
(Intercept)	-2.95	-11.86–5.97		0.499
APO ϵ 4 status	1.93	0.66 – 3.20	0.65	0.005**
age	0.07	-0.05 – 0.20	0.27	0.220
sex	0.38	-0.81 – 1.56	0.12	0.516
Total cholesterol				
Observations: 32, R^2 : 0.204 F(3,28)=2.395				
Predictors	β coefficient	Confidence Intervals	Standardized β coefficient	p-value
(Intercept)	3.31	-5.19–11.80		0.432
APO ϵ 4 status [carriers]	1.42	0.25 – 2.59	0.48	0.019*
age	0.04	-0.08 – 0.15	0.12	0.533
sex	-0.26	-1.36 – 0.84	-0.08	0.634

Table 7.26 Multivariate regression results, Triglycerides and High-density lipoprotein

Triglycerides				
Observations: 31, R^2 : 0.153 F(3,27)=1.630				
Predictors	β coefficient	Confidence Intervals	Standardized β coefficient	p-value
(Intercept)	4.60	-2.45 – 11.66		0.192
APO ϵ 4 status [carriers]	-0.85	-1.81 – 0.11	-0.39	0.080
age	-0.02	-0.12 – 0.08	-0.08	0.220
sex	-0.43	-1.29 – 0.42	-0.19	0.516
HDL				
Observations: 32, R^2 : 0.08 F(3,28)=0.531				
Predictors	β coefficient	Confidence Intervals	Standardized β coefficient	p-value
(Intercept)	3.03	0.21 – 5.84		0.036
APO ϵ 4 status [carriers]	-0.07	-0.46 – 0.32	-0.07	0.720
age	-0.01	-0.05 – 0.02	-0.17	0.444
sex	-0.26	-0.62 – 0.11	-0.27	0.162

Microbiome results of Apolipoprotein E cohorts

Table 7.27 Alpha diversity by taxonomic level between the Apolipoprotein E groups at baseline (T1), 6-months follow-up (T2), 12-months follow-up (T3)

Taxonomic level	Measure – Alpha diversity	T1 - Baseline			T2 – 6 months			T3 – 12 months		
		APOε4 non-carriers [n=40] mean (SD)	APOε4 carriers [n=39] mean (SD)	p-value (Wilcox rank sum test)	APOε4 non-carriers [n=36] mean (SD)	APOε4 carriers [n=37] mean (SD)	p-value (Wilcox rank sum test)	APOε4 non-carriers [n=39] mean (SD)	APOε4 carriers [n=37] mean (SD)	p-value (Wilcox rank sum test)
Kingdom	Shannon	0.08 (0.10)	0.04 (0.09)	0.005**	0.08 (0.12)	0.07 (0.15)	0.555	0.11 (0.13)	0.07 (0.16)	0.011*
	Simpson	0.03 (0.05)	0.02 (0.05)	0.004**	0.04 (0.07)	0.04 (0.10)	0.574	0.06 (0.08)	0.04 (0.10)	0.012*
	Inv. Simpson	1.04 (0.07)	1.02 (0.06)		1.05 (0.10)	1.05 (0.15)		1.07 (0.10)	1.06 (0.18)	
Phylum	Shannon	0.96 (0.18)	0.91 (0.17)	0.141	0.98 (0.23)	0.97 (0.22)	0.543	0.98 (0.17)	0.98 (0.18)	0.122
	Simpson	0.52 (0.09)	0.51 (0.08)	0.382	0.52 (0.12)	0.53 (0.10)	0.730	0.53 (0.09)	0.52 (0.10)	0.495
	Inv. Simpson	2.09 (0.42)	2.09 (0.34)		2.22 (0.56)	2.26 (0.60)		2.22 (0.40)	2.15 (0.42)	
Class	Shannon	1.15 (0.21)	1.09 (0.23)	0.317	1.14 (0.26)	1.14 (0.26)	0.822	1.15 (0.21)	1.10 (0.21)	0.263
	Simpson	0.58 (0.09)	0.56 (0.09)	0.473	0.56 (0.12)	0.58 (0.10)	0.713	0.58 (0.09)	0.57 (0.09)	0.482
	Inv. Simpson	2.46 (0.56)	2.40 (0.54)		2.46 (0.68)	2.55 (0.76)		2.53 (0.60)	2.43 (0.54)	
Order	Shannon	1.19 (0.23)	1.13 (0.23)	0.267	1.21 (0.28)	1.18 (0.27)	0.507	1.19 (0.22)	1.13 (0.22)	0.263
	Simpson	0.58 (0.09)	0.57 (0.09)	0.575	0.57 (0.12)	0.58 (0.10)	0.935	0.59 (0.09)	0.57 (0.09)	0.476
	Inv. Simpson	2.48 (0.58)	2.42 (0.54)		2.55 (0.77)	2.57 (0.77)		2.54 (0.61)	2.44 (0.55)	
Family	Shannon	2.05 (0.21)	1.98 (0.21)	0.135	2.01 (0.25)	2.01 (0.18)	0.697	2.04 (0.21)	2.04 (0.21)	0.234
	Simpson	0.82 (0.05)	0.81 (0.04)	0.263	0.81 (0.06)	0.81 (0.04)	0.713	0.82 (0.04)	0.81 (0.04)	0.115
	Inv. Simpson	5.78 (1.47)	5.47 (1.34)		5.69 (1.63)	5.57 (1.13)		5.88 (1.32)	5.46 (1.08)	
Genus	Shannon	2.52 (0.27)	2.46 (0.25)	0.263	2.48 (0.30)	2.49 (0.22)	0.926	2.54 (0.20)	2.44 (0.22)	0.103
	Simpson	0.87 (0.05)	0.87 (0.5)	0.267	0.87 (0.07)	0.87 (0.5)	0.595	0.88 (0.03)	0.87 (0.04)	0.105
	Inv. Simpson	8.85 (2.87)	8.21 (2.67)		8.69 (2.86)	8.39 (2.20)		8.93 (2.36)	8.00 (2.12)	
Species	Shannon	3.15 (0.25)	3.09 (0.24)	0.157	3.05 (0.31)	3.09 (0.31)	0.507	3.19 (0.21)	3.08 (0.29)	0.044*
	Simpson	0.92 (0.04)	0.92 (0.04)	0.398	0.91 (0.05)	0.91 (0.05)	0.763	0.93 (0.02)	0.91 (0.04)	0.210
	Inv. Simpson	13.90 (4.03)	13.40 (4.25)		12.73 (4.09)	13.18 (4.66)		14.81 (3.75)	13.38 (4.33)	

Table 7.28 Post-hoc analysis. Variance of between-sample diversity (Bray-Curtis dissimilarity distances, 999 permutations) explained by each variable assessed with cross-sectional PERMANOVA for T1 samples

Taxon. level	Source	Df	Sums Sq	R²	F-value	p-value (Bray)
Kingdom	APOε4 status	1	0.001	0.012	0.769	0.394
	age group	2	0.000	0.008	0.257	0.869
	sex	1	0.000	0.006	0.357	0.653
	Residual	60	0.052	0.968		
	Total	64	0.053	1.000		
Phylum	APOε4 status	1	0.000	0.000	-0.008	0.975
	age group	2	0.025	0.017	0.536	0.736
	sex	1	0.016	0.011	0.685	0.499
	Residual	60	1.417	0.972		
	Total	64	1.458	1.000		
Class	APOε4 status	1	0.007	0.003	0.199	0.942
	age group	2	0.047	0.023	0.724	0.662
	sex	1	0.013	0.006	0.401	0.791
	Residual	60	1.963	0.966		
	Total	64	2.033	1.000		
Order	APOε4 status	1	0.007	0.004	0.221	0.944
	age group	2	0.044	0.021	0.651	0.727
	sex	1	0.016	0.008	0.487	0.727
	Residual	60	2.030	0.966		
	Total	64	2.101	1.000		
Family	APOε4 status	1	0.066	0.013	0.803	0.607
	age group	2	0.144	0.028	0.884	0.576
	sex	1	0.120	0.023	1.468	0.140
	Residual	60	4.893	0.938		
	Total	64	5.216	1.000		
Genus	APOε4 status	1	0.114	0.015	0.970	0.479
	age group	2	0.198	0.026	0.841	0.661
	sex	1	0.155	0.021	1.312	0.195
	Residual	60	7.077	0.940		
	Total	64	7.532	1.000		
Species	APOε4 status	1	0.161	0.013	0.817	0.720
	age group	2	0.316	0.025	0.804	0.809
	sex	1	0.229	0.018	1.167	0.242
	Residual	60	11.801	0.943		
	Total	64	12.510	1.000		

Running PERMANOVA on Jaccard distance index generated similar results.

Table 7.29 Variance of between-sample diversity (Bray-Curtis dissimilarity distances, 999 permutations) explained by each variable assessed with cross-sectional PERMANOVA for T2 samples

Taxon. level	Source	Df	Sums Sq	R ²	F-value	p-value	stress value of NMDS
Kingdom	APOε4 status	1	0.001	0.005	0.328	0.825	0.00
	age group	2	0.003	0.014	0.472	0.799	
	sex	1	0.000	0.001	0.078	0.955	
	residual	68	0.217	0.980			
	total	72	0.222	1.000			
Phylum	APOε4 status	1	0.108	0.039	2.889	0.024*	0.10
	age group	2	0.061	0.022	0.814	0.561	
	sex	1	0.053	0.019	1.417	0.220	
	residual	68	2.535	0.928			
	total	72	2.731	1.000			
Class	APOε4 status	1	0.127	0.038	2.778	0.023*	0.13
	age group	2	0.083	0.024	0.902	0.497	
	sex	1	0.088	0.026	1.931	0.087	
	residual	68	3.109	0.922			
	total	72	3.371	1.000			
Order	APOε4 status	1	0.120	0.034	2.505	0.030*	0.14
	age group	2	0.081	0.023	0.850	0.850	
	sex	1	0.088	0.024	1.833	0.092	
	residual	68	3.247	0.927			
	total	72	3.502	1.000			
Family	APOε4 status	1	0.118	0.017	1.239	0.245	0.21
	age group	2	0.150	0.022	0.779	0.700	
	sex	1	0.190	0.028	2.003	0.033*	
	residual	68	6.457	0.938			
	total	72	6.887	1.000			
Genus	APOε4 status	1	0.167	0.017	1.233	0.242	0.23
	age group	2	0.201	0.020	0.741	0.802	
	sex	1	0.265	0.027	1.958	0.023*	
	residual	68	9.206	0.939			
	total	72	9.801	1.000			
Species	APOε4 status	1	0.282	0.020	1.421	0.085	0.24
	age group	2	0.294	0.020	0.741	0.893	
	sex	1	0.380	0.026	1.913	0.009**	
	residual	68	13.491	0.936			
	total	72	14.414	1.000			

Significance codes: 0 ***, 0.001**, 0.01*; stress value indicates reliability of ordination

Table 7.30 Variance of between-sample diversity (Bray-Curtis dissimilarity distances, 999 permutations) explained by each variable assessed with cross-sectional PERMANOVA of T3 samples

Taxon. level	Source	Df	Sums Sq	R ²	F-value	p-value (Bray)	stress value
Kingdom	APOε4 status	1	0.000	0.000	0.037	0.850	0.00
	age group	2	0.023	0.079	3.064	0.038*	
	sex	1	0.000	0.000	0.033	0.901	
	Residual	71	0.270	0.920			
	Total	75	0.294	1.000			
Phylum	APOε4 status	1	0.010	0.005	0.399	0.752	0.10
	age group	2	0.050	0.027	0.997	0.420	
	sex	1	0.004	0.002	0.151	0.933	
	Residual	71	1.792	0.966			
	Total	75	1.856	1.000			
Class	APOε4 status	1	0.020	0.007	0.519	0.707	0.12
	age group	2	0.081	0.029	1.067	0.365	
	sex	1	0.009	0.003	0.247	0.916	
	Residual	71	2.679	0.961			
	Total	75	2.786	1.000			
Order	APOε4 status	1	0.027	0.009	0.697	0.572	0.12
	age group	2	0.082	0.029	1.064	0.364	
	sex	1	0.008	0.003	0.195	0.953	
	Residual	71	2.733	0.960			
	Total	75	2.848	1.000			
Family	APOε4 status	1	0.082	0.013	0.983	0.437	0.21
	age groups	2	0.136	0.022	0.816	0.683	
	sex	1	0.201	0.032	2.418	0.013*	
	residual	71	5.893	0.936			
	total	75	6.299	1.000			
Genus	APOε4 status	1	0.149	0.017	1.252	0.242	0.20
	age group	2	0.197	0.022	0.825	0.802	
	sex	1	0.222	0.025	1.857	0.023*	
	residual	71	8.473	0.940			
	total	75	9.015	1.000			
Species	APOε4 status	1	0.217	0.015	1.104	0.315	0.24
	age group	2	0.398	0.027	1.011	0.446	
	sex	1	0.295	0.020	1.496	0.052	
	Residual	71	13.982	0.940			
	Total	75	14.867	1.000			

Significance codes: 0 ***, 0.001**, 0.01*; stress value indicates reliability of ordination (k=2 unless otherwise indicated)

Table 7.31 Univariate differential abundance results of Apolipoprotein ε4 non-carriers for T1-T3. Significant associations in green

Time-point	Significant associations with APOε4 non-carriers
Baseline (T1)	<p>k_Archaea p_Euryarchaeota c_Methanobacteria o_Methanobacteriales f_Methanobacteriaceae g_Methanobrevibacter s_Methanobrevibacter_smithii t_Methanobrevibacter_smithii_unclassified</p> <p>k_Bacteria p_Actinobacteria c_Actinobacteria o_Actinomycetales f_Propionibacteriaceae g_Propionibacteriaceae_unclassified</p> <p>k_Bacteria p_Actinobacteria c_Actinobacteria o_Coriobacteriales f_Coriobacteriaceae g_Collinsella s_Collinsella_aerofaciens t_GCF_000169035</p> <p>k_Bacteria p_Bacteroidetes c_Bacteroidia o_Bacteroidales f_Bacteroidaceae g_Bacteroides s_Bacteroides_eggerthii t_Bacteroides_eggerthii_unclassified</p> <p>k_Bacteria p_Bacteroidetes c_Bacteroidia o_Bacteroidales f_Bacteroidaceae g_Bacteroides s_Bacteroides_uniformis t_GCF_000154205</p> <p>k_Bacteria p_Bacteroidetes c_Bacteroidia o_Bacteroidales f_Bacteroidaceae g_Bacteroides s_Bacteroides_stercoris t_Bacteroides_stercoris_unclassified</p> <p>k_Bacteria p_Bacteroidetes c_Bacteroidia o_Bacteroidales f_Porphyrionadaceae</p> <p>k_Bacteria p_Bacteroidetes c_Bacteroidia o_Bacteroidales f_Rikenellaceae g_Alistipes s_Alistipes_nderdonkii t_GCF_000374505</p> <p>k_Bacteria p_Firmicutes c_Erysipelotrichia o_Erysipelotrichales f_Erysipelotrichaceae g_Holdemania s_Holdemania_filiformis t_GCF_000157995</p> <p>k_Bacteria p_Proteobacteria c_Betaproteobacteria o_Burkholderiales f_Sutterellaceae g_Sutterellaceae_unclassified</p>
6-months follow-up (T2)	<p>k_Bacteria p_Actinobacteria c_Actinobacteria o_Actinomycetales f_Actinomycetaceae g_Actinomyces s_Actinomyces_graevenitzii t_Actinomyces_graevenitzii_unclassified</p> <p>k_Bacteria p_Actinobacteria c_Actinobacteria o_Coriobacteriales f_Coriobacteriaceae g_Atopobium s_Atopobium_parvulum t_GCF_000024225</p> <p>k_Bacteria p_Actinobacteria c_Actinobacteria o_Coriobacteriales f_Coriobacteriaceae g_Collinsella s_Collinsella_aerofaciens t_GCF_000169035</p> <p>k_Bacteria p_Firmicutes c_Clostridia o_Clostridiales f_Clostridiaceae g_Clostridium s_Clostridium_methylpentosum t_GCF_000158655</p>
12- months follow-up (T3)	<p>k_Archaea p_Euryarchaeota c_Methanobacteria o_Methanobacteriales f_Methanobacteriaceae g_Methanobrevibacter s_Methanobrevibacter_smithii t_Methanobrevibacter_smithii_unclassified</p> <p>k_Bacteria p_Actinobacteria c_Actinobacteria o_Coriobacteriales f_Coriobacteriaceae g_Collinsella s_Collinsella_aerofaciens t_GCF_000169035</p> <p>k_Bacteria p_Actinobacteria c_Actinobacteria o_Coriobacteriales f_Coriobacteriaceae g_Slackia s_Slackia_piriformis t_GCF_000296445</p> <p>k_Bacteria p_Bacteroidetes c_Bacteroidia o_Bacteroidales f_Bacteroidaceae g_Bacteroides s_Bacteroides_intestinalis t_GCF_000172175</p> <p>k_Bacteria p_Bacteroidetes c_Bacteroidia o_Bacteroidales f_Bacteroidaceae g_Bacteroides s_Bacteroides_stercoris t_Bacteroides_stercoris_unclassified</p> <p>k_Bacteria p_Firmicutes c_Clostridia o_Clostridiales f_Clostridiales_Family_XI_Incertae_Sedis g_Finegoldia s_Finegoldia_magna t_Finegoldia_magna_unclassified</p> <p>k_Bacteria p_Firmicutes c_Clostridia o_Clostridiales f_Eubacteriaceae g_Eubacterium s_Eubacterium_siraeum t_Eubacterium_siraeum_unclassified</p> <p>k_Bacteria p_Firmicutes c_Clostridia o_Clostridiales f_Lachnospiraceae g_Dorea s_Dorea_formicigenerans t_Dorea_formicigenerans_unclassified</p> <p>k_Bacteria p_Firmicutes c_Clostridia o_Clostridiales f_Lachnospiraceae g_Lachnospiraceae_noname s_Lachnospiraceae_bacterium_8_1_57FAA t_GCF_000185545</p> <p>k_Bacteria p_Firmicutes c_Clostridia o_Clostridiales f_Lachnospiraceae g_Lachnospiraceae_noname s_Lachnospiraceae_bacterium_2_1_58FAA t_GCF_000218465</p> <p>k_Bacteria p_Firmicutes c_Negativicutes o_Selenomonadales f_Acidaminococcaceae g_Acidaminococcus s_Acidaminococcus_unclassified</p> <p>k_Bacteria p_Firmicutes c_Negativicutes o_Selenomonadales f_Veillonellaceae g_Dialister s_Dialister_succinatiphilus t_GCF_000242435</p>

* Associations that survived further lowering of alpha error in bold. Prefix indicates taxonomic level: ‘k__’: kingdom-level, ‘p__’: phylum-level, ‘c__’: class-level, ‘o__’: order-level, ‘f__’: family-level, ‘g__’: genus-level, ‘s__’: species-level, ‘t__’: strain-level

Table 7.32 Univariate differential abundance results of Apolipoprotein ε4 carriers for T1-T3. Significant associations in red

Timepoint	Significant associations with APOε4 carriers
Baseline (T1)	<p>k_Bacteria p_Bacteroidetes c_Bacteroidia o_Bacteroidales f_Bacteroidaceae g_Bacteroides s_Bacteroides_cellulosilyticus t_Bacteroides_cellulosilyticus_unclassified</p> <p>k_Bacteria p_Bacteroidetes c_Bacteroidia o_Bacteroidales f_Bacteroidaceae g_Bacteroides s_Bacteroides_intestinalis t_GCF_000172175</p> <p>k_Bacteria p_Firmicutes c_Clostridia o_Clostridiales f_Lachnospiraceae g_Anaerostipes s_Anaerostipes_hadrus t_GCF_000332875</p> <p>k_Bacteria p_Firmicutes c_Clostridia o_Clostridiales f_Lachnospiraceae g_Lachnospiraceae_noname s_Lachnospiraceae_bacterium_5_1_63FAA t_GCF_000185525</p> <p>k_Bacteria p_Firmicutes c_Clostridia o_Clostridiales f_Lachnospiraceae g_Lachnospiraceae_noname s_Lachnospiraceae_bacterium_1_1_57FAA t_GCF_000218445</p>
6-months follow-up (T2)	<p>k_Bacteria p_Bacteroidetes c_Bacteroidia o_Bacteroidales f_Bacteroidaceae g_Bacteroides s_Bacteroides_plebeius t_GCF_000187895</p> <p>k_Bacteria p_Firmicutes c_Clostridia o_Clostridiales f_Lachnospiraceae g_Blautia s_Ruminococcus_obeum t_Ruminococcus_obeum_unclassified</p>
12-months follow-up (T3)	<p>k_Bacteria p_Actinobacteria c_Actinobacteria o_Coriobacteriales f_Coriobacteriaceae g_Eggerthella s_Eggerthella_unclassified</p> <p>k_Bacteria p_Bacteroidetes c_Bacteroidia o_Bacteroidales f_Bacteroidaceae g_Bacteroides s_Bacteroides_plebeius t_GCF_000187895</p> <p>k_Bacteria p_Firmicutes c_Clostridia o_Clostridiales f_Clostridiaceae g_Clostridium</p> <p>k_Bacteria p_Firmicutes c_Bacilli o_Lactobacillales f_Streptococcaceae g_Streptococcus s_Streptococcus_australis t_Streptococcus_australis_unclassified</p> <p>k_Bacteria p_Firmicutes c_Bacilli o_Lactobacillales f_Streptococcaceae g_Streptococcus s_Streptococcus_vestibularis t_Streptococcus_vestibularis_unclassified</p> <p>k_Bacteria p-Proteobacteria c_Gammaproteobacteria o_Enterobacteriales f_Enterobacteriaceae g_Escherichia</p> <p>k_Viruses_noname p_Virus_noname c_Viruses_noname o_Caudovirales f_Siphoviridae g_C2likevirus s_C2likevirus_unclassified</p>

* Associations that survived further lowering of alpha error in bold. Prefix indicates taxonomic level: ‘k__’: kingdom-level, ‘p__’: phylum-level, ‘c__’: class-level, ‘o__’: order-level, ‘f__’: family-level, ‘g__’: genus-level, ‘s__’: species-level, ‘t__’: strain-level

Table 7.33 Multivariate linear regression results showing features significantly associated with Apolipoprotein ε4 status, after accounting for the effect of gender and age at baseline

Taxonomic level	feature	coef	stderr	N	pval	qval
Phylum	<i>p__Verrucomicrobia</i>	-0.304	0.092	79	0.002	0.009
Class	<i>c__Verrucomicrobiae</i>	-0.304	0.092	79	0.002	0.018
Order	<i>o__Verrucomicrobiales</i>	-0.304	0.092	79	0.002	0.025

coef = beta coefficient, stderr = standard error of the model, N= number of samples in this model, pval = nominal p-value (two-sided), qval = FDR-corrected p-values

Table 7.34 Multivariate linear regression results showing features significantly associated with Apolipoprotein ε4 status, after accounting for the effect of gender and age at T2

Taxonomic level	feature	coef	stderr	N	pval	qval
Phylum	<i>p__Bacteroidetes</i>	3.424	1.347	73	0.013	0.046
	<i>p__Actinobacteria</i>	-0.759	1.287	73	0.005	0.033

coef = beta coefficient, stderr = standard error of the model, N= number of samples in this model, pval = nominal p-value (two-sided), qval = FDR-corrected p-values

Table 7.35 Multivariate linear regression results showing features significantly associated with Apolipoprotein ε4 status, after accounting for the effect of gender and age at T3

Taxonomic level	feature	coef	stderr	N	pval	qval
Kingdom	<i>k__Archaea</i>	0.148	0.042	76	0.001	0.002
Phylum	<i>p__Euryarchaeota</i>	0.148	0.042	76	0.001	0.005
Class	<i>c__Methanobacteria</i>	0.148	0.042	76	0.001	0.010
Order	<i>o__Methanobacteriales</i>	0.148	0.042	76	0.001	0.014
Family	<i>f__Methanobacteriaceae</i>	0.148	0.042	76	0.001	0.030

coef = beta coefficient, stderr = standard error of the model, N= number of samples in this model, pval = nominal p-value (two-sided), qval = FDR-corrected p-values

Table 7.36 Multivariate linear regression results showing features significantly associated with Apolipoprotein ε4 status, after accounting for the effect of gender and age across all three timepoints, subject ID as random effect

Taxonomic level	feature	coef	stderr	N	pval	qval
Family	<i>f__Prevotellaceae</i>	-6.082	1.752	288	>0.001	0.031
Genus	<i>g__Prevotella</i>	-6.333	1.771	288	>0.001	0.044
Species	<i>s__Ruminococcus_obenum</i>	-0.321	0.077	288	>0.001	0.013

coef = beta coefficient, stderr = standard error of the model, N= number of samples in this model,

pval = nominal p-value (two-sided), qval = FDR-corrected p-values

Table 7.37 Kyoto Encyclopedia of Genes and Genomes modules associated with Apolipoprotein ε4 status

related metabolism*	KEGG modules		value	coef	p-value	q-value
decreased (↓) in APOε4 carriers compared to APOε4 non-carriers						
6 –	Acylglycerol degradation	M00098	carrier	-0.00003	0.003	0.553
4 –	Formaldehyde assimilation, serine pathway	M00346	carrier	-7.8E-05	0.006	0.650
7 –	C1-unit interconversion, eukaryotes	M00141	carrier	-0.0002	0.010	0.670
5 –	N-glycosylation by oligosaccharyltransferase	M00072	carrier	-1.5E-05	0.030	0.670
10 –	Uridine monophosphate biosynthesis, glutamine (+ PRPP) => UMP	M00051	carrier	-0.00016	0.038	0.670
5 –	N-glycan biosynthesis, complex type	M00075	carrier	-3.1E-06	0.039	0.670
6 –	Phosphatidylethanolamine (PE) biosynthesis, ethanolamine => PE	M00092	carrier	-7.2E-06	0.044	0.670
enriched (↑) in APOε4 carriers compared to APOε4 non-carriers						
4 –	Assimilatory sulfate reduction, sulfate => H2S	M00176	carrier	0.0002	0.019	0.670
3 –	Pentose phosphate pathway, archaea, fructose 6P => ribose 5P	M00580	carrier	0.0001	0.021	0.670
4 –	Dissimilatory nitrate reduction, nitrate => ammonia	M00530	carrier	0.0001	0.024	0.670
4 –	Assimilatory nitrate reduction, nitrate => ammonia	M00531	carrier	6.04E-05	0.027	0.670
2 –	Monolignol biosynthesis, phenylalanine/tyrosine => monolignol	M00039	carrier	3.04E-05	0.039	0.670
9 –	Capsaicin biosynthesis, L-Phenylalanine => Capsaicin	M00350	carrier	7.29E-05	0.039	0.670
4 –	Denitrification, nitrate => nitrogen	M00529	carrier	5.62E-05	0.044	0.670

*1: Amino acid metabolism, 2: Biosynthesis of other secondary metabolites, 3: Carbohydrate metabolism, 4: Energy metabolism, 5: Glycan biosynthesis and metabolism, 6: Lipid metabolism, 7: Metabolism of cofactors and vitamins, 8: Metabolism of other amino acids, 9: Metabolism of terpenoids and polyketides, 10: Nucleotide metabolism, 11: Xenobiotics biodegradation and metabolism

Table 7.38 Kyoto Encyclopedia of Genes and Genomes pathways associated with Apolipoprotein ε4 status

related metabolism*	KEGG pathways		value	coef	p-value	q-value
decreased (↓) in APOε4 carriers compared to APOε4 non-carriers						
1 –	Glycine, serine and threonine metabolism	ko00260	carrier	-0.0001	0.014	0.893
9 –	Biosynthesis of ansamycins	ko01051	carrier	-0.0001	0.028	0.893
enriched (↑) in APOε4 carriers compared to APOε4 non-carriers						
3 –	Fructose and mannose metabolism	ko00051	carrier	0.0003	0.039	0.893
2 –	Aflatoxin biosynthesis	ko00254	carrier	0.0000	0.040	0.893
6 –	Linoleic acid metabolism	ko00591	carrier	0.0000	0.037	0.893
4 –	Sulfur metabolism	ko00920	carrier	0.0001	0.035	0.893

*1: Amino acid metabolism, 2: Biosynthesis of other secondary metabolites, 3: Carbohydrate metabolism, 4: Energy metabolism, 5: Glycan biosynthesis and metabolism, 6: Lipid metabolism, 7: Metabolism of cofactors and vitamins, 8: Metabolism of other amino acids, 9: Metabolism of terpenoids and polyketides, 10: Nucleotide metabolism, 11: Xenobiotics biodegradation and metabolism

Table 7.39 HUMAnN3 Stratified pathways in Apolipoprotein E cohorts

	Feature	coef	stderr	N	p-value	q-value
enriched (↑) in APOε4 carriers	UNINTEGRATED_g__Prevotella s__Prevotella_copri_CAG_164	0.022	0.005	228	0.000	0.002
	UNINTEGRATED_g__Prevotella s__Prevotella_copri	0.017	0.005	228	0.002	0.011
decreased (↓) in APOε4 carriers	UNINTEGRATED_g__Bifidobacterium s__Bifidobacterium_adolescentis	-0.006	0.002	228	0.020	0.029

q-value = BH-corrected value

Table 7.40 HUMAnN3 Unstratified pathways in Apolipoprotein E cohorts

	Feature	coef	stderr	N	p-value	q-value
enriched (↑) in APOε4 carriers	PWY-7539: 6-hydroxymethyl-dihydropterin diphosphate biosynthesis III (Chlamydia)	5.73E-05	1.7E-05	228	0.001	0.012
	PWY-6147: 6-hydroxymethyl-dihydropterin diphosphate biosynthesis I	5.69E-05	1.7E-05	228	0.002	0.012
	ASPASN-PWY: superpathway of L-aspartate and L-asparagine biosynthesis	3.33E-05	1.3E-05	228	0.014	0.045
	PHOSLIPSYN-PWY: superpathway of phospholipid biosynthesis I (bacteria)	4.54E-05	1.8E-05	228	0.015	0.045
	PWY-1269: CMP-3-deoxy-D-manno-octulosonate (CMP-Kdo) biosynthesis I	2.36E-05	1E-05	228	0.022	0.045
	PWY4FS-7: phosphatidylglycerol biosynthesis I (plastidic)	4.08E-05	1.8E-05	228	0.025	0.045
	PWY4FS-8: phosphatidylglycerol biosynthesis II (non-plastidic)	4.08E-05	1.8E-05	228	0.025	0.045
decreased (↓) in APOε4 carriers	PWY-7383: anaerobic energy metabolism (invertebrates, cytosol)	-2.2E-05	6.2E-06	228	0.001	0.012
	PWY66-399: gluconeogenesis III	-1.4E-05	5.1E-06	228	0.006	0.031
	PWY-6124: inosine-5'-phosphate biosynthesis II	-2.4E-05	9.6E-06	228	0.016	0.045
	PWY-6123: inosine-5'-phosphate biosynthesis I	-2.3E-05	9.4E-06	228	0.018	0.045
	PWY-4981: L-proline biosynthesis II (from arginine)	-2.9E-05	1.3E-05	228	0.029	0.046
	HISDEG-PWY: L-histidine degradation I	-1.8E-05	8.3E-06	228	0.030	0.046
	PWY-3841: folate transformations II	-2.8E-05	1.3E-05	228	0.034	0.046

q-value = BH-corrected value

Table 7.41 Variance of between-sample functional diversity (Jaccard dissimilarity distances, 999 permutations) explained by each variable assessed with cross-sectional PERMANOVA

KEGG level	Source	Df	Sums Sq	R²	F-value	p-value (Jaccard)	stress value
KEGG metabolism	APOε4 status	1	0.008	0.001	0.169	0.875	0.144
	age	1	0.070	0.007	1.466	0.193	
	sex	1	0.026	0.002	0.535	0.544	
	Residual	213	10.190	0.989			
	Total	216	10.299	1.000			
KEGG modules	APOε4 status	1	0.010	0.001	0.214	0.859	0.183
	age	1	0.068	0.007	1.401	0.205	
	sex	1	0.028	0.003	0.567	0.529	
	Residual	213	10.377	0.989			
	Total	216	10.489	1.000			
KEGG pathways	APOε4 status	1	0.008	0.001	0.169	0.875	0.197
	age	1	0.070	0.007	1.466	0.193	
	sex	1	0.026	0.002	0.535	0.544	
	Residual	213	10.190	0.989			
	Total	216	10.299	1.000			

Significance codes: 0 ***, 0.001**, 0.01*; stress value indicates reliability of ordination for k=2

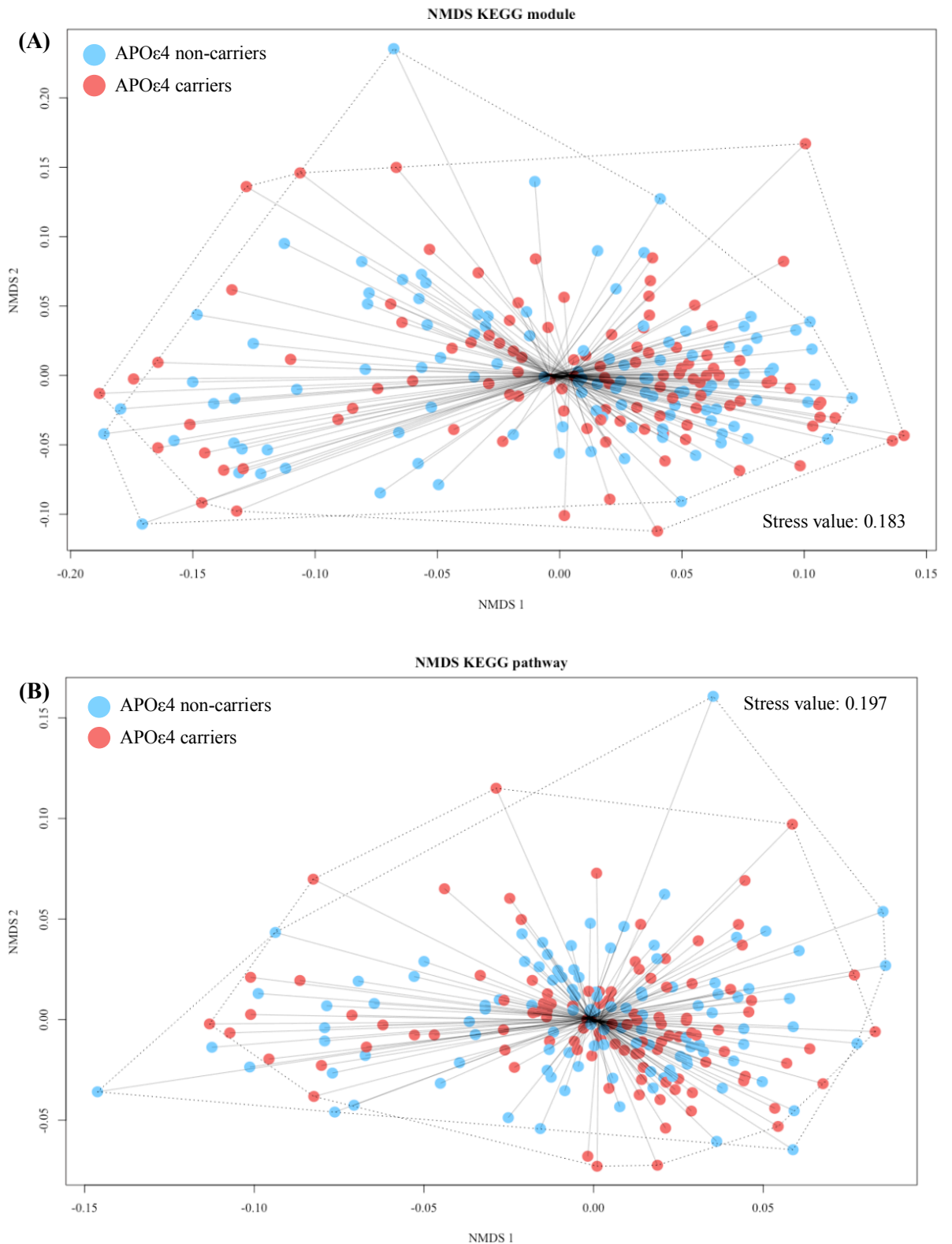


Figure 7.12 Non-metric Multidimensional Scaling on beta diversity (Jaccard index) between the predicted (A) KEGG module and (B) KEGG pathways by group (light blue = Apolipoprotein ϵ 4 non-carriers, red = Apolipoprotein ϵ 4 carriers). Each point denotes a sample in a reduced dimensional space and is connected with a line to the group centroid

Neuropsychological results of the Alzheimer's Disease patient group

Addenbrooke's Cognitive Examination-III

Table 7.42 Multivariate regression results, Addenbrooke's Cognitive Examination-III

Predictors	Estimates for beta values	Confidence Intervals	Standardized beta values	p-value
(Intercept)	74.32	60.16 – 88.84		<0.001
Age	-0.04	-0.23 – 0.14	-0.03	0.638
Group [APOε4 non-carriers]	23.98	20.20 – 27.76	1.31	<0.001
Group [APOε4 carriers]	-23.59	19.55 – 27.62	1.28	<0.001
Educational attainment [College]	-1.99	-4.90 – 0.92	-0.10	0.177
Educational attainment [University]	1.15	-1.53 – 3.83	0.06	0.396

$F(5,78)=44.52$, $p<0.001$, $R^2=0.74$

Rey-Osterrich-Complex Figure

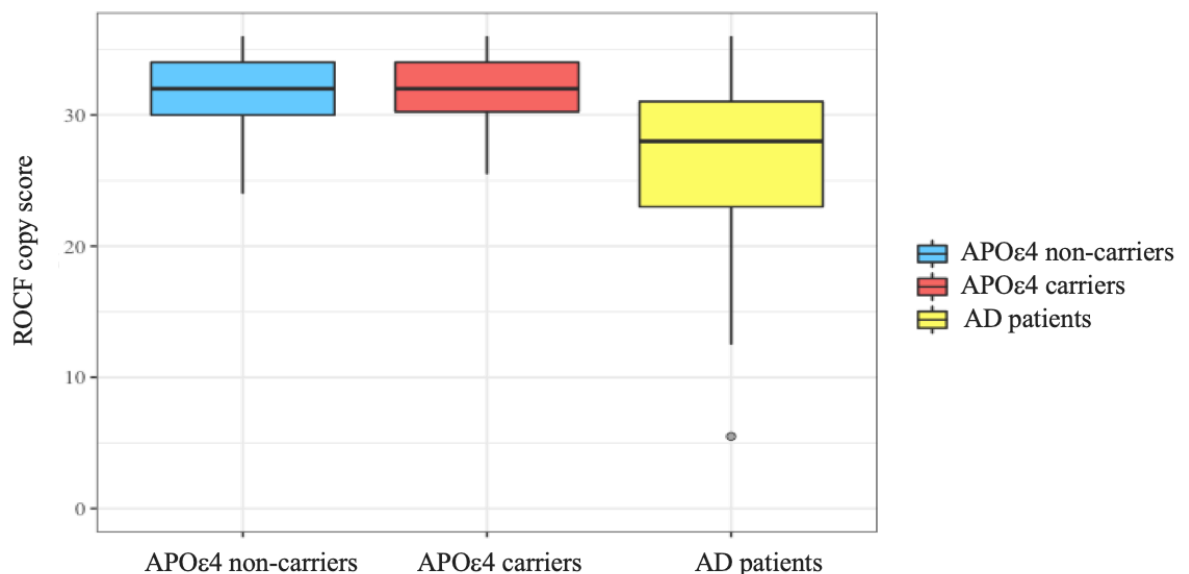


Table 7.43 Boxplot of Rey-Osterrich Complex Figure copy score by group

Table 7.44 Multivariate regression results, Rey-Osterrich Complex Figure: Copy score

Predictors	Estimates for beta values	Confidence Intervals	Standardized beta values	p-value
(Intercept)	29.77	17.40 – 42.14		<0.001
Age	-0.05	-0.21 – 0.11	-0.07	0.522
Group [APOε4 non-carriers]	6.34	3.04 – 9.64	0.69	<0.001
Group [APOε4 carriers]	6.74	3.22 – 10.25	0.73	<0.001
Educational attainment [College]	-1.18	-3.71 – 1.35	-0.12	0.357
Educational attainment [University]	-1.65	-4.00 – 0.70	-0.18	0.167

$F(5,77)=4.319$, Observations: 83, $R^2: 0.219$

Table 7.45 Multivariate regression results, Rey-Osterrich Complex Figure: Recall score

Predictors	Estimates for beta values	Confidence Intervals	Standardized beta values	p-value
(Intercept)	16.33	0.15 – 32.51		0.048
Age	-0.14	-0.35– 0.08	-0.13	0.202
Group [APOε4 non-carriers]	11.58	7.26 – 15.89	0.87	<0.001
Group [APOε4 carriers]	11.22	6.62 –15.82	0.84	<0.001
Educational attainment [College]	-0.33	-3.64 – 2.99	-0.02	0.846
Educational attainment [University]	0.13	-2.95 – 3.21	0.01	0.934

$F(5,77)=8.798$, Observations: 83, R^2 : 0.364

Table 7.46 Multivariate regression results, Rey-Osterrich Complex Figure: Copy time

Predictors	Estimates for beta values	Confidence Intervals	Standardized beta values	p-value
(Intercept)	177.29	-103.02 – -457.60		0.212
Age	1.65	-2.03 – 5.33	0.11	0.375
Group [APOε4 non-carriers]	-102.79	-177.57 – -28.00	0.87	0.008
Group [APOε4 carriers]	-86.18	-165.88 – -6.48	0.84	0.034
Educational attainment [College]	-18.47	-75.89 – 38.95	-0.02	0.524
Educational attainment [University]	-11.17	-64.49 – 42.16	0.01	0.678

$F(5,77)= 2.426$, Observations: 83, R^2 : 0.136

Trail Making Test

Table 7.47 Multivariate regression results, Trail Making Test-A

Predictors	Estimates for beta values	Confidence Intervals	Standardized beta values	p-value
(Intercept)	24.98	-14.46 – 64.42	0.00	0.211
Age	0.45	-0.08 – 0.97	0.19	0.095
Group [APOε4 non-carriers]	-20.29	-31.68 – -8.90	-0.69	<0.001
Group [APOε4 carriers]	-21.28	-33.24 – -9.31	-0.72	<0.001
Educational attainment [College]	-1.19	-9.73 – 7.36	-0.04	0.783
Educational attainment [University]	1.61	-6.14 – 9.36	0.05	0.681

$F(5,73)=4.446$, $p=0.001$, $R^2=0.233$

Table 7.48 Multivariate regression results, Trail Making Test-B

Predictors	Estimates for beta values	Confidence Intervals	Standardized beta values	p-value
(Intercept)	95.33	-7.69 – 198.34		0.069
Age	1.65	0.28 – 3.02	0.19	0.019
Group [APOε4 non-carriers]	-129.75	-159.50 – -100.00	-1.20	<0.001
Group [APOε4 carriers]	-135.60	-166.86 – -104.34	-1.25	<0.001
Educational attainment [College]	-8.58	-30.89 – 13.74	-0.07	0.446
Educational attainment [University]	-3.94	-24.19 – 16.30	-0.04	0.699

$F(5,73)=23.18$, $p<0.001$, $R^2=0.614$

Generalized Anxiety Disorder-7

Table 7.49 Multivariate regression results, Generalized Anxiety Disorder-7

Predictors	Estimates for beta values	Confidence Intervals	Standardized beta values	p-value
(Intercept)	7.09	0.71– 13.46		0.030
Age	-0.04	-0.12 – 0.05	-0.10	0.377
Group [APOε4 non-carriers]	-3.21	-4.90 – -1.53	-0.70	<0.001
Group [APOε4 carriers]	-3.18	-4.97 – -1.39	-0.68	0.001
Educational attainment [College]	-0.62	-1.91 – 0.67	-1.22	0.339
Educational attainment [University]	0.07	-1.91 – 0.50	-0.15	0.250

$F(5,75)=3.773$, $p=0.005$, $R^2=0.199$

Patient Health Questionnaire-9

Table 7.50 Multivariate regression results, Patient Health Questionnaire-9

Predictors	Estimates for beta values	Confidence Intervals	Standardized beta values	p-value
(Intercept)	9.11	0.49 – 17.73		0.039
Age	-0.06	-0.17 – 0.05	-0.13	0.288
Group [APOε4 non-carriers]	-3.64	-5.92 – -1.37	-0.61	0.002
Group [APOε4 carriers]	-3.79	-6.21 – -1.36	-0.63	0.003
Educational attainment [College]	0.35	-1.39 – 2.09	0.05	0.688
Educational attainment [University]	0.71	-0.92 – 2.34	0.12	0.390

$F(5,75)=2.222$, $p=0.061$, $R^2=0.129$

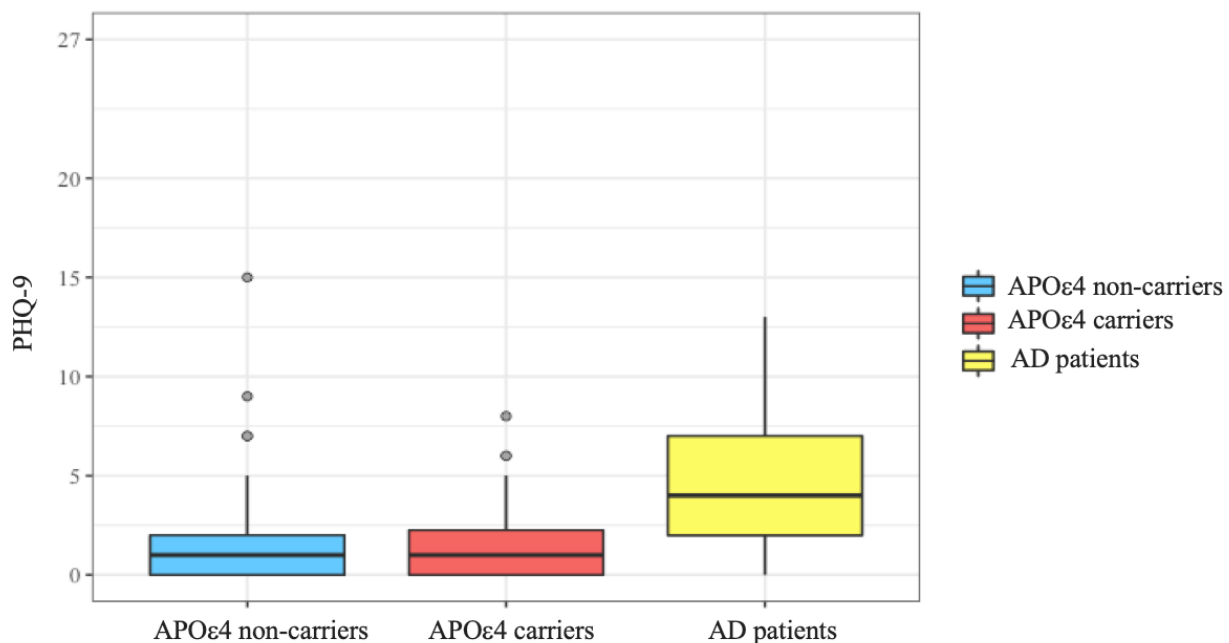


Figure 7.13 Patient Health Questionnaire-9 score by group, depression severity= none (<4), mild (5-9), moderate (10-14), moderately severe (15-19), severe (20-27)

Table 7.51 Multivariate regression results, Cambridge Behavioural Inventory-Revised: Domain Frequency Score

Predictors	Estimates for beta values	Confidence Intervals	Standardized beta values	p-value
(Intercept)	34.19	12.35 – 56.02	0.00	0.003
Age	-0.11	-0.40 – 0.17	-0.07	0.434
Group [APOε4 non-carriers]	-22.13	-27.83 – 16.43	-1.11	<0.001
Group [APOε4 carriers]	-24.19	-30.28 – -18.09	-1.18	<0.001
Educational attainment [College]	0.92	-3.44– 5.28	0.04	0.674
Educational attainment [University]	0.22	-3.90 – 4.35	0.01	0.914

$F(5,73)=15.55$, $p<0.001$, $R^2=0.516$

Alpha diversity

Table 7.52 Alpha diversity by taxonomic level between the two Apolipoprotein E cohorts and the Alzheimer's Disease patient group

Taxonomic level	Measure – Alpha diversity	APOε4 non-carriers [n=36] mean (SD)	APOε4 carriers [n=37] mean (SD)	AD patient group [n=9] mean (SD)	p-value (Wilcox rank sum test) for each group comparison		
					APOε4 carriers vs non-carriers	AD vs APOε4 non-carriers	AD vs APOε4 carriers
Kingdom	Shannon	0.08 (0.12)	0.07 (0.15)	0.19 (0.24)	0.555	0.076	0.017
	Simpson	0.04 (0.07)	0.04 (0.10)	0.11 (0.16)	0.574	0.072	0.017
	Inv. Simpson	1.05 (0.10)	1.05 (0.15)	1.17 (0.26)			
Phylum	Shannon	0.98 (0.23)	0.97 (0.22)	0.96 (0.20)	0.543	0.665	0.935
	Simpson	0.52 (0.12)	0.53 (0.10)	0.52 (0.11)	0.730	0.944	0.786
	Inv. Simpson	2.22 (0.56)	2.26 (0.60)	2.18 (0.53)			
Class	Shannon	1.14 (0.26)	1.14 (0.26)	1.25 (0.29)	0.822	0.320	0.325
	Simpson	0.56 (0.12)	0.58 (0.10)	0.60 (0.13)	0.713	0.442	0.531
	Inv. Simpson	2.46 (0.68)	2.55 (0.76)	2.80 (0.97)			
Order	Shannon	1.21 (0.28)	1.18 (0.27)	1.36 (0.28)	0.507	0.191	0.129
	Simpson	0.57 (0.12)	0.58 (0.10)	0.63 (0.13)	0.935	0.306	0.261
	Inv. Simpson	2.55 (0.77)	2.57 (0.77)	2.97 (0.98)			
Family	Shannon	2.01 (0.25)	2.01 (0.18)	1.87 (0.37)	0.697	0.211	0.250
	Simpson	0.81 (0.06)	0.81 (0.04)	0.75 (0.13)	0.713	0.191	0.238
	Inv. Simpson	5.69 (1.63)	5.57 (1.13)	4.80 (1.98)			
Genus	Shannon	2.48 (0.30)	2.49 (0.22)	2.19 (0.46)	0.926	0.086	0.039
	Simpson	0.87 (0.07)	0.87 (0.5)	0.79 (0.15)	0.595	0.054	0.042
	Inv. Simpson	8.69 (2.86)	8.39 (2.20)	6.43 (3.25)			
Species	Shannon	3.05 (0.31)	3.09 (0.31)	2.72 (0.59)	0.507	0.028	0.012
	Simpson	0.91 (0.05)	0.91 (0.05)	0.85 (0.15)	0.763	0.033	0.029
	Inv. Simpson	12.73 (4.09)	13.18 (4.66)	9.97 (5.28)			

Beta diversity

Table 7.53 Variance of between-sample diversity (Bray-Curtis dissimilarity distances, 999 permutations) explained by each variable assessed with cross-sectional PERMANOVA

Taxon. level	Source	Df	Sums Sq	R²	F-value	p-value	stress value
Kingdom	group	2	0.045	0.056	2.423	0.071	0.00
	age groups	2	0.011	0.013	0.577	0.564	
	sex	1	0.001	0.001	0.066	0.929	
	residual	76	0.703	0.890			
	total	81	0.791	1.000			
Phylum	group	2	0.390	0.099	4.337	0.001***	0.12
	age groups	2	0.088	0.022	0.980	0.447	
	sex	1	0.051	0.013	1.142	0.327	
	residual	76	3.417	0.869			
	total	81	3.931	1.000			
Class	group	2	0.622	0.123	5.606	0.001***	0.14
	age	2	0.117	0.023	1.055	0.395	
	sex	1	0.082	0.016	1.472	0.180	
	residual	76	4.216	0.835			
	total	81	5.052	1.000			
Order	group	2	0.626	0.118	5.322	0.001***	0.15
	age	2	0.115	0.022	0.997	0.432	
	sex	1	0.082	0.016	1.414	0.197	
	residual	76	4.398	0.840			
	total	81	5.236	1.000			
Family	group	2	0.568	0.064	2.728	0.001***	0.21
	age groups	2	0.203	0.023	0.977	0.454	
	sex	1	0.158	0.018	1.518	0.133	
	residual	76	7.907	0.889			
	total	81	8.889	1.000			
Genus	group	2	0.732	0.060	2.555	0.001***	0.22
	age groups	2	0.256	0.021	0.894	0.585	
	sex	1	0.268	0.022	1.871	0.029*	
	residual	76	10.890	0.893			
	total	81	12.189	1.000			
Species	group	2	0.926	0.053	2.244	0.001***	0.23
	age groups	2	0.332	0.019	0.805	0.838	
	sex	1	0.380	0.022	1.838	0.023*	
	residual	76	15.698	0.903			
	total	81	17.379	1.000			

Significance codes: 0 ***, 0.001**, 0.01*; stress value indicates reliability of ordination for k=2

Table 7.54 Post-hoc analysis, pairwise comparisons for all pairs of level for ‘group’ using PERMANOVA

Taxon. level	Pairwise comparison	Sums Sq	R²	F-value	p-value	p-value corrected (FDR)
Kingdom	AD patients vs carriers	0.069	0.097	4.700	0.041*	0.062
	AD patients vs non-carriers	0.065	0.105	5.026	0.034*	0.062
	non-carriers - vs carriers	0.001	0.006	0.422	0.745	0.745
Phylum	AD patients vs carriers	0.358	0.155	8.076	0.001***	0.003**
	AD patients vs non-carriers	0.183	0.068	3.142	0.022*	0.033*
	non-carriers - vs carriers	0.086	0.032	2.314	0.073	0.073
Class	AD patients vs carriers	0.588	0.188	10.192	0.001***	0.003**
	AD patients vs non-carriers	0.411	0.120	5.875	0.004**	0.006**
	non-carriers - vs carriers	0.096	0.029	2.088	0.077	0.077
Order	AD patients vs carriers	0.590	0.181	9.736	0.001***	0.003**
	AD patients vs non-carriers	0.424	0.120	5.869	0.002**	0.003**
	non-carriers - vs carriers	0.091	0.026	1.893	0.095	0.095
Family	AD patients vs carriers	0.567	0.106	5.203	0.001***	0.003**
	AD patients vs non-carriers	0.403	0.075	3.507	0.005**	0.008**
	non-carriers - vs carriers	0.091	0.013	0.949	0.481	0.481
Genus	AD patients vs carriers	0.682	0.100	4.652	0.001***	0.003**
	AD patients vs non-carriers	0.429	0.068	3.134	0.003**	0.005**
	non-carriers - vs carriers	0.131	0.013	0.963	0.479	0.479
Species	AD patients vs carriers	0.775	0.079	3.750	0.001***	0.003**
	AD patients vs non-carriers	0.552	0.055	2.480	0.002**	0.003**
	non-carriers - vs carriers	0.250	0.017	1.254	0.184	0.184

Significance codes: 0 ***, 0.001**, 0.01*

Table 7.55 Significant associations from univariate differential abundance analysis per group

Taxonomic level	↑ in AD GROUP*	↑ in APOE4 CARRIERS *	↑ in APOE4 NON-CARRIERS *
Phylum	↑ <i>Actinobacteria</i>	↑ <i>Bacteroidetes</i>	
Class	↑ <i>Actinobacteria</i>	↑ <i>Bacteroidia</i>	
Order	↑ <i>Coriobacteriales</i> ↑ <i>Actinomycetales</i>	↑ <i>Bacteroidales</i>	
Family	↑ <i>Coriobacteriaceae</i> ↑ <i>Actinomycetacea</i> ↑ <i>Bacillales_noname</i>		
Genus	↑ <i>Actinomyces</i> ↑ <i>Gemella</i>		↑ <i>Collinsella</i>
Species (strain)	↑ <i>Atopobium parvulum</i> (GCF_000024225) ↑ <i>Actinomyces viscosus</i> (GCF_000175315) ↑ <i>Actinomyces johnsonii</i> (unclassified strain) ↑ <i>Lactobacillus casei paracasei</i> (unclassified strain) ↑ <i>Clostridium methylpentosum</i> (GCF_000158655)	↑ <i>Streptococcus cristatus</i> (unclassified strain) ↑ <i>Streptococcus australis</i> (unclassified strain) ↑ <i>Eubacterium eligens</i> (GCF_000146185) ↑ <i>Ruminococcus callidus</i> (GCF_000468015) ↑ (GCF_000166035) ↑ <i>Ruminococcus obeum</i> (unclassified strain) ↑ <i>Bacteroides plebeius</i> (GCF_000187895)	↑ <i>Eubacterium ramulus</i> (GCF_000469345) ↑ <i>Collinsella aerofaciens</i> (GCF_000169035) ↑ <i>Bacteroides stercoris</i> (unclassified strain)

* compared to all other groups

Table 7.56 (Part 1) Multivariate analysis with significant associations for ‘group’, model accounts for the effect of ‘age’ and ‘sex’.

Alzheimer’s Disease patient group as baseline contrast compared against Apolipoprotein ε4 carriers (contrast: carriers) and compared against the Apolipoprotein ε4 non-carriers (contrast: non-carriers)

Taxonomic level	feature	N	N.not.0	contrast	coef	stderr	pval	qvalue2	contrast	coef	stderr	pval	qval
Kingdom	<i>k Viruses</i>	82	57	carriers	-0.247	0.095	0.012	0.023	non-carriers	-0.232	0.089	0.011	0.023
Phylum	<i>p Actinobacteria</i>	82	82	carriers	-21.533	5.239	0.000	0.001	non-carriers	-14.28	4.815	0.004	0.014
	<i>p Bacteroidetes</i>	82	82	carriers	20.686	4.897	0.000	0.001	non-carriers	13.602	4.501	0.003	0.014
	<i>p Viruses noname</i>	82	57	carriers	-0.247	0.095	0.012	0.047	non-carriers	-0.232	0.089	0.011	0.047
Class	<i>c Actinobacteria</i>	82	82	carriers	-21.533	5.239	0.000	0.001	non-carriers	-14.28	4.815	0.004	0.016
	<i>c Bacteroidia</i>	82	81	carriers	1.487	0.263	0.000	0.000	non-carriers	1.123	0.242	0.000	0.000
	<i>c Bacilli</i>	82	28	carriers	-0.852	0.316	0.009	0.035	non-carriers	-1.067	0.291	0.000	0.003
	<i>c Betaproteobacteria</i>	82	11	carriers	1.641	0.536	0.003	0.018	non-carriers	1.855	0.493	0.000	0.003
	<i>c Clostridia</i>	82	82	carriers	0.180	0.071	0.013	0.039	non-carriers	0.185	0.065	0.006	0.024
Order	<i>o Actinomycetales</i>	82	76	carriers	-0.210	0.065	0.002	0.012	non-carriers	-0.192	0.060	0.002	0.012
	<i>o Bacteroidales</i>	82	82	carriers	20.686	4.897	0.000	0.001	non-carriers	13.602	4.501	0.003	0.013
	<i>o Bifidobacteriales</i>	82	82	carriers	-18.955	4.672	0.000	0.001	non-carriers	-13.22	4.294	0.003	0.012
	<i>o Burkholderiales</i>	82	62						non-carriers	0.470	0.161	0.005	0.030
	<i>o Caudovirales</i>	82	56	carriers	-0.251	0.096	0.011	0.038	non-carriers	-0.233	0.089	0.011	0.038
	<i>o Clostridiales</i>	82	82	carriers	0.438	0.173	0.014	0.043	non-carriers	0.438	0.159	0.007	0.033
	<i>o Lactobacillales</i>	82	82	carriers	-4.654	1.501	0.003	0.012	non-carriers	-5.776	1.380	0.000	0.001
	<i>o Pasteurellales</i>	82	57	carriers	0.146	0.053	0.007	0.021	non-carriers	0.143	0.049	0.004	0.015
Family	<i>f Selenomonadales</i>	82	44	carriers	-0.515	0.186	0.009	0.038					
	<i>f Actinomycetaceae</i>	82	72	carriers	-0.197	0.061	0.002	0.032	non-carriers	-0.182	0.056	0.002	0.032
	<i>f Bacteroidaceae</i>	82	80	carriers	0.960	0.298	0.002	0.027					
	<i>f Bifidobacteriaceae</i>	82	82	carriers	-18.955	4.672	0.000	0.009	non-carriers	-13.22	4.294	0.003	0.035
	<i>f Clostridiales Family XIII Incertae Sedis</i>	82	28	carriers	-0.056	0.018	0.003	0.030	non-carriers	-0.052	0.017	0.003	0.030
	<i>f Lactobacillaceae</i>	82	44	carriers	-2.087	0.657	0.002	0.032	non-carriers	-2.328	0.604	0.000	0.009
	<i>f Pasteurellaceae</i>	82	57	carriers	0.287	0.086	0.001	0.022	non-carriers	0.273	0.079	0.001	0.020
	<i>f Porphyromonadaceae</i>	82	74	carriers	0.835	0.241	0.001	0.027	non-carriers	0.730	0.221	0.001	0.027
<i>f Rikenellaceae</i>	82	75	carriers	1.067	0.266	0.000	0.003	non-carriers	0.967	0.245	0.000	0.003	

Table 7.56 (Part 2) Multivariate analysis with significant associations for ‘group’, model accounts for the effect of ‘age’ and ‘sex’. Alzheimer’s Disease patient group as baseline contrast compared against Apolipoprotein ε4 carriers (contrast: carriers) and compared against the Apolipoprotein ε4 non-carriers (contrast: non-carriers)

Genus	<i>g_Actinomyces</i>	81	71	carriers	-0.220	0.063	0.001	0.018	non-carriers	-0.206	0.058	0.001	0.018
	<i>g_Alistipes</i>	81	74	carriers	1.146	0.276	0.000	0.003	non-carriers	1.044	0.255	0.000	0.003
	<i>g_Bacteroides</i>	81	81	carriers	1.011	0.309	0.002	0.015	non-carriers	0.461	0.159	0.005	0.032
	<i>g_Barnesiella</i>	81	33	carriers	1.852	0.517	0.001	0.009	non-carriers	1.582	0.478	0.001	0.011
	<i>g_Bifidobacterium</i>	81	81	carriers	-20.198	4.850	0.000	0.005	non-carriers	-14.45	4.481	0.002	0.035
	<i>g_Coprococcus</i>	81	67	carriers	0.809	0.292	0.007	0.035					
	<i>g_Eggerthella</i>	81	71	carriers	-0.796	0.210	0.000	0.011	non-carriers	-0.796	0.194	0.000	0.005
	<i>g_Faecalibacterium</i>	81	80	carriers	1.141	0.313	0.000	0.007	non-carriers	0.997	0.289	0.001	0.010
	<i>g_Haemophilus</i>	81	57	carriers	0.298	0.090	0.001	0.029	non-carriers	0.284	0.083	0.001	0.028
	<i>g_Lactobacillus</i>	81	43	carriers	-2.338	0.677	0.001	0.019	non-carriers	-2.575	0.625	0.000	0.005
	<i>g_Odoribacter</i>	81	65	carriers	0.520	0.140	0.000	0.027	non-carriers	0.518	0.130	0.000	0.022
	<i>g_Parabacteroides</i>	81	33	carriers	1.231	0.428	0.005	0.033	non-carriers	1.130	0.396	0.006	0.033
<i>g_Roseburia</i>	81	81	carriers	2.468	0.794	0.003	0.044						
Species	<i>s_Actinomyces_oris</i>	82	22	carriers	-0.020	0.004	0.000	0.000	non-carriers	-0.018	0.004	0.000	0.000
	<i>s_Actinomyces_viscosus</i>	82	42	carriers	-0.023	0.005	0.000	0.002	non-carriers	-0.021	0.005	0.000	0.002
	<i>s_Alistipes_putredinis</i>	82	57	carriers	2.099	0.557	0.000	0.010	non-carriers	1.809	0.512	0.001	0.014
	<i>s_Alistipes_nderdonkii</i>	82	16	carriers	1.663	0.455	0.000	0.012	non-carriers	1.784	0.418	0.000	0.003
	<i>s_Barnesiella_intestinihominis</i>	82	33	carriers	1.650	0.502	0.002	0.023	non-carriers	1.383	0.462	0.004	0.044
	<i>s_Bacteroides_stercoris</i>	82	21	carriers	2.126	0.671	0.002	0.029	non-carriers	2.655	0.617	0.000	0.003
	<i>s_Bifidobacterium_longum</i>	82	82	carriers	-10.022	2.210	0.000	0.002	non-carriers	-8.898	2.032	0.000	0.002
	<i>s_Eggerthella_unclassified</i>	82	70	carriers	-0.487	0.120	0.000	0.006	non-carriers	-0.479	0.110	0.000	0.002
	<i>s_Eubacterium_eligens</i>	82	32	carriers	1.573	0.398	0.000	0.007	non-carriers	1.400	0.366	0.000	0.010
	<i>s_Faecalibacterium_prausnitzii</i>	82	82	carriers	1.028	0.305	0.001	0.043	non-carriers	0.637	0.176	0.001	0.013
	<i>s_Haemophilus_parainfluenzae</i>	82	57	carriers	0.278	0.082	0.001	0.032	non-carriers	0.261	0.075	0.001	0.028
	<i>s_Odoribacter_splanchnicus</i>	82	60	carriers	0.513	0.140	0.000	0.016	non-carriers	0.504	0.129	0.000	0.009
	<i>s_Parabacteroides_merdae</i>	82	15	carriers	1.696	0.552	0.003	0.036	non-carriers	1.475	0.507	0.005	0.048
	<i>s_Streptococcus_thermophilus</i>	82	67	carriers	-1.698	0.476	0.001	0.021	non-carriers	-1.640	0.437	0.000	0.014

Table 7.57 KEGG metabolisms in Alzheimer's Disease vs Apolipoprotein E cohorts

KEGG metabolism	value	coef	p-value	q-value	value	coef	p-value	q-value
Carbohydrate metabolism	↑AD vs carriers	-0.0039	0.001	0.009	↑AD vs non-c.	-0.0039	0.0003	0.007
Metabolism of cofactors and vitamins	↓AD vs carriers	0.0040	0.013	0.040	↑AD vs non-c.	-0.0017	0.0018	0.014

If the coef is a negative number, then the AD patient group has higher values than the controls, Apolipoprotein ε4 carriers = carriers, Apolipoprotein ε4 non-carriers = non-c.

Table 7.58 KEGG modules that are enriched (↑) in Alzheimer's Disease vs Apolipoprotein E cohorts

Related KEGG metabolism	KEGG modules		value	coef	p-value	q-value	value	coef	p-value	q-value
3 –	Glycolysis (Embden-Meyerhof pathway)	M00001	carriers	-0.0004	0.0003	0.0051	non-c.	-0.000	0.001	0.015
3 –	Pentose phosphate pathway (Pentose phosphate cycle)	M00004	carriers	-0.0008	0.0000	0.0013	non-c.	-0.001	0.000	0.005
3 –	Pentose phosphate pathway, oxidative phase, glucose 6P => ribulose 5P	M00006					non-c.	-0.001	0.002	0.020
3 –	Pentose phosphate pathway, non-oxidative phase, fructose 6P => ribose 5P	M00007	carriers	-0.0014	0.0001	0.0035	non-c.	-0.001	0.005	0.034
3 –	Entner-Doudoroff pathway, glucose-6P, glucose-6P => glyceraldehyde-3P + pyruvate	M00008					non-c.	-0.001	0.009	0.040
3 –	Glucuronate pathway (uronate pathway)	M00014	carriers	-0.0009	0.0000	0.0014	non-c.	-0.001	0.000	0.005
1 –	Lysine biosynthesis, succinyl-DAP pathway	M00016	carriers	-0.0005	0.0002	0.0037	non-c.	-0.000	0.001	0.011
1 –	Lysine biosynthesis, DAP aminotransferase pathway	M00027					non-c.	-0.000	0.005	0.035
10 –	Guanine ribonucleotide biosynthesis	M00050	carriers	-0.0007	0.0004	0.0059	non-c.	-0.001	0.002	0.016
7 –	Tocopherol/tocotrienol biosynthesis	M00112	carriers	-0.0002	0.0051	0.0344				
1 –	GABA biosynthesis, eukaryotes	M00135	carriers	-0.0005	0.0021	0.0189				
4 –	Reductive pentose phosphate cycle (Calvin cycle)	M00165	carriers	-0.0006	0.0034	0.0260				
4 –	Reductive pentose phosphate cycle, glyceraldehyde-3P => ribulose-5P	M00167	carriers	-0.0008	0.0009	0.0102				
4 –	Nitrogen fixation, nitrogen => ammonia	M00175	carriers	-0.0005	0.0000	0.0013	non-c.	-0.0005	0.0000	0.0006
4 –	Formaldehyde assimilation, xylulose monophosphate pathway	M00344	carriers	-0.0014	0.0000	0.0014	non-c.	-0.0010	0.0014	0.0150
4 –	Formaldehyde assimilation, ribulose monophosphate pathway	M00345	carriers	-0.0009	0.0003	0.0054	non-c.	-0.0007	0.0009	0.0102
1 –	Lysine biosynthesis, acetyl-DAP pathway	M00525	carriers	-0.0007	0.0004	0.0060	non-c.	-0.0005	0.0038	0.0274
11 –	Carbazole degradation	M00544	carriers	-0.0002	0.0001	0.0018	non-c.	-0.0001	0.0004	0.0060
3 –	Nucleotide sugar biosynthesis	M00549	carriers	-0.0011	0.0001	0.0035	non-c.	-0.0009	0.0007	0.0088
3 –	Ascorbate degradation	M00550	carriers	-0.0011	0.0000	0.0003	non-c.	-0.0010	0.0000	0.0003
3 –	D-Galacturonate degradation (fungi)	M00630	carriers	-0.0001	0.0001	0.0018	non-c.	-0.0001	0.0002	0.0039

1: Amino acid metabolism, 2: Biosynthesis of other secondary metabolites, 3: Carbohydrate metabolism, 4: Energy metabolism, 5: Glycan biosynthesis and metabolism, 6: Lipid metabolism, 7: Metabolism of cofactors and vitamins, 8: Metabolism of other amino acids, 9: Metabolism of terpenoids and polyketides, 10: Nucleotide metabolism, 11: Xenobiotics biodegradation and metabolism, Apolipoprotein ε4 carriers = carriers, Apolipoprotein ε4 non-carriers = non-c.

Table 7.59 KEGG modules that are decreased (↓) in Alzheimer's Disease vs Apolipoprotein E cohorts

Related KEGG metabolism	KEGG modules		value	coef	p-value	q-value	value	coef	p-value	q-value
1 –	Lysine biosynthesis, AAA pathway, 2-oxoglutarate	M00030	carriers	0.0002	0.0008	0.0096				
1 –	Histidine degradation, histidine	M00045	carriers	0.0006	0.0028	0.0215				
10 –	Pyrimidine ribonucleotide biosynthesis	M00052	carriers	0.0007	0.0022	0.0193	non-c.	0.001	0.002	0.016
5 –	KDO2-lipid A biosynthesis, Raetz pathway	M00060	carriers	0.0009	0.0002	0.0039	non-c.	0.001	0.001	0.008
5 –	CMP-KDO biosynthesis	M00063	carriers	0.0076	0.0048	0.0290				
5 –	ADP-L-glycero-D-manno-heptose biosynthesis	M00064	carriers	0.0005	0.0076	0.0472	non-c.	0.001	0.003	0.022
5 –	Lipopolysaccharide biosynthesis	M00080	carriers	0.0002	0.0070	0.0442	non-c.	0.000	0.007	0.044
3 –	Pectin degradation	M00081	carriers	0.0018	0.0000	0.0001	non-c.	0.001	0.000	0.000
6 –	beta-Oxidation, acyl-CoA synthesis	M00086	carriers	0.0019	0.0082	0.0495	non-c.	0.002	0.004	0.026
9 –	C5 isoprenoid biosynthesis, non-mevalonate pathway	M00096	carriers	0.0011	0.0007	0.0094	non-c.	0.001	0.000	0.004
7 –	Pantothenate biosynthesis	M00119	carriers	0.0006	0.0041	0.0289				
7 –	Coenzyme A biosynthesis	M00120	carriers	0.0004	0.0084	0.0498				
7 –	Biotin biosynthesis, pimeloyl-ACP/CoA	M00123	carriers	0.0010	0.0028	0.0215				
7 –	Pyridoxal-P biosynthesis	M00124	carriers	0.0004	0.0052	0.0344				
7 –	Riboflavin biosynthesis	M00125	carriers	0.0008	0.0003	0.0054	non-c.	0.0007	0.0017	0.0161
2 –	Flavanone biosynthesis, phenylalanine => naringenin	M00137	carriers	0.0000	0.0027	0.0215				
4 –	Assimilatory sulfate reduction	M00176	carriers	0.0005	0.0083	0.0495				
4 –	F420 biosynthesis	M00378	carriers	0.0053	0.0032	0.0239	non-c.	0.0048	0.0037	0.0262
11 –	Benzoyl-CoA degradation	M00541					non-c.	0.0033	0.0038	0.0262
7 –	Biotin biosynthesis, BioI pathway	M00573	carriers	0.0008	0.0028	0.0215				
7 –	Biotin biosynthesis, BioW pathway	M00577	carriers	0.0009	0.0019	0.0173				

1: Amino acid metabolism, 2: Biosynthesis of other secondary metabolites, 3: Carbohydrate metabolism, 4: Energy metabolism, 5: Glycan biosynthesis and metabolism, 6: Lipid metabolism, 7: Metabolism of cofactors and vitamins, 8: Metabolism of other amino acids, 9: Metabolism of terpenoids and polyketides, 10: Nucleotide metabolism, 11: Xenobiotics biodegradation and metabolism, Apolipoprotein ε4 carriers = carriers, Apolipoprotein ε4 non-carriers = non-c.

Table 7.60 KEGG pathways that are enriched (↑) in Alzheimer's Disease vs Apolipoprotein E cohorts

Related KEGG metabolism	KEGG reference pathway	value	coef	p-value	q-value	value	coef	p-value	q-value
3 – Glycolysis/ Gluconeogenesis	ko00010	carriers	-0.0007	0.002	0.018	non-c.	-0.0006	0.004	0.033
3 – Pentose phosphate pathway	ko00030	carriers	-0.0006	0.004	0.032				
3 – Fructose and mannose metabolism	ko00051	carriers	-0.0013	0.002	0.016	non-c.	-0.0013	0.001	0.013
3 – Galactose metabolism	ko00052					non-c.	-0.0010	0.002	0.020
3 – Ascorbate and aldarate metabolism	ko00053	carriers	-0.0005	0.000	0.006	non-c.	-0.0005	0.000	0.002
6 – Steroid biosynthesis	ko00100	carriers	-0.0000	0.002	0.016	non-c.	-0.0000	0.003	0.024
2 – Penicillin and cephalosporin biosynthesis	ko00311	carriers	-0.0003	0.002	0.020	non-c.	-0.0003	0.001	0.007
2 – Neomycin, kanamycin and gentamicin biosynthesis	ko00524	carriers	-0.0005	0.000	0.004	non-c.	-0.0004	0.001	0.007
6 – Glycerolipid metabolism	ko00561	carriers	-0.0006	0.000	0.004				
11 – Chloroalkane and chloroalkene degradation	ko00625	carriers	-0.0008	0.000	0.001	non-c.	-0.0006	0.000	0.002
11 – Naphthalene degradation	ko00626	carriers	-0.0005	0.001	0.007	non-c.	-0.0004	0.002	0.017
7 – Retinol metabolism	ko00830	carriers	-0.0002	0.000	0.000	non-c.	-0.0002	0.000	0.000
11 – Metabolism of xenobiotics by cytochrome P450	ko00980	carriers	-0.0003	0.000	0.000	non-c.	-0.0003	0.000	0.001
11 – Drug metabolism - cytochrome P450	ko00982	carriers	-0.0005	0.000	0.000	non-c.	-0.0004	0.000	0.000
11 – Steroid degradation	ko00984	carriers	-0.0001	0.001	0.010				
9 – Biosynthesis of ansamycins	ko01051	carriers	-0.0004	0.003	0.026				

1: Amino acid metabolism, 2: Biosynthesis of other secondary metabolites, 3: Carbohydrate metabolism, 4: Energy metabolism, 5: Glycan biosynthesis and metabolism, 6: Lipid metabolism, 7: Metabolism of cofactors and vitamins, 8: Metabolism of other amino acids, 9: Metabolism of terpenoids and polyketides, 10: Nucleotide metabolism, 11: Xenobiotics biodegradation and metabolism, Apolipoprotein ε4 carriers = carriers, Apolipoprotein ε4 non-carriers = non-c.

Table 7.61 KEGG pathways that are decreased (↓) in Alzheimer's Disease vs Apolipoprotein E cohorts

Related KEGG metabolism	KEGG reference pathway	value	coef	p-value	q-value	value	coef	p-value	q-value
5 – Lipopolysaccharide biosynthesis	ko00540	carriers	0.0012	0.000	0.004	non-c	0.0011	0.000	0.006
7 – One carbon pool by folate	ko00670	carriers	0.0009	0.001	0.013	non-c	0.0009	0.000	0.005
7 – Riboflavin metabolism	ko00740	carriers	0.0009	0.000	0.001	non-c	0.0007	0.000	0.004
7 – Biotin metabolism	ko00780	carriers	0.0012	0.000	0.006	non-c	0.0009	0.005	0.038
9 – Terpenoid backbone biosynthesis	ko00900					non-c	0.0006	0.001	0.007

1: Amino acid metabolism, 2: Biosynthesis of other secondary metabolites, 3: Carbohydrate metabolism, 4: Energy metabolism, 5: Glycan biosynthesis and metabolism, 6: Lipid metabolism, 7: Metabolism of cofactors and vitamins, 8: Metabolism of other amino acids, 9: Metabolism of terpenoids and polyketides, 10: Nucleotide metabolism, 11: Xenobiotics biodegradation and metabolism, Apolipoprotein ε4 carriers = carriers, Apolipoprotein ε4 non-carriers = non-c.

Table 7.62 HUMAnN3 Stratified pathways enriched in Alzheimer's Disease vs Apolipoprotein E cohorts

feature	value	coef	pval	qvalue	value	coef	pval	qvalue
UNINTEGRATED_g_Actinomyces.s_Actinomyces_naeslundii	carriers	-0.0003	0.000	0.034	non-c.	-0.0003	0.001	0.044
UNINTEGRATED_g_Bifidobacterium.s_Bifidobacterium_dentium					non-c.	-0.0005	0.001	0.046
UNINTEGRATED_g_Streptococcus.s_Streptococcus_thermophilus	carriers	-0.0072	0.001	0.046	non-c.	-0.0070	0.001	0.044
UNINTEGRATED_g_Streptococcus.s_Streptococcus_thermophilus_CAG_236	carriers	-0.0030	0.001	0.044	non-c.	-0.0028	0.001	0.044
UNINTEGRATED_g_Bifidobacterium.s_Bifidobacterium_bifidum	carriers	-0.0152	0.002	0.046				
UNINTEGRATED_g_Bifidobacterium.s_Bifidobacterium_bifidum_CAG_234	carriers	-0.0028	0.001	0.046				

Note: UNINTEGRATED means that the identified species did not contribute to a known pathway.

Table 7.63 HUMAnN3 Stratified pathways decreased in Alzheimer's Disease vs Apolipoprotein E cohorts

feature	value	coef	pval	qvalue
UNINTEGRATED_g_Roseburia.s_Roseburia_intestinalis	carriers	0.0104	0.002	0.046

Table 7.64 HUMAnN3 Unstratified pathways enriched Alzheimer's Disease vs Apolipoprotein E cohorts

feature	value	coef	pval	qvalue	value	coef	pval	qvalue
GLYCOCAT-PWY: glycogen degradation I (bacterial)	carriers	-0.0002	0.000	0.000	non-c.	-0.0001	0.000	0.000
PWY-7328: superpathway of UDP-glucose-derived O-antigen building blocks biosyn.	carriers	-0.0001	0.000	0.000	non-c.	-0.0001	0.000	0.000
PWY-622: starch biosynthesis unclassified	carriers	-0.0001	0.000	0.001	non-c.	-0.0001	0.000	0.003
PWY-5384: sucrose degradation IV (sucrose phosphorylase)	carriers	-0.0001	0.000	0.001	non-c.	-0.0001	0.000	0.003
PWY-7198: pyrimidine deoxyribonucleotides de novo biosynthesis IV	carriers	-0.0001	0.000	0.001	non-c.	-0.0001	0.000	0.002
DAPLYSINESYN-PWY: L-lysine biosynthesis I	carriers	-0.0001	0.000	0.001	non-c.	-0.0001	0.001	0.010
PWY-7234: inosine-5'-phosphate biosynthesis III	carriers	-0.0002	0.000	0.001	non-c.	-0.0001	0.000	0.003
P4-PWY: superpathway of L-lysine, L-threonine and L-methionine biosynthesis I	carriers	-0.0001	0.000	0.002	non-c.	-0.0001	0.001	0.007
PWY-6270: isoprene biosynthesis I	carriers	-0.0001	0.000	0.002	non-c.	-0.0001	0.001	0.010
PWY-7560: methylerythritol phosphate pathway II	carriers	-0.0001	0.000	0.002	non-c.	-0.0001	0.001	0.010
P124-PWY: Bifidobacterium shunt	carriers	-0.0001	0.000	0.002	non-c.	-0.0001	0.003	0.022
HOMOSER-METSYN-PWY: L-methionine biosynthesis I	carriers	-0.0001	0.000	0.005	non-c.	-0.0001	0.000	0.002
PWY-4041: γ -glutamyl cycle	carriers	-0.0001	0.000	0.002	non-c.	-0.0001	0.000	0.005
PWY0-781: aspartate superpathway	carriers	-0.0001	0.000	0.002	non-c.	-0.0001	0.001	0.010
PWY-5100: pyruvate fermentation to acetate and lactate II	carriers	-0.0001	0.000	0.003	non-c.	-0.0001	0.003	0.019
MET-SAM-PWY: superpathway of S-adenosyl-L-methionine biosynthesis	carriers	-0.0001	0.001	0.006	non-c.	-0.0001	0.000	0.003

PWY-5484: glycolysis II (from fructose 6-phosphate)	carriers	-0.0001	0.000	0.003	non-c.	-0.0001	0.002	0.018
GLYCOLYSIS: glycolysis I (from glucose 6-phosphate)	carriers	-0.0001	0.000	0.003	non-c.	-0.0001	0.006	0.034
ANAEROFRUCAT-PWY: homolactic fermentation	carriers	-0.0001	0.000	0.005	non-c.	-0.0001	0.005	0.034
PWY-7117: C4 photosynthetic carbon assimilation cycle, PEPCK type	carriers	-0.0001	0.000	0.005	non-c.	-0.0001	0.002	0.019
NONMEVIPP-PWY: methylerythritol phosphate pathway I	carriers	-0.0002	0.000	0.006	non-c.	-0.0001	0.008	0.045
PWY-7220: adenosine deoxyribonucleotides de novo biosynthesis II	carriers	-0.0001	0.000	0.006	non-c.	-0.0001	0.001	0.010
PWY-7222: guanosine deoxyribonucleotides de novo biosynthesis II	carriers	-0.0001	0.000	0.006	non-c.	-0.0001	0.001	0.010
PWY-1861: formaldehyde assimilation II (RuMP Cycle)	carriers	-0.0001	0.001	0.006				
PWY-5913: TCA cycle VI (obligate autotrophs)	carriers	-0.0001	0.001	0.007	non-c.	-0.0001	0.004	0.025
PWY-5347: superpathway of L-methionine biosynthesis (transsulfuration)	carriers	-0.0001	0.003	0.021	non-c.	-0.0001	0.001	0.008
PWY0-162: superpathway of pyrimidine ribonucleotides de novo biosynthesis	carriers	-0.0001	0.002	0.016				
PWY66-400: glycolysis VI (metazoan)	carriers	-0.0001	0.002	0.018				
SER-GLYSYN-PWY: superpathway of L-serine and glycine biosynthesis I	carriers	-0.0001	0.002	0.018				
PWY-7211: superpathway of pyrimidine deoxyribonucleotides de novo biosynthesis	carriers	0.0000	0.002	0.019	non-c.	0.0000	0.002	0.019
PWY-6124: inosine-5'-phosphate biosynthesis II	carriers	-0.0001	0.002	0.019				
PWY-2942: L-lysine biosynthesis III	carriers	-0.0001	0.003	0.019				
PWY-6123: inosine-5'-phosphate biosynthesis I	carriers	-0.0001	0.003	0.019				
UDPNAGSYN-PWY: UDP-N-acetyl-D-glucosamine biosynthesis I	carriers	-0.0001	0.003	0.019				
PWY-241: C4 photosynthetic carbon assimilation cycle, NADP-ME type	carriers	-0.0001	0.005	0.030				
PWY0-166: superpathway of pyrimidine deoxyribonucleotides de novo biosynthesis (E. coli)	carriers	-0.0001	0.005	0.030				
THRESYN-PWY: superpathway of L-threonine biosynthesis	carriers	-0.0001	0.005	0.031				
PWY-7187: pyrimidine deoxyribonucleotides de novo biosynthesis II	carriers	-0.0001	0.006	0.035				
PYRIDNUCSAL-PWY: NAD salvage pathway I	carriers	-0.0001	0.006	0.035	non-c.	-0.0001	0.005	0.032
P461-PWY: hexitol fermentation to lactate, formate, ethanol and acetate	carriers	-0.0001	0.008	0.043	non-c.	0.0000	0.007	0.039
PWY-7242: D-fructuronate degradation	carriers	-0.0001	0.007	0.039				
ANAGLYCOLYSIS-PWY: glycolysis III (from glucose)	carriers	-0.0001	0.008	0.043				
PWY-3001: superpathway of L-isoleucine biosynthesis I	carriers	-0.0001	0.008	0.043				

Table 7.65 HUMAnN3 Unstratified pathways decreased in Alzheimer's Disease vs Apolipoprotein E cohorts

feature	value	coef	pval	qvalue	value	coef	pval	qvalue
RIBOSYN2-PWY: flavin biosynthesis I (bacteria and plants)	carriers	0.0001	0.004	0.024	non-c.	0.0001	0.007	0.042
THISYN-PWY: superpathway of thiamin diphosphate biosynthesis I	carriers	0.0001	0.008	0.045				

Table 7.66 Post-hoc analysis. Variance of between-sample functional diversity (Jaccard dissimilarity distances, 999 permutations) explained by each variable assessed with cross-sectional PERMANOVA for T2 and Alzheimer’s Disease patient samples

KEGG level	Source	Df	Sums Sq	R ²	F-value	p-value (Jaccard)	stress value
KEGG metabolism	group	2	0.308	0.071	3.018	0.027*	0.159
	age	1	0.051	0.012	0.993	0.363	
	sex	1	0.015	0.003	0.291	0.762	
	Residual	78	3.980	0.918			
	Total	82	4.335	1.000			
KEGG modules	group	2	0.326	0.074	3.150	0.026*	0.155
	age	2	0.051	0.012	0.991	0.361	
	sex	1	0.019	0.004	0.367	0.712	
	Residual	78	4.032	0.913			
	Total	82	4.415	1.000			
KEGG pathways	group	2	0.303	0.070	2.978	0.028*	0.171
	age	1	0.050	0.012	0.984	0.365	
	sex	1	0.017	0.004	0.336	0.743	
	Residual	78	3.968	0.918			
	Total	82	4.321	1.000			

Significance codes: 0 ***, 0.001**, 0.01*; stress value indicates reliability of ordination for k=2

Table 7.67 Post-hoc analysis, pairwise comparisons for all pairs of level for “group” using PERMANOVA

KEGG level	Pairwise comparison	Sums Sq	F-value	R ²	p-value	p-value corrected (FDR)
KEGG metabolism	APOε4 non-carriers vs carriers	0.082	1.748	0.024	0.165	0.165
	AD patients vs APOε4 non-carriers	0.266	5.934	0.121	0.006**	0.018*
	AD patients vs APOε4 carriers	0.126	2.039	0.043	0.113	0.165
KEGG modules	APOε4 non-carriers vs carriers	0.081	1.697	0.023	0.174	0.174
	AD patients vs APOε4 non-carriers	0.289	6.320	0.128	0.006**	0.018*
	AD patients vs APOε4 carriers	0.147	2.357	0.050	0.089	0.134
KEGG pathways	APOε4 non-carriers vs carriers	0.082	1.748	0.023	0.164	0.164
	AD patients vs APOε4 non-carriers	0.262	5.864	0.120	0.006**	0.018*
	AD patients vs APOε4 carriers	0.124	2.017	0.043	0.113	0.164

Significance codes: 0 ***, 0.001**, 0.01*; stress value indicates reliability of ordination for k=2

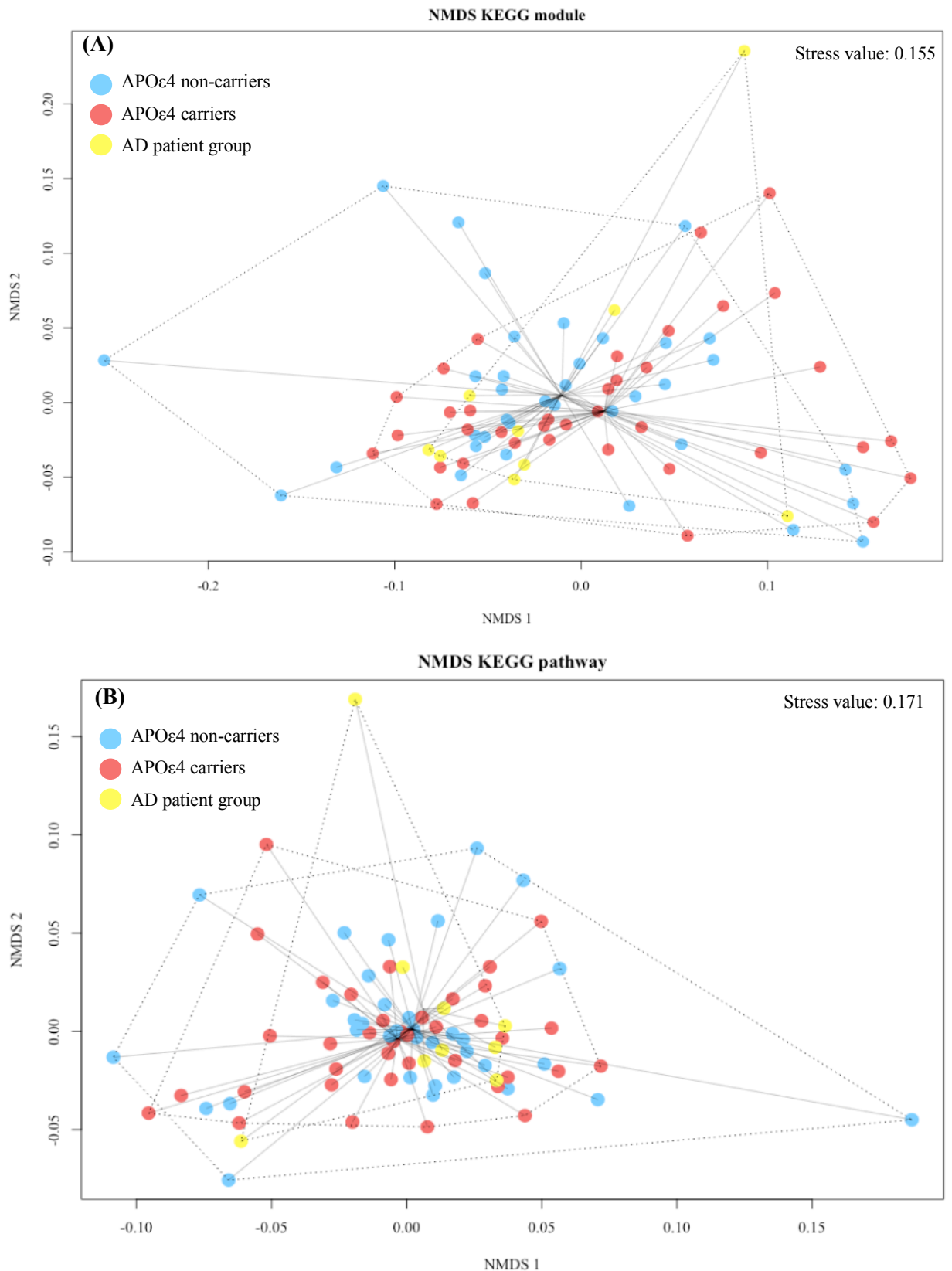


Figure 7.14 Non-metric Multidimensional Scaling (Jaccard diversity index) between the predicted (A) KEGG module and (B) KEGG pathways by group (light blue = Apolipoprotein ϵ 4 non-carriers, red = Apolipoprotein ϵ 4 carriers, yellow = Alzheimer's Disease patients). Each point denotes a sample in a reduced dimensional space and is connected with a line to the group centroid